# Rôle des corps nucléaires PML et du complexe chaperon d'histones HIRA dans la dynamique de la chromatine

Constance Kleijwegt

N°d'ordre NNT :
2021LYSE1112

# THESE de DOCTORAT DE L'UNIVERSITE DE LYON

opérée au sein de
**l'Université Claude Bernard Lyon 1**

**Ecole Doctorale** N°40
**Biologie Moléculaire, Intégrative et Cellulaire**

**Spécialité de doctorat** : Biologie cellulaire/épigénétique

Soutenue publiquement le 01/07/2021, par :
**Constance KLEIJWEGT**

---

# Rôle des corps nucléaires PML et du complexe chaperon d'histones HIRA dans la dynamique de la chromatine

---

Devant le jury composé de :

| | |
|---|---|
| **SCHAEFFER, Laurent**, Professeur des Universités-Praticien Hospitalier<br>Université Claude Bernard Lyon 1 | **Président** |
| **JULIEN, Eric**, Directeur de recherche CNRS,<br>Université de Montpellier | **Rapporteur** |
| **LALLEMAND-BREITENBACH, Valérie**, Directrice de recherche INSERM<br>Collège de France | **Rapporteure** |
| **NISOLE, Sébastien**, Chargé de recherche INSERM<br>Université de Montpellier | **Examinateur** |
| **POLO, Sophie**, Directrice de recherche INSERM<br>Université Paris Diderot | **Examinatrice** |
| **CORPET, Armelle**, Maître de conférence<br>Université Claude Bernard Lyon 1 | **Directrice de thèse** |
| **LOMONTE, Patrick,** Directeur de recherche CNRS<br>Université Claude Bernard Lyon 1 | **Co-directeur de thèse** |

# Université Claude Bernard – LYON 1

| | |
|---|---|
| Président de l'Université | M. Frédéric FLEURY |
| Président du Conseil Académique | M. Hamda BEN HADID |
| Vice-Président du Conseil d'Administration | M. Didier REVEL |
| Vice-Président du Conseil des Etudes et de la Vie Universitaire | M. Philippe CHEVALLIER |
| Vice-Président de la Commission de Recherche | M. Petru MIRONESCU |
| Directeur Général des Services | M. Pierre ROLLAND |

## COMPOSANTES SANTE

| | |
|---|---|
| Département de Formation et Centre de Recherche en Biologie Humaine | Directrice : Mme Anne-Marie SCHOTT |
| Faculté d'Odontologie | Doyenne : Mme Dominique SEUX |
| Faculté de Médecine et Maïeutique Lyon Sud - Charles Mérieux | Doyenne : Mme Carole BURILLON |
| Faculté de Médecine Lyon-Est | Doyen : M. Gilles RODE |
| Institut des Sciences et Techniques de la Réadaptation (ISTR) | Directeur : M. Xavier PERROT |
| Institut des Sciences Pharmaceutiques et Biologiques (ISBP) | Directrice : Mme Christine VINCIGUERRA |

## COMPOSANTES & DEPARTEMENTS DE SCIENCES & TECHNOLOGIE

| | |
|---|---|
| Département Génie Electrique et des Procédés (GEP) | Directrice : Mme Rosaria FERRIGNO |
| Département Informatique | Directeur : M. Behzad SHARIAT |
| Département Mécanique | Directeur M. Marc BUFFAT |
| Ecole Supérieure de Chimie, Physique, Electronique (CPE Lyon) | Directeur : Gérard PIGNAULT |
| Institut de Science Financière et d'Assurances (ISFA) | Directeur : M. Nicolas LEBOISNE |
| Institut National du Professorat et de l'Education | Administrateur Provisoire : M. Pierre CHAREYRON |
| Institut Universitaire de Technologie de Lyon 1 | Directeur : M. Christophe VITON |
| Observatoire de Lyon | Directrice : Mme Isabelle DANIEL |
| Polytechnique Lyon | Directeur : Emmanuel PERRIN |
| UFR Biosciences | Administratrice provisoire : Mme Kathrin GIESELER |
| UFR des Sciences et Techniques des Activités Physiques et Sportives (STAPS) | Directeur : M. Yannick VANPOULLE |
| UFR Faculté des Sciences | Directeur : M. Bruno ANDRIOLETTI |

*« Ne te contente pas du ‘qu’est-ce que c’est’,*
*mais essaie de savoir le ‘pourquoi’ et le ‘comment’. »*

Lord Robert Baden-Powell

# Remerciements

A l'aube de ma soutenance de thèse, il est temps pour moi de remercier toutes les personnes qui ont contribué de près ou de loin au bon déroulement de mon doctorat (et c'est assez incroyable le nombre de personnes qui croisent notre route en l'espace de 4 ans) :

Armelle Corpet, ma directrice de thèse, pour m'avoir fait confiance et donné ma chance, en tant que stagiaire puis en tant que doctorante. Je voudrais te remercier pour ton soutien, tes conseils, ta bienveillance et ton enthousiasme. Il m'est difficile d'écrire tout ce tu m'as transmis et j'espère que tu réalises à quel point travailler pendant 4 ans à tes côtés m'a tant apporté professionnellement et humainement. Tu m'as transmis ton amour de la recherche et du partage de connaissance et c'est en partie grâce à toi que je souhaite poursuivre dans cette voie. J'étais ta première étudiante en thèse et j'espère que de nombreux autres auront la chance de t'avoir comme mentor.

Patrick Lomonte, mon co-directeur de thèse, pour m'avoir accueilli dans ton équipe et pour avoir accepté de co-diriger ma thèse. Je te remercie pour ton regard critique et constructif sur mes travaux, toujours rempli de bienveillance. Tu m'as appris à prendre de la hauteur et à m'intéresser à d'autres sujets *a priori* éloignés du mien. Je suis d'ailleurs admirative de ton immense curiosité scientifique et espère que cette qualité saura m'inspirer tout au long de ma carrière.

Valérie Lallemand-Breitenbach et Éric Julien pour avoir accepté de lire et d'évaluer ce manuscrit, Sébastien Nisole et Laurent Schaeffer pour avoir accepté de participer à mon jury de thèse, ainsi que Sophie Polo qui, après m'avoir accompagnée et conseillée en tant que membre de mon comité de suivi de thèse, a également accepté de faire partie de mon jury. Je tiens aussi à remercier Benjamin Loppin, second membre de mon comité de suivi de thèse, pour m'avoir suivie pendant ces 4 années. Merci pour votre regard critique et vos conseils qui ont été d'une aide précieuse.

Caroline Schluth-Bolard pour l'optimisation du FISH, Séverine Croze pour ton aide dans l'analyse de la fragmentation de la chromatine et Thomas Simonet pour ton aide dans l'analyse du ChIP seq,

L'Ecole Doctorale BMIC et l'Université Claude Bernard Lyon 1 pour avoir financé mes trois premières années de thèse et pour avoir proposé de nombreuses formations qui me seront très utiles dans ma carrière et dans ma vie, ainsi que la FRM pour avoir accepté de financer ma quatrième année de thèse.

L’équipe de choc qu’est l’équipe Lomonte sans qui ces 4 ans n’auraient pas eu la même saveur : les anciens membres de l’équipe, Karine, Camille, Boris et Soraya ainsi et les membres actuels, Olivier, Simon, Pascale, Franceline, Florent, Clément et Faouzi. Merci pour les rires, l’entraide, les conseils, les sorties Yafa, les pauses mots fléchés, les initiations yoga et escalades… et tant d’autres choses.

Mes camarades doctorants de l’INMG, désormais docteurs, pour avoir partagé avec moi les joies et les doutes de la thèse : Dounia, pour ton immense gentillesse et ton soutien, Laurent pour ta bonne humeur et les discussions au Chemidoc ainsi que Thibault et Hugo pour votre humour, votre légèreté et évidemment pour les bières.

Mon ancien colocataire et ami de très longue date, Florian, pour ton amitié et ta présence dans les bons comme les mauvais moments, ainsi que mon amie de moins longue date mais tout aussi importante, Mélanie, pour ton soutien et ton écoute qui ont également été très précieux pour moi. Merci pour les Blind test, les karaokés, les après-midi jeux de société et tout ce que nous avons pu partager ensemble.

Thomas, mon ami fidèle pour ta présence malgré la distance. Merci pour ta bonne humeur et ton amour, si chers à mon cœur.

Mes amis lyonnais pour avoir contribué à ma vie sociale pendant ces 4 ans et pour avoir su apporter de la fraîcheur dans mon quotidien : Amandine, Tony, Maxence, Gaëlle, Clotilde, Daniela, Étienne, Guillaume, Nicolas et Wilhelm.

Mes amis poitevins pour votre présence quand je rentrais au pays : ma famille scoute Laura, Anne-Charlotte et Matthieu ainsi que Ludivine, Mathilde, Grégoire et Charles.

Mes amis Erasmus, qui malgré la distance auront toujours une place particulière dans mon cœur : Andi, Marie, Matthieu et Ross.

Évidemment, ma famille, mes parents, mon frère, Marianna, Florence qui m’ont soutenue et accompagnée pendant cette thèse. Merci pour votre confiance et votre amour.

Enfin, Clément pour être entré dans ma vie il y a maintenant 2 ans. Merci pour ton amour, ton soutien, ton humour, pour les voyages, les films, les musées, les balades, les restaurants, les verres en terrasse… et tout ce que nous avons partagé ensemble.

# Résumé

Au sein du noyau des cellules eucaryotes, l'ADN s'enroule autour de protéines histones pour former une structure appelée la chromatine. Cette organisation permet notamment la compaction d'un génome de 2 mètres dans un noyau d'une dizaine de micromètres. Elle permet également de réguler l'expression des gènes. En effet, la chromatine est porteuse d'une information appelée l'information épigénétique et la modulation de sa structure peut avoir des conséquences importantes sur le programme transcriptionnel d'une cellule. Le complexe chaperon d'histones HIRA est impliqué dans le dépôt du variant d'histone H3.3 dans des régions d'euchromatine ou dans des régions dépourvues de nucléosomes afin d'assurer l'intégrité de la chromatine et de l'information épigénétique. En conditions normales, le complexe HIRA localise de façon homogène dans le noyau cellulaire ; en revanche, dans certaines conditions de stress, comme lors de l'inflammation, de l'entrée des cellules en sénescence ou, comme je l'ai montré dans ma thèse, lors de l'induction de cassures double-brin de l'ADN, le complexe HIRA s'accumule avec H3.3 dans des organelles nucléaires sphériques sans membrane appelés corps nucléaires PML. L'impact fonctionnel d'une telle accumulation est encore mal compris. Lors de ma thèse, j'ai cherché à comprendre comment et pourquoi le complexe HIRA localisait dans ces organelles. En particulier, j'ai cherché à analyser l'impact fonctionnel de cette localisation sur le dépôt d'H3.3 en des régions particulières de la chromatine.

Dans un premier temps, j'ai investigué les mécanismes et le rôle de la relocalisation de HIRA lors de l'inflammation induite en réponse de la signalisation interféron de type I (IFN-I), une cytokine pro-inflammatoire. Mes travaux ont permis de montrer que le complexe HIRA relocalise au sein des corps nucléaires PML d'une façon dépendante des interactions entre la modification SUMO et un motif d'interaction avec cette modification (SIM). De plus, j'ai montré que le complexe HIRA et les corps nucléaires PML étaient importants dans la régulation de l'expression des gènes stimulés par l'IFN-I (ISGs), en participant à l'incorporation du variant d'histone H3.3 dans ces loci géniques. Leur action pourrait permettre de mieux contrôler la réponse inflammatoire afin d'assurer son homéostasie. Dans un second temps, je me suis intéressée à la relocalisation d'HIRA dans les corps nucléaires PML induite par les cassures double-brin, jamais décrite auparavant. J'ai montré que cette relocalisation est indépendante de la signalisation IFN-I et dépend probablement de la signalisation en réponse aux dommages à l'ADN. Le recrutement d'HIRA est également dépendant d'interactions SIM-SUMO. De façon intéressante, le complexe HIRA dans les corps nucléaires PML juxtapose à proximité des sites de cassures, et cela pourrait servir à incorporer de nouvelles histones après la réparation et ainsi assurer le rétablissement de la structure chromatinienne.

# Abstract

Within the nucleus of eucaryotic cells, DNA is wrapped around histone proteins in order to form a structure called chromatin. This organization allows the compaction of a genome of 2 meters in a nucleus of around ten micrometers. It also allows the regulation of gene expression. Indeed, chromatin carries a source of information called epigenetic information and the modulation of its structure has important consequences on the transcriptional program. The histone chaperone complex HIRA is involved in the deposition of the histone variant H3.3 in euchromatin regions and in regions devoid of nucleosomes, in order to ensure chromatin and epigenetic integrity. Under normal conditions, the HIRA complex localizes homogeneously in the cell nucleus; on the other hand, under certain stressful conditions, such as during inflammation, the entry of cells into senescence or, as I showed in my thesis, during the induction of double-strand DNA breaks, the HIRA complex accumulates with H3.3 in spherical nuclear membrane-less organelles called PML nuclear bodies. The functional impact of such accumulation is still poorly understood. During my thesis, I sought to understand how and why the HIRA complex localizes in these organelles. In particular, I sought to analyse the functional impact of this localization on the deposition of H3.3 in particular regions of the chromatin.

First, I investigated the mechanisms and role of HIRA relocalization during inflammation response to type I interferon (IFN-I) treatment, a pro-inflammatory protein. My work has shown that the HIRA complex relocalizes within PML nuclear bodies in a manner dependent on interactions between SUMO modifications and a SUMO-interacting motif (SIM). In addition, I have shown that the HIRA complex and PML nuclear bodies are important in the regulation of the expression of IFN-I-stimulated genes (ISGs), by participating in the incorporation of the histone variant H3 .3 in these gene loci. Their action could allow better control of the inflammatory response in order to ensure its homeostasis. Secondly, I was interested in the relocalization of HIRA within PML nuclear bodies induced by double-strand breaks, never described before. I have shown that this relocalization is independent of IFN-I signaling and probably depends on signaling in response to DNA damage. Recruitment of HIRA is also dependent on SIM-SUMO interactions. Interestingly, the HIRA complex in PML nuclear bodies juxtaposes near the sites of damage, and this could serve to incorporate new histones after repair and thus ensure the reestablishment of the chromatin structure.

# Table des matières

# Table des figures et des tableaux

**Figures :**

## Tableaux :

# Liste des abréviations

### A

| | |
|---|---|
| **ADN** | Acide désoxyribonucléique |
| **ADNdb** | ADN double brin |
| **ADNsb** | ADN simple brin |
| **ALR** | AIM2-like receptor |
| **ALT** | Alternative lenghtening of telomeres |
| **Alt-EJ** | Alternative end-joining |
| **APB** | ALT-associated PML NB |
| **APL** | Acute promyelocytic leukemia |
| **ARN** | Acide ribunucléique |
| **ARNdb** | ARN double brin |
| **ARNsb** | ARN simple brin |
| **ASF1** | Anti-silencing function protein 1 |
| **ATM** | Ataxia telangiectasia mutated |
| **ATP** | Adénosine triphosphate |
| **ATR** | Ataxia telangiectasia mutated and Rad3-related homolog |
| **ATRX** | Alpha thalassemia/mental retardation syndrome X-linked protein |

### B

| | |
|---|---|
| **BER** | Base excision repair |
| **BLM** | Bloom syndrome protein |
| **BRCA** | Breast cancer susceptibility protein |
| **BRD4** | Bromodomain-containing protein 4 |

### C

| | |
|---|---|
| **CABIN1** | Calcineurin binding protein 1 |
| **Càd** | C'est-à-dire |
| **CAF-1** | Chromatin associated factor 1 |
| **CBP** | CREB-binding protein |
| **CDK** | Cyclin-dependent kinase |
| **CENP** | Centromere protein |
| **cGAMP** | Cyclic GMP-AMP |
| **cGAS** | Cyclic GMP-AMP synthase |
| **CHD** | Chromodomain helicase DNA-binding |
| **CHK** | Checkpoint kinase |
| **CLR** | C-type lectin receptor |
| **CRKL** | CRK-like protein |
| **CTCF** | CCCTC-binding factor |
| **CXCR** | C-X-C chemokine receptor |

### D

| | |
|---|---|
| **DAMP** | Damage-associated molecular pattern |
| **DAXX** | Death domain-associated protein 6 |
| **DDR** | DNA damage response |
| **dHJ** | Double Holliday junction |
| **DNA-PK** | DNA-dependent protein kinase |
| **DNMT** | DNA methyltransferase |
| **DSB** | Double srand break |

### E

| | |
|---|---|
| **ES cells** | Embryonic stem cell |

### F

| | |
|---|---|
| **FA** | Fanconi anemia |
| **FACT** | Facilitated chromatin transcription complex |
| **FISH** | Fluorescent *in situ* hybridization |

### G

| | |
|---|---|
| **GG-NER** | Global genomic NER |
| **γH2AX** | Phosphorylation de la sérine 139 de H2AX |
| **GHRL** | Ghrelin |
| **GSK** | Glycogen synthase kinase |

### H

| | |
|---|---|
| **H2BK120** | Lysine 120 de l'histone H2B |
| **H2BK120ub** | Ubiquitination de H2BK120 |
| **H3.3S31** | Sérine 31 de l'histone H3.3 |
| **H3.3S31ph** | Phosphorylation de H3.3S31 |
| **H3K27** | Lysine 27 de l'histone H3 |
| **H3K27me3** | Triméthylation de H3K27 |
| **H3K36** | Lysine 36 de l'histone H3 |
| **H3K36me3** | Triméthylation de H3K36 |
| **H3K4** | Lysine 4 de l'histone 3 |
| **H3K4me1** | Monométhylation de H3K4 |
| **H3K9** | Lysine 9 de l'histone H3 |
| **H3K9me2** | Diméthylation de H3K9 |
| **H3K9me3** | Triméthylation de H3K9 |
| **HAT** | Histone acetyltransferase |
| **HDAC** | Histone deacetylase |
| **HEK 293** | Human embryonic kidney cells 293 |
| **HIRA** | Histone regulator A |
| **HR** | Homologous recombination |
| **HSV-1** | Herpes simplex virus 1 |

### I

| | |
|---|---|
| **IFN** | Interferon |
| **IFNAR** | Type I IFN receptor |
| **IFIT2/ISG54** | Interferon-induced protein with tetratricopeptide repeats 2 |
| **IL-(n)** | Interleukin-(n) |
| **IL(n)R** | Interleukin-(n) receptor |
| **IRF** | Interferon regulatory factor |
| **IRG** | Interferon regulated gene |
| **ISG** | Interferon stimulated gene |
| **ISWI** | Imitation switch |

### J

| | |
|---|---|
| **JAK** | Janus kinase |

### L

| | |
|---|---|
| **LAD** | Lamina associated domain |
| **LAMP** | Lifestyle-associated molecular pattern |
| **LLPS** | Liquid-liquid phase separation |
| **lncRNA** | Long non-coding RNA |

## M

**MAPK** Mitogen-activated protein kinase
**MBD** Methyl-CpG-binding domain protein
**MEF** Murine embryonnic fibroblast
**MGMT** Methylguanine methyltransferase
**MHC** Major histocompatibility complex
**MRE11** Meiotic recombination 11
**MRN** Complexe MRE11, RAD50 et NSB1
**mTOR** Mammalian target of rapamycin
**MX1** Myxoma resistance protein 1
**MyD88** Myeloid differentiation primary response protein 8
**MyoD** Myoblast determination protein

## N

**NAD** Nucleolus associated domain
**NASP** Nuclear autoantigenic sperm protein
**NBS1** Nijmegen breakage syndrome protein 1
**NER** Nucleotide excision repair
**NF-κB** Nuclear factor kappa B
**NHEJ** Non-homologous end-joining
**NLR** NOD-like receptor

## O

**OAS1** 2'-5'-oligoadenylate synthase 1

## P

**PAD** PML associated domain
**PAMP** Pathogen-associated molecular pattern
**PARP** Poly(ADP) ribose polymerase
**PI3K** Phosphoinositide 3-kinase
**PML** Promyelocytic leukemia
**PML NB** PML nuclear body
**pRB** Retinoblastoma-associated protein
**PRR** Pattern recognition receptor
**PTM** Post-translational modification

## R

**RARα** Retinoic acid receptor alpha
**RLR** RIG-I-like receptor
**RNF** RING finger protein
**RNS** Reactive nitrogen species
**ROS** Reactive oxygen species
**RPA** Replication protein A

## S

**SAE** SUMO-activating enzyme
**SAHF** Senescence-associated heterochromatin foci
**SASP** Senescence-associated secretory phenotype
**SDSA** Synthesis-dependent strand annealing
**SENP** Sentrin-specific protease
**SETD** SET domain protein
**SETDB** SET domain bifurcated protein
**SSA** Single-strand annealing
**STAT** Signal transducer and activator of transcription
**STING** Stimulator of interferon genes protein
**SUMO** Small ubiquitin-like modifier
**SWI/SNF** Switch/sucrose non-fermentable

## T

**TAD** Topologically associated domain
**TC-NER** Transcription-coupled NER
**TLR** Tolll-like receptor
**TLS** Translesion synthesis
**TNFα** Tumor necrosis factor alpha
**TNFR** Tumor necrosis factor receptor
**TOP** DNA topoisomerase
**TOPBP** Topoisomerase binding protein
**TRIF/TICAM1** TIR domain-containing adaptator molecule 1
**TYK** Tyrosine-protein kinase

## U

**UBC9** Ubiquitin carrier protein 9
**UBN1** Ubinuclein 1
**UHRF** Ubiquitin-like with PHD and RING finger domain-containing protein
**USP** Ubl carboxyl-terminal hydrolase

## V

**vDCP NB** Viral DNA-containing PML NB

## Z

**ZMYND11** Zinc-finger MYND domain-containing protein 11
**ZNF** Zinc-finger protein

# Introduction

# I. La chromatine, source d'information épigénétique

Au sein du noyau des cellules eucaryotes, l'ADN constitue le support de l'information génétique. Il est associé avec des protéines appelées histones pour former une structure nucléoprotéique, la chromatine (Kornberg, 1977). Cette organisation permet notamment la compaction d'un génome d'environ 2 mètres de long au sein du noyau cellulaire d'une dizaine de micromètres de diamètre. L'organisation de la chromatine est aussi porteuse d'une information supplémentaire à l'information génétique : l'information épigénétique. Après un bref historique sur la définition de l'épigénétique, je décrirai dans ce chapitre la structure de la chromatine et comment certaines modifications peuvent influer sur son organisation et être source d'information épigénétique. Je terminerai cette partie sur le variant d'histone H3.3 et le complexe chaperon d'histone HIRA, au cœur de mes travaux de thèse.

## I.1. La définition de l'épigénétique

La définition de l'épigénétique est complexe et largement débattue au sein de la communauté scientifique (pour revue, voir Nicoglou and Merlin, 2017). La notion d'épigénétique fut tout d'abord utilisée dans le domaine de la biologie développementale. Elle est pour la première fois introduite par Conrad Waddington dans les années 1940 (Waddington, 1940). Il définit alors l'épigénétique comme « l'étude des mécanismes par lesquels le génotype mène au phénotype » dans le contexte du développement. Il choisit le terme 'épigénétique' en référence à la théorie de l'épigénèse (càd. développement progressif des tissus de l'embryon), qui s'oppose à la théorie de la préformation (càd. organes déjà présents chez l'embryon qui est considéré comme un être vivant miniature). Dix-huit ans plus tard, le biologiste David Nanney donne une nouvelle définition du terme 'épigénétique' (Nanney, 1958) . Dans ses écrits, il associe le génome à « une librairie de spécificités » et définit comme « systèmes de contrôle épigénétique » les mécanismes employés pour l'expression spatiale et temporelle de ces spécificités. Il introduit pour la première fois la condition d'héritabilité des marques épigénétiques ; en effet, selon lui, ces « systèmes de contrôle épigénétique » sont stables mitotiquement grâce à une « mémoire cellulaire » qui permet aux cellules de maintenir leurs différences concernant leur profil d'expression génétique afin de participer à la construction de différents tissus et organes au cours du développement embryonnaire. Dans la lignée des travaux de Nanney, dans les années 90, Robin Holliday et Arthur Riggs proposent une nouvelle définition de l'épigénétique, définition actuellement la plus populaire au sein de la communauté scientifique (Holliday, 1994; Riggs et al., 1996). En se basant sur leurs travaux sur la méthylation de l'ADN (Holliday and Pugh, 1975; Riggs, 1975), ils définissent l'épigénétique comme « l'étude des changements dans la fonction des gènes, mitotiquement et/ou

méiotiquement héritables, qui ne peuvent pas être expliqués par des changements de la séquence ADN » (définition issue de Riggs et al., 1996).

Cependant, les recherches sur les modifications d'histones et sur les ARN non codants tendent à assouplir la définition d'épigénétique. En effet, beaucoup d'études utilisent désormais le terme 'épigénétique' pour définir « l'étude des mécanismes moléculaires qui modifient l'activité des gènes indépendamment de changements dans la séquence ADN sans condition d'héritabilité des marques » (Nicoglou and Merlin, 2017). Cette définition considère ainsi comme processus épigénétiques les modifications transitoires de l'organisation de la chromatine participant à la signalisation cellulaire. Dans une revue récente, Giacomo Cavalli et Edith Heard argumentent en faveur de cette définition moins stricte de l'épigénétique, considérant qu'elle permet également d'englober les changements chromatiniens observés dans les cellules post-mitotiques et ne se focalise pas uniquement sur l'expression des gènes de l'ADN génomique mais sur l'entièreté de l'ADN de l'organisme, y compris l'ADN du microbiote (Cavalli and Heard, 2019). Dans le cadre de ma thèse, j'emploierai donc le terme 'épigénétique' en me référant à cette dernière définition, et en écartant la condition d'héritabilité des marques épigénétiques que j'étudierai.

L'information épigénétique est portée par des modifications de la chromatine. Dans la prochaine partie, je détaillerai les différents niveaux d'organisation de cette structure nucléoprotéique, de l'unité de base que constitue le nucléosome au niveau le plus compacté au moment de la mitose cellulaire, le chromosome.

## I.2. La structure de la chromatine

### *I.2.i. Le nucléosome, unité de base de la chromatine*

Le nucléosome est constitué d'une particule cœur, le noyau nucléosomique et, de chaque côté, de l'ADN internucléosomal, dit ADN de liaison dont la longueur varie en fonction de espèces et des types cellulaires (***Figure 1***) (Kornberg, 1977). Le noyau nucléosomique est formé d'un octamère d'histones autour duquel s'enroule 147 paires de bases de la double hélice d'ADN, effectuant 1,65 tours. L'axe de symétrie du nucléosome est appelé la dyade. L'octamère d'histones consiste en l'assemblage de deux dimères d'histones H2A-H2B avec un tétramère d'histones $(H3\text{-}H4)_2$. Le noyau nucléosomique est fréquemment lié par une cinquième histone, l'histone de liaison H1, qui lie 20 paires de bases d'ADN au site d'entrée et de sortie à la surface du noyau nucléosomique au niveau de la dyade du nucléosome (Simpson, 1978). Le noyau nucléosomique associé à l'histone de liaison forme une structure appelée chromatosome (***Figure 1***) (Simpson, 1978).

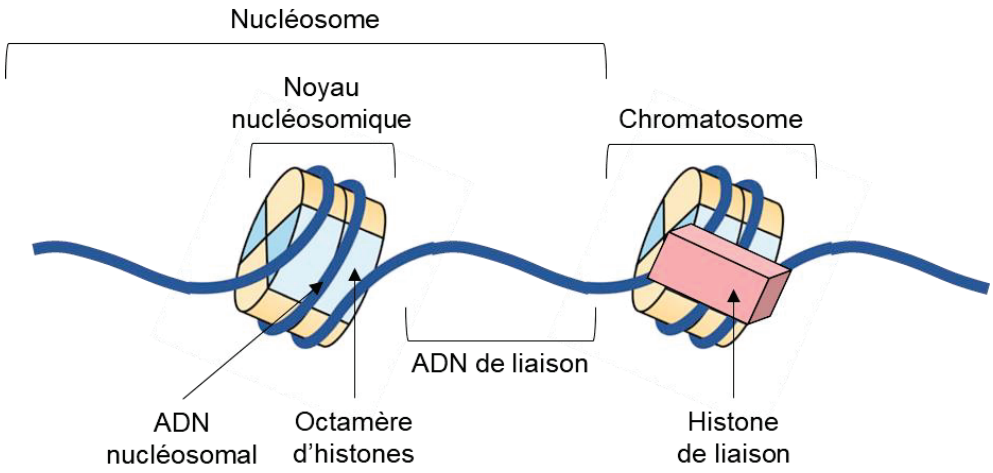


**Figure 1. Le nucléosome, unité de base de la chromatine.** Le nucléosome est constitué d'un noyau nucléosomique et d'ADN de liaison. Le noyau nucléosomique comprend un octamère d'histone autour duquel s'enroule l'ADN nucléosomale. Lorsqu'une histone de liaison se lie au noyau nucléosomique, on parle alors de chromatosome

Les histones sont de petites protéines d'environ 15kDa dont la charge positive permet leur interaction avec l'ADN. Il en existe 5 classes : les histones H2A, H2B, H3 et H4 (histones cœur) et l'histone de liaison H1. Les quatre protéines d'histones cœur (H2A, H2B, H3 et H4) sont très conservées au sein des eucaryotes. Elles possèdent un motif globulaire central appelé le domaine « histone-fold », composé de trois hélices alpha permettant la formation des dimères. Les régions intermédiaires entre les hélices alpha forment des ponts bêta présentant des résidus d'acides aminés chargés positivement servant de point d'ancrage à la double hélice d'ADN chargée négativement (Luger et al., 1997). Les histones cœur possèdent également une queue désorganisée riche en arginines et lysines en position N-terminale pour les histones H2B, H3 et H4 et en positions N- et C-terminales pour l'histone H2A. Ces queues d'histones sont à l'extérieur du noyau nucléosomique et sont donc accessibles et modifiables post-traductionnellement par des enzymes (***Figure 2***) (Luger and Richmond, 1998) (cf. partie *I.3.ii*).

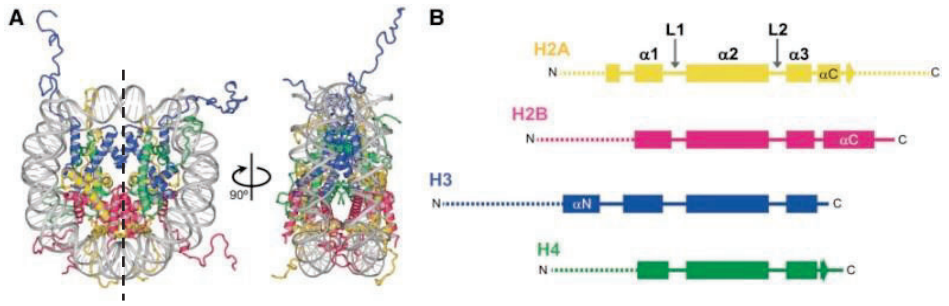


**Figure 2. L'organisation du noyau nucléosomique.** (Koyama and Kurumizaka, 2018) **A.** Structure globale du noyau nucléosomique. La double hélice d'ADN nucléosomique est représentée en gris, l'octamère d'histones est représenté en couleur (H2A=jaune ; H2B=rose ; H3=bleu ; H4=vert). La dyade est représentée par l'axe en pointillé noir. **B.** Visualisation des domaines des 4 histones cœur. Les boîtes correspondent à des hélices alpha, les lignes représentent les ponts bêta, les pointillés correspondent aux queues désorganisées.

L'histone de liaison H1 permet de stabiliser le nucléosome et de faciliter l'organisation de la chromatine en structures d'ordre supérieur. Elle influe également sur l'espacement des nucléosomes le long de la chromatine. La séquence protéique de l'histone H1 est plus variable au sein des eucaryotes ; cependant, on observe une structure redondante en trois domaines : un court domaine N-terminal, un domaine central globulaire et un domaine C-terminal (Cutter and Hayes, 2017). Le domaine central globulaire est le plus conservé. Il contient un motif « winged-helix fold » qui permet la liaison à l'ADN et est nécessaire pour la reconnaissance du noyau nucléosomique. Le domaine C-terminal est important pour la stabilisation du chromatosome et de la chromatine en structures d'ordre supérieur. Enfin, la queue N-terminale n'est pas essentielle pour la formation du chromatosome mais ses modifications post-traductionnelles influent sur l'affinité de l'histone de liaison avec le noyau nucléosomique (Roque et al., 2016).

### *I.2.ii. Les structures d'ordre supérieur de la chromatine*

La répétition de nucléosomes forme une structure en « collier de perle » appelée fibre nucléosomale ou fibre de 11nm, en référence à son diamètre. Cette fibre constitue le premier niveau de compaction de la chromatine (Kornberg, 1974, 1977). L'espacement régulier des nucléosomes est assuré par des ATPases de remodelage de la chromatine de la famille des ISWI (Imitation SWItch) et CHD (Chromodomain Helicase DNA-binding) (Clapier et al., 2017). Les ATPases de remodelage de la famille des SWI/SNF (SWItch/Sucrose Non-Fermentable) peuvent quant à elles faire glisser ou éjecter des nucléosome, favorisant la liaison de certains facteurs à l'ADN (par ex. facteurs de transcription, machinerie de réparation de l'ADN…) (Clapier et al., 2017).

Par la suite, la chromatine subit des niveaux de compaction supérieurs, jusqu'à atteindre sa forme la plus compactée au moment de la mitose, le chromosome (***Figure 3***). Jusqu'à récemment, le modèle de repliement hiérarchique de la chromatine était le plus répandu et le plus accepté pour expliquer l'architecture des chromosomes: la liaison de l'histone H1 aux fibres de 11nm favoriserait une interaction entre les nucléosomes voisins et mènerait à la formation de fibres organisées de 30nm ; un enroulement supplémentaire mènerait à la formation de fibres de 100-130nm appelées fibres de chromonema ; enfin, lors de l'entrée en mitose, avec l'aide d'autres protéines structurales (càd. condensines et topoisomérase II), les fibres de chromonema se compacteraient d'avantage pour former les chromatides du chromosome (Kireeva et al., 2004). Cependant, des études récentes de microscopie électronique et à super-résolution semblent démontrer que la fibre de 30nm et le modèle d'organisation de repliement hiérarchique observés *in vitro* n'existent pas *in vivo* (Ou et al., 2017; Ricci et al., 2015) *(*pour revue, voir Maeshima et al., 2019).

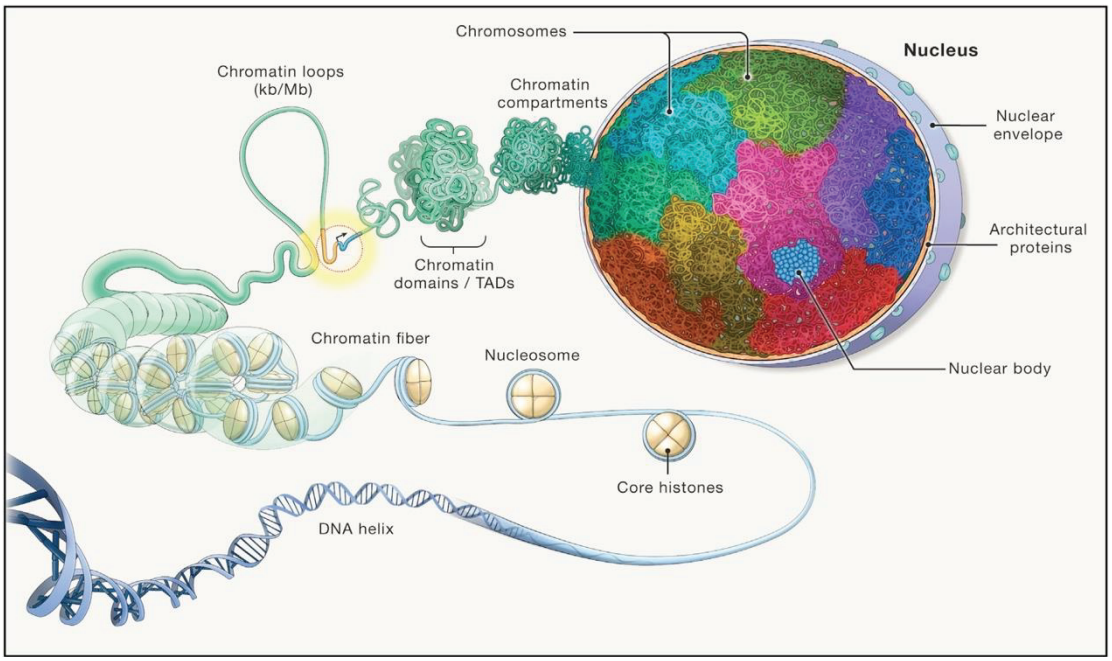


**Figure 3. L'organisation du génome eucaryote.** *(Misteli, 2020)* Le génome s'organise en plusieurs niveau dans le noyau des cellules eucaryotes. L'ADN s'enroule autour d'octamères d'histones pour former des nucléosomes. La répétition de nucléosome forme la fibre de 11 nm. Les nucléosomes s'associent en grappes pour former une fibre de chromatine de 5 à 24 nm. Par la suite, la chromatine s'organise en boucles et en domaines topologiquement associés, les TADs. Les TADs, en fonction de leur activité, se regroupe en compartiments A d'euchromatine et B d'hétérochromatine. Chaque chromosome occupe son territoire propre dans le noyau, un territoire chromosomique.

Un nouveau modèle a donc été récemment proposé dans lequel les nucléosomes s'associent de manière désordonnée et forment des grappes de nucléosomes, ou des nano-domaines, variables en taille (diamètre entre 5 et 24nm) (Ou et al., 2017). Ces nano-domaines sont ensuite associés entre eux grâce à un anneau de cohésine pour former des boucles de chromatine afin de favoriser, entre autres, la communication entre des éléments régulateurs. Le mécanisme de formation de ces boucles est encore incertain. Le modèle le plus populaire est l'extrusion de boucle de chromatine dans lequel l'anneau de cohésine avance progressivement autour de la boucle de chromatine qui s'élargit peu à peu (Banigan and Mirny, 2020). Ce modèle est néanmoins remis en question par l'encombrement stérique résultant de l'organisation de la chromatine en nano-domaines (Banigan and Mirny, 2020; Maeshima et al., 2019) et nécessite actuellement une validation *in vivo*.

Le génome est ensuite organisé en domaines topologiquement associés (TADs ou 'Topologically Associated Domains') délimités par la protéine isolatrice CTCF (CCCTC-binding Factor), au sein desquels la fréquence de contact est plus élevée que la fréquence de contact inter-TADs (Dixon et al., 2012; Nora et al., 2012). Les TADs peuvent être considérés comme des domaines fonctionnels dans lesquels on observe une dynamique et un état chromatinien similaires. De plus, les TADs pourraient constituer des unités régulatrices de réplication (Pope et al., 2014). Ces domaines ont tendance à s'associer

entre eux en fonction de la compaction de la chromatine les constituant et de son activité transcriptionnelle, formant 2 types de compartiments distincts : les compartiments A et B (Lieberman-Aiden et al., 2009) (subdivisés plus récemment en 6 sous-compartiments A1, A2, B1, B2, B3 et B4 en fonction de la signature moléculaire et de la vitesse de réplication des domaines associés (Rao et al., 2014)). Les compartiments A correspondent au rassemblement de domaines lâches et actifs dits d'euchromatine, tandis que les compartiments B correspondent au regroupement de domaines compactés et silencieux dits d'hétérochromatine (Lieberman-Aiden et al., 2009).

Le dernier niveau d'organisation de la chromatine est le chromosome, visible seulement en mitose. Lors de l'entrée en prophase, les compartiments et les TADs sont perdus et la chromatine s'organise en boucles autours d'un axe de condensine/topoisomérase II, permettant la très grande compaction de la chromatine (environ 10 000 fois) et la formation des chromatides sœurs pour assurer la division équitable du matériel génétiques dans les 2 cellules filles (Gibcus et al., 2018).

### I.3. Les différentes sources d'information épigénétique

La compaction de la chromatine influe sur l'accessibilité de l'ADN et a donc un impact sur divers processus tels que la transcription, la réparation de l'ADN ou encore la réplication ; sa régulation apporte de ce fait une information épigénétique et diffère entre les individus, les types cellulaires et dans le temps. Les différentes sources d'information épigénétique sont les suivantes (***Figure 4***) : *(i)* la méthylation de l'ADN, *(ii)* les modifications post-traductionnelles des histones, *(iii)* la composition des nucléosomes en variants d'histones, *(iv)* l'interaction de la chromatine avec des longs ARN non-codants, et enfin *(v)* le positionnement nucléaire des régions chromatiniennes (Allis and Jenuwein, 2016; Probst et al., 2009). Les différentes sources d'informations épigénétiques sont étroitement liées entre elles et la mise en place d'une marque peut favoriser la mise en place d'une autre afin de renforcer l'état chromatinien. Cette partie détaillera ces différents niveaux de régulation de la compaction de la chromatine et de l'information épigénétique.

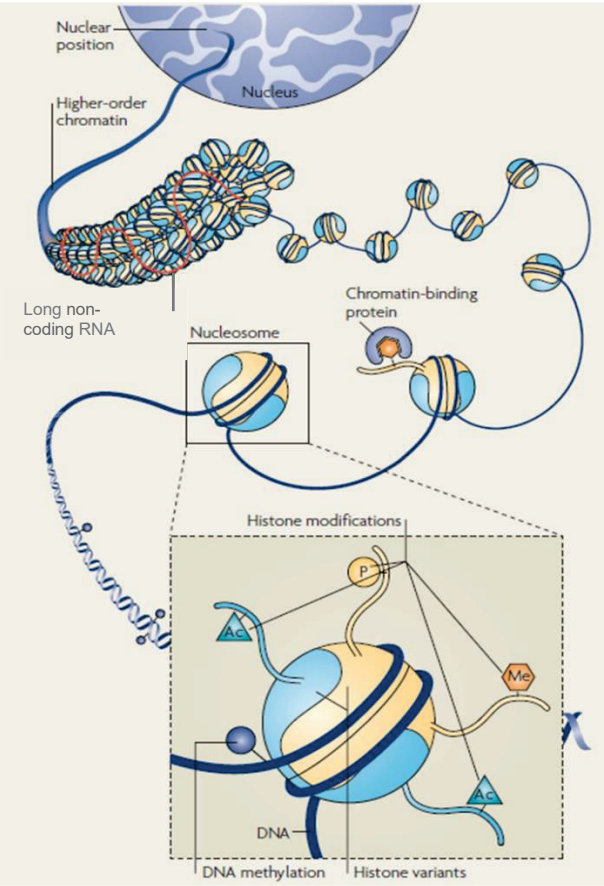


**Figure 4. Les différentes sources d'information épigénétique.** (adaptée de *Probst et al., 2009*) La chromatine subit des modifications impactant sa compaction et apportant une source d'information épigénétique. L'ADN peut être méthylé et reconnu par la suite par des protéines spécifiques. Les queues des histones peuvent subir différentes modifications influant sur la stabilité du nucléosome ou pouvant être reconnues par des protéines spécifiques, appelées 'readers'. La composition du nucléosome en variant d'histone peut aussi avoir un impact sur sa stabilité et confère de nouvelles cibles de modifications post-traductionnelles. Les longs ARNs non-codants participent également à la mise en place d'une signature épigénétique. Enfin la position nucléaire d'une région génomique influe sur sa compaction et son activité.

### I.3.i. *La méthylation de l'ADN*

La méthylation de l'ADN constitue historiquement la première source d'information épigénétique décrite (Hotchkiss, 1948). Chez les mammifères, elle est principalement observée sur les bases cytosines des dinucléotides CpG (Lister et al., 2009) ; ainsi dans cette partie, je décrirai particulièrement l'établissement et la fonction de la méthylation CpG. Cependant, la méthylation de l'ADN est également observée dans d'autres contextes, comme sur les cytosines de régions riches en motifs CHG ou CHH (où H = C, A ou T) (Lister et al., 2009) ou encore sur des bases adénines (pour revue, voir Iyer et al., 2016).

La méthylation des dinucléotides CpG consiste au transfert de manière covalente d'un groupement méthyle provenant de la S-adénosylméthionine (SAM) sur le cinquième carbone de l'anneau pyrimidine de la cytosine pour former une base 5mC (5-méthylcytosine) (***Figure 5***). Ce transfert est catalysé par une ADN-méthyltransférase (DNMT pour 'DNA Methyltransferase') (pour revue, voir Kumar et al., 1994). Chez les mammifères, DNMT3a et DNMT3b permettent une méthylation de l'ADN *de novo* (Okano et al., 1999), tandis que DNMT1 est impliquée dans la maintenance du paysage de méthylation après le processus de réplication (Hermann et al., 2004). La méthylation des CpG peut par la suite être reconnue par trois familles de protéines : les familles de

protéines MBD (Methyl-CpG-Binding Domain) et ZNF (Zinc-Finger) qui participent à la répression de la transcription décrite plus bas (Du et al., 2015; Filion et al., 2006; Lopes et al., 2008; Prokhortchouk et al., 2001; Yoon et al., 2003) et la famille des protéines UHRF (Ubiquitin-like with PHD and RING Finger domain-containing proteins) qui participent à la maintenance de la méthylation en favorisant la liaison de DNMT1 avec l'ADN hémi-méthylé (Bostick et al., 2007; Sharif et al., 2007).

Pendant de nombreuses années, la méthylation de l'ADN était considérée comme irréversible et il était admis que seule sa dilution par réplication induisait la perte de la marque au niveau d'une région génomique. Cependant, des processus de déméthylation actifs par les enzymes AID/APOBEC (Activation-Induced cytidine Deaminase/Alipo-protein B mRNA-editing) et TET (Ten-Eleven Translocation) ont récemment été mis en évidence (pour revue, voir Moore et al., 2013) (***Figure 5***).

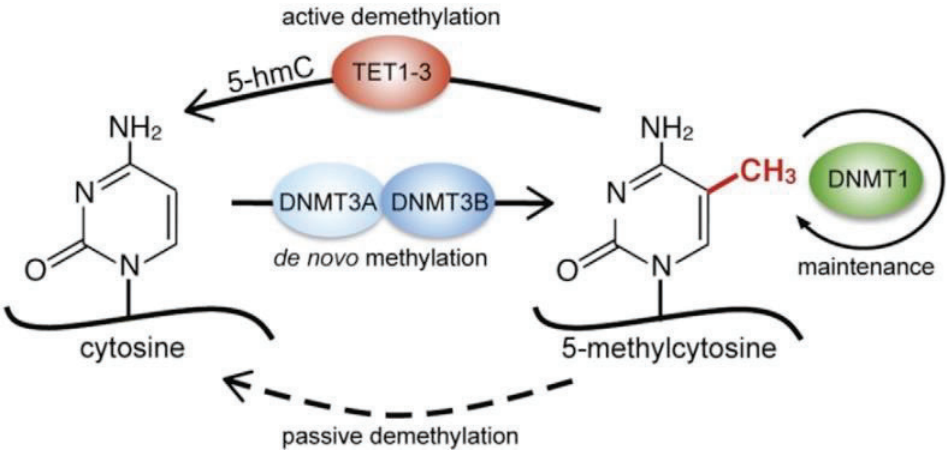


**Figure 5. La méthylation des cytosines.** (Ambrosi et al., 2017) La méthylation des cytosines de l'ADN est médiée par l'action des DNMT, DNMT3A/3B pour la méthylation de novo et DNMT1 pour la maintenance du profil de méthylation. La méthylation est réversible, soit passivement par dilution lors de la réplication, soit activement par l'action de différentes enzymes (e.g. enzymes TET ici représentées).

Bien que la découverte de la marque 5mC remonte à la fin des années 1940 (Hotchkiss, 1948), son rôle exact est encore incertain et semble dépendre de la région génomique où elle se situe : régions promotrices, corps des gènes ou régions régulatrices (pour revue, voir Jones, 2012). Ainsi, alors que la méthylation de l'ADN est principalement répressive lorsqu'elle se situe au niveau des promoteurs et des enhancers (par ex. Schmidl et al., 2009; Song et al., 2005a; Wutz et al., 1997), elle ne semble pas inhiber la transcription lorsqu'elle se situe dans des régions intragéniques. Dans ce contexte, elle joue notamment un rôle dans le processus d'épissage alternatif (par ex. Laurent et al., 2010) (pour revue, voir Maor et al., 2015).

### *I.3.ii. Les modifications post-traductionnelles des histones*

En 1964, Allfrey *et al*. ont démontré la présence de résidus acétylés ou méthylés au niveau des histones (Allfrey et al., 1964) ; depuis lors, avec le développement des techniques de protéomique, plusieurs études sont venues compléter ces premières observations, avec de nombreuses nouvelles modifications post-traductionnelles (PTMs pour 'Post-Translational Modifications') des histones mises en évidence, majoritairement au niveau des queues N et C-terminales (par ex. acétylation, phosphorylation, méthylation pour les plus étudiées) (pour une liste plus exhaustive des différentes modifications d'histones, voir Arnaudo and Garcia, 2013; Bannister and Kouzarides, 2011; Kouzarides, 2007). Les PTMs d'histones sont médiées par différentes enzymes appelées classiquement les 'writers' ou 'auteurs' (***Figure 6***). Elles sont généralement réversibles par l'action d'autres enzymes qu'on surnomme les 'erasers' ou 'effaceurs'.

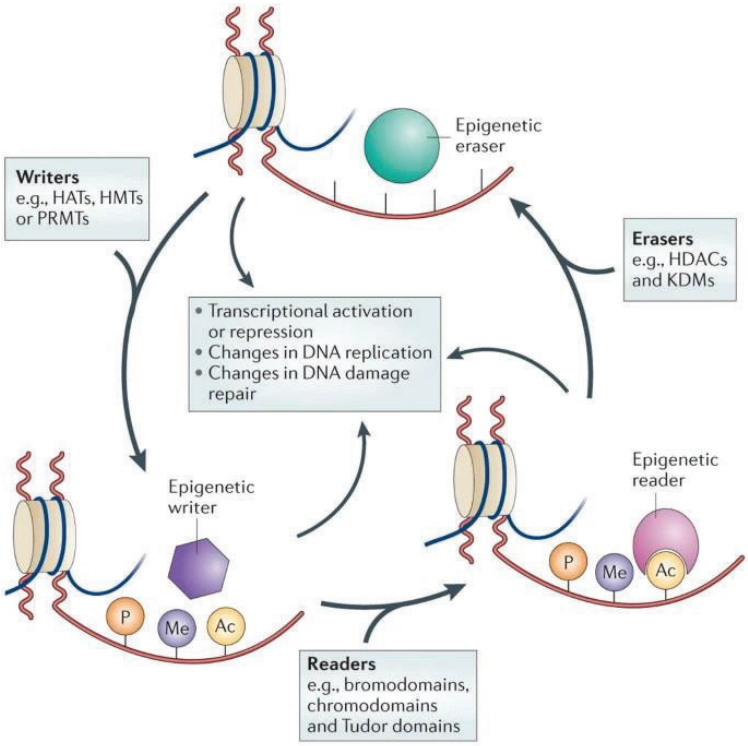


**Figure 6. Les modifications post-traductionnelles d'histones.** *(Falkenberg and Johnstone, 2014)* Le profil de modifications post-traductionnelles sur les queues d'histones a une influence sur différents processus tels que la transcription, la réplication ou la réparation de l'ADN. Les protéines 'writers' permettent l'établissement des marques ; les protéines 'readers' reconnaissent les modifications et provoquent une cascade d'évènements ; les protéines 'erasers' retirent les modifications post-traductionnelles.

Les modifications d'histones ont des conséquences très variées et interviennent dans divers processus cellulaires tels que la régulation de la transcription, de la réparation de l'ADN ou encore de la réplication. Le paysage de marques varie ainsi grandement entre les régions génomiques mais aussi au cours du développement et en fonction du type cellulaire (pour des revues plus complètes sur la fonction des marques d'histones, voir

Zhang et al., 2015; Zhao and Garcia, 2015). Il existe par ailleurs un phénomène de 'dialogue croisé' entre les marques d'histones, avec la co-occurrence ou l'antagonisme de certaines, permettant le renforcement de la signature épigénétique d'une région génomique.

La fonction des PTMs résulte de l'effet de chaque marque sur la structure de la chromatine (pour revue, voir Bannister and Kouzarides, 2011). Les PTMs d'histones peuvent tout d'abord induire une déstabilisation du nucléosome, induisant par conséquence un relâchement de la région. C'est le cas par exemple de l'acétylation qui réduit la charge positive de l'histone et peut perturber l'interaction électrostatique de l'histone avec la double hélice d'ADN (Iwasaki et al., 2011). Les PTMs d'histones peuvent être également reconnues par diverses protéines ou complexes protéiques appelées communément 'readers' ou 'lecteurs', au cœur de l'hypothèse du 'code d'histone' proposée par Brian D. Strahl, C. David Allis et Thomas Jenuwein dans les années 2000 (Jenuwein and Allis, 2001; Strahl and Allis, 2000). L'effet de la liaison d'un 'reader' à une PTM d'histone dépend de sa nature. Certains peuvent par exemple se dimériser, induisant une compaction locale de la chromatine (par ex. HP1, L3MBTL1 (Bannister et al., 2001; Lachner et al., 2001; Trojer et al., 2007)). D'autres 'readers' possèdent une activité de remodelage de la chromatine, ou recrutent des remodeleurs, induisant le repositionnement des nucléosomes et un changement dans la compaction de la chromatine (ex. reconnaissance d'histones acétylées par le complexe SWI/SNF (Hassan et al., 2002)). Enfin, certains possèdent une activité enzymatique 'writer' ou 'eraser' (ou permettent le recrutement d'un 'writer' ou d'un 'eraser') entraînant par la suite la modification du paysage de PTMs environnant (par ex. reconnaissance de H3K4me3 par le complexe désacétylase mSin3a-HDAC1 en réponse aux dommages à l'ADN (Shi et al., 2006)).

Le paysage de modifications d'histones est intimement lié à la composition du nucléosome en variants d'histones. La prochaine partie détaille les différents variants d'histones et leurs spécificités.

#### *I.3.iii. Les variants d'histones*

La composition du nucléosome en variants d'histones (isoformes des histones conventionnelles dites canoniques), apporte une information épigénétique supplémentaire et peut avoir une influence sur les processus de transcription, de réplication ou de réparation de l'ADN. Les variants peuvent différer de l'histone canonique par la substitution de quelques acides aminés ou par l'ajout/la perte d'une partie de la protéine (***Figure 7***). Certains variants sont très conservés entre les espèces alors que d'autres sont spécifiques à une famille d'espèces. Ainsi, chez les hominidés, chaque protéine d'histone

possède des variants : l'histone de liaison H1 possède 11 variants (H1.0, H1.1 à 5, H1x, H1t, H1T2, H1.5 et H1oo), l'histone H2A possède 6 variants (H2A.X, macroH2A, H2A.Z, H2A.B, H2A.L et H2A.P), l'histone H2B possède 3 variants (H2BE, H2B.W et TH2B), l'histone H3 (H3.1/H3.2) possède 6 variants (H3.3, H3.4, H3.5, CENP-A, H3.Y1 et H3.Y2) et l'histone H4 possède un variant, H4-G, mis en évidence très récemment (Buschbeck and Hake, 2017; Fyodorov et al., 2018; Martire and Banaszynski, 2020). Les variants sont exprimés tout au long du cycle cellulaire, contrairement aux histones canoniques dont l'expression est limitée à la phase S. Leur expression peut être ubiquitaire ou spécifique à un type de tissus, comme les testicules ou le cerveau. Le trafic cellulaire, l'incorporation et l'éviction de la chromatine des différents variants sont médiés par l'action de complexes

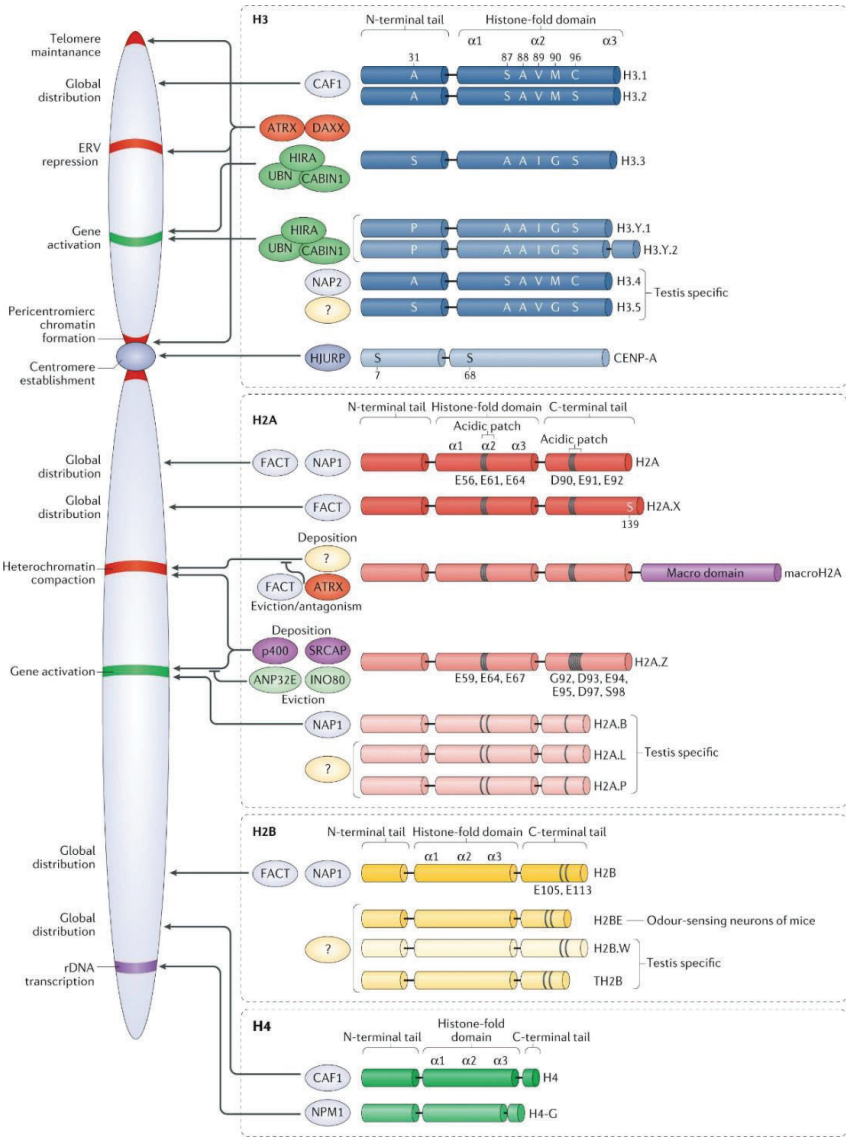


**Figure 7. Les variants d'histones et leurs chaperons.** *(Martire and Banaszynski, 2020)*. Les différents variants des 4 histones cœurs sont représentés. Ils peuvent différer de l'histone canonique de quelques acides aminés jusqu'à l'ajout/la suppression d'une partie de la protéine. L'incorporation ou l'éviction d'un variant est médiée par l'action des complexes chaperons d'histones ou des enzymes remodeleur de la chromatine de la famille INO80. L'incorporation d'un variant au niveau de la chromatine peut être globale ou associée à une région spécifique, et peut avoir diverses conséquences (e.g. activation, répression, signalisation).

protéiques appelés chaperons d'histones ou par celle d'ATPase de remodelage de la chromatine de la famille des INO80 (***Figure 7***) (pour revue sur les chaperons d'histones, voir Gurard-Levin et al., 2014).

L'incorporation d'un ou plusieurs variants d'histones au niveau des nucléosomes d'une région génomique a de multiples conséquences sur l'accessibilité de la chromatine (pour revue, voir Buschbeck and Hake, 2017; Fyodorov et al., 2018; Martire and Banaszynski, 2020). Tout d'abord, la composition du nucléosome avec certains variants peut renforcer (par ex. CENP-A (Melters et al., 2019; Tachiwana et al., 2011)) ou affaiblir (par ex. H2A.B (Arimura et al., 2013)) la stabilité du nucléosome, facilitant respectivement la compaction ou le relâchement de la chromatine. Certaines différences en acides aminés des variants peuvent conduire à l'apparition ou la disparition de PTMs d'histones, impactant également l'activité de la région génomique. Enfin, l'incorporation d'un variant peut avoir un effet plus indirect en favorisant de recrutement de 'writers' ou de 'readers'.

#### *I.3.iv. Les longs ARNs non-codants*

Longtemps considéré comme de l'ADN « poubelle », l'ADN intergénique est pourtant porteur d'informations essentielles pour le fonctionnement cellulaire. Une partie importante du génome est transcrite en ARNs non codants. Parmi eux, les longs ARNs non-codants (lncRNAs pour 'long non-coding RNAs') participent notamment à des régulations épigénétiques permissives ou répressives du génome et leur transcription est régulée dans l'espace et le temps (pour revue, voir Balas and Johnson, 2018; Wang and Chang, 2011). L'exemple le plus extrême de l'action d'un lncRNA est l'inactivation d'un des chromosome X chez les femelles mammifères initiée par la transcription du lncRNA *Xist* (pour revue, voir Boeren and Gribnau, 2021).

On distingue 3 fonctions non-exclusives des lncRNAs (***Figure 8***). Ils peuvent tout d'abord servir de guides pour des complexes modificateurs de la chromatine ou des facteurs de transcription afin de les cibler sur des régions spécifiques du génome. Par exemple, pendant la différenciation musculaire, la déméthylase LSD1 favorise la transcription de l'ARN non codant CEeRNA au niveau de l'enhancer du gène MyoD (Scionti et al., 2017). Ce dernier se lie à la région promotrice du gène où il participe à l'établissement d'un environnement chromatinien permettant le recrutement de l'ARN polymérase II et l'expression de MyoD (Mousavi et al., 2013). Les lncRNAs peuvent également servir d'échafaudages pour assembler transitoirement plusieurs complexes ou cofacteurs pour une action conjointe. Le lncRNA KCNQ1OT1 sert par exemple chez la souris de plateforme pour les méthyltransférases G9a et PRC2 et la mise en place concomitante des marques H3K9me3 et H3K27me3 (Pandey et al., 2008). Enfin, les lncRNAs peuvent

servir de leurres, détournant des complexes modificateurs de chromatine ou des facteurs de transcription de leurs cibles. En réponse à de faibles dommages à l'ADN, PANDA prévient notamment la liaison du facteur de transcription pro-apoptotique NF-YA et favorise la survie cellulaire de fibroblastes humains (Hung et al., 2011).

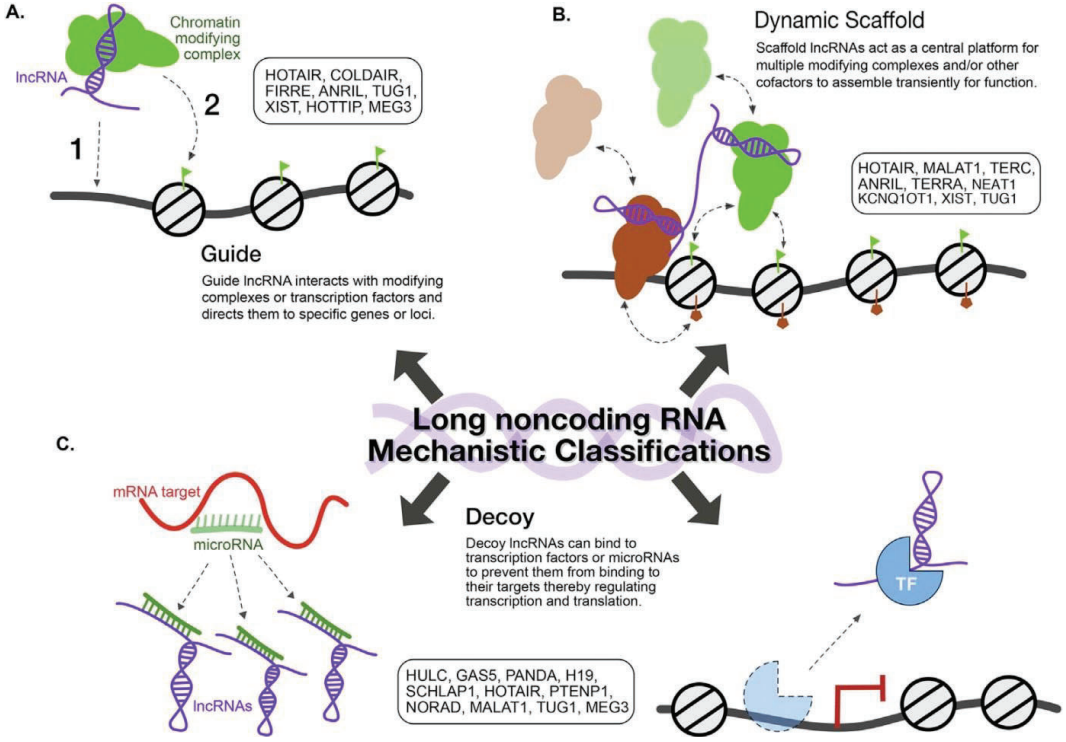


**Figure 8. Les mécanismes d'action des ARN longs non codants.** *(Balas and Johnson, 2018)* Les fonctions des ARNs longs non codants peuvent être classifier en 3 catégories non-exclusives : une fonction de guide, une fonction d'échafaudage et une fonction de leurre.

### *I.3.v. La position nucléaire*

Le noyau des cellules eucaryotes est une structure très organisée et dynamique, permettant d'accomplir différentes réactions dans l'espace et dans le temps. Il est entouré d'une enveloppe nucléaire constitué d'une bicouche lipidique qui enferme ses différents composants : la lamina nucléaire tapissant la membrane interne de l'enveloppe nucléaire, la chromatine répartie en territoires chromosomiques, et enfin, différents organelles nucléaires appelés corps nucléaire (***Figure 9***).

Le positionnement nucléaire d'une région chromatinienne a une influence sur son accessibilité et par conséquent sur sa transcription. La position radiale de la chromatine constitue un parfait exemple (pour revue, voir Crosetto and Bienko, 2020). Ainsi, les régions se situant en périphérie et associées à la lamina nucléaire (càd. 'Lamin-Associated Domains' ou LADs) seront généralement plus réprimées que les régions se situant dans le centre du noyau (Guelen et al., 2008). De plus, le ciblage d'un chromosome ou d'un gène rapporteur à la membrane interne du noyau induit généralement la répression des gènes (Finlan et al., 2008; Kumaran and Spector, 2008; Reddy et al., 2008). Ce

positionnement des gènes à la lamina est dynamique dans le temps et permet de réguler l'expression de certains gènes (par ex. lors du processus de différenciation cellulaire (Peric-Hupkes et al., 2010), ou lors de l'activation des lymphocytes T (Robson et al., 2017)).

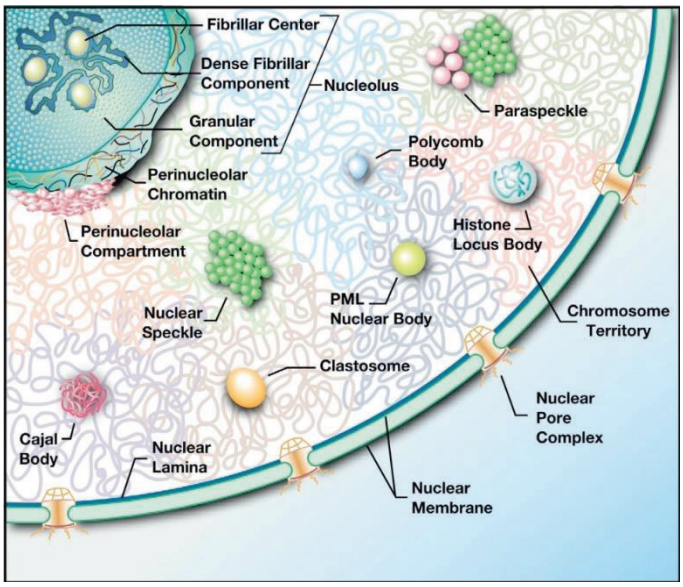


**Figure 9. Les différents corps nucléaires et leurs fonctions.** *(Mao et al., 2011)* Le noyau des cellules eucaryotes est entouré d'une enveloppe nucléaire, tapissée à l'intérieur par la lamina. Les pores nucléaires permettent les échanges entre le noyau et le cytoplasme. A l'intérieur du noyau, on trouve l'ADN sous forme de chromatine répartie en territoires chromosomiques dans lesquels s'intercalent les corps nucléaires. Le tableau résume les différents corps nucléaires retrouvé dans le noyau et leurs fonctions.

| Body name | (Putative) Functions |
|---|---|
| Cajal body | Involved in snRNAs and snoRNAs modification, and assembly and trafficking of snRNPs and snoRNPs. Also plays a role in telomerase assembly and telomere length regulation. |
| Clastosome | Contains 20S and 19S proteasomes, ubiquitin conjugates, and protein substrates of the proteasome. Forms in response to stimuli that activate proteasome-dependent proteolysis. |
| Histone locus body | Involved in the transcription and processing of histone pre-mRNAs. |
| Nuclear speckle | Involved in the storage, assembly, and modification of pre-mRNA splicing factors. |
| Nuclear stress body | Contains satellite III ncRNAs and is a part of the general response to stress. Precise function not yet determined. |
| Nucleolus | Involved in the transcription and processing of rRNA and the assembly of ribosomal subunits. Plays roles in the modification and assembly of other nuclear RNAs and RNPs. Regulates cell cycle progression by sequestering and modifying many proteins. |
| Paraspeckle | Involved in nuclear retention of some A-to-I hyperedited mRNAs. |
| Perinucleolar compartment | Precise functions are unknown but its prevalence positively correlates with metastatic capacity. |
| PML-nuclear body | Involved in response to many forms of stress, viral defense, and genome stability by the sequestration, modification, and degradation of many partner proteins. |
| Polycomb body | Involved in Polycomb proteins-mediated gene paring and silencing in *Drosophila*. Precise function in mammalian cells remains to be determined. |

La proximité d'une région chromatinienne avec certains corps nucléaires peut également influer sur sa compaction et son activité. Les speckles s'associent ainsi avec des régions actives de la chromatine car ils constituent des centres de transcription (Chen and Belmont, 2019), tandis que les nucléoles sont entourés d'hétérochromatine principalement péricentrique (càd. 'Nucleoli-Associated Domains' ou NADs) (Padeken and Heun, 2014). Finalement, il a été montré récemment que les corps nucléaires PML (ou PML NBs pour 'PML Nuclear Bodies') des cellules ES murines étaient majoritairement entourés par des régions régulatrices de gènes transcriptionnellement actifs (càd. promoteurs et

enhancers) bien que le mécanisme derrière cette association reste à investiguer (Kurihara et al., 2020).

Cette partie a permis d'apporter une vision large des modifications de la chromatine et des facteurs contribuant à définir l'information épigénétique. Au cours de ma thèse, je me suis plus particulièrement intéressée à un variant spécifique de l'histone H3, le variant H3.3. Dans la partie suivante, je vais donc me focaliser sur ce variant et ses caractéristiques.

## I.4. Le variant d'histone H3.3

Le variant d'histone H3.3 est un variant de l'histone H3, conférant à la chromatine des propriétés particulières. Son incorporation par divers chaperons est donc source d'une information épigénétique. Dans cette partie, je décrirai premièrement les propriétés du variant H3.3 par rapport aux histones canoniques. Je détaillerai ensuite l'impact de son incorporation dans la chromatine et l'information qu'il confère. Enfin, je terminerai sur l'implication du variant H3.3 et de ses chaperons dans des processus physiologiques et pathologiques.

### *I.4.i. Les propriétés du variant H3.3 par rapport aux histones canoniques*

Le variant d'histone H3.3 diffère des histones canoniques H3.1 et H3.2 de 5 et 4 acides aminés respectivement (***Figure 10***). Les acides aminés en position 87 à 90 confèrent la spécificité de liaison du variant avec ses différents chaperons (Elsässer et al., 2012; Liu et al., 2012; Ricketts et al., 2015). La sérine en position 31 peut quant à elle être phosphorylée dans certains contextes (cf. partie *I.4.i*) (Hake et al., 2005). Enfin la différence d'acide aminé en position 96 (cystéine pour H3.1, sérine pour H3.2 et H3.3) n'est pas encore fonctionnellement comprise.

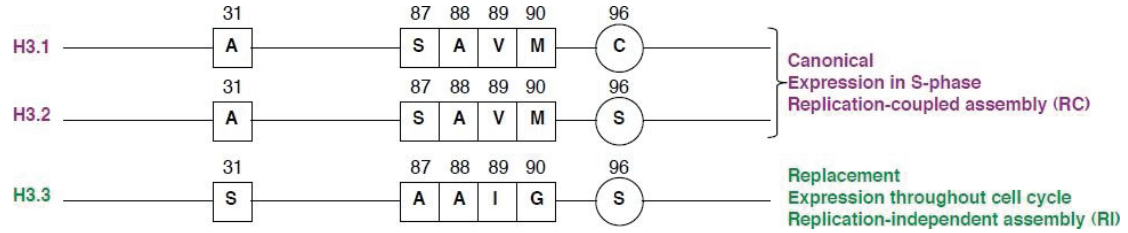


**Figure 10. Représentation schématique des différences protéiques entre les histones canoniques H3.1/H3.2 et le variant d'histone H3.3.** Les histones canoniques H3.1 et H3.2 (violet) sont exprimées exclusivement lors de la phase S et sont incorporées à la chromatine de façon dépendante du processus de réplication. Elles diffèrent d'un acide aminé en position 96 (C ou S) dont l'importance n'est pas connue. Le variant d'histone H3.3 (vert) est exprimé tout au long du cycle cellulaire et est incorporé à la chromatine indépendamment à la synthèse d'ADN. Il diffère des histones canoniques de 6 ou 5 acides aminés : l'alanine en position 31 devient une sérine phosphorylable, la séquence SAVM en position 87 à 90 devient AAIG, conférant la spécificité de liaison aux chaperons d'histones. Enfin, la cystéine 96 d'H3.1 devient une sérine, comme pour H3.2.

Le variant H3.3 est extrêmement conservé au sein des eucaryotes et constitue même l'unique variant chez les ascomycètes. L'émergence plus tardive des histones canoniques H3.1 et H3.2 dans l'arbre du vivant suggère que ces dernières dérivent d'un ancêtre

commun proche d'H3.3 et que la spécialisation de leurs fonctions s'est faite au cours de l'évolution (Szenker et al., 2011; Talbert and Henikoff, 2010).

Les gènes encodant pour les histones canoniques de l'histone H3 sont présents en copies multiples et organisés en clusters. Ils ne possèdent pas d'introns et leurs transcrits ne sont pas poly-adénylés mais se terminent par une structure en épingle à cheveux. Ces particularités expliquent un pic d'expression de ces gènes au cours de la phase S, de façon dépendante à la synthèse d'ADN, et une extinction rapide de ces gènes après la réplication (Marzluff et al., 2002; Osley, 1991). A l'inverse, chez la souris, l'homme et la drosophile, seulement 2 gènes encodent pour le variant H3.3 : le gène *H3F3A* en position 1q41 et le gène *H3F3B* en position 1q25. Ces deux derniers possèdent des introns et leurs transcrits sont poly-adénylés, permettant une expression continue au cours du cycle cellulaire, indépendamment de la synthèse d'ADN (Krimer et al., 1993; Wu et al., 1982).

Par sa spécificité de séquence en position 87 à 90, le variant H3.3 s'associe à des chaperons d'histones différents de ceux liant l'histone H3.1 et impliqués dans le dépôt du variant H3.3 dans la chromatine de façon indépendant du processus de réplication (Ahmad and Henikoff, 2002).

#### *I.4.ii. Les chaperons d'histones associées à H3.3*

Le trafic cellulaire et l'incorporation du variant H3.3 sont médiés par l'action de protéines ou complexes chaperons d'histones (pour revue Gurard-Levin et al., 2014). Certains reconnaissent à la fois les histones canoniques et le variant H3.3. C'est le cas des protéines NASP (Nuclear Autoantigenic Sperm Protein) et ASF1 (Anti-Silencing Function Protein 1) (Tagami et al., 2004). La protéine NASP assure la protection des dimères H3-H4 de la dégradation et permet de constituer un réservoir d'histones solubles disponibles pour être incorporées à la chromatine (Cook et al., 2011). Le chaperon ASF1 permet quant à lui d'acheminer le dimère H3-H4 vers le complexe de dépôt pour l'incorporation de l'histone à la chromatine (Alvarez et al., 2011). Les complexes chaperons HIRA/UBN1/CABIN1 (Histone Regulator A/Ubinuclein 1/Calcineurin Binding protein 1) ou complexe HIRA et le complexe DAXX/ATRX (Death domain-Associated protein 6/Alpha Thalassemia/mental Retardation syndrome X-linked protein) sont des chaperons de dépôt qui, contrairement à NASP et ASF1, sont spécifiques au variant H3.3 (Drané et al., 2010; Goldberg et al., 2010; Lewis et al., 2010; Ricketts et al., 2019; Tagami et al., 2004). Leurs spécificités respectives seront détaillées dans la partie suivante (cf. partie *I.4.iii*).

De façon notable, une étude *in vitro* sur la protéine DEK de drosophile ou humaine purifiée a montré sa capacité à lier spécifiquement le variant H3.3 et à former une fibre nucléosomale (Sawatsubashi et al., 2010). Cependant, le rôle de chaperon de cette

protéine est encore incertain et une étude de 2014 suggère plutôt un rôle de DEK dans la régulation du dépôt d'H3.3 par les complexes HIRA et DAXX/ATRX, indépendamment de sa liaison à H3.3 (Ivanauskiene et al., 2014).

Enfin, des études sur les remodeleurs de la chromatine de type CHD ont montré qu'ils pouvaient s'associer avec le variant H3.3 et médier son incorporation à la chromatine dans certaines conditions. Chez la drosophile, le remodeleur CHD1 est requis pour le dépôt d'H3.3 pendant le développement embryonnaire de façon indépendante de HIRA (Konev et al., 2007). Chez les mammifères, le remodeleur CHD2 participe à la différenciation musculaire en incorporant H3.3 au niveau des promoteurs des gènes de myogenèse en se liant au facteur de transcription MyoD (Harada et al., 2012; Siggens et al., 2015). De même, dans les cellules souches embryonnaires de souris, CHD2 se lie à Oct3/4 pour déposer H3.3 au niveau des promoteurs de gènes de développement et permettre leur expression (Semba et al., 2017). CHD2 est également recruté au niveau de certaines cassures double-brin par PARP1 dans des cellules humaines où il participe à la réparation par ligature d'extrémités non-homologues (NHEJ pour 'Non-Homologous End-Joining') (Luijsterburg et al., 2016).

### *I.4.iii. L'enrichissement d'H3.3 en fonction du contexte cellulaire et des régions de la chromatine*

Le variant H3.3 agit premièrement comme une histone de remplacement des histones canoniques en dehors de la phase de réplication (Ahmad and Henikoff, 2002). Ce rôle de remplacement est particulièrement important lors du processus de fertilisation. En effet, les protamines présentes dans le noyau du spermatozoïde sont remplacées par H3.3 après son entrée dans l'oocyte et avant la formation du zygote grâce au complexe HIRA en collaboration avec la protéine de remodelage de la chromatine CHD1 (Konev et al., 2007; Loppin et al., 2005; Torres-Padilla et al., 2006). De même, dans les cellules somatiques, le chaperon d'histone HIRA peut reconnaître l'ADN nu et peut ainsi incorporer H3.3 à la chromatine dans les régions dépourvues en nucléosomes afin d'assurer le maintien de l'intégrité de la chromatine (Ray-Gallet et al., 2011; Schneiderman et al., 2012).

En plus de son rôle d'histone de remplacement, de nombreuses études ont démontré un enrichissement particulier du variant H3.3 dans certaines régions génomiques des cellules (***Figure 11***). Le variant H3.3 a d'abord été décrit comme particulièrement enrichi dans des régions d'euchromatine. Plus particulièrement, chez la drosophile, il a été observé un co-enrichissement d'H3.3 avec l'ARN polymérase II et la marque H3K4me2, marqueurs des promoteurs de gènes actifs (Mito et al., 2005). Cet enrichissement est aussi observable

dans le corps de ces gènes, suggérant que le dépôt d'H3.3 est associé à l'élongation transcriptionnelle (Schwartz and Ahmad, 2005). De plus, en 2013, Chen *et al.* ont démontré un enrichissement du variant H3.3 au niveau des régions régulatrices de type enhancer dans des cellules ES murines, permettant de maintenir la chromatine dans une conformation relativement ouverte et accessible pour la liaison de facteurs de transcription (Chen et al., 2013). Ces études suggéraient ainsi que le variant H3.3 constituait une marque de la chromatine active. Cependant, et de façon surprenante, un enrichissement de H3.3 a également été démontré dans des régions d'hétérochromatine. Ainsi, chez la souris, le variant H3.3 est enrichi au niveau des régions télomériques des cellules souches embryonnaires (cellules ES) (Goldberg et al., 2010; Wong et al., 2009) et dans les régions péricentriques (Drané et al., 2010). Le variant H3.3 est également retrouvé au niveau des régions réprimées des rétrotransposons de type ERV et des gènes soumis à empreinte dans les cellules ES de souris (Elsässer et al., 2015; Sadic et al., 2015; Voon et al., 2015). Ainsi, la fonction de marque active du variant H3.3 est à reconsidérer et le rôle de son incorporation dans la chromatine semble plus complexe et dépend de l'environnement chromatinien.

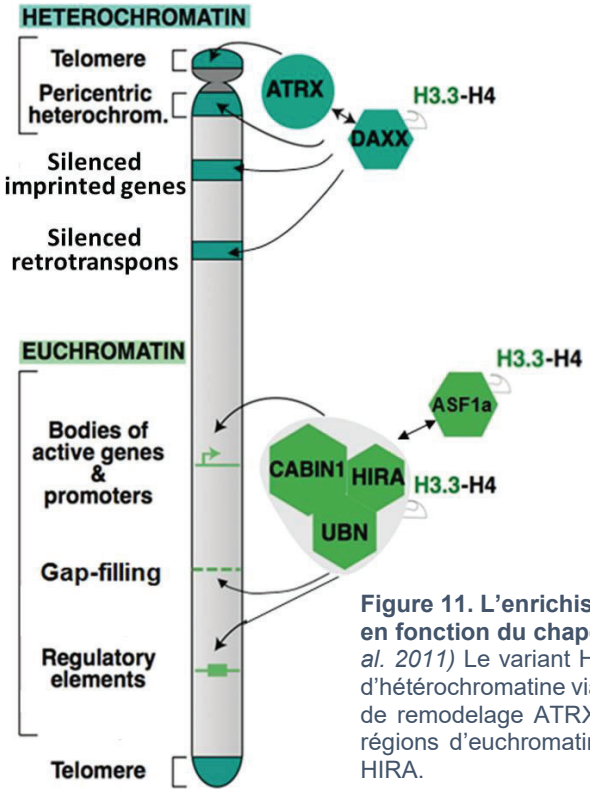


**Figure 11. L'enrichissement spécifique d'H3.3 dans certaines régions en fonction du chaperon le prenant en charge.** *(*adaptée de *Szenker et al. 2011)* Le variant H3.3 se retrouve d'une part enrichi dans des régions d'hétérochromatine via le chaperon DAXX en collaboration avec la protéine de remodelage ATRX. On retrouve également le variant H3.3 dans des régions d'euchromatine. Ce dépôt est médié par le complexe chaperon HIRA.

Cet enrichissement d'H3.3 à la fois dans des régions d'euchromatine et d'hétérochromatine semble dépendre du complexe chaperon prenant en charge le variant (***Figure 11***) (pour revue, voir Szenker et al., 2011) Le complexe HIRA semble permettre l'incorporation d'H3.3 au niveau des régions d'euchromatine, au niveau de gènes transcriptionnellement actifs ; cette spécificité peut en partie s'expliquer par la liaison de

HIRA avec le complexe RPA (Replication Protein A) et de facteurs de transcription au niveau des éléments régulateurs (Soni et al., 2014; Zhang et al., 2017) et avec la machinerie transcriptionnelle au niveau du promoteurs et du corps du gène (Ray-Gallet et al., 2011; Sarai et al., 2013). Le complexe DAXX/ATRX semble quant à lui impliqué dans l'incorporation d'H3.3 dans des régions d'hétérochromatine. La reconnaissance de G-quadruplexes (retrouvés fréquemment dans ces régions) et de la marque H3K9me3 par ATRX peut expliquer ce ciblage particulier (Law et al., 2010), bien que l'importance d'ATRX dans le dépôt d'H3.3 est encore débattue dans certains contextes (Hoelper et al., 2017).

### *I.4.iv. L'impact de l'incorporation d'H3.3 à la chromatine*

Le variant H3.3 est enrichi dans des régions d'euchromatine où la chromatine est plus lâche et la dynamique des histones plus importante. L'incorporation d'H3.3 semble participer à cet état. Premièrement, la présence d'H3.3 inhibe la liaison d'H1 avec la chromatine chez la drosophile (Braunschweig et al., 2009). De plus, des études sur des érythrocytes de poulet ont montré que l'incorporation d'H3.3 dans la chromatine réduit la stabilité du nucléosome (Jin and Felsenfeld, 2007). Étant donné sa différence de seulement 5 acides aminés avec les histones canoniques, il semble peu probable que la séquence d'H3.3 en elle-même réduise son interaction avec l'ADN ou les autres histones de l'octamère cœur. En revanche, la présence d'une sérine phosphorylable en position 31 peut expliquer l'instabilité du nucléosome. En effet, il a été montré que la marque H3.3S31ph favorise l'activité de l'histone acétyltransférase p300 et l'apparition de la marque H3K27ac (Martire et al., 2019; Sitbon et al., 2020).

Comme les histones canoniques, le variant H3.3 peut être triméthylé sur sa lysine 36. La marque H3.3K36me3 peut être spécifiquement reconnue par le 'reader' ZMYND11 (Guo et al., 2014b; Wen et al., 2014). Ce dernier a été identifié comme un répresseur de l'élongation transcriptionnelle (Wen et al., 2014). Il semble également impliqué dans la rétention d'intron lors de l'épissage alternatif (Guo et al., 2014b). Un papier récent montre un lien entre les marques H3.3K36me3 et H3.3S31ph : lors de la stimulation de cellules de l'immunité, la marque H3.3S31ph est établie au niveau des gènes induits et permet le recrutement de SETD2 et l'établissement de la marque H3.3K36me3 (Armache et al., 2020). Cependant, des études biochimiques ont montré que H3.3S31ph réduit l'association de ZMYND11 et H3.3K36me3 (Armache et al., 2020; Guo et al., 2014b) et des analyses cinétiques sont encore nécessaires pour mieux comprendre la relation entre les deux marques.

Des études sur le singe et l'humain montrent un enrichissement de la marque H3.3S31ph au niveau de l'hétérochromatine péricentrique au moment de la mitose, de la fin de la prométaphase à la métaphase (Hake et al., 2005; Hinchcliffe et al., 2016). En condition normale, cette marque disparaît au moment de l'anaphase mais elle peut se répandre tout le long des bras du chromosome en cas de mauvaise ségrégation des chromatides (Hinchcliffe et al., 2016). L'établissement de cette marque permet par la suite l'activation de p53 et l'arrêt du cycle de la cellule aneuploïde (Hinchcliffe et al., 2016). De façon intéressante, les cellules souches embryonnaires de souris présentent également la marque H3.3S31ph au moment de la mitose mais l'enrichissement se situe cette fois-ci au niveau des télomères (Wong et al., 2009). La fonction de cette marque dans les cellules pluripotentes et la raison de son changement de position après la différenciation ne sont pour le moment pas connues. Enfin, la présence de la marque H3.3S31ph au moment de la mitose est importante pour les cellules cancéreuses utilisant le mécanisme de l'élongation alternative des télomères (ALT pour 'Alternative Lenghtening of Telomeres') (Chang et al., 2015). En effet, dans ces cellules, H3.3S31ph est retrouvée tout le long des bras des chromosomes et est impliquée dans le maintien de l'intégrité de la chromatine et la survie de ces cellules.

### *I.4.v. Le variant H3.3 et ses chaperons dans les processus physiologiques et pathologiques*

L'importance du variant H3.3 et de ses chaperons au cours du développement est variable entre les organismes. Ainsi, les drosophiles inactivées pour H3.3 ne présentent pas de défaut dans le développement et sont viables mais la perte d'H3.3 conduit à la stérilité des mâles et des femelles (Hödl and Basler, 2009). Chez le xénope en revanche, l'inactivation de l'histone H3.3 et du chaperon HIRA conduit à la mort des embryons à la suite d'un défaut dans les étapes tardives de la gastrulation dans l'induction mésodermique (Szenker et al., 2012). De même, chez la souris, la double inactivation de *H3f3a* et *H3f3b* est létale, due à de sévères défauts développementaux (Jang et al., 2015). En effet, l'absence totale d'histones H3.3 augmente la mortalité cellulaire et décroit la prolifération cellulaire chez l'embryon, conduisant à sa mort précoce (dès le stade embryonnaire E6.5). L'inactivation d'un seul des gènes est quant à elle viable et les souris ne présentent globalement pas de défaut, bien que dans certains contextes on observe une stérilité des mâles (chez les mâles (*H3f3a*$^{-/+}$ ; *H3f3b*$^{-/-}$)). L'inactivation chez la souris des gènes codants les chaperons du variant H3.3 conduit également à une mortalité embryonnaire. Ainsi, les embryons *Hira*$^{-/-}$ présentent un défaut de gastrulation et meurent au stade embryonnaire E10-E11 (Roberts et al., 2002) et les embryons *Daxx*$^{-/-}$ et *Atrx*$^{-/-}$ meurent au stade embryonnaire E9.5 à la suite d'un défaut de différenciation (Michaelson et al., 1999) et de développement

du trophoblaste (Garrick et al., 2006). Le variant H3.3 et ses chaperons ont aussi une importance plus tardive dans le développement murin, au niveau de l'organogenèse. HIRA et H3.3 sont par exemple importants dans le processus de myogenèse car ils permettent l'expression du facteur de transcription myogénique MyoD (Yang et al., 2011a, 2011b, 2016). De plus, H3.3 est important pour l'expression des gènes cibles de MyoD, indépendamment de la présence du complexe HIRA (Harada et al., 2012). Dans le cerveau, ATRX est important pour la survie cellulaire dans les étapes précoce de différenciation neuronale et DAXX permet l'incorporation de H3.3 et l'expression des gènes dépendants de l'activité neuronale (Michod et al., 2012). L'implication du variant H3.3 et de ses chaperons dans le développement murins est illustrée en ***Figure12A.***

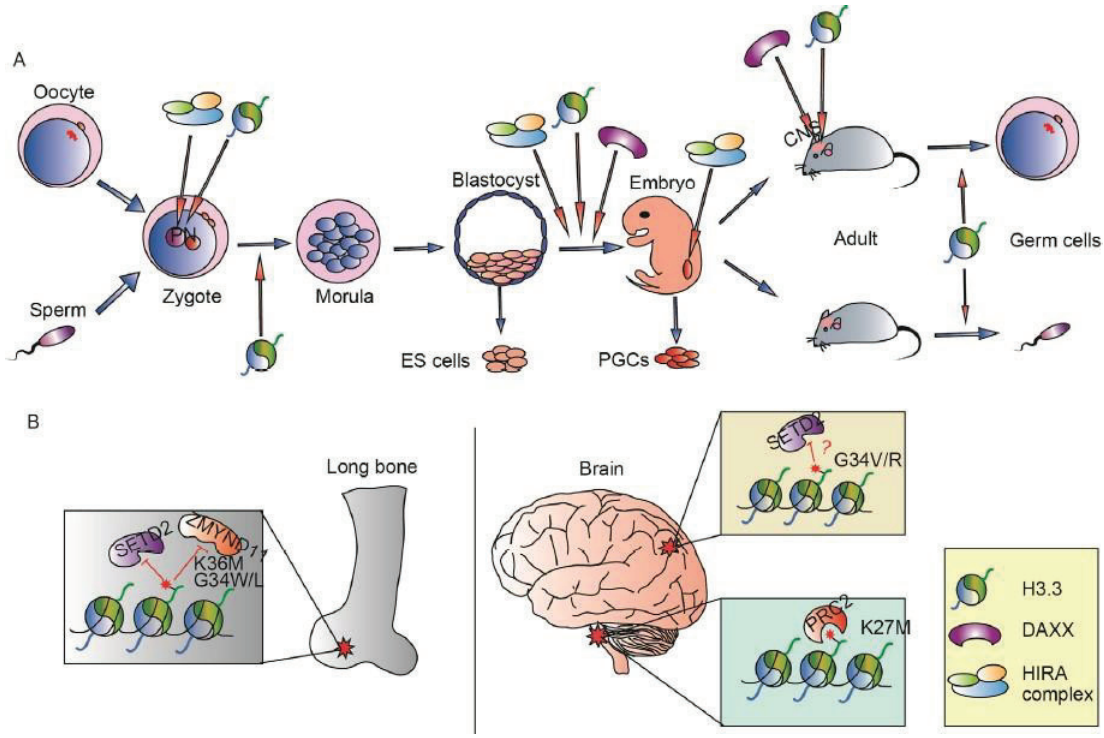


**Figure 12. Les rôles du variant H3.3 dans le développement et de ses mutations dans certains cancers.** *(Xiong et al., 2016)* A. Le variant H3.3 et ses chaperons participent à différentes étapes du développement chez les mammifères. B. On retrouve des mutations du variant H3.3 dans certains cancers : H3.3K36M et H3.3G34W/L dans des tumeurs de l'os et H3.3K27M et G34R/V dans des glioblastomes. Ces mutations perturbent la reconnaissance de l'histone par des readers ou writers et modifient le paysage épigénétique de la région où ils sont incorporés.

Comme je le développerai dans cette thèse, H3.3 et le chaperon HIRA semblent être également impliqués dans la réponse à divers stress cellulaires tels que la réponse à l'inflammation (Kamada et al., 2018) ou encore la réponse aux dommages à l'ADN (Adam et al., 2013). De plus, le complexe HIRA participerait au processus de sénescence et prévient la tumorigenèse (Rai et al., 2014; Ye et al., 2007a; Zhang et al., 2005).

L'histone H3, et plus particulièrement le variant H3.3, est retrouvée mutée dans plusieurs glioblastomes pédiatriques et certaines tumeurs osseuses (***Figure12B***) (pour revue, voir Lowe et al., 2019; Qiu et al., 2018; Shi et al., 2017). Ainsi, les mutations faux-sens K27M

et G34R/V sont retrouvées dans les glioblastomes pédiatriques (Schwartzentruber et al., 2012), la mutation faux-sens K36M dans des chondroblastomes et les mutations faux-sens G34W/L dans des tumeurs à cellules géantes de l'os (TCGO) (Behjati et al., 2013). La mutation K27M prévient la modification post-traductionnelle répressive H3K27me3 en séquestrant la sous-unité EZH2 du complexe PRC2, induisant la dérépression de ses gènes cibles (Lewis et al., 2013). Dans les chondroblastomes, la mutation K36M inhibe la marque H3K36me3, une augmentation de la marque H3K27me3 dans les régions intergéniques, un détournement du complexe PRC1 et une augmentation de l'expression de ses gènes cibles (Lu et al., 2016). A l'inverse de K27 et K36, G34 n'est pas un acide aminé modifié post-traductionnellement ; en revanche, sa mutation altère le recrutement de SETD2 et la méthylation de H3K36 sur la même queue d'histone (Lewis et al., 2013; Shi et al., 2018). De plus, la déméthylase KDM4 montre une plus forte affinité pour le mutant G34R et participe à la déméthylation de H3K36 (Voon et al., 2018). Sachant que le 'reader' ZMYND11, un suppresseur de tumeur, reconnaît spécifiquement H3.3K36me3 (Guo et al., 2014b; Wen et al., 2014), on peut supposer que la mutation K36M ou les mutations sur G34 impactent sur sa liaison et que cela participe au processus de tumorigenèse. Supportant cette hypothèse, les mutations G34R/V empêchent la liaison de ZMYND11 au peptide H3.3K36me3 (Wen et al., 2014).

Outre le variant en lui-même, ses chaperons sont également impliqués dans certaines pathologies. *HIRA* est par exemple un gène candidat pour le syndrome de DiGeorge (cf. Orphanet ORPHA:567). Cette maladie résulte de la délétion d'un large fragment d'ADN dans la région 2q11.2, comportant plusieurs gènes dont *HIRA*. Peu de choses sont pour le moment connues sur une implication éventuelle du chaperon dans le développement de la maladie, mais une étude récente suggère que la perte de HIRA participe à l'immunodéficience et la thrombocytopénie observées chez les patients résultant d'un défaut d'hématopoïèse (Chen et al., 2020). Le gène *ATRX* est quant à lui impliqué dans le syndrome d'ATR-X (cf. Orphanet ORPHA:847) et des mutations de *ATRX* et *DAXX* sont retrouvées dans des cancers utilisant le mécanisme de prolongation alternative des télomères (ALT pour 'Alternative Lenghtening of Telomeres') (Clynes et al., 2013; Dyer et al., 2017). L'absence de DAXX et ATRX et le défaut d'incorporation d'H3.3 induit un stress réplicatif au niveau des télomères et l'activation de la voie de réparation de l'ADN, impliquée dans le phénomène de ALT (Li et al., 2019).

Dans la partie suivante, j'introduirai plus en détail la composition et le fonctionnement du complexe chaperon d'histone HIRA, complexe au cœur de mes investigations de thèse.

## I.5. Le complexe chaperon d'histones HIRA

La découverte du chaperon d'histone HIRA remonte à l'identification il y a 30 ans de son homologue chez *Saccharomyces cerevisiae,* le complexe HIR. Ses membres furent alors identifiés comme réprimant la transcription des paires de gènes d'histones (Osley and Lycan, 1987; Xu et al., 1992). Le complexe est composé des protéines Hir1, Hir2, Hir3 et Hcp2 et est décrit comme un complexe répresseur de la transcription (Green et al., 2005; Prochasson et al., 2005). Les membres du complexe HIRA sont très conservés dans le règne animal où ils sont impliqués dans la formation du nucléosome (Amin et al., 2012). Chez les mammifères, le complexe HIRA permet le dépôt du variant H3.3 dans des régions d'euchromatine et assure le maintien de l'intégrité de la chromatine dans des régions transitoirement dépourvues de nucléosomes (Chen et al., 2013; Mito et al., 2005; Ray-Gallet et al., 2011; Schneiderman et al., 2012; Schwartz and Ahmad, 2005). Dans cette partie, je détaillerai la composition et l'assemblage du complexe HIRA et les modèles proposés pour le dépôt d'H3.3 dans les cellules humaines.

### *I.5.i. La composition du complexe HIRA*

Le complexe HIRA est constitué de 3 protéines, la protéine HIRA (homologue de Hir1 et Hir2) (1017 a.a.), la protéine UBN1 (homologue de Hcp2) (1134 a.a.) et la protéine CABIN1 (homologue de Hir3) (2220 a.a.), transitoirement associées à la protéine ASF1a (204 a.a.) qui fournit le dimère H3.3-H4 au complexe avant son incorporation dans la chromatine (***Figure 13***) (Banumathy et al., 2009; Bonnefoy et al., 2007; Rai et al., 2011; Ray-Gallet et al., 2007; Ricketts and Marmorstein, 2016; Tagami et al., 2004; Tang et al., 2006). La protéine HIRA sert d'échafaudage au complexe (Ricketts and Marmorstein,

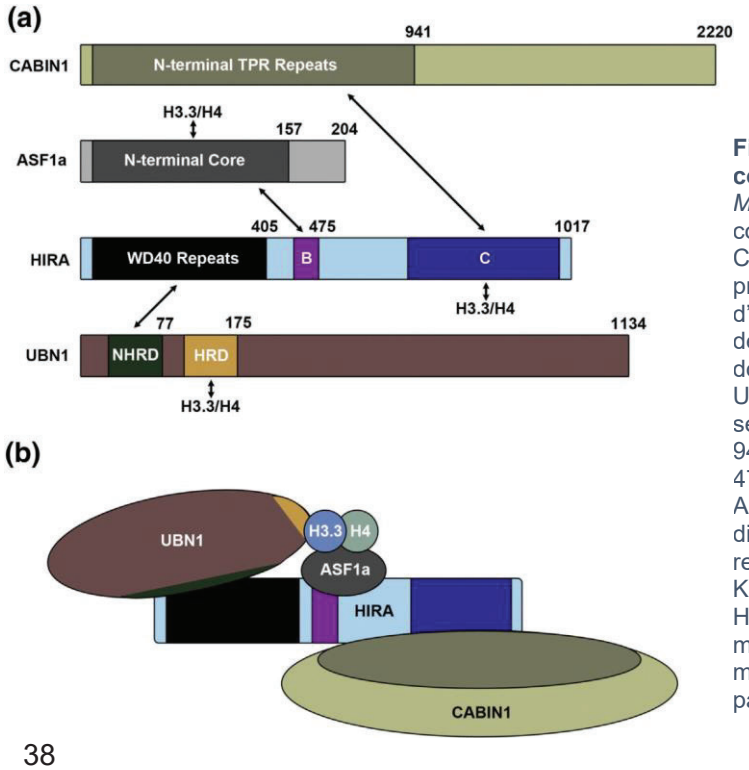


**Figure 13. Modèle d'assemblage du complexe HIRA.** *(Ricketts and Marmorstein, 2016)* Le complexe HIRA se compose de trois protéines, HIRA, UBN1 et CABIN1 et est transitoirement associé à la protéine ASF1a. La protéine HIRA sert d'échafaudage au complexe : son domaine de répétitions WD40 (1-405) se lie au domaine NHRD (41-77) de la protéine UBN1, son domaine C-terminal (763-793) se lie au domaine de répétitions TPR (1-941) de CABIN1 et son domaine B (439-475) se lie à la région N-terminale de ASF1a. ASF1a et UBN1 lient également le dimère H3.3-H4 via leurs domaines respectifs N-terminal et HRD. En 2011, Kang *et al.* ont démontré une interaction de HIRA et du dimère H3.3-H4 favorisée par la modification H4S37ph (Kang et al., 2011), mais ces résultats n'ont pas été approfondis par la suite.

2016); en effet, elle interagit avec UBN1 *via* son domaine de répétitions WD40 dans la région N-terminale (Banumathy et al., 2009) et avec CABIN1 *via* son domaine C-terminal (Rai et al., 2011). HIRA interagit également avec ASF1a *via* son domaine B (Tang et al., 2006). La protéine UBN1 reconnaît spécifiquement le dimère H3.3-H4 grâce à son domaine HRD (Hpc2-Related Domain) et peut reconnaître l'ADN (Ricketts et al., 2015, 2019). Elle constitue ainsi l'unité fonctionnelle du complexe et permet d'incorporer d'H3.3 à la chromatine. Le rôle de la protéine CABIN1 dans le complexe HIRA est encore mal compris ; elle semble dispensable pour le bon fonctionnement du complexe et permettrait simplement de le stabiliser (Rai et al., 2011; Ray-Gallet et al., 2011). Récemment, il a été montré que l'activité fonctionnelle du complexe HIRA nécessite l'homotrimérisation de la protéine HIRA (Ray-Gallet et al., 2018). Le trimère est associé à 2 protéines CABIN1 *in vitro* tandis que l'association avec plusieurs protéines UBN1 n'est pas connu (Ray-Gallet et al., 2018).

### *I.5.ii. Mécanismes de dépôt d'H3.3 par le complexe HIRA*

La mise en évidence du rôle du complexe HIRA dans le dépôt d'H3.3 étant relativement récente, les mécanismes sous-jacents sont encore en cours d'investigation. Cependant, plusieurs études permettent de proposer un modèle sur l'incorporation dans la chromatine du tétramère $(H3.3\text{-}H4)_2$, associé avec deux dimères H2A-H2B. On distingue actuellement deux mécanismes : le dépôt d'histones H3.3 nouvellement synthétisées (***Figure 14***) et le recyclage d'anciennes histones, servant de modèles pour le maintien de marques épigénétiques après le processus de transcription (***Figure 15***).

Les histones H3 et H4 nouvellement traduites dans le cytoplasme sont principalement trouvées sous forme de dimères H3-H4 (Tagami et al., 2004). Ainsi, pour le dépôt *de novo* des tétramères $(H3\text{-}H4)_2$, on peut distinguer 3 étapes : le transit cytoplasme/noyau, la tétramérisation $(H3\text{-}H4)_2$ et la formation du nucléosome. Dans le cas du variant H3.3, le dimère H3.3-H4 interagit avec ASF1a et l'importine 4 qui permettent son passage à travers les pores nucléaires (Alvarez et al., 2011; Jasencakova et al., 2010). ASF1a est également retrouvée en complexe avec les membres du complexe HIRA. Sa nécessité pour l'association d'H3.3 avec la chromatine est incertaine : une étude de Galvani *et al.* sur des lignées humaines a montré qu'elle est requise (Galvani et al., 2008) alors que d'autres études *in vitro* et dans des lignées humaines ont montré qu'elle est dispensable (Adam et al., 2013; Ray-Gallet et al., 2007). Les travaux de Daniel Ricketts ont montré que la protéine UBN1 lie le complexe H3.3-H4-ASF1a via son domaine HRD (Ricketts et al., 2015) mais peut également lier H3.3-H4 via son domaine central, les deux liaisons étant mutuellement exclusives (Ricketts et al., 2019). L'auteur suggère ainsi que ASF1a transmet le dimère H3.3-H4 au complexe HIRA en liant le domaine HRD d'UBN1, puis est

éjectée lorsque H3.3-H4 lie le domaine central d'UBN1 (***Figure 14***) (Ricketts et al., 2019). Le domaine central d'UBN1 permet également sa dimérisation, ce qui permettrait la tétramérisation $(H3.3\text{-}H4)_2$ (Ricketts et al., 2019). Par la suite, UBN1 lierait ensuite l'ADN pour déposer le tétramère d'histones. Deux dimères H2A-H2B y sont alors associés pour former le nucléosome (Ricketts et al., 2019).

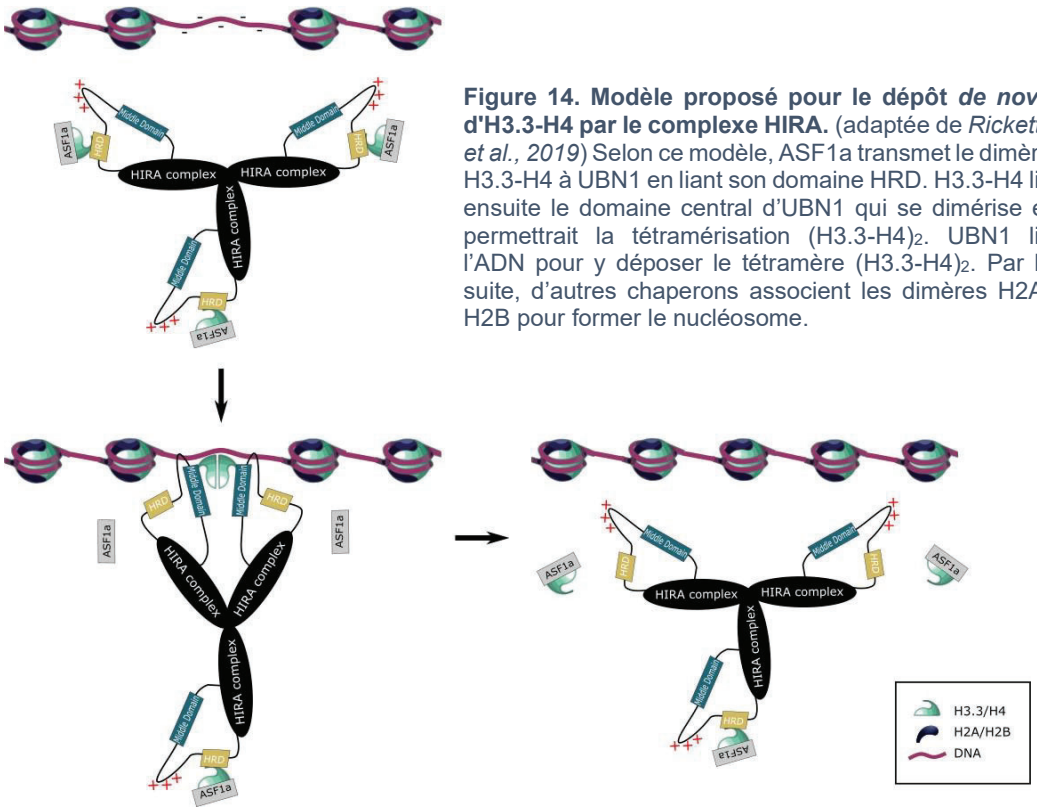


**Figure 14. Modèle proposé pour le dépôt *de novo* d'H3.3-H4 par le complexe HIRA.** (adaptée de *Ricketts et al., 2019*) Selon ce modèle, ASF1a transmet le dimère H3.3-H4 à UBN1 en liant son domaine HRD. H3.3-H4 lie ensuite le domaine central d'UBN1 qui se dimérise et permettrait la tétramérisation $(H3.3\text{-}H4)_2$. UBN1 lie l'ADN pour y déposer le tétramère $(H3.3\text{-}H4)_2$. Par la suite, d'autres chaperons associent les dimères H2A-H2B pour former le nucléosome.

Dans une étude récente, Torné *et al*. se sont intéressés au devenir des anciennes histones éjectées après le passage de l'ARN polymérase II lors du processus de transcription (Torné et al., 2020). Ils ont montré que ces histones sont recyclées et sont ré-incorporées à la chromatine afin d'assurer le maintien de l'information épigénétique. Cette étude a également montré que le dépôt des histones recyclées ne semble pas reposer sur le mécanisme précédemment décrit (***Figure 15***) : ainsi, ce dépôt est indépendant de UBN1

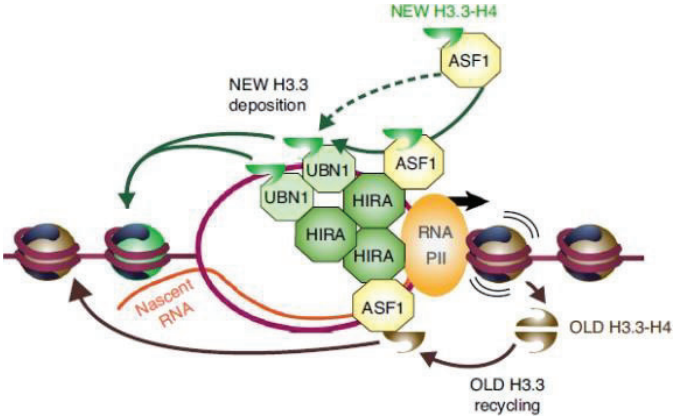


**Figure 15. Modèle proposé pour le dépôt des anciens dimères H3.3-H4 par HIRA et ASF1a après le processus de transcription.** (*Torné et al., 2020)* Contrairement au dépôt *de novo*, le dépôt des histones recyclées ne nécessite pas UBN1 ou la trimérisation. Elle repose en revanche sur l'interaction de HIRA et ASF1a. Le recyclage des histones permet d'assurer le maintien du paysage épigénétique de la région transcrite.

et de la trimérisation de HIRA ; il nécessite en revanche l'interaction de HIRA et d'ASF1a. Comment le tétramère $(H3.3\text{-}H4)_2$ se forme dans ce contexte reste encore à investiguer.

Le complexe HIRA peut localiser dans les structures nucléaires PML NBs bien que le rôle de cette localisation soit encore largement non compris. Dans le prochain chapitre, je présenterai la composition des PML NBs et leurs différents rôles. Je m'intéresserai ensuite aux différents éléments pouvant expliquer un rôle de la localisation du complexe HIRA au sein des PML NBs.

# II. Les corps nucléaires PML

Les corps nucléaires PML ou PML NBs sont des organelles sans membrane retrouvés dans la majorité des noyaux des cellules de mammifères (Lallemand-Breitenbach and de Thé, 2018). Il s'agit de sphères de 0,1 à 1μm de diamètre dans lesquelles transitent différents types de protéines (Lallemand-Breitenbach and de Thé, 2018). On compte en général 10 à 30 PML NBs par noyau et leur nombre et taille varient grandement en fonction du type cellulaire, du cycle cellulaire ou de l'état physiologique de la cellule (Bernardi and Pandolfi, 2007). Dans ce chapitre, je décrirai premièrement le mécanisme de formation des PML NBs avant de discuter de la fonction de ces corps nucléaires dans divers processus cellulaires. Enfin, dans un troisième temps, par le biais d'une revue scientifique publiée en octobre 2020 dans Nucleic Acids Research à laquelle j'ai participé (Corpet et al., 2020), les liens entre les PML NBs et la dynamique de la chromatine seront détaillés.

## II.1. La formation des PML NBs

### *II.1.i. La protéine PML*

La protéine PML ou protéine de la leucémie promyélocytaire fut pour la première fois décrite comme fusionnée avec le récepteur de l'acide rétinoïque alpha (RARα) dans la majorité des cas de leucémie aiguë promyélocytaire (APL), à la suite d'une translocation *de novo* t(15,17) (cf. Orphanet ORPHA:520) (de Thé et al., 1990, 2012). On distingue plus d'une quinzaine d'isoformes de la protéine PML résultant d'un épissage alternatif des exons 4 à 9 dans la région C-terminale (pour revue sur les différentes isoformes de PML, voir Bernardi and Pandolfi, 2007; Jensen et al., 2001; Nisole et al., 2013). Les 7 isoformes majeures sont notées PML-I à VII et sont présentées en ***Figure 16***. D'autres isoformes moins répandues peuvent résulter de l'épissage alternatif des exons 4, 5 et 6 ; ainsi on ajoutera la lettre 'a' pour les isoformes sans exon 5, la lettre 'b' pour les isoformes dans l'exon 5 et 6 et la lettre 'c' pour les isoformes sans les exons 4, 5 et 6. La protéine PML appartient à la famille des protéines contenant un motif tripartite (protéines TRIM). Le motif TRIM ou RBCC consiste en un domaine *RING finger* (R) suivi d'un ou deux domaines *B-box* (B) et d'un domaine *coiled-coil* (CC) en hélice alpha (Borden, 1998; Jensen et al., 2001; Saurin et al., 1996). Le motif RBCC de PML se situe dans la région N-terminale de la protéine, conservée par toutes les isoformes. Mis à part l'isoforme PML-VII et les isoformes 'b' et 'c', les isoformes de PML localisent principalement dans le noyau cellulaire ; en effet, on retrouve une séquence de signal de localisation nucléaire (NLS) au niveau de l'exon 6. L'isoforme PML-I possède également une séquence de signal d'export nucléaire (NES) ; elle présente donc une localisation nucléaire ou cytoplasmique en fonction du contexte cellulaire.

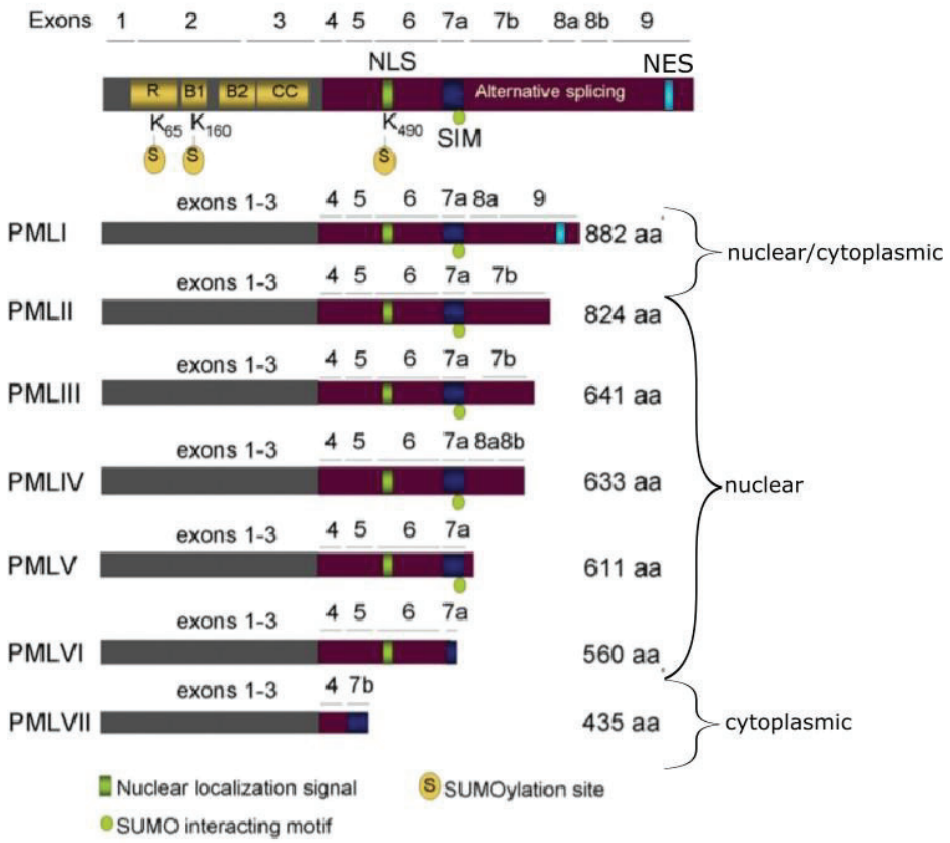


**Figure 16. Les isoformes majeures de la protéine PML.** (adaptée de *Maroui et al., 2011*) Le gène *PML* code pour une protéine de 11 exons. L'épissage alternatif de la région C-terminale conduit à générer 7 isoformes de la protéine (PML-I à PML-VII). En fonction de la présence de signaux NLS et NES dans la séquence protéique de l'isoforme, cette dernière peut présenter une localisation nucléaire ou cytoplasmique, la majorité des isoforme localisant dans le noyau. PML présente 3 sites principaux de SUMOylation (K65, K160 et K490), ainsi qu'un motif SIM.

L'expression du gène *PML* est stimulée par différents facteurs. Sa région promotrice possède un élément de réponse stimulé par les interférons de type I (IFNs) (ISRE pour 'Type I IFN stimulated response element') ainsi qu'un site d'activation par IFNγ (GAS pour 'IFN-gamma activated site'), augmentant l'expression de *PML* en réponse à une stimulation aux IFNs et à la liaison des protéines STAT (Signal-Transducer and Activator of Transcription) 1 et 2 au niveau du promoteur (Chelbi-Alix et al., 1995; Lavau et al., 1995; Stadler et al., 1995). Le facteur de nécrose tumorale TNFα et la cytokine IL-6 peuvent également stimuler l'expression de *PML*, respectivement à travers la liaison au promoteur des protéines STAT1 et STAT3 (Cheng et al., 2012; Gao et al., 2008; Hubackova et al., 2012). Un traitement de fibroblastes humains avec la cytokine IL-1 semble également augmenter l'expression de *PML*, mais le mécanisme moléculaire n'est pas connu (Heuser et al., 1998). Outre l'augmentation de l'expression de *PML* induite dans un contexte inflammatoire, l'induction d'un stress oncogénique stimule également sa transcription, en partie *via* l'activation et la liaison au promoteur du facteur de transcription p53 (Ferbeyre et al., 2000; de Stanchina et al., 2004). Ces différentes régulations positives de la

transcription de *PML* favorisent la formation des PML NBs et le recrutement des protéines associées, décrits en partie *II.1.iii*.

### *II.1.ii. Les modifications post-traductionnelles de PML : focus sur la SUMOylation*

La protéine PML est sujette à diverses PTMs (pour revue, Cheng and Kao, 2013; Hsu and Kao, 2018). Dans cette partie, je ne m'intéresserai qu'à la SUMOylation, modification la plus importante de PML. Elle participe ainsi à la maturation des PML NBs mais peut également induire la dégradation de PML par le protéasome. Il est néanmoins important de noter que la protéine PML peut également subir d'autres types de PTMs qui ne seront pas détaillées dans cette thèse. Ainsi la protéine PML possède de nombreux sites de phosphorylation, importants pour la réponse cellulaire à divers stimuli extérieurs. L'acétylation de PML régule sa SUMOylation. Enfin, la protéine PML pourrait être sujette à l'ISGylation qui entrainerait sa dégradation.

#### II.1.ii.a. La SUMOylation : généralités

La SUMOylation est une PTM consistant en la liaison covalente de protéines SUMO (Small Ubiquitin-like Modifier) sur des résidus lysines des protéines cibles (pour revue, voir Chang and Yeh, 2020; Wilkinson and Henley, 2010; Wilson, 2017). Les protéines SUMO, aussi appelées Sentrin, sont de petites protéines d'environ 11kDa présentant de fortes similitudes de séquence et de structure avec la protéine d'ubiquitine (Boddy et al., 1996; Matunis et al., 1996; Okura et al., 1996; Shen et al., 1996). Chez les vertébrés, on compte actuellement 5 paralogues différents de SUMO, notés SUMO-1 à 5. Les protéines SUMO-1, 2 et 3 sont les plus étudiées (Boddy et al., 1996; Kamitani et al., 1998a; Matunis et al., 1996; Okura et al., 1996; Shen et al., 1996). Elles peuvent être retrouvées sous formes monomériques (principalement SUMO-1) ou, de manière similaire à l'ubiquitine, former des chaînes poly-SUMO (principalement constituées de SUMO-2 et 3) (Tatham et al., 2001). SUMO-2 et 3 présentent des séquences protéiques proches, les rendant indifférenciables par western-blot (Saitoh and Hinchey, 2000). Elles sont donc généralement notées SUMO-2/3. La protéine SUMO-4, contrairement au 3 précédentes, n'est pas ubiquitaire et est uniquement retrouvée dans des organes bien spécifiques tels que les reins, la rate ou les ganglions lymphatiques (Bohren et al., 2004). Du fait de la présence d'une proline en position 90, SUMO-4 n'est pas pris en charge par la machinerie enzymatique impliquée dans la SUMOylation (expliquée plus bas) et ne peut pas être conjuguée à un substrat (Owerbach et al., 2005). Enfin, la protéine SUMO-5 n'a été découverte que très récemment et peu de choses sont pour le moment connues à son sujet (Liang et al., 2016). Elle est spécifique à l'ordre des primates et est exprimée dans des tissus particuliers comme les tissus pulmonaires ou la rate.

La conjugaison de protéines SUMO à une lysine cible requiert l'action d'un processus enzymatique de plusieurs étapes (décrit dans Chang and Yeh, 2020; Wilkinson and Henley, 2010; Wilson, 2017). Les protéines SUMO sont traduites sous forme de précurseurs dont la maturation nécessite l'action protéolytique des enzymes SENPs (SENtrin-specific Proteases) au niveau de la partie C-terminale, permettant l'exposition d'un motif di-glycine (GG). Les protéines SUMO matures sont ensuite liées avec l'hétérodimère enzymatique d'activation E1 constitué des protéines SAE1 et SAE2 (SUMO-Activating Enzymes 1 et 2), une étape qui implique l'hydrolyse d'ATP. SUMO est alors transféré à l'enzyme de conjugaison E2, la protéine UBC9 (Ubiquitin Carrier protein 9) qui, avec l'aide d'enzymes ligases E3 (par ex. les ligases de la famille des PIAS (Protein Inhibitor of Activated STAT) ou l'enzyme RanBP2), le conjugue à une lysine. Les lysines SUMOylables résident la plupart du temps au milieu d'un motif consensus ψKx(E/D) reconnu par UBC9 où ψ correspond à un acide aminé hydrophobe et x un acide aminé quelconque (Bergink and Jentsch, 2009; Gareau and Lima, 2010; Hendriks et al., 2015). La SUMOylation est réversible et peut-être retirée par les protéases SENPs (Mukhopadhyay and Dasso, 2007).

La SUMOylation d'une protéine peut conduire à l'altération de la fonction de la protéine cible en masquant des sites d'interactions ou en induisant un changement de conformation (Wilkinson and Henley, 2010) (par ex. Hardeland et al., 2002; Pichler et al., 2005). La SUMOylation peut aussi favoriser des interactions entre protéines. En effet, les protéines SUMO conjuguées peuvent être reconnues par des domaines protéiques, appelés SIM (SUMO-interacting motif). Ces domaines sont caractérisés par un groupe d'acides aminés hydrophobes (V/I/L)x(V/I/L)(V/I/L) ou (V/I/L)(V/I/L)x(V/I/L), souvent entourés par des résidus acides ou des sérines phosphorylables (Beauclair et al., 2015; Hecker et al., 2006; Kerscher, 2007; Song et al., 2005b). Les interactions SIM-SUMO peuvent également conduire au recrutement d'effecteurs sur la protéine SUMOylée. Par exemple, certaines ubiquitine-ligases reconnaissent les chaînes poly-SUMO (RNF4 et RNF11 chez l'humain), conduisant à l'ubiquitination des protéines SUMOylées et finalement à leur dégradation par le protéasome (Erker et al., 2013; Tatham et al., 2008).

#### II.1.ii.b. La SUMOylation de PML

La protéine PML contient plusieurs sites de SUMOylation. On retrouve notamment trois sites de SUMOylation principaux, les lysines K65, K160 et K490 (Kamitani et al., 1998b) (***Figure 16***), ainsi que d'autres sites de SUMOylation moins étudiés, comme la lysine K616 (Cuchet-Lourenço et al., 2011; Vertegaal et al., 2006). Plusieurs stimuli extracellulaires peuvent réguler la SUMOylation de PML. Ainsi, un traitement court au trioxyde d'arsenic ($As_2O_3$) entraîne une augmentation importante de la SUMOylation, particulièrement au

niveau des lysines 65 et 160, menant à la dégradation des protéines par ubiquitination quand le traitement est prolongé (Lallemand-Breitenbach et al., 2001; Müller et al., 1998; Sahin et al., 2014a). L'$As_2O_3$ est d'ailleurs utilisé pour dégrader l'oncoprotéine PML/RAR$\alpha$ chez les patients atteints d'APL (de Thé et al., 2012).

De nombreuses protéines reconnaissent à travers des motifs SIM les lysines SUMOylées et poly-SUMOylées de PML, et principalement la SUMOylation de K160 (Ishov et al., 1999; Lallemand-Breitenbach et al., 2001; Zhong et al., 2000; Zhu et al., 2005). La protéine PML elle-même possède un motif SIM en position 556-562 lui permettant d'interagir avec d'autres protéines PML SUMOylées (Shen et al., 2006) (***Figure 16***). Les interactions SIM-SUMO sont particulièrement importantes pour la maturation des PML NBs et pour le recrutement de protéines associées (Sahin et al., 2014a) (cf. partie *II.1.iii*).

Dans les deux dernières parties, j'ai donné un aperçu de la structure de la protéine PML et des PTMs pouvant modifier son activité ou sa stabilité. Dans la prochaine partie, je développerai les différentes étapes impliquées dans la formation des PML NBs et comment l'étape de maturation pourrait reposer sur le processus de séparation de phase liquide-liquide (LLPS pour 'Liquid-Liquid Phase Separation').

### *II.1.iii. Les différentes étapes de la formation des PML NB et l'éventuelle implication de la séparation de phase liquide-liquide (LLPS)*

La première étape de formation des PML NBs consiste en la multimérisation de plusieurs protéines PML. Cette multimérisation est médiée à la fois par des liaisons faibles entre les motifs RBCC et par l'établissement de ponts disulfures à la suite de l'oxydation de PML (Jeanne et al., 2010; Lallemand-Breitenbach et al., 2001; Sahin et al., 2014a). Toutes les isoformes nucléaires de PML sont capables de former des PML NBs en l'absence de PML endogène (Brand et al., 2010) et on observe une co-localisation des différentes isoformes *in vivo*, suggérant qu'un PML NB résulte de l'association de plusieurs isoformes (Condemine et al., 2006). Il est important de noter que seule une faible proportion de protéines PML forment des PML NBs, la large majorité (environ 90%) présentent une localisation nucléaire diffuse (Lallemand-Breitenbach and de Thé, 2010; Lallemand-Breitenbach et al., 2001). La multimérisation des motifs RBCC permet par la suite le recrutement de l'enzyme de conjugaison de SUMO UBC9 (Wang et al., 2018b). La SUMOylation de PML par UBC9 renforce les interactions PML-PML *via* des liaisons intermoléculaires SIM/SUMO (Lallemand-Breitenbach et al., 2001; Sahin et al., 2014a; Shen et al., 2006; Zhong et al., 2000). La SUMOylation de PML est donc importante pour la maturation des PML NBs ; elle est également essentielle pour le recrutement de

protéines dites protéines clientes *via* des interactions SIM/SUMO qui participeront aux diverses fonctions des PML NBs (Banani et al., 2016; Sahin et al., 2014a).

Bien que l'initiation de la formation des PML NBs repose sur des liaisons covalentes de type ponts disulfures, plusieurs éléments mènent à penser que la maturation des PML NBs et le recrutement des protéines clientes reposent sur le processus de LLPS qui stipule qu'au-dessus d'une certaine concentration, certaines protéines peuvent former des gouttelettes avec une composition distincte de l'environnement immédiat, à la manière de gouttes d'huile dans un verre d'eau (A and Weber, 2019; Banani et al., 2017; McSwiggen et al., 2019). Plusieurs critères définissent la LLPS, dont certains sont remplis ou partiellement remplis par les PML NBs matures (forme sphérique (Hoischen et al., 2018; Lallemand-Breitenbach and de Thé, 2010; Lang et al., 2010; Sahin et al., 2014a), évènements de fusion et de fission (Dellaire et al., 2006a, 2006b; Hoischen et al., 2018), haute mobilité interne des protéines clientes (Boisvert et al., 2001; Weidtkamp-Peters et al., 2008), taille dépendante de la concentration de PML (Chelbi-Alix et al., 1995; Ferbeyre et al., 2000; Hancock, 2004; Lavau et al., 1995; Stadler et al., 1995), multivalence de la protéine PML (Banani et al., 2016; Sahin et al., 2014a)) (***Figure 17***). Cependant, de nouvelles investigations sont nécessaires pour déterminer si les PML NBs répondent à

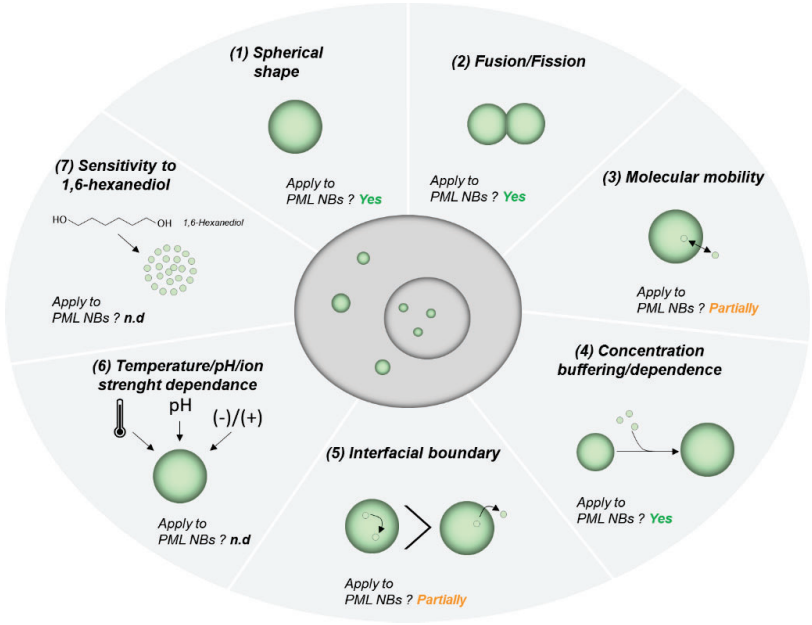


**Figure 17. Les différents critères de la transition de phase liquide-liquide (LLPS).** (adaptée de *Corpet et al., 2020*) Ce schéma résume les différents critères de la LLPS et s'ils sont remplis par les PML NBs. (1) Les gouttelettes liquides présentent tout d'abord une forme sphérique entrainée par la tension de surface ; (2) les gouttelettes ont la capacité de fusionner et de fissionner ; (3) les protéines constituant les gouttes présentent une forte mobilité interne; (4) une fois la concentration critique requise pour la formation des gouttes atteinte, la production de plus de protéines augmente la taille des gouttelettes sans changer la concentration dans les phases ; (5) les protéines effectuant de la séparation de phase se déplacent préférentiellement à l'intérieur de la goutte, la présence d'une limite de phase réduit la diffusion à travers elle ; (6) la formation de la gouttelette montre une dépendance à la température, le pH ou la concentration en ions ; (7) le 1,6-hexanediol perturbe les liaisons faibles hydrophobiques, notamment impliquées dans la LLPS. Les PML NBs répondent à plusieurs de ces critères, d'autres ont été partiellement démontrés et d'autres n'ont pas encore été déterminés (cf. tableau 1, Corpet *et al*., 2020, en partie *II.3.*).

d'autres critères définissant la LLPS et si ce mécanisme est effectivement impliqué dans la maturation des PML NBs. Plus de détails sur le possible lien entre la LLPS et les PML NBs sont donnés dans la revue Corpet et al., 2020, introduite dans la partie *II.3.i* et présentée en ***Annexe 1*** (Corpet et al., 2020).

## II.2. L'importance fonctionnelle des PML NBs

### *II.2.i. Les différents rôles potentiels des PML NBs*

Plus de 170 protéines ont été décrites comme résidant de manière constitutive ou transitoire au sein des PML NBs (Van Damme et al., 2010). Les conséquences biologiques de leur localisation dans les PML NBs ne sont pas encore connues pour toutes mais on peut envisager 3 rôles non-exclusifs des PML NBs (Corpet et al., 2020) : (1) les PML NBs pourraient servir de lieux de modifications post-traductionnelles pouvant moduler l'activité des protéines transitant à l'intérieur ou entraîner leur dégradation ; (2) les PML NBs pourraient permettre de séquestrer ou tamponner des protéines nucléaires, les détournant de leur site d'action ; (3) enfin, les PML NBs pourraient permettre d'organiser certains domaines chromatiniens.

(1) La présence dans les PML NBs de différentes enzymes suggèrent que les PML NBs constituent un haut lieu de modifications post-traductionnelles des protéines (Schmitz and Grishina, 2012) (***Figure 18***). Comme évoqué précédemment, on retrouve notamment la protéine UBC9 au sein des PML NBs qui induit la SUMOylation de plusieurs protéines clientes des PML NBs (Sahin et al., 2014a). Cette dernière peut favoriser ensuite la dégradation de certaines protéines par le protéasome à la suite de leur poly-ubiquitination par l'ubiquitine ligase RNF4 (Sahin et al., 2014a). Au sein des PML NBs, on retrouve également des enzymes impliqués dans la phosphorylation ou l'acétylation ; ainsi, la phosphorylation puis l'acétylation de la protéine suppresseur de tumeur p53 (nécessaires à son activité) reposent sur le recrutement des enzymes HIPK2 et CBP (CREB-binding protein) au sein des PML NBs (D'Orazi et al., 2002; Hofmann et al., 2002; Pearson et al., 2000).

(2) La SUMOylation des protéines clientes peut renforcer leur résidence au sein des PML NBs *via* des interaction SIM-SUMO et favoriser ainsi leur séquestration (Sahin et al., 2014a) (***Figure 18***). Ainsi, on peut par exemple mentionner les facteurs de transcription E2Fs qui sont séquestrés avec pRB (Retinoblastoma-associated protein) dans les PML NBs lors de l'entrée en sénescence, les empêchant d'induire la transcription de leurs gènes cibles (Vernier et al., 2011). De même, le chaperon d'histone DAXX est retrouvé séquestré dans les cellules entrant en apoptose,

permettant la dérépression des gènes pro-apoptotiques (Li et al., 2000; Zhong et al., 2000)

(3) Enfin, la proximité des PML NBs avec certaines régions de chromatine suggère qu'ils pourraient participer à l'organisation de ces domaines (Corpet et al., 2020). De plus, le transit de plusieurs facteurs chromatiniens au sein des PML NBs mènent à penser que les PML NBs pourraient servir de point de rencontre pour ces facteurs et permettre leur ciblage précis sur une région chromatinienne (Corpet et al., 2020). Le lien entre les PML NBs et la dynamique de la chromatine sera développée dans la partie *II.3*.

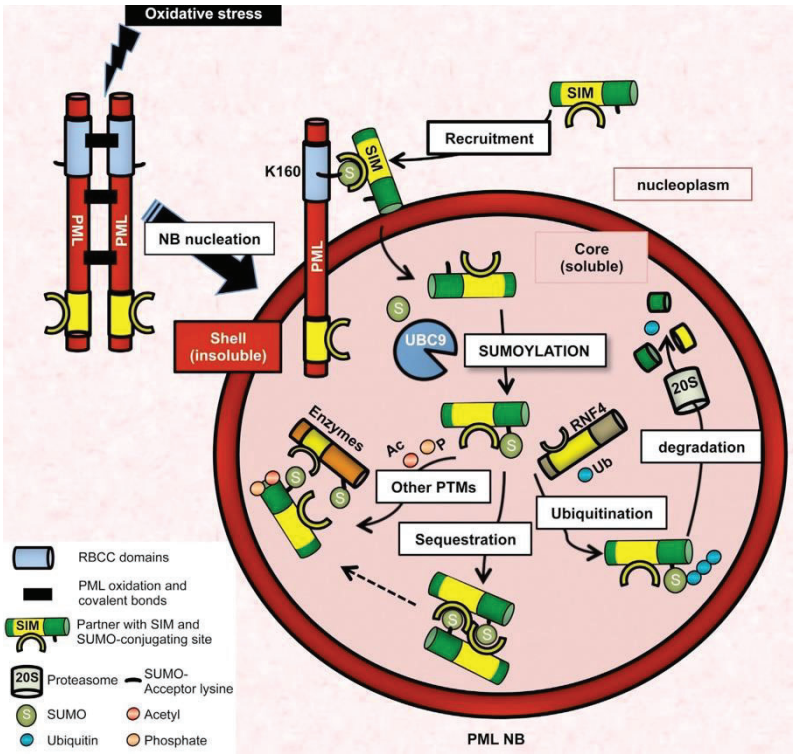


**Figure 18. Les PML NBs comme centre de modifications post-traductionnelles.** *(Sahin et al., 2014a)* Les PML NBs se forment tout d'abord par l'établissement de liaisons covalentes entre les protéines PML. ; par la suite la SUMOylation de PML et les liaisons SIM/SUMO renforcent la structure. La SUMOylation de PML permet également le recrutement de protéines clientes. A l'intérieur des PML NBs, on retrouve plusieurs enzymes impliquées dans diverses modifications post-traductionnelles telles que la SUMOylation, l'ubiquitination, l'acétylation ou encore la phosphorylation.

### *II.2.ii. Les implications physiologiques et pathologiques des PML NBs*

Du fait de leur rôle comme centre de modifications post-traductionnelles, de séquestration de protéines et leur rôle dans la dynamique de la chromatine, les PML NBs sont impliqués dans divers processus physiologiques et pathologiques (pour revue, voir Bernardi and Pandolfi, 2007; Hsu and Kao, 2018). Le *knock-out* de *Pml* chez la souris n'est pas létal mais ces souris sont plus sujettes aux infections au staphylocoque doré et aux tumeurs (Wang et al., 1998a). Elles présentent également un défaut dans la maturation terminale

des cellules myéloïdes (Wang et al., 1998a) ainsi que dans le développement du néocortex (Regad et al., 2009). Le ***Tableau 1*** résume les différentes implications de la protéine PML et des PML NBs retrouvées dans la littérature.

Les PML NBs possèdent une activité antitumorale. Ainsi, ces derniers participent à la promotion de la sénescence et de la mort par apoptose (Pearson et al., 2000; Wang et al., 1998b). Ils sont également importants pour inhiber l'angiogenèse, prévenant ainsi la progression tumorale (Bernardi et al., 2006). Les PML NBs participent à la reconnaissance et la réparation des dommages à l'ADN et jouent un rôle dans le maintien de l'intégrité de la chromatine (Chang et al., 2018). Enfin, la protéine PML sert de senseur cellulaire pour le contrôle des espèces réactives de l'oxygène (ROS pour 'Reactive Oxygen Species') (Guo et al., 2014c; Niwa-Kawakita et al., 2017). En effet, ces dernières stimulent la formation des PML NBs et l'activation de p53 (Niwa-Kawakita et al., 2017). Ce processus permet notamment la production d'antioxydants afin de contrôler le niveau de ROS dans la cellule ; lorsque le stress oxydant est trop important, l'augmentation intense de la formation des PML NBs favorise la mort cellulaire par apoptose ou l'entrée des cellules en sénescence (Niwa-Kawakita et al., 2017).

A l'inverse, certaines fonctions des PML NBs dans la physiologie, l'homéostasie cellulaire et le développement, confèrent un rôle pro-oncogénique aux PML NBs. Par exemple, alors que les PML NBs sont importants pour le renouvellement des cellules souches hématopoïétiques (Ito et al., 2012), ils favorisent également le renouvellement des cellules initiatrices de cancer (Ito et al., 2008; Martín-Martín et al., 2016). De même, les PML NBs favorisent l'oxydation des acides gras (FAO pour 'Fatty Acid Oxydation'), une voie métabolique importante pour la progression tumorale (Carracedo et al., 2012; Ito et al., 2012).

Les PML NBs ont un rôle très important dans l'immunité contre les virus à ADN et ARN (pour revue, voir Everett and Chelbi-Alix, 2007; Geoffroy and Chelbi-Alix, 2011; Scherer and Stamminger, 2016). Ainsi, lors de l'infection virale, de nombreux génomes viraux parentaux se retrouvent à proximité ou au sein des PML NBs (Everett, 2006; Lomonte, 2017). Les PML NBs sont ensuite dégradés ou déstabilisés par certaines protéines virales (Geoffroy and Chelbi-Alix, 2011; Scherer and Stamminger, 2016), mais dans des modèles de latence du virus de l'herpès simplex 1 (HSV-1) où la protéine ICP0 responsable de la dégradation des PML NBs est inactivée, le génome viral se retrouve enfermé et réprimé au sein des PML NBs (structures appelées dans notre équipe vDCP NBs pour 'viral DNA-Containing PML NBs') (Alandijany et al., 2018; Catez et al., 2012; Cohen et al., 2018; Everett et al., 2007; Maroui et al., 2016). Les PML NBs peuvent également séquestrer des

protéines virales importantes pour le cycle de réplication des virus ; par exemple, la 3D polymérase du virus de l'encéphalomyocardite (EMCV) est emprisonnée au sein des PML NBs (Maroui et al., 2011). Enfin, la protéine PML et les PML NBs sont d'importants médiateurs de la réponse immunitaire innée (Maarifi et al., 2014). Ils stimulent ainsi la sécrétion de nombreuses cytokines et potentialisent leur effet et la transcription de nombreux gènes cibles.

Pour finir, les PML NBs jouent un rôle important dans la régulation de la transcription et plus largement dans l'accessibilité de la chromatine. Plusieurs acteurs chromatiniens et facteurs de transcription transitent ainsi dans les PML NB et ces derniers pourraient favoriser la formation de domaines chromatiniens permissifs ou réfractaires à la transcription (Corpet et al., 2020). Plusieurs virus profitent d'ailleurs de l'environnement qu'offrent les PML NBs pour accomplir leur propre réplication avant de dégrader les PML NBs pour éviter leur action antivirale (Bell et al., 2000a; Day et al., 2004; Sourvinos and Everett, 2002; Swindle et al., 1999; Tang et al., 2003). La relation des PML NBs avec la dynamique de la chromatine fait l'objet de la revue Corpet A., Kleijwegt C., et al., publiée en 2020 dans Nucleic Acids Research, présentée dans la prochaine partie.

**Tableau 1. Fonctions de la protéine PML et des PML NBs.** Ce tableau reprend divers travaux établissant un lien entre la protéine PML ou les PML NBs et divers processus physiologiques et pathologiques. La littérature utilisée pour se tableau se veut la plus large et exhaustive possible, mais des oublis ont pu être commis. Les abréviations utilisées sont détaillées à la fin du tableau.

| Fonctions | | Implication de PML ou des PML NBs | Ref |
|---|---|---|---|
| Suppression de tumeur | Promotion de la sénescence | • Meilleure résistance des cellules PML$^{-/-}$ à la OIS[a]<br>• Entrée en sénescence des cellules surexprimant PML<br>• Induction de PML par p53 en réponse à un stress oncogénique<br>• Stimulation de la formation des PML NBs par les ROS[b], induction de la sénescence ou de l'apoptose en réponse à un stress oxydant aigu<br>• Activation de p53 (acétylation et phosphorylation) dans les PML NBs<br>• Séquestration du complexe pRB-E2F dans les PML NBs → arrêt du cycle cellulaire<br>• Relocalisation des membres du complexe HIRA → formation des SAHF[c] | (Banumathy et al., 2009; D'Orazi et al., 2002; Ferbeyre et al., 2000; Hofmann et al., 2002; Niwa-Kawakita et al., 2017; Pearson et al., 2000; Rai et al., 2011; Vernier et al., 2011; Zhang et al., 2005) |

| | | | |
|---|---|---|---|
| | Promotion de l'apoptose | • Meilleure résistance des souris PML$^{-/-}$ à l'apoptose induites par différents signaux (DNA-damage, Fas, céramides, TNF$\alpha$, type I and II IFNs)<br>• Induction de PML par p53 en réponse à un stress oncogénique<br>• Stimulation de la formation des PML NBs par les ROS[b], induction de la sénescence ou de l'apoptose en réponse à un stress oxydant aigu<br>• Activation de p53 (acétylation et phosphorylation) dans les PML NBs. Stabilisation de p53 *via* la séquestration de MDM2 dans le nucléole par PML<br>• Promotion de l'autophosphorylation de CHK2 par PML<br>• Séquestration de DAXX dans les PML NBs → expression des gènes pro-apoptotiques | (Bernardi et al., 2004; D'Orazi et al., 2002; Hofmann et al., 2002; Li et al., 2000; Niwa-Kawakita et al., 2017; Pearson et al., 2000; Wang et al., 1998b; Yang et al., 2002, 2006; Zhong et al., 2000) |
| | Inhibition de l'angiogenèse | • Meilleure récupération des souris PML$^{-/-}$ à une ischémie<br>• Augmentation de l'angiogenèse dans les tumeurs PML$^{-/-}$<br>• Séquestration de mTOR (favorisant l'angiogenèse) dans les PML NBs sous hypoxie<br>• Régulation de STAT1/2 et 3 par PML → promotion de la fonction anti-angiogenèse d'IFN$\alpha$ | (Bernardi et al., 2006; Hsu et al., 2017) |
| | Régulation de l'autophagie | • Promotion du transfert calcique du réticulum endoplasmique à la mitochondrie par PML cytoplasmique → répression de l'autophagie<br>• Séquestration de mTOR dans les PML NBs dans les cellules leucémiques → promotion de l'autophagie et mort cellulaire | (Laane et al., 2009; Missiroli et al., 2016) |
| | Réparation de l'ADN (Cf. Partie *IV.1.iv*) | • Juxtaposition des PML NBs avec des sites de DSBs[d] et de dommages au UV-C<br>• Augmentation du nombre de PML NBs lors de l'induction de DSB[d]<br>• Défaut de réparation des DSBs[d] dans les leucémies aiguës promyélocytaires sans PML NBs. Plus grande sensibilité aux DSBs[c] dans les cellules PML$^{-/-}$<br>• Localisation de plusieurs protéines impliquées dans la reconnaissance et la réparation des DSBs[d] avant et après l'induction de cassures : complexe MRN, TOPBP1, ATR, ATM, CHK2, BLM, BRCA1, RAD51, RAD52, WRN, RPA...<br>• Implication des PML NBs dans la réparation par recombinaison homologue | (Carbone et al., 2002; Chang et al., 2018; Dellaire and Bazett-Jones, 2004; Dellaire et al., 2006a; di Masi et al., 2016; Seker et al., 2003; Vancurova et al., 2019; Yeung et al., 2012) |
| Rôle pro-oncogénique | Régulation du métabolisme | • Promotion de la FAO[e] par PML dans des cellules de cancer du sein *via* la voie PGC$\alpha$/PPAR$\delta$ | (Carracedo et al., 2012) |

| | | | |
|---|---|---|---|
| | Renouvellement des cellules souches | • Promotion par PML du renouvellement des LICs[f] dans la leucémie et des CICs[g] dans le cancer du sein | (Ito et al., 2008; Martín-Martín et al., 2016) |
| | Résistance au médicaments | • Inhibition de la voie PI3K/Akt/mTOR par PML → résistance aux thérapies ciblant cette voie pour le traitement des glioblastomes (Iwanami et al., 2013) | (Iwanami et al., 2013) |
| | Promotion des métastases | • Promotion des métastases par PML dans le cancer du sein<br>• Promotion de la EMT[h] par PML cytoplasmique dans le cancer de la prostate | (Buczek et al., 2016; Martín-Martín et al., 2016; Ponente et al., 2017) |
| | Promotion de l'élongation alternative des télomères (ALT[h]) | • Localisation des télomères des cellules ALT[i] au sein des PML NBs → formation des APBs[j]<br>• Promotion du processus de ALT[i] par les PML NBs en promouvant la recombinaison homologue et en facilitant le recrutement du complexe BLM-TOP3A-RMI (BTR) au niveau des télomères | (Loe et al., 2020; Osterwald et al., 2015; Yeager et al., 1999) |
| Immunité et inflammation | Fonction antivirale | • Moins bonne résistance des souris ou cellules PML$^{-/-}$ aux infections par différents virus (LCMV[k], VSV[l], EMCV[m] et virus de la rage)<br>• Localisation proche des PML NBs des génomes parentaux et des complexes de réplication de plusieurs virus à ADN (herpesviruses, adenovirus, SV40[n], polyovirus et AAV[o])<br>• Répression épigénétique du génome de HSV-1[p] favorisée par les PML NBs dans des modèles de latence<br>• Séquestration dans les PML NBs des nucléocapsides de VZV[q]<br>• Séquestration dans les PML NBs de la 3D polymérase d'EMCV[m]<br>• Restriction de HBV[r] par le complexe SMC5/SMC6 dans les PML NBs avant l'expression de la protéine HBx<br>• Co-localisation de la protéine virale L-HDAg et des ARN antigénomiques de HDV[s] avec les PML NBs<br>• Relocalisation des PML NBs en corps cytoplasmique à la suite d'une infection par HIV-1[t] → répression de la transcription inverse<br>• Contrôle de la latence rétrovirale par les PML NBs *via* une répression épigénétique<br>• Promotion de l'activation des gènes de cyokines par les PML NBs à la suite d'une infection virale → induction d'une réponse immunitaire innée<br>• Dégradation/perturbation des PML NBs et/ou protéines associées par beaucoup de facteurs viraux | (Alandijany et al., 2018; Bell et al., 2000b; Blondel et al., 2002; Bonilla et al., 2002; Catez et al., 2012; Cohen et al., 2018; Dutrieux et al., 2015; El Mchichi et al., 2010; Everett, 2006; Everett et al., 2007; Geoffroy and Chelbi-Alix, 2011; Kahle et al., 2015; Lusic et al., 2013; Maroui et al., 2011, 2016; Niu et al., 2017; Rai et al., 2017; Reichelt et al., 2011; Scherer and Stamminger, 2016; Shalginskikh et al., 2013) |

| | | | |
|---|---|---|---|
| | Immunité innée et réponse inflammatoire | • Développement d'une sévère inflammation granulomateuse par les souris PML-/- → mauvais fonctionnement des macrophages et mauvaise élimination des pathogènes<br>• Importance de PML pour la différenciation des cellules GMP[u] en macrophage ou granulocyte chez la souris<br>• Expression de *PML* induite par les IFNs de type I et II, l'IL-6, le TNFα et l'IL-1<br>• Régulation de l'expression d'IL-6 par PML dans les myélomes multiples<br>• Promotion de l'activation de NLRP3 et la formation de l'inflammasome par PML → production d'IL-1β<br>• Promotion de la phosphorylation de STAT1 et de l'expression des ISGs[v] cibles par PML nucléaire → potentialisation de la signalisation à l'IFNγ<br>• Inhibition de la dégradation de IRF3 par PML-IV *via* la séquestration de Pin1 à la suite d'une infection par VSV[k] → augmentation de la production d'IFNβ<br>• Promotion de la signalisation TGFβ par PML cytoplasmique<br>• Régulation par PML de l'accumulation des formes actives de STAT1 et STAT2 et de leur interaction avec les protéines HDACs au niveau des promoteurs des ISGs[v] → potentialisation de la signalisation à l'IFN de type I<br>• Rapprochement spatial entre les PML NBs et le cluster de gènes MHC-II[w] induit par un traitement à l'IFNγ. Importance de PML pour la transcription de MHC-II[w] | (Cheng et al., 2012; El Asmi et al., 2014; El Bougrini et al., 2011; Gao et al., 2008; Gialitakis et al., 2010; Heuser et al., 1998; Hubackova et al., 2012; Khalfin-Rabinovich et al., 2011; Kim and Ahn, 2015; Lin et al., 2004; Lo et al., 2013; Lunardi et al., 2011; Maarifi et al., 2014; Ohgiya et al., 2012; Stadler et al., 1995; Ulbricht et al., 2012) |
| Développement et physiologie | Développement neuronal | • Plus petits cerveaux observés chez les souris PML$^{-/-}$<br>• Séquestration du complexe pRB-E2F dans les PML NBs. Prolifération des NPCs[x] et altération de la sortie du cycle cellulaire et de la différenciation favorisées par la perte de PML<br>• Promotion de la formation des PML NBs et de la répression de GluA1 par la localisation nucléaire d'Arc murin → promotion de la plasticité synaptique | (Korb et al., 2013; Regad et al., 2009) |
| | Développement des glandes mammaires | • Importance de PML pour la morphogenèse ductale chez la souris<br>• Régulation par PML de la prolifération des progéniteurs mammaires<br>• Régulation de l'expression de PML par la famille des STAT durant la grossesse des souris | (Li et al., 2009) |

| | | | |
|---|---|---|---|
| | Renouvellement des cellules souches hématopoïetiques | • Importance de PML pour le maintien de la quiescence des HSCs[y] | (Ito et al., 2008, 2012) |
| | Régulation de la transcription | • Présence des PML NBs sont présents dans des régions à haute activité transcriptionnelle<br>• Régulation de la transcription par les PML NBs *via* l'activation ou la séquestration de facteurs de transcription (par ex. p53 ou E2Fs) ou la régulation de l'action de protéines associées à la chromatine (HDACs, DAXX, complexe HIRA)<br>• Promotion potentielle par les PML NBs de la formation de domaines de chromatine permissifs ou réfractaires à la transcription | (Corpet et al., 2020; Kurihara et al., 2020; Wang et al., 2004) |
| Homéostasie | Dégradation des aggrégats protéiques | • Co-localisation d'agrégats protéiques avec les PML NBs dans des maladies d'expansion de polyglutamine. Exacerbation de l'expansion dans un modèle d'ataxie spinocérébelleuse déficient pour PML<br>• Promotion par PML de la SUMOylation des protéines mal-conformées, leur ubiquitination par RNF4 et leur dégradation par le protéasome | (Guo et al., 2014a; Janer et al., 2006) |
| | Métabolisme | • Inhibition de la glycolyse par PML cytoplasmique<br>• Interaction de FoxO avec les PML NBs et la désacétylase SIRT1 pour induire l'expression des facteurs de transcription NeuroD et MafA → protection des cellules β au stress oxydant induit par l'hyperglycémie<br>• Contrôle par PML de l'homéostasie des ROS[b] Incapacité des cellules déficientes pour PML à contrôler le niveau de ROS[b].<br>• Promotion de la FAO[e] par les PML NBs en favorisant l'activation de la voie PGCα/PPARδ<br>• Relation entre PML et obésité → résultats contradictoires montrant soit une protection ou une prédisposition contre/à l'obésité en l'absence de PML | (Carracedo et al., 2012; Cheng et al., 2013; Guo et al., 2014c; Ito et al., 2012; Kim et al., 2011; Kitamura et al., 2005; Shimada et al., 2008) |
| | Cycle circadien | • Réduction de la précision et de la stabilité du rythme circadien des souris PML$^{-/-}$<br>• Localisation du régulateur d'horloge PER2 dans les PML NBs | (Miki et al., 2012) |

a: Oncogene Induced Senescence (OIS); b: Reactive Oxygen Species (ROS); c: Senescence-Associated Heterochromatin Foci (SAHF); d: Double Strand Breaks (DSBs); e: Fatty Acid Oxidation (FAO); f: Leukemia Inducting Cells (LICs); g: Cancer Initiating Cells (CICs); h: Epithelial-Mesenchymal Transition (EMT); i: Alternative Lengthening of Telomeres (ALT); j: ALT-associated PML Bodies (APBs); k: Lymphocytic choriomeningitis virus (LCMV); l: Vesicular stomatitis virus (VSV); m: Encephalomyocarditis virus (EMCV); n: Simian virus 40 (SV40); o: Adeno-associated virus (AAV); p: Herpes simplex virus 1 (HSV-1); q: Varicella-zoster virus (VZV); r: Hepatitis B virus (HBV); s: Hepatitis D virus (HDV); t: Human immunodeficiency virus 1 (HIV-1); u: Granulocyte/monocyte progenitor (GMP); v: Interferon Stimulated Genes (ISGs); w: Major Histocompatibility Complex II (MHC-II); x: Neural Progenitor Cells (NPCs); y: Hematopoietic Stem Cells (HSCs);

## II.3. Les PML NBs et la dynamique de la chromatine

### *II.3.i. "PML nuclear bodies and chromatin dynamics: catch me if you can !". Nucleic Acids Research. 2020 (Annexe 1)*

Au cours de ma 3ème année de thèse, mes directeurs de thèse Armelle Corpet et Patrick Lomonte m'ont proposé de participer à la rédaction d'un article de revue sur le sujet des corps nucléaires PML et de la dynamique de la chromatine (***Annexe 1***). J'ai accepté cette expérience et ai participé avec enthousiasme à la rédaction des 3 dernières sous-parties de la revue, portant sur l'implication des PML NBs dans la dynamique de l'hétérochromatine. La revue est parue en octobre 2020 dans le journal Nucleic Acids Research et est disponible en ***Annexe 1***.

La première partie de la revue focalise sur la structure et la formation des PML NBs, notions déjà introduites précédemment. La deuxième partie résume les liens entre les PML NBs et la chromatine. Plusieurs éléments suggèrent un rôle important des PML NBs dans la régulation de la dynamique de la chromatine. Premièrement, plusieurs protéines associées à la chromatine, y compris des histones et des chaperons d'histones, sont retrouvées dans les PML NBs. Les PML NBs sont également retrouvées associées avec certaines régions chromatiniennes et dans certains cas, de l'ADN ou de la chromatine peuvent être retrouvés à l'intérieur des PML NBs (par ex. les télomères des cellules cancéreuses ALT, certains péricentromères dans la pathologie de l'ICF (Immunodeficiency, Centromeric region instability and Facial anomalies syndrome) ainsi que le génome latent hétérochromatinisé du virus HSV-1). Enfin, la troisième et la quatrième partie s'intéressent à l'implication des PML NBs dans la dynamique de la chromatine virale et cellulaire respectivement.

### *II.3.ii. La relation entre les PML NBs, le variant H3.3 et le complexe HIRA*

#### II.3.ii.a. Les PML NBs et la dynamique d'H3.3

Contrairement à une localisation pan-nucléaire des histones H3 canoniques, il a été montré que les dimères H3.3-H4 nouvellement synthétisés localisent au sein des PML NBs (Corpet et al., 2014; Delbarre et al., 2013; Drané et al., 2010). Cette accumulation dans les corps nucléaires est dépendante du chaperon d'histone DAXX (Corpet et al., 2014; Delbarre et al., 2013; Drané et al., 2010) et semble importante pour le dépôt d'H3.3 dans les régions péricentriques (Corpet et al., 2014). Plus globalement, les PML NBs pourraient servir de plateforme de rencontre entre le variant H3.3 et d'autres partenaires et notamment le complexe HIRA qui peut également transiter dans ces corps nucléaires dans des conditions de stress.

Des études d'immunoprécipitation de la chromatine (ChIP pour 'Chromatin Immunoprecipitation') sur la protéine PML dans des fibroblastes embryonnaires murins ont montré qu'elle était associée avec des régions globalement pauvres en H3.3 et enrichies pour la marque d'hétérochromatine H3K9me3 (appelés PADs pour 'PML Associated domains') (Delbarre et al., 2017). De plus, la délétion de PML dans ces cellules induit une augmentation de l'incorporation de H3.3 et une baisse de la marque H3K9me3 (Delbarre et al., 2017; Shastrula et al., 2019). Ces études suggèrent ainsi que la liaison de PML à la chromatine prévient l'incorporation de H3.3 et permet l'établissement de régions d'hétérochromatine associées à la marque H3K9me3. Ces résultats semblent à première vue en contradiction avec l'idée d'une accumulation d'H3.3 dans les PML NBs. Cependant, les expériences de ChIP ne permettent pas de faire la distinction entre les protéines PML nucléoplasmiques et celles associées aux PML NBs et la visualisation par immunofluorescence combinée une hybridation *in situ* par fluorescence (FISH pour 'Fluorescent *In Situ* Hybridization') montre que les PADs ne localisent pas à proximité des PML NBs. Ainsi, l'exclusion d'H3.3 des PADs pourrait être liée à la forme nucléoplasmique de PML et indépendante des PML NBs.

#### II.3.ii.b. Le complexe HIRA relocalise dans les PML NBs en condition de stress

En conditions normales, le complexe HIRA présente une localisation pan-nucléaire ; cependant, dans certains contextes, comme lors d'une infection virale ou l'entrée des cellules en sénescence, le complexe HIRA s'accumule dans les PML NBs (***Figure 19***) (Banumathy et al., 2009; Cohen et al., 2018; McFarlane et al., 2019; Rai et al., 2011, 2017; Zhang et al., 2005). Cette localisation spécifique est encore mal comprise et est au cœur de mes travaux de thèse. Cette partie vise à présenter l'état de l'art sur le mécanisme et

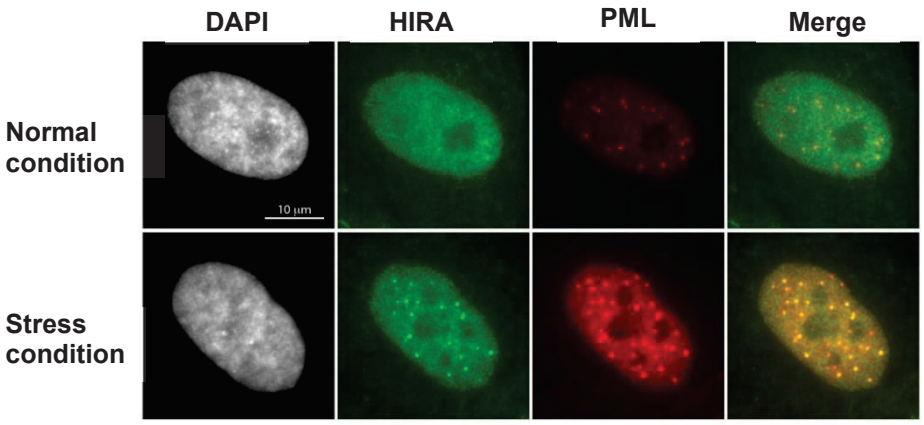


**Figure 19. L'accumulation de HIRA au sein des PML NBs en condition de stress (ici, stimulation à l'IFNβ).** Sur cette immunofluorescence, la protéine HIRA (vert) forme des foyers co-localisant avec les PML NB (rouge) lorsqu'elle est soumise à un stress (infection virale, traitement IFN ou entrée en sénescence). Les autres membres du complexe (UBN1, CABIN1 et ASF1a) se comportent de manière identique.

le rôle potentiel de cette accumulation, d'une part dans les cellules sénescentes et dans un second temps dans un contexte infectieux.

Le complexe HIRA relocalise au sein des PML NBs lors de l'entrée en sénescence :

La sénescence se définit par un arrêt permanent du cycle cellulaire et constitue un processus physiologique impliqué notamment dans la prévention de la formation de tumeurs (Braig et al., 2005; Chen et al., 2005), la cicatrisation (Krizhanovsky et al., 2008), le développement embryonnaire (Muñoz-Espín et al., 2013; Storer et al., 2013) ou encore le vieillissement de l'organisme (Baker et al., 2016). Initialement découverte comme résultant du raccourcissement progressif des télomères au cours des divisions cellulaires (sénescence réplicative) (Hayflick, 1965; Hayflick and Moorhead, 1961), la sénescence peut également être induite par différents types de signaux tels qu'un dommage à l'ADN, un stress oxydant ou l'activation d'un oncogène, constituant ainsi un mécanisme de défense contre la transformation cellulaire (Rai and Adams, 2012). L'entrée des cellules en sénescence et l'arrêt du cycle cellulaire est la résultante de l'activation des voies de signalisation p53/p21 et p16/pRb (Campisi, 2005).

Les cellules sénescentes présentent des caractéristiques spécifiques par rapport aux cellules proliférantes, dont les plus notables sont la sécrétion d'un cocktail de facteurs appelés le SASP ou 'Senescence-Associated Secretory Phenotype' (Coppé et al., 2008) ainsi qu'une réorganisation globale de la chromatine avec la formation de foyers d'hétérochromatine appelés SAHF ou 'Senescence-Associated Heterochromatin Foci' (Rai and Adams, 2012). Les SAHF permettent notamment l'extinction des gènes de prolifération et participent à maintenir la cellule dans un état sénescent (Rai and Adams, 2012). Dans les cellules sénescentes, on observe également une accumulation des membres du complexe HIRA au sein des PML NBs, importante pour la formation des SAHF (Banumathy et al., 2009; Rai et al., 2011; Zhang et al., 2005). On pourrait supposer que le complexe HIRA, en collaboration avec d'autres acteurs, participe directement à la formation des SAHF en y incorporant le variant H3.3 après son passage dans les PML NBs ; cependant, l'étude épigénétique des SAHF montre qu'il n'y a pas d'accumulation du variant H3.3 dans ces régions d'hétérochromatine (Corpet et al., 2014). De plus, les SAHF ne localisent pas à proximité des PML NBs. Ainsi, l'implication du complexe HIRA et de sa localisation dans les PML NBs dans la formation des SAHF, et plus largement dans l'établissement de l'état sénescent, semble être indirecte et des études supplémentaires seront nécessaires pour comprendre ce mécanisme.

La relocalisation du complexe HIRA au sein des PML NBs dans les cellules sénescentes ne dépend pas des voies de signalisation de mises en place au cours de la sénescence à

savoir les voies p21/p53 et p16/pRb, bien que ces dernières soient requises pour la formation des SAHF (Ye et al., 2007a). En revanche, la répression de la voie Wnt observée dans les cellules sénescentes est importante pour la relocalisation : en effet, cette répression permet l'activation de la kinase GSK3β (Glycogen Synthase Kinase 3β), requise pour la relocalisation du complexe et la formation des SAHF lors de l'induction de la sénescence (Ye et al., 2007b). La phosphorylation de la sérine 697 de la protéine HIRA par GSK3β induirait son recrutement au sein des PML NBs (Ye et al., 2007b); cependant, la mutation de S697 de cette étude a été effectuée sur une version tronquée de la protéine HIRA exprimée de façon ectopique, et la même mutation dans le contexte de la sur-expression de la protéine totale effectuée au cours de ma thèse n'a pas permis de reproduire ces résultats. Enfin, le SASP des cellules sénescentes est en partie constitué de cytokines pro-inflammatoires dont l'IFN de type I (Novakova et al., 2010). L'IFN de type I a été montré comme responsable de la relocalisation du complexe HIRA au sein des PML NBs dans le cas des infections virales (cf. ci-dessous) (McFarlane et al., 2019; Rai et al., 2017); il est ainsi envisageable que cette voie est également impliquée dans la relocalisation du complexe dans les cellules sénescentes. Cependant, l'IFN de type I est sécrété tardivement par les cellules sénescentes (Cecco et al., 2019) tandis que la relocalisation d'HIRA est relativement précoce (Zhang et al., 2005) ; ainsi une autre voie pourrait être impliquée dans la relocalisation du complexe HIRA lors de l'entrée des cellules en sénescence.

<u>Le complexe HIRA relocalise au sein des PML NBs à la suite d'une infection virale et de manière dépendante de la signalisation IFN</u> :

Le virus de l'herpès simplex 1 (HSV-1) est un pathogène humain neurotrope, responsable notamment des boutons de fièvre mais aussi de pathologies plus sévères comme les encéphalites herpétiques. Deux cycles se distinguent lors d'une infection HSV-1 : le cycle lytique et le cycle latent. Lors du cycle lytique, tous les gènes viraux sont exprimés conduisant à l'excrétion virale et la mort de la cellule hôte. Le cycle latent se déroule uniquement dans les neurones. La majorité des gènes viraux sont éteints *via* l'hétérochromatinisation du génome viral (Bloom et al., 2010; Cliffe et al., 2009; Deshmane and Fraser, 1989; Kwiatkowski et al., 2009) et son enfermement dans les PML NBs, formant les vDCP-NBs (Catez et al., 2012; Everett et al., 2007; Maroui et al., 2016). Dans un modèle d'infection avec un virus HSV-1 atténué dans des fibroblastes primaires humains permettant de reproduire la latence, le complexe HIRA relocalise avec le génome viral dans les PML NBs (Cohen et al., 2018; Rai et al., 2017). Le complexe HIRA est notamment important pour la chromatinisation du génome d'HSV-1 latent avec le variant H3.3 (Cohen et al., 2018). Rai *et al.* ont également montré que la transfection des cellules

avec un plasmide induit la relocalisation du complexe HIRA au sein des PML NBs et la chromatinisation du plasmide avec le variant H3.3, permettant d'étendre les résultats à de l'ADN nu étranger (Rai et al., 2017). En revanche, aucune des deux études n'a démontré un lien direct entre l'évènement de relocalisation dans les PML NBs et le processus de chromatinisation.

La relocalisation du complexe HIRA dans les vDCP NBs est dépendante de la signalisation IFN (signalisation décrite en partie *III.3*). En effet, l'inhibition de la voie IFN prévient la relocalisation du complexe suite à une infection par HSV-1 (McFarlane et al., 2019) et la stimulation de cellules non-infectées avec de l'IFN (type I et II) induit la relocalisation du complexe HIRA au sein des PML NBs (McFarlane et al., 2019; Rai et al., 2017). Cette relocalisation n'est pas observée dans la plupart cellules cancéreuses (Rai et al., 2017). Ainsi, la signalisation induisant la relocalisation semble défectueuse dans les cellules transformées. En plus de son rôle dans la chromatinisation du génome viral, le complexe HIRA semble important pour l'induction des gènes stimulés par l'interféron (ISGs pour 'Interferon Stimulated Genes') (McFarlane et al., 2019). Ainsi, le complexe HIRA participerait à la réponse cellulaire antivirale. Supportant cette hypothèse, une étude portant sur le virus du SARS-Cov-2 (Severe Acute Respitory Syndrome Coronavirus 2) indique que la protéine HIRA a une activité antivirale (Wei et al., 2021). Une autre étude sur un autre modèle cellulaire a à l'inverse montré une activité provirale de la protéine HIRA suite à une infection par SARS-Cov-2 (Schneider et al., 2021). Plus largement, l'IFN est une cytokine sécrétée lors de l'inflammation, y compris dans des maladies chroniques (par ex. le lupus érythémateux systémique (SLE pour 'Systemic Lupus Erythematosus') ou certaines myopathies inflammatoires). On pourrait ainsi supposer que le complexe HIRA, en relocalisant dans les PML NBs, participe à ce contexte inflammatoire.

Un des objectifs de ma thèse a été de caractériser le rôle de la relocalisation du complexe HIRA dans les PML NBs dans le cadre de la réponse inflammatoire. Dans le prochain chapitre, j'introduirai le processus de l'inflammation, les voies de signalisation et les différents médiateurs impliqués. Je m'intéresserai ensuite plus particulièrement à la voie de l'IFN, impliquée dans la relocalisation du complexe HIRA à la suite d'une infection virale. J'évoquerai aussi les liens découverts précédemment entre le complexe chaperon d'histone HIRA et la régulation de l'expression des ISGs en réponse à une signalisation à l'IFN de type I.

# III. L'inflammation

L'inflammation est un processus physiologique complexe et multifactoriel mis en place par l'organisme pour s'assurer de l'élimination de facteurs nocifs, enclencher une réponse immunitaire et favoriser la réparation des tissus endommagés (Medzhitov, 2008). Ainsi, une réponse inflammatoire maîtrisée permet de maintenir l'homéostasie de l'organisme ; en revanche, un dérèglement de la réponse inflammatoire peut conduire à de sérieux dommages, comme cela peut être observé à la suite de certaines infections virales (par ex. syndrome de détresse respiratoire aigüe induit notamment par les coronavirus (Channappanavar and Perlman, 2017; Coperchini et al., 2020; Mahmudpour et al., 2020)) ou dans des pathologies inflammatoires (par ex. les myopathies inflammatoires (Rayavarapu et al., 2013) ou la polyarthrite rhumatoïde (Guo et al., 2018)). L'inflammation d'un tissu est généralement caractérisée par 5 symptômes : la rougeur, l'enflure, la chaleur, la douleur et la perte de fonction du tissu (Hurley, 1972; Punchard et al., 2004). Ces symptômes sont le reflet d'une augmentation de la perméabilité de l'endothélium vasculaire, une fuite des composants du sérum et l'infiltration des cellules de l'immunité (Punchard et al., 2004). Dans ce chapitre, j'exposerai les différents inducteurs de l'inflammation ainsi que les facteurs nucléaires impliqués dans leur reconnaissance. Je détaillerai ensuite les différents médiateurs de la réponse inflammatoire. Par soucis de simplicité, je n'évoquerai dans cette partie que les médiateurs cytokiniques et chemoattractants impliqués dans l'inflammation mais il est important de noter que de nombreux autres médiateurs participent au processus inflammatoire, notamment les amines et peptides vasoactifs (par ex. l'histamine), les anaphylatoxines, les médiateurs lipidiques (càd. les eicosanoïdes et les facteurs d'activation plaquettaire) ou encore les enzymes protéolytiques (pour revue, voir Medzhitov, 2008). Dans une dernière partie, je m'intéresserai particulièrement à la signalisation de l'IFN de type I, qui semble particulièrement impliquée dans la relocalisation du complexe HIRA au sein des PML NBs après une infection virale.

## III.1. Les différents inducteurs de l'inflammation et leurs senseurs

Les inducteurs de l'inflammation peuvent être classifiés en plusieurs catégories et sous-catégories (***Figure 20***) (Medzhitov, 2008; Zindel and Kubes, 2020). Ces inducteurs peuvent tout d'abord être exogènes et provenant de l'environnement immédiat de l'organisme subissant l'inflammation. On compte parmi eux les inducteurs microbiens qui possèdent de nombreuses structures moléculaires conservées appelées PAMPs pour 'Pathogen-Associated Molecular Patterns' ainsi que des facteurs de virulence participant à l'induction de l'inflammation (Medzhitov, 2008). Les inducteurs exogènes peuvent être aussi non-microbiens comme des particules étrangères retrouvées dans l'air ou dans

l'alimentation (appelés LAMPs exogènes pour 'Lifestyle-associated Molecular Patterns') ou des allergènes (Medzhitov, 2008; Zindel and Kubes, 2020). Les inducteurs endogènes (appelés DAMPs pour 'Damage-associated Molecular Patterns') proviennent eux du stress, endommagement ou mauvais fonctionnement d'un tissu, induisant la présence intra- et extracellulaire de molécules reconnues comme signal de danger par l'organisme. Ainsi, l'apoptose ou la nécrose d'une cellule induit la libération de nombreuses molécules dans l'environnement, normalement indétectables car intracellulaires (Medzhitov, 2008; Zindel and Kubes, 2020). Plus récemment, il a également été montré que la présence d'ADN cytoplasmique du soi, suite à des dommages à l'ADN ou dans les cellules sénescentes, pouvait également induire une réponse inflammatoire (Dou et al., 2017; Glück et al., 2017; Harding et al., 2017; Mackenzie et al., 2017; Yang et al., 2017). De plus, la protéine ATM, impliquée dans la réponse au cassures double-brin est également capable d'induire la production d'IFN de type I (Brzostek-Racine et al., 2011; Yu et al., 2015). Il existe également des LAMPs endogènes, par exemple des cristaux de cholestérol résultant d'une alimentation trop riche en matières grasses (Zindel and Kubes, 2020).

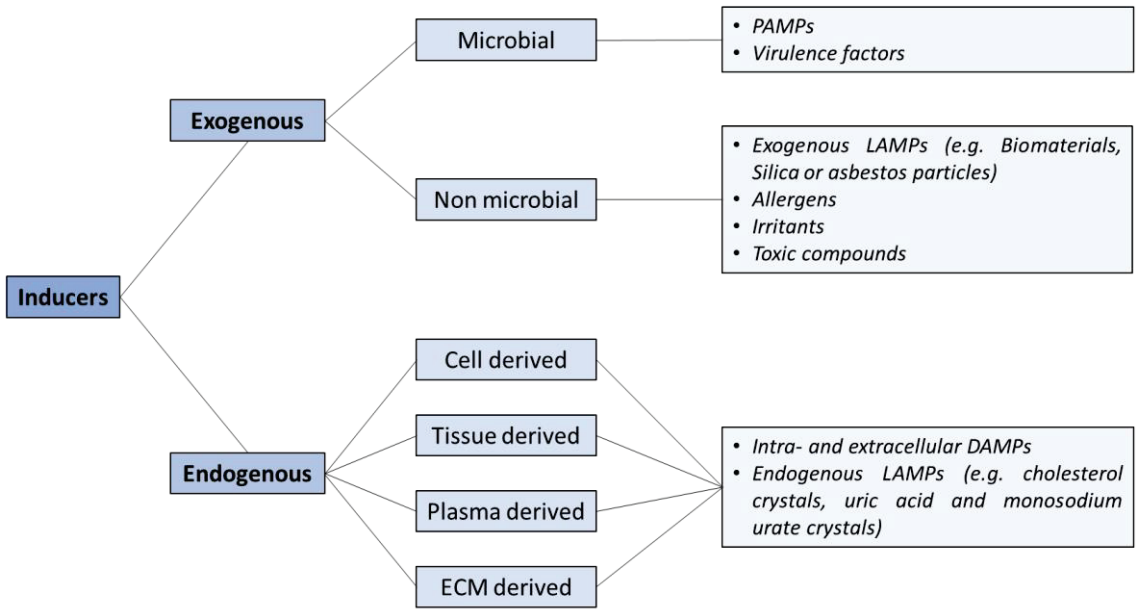


**Figure 20. Les différents types d'inducteurs de l'inflammation.** (adaptée de *Medhzitov, 2008* et *Zindel and Kubes, 2020*). Les inducteurs de l'inflammation peuvent être exogènes ou endogènes. Parmi les inducteurs exogènes, on peut retrouver des inducteurs microbiens ou non-microbiens provenant de l'environnement. Les inducteurs endogènes dérivent de tissus stressés, endommagés ou défaillants. ECM: Extracellular Matrix; PAMPs: Pathogen-Associated Molecular Patterns; LAMPs: Lifestyle-Associated Molecular Patters; DAMPs: Damage-Associated Molecular Patterns.

Une large majorité des inducteurs de l'inflammation sont reconnus par des récepteurs appelés PRRs pour 'Pattern Recognition Receptors'. Les différents PRRs peuvent être classés dans différentes familles en fonction de l'homologie de leurs domaines protéiques : les récepteurs Toll-like (TLRs), les récepteurs à lectin de type C (CLRs), les récepteurs NOD-like (NLRs), les récepteurs RIG-I-like (RLRs), les récepteurs AIM2-like

(ALRs) et d'autres récepteurs d'ADN intracellulaires comme la protéine cGAS (***Tableau 2***) (Brubaker et al., 2015; Takeuchi and Akira, 2010). Les PRRs reconnaissent différents types de molécules et permettent de répondre de manière adéquate aux divers PAMPs, DAMPs et LAMPs présents dans l'environnement tissulaire. La reconnaissance d'un ligand par un PRR induit par la suite l'activation d'une ou plusieurs voies de signalisation et la transcription de gènes clés dans le processus inflammatoire.

**Tableau 2. Les différentes familles de PRRs.** Ce tableau, adapté de *Brubaker et al., 2015* et *Takeuchi and Akira, 2010* résume les différentes familles de PRRs, leurs membres, les domaines qu'il partagent et la nature des ligands qu'ils reconnaissent.

| | **Familles de PRRs** | **PRRs membres** | **Domaines partagés** | **Ligands** | **Origines des ligands** |
|---|---|---|---|---|---|
| Récepteurs liés à la membrane | Toll-like receptors (TLRs) | TLR1-10 chez l'homme, TLR1-9 et 11-13 chez la souris | LRR, TIR | Lipoprotéines, Lipopolysaccharide, Flagelline, Protéines d'enveloppe virale, ARNsb, ARNdb, ADN CpG, LAMPs … | Bactéries, virus, champignons, protozoaires, soi, environnement |
| | C-type lectin receptors (CLRs) | Des centaines de CLRs recensés subdivisés en 17 groupes Ex : Dectin-1, Dectin-2… | C-type lectin | Carbohydrates | Bactéries, virus, champignons |
| Récepteurs intracellulaires non liés à la membrane | NOD-like receptors (NLRs) | NOD1, NOD2, NLRC3-5, NLRP1-9 et 11-14, NAIP1,-2,-5 et -6 | Nucleotide binding, LRR | Peptydoglycan, Flagellin, Toxines, acides nucléiques viraux, LAMPs… | Bactéries, virus, soi, environnement |
| | RIG-I-like receptors (RLRs) | RIG-I, MDA5, LGP2 | DExD/H helicase | ARNdb, ADNdb (*via* l'activité de l'ARN Pol III) | Essentiellement virus à ARN, mais peut reconnaître de l'ADN viral, bactérien ou du soi *via* l'activité de l'ARN Pol III |
| | AIM2-like receptors (ALRs) | AIM2, IFI16 | PYRIN, HIN-200 | ADNdb | Bacteries, virus, soi |
| | Others | cGAS, DAI, DNA-PK, MRE11, ATM | n.a. | ADNdb, DSBs | Bactérie, virus, soi |

## III.2. Les différents médiateurs de l'inflammation

### *III.2.i. Les voies de signalisation sous les PRRs*

Différentes voies de signalisation sont activées à la suite de la reconnaissance de ligands en fonction des types de PRRs entrant en action. Ces dernières sont brièvement présentées ci-dessous et représentées en ***Figure 21***.

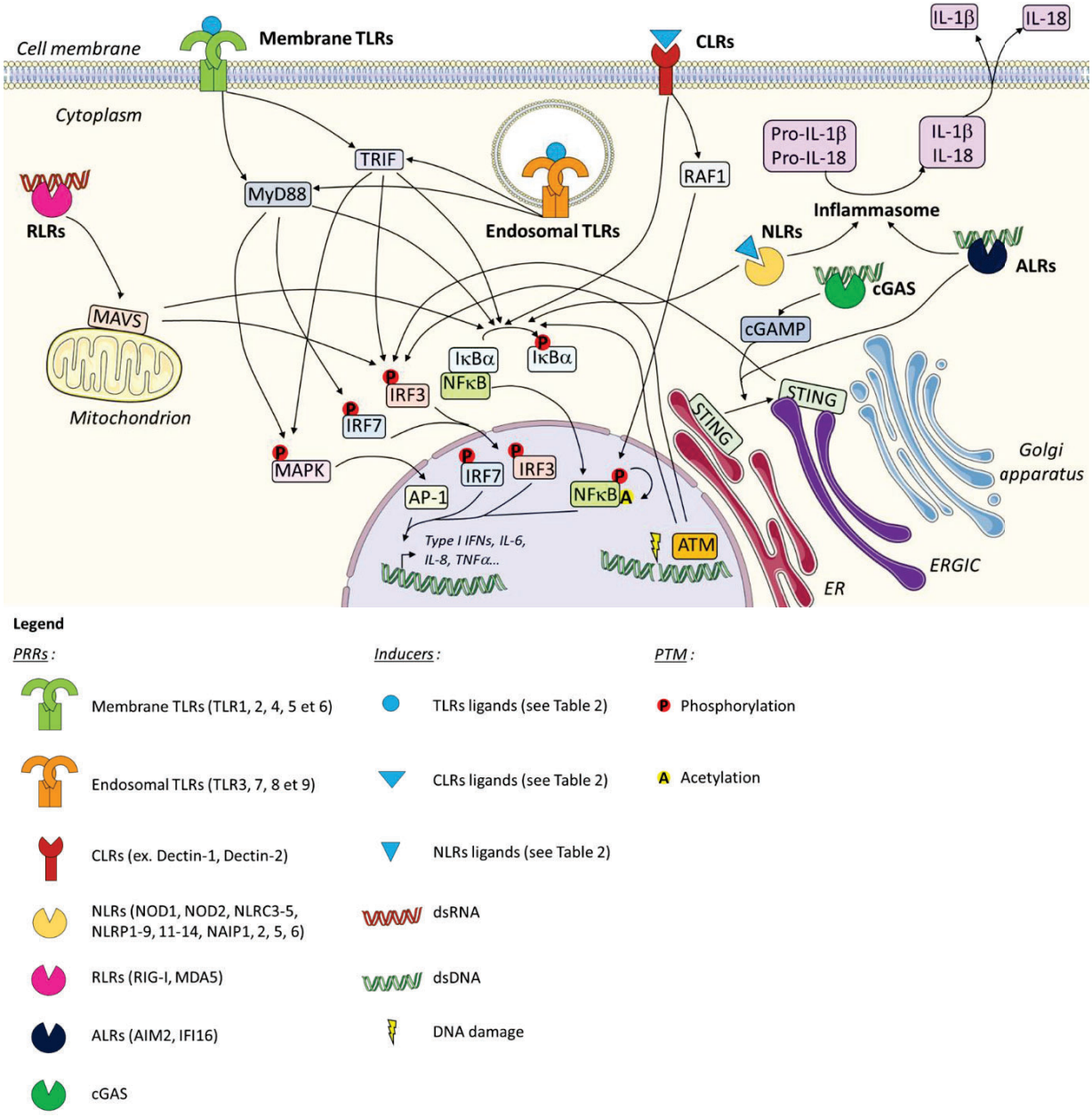


**Figure 21. Les différentes voies de signalisation en aval des PRRs.** Cette figure résume les différentes voies de signalisation stimulées par l'activation des PRRs. Par soucis de clarté, toutes les protéines impliquées dans les voies ne figurent pas sur le schéma. Brièvement, les récepteurs TLRs membranaires et endosomaux activent les voies MyD88 et TRIF, conduisant à l'activation de NF-κB, AP-1, IRF3 et IRF7. Les récepteurs CLRs membranaires activent la voie NF-κB et stimulent son activité *via* sa phosphorylation et son acétylation subséquente. Les récepteurs NLRs, en fonction de leur nature, peuvent activer la voie NF-κB ou participer à la formation d'un inflammasome et la maturation d'IL-1β et IL-18. Les RLRs RIG-I et MDA5 activent la voie MAVS et permettent l'activation de NF-κB et IRF3. Les ALR AIM2 et IFI16 peuvent permettre la formation d'un inflammasome et IFI16 stimule également la voie STING permettant la translocation nucléaire d'IRF3. De même, le récepteur d'ADN cytoplasmique cGAS participe également à l'activation de la voie STING en synthétisant cGAMP. ER: Endoplasmic reticulum; ERGIC: Endoplasmic reticulum-Golgi Intermediate Compartment.

La signalisation des TLRs *(Brubaker et al., 2015; Takeuchi and Akira, 2010)* :

Les récepteurs TLRs se situent à la membrane cytoplasmique (TLR1, 2, 4, 5 et 6) ou dans des endosomes (TLR3, 7, 8 et 9). Les voies de signalisation en aval des récepteurs TLRs sont les voies MyD88 (Myeloid Differenciation primary response protein 88) et TRIF (ou TICAM1 pour 'TIR domain-containing adaptator molecule 1'). La voie MyD88 répond à l'activation de tous les TLRs à l'exception de TLR3 tandis que la voie TRIF est activée par la stimulation des récepteurs TLR3 et TLR4 qui reconnaissent respectivement de l'ARN double-brin (ARNdb) et des lipopolysaccharides/des protéines d'enveloppe virale. La stimulation de ces voies permet d'activer les facteurs de régulation de l'IFN IRF (Interferon Regulatory Factor) 3 et 7, le facteur de transcription NF-κB et la voie MAPK (Mitogen-Activated Protein Kinase), entraînant l'expression de nombreux facteurs pro-inflammatoires.

La signalisation des CLRs *(Geijtenbeek and Gringhuis, 2009)* :

La famille des récepteurs CLRs étant très large, la liaison d'un ligand à ces derniers conduit à diverses conséquences. Les CLRs semblent néanmoins principalement activer directement NF-κB (par ex. Dectin-1, Dectin-2 ou Mincle) ou moduler positivement (par ex., DC-SIGN) ou négativement (par ex. BDAC2, DCIR ou MICL) les signalisations médiées par les TLRs.

La signalisation des NLRs *(Mariathasan and Monack, 2007; Philpott and Girardin, 2010; Takeuchi and Akira, 2010)* :

C'est la portion N-terminale des NLRs qui définit la signalisation que leur activation va induire. Ainsi les NLRs NOD (Nucleotide binding Oligomerization Domain-containing) 1 et 2 possèdent des domaines CARDs (Caspase Recruitment Domain) qui stimule la translocation de NF-κB dans le noyau. D'autres NLRs (NLRPs, NAIPs et NLRC4) possèdent des domaines pyrines ou BIR (Baculovirus IAP Repeat) et s'associent avec la caspase-1 et la protéine ASC (Apoptosis-associated Speck-like protein containg a CARD) permettant l'activation de la caspase-1, pour former complexes appelés inflammasomes. Le nom de chaque inflammasome est défini par le NLR le constituant ; ainsi, un inflammasome constitué du NLR NLRP3 sera nommé inflammasome NLRP3. La caspase-1 activée permet la maturation des protéines pro-IL-1β et pro-IL-18 pour former respectivement les cytokines IL-1β et IL-18.

La signalisation des RLRs *(Takeuchi and Akira, 2010; Wu and Chen, 2014)* :

Les récepteurs RLRs sont principalement impliqués dans la reconnaissance des ARN viraux double brins et les intermédiaires de réplication double brins des ARN viraux simple-brin. On compte actuellement 3 membres dans cette famille : RIG-I (Retinoic acid Inducible Gene I), MDA5 (Melanoma Differenciation-Associated gene 5) et LGP2 (Laboratory of Genetics and Physiology 2). RIG-I reconnaît des ARNdb relativement courts et la présence d'un triphosphate ou diphosphate à l'extrémité 5' augmente son activité. Cette spécificité n'est pas retrouvée sur les ARN messagers (ARNm) de l'hôte et permet de distinguer les ARNs exogènes des ARNs du soi, prévenant ainsi une activation inadaptée de la voie. RIGI peut également reconnaître de l'ARN 5'PPP résultant de la transcription d'ADN riche en AT par l'ARN Polymérase III. Le récepteur MDA5 reconnaît lui plutôt de longs ARNs double brins (> à 2kb) ou des structures ARN à haut poids moléculaire constitué d'ARN simple-brin et d'ARN double-brin (retrouvés dans les virus EMCV ou de la vaccine). La liaison d'un ligand avec RIG-I ou MDA5 entraînent un réarrangement structural des protéines et la révélation de leurs domaines CARDs. Ces derniers peuvent interagir avec le domaine CARD de la protéine MAVS (Mitochrondial Antiviral Signaling protein) à la membrane externe mitochondriale. Cette interaction permet la polymérisation et l'agrégation de plusieurs protéines MAVS, favorisant la translocation nucléaire de NF-$\kappa$B et IRF3. Le rôle de LGP2, le troisième RLR de la famille, ne semble pas induire de voie de signalisation par lui-même. En effet, il ne possède pas de domaines CARDs. En revanche, une étude montre que LGP2 régule positivement l'activité de RIG-I et MDA5 en facilitant la reconnaissance d'ARN viraux (Satoh et al., 2010).

La signalisation des ALRs *(Brubaker et al., 2015; Wu and Chen, 2014)* :

Les récepteurs ALRs reconnaissent de l'ADN double-brin. Le récepteur AIM2 (Absent In Melanoma 2) interagit avec l'adaptateur ASC permettant la formation d'un inflammasome après la reconnaissance d'ADN cytoplasmique et la génération d'IL-1$\beta$ et d'IL-18. Le deuxième membre de la famille, IFI16 (Interferon gamma Inducible protein 16) possède deux fonctions dans le cytoplasme. Comme AIM2, il peut également former un inflammasome ; il participe également à induire la relocalisation de la protéine STING (Stimulator of Interferon Genes protein) du réticulum endoplasmique (RE) au compartiment intermédiaire RE/Golgi (CIREG ou ERGIC). STING va alors s'associer avec TBK1 (TANK Binding Kinase 1) et permettre la phosphorylation et la translocation de IRF3 dans le noyau et l'activation des gènes d'IFN de type I. Contrairement à AIM2 qui se situe uniquement dans le cytoplasme, IFI16 peut également être retrouvé dans le noyau

cellulaire où il participe notamment à la répression épigénétique de plusieurs ADN viraux épisomaux (HSV-1, KSHV, HCMV et HPV-18) (Roy et al., 2019). Le mécanisme de distinction dans le noyau entre l'ADN étranger et l'ADN du soi n'est pas encore connu.

La signalisation des autres senseurs de l'ADN cytoplasmique *(Wu and Chen, 2014)* :

On retrouve d'autres senseurs de l'ADN cytoplasmique étranger ou du soi (mauvaise ségrégation chromosomique, sénescence cellulaire) et pouvant être impliqués dans l'induction de l'inflammation. DAI (DNA-dependent Activator of IFN-regulatory factors) fut le premier senseur décrit pouvant potentiellement induire la production d'IFN de type I. En effet, sa surexpression induit une augmentation de l'induction d'IFN à la suite d'une stimulation avec de l'ADN. De plus DAI s'associe avec TBK1 et IRF3. Cependant, l'absence de DAI n'impacte pas la capacité des cellules ou des souris à induire une réponse IFN. Des études d'inactivation des facteurs de réparation de l'ADN DNA-PK (DNA-dependent Protein Kinase) et MRE11 (Meiotic Recombination 11) ont montré qu'ils pourraient également être impliqués dans l'induction d'une réponse IFN en présence d'ADN cytoplasmique mais aucun mécanisme n'a pour le moment été décrit.

En 2013, deux études ont mis en évidence la présence d'un nouveau senseur de l'ADN dans le cytoplasme : la protéine cGAS, une synthase de GMP-AMP cyclique (cGAMP) (Sun et al., 2013; Wu et al., 2013) (pour revue, voir Hopfner and Hornung, 2020). cGAS est une protéine d'environ 520 acides aminés possédant un domaine catalytique organisé en deux lobes structuraux avec un site actif à leur interface. L'activité catalytique du domaine n'est induite que lors de la liaison de cGAS avec de l'ADN résultant en un changement conformationnel. De plus, pour adopter une conformation active stable, cGAS doit s'assembler en homodimère, reconnaissant deux hélices d'ADN prise en sandwich entre les deux protéines cGAS. Les protéines cGAS possèdent deux sites de liaison à l'ADN, les sites A et B couvrant environ 16 à 18 pb d'ADN (***Figure 22***). L'activation de cGAS est dépendante de la longueur de l'ADN reconnu et les ADN courts n'induisent qu'une faible réponse. Les dimères de cGAS peuvent s'oligomériser et former des condensats, renforçant l'activité de cGAS (Du and Chen, 2018). La catalyse de cGAMP par cGAS implique deux réactions chimiques distinctes. Premièrement, cGAS récupère de l'ATP et du GTP comme substrat et transfère l'ATP sur le 2'OH du GTP. La deuxième réaction consiste au transfert du GTP sur le 3'OH de l'ATP. Une fois synthétisé, cGAMP est reconnu par la protéine STING qui transite du RE au CIREG. Comme décrit plus haut, l'activation de STING induit le recrutement de TBK1. TBK1 phosphoryle STING et permet le recrutement de IRF3 qui est également phosphorylé. IRF3 transloque alors dans le noyau et promeut la transcription des gènes d'IFN de type I. De façon moins importante

que les autres voies des PRRs, la stimulation de STING peut également activer les voies MAPK et NF-κB (de Oliveira Mann et al., 2019). La protéine cGAS localise de manière constitutive principalement dans le noyau cellulaire dans lequel elle est séquestrée et inactivée par sa liaison aux nucléosomes (Boyer et al., 2020; Jiang et al., 2019; Kujirai et al., 2020; Michalski et al., 2020; Pathare et al., 2020; Volkman et al., 2019). En effet, sa liaison à un nucléosome masque le site de liaison à l'ADN B et empêche son activation catalytique (***Figure 22***). Son exportation du noyau vers le cytoplasme, et de ce fait son activation catalytique, nécessite l'action de la protéine CRM1 (Chromosome Region Maintenance 1) en réponse à la présence d'ADN cytoplasmique (Sun et al., 2021). De façon intéressante, la protéine cGAS nucléaire, du fait de sa liaison à la chromatine, prévient le processus de recombinaison homologue (Jiang et al., 2019; Liu et al., 2018).

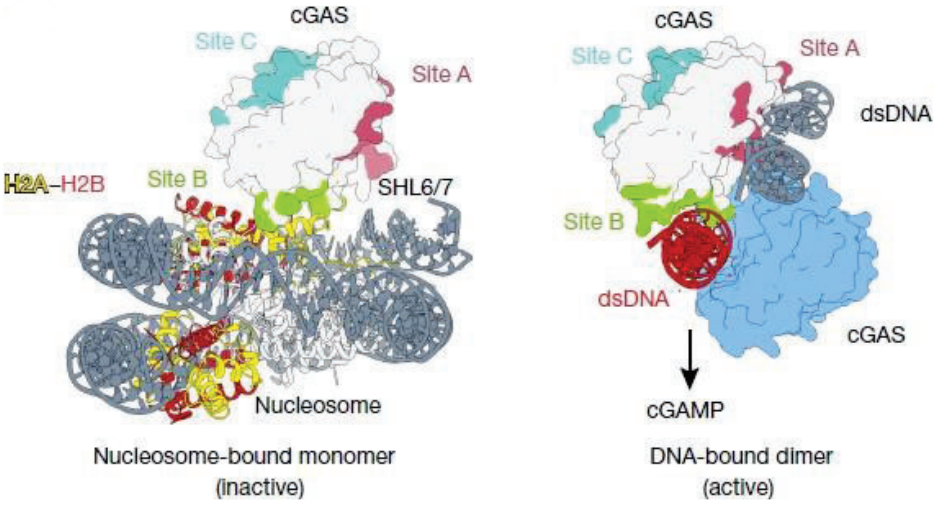


**Figure 22. L'inactivation de cGAS par sa liaison à un nucléosome.** (*Michalski et al., 2020*) Cette figure représente les deux formes de cGAS : la forme monomérique, inactive, lié au nucléosome dans le noyau (à gauche) et la forme dimérique, active, liée à l'ADN cytoplasmique (à droite). La liaison du domaine catalytique de cGAS aux histones H2A-H2B masque le site de liaison à l'ADN B (vert), empêche la reconnaissance d'ADN double brin et prévient l'activation catalytique de cGAS.

### *III.2.ii. Les cytokines et chémokines médiatrices de l'inflammation*

La reconnaissance de ligands par les différents PRRs mène à l'activation de l'inflammasome et des facteurs de transcription NF-κB et AP-1. Ces derniers permettent l'expression et la sécrétion de nombreuses protéines participant au processus inflammatoire en promouvant la différenciation des cellules de l'immunité, en favorisant l'extravasation ou encore en stimulant la cicatrisation des tissus. Parmi les protéines sécrétées on retrouve notamment les cytokines et chémokines IL-1, IL-6, IL-8, IL-12 et TNFα. Ces protéines sont sécrétées par les cellules infectées, les cellules de l'immunité innée mais aussi par des cellules endommagées ou les cellules sénescentes (sécrétion du SASP). Le ***Tableau 3*** donne un bref aperçu des effets de ces diverses cytokines dans

le processus inflammatoire. Plus de détails sont donnés ensuite pour les molécules IL-6, IL-8 et TNFα, toutes les trois utilisées dans mes travaux de thèse.

**Tableau 3. Les cytokines et chémokines de l'inflammation.** Ce tableau résume les différentes cytokines et chémokines impliquées dans le processus inflammatoire, leurs récepteurs ainsi que leurs effets. Plus de détails sont donnés dans le texte pour les protéines IL-6, IL-8 et TNFα.

| Cytokine/chémokine | Récepteur (cellules réceptrices) | Effets | Ref |
|---|---|---|---|
| IL-1α et IL-1β | IL-1R (plupart des types cellulaires) | • Induction d'une signalisation MyD88 → expression de cytokines pro-inflammatoires et d'IFN de type I<br>• Promotion de la fièvre, la douleur, la vasodilatation et l'hypotension *via* la production de prostaglandine-E2, du facteur d'activation plaquettaire et de monoxyde d'azote<br>• Promotion de l'infiltration des cellules de l'immunité *via* l'induction de l'expression des molécules d'adhésion)<br>• Promotion de l'angiogenèse | (Dinarello, 2009; Mantovani et al., 2019) |
| IL-33 | ST2 (cellules lymphoïdes de type II, lymphocytes Th2 et macrophages M2) | • Induction d'une signalisation MyD88 → expression de cytokines pro-inflammatoires et d'IFN de type I<br>• Stimulation d'une réponse immunitaire de type II | (Mantovani et al., 2019) |
| IL-18 | IL-18R (cellules lymphoïdes de type I et cellules NK) | • Induction d'une signalisation MyD88 → expression de cytokines pro-inflammatoires et d'IFN de type I<br>• Stimulation de la production d'IFNγ<br>• Stimulation d'une réponse immunitaire de type I | (Mantovani et al., 2019) |
| IL-36α, β et γ | IL-36R (particulièrement au niveau des cellules de la peau, des poumons et des intestins) | • Induction d'une signalisation MyD88 → expression de cytokines pro-inflammatoires et d'IFN de type I | (Queen et al., 2019) |
| IL-6 (cf. texte principal) | IL-6R membranaire (macrophages, neutrophiles, cellules T et hépatocytes) ou IL-6R soluble + gp130 (tous les types cellulaires) | • Effet anti-inflammatoire de l'activation d'IL-6R membranaire → promotion de la régénération<br>• Effet pro-inflammatoire de l'activation d'IL-6R soluble → expression de chémokines, de molécules d'adhésion des lymphocytes, différenciation des cellules de l'immunité | (Heinrich et al., 2003; Scheller et al., 2011) |
| IL-8 (aussi appelée CXCL8) (cf. texte principal) | CXCR1 ou CXCR2 (leucocytes et quelques cellules non leucocytaires) | • Pouvoir chimiotactique pour les cellules de l'immunité<br>• Activation de NF-kB et expression des gènes associés<br>• Promotion de la dégranulation et de l'explosion oxydative des neutrophiles | (Ha et al., 2017; Koch et al., 1992; Russo et al., 2014) |

| | | | |
|---|---|---|---|
| IL-12 | IL-12R (cellules NK et lymphocytes T) | • Pouvoir chimiotactique pour les cellules NK<br>• Différenciation des cellules NK et des lymphocytes T cytotoxiques<br>• Stimulation de la production d'IFNγ par les cellules NK et Th1 | (Gee et al., 2009) |
| TNFα (cf. texte principal) | TNFR1 (tous les types cellulaires) ou TNFR2 (cellules de l'immunité, neurones et cellules endothéliales) | • Activation de NF-κB et de la voie MAPK et expression des gènes associés<br>• Possible induction de mort par apoptose ou nécroptose par l'activation de TNFR1<br>• Stimulation de la production d'IFNβ<br>• Promotion de l'infiltration des cellules de l'immunité → promotion de la vasodilatation et de l'expression de molécules d'adhésion au niveau des cellules endothéliales<br>• Expansion et activation des lymphocytes T | (Bradley, 2008; Holbrook et al., 2019; Wajant et al., 2003; Yarilina and Ivashkiv, 2010) |

La cytokine IL-6 :

La signalisation IL-6 est médiée par un complexe récepteur transmembranaire constitué d'une protéine de reconnaissance IL-6R et de deux protéines de transduction gp130 (signalisation décrite dans Heinrich et al., 2003). Lorsque la cytokine IL-6 est sécrétée, elle est d'abord reconnue par IL-6R. Le complexe IL-6/IL-6R s'associe ensuite avec les deux protéines gp130. Cela permet ensuite le recrutement par gp130 des kinases JAK (Janus Kinase) et la phosphorylation du facteur de transcription STAT3 et dans une moindre mesure du facteur STAT1. Les facteurs STATs se dimérisent et transloquent dans le noyau pour induire l'expression de leurs gènes cibles. JAK permet également la phosphorylation de la tyrosine 759 de gp130, le recrutement de la phosphatase SHP2 et l'activation de la cascade de signalisation MAPK. La protéine gp130 est ubiquitaire ; en revanche, IL-6R n'est exprimée que sur un nombre limité de cellules, à savoir les macrophages, les neutrophiles, quelques types de cellules T et les hépatocytes (Scheller et al., 2011). Le récepteur IL-6R peut également être trouvé sous forme soluble grâce à l'action des protéases ADAM (A Disintegrin And Metalloproteinase) 10 et 17. ADAM10 est responsable de la lente digestion constitutive d'IL-6R tandis que ADAM17 est activée notamment par le contexte inflammatoire et permet la production massive d'IL-6R soluble dans ce contexte (Scheller et al., 2011). La forme soluble d'IL-6R reconnaît de la même manière IL-6 et peut former un complexe avec les protéines gp130 ; elle permet ainsi d'élargir le panel de cellules répondant à IL-6. Ainsi, on distingue deux types de signalisation médiée par IL-6 : la signalisation classique *via* le récepteur IL-6R membranaire et la signalisation trans *via* le récepteur IL-6R soluble (Scheller et al., 2011).

La signalisation classique est considérée comme anti-inflammatoire car promouvant la régénération. La signalisation trans, elle, joue un rôle pro-inflammatoire. En effet, elle permet de promouvoir le recrutement des monocytes au site de lésion en augmentant l'expression des chémokines les attirant. Elle augmente également l'expression des molécules d'adhésion des lymphocytes et des chémokines qu'ils reconnaissent, favorisant la transmigration de ces derniers. Le récepteur IL-6R soluble joue également un rôle important dans la différenciation des cellules de l'immunité (monocyte vers macrophage, lymphocytes B naïf vers plasmocytes, lymphocytes Thelper naïfs vers Th2 et Th17) (Scheller et al., 2011).

La chémokine IL-8 :

La chémokine IL-8, aussi appelée CXCL8 fut l'une des premières chémokines identifiées. Elle se lie à deux récepteurs couplés à la protéine G, les récepteurs CXCR1 et CXCR2 (Ha et al., 2017). L'activation des récepteurs par IL-8 induit le détachement de la protéine G du récepteur et la dissociation des sous-unités $G\beta\gamma$ de la sous-unité $G\alpha$ de la protéine G. La présence de $G\beta\gamma$ dans le cytosol, induit l'activation de nombreuses voies de signalisation et l'activation de nombreuses kinases de stress et de croissance, dont MAPK, ERK1/2 (Extracellular signal-regulated kinase 1/2) ou JNK1 (c-Jun N-terminal Kinase 1), ainsi que le relargage de calcium, essentiel pour le chimiotaxie. Elle induit également l'activation de NF-$\kappa$B. Enfin, à la suite de l'activation de CXCR1 et non CXCR2, $G\beta\gamma$ stimule la production de ROS en activant la phospholipase D (Ha et al., 2017). Les récepteurs CXCR1 et CXCR2 sont particulièrement exprimés à la surface des leucocytes tels que les neutrophiles, les monocytes, les lymphocytes T cytotoxiques, les mastocytes, les basophiles, les cellules NK (Natural Killer) et les cellules myéloïdes suppressives (Russo et al., 2014). La détection d'IL-8 par ces cellules permet leur recrutement au site d'infection en suivant le gradient de chémokine. La cytokine IL-8 promeut également la dégranulation des neutrophiles. Enfin, l'activation de CXCR1 et l'augmentation de ROS dans les neutrophiles induit leur explosion oxydative (càd. la libération extracellulaire des ROS). Les récepteurs CXCR1 et CXCR2 sont également exprimés par des cellules non leucocytaires (Russo et al., 2014). L'activation des récepteurs sur ces cellules pourraient participer à plusieurs actions. Notamment, il a été montré que la cytokine IL-8 pouvait attirer les cellules endothéliales et ainsi promouvoir le phénomène d'angiogenèse (Koch et al., 1992).

Le facteur de nécrose tumorale TNF$\alpha$ :

Le facteur TNF$\alpha$ présente une forme transmembranaire exprimée à la surface des cellules et une forme soluble active, médiée par le clivage de la forme membranaire par la

métalloprotéase TACE (Tumor necrosis factor Alpha Converting Enzyme) (Holbrook et al., 2019; Wajant et al., 2003). Le facteur TNFα est reconnu par deux récepteurs transmembranaires : le récepteur TNFR1, exprimé de façon ubiquitaire, et le récepteur TNFR2, exprimé principalement à la surface des cellules de l'immunité, des neurones et des cellules endothéliales (Holbrook et al., 2019). Les deux récepteurs possèdent un site de reconnaissance du ligand similaire mais diffèrent par leur structure intracellulaire et leur liaison avec des protéines adaptatrices. Ainsi, le récepteur TNFR1 possède un 'death domain' DD permettant le recrutement de la protéine TRADD (TNFRSF1A Associated via Death Domain). Le récepteur TNFR2 ne possède lui pas de domaine DD et recrute à la place les protéines TRAF1 et TRAF2 (Holbrook et al., 2019; Wajant et al., 2003). Les deux récepteurs induisent l'activation des voies NF-κB et MAPK, promouvant plutôt l'expression de leurs gènes cibles. Par ces voies, TNFα favorise également la prolifération et la survie cellulaire (Holbrook et al., 2019). Le récepteur TNFR1, grâce à sa liaison à TRADD, peut induire la mort cellulaire par apoptose ou nécroptose en fonction des circonstances physiologiques (Holbrook et al., 2019; Wajant et al., 2003). Il a également été montré que le traitement de macrophages avec du TNFα induisait la production d'IFNβ via le facteur de transcription IRF1 (Yarilina and Ivashkiv, 2010). Le rôle pro-inflammatoire de TNFα s'explique essentiellement par son impact sur les cellules endothéliales et la promotion du recrutement des cellules de l'immunité (Bradley, 2008). En effet, il favorise la vasodilatation et permet d'induire l'expression de différentes molécules d'adhésion à la surface des cellules endothéliales. Enfin, le TNFα participe à l'expansion et l'activation des lymphocytes T (Holbrook et al., 2019).

L'activation des PRRs par un ligand induit également la phosphorylation et la translocation des facteurs de régulation des gènes d'IFN de type I, IRF3 et IRF7. Leur translocation dans le noyau permet l'expression des IFNs de type I, particulièrement impliqués dans l'immunité antivirale en interférant avec la réplication virale. Ces derniers sont également impliqués dans la réponse inflammatoire en promouvant par exemple la production de cytokines, les activités cytotoxiques des cellules NK et des lymphocytes T cytotoxiques ou en encore augmentant la présentation d'antigène pour stimuler l'immunité. Dans la prochaine partie, je détaillerai la voie de signalisation induite par les IFNs de type I et les gènes régulés par l'activation de cette dernière. Enfin, je reviendrai plus en détail sur le lien entre la réponse IFN et les régulations épigénétiques, et en particulier, l'implication éventuelle du complexe chaperon d'histone HIRA.

## III.3. La signalisation IFN de type I

Les interférons forment une famille de molécules qui se subdivisent en 3 classes (Type I, II, III) en fonction de leur homologie de séquence et du récepteur auquel ils se lient. La plus grande classe, les IFNs de type I, inclut plusieurs variants de l'IFNα (13 variants chez l'humain, 14 chez la souris), l'IFNβ, l'IFNω, l'IFNε et l'IFNκ. Il n'y a qu'un seul IFN de type II, l'IFNγ. Enfin, les IFNs de type III regroupent 4 variants de l'IFNλ. Les IFNα et l'IFNβ sont les IFNs de type I les plus étudiés car ils possèdent une action ubiquitaire, tandis que les IFN-ω, -ε et -κ ont une action limitée à certains organes. Dans cette partie, le terme 'IFNs de type I' désignera les IFNs α et β.

### *III.3.i. Les voies de signalisation activées par les IFNs de type I*

Les IFNs de type I se lient au récepteur IFNAR, un récepteur transmembranaire composé de 2 sous-unités, IFNAR1 et IFNAR2. La partie cytoplasmique de IFNAR1 est associée avec la kinase TYK2 (Tyrosne-protein Kinase 2) et celle de IFNAR2 est associée avec la kinase JAK1 (Janus Kinase 1). La dimérisation de IFNAR1 et IFNAR2 après la reconnaissance de l'IFN de type I permet l'interaction de TYK2 et JAK1 et leur activation par cross-phosphorylation. La liaison du ligand au récepteur IFNAR induit son internalisation par endocytose, importante pour induire une signalisation en aval. Les mécanismes impliqués dans l'endocytose du récepteur sont détaillés dans la revue Zanin et al., 2021.

L'activation des kinases TYK2 et JAK1 favorisent l'induction de plusieurs voies de signalisation (***Figure 23***) (González-Navajas et al., 2012; Mazewski et al., 2020; Platanias, 2005). La voie classique consiste en l'activation des protéines de la famille des STATs. En particulier, les kinases phosphorylent STAT1 et STAT2 qui hétérodimérisent et s'associent avec la protéine IRF9 pour former le complexe ISGF3 (IFN-stimulated gene factor 3). Ce dernier transloque dans le noyau où il se lie aux séquences ISRE (IFN-stimulated response éléments) au niveau des promoteurs de certains gènes régulés par l'IFN (dont les ISGs pour IFN-stimulated genes). Les protéines STAT1 phosphorylées peuvent également s'homodimériser et se lier à des séquences GAS (IFNγ-activated sites), régulant la transcription de certains ISGs. TYK2 et JAK1 peuvent également phosphoryler les autres protéines STATs (STAT3, STAT4, STAT5 et STAT6) ; la phosphorylation et l'homodimérisation de STAT3 permettent par exemple sa liaison aux séquences SBE (STAT3-binding éléments), pour l'induction d'autres types d'ISGs. TYK2 et JAK1 favorisent également l'activation de voies non-canoniques, telles que les voies MAPK, mTOR et CRKL (CRK-like protein). L'activation des voies MAPK et mTOR régule positivement la transcription et la traduction des ISGs tandis que CRKL promeut l'activation de RAP1 et inhibe le cycle cellulaire.

La signalisation IFN de type I est maintenue pendant une vingtaine de minutes après l'endocytose du récepteur IFNAR. La sous-unité IFNAR1 est ensuite dégradée dans les lysosome tandis que IFNAR2 est recyclée à la membrane ; la signalisation est alors rompue (Zanin et al., 2021).

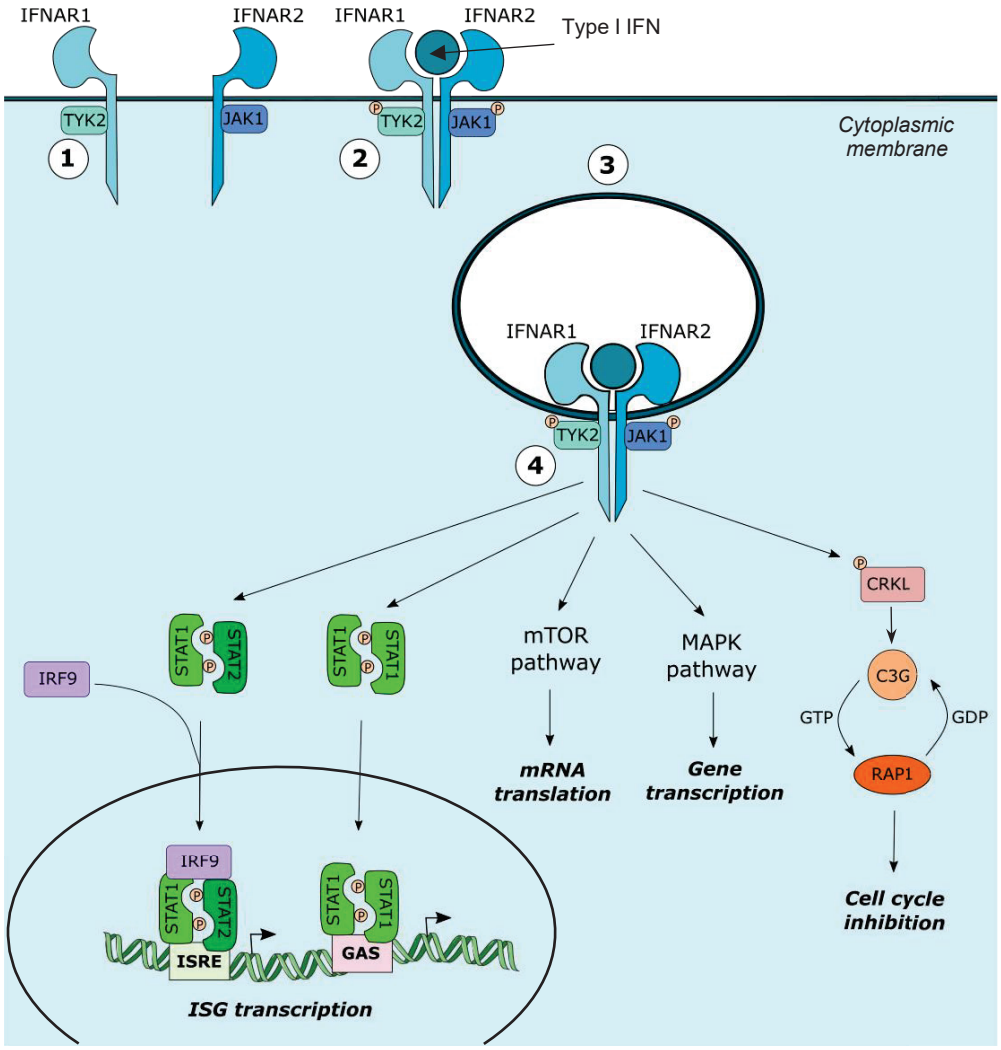


**Figure 23. Les voies de signalisation induites par le récepteur IFNAR.** Ce schéma résume les différentes voies de signalisation induite à la suite de la reconnaissance d'un IFN de type I par le récepteur IFNAR. (1) Les sous-unités IFNAR1 et IFNAR2 se situent à la membrane cytoplasmique. Elles sont respectivement associées avec les kinases TYK2 et JAK1. (2) La dimérisation des récepteurs à la suite de leur liaison avec l'IFN de type I induit la cross-phosphorylation et l'activation des kinases. (3) Le récepteur est internalisé par endocytose. (4). Les kinases TYK2 et JAK1 activent plusieurs protéines cibles et plusieurs voies de signalisation. La phosphorylation de STAT1 et STAT2 induit leur hétérodimérisation, leur association avec IRF9, la translocation du complexe dans le noyau et sa liaison aux séquences ISRE, induisant la transcription de certains ISGs. Les protéines STAT1 dimérisées peuvent également se lier aux séquences GAS, permettant également la transcription de certains ISGs. JAK1 et TYK2 peuvent également activer les voies mTOR, MAPK et CRKL promouvant respectivement la traduction d'ARNm, la transcription et l'arrêt du cycle cellulaire.

Plusieurs mécanismes de régulation sont mis en place par la cellule afin de prévenir une réponse trop élevée à l'IFN de type I (Schneider et al., 2014; Schreiber, 2017). Comme mentionné plus haut, l'endocytose et la dégradation lysosomale de IFNAR1 constitue une première couche de régulation. De plus, la protéine USP18, dont la transcription est

stimulée par les IFNs de type I, se lie à IFNAR2 et prévient sa dimérisation avec IFNAR1, réduisant l'induction de la signalisation. L'inhibiteur de kinase SOCS1 (Suppressor Of Cytokine Signaling 1), un ISG, se lie à TYK2 et prévient son action. Enfin, les protéines PIAS se lient aux STATs phosphorylées et préviennent leur dimérisation.

La signalisation IFNAR induit l'expression de nombreux gènes ISGs à la suite de liaison des protéines STATs sur les séquences ISRE et GAS au niveau du promoteur (Shaw et al., 2017; Veer et al., 2001). Les rôles de ces différents ISGs seront détaillés dans la prochaine partie. Beaucoup d'études se focalisent sur l'induction des ISGs mais il est important de noter qu'un certain nombre de gènes sont aussi régulés négativement par la signalisation IFNAR, les IRGs (IFN-Repressed Genes) (Der et al., 1998) et leur répression pourrait également jouer un rôle dans la réponse cellulaire à l'IFN de type I.

#### *III.3.ii. Les gènes induits par l'IFN (ISGs)*

Le nombre d'ISGs varie en fonction du type cellulaire et de l'espèce étudiés. L'ensemble des ISGs décrits dans la littérature (en fonction du type cellulaire, de l'espèce, du type d'IFN, de la dose, du temps de traitement) sont d'ailleurs répertoriés sur la base de données Interferome (www.interferome.org, Hertzog et al., 2011; Rusinova et al., 2013).

Les premières études sur puces avec des cellules humaines et murines estimaient à plus de 300 gènes dont le niveau augmente d'au moins 2 fois à la suite d'une stimulation à l'IFN de type I ou II (Veer et al., 2001). Plus récemment, une étude des ISGs conduite sur les fibroblastes de différents vertébrés répertorie chez l'humain un peu plus de 2000 gènes régulés positivement par l'IFN de type I, soit environ 10% des gènes humains (Shaw et al., 2017). Contrairement à la plupart des études, cette dernière ne fixe pas de seuil pour le taux d'augmentation mais un seuil statistique avec un taux d'erreur inférieur à 5%. Dans cette même étude, les auteurs ont comparé les ISGs chez 10 espèces différentes de vertébrés et n'ont retrouvé que 62 ISGs communs, appelés ISGs cœurs, qui représentent les fonctions ancestrales du système IFN.

L'analyse de la fonction des ISGs ont permis de les regrouper dans différentes catégories fonctionnelles (***Figure 24***) (Shaw et al., 2017; Veer et al., 2001). L'étude des 62 ISGs cœurs indique que les protéines qu'ils encodent sont principalement impliquées (1) dans la stimulation de la réponse immunitaire acquise en stimulant la présentation d'antigène (par ex. protéines HLA), la migration des leukocytes (par ex. CD47), l'activation des cellules cytotoxiques (par ex. IL15RA), (2) dans la modulation positive ou négative de la réponse IFN (par ex. certains PRRs, MyD88 ou STAT1/STAT2 pour la régulation positive et SOCS1 ou UPS18 pour la régulation négative), (3) dans l'ubiquitination et la dégradation des protéines (par ex. RNF213, RNF19B…) et (4) dans la réponse antivirale

en stimulant l'expression de gènes inhibant différentes étapes du cycle de réplication viral (par ex. PML, MX1, OAS1, ISG54/IFIT2…). On retrouve également certains gènes codant des protéines reliées au fonctionnement cellulaire, comme DNAJC13 impliquée dans le trafic des endosomes, FMR1 impliquée dans le transport intracellulaire des ARN et dans la régulation de la traduction des ARNm ou des facteurs de modification de la chromatine comme l'histone méthyltransférase SETDB2 d'H3K9 ou le complexe ligase E3 d'ubiquitine PARP9-DTX3L permettant l'ubiquitination de H2B, une marque épigénétique activatrice (Kroetz et al., 2015; Zhang et al., 2015b) (cf. partie *III.3.iii*). Enfin, la signalisation IFN induite par les dommages à l'ADN peut favoriser l'expression des cytokines du SASP et semble participer à l'induction de la sénescence cellulaire (Glück et al., 2017; Moiseeva et al., 2006; Yang et al., 2017; Yu et al., 2015).

La stimulation à l'IFN peut également induire la transcription d'ARNs non codants et notamment des microARNs et des longs ARNs non-codants (lncRNAs), comme *NeST*, qui promeut la marque H3K4me3 au niveau du promoteur du gène codant pour IFNγ et favorise sa transcription (Gomez et al., 2013; Schneider et al., 2014).

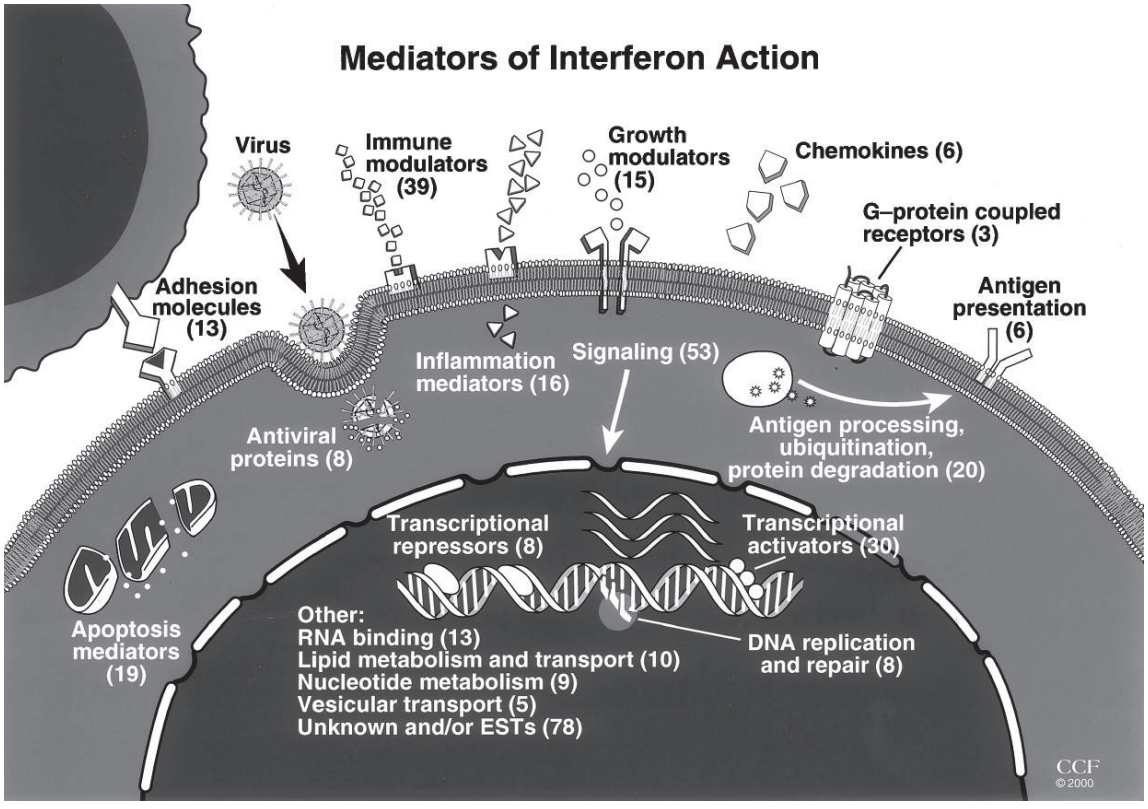


**Figure 24. Les différentes classes d'ISGs.** *(Veer et al., 2001)* Cette figure récapitule les fonctions des différents gènes induits par les IFNs de type I et II chez l'homme et la souris. Dans cette étude, Veer *et al.* ont regroupé 335 gènes dont l'expression augmente d'au moins 2 fois à la suite d'un traitement IFN. Ils ont ensuite classé ces gènes en différentes catégories selon leur fonction. Les nombres entre parenthèses correspondent au nombre de gènes regroupés dans cette catégorie.

### *III.3.iii. Régulations épigénétiques induites par la signalisation IFN*

La signalisation IFN induit de nombreux changements chromatiniens au niveau des éléments régulateurs des ISGs mais aussi d'autres gènes dont l'expression n'est pas stimulée directement par la signalisation IFN. Ces différentes régulations permettent d'induire une réponse appropriée à la stimulation IFN et, dans certains contextes, favorisent une réponse plus rapide et plus forte lors d'une restimulation (pour revue, voir Barrat et al., 2019; Chen et al., 2017; Ivashkiv, 2018).

A l'état quiescent, la plupart des promoteurs des ISGs sont hyperméthylés au niveau des CpG et présentent la marque d'histone répressive H3K9me2 médiée par la présence de la méthyltransférase G9a (***Figure 25***) (Chen et al., 2017; Coit et al., 2013, 2015; Fang et al., 2012). Ces marques permettent de maintenir ces gènes silencieux lorsqu'ils n'ont pas besoin d'être activés. De manière intéressante, chez les patients atteint de lupus érythémateux disséminé (SLE), les promoteurs des ISGs dans les neutrophiles et les lymphocytes T $CD4^+$ sont significativement hypométhylés, résultant en une réponse plus importante à la signalisation IFN chez ses personnes (Coit et al., 2013, 2015). La méthyltransférase G9a est, elle, plus exprimée dans les fibroblastes que dans les cellules

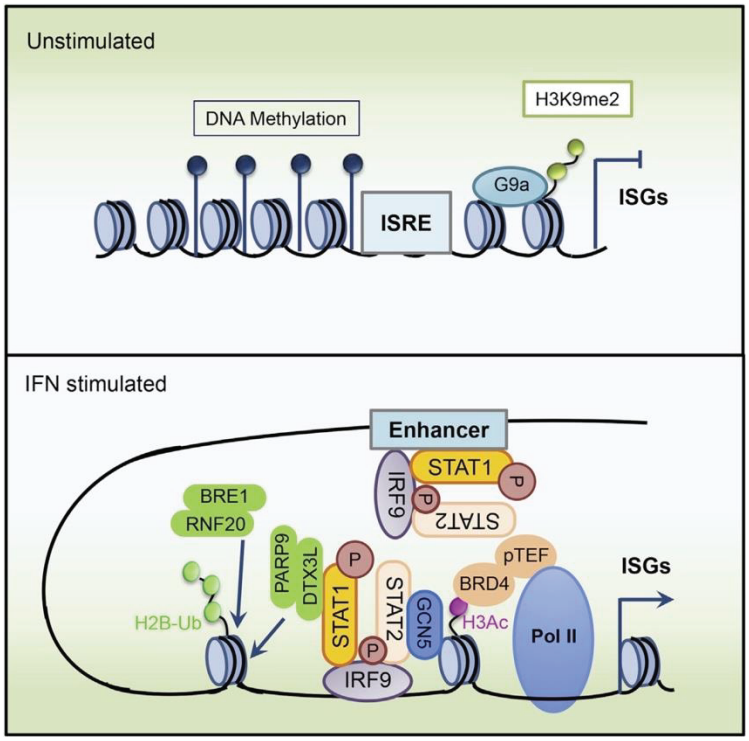


**Figure 25. Les changements chromatiniens au niveau des promoteurs des ISGs à la suite d'une stimulation IFN de type I.** (*Chen et al., 2017*) Les promoteurs des ISGs à l'état quiescent sont méthylés au niveau des CpG et sont enrichis en H3K9me2 mis en place par G9a. Suite à la stimulation, les marques répressives laissent place à des marques permissives de la transcription. Ainsi, STAT2 recrute l'acétyltransférase GCN5 et permet l'acétylation d'H3. Le complexe DTX3L/PPAR9 en collaboration avec BRE1/RNF20 induisent l'ubiquitination de H2B, une marque favorisant la transcription.

dendritiques, permettant une meilleure réponse de ces dernières à une stimulation IFN. La suppression de G9a dans les fibroblastes induit une augmentation de l'expression des ISGs à la suite d'une stimulation IFN et résulte en une réponse antivirale plus forte (Fang et al., 2012). Les ISGs sont également réprimés dans les macrophages par le long ARN non codant LincRNA-EPS et son interaction avec la protéine hnRNPL (Atianand et al., 2016). Lors de l'activation du PRRs TLR2, l'expression de LincRNA-EPS est diminuée et l'inhibition est levée.

Lors de l'activation du récepteur IFNAR, les marques répressives sont perdues (mécanisme non décrit) et des marques permissives sont mises en place (***Figure 25***). La protéine STAT2 recrute l'acétyltransférase GCN5 (General Control of amino acid protein 5) au niveau des promoteurs, qui y établit des marques H3ac. Le 'reader' BRD4 (Bromodomain protein 4) est ensuite recruté, facilitant l'élongation transcriptionnelle en se liant au facteur P-TEFb (Positive Transcription Elongation Factor) (Patel et al., 2013; Paulson et al., 2002). De plus, sous stimulation IFN de type I, la marque activatrice H2Bub est augmentée au niveau des promoteurs, rendant la chromatine plus accessible pour le processus de transcription (Zhang et al., 2015b). Enfin, les complexes remodeleurs de la chromatine BRG1 (BRM/SWI2-Related Gene 1) et BAF (BRG1-Associated Factor) sont également recrutés au niveau de certains ISGs, permettant l'ouverture de la chromatine et facilitant la transcription (Huang et al., 2002; Liu et al., 2002).

Comme mentionné plus haut, l'IFN de type I induit la transcription du long ARN non codant *NeST*. Dans les lymphocytes T $CD8^+$, ce dernier interagit avec la méthyltransférase WDR5 qui catalyse la marque H3K4me3 au niveau du promoteur du gène codant pour IFN$\gamma$, favorisant sa transcription et une meilleure résistance de l'hôte aux infections à *Salmonella enterica*. En revanche, *NeST* favorise dans le même temps la persistance du virus de l'encéphalomyélite murine de Theiler (TMEV), dû à une altération de la magnitude ou du timing de la réponse inflammatoire (Gomez et al., 2013).

Certains mécanismes épigénétiques de régulation négative de la réponse IFN existent également. Ainsi, la méthyltransférase SETDB2 est exprimée en réponse à l'IFN de type I dans des macrophages humains et murins, conduisant à l'augmentation de la marque H3K9me3 au niveau des promoteurs de ISGs et l'inhibition de la transcription de ces gènes (Kroetz et al., 2015). De même, l'expression du long ARN non-codant lincRNA-Cox2 est augmentée dans les macrophages dérivés de la moëlle épinière dans lesquels il joue un rôle inhibiteur sur l'expression de nombreux gènes, y compris certains ISGs (Carpenter et al., 2013). Cette inhibition est médiée par son interaction avec les protéines hnRNP-A/B et hnRNP-A2/B1.

La signalisation IFN induit également des changements chromatiniens au niveau des gènes non-ISGs. Par exemple, les gènes stimulés par le TNFα (*IL6*, *TNF*) sont généralement exprimés de manière transitoire puis sont fortement réprimés, un état appelé la tolérance. L'état de tolérance peut être prévenu dans des macrophages humains par une co-stimulation avec l'IFNα ; ce dernier permet la liaison coordonnée d'IRFs et de NF-κB au niveau des enhancers et des promoteurs, permettant d'augmenter l'accessibilité de la chromatine et les marques d'histones positives comme H3K4me3. La chromatine est ainsi prête à la transcription, on parle de 'primed chromatin'. Par la suite, la stimulation d'un TLR, même très faible, permettra une forte induction de l'expression des gènes stimulés par le TNFα (Park et al., 2017). Ce mécanisme de priming est aussi observable dans des monocytes humains stimulées à l'IFNγ *via* l'action de STAT1 et IRF1 (Qiao et al., 2013). Leur liaison aux enhancers des gènes cibles de NF-κB permettra ensuite une stimulation rapide ou importante de gènes inflammatoires lors de la stimulation d'un TLR. De manière intéressante, dans des macrophages murins, l'IFNγ peut également induire l'apparition de nouveaux enhancers (appelés enhancers latents) en favorisant la liaison coopérative des facteurs STATs ou IRFs avec le facteur PU.1 (Ostuni et al., 2013). Ces derniers favorisent l'ouverture de la chromatine et l'établissement de la marque H3K4me1. Les enhancers latents persistent au moins 48h après le traitement IFNγ et permettent l'induction des gènes associés après une stimulation cytokinique, conférant une mémoire transcriptionnelle à court terme.

Le concept de mémoire transcriptionnelle lié à une stimulation IFN a également été mis en évidence récemment sur certains ISGs (Kamada et al., 2018). En effet, dans leur étude de 2018, Kamada *et al.* ont montré qu'environ la moitié des ISGs stimulés par l'IFNβ possèdent une mémoire transcriptionnelle dans des fibroblastes murins, permettant une transcription plus rapide et plus importante de ses gènes à la suite d'une re-stimulation. Ils définissent ces ISGs comme des ISGs mémoires. Contrairement au mécanisme décrit avant, cette mémoire transcriptionnelle n'est pas médiée par la rétention de facteurs de transcription au niveau des enhancers des ISGs ; dans ce contexte, elle coïncide avec l'acquisition du variant d'histone H3.3 et de la marque H3K36me3, plus particulièrement dans les parties TES des ISGs mémoires. La perte de ces marques réduit significativement la réponse mémoire de ces ISGs. Ils ont également montré que l'effet mémoire s'explique par un recrutement de l'ARN polymérase II plus rapide et à des niveaux plus importants sur les ISGs mémoires au moment de la restimulation. Enfin, les auteurs ont montré que le mécanisme de mémoire transcriptionnelle de certains ISGs est conservé dans les macrophages murins stimulés par l'IFNγ. Une étude similaire sur des cellules HeLa a en revanche démontré que H3.3 n'était conservée que temporairement

au niveau des ISGs mémoires (jusqu'à 2 jours après un traitement à l'IFNγ quand la mémoire transcriptionnelle est maintenue jusqu'à 14 jours) (Siwek et al., 2020). Le mécanisme moléculaire derrière l'établissement des marques H3.3 et H3K36me3 est encore à définir mais le complexe chaperon d'histones HIRA, impliqué dans l'incorporation d'H3.3 dans des régions d'euchromatine, pourrait potentiellement jouer un rôle dans ce contexte. Étant donné sa relocalisation dans les PML NBs sous IFN, il est également envisageable que ces derniers servent de plateforme pour le dépôt d'H3.3 au niveau des ISGs mémoires. Cette hypothèse est supportée par l'observation d'un rapprochement spatial entre le cluster de gènes du complexe majeur d'histocompatibilité MHC-II (Major Histocompatibility Complex II) et les PML NBs lors du traitement à l'IFNγ de cellules HeLa (Gialitakis et al., 2010). Dans cette même étude, les auteurs ont également montré l'importance de la protéine PML pour la transcription des gènes du complexe MHC-II et pour l'établissement d'une mémoire transcriptionnelle.

Comme évoqué précédemment, les membres du complexe HIRA relocalisent dans les PML NBs également dans le contexte de la sénescence cellulaire. La signalisation derrière cette relocalisation est encore mal comprise. Les cellules sénescentes présentent des fragments d'ADN cytosoliques conduisant à la sécrétion d'IFN de type I (Dou et al., 2017; Glück et al., 2017). On pourrait donc imaginer que, comme dans le cas des infections virales par HSV-1, la relocalisation du complexe dans les cellules sénescentes soit induite par la voie de signalisation de l'IFN. Cependant, la production d'IFN de type I intervient tardivement dans le processus de sénescence (Cecco et al., 2019) tandis que la relocalisation du complexe HIRA a lieu dans les étapes précoces (Zhang et al., 2005). Ainsi, dans ces cellules, on peut supposer qu'une autre voie de signalisation est responsable la relocalisation. Les voies de réparation des cassures double-brin pourraient notamment être impliquées. En effet, les cellules sénescentes présentent une activation importantes de ces voies de réparation (Bartkova et al., 2006; Micco et al., 2006). Dans le cadre de ma thèse, j'ai donc cherché à savoir si l'induction de cassures double-brin pouvait induire la relocalisation du complexe HIRA dans les PML NBs. Le prochain chapitre vise à introduire les différents types de dommages à l'ADN auxquels une cellule peut être soumise. Je m'intéresserai ensuite plus particulièrement aux cassures double-brin et aux mécanismes cellulaires impliqués dans leur reconnaissance et leur résolution. Enfin je m'intéresserai aux mécanismes impliqués dans la reformation de la chromatine après la réparation de l'ADN.

# IV. Les dommages à l'ADN

## IV.1. Les dommages à l'ADN et la réparation

Les molécules d'ADN, bien que potentiellement protégées par leur organisation en chromatine, sont soumises à des dizaines de milliers de lésions par jour (Ciccia and Elledge, 2010). Ces dommages peuvent interférer avec les processus de transcription et de réplication, induire la mort cellulaire ou introduire des mutations pouvant être délétères pour l'organisme. Pour assurer la stabilité du génome face à ces attaques, les cellules possèdent différents mécanismes de reconnaissance et de réparation, les mécanismes de DDR (DNA Damage Response), dont la nature dépend du type de dommages auquel l'ADN est soumis.

### *IV.1.i. Les différents types de dommages à l'ADN*

Les agents inducteurs de dommages peuvent être endogènes (en majorité) mais peuvent également exogènes, issus de l'environnement, de l'alimentation ou de traitements avec certains médicaments (***Figure 26***) (pour revue, voir Chatterjee and Walker, 2017; Dexheimer, 2013). La première source de dommages endogènes est l'hydrolyse spontanée des bases de l'ADN (Lindahl, 1993). L'hydrolyse de la liaison N-glycosidique entre la base et le désoxyribose produit un site abasique. On estime cette réaction à environ 10 000/cellule/jour. Les bases possédant un groupe amine exocyclique, comme la cytosine (C), l'adénine (A), la guanine (G) ou la 5-methyl cytosine (5mC) peuvent

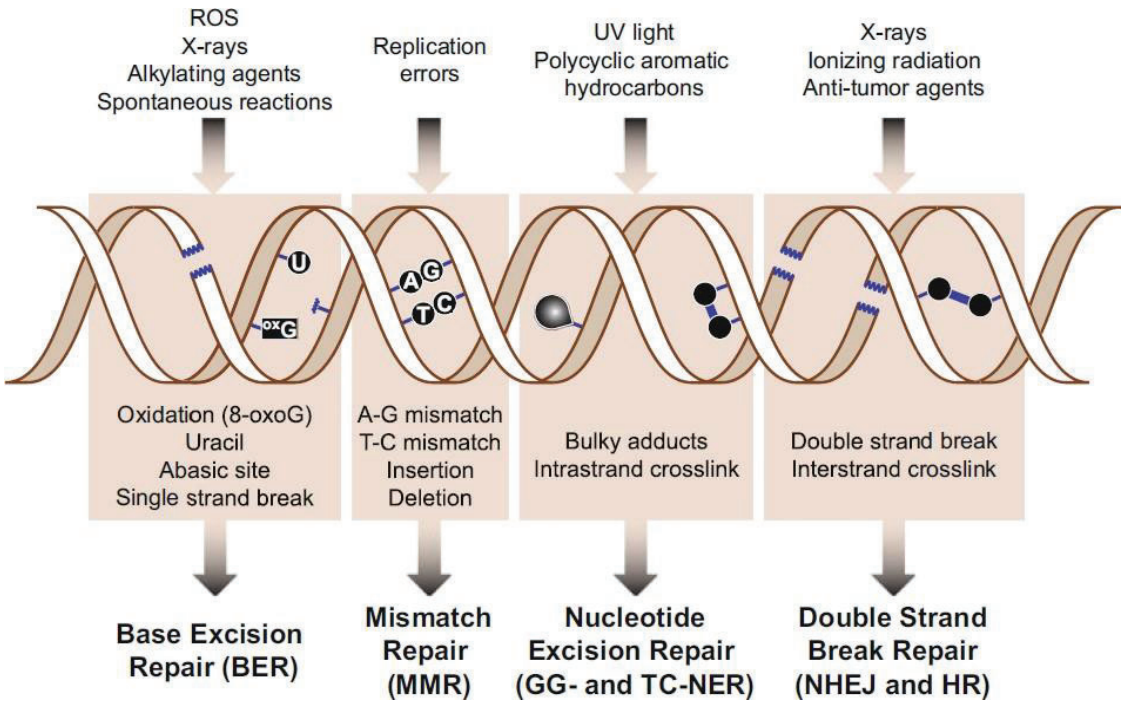


**Figure 26. Les différents types de dommages à l'ADN et les voies de réparation qu'ils activent.** (Dexheimer, 2013) Cette figure résume les différents agents inducteurs de dommages et les différents types de dommages qu'ils induisent. Par la suite, les différents dommages sont reconnus et réparés par les voies de réparation indiquées.

également être hydrolysées, un phénomène qu'on appelle la déamination, conduisant respectivement à la formation d'uracile, d'hypoxanthine et de thymine.

L'ADN est également sensible aux dommages induits par les molécules réactives produites naturellement par le métabolisme cellulaire, comme les ROS ou les espèces réactives de l'azote (RNS pour 'Reactive Nitrogen Species') (Cadet et al., 1997). Ces molécules génèrent différents dommages oxydatifs comme des modifications de bases, la génération de sites abasiques, des cassures simple- et double-brin ou la liaison covalente de protéines à l'ADN (dommage DPC (DNA-Protein Crosslink)). En plus des dommages oxydatifs, les bases d'ADN sont sujettes à l'alkylation par des agents endogènes, consistant en l'ajout d'un groupe alkyl (méthyl, chloroéthyl, etc…) sur les atomes azotes de l'anneau ou sur les atomes oxygènes extracycliques (Fu et al., 2012).

Les dommages endogènes peuvent également résulter d'une erreur de réplication de la polymérase, générant des incompatibilités de bases, des insertions et des délétions (McCulloch and Kunkel, 2008). De même, certains mécanismes de DDRs cités plus bas peuvent être sources d'erreurs.

Plusieurs agents exogènes sont également susceptibles de causer des dommages à l'ADN (Chatterjee and Walker, 2017; Dexheimer, 2013). On peut citer par exemple les rayons UV (ultraviolets), causant la dimérisation covalente de bases pyrimidines adjacentes. Les radiations ionisantes (IR), retrouvées dans la nature mais aussi dans certains traitements médicaux comme la radiothérapie, induisent diverses lésions de l'ADN dont les plus sévères sont les cassures double-brin (DSBs pour 'Double-Strand Breaks). Plusieurs médicaments utilisés dans le traitement de diverses pathologies dont le cancer, ont également été développés pour induire des dommages à l'ADN et provoquer la mort cellulaire. Parmi ces traitements, les agents alkylants (par ex. le méthyl méthane sulfonate ou le témozolomide) et les inhibiteurs de topoisomérase I ou II (par ex. respectivement, la camptothécine ou l'étoposide), causent des cassures simple- et double-brin. Enfin, l'ADN peut être endommagé par des facteurs retrouvés dans l'alimentation dont les N-nitrosamines, les amines hétérocycliques et des hydrocarbones aromatiques. Ces derniers sont également retrouvés dans les émissions atmosphériques comme dans la fumée de cigarette ou les gaz d'échappement des voitures.

#### *IV.1.ii. Les différentes voies de réparation de l'ADN : les DNA-damage response (DDR)*

Chez les mammifères, on répertorie au moins 10 voies pour la réparation des différentes lésions citées plus haut : la réparation d'incompatibilités (MMR pour 'Mismatch Repair'), l'excision de bases (BER pour 'Base Excision Repair'), l'excision de nucléotides (NER

pour ‘Nucleotide Excision Repair’), la réparation par la méthylguanine méthyltransférase (MGMT), la voie de l’anémie de Fanconi (FA pour ‘Fanconi Anemia’), la synthèse translésionnelle (TLS pour ‘Translesion Synthesis’), la ligature d’extrémités non-homologues (NHEJ pour ‘Non-Homologous End Joining’), la recombinaison homologue (HR pour ‘Homologous Recombination’), l’hybridation simple-brin (SSA pour ‘Single-Strand Annealing’) et la ligature d’extrémités non-homologues alternative (alt-EJ pour ‘Alternative End Joining’)

La voie MMR reconnaît les incompatibilités, les insertions et délétions pour éviter la propagation de mutations avec les divisions cellulaires (Liu et al., 2017). La voie BER permet quant à elle la réparation de bases d’ADN endommagées n’impactant pas la structure de l’hélice d’ADN (Zharkov, 2008). Typiquement, la voie BER est impliquée dans la reconnaissance et réparation des bases modifiées (oxydation, alkylation), des sites abasiques ou des cassures simple-brin. La voie NER reconnaît les dommages induisant une distorsion de l’hélice d’ADN, comme les lésions induites par les rayons UV (Schärer, 2013). Elle est subdivisée en 2 sous-voies : la NER couplée à la transcription (TC-NER pour ‘Transcription coupled NER’) et la NER du génome global (GG-NER pour ‘Global Genomic NER). L’enzyme MGMT est impliquée dans la réparation des guanines méthylées provoquées par les agents alkylants (Soll et al., 2017; Yu et al., 2020). Elle joue d’ailleurs un rôle important dans la résistance aux chimiothérapies aux agents alkylants et constitue une cible intéressante pour le traitement des tumeurs. La voie FA permet la réparation des liaisons covalentes inter-brins (ICLs pour ‘Interstrand Crosslink’) (Ceccaldi et al., 2016a). Cette voie est perturbée dans l’anémie de Fanconi, une maladie génétique résultant en une plus grande sensibilité aux ICLs et une prédisposition à l’insuffisance médullaire et au développement de cancers. La voie TLS est une voie particulière dans le sens qu’elle ne corrige pas le dommage mais permet la tolérance du dommage au moment de la réplication grâce à l’action de polymérases, principalement celles de la famille Y et de la polymérase ζ (Sale, 2013). Ce mécanisme permet notamment d’éviter l’arrêt du cycle cellulaire provoqué par les autres processus de réparation de l’ADN. Enfin, les voies HR, SSA, NHEJ et alt-EJ sont impliquées dans la réparation des DSBs. Leurs mécanismes moléculaires seront décrits dans la prochaine partie.

#### *IV.1.iii. Les cassures double-brin : reconnaissance et réparation*

Les DSBs sont des lésions hautement toxiques pour les cellules. Pour assurer la réparation de ces cassures, les cellules de vertébrés possèdent plusieurs voies de réparation, dont la mobilisation semble en partie dépendre du cycle cellulaire et du contexte chromatinien (pour revue, voir Scully et al., 2019). On compte 4 voies de réparation des cassures double-brin dont deux principales, la NHEJ et la HR, et deux plus

accessoires, la SSA et la alt-EJ (***Figure 27***). Les protéines impliquées dans les différentes voies de réparation et leurs fonctions sont résumées dans le ***Tableau 4***.

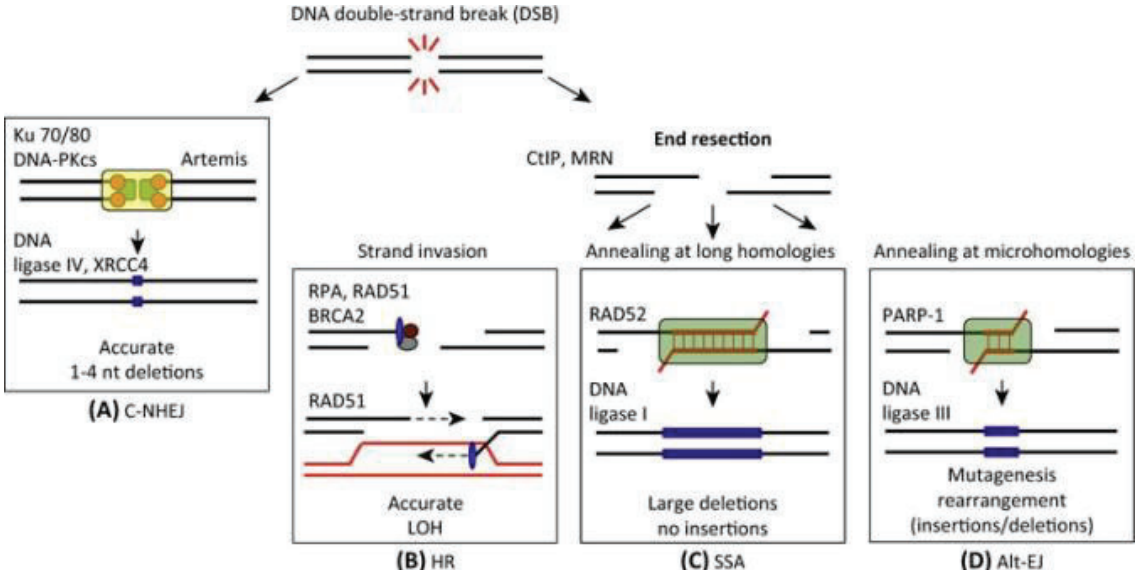


**Figure 27. Les différentes voies de réparation des cassures double-brins (DSBs).** *(Ceccaldi et al., 2016b)* Les DSBs peuvent être réparées par 4 voies de réparation. (A) La NHEJ (non-homologous end joining) permet la ligation des extrémités n'ayant pas subit la résection. (B) La HR (homologous recombination) nécessite la résection des extrémités. Elle repose sur la recombinaison entre les chromatides sœurs du chromosome en phase S et G2. (C) La SSA (single-strand annealing) repose sur l'homologie de deux séquences répétées. (D) L'alt-EJ (alternative end joining) repose la plupart du temps sur la recherche de microhomologies entre les deux brins, bien qu'elles ne soient pas nécessaires.

**Tableau 4. Les différentes protéines impliquées dans la réparation des DSBs et leurs fonctions.** *(basé sur Pannunzio et al., 2018; Wright et al., 2018; Sallmyr and Tomkinson, 2018)* Ce tableau résume les protéines impliquées dans les différentes voies de réparation des DSB et leurs fonctions. Les abréviations des différentes protéines sont détaillées à la fin du tableau.

| Voie de réparation | Protéines impliquées → *Fonction* |
|---|---|
| **Non-homologous end-joining (NHEJ)** | • **Ku70-Ku80** → *reconnaissance des extrémités, inhibition de la résection*<br>• **DNA-PK** → *activation de Artemis + établissement de la marque γH2AX*<br>• **Artemis** → *génération d'une coupe franche*<br>• **LIG4** → *ligation des extrémités*<br>• **XRCC4** et **XLF** → *protéines d'échafaudage pour la réparation* |
| **Homologous recombination (HR)** | • **Complexe MRN (MRE11, RAD50** et **NBS1)** → *initiation de la résection des extrémités, recrutement et activation de ATM*<br>• **CtIP** → *initiation résection des extrémités*<br>• **ATM** → *stimulation de la résection, établissement de la marque γH2AX, activation de des voies IFN, p53 et CHK2 associées aux DSBs*<br>• **EXO1, BLM** et **complexe BRCA1/BARD1** → *poursuite de la résection des extrémités*<br>• **RPA** → *prévention d'un mauvais appariement, point d'ancrage pour ATR*<br>• **ATR** → *établissement de la marque γH2AX, activation de la voie CHK1 associée aux DSBs*<br>• **Complexe BRCA2-DSS1** → *déplacement des protéines RPA* |

| | |
|---|---|
| | • **Filaments de RAD51** → *recherche d'homologie de séquence par invasion de la chromatide sœur et formation de la D-loop*<br>• **ADN polymérase δ** → *extension du brin envahisseur*<br>• **FANCM, BLM** et **RTEL1** → *désassemblage de la D-loop* |
| **Single-strand annealing (SSA)** | • **Complexe MRN, CtIP, ATM, RPA et ATR** → *cf. HR*<br>• **RAD52** → *déplacement des protéines RPA et rapprochement des extrémités pour la recherche d'homologie entre les séquences répétées*<br>• **ERCC1/XPF** → *clivage des extrémités 3' non complémentaires*<br>• **Ligase I** → *ligation des extrémités* |
| **Alternative end-joining (alt-EJ)** | • **Complexe MRN, CtIP, ATM, RPA et ATR** → *cf. HR*<br>• **PARP-1** → *rapprochement des extrémités*<br>• **ADN polymérase θ** → *déplacement des protéines RPA et extension de l'ADN*<br>• **Complexe LigIII/XRCC1** → *ligation des extrémités* |
| **DNA-PK:** DNA-dependent Protein Kinase; **LIG4:** Ligase IV; **XRCC4:** X-ray Repair Cross-Complementing 4; **XLF:** XRCC4-Like Factor; **MRE11:** Meiotic Recombination 11; **NBS1:** Nijmegen Breakage Syndrome 1; **CtIP:** CTBP-Interacting Protein; **ATM:** Ataxia Telangiectasia Mutated; **EXO1**: Exonuclease 1; **BLM:** Bloom syndrome protein; **BRCA1:** Breast Cancer susceptibility 1 protein; **BARD1:** BRCA1 Associated RING Domain 1; **RPA:** Replication Protein A; **ATR:** Ataxia Telangiectasia mutated and Rad3 related; **BRCA2:** Breast Cancer susceptibility 2 protein; **DSS1:** Deleted in Split hand/Split foot protein 1; **FANCM:** Fanconi Anemia Complementation Group M; **RTEL1:** Regulator of Telomere Elongation helicase 1; **ERCC1:** Excision Repair Cross-Complementing 1; **XPF:** Xeroderma Pigmentosum complementation group F; **PARP-1:** Poly(ADP-Ribose) Polymerase 1; **XRCC1:** X-ray Repair Cross-Complementing 1 | |

La NHEJ (***Figure 27(A)***) (Pannunzio et al., 2018) est initiée par la liaison de complexes Ku70-Ku80 à chaque extrémité de la cassure et préviennent la résection des extrémités (càd. la digestion par une nucléase d'un des brins pour générer de l'ADN simple-brin). Cette étape est suivie par la génération d'une coupe franche par la nucléase Artemis et la ligation des extrémités cohésives par la LIG4. La délétion ou l'insertion de quelques nucléotides pour générer des extrémités cohésives font de la NHEJ une voie potentiellement mutagène.

La réparation par HR (***Figure 27(B)***) (Wright et al., 2018) se base sur la recherche d'homologie. Elle nécessite donc la présence d'un modèle trouvé au niveau de la chromatide sœur du chromosome. Ainsi, à l'inverse de la NHEJ qui est active tout au long du cycle cellulaire, la réparation par HR est restreinte aux phases S et G2. La HR permet la réparation des cassures à la suite de la résection des extrémités et la génération d'ADN simple-brin. La résection est suivie d'une étape de recombinaison entre les deux chromatides. Des filaments de protéines RAD51 se lient à l'ADN simple brin et permettent la recherche d'homologie par l'invasion de la chromatide sœur. Si une homologie est trouvée, le brin de la chromatide sœur non apparié est déplacé pour former une boucle de déplacement (ou D-loop). Le brin envahisseur est étendu par l'ADN polymérase δ. Il existe

2 sous-voies dans la HR : la voie SDSA (Synthesis-Dependent Strand Annealing) où le brin envahisseur ne provient que d'une extrémité de la cassure, et la dHJ (Double Holliday Junction), où les brins résectés des deux extrémités envahissent la chromatide sœur. La HR par dHJ peut conduire à des crossing-over entre les chromatides ; néanmoins, la réparation par HR est plus fiable que la NHEJ et moins mutagène. La réparation par HR peut être inhibée par la présence de cGAS nucléaire liée à la chromatine (Jiang et al., 2019; Liu et al., 2018). En effet, cGAS est capable d'oligomériser, compactant ainsi la chromatine liée et empêchant ainsi l'invasion médiée par les filaments de RAD51 (Jiang et al., 2019). Ainsi, lorsqu'elle est nucléaire, la protéine cGAS favorise l'instabilité génomique et est promotrice de tumeur (Jiang et al., 2019; Liu et al., 2018).

Les voies SSA et alt-EJ (***Figure 27(C) et (D)***) sont des voies de réparation plus alternatives car elles génèrent automatiquement des délétions ou des insertions et sont donc sources de mutations (Sallmyr and Tomkinson, 2018). Les deux voies reposent comme la HR sur la résection des extrémités au niveau du site de cassure et la recherche d'homologie. La SSA repose sur la rechercher d'homologies entre deux séquences répétées, l'alt-EJ repose elle sur la recherche de micro-homologie.

Le choix de la voie de réparation des DSBs dépend de plusieurs facteurs (Ceccaldi et al., 2016; Scully et al., 2019). La voie NHEJ est la voie de réparation principale, car la plus rapide. Elle est favorisée par l'action de 53BP1 qui prévient la résection des extrémités et facilite la liaison de Ku70-Ku80. A l'inverse, les kinases CDK, dont l'expression augmentent au moment de la phase S, facilitent l'initiation de la résection. De même l'expression des gènes impliqués dans la HR est augmentée entre la phase G1 et S. Le choix de la voie de réparation semble aussi dépendre du contexte chromatinien. Ainsi, les régions d'hétérochromatine et les régions transcriptionnellement actives semblent être préférentiellement réparées par HR, les marques épigénétiques spécifiques à ces régions permettant le recrutement de protéines impliquées dans cette voie de réparation (Aymard et al., 2014; Ferrand et al., 2021; Goodarzi et al., 2008).

Comment les protéines impliquées dans la réparation des DSBs sont-elles ciblées aux sites de cassures ? Les études sur les PML NBs laissent supposer que ces structures jouent un rôle important dans la reconnaissance des DSBs et dans le processus de réparation, plus particulièrement par HR (***Tableau 1*** en partie *II.2.ii*) (Carbone et al., 2002; Chang et al., 2018; Dellaire and Bazett-Jones, 2004; Dellaire et al., 2006a; di Masi et al., 2016; Vancurova et al., 2019; Yeung et al., 2012). Dans la prochaine partie, j'aborderai ainsi les différentes études suggérant une implication des PML NBs dans le processus de HR.

### *IV.1.iv. L'implication des PML-NBs dans la recombinaison homologue*

L'idée d'une implication des PML NBs dans la réparation des DSBs vient initialement de la description de la localisation de nombreuses protéines de la réparation au sein de ces structures nucléaires avant et/ou après l'induction de DSBs (répertoriées dans Dellaire and Bazett-Jones, 2004). Ainsi, comme évoqué dans le ***Tableau 1*** en partie *II.2.ii*, les protéines BLM, RAD51, RPA et ATR localisent dans une fraction de PML NBs avant et après l'induction de dommages (Barr et al., 2003; Bischof et al., 2001; Wang et al., 2001; Zhong et al., 1999). Les membres MRE11 et NSB1 du complexes MRN localisent dans les PML NBs dans les cellules non endommagées (Mirzoeva and Petrini, 2001). Lors d'une irradiation, les protéines quittent les corps nucléaires pour relocaliser sur les sites de cassures (Mirzoeva and Petrini, 2001). Une étude plus précise de la dynamique de MRE11 a montré que la protéine co-localise de nouveau avec les PML NBs à partir de 8-12h après l'irradiation et est co-localise complètement après 24h (Carbone et al., 2002). Pour finir, les protéines ATM et BRCA1 relocalisent dans les PML NBs avec la protéine de signalisation TOPBP1 après l'induction de DSBs par irradiation (les trois protéines co-localisent à 8h post-irradiation, les temps plus précoces n'ayant pas été investigués) (Xu et al., 2003).

Dans les années 2000, des observations de microscopie ont montrés que les PML NBs augmentent en nombre suite à l'induction de DSBs et sont juxtaposées aux sites de cassures (Carbone et al., 2002; Dellaire and Bazett-Jones, 2004; Dellaire et al., 2006a). Les PML NBs sont alors qualifiés de senseurs des cassures double-brin. La juxtaposition des PML NBs avec les sites de cassures augmente graduellement après l'induction du dommage : ainsi, environ 20% des PML NBs juxtaposent des sites de dommages 2 à 4h après une irradiation et ce pourcentage atteint les 60% après 8h (Carbone et al., 2002). Des études plus précises sur l'implication des PML NBs dans la réparation des dommages ont montré que ces derniers sont importants pour la réparation par HR et non la réparation par NHEJ (Vancurova et al., 2019; Yeung et al., 2012). Plus précisément, les PML NBs ne sont pas impliqués dans la reconnaissance des cassures double-brin ou la formation des foyers RAD51 mais sont essentiels pour le bon déroulement des étapes tardives de la HR (Yeung et al., 2012), pouvant expliquer leur association graduelle avec les sites de dommages.

Le rôle important des PML NBs dans la réparation des DSBs est supporté par l'observation d'un défaut de réparation des DSBs dans les cellules de patients atteints d'APL, maladie dans laquelle la protéine PML est fusionnée avec la protéine RAR$\alpha$ (di Masi et al., 2016). De plus, des cellules épithéliales humaines PML$^{-/-}$ montrent une plus grande sensibilité

aux faibles doses d'IR et aux dommages induits par la mitomycine C, la cisplatine ou la camptothécine (Vancurova et al., 2019).

Le mécanisme moléculaire derrière le recrutement des PML NBs aux sites de cassures semble reposer sur le recrutement de 53BP1 au site de dommage (Vancurova et al., 2019). En effet, la suppression de 53BP1 et de RNF168 (protéine requise pour le recrutement de 53BP1), induit une diminution de la juxtaposition des PML NBs et des sites de cassures. L'augmentation du nombre de PML NBs est quant à elle dépendante de l'expression des protéines ATR, ATM, NBS1 et de la protéine checkpoint kinase CHK2 (voir ci-dessous) (Dellaire et al., 2006a).

#### *IV.1.v. Les différentes voies de signalisation induites par les cassures double-brin*

L'induction de DSBs induit une cascade de signalisation en grande partie grâce à l'activation des protéines ATR (Ataxia Telangiectasia mutated and Rad3-related homolog) et ATM (Ataxia Telangiectasia Mutated) (***Figure 28***) (Awasthi et al., 2015; Blackford and Jackson, 2017). Tout d'abord, ATR et ATM phosphorylent respectivement les protéines checkpoint kinases 1 et 2 (CHK1 et CHK2) (Chaturvedi et al., 1999; Guo et al., 2000; Hekmat-Nejad et al., 2000; Liu et al., 2000; Matsuoka et al., 1998, 2000; Zhao and Piwnica-Worms, 2001). L'activation de CHK1 et CHK2 conduit à un arrêt temporaire du cycle cellulaire afin de procéder à la réparation des cassures. La protéine ATM est également capable de phosphoryler la protéine p53 (Banin et al., 1998; Canman et al., 1998; Siliciano et al., 1997), promouvant l'arrêt du cycle cellulaire temporaire ou permanent (la sénescence cellulaire) ou pouvant promouvoir la mort cellulaire par apoptose. ATM régule également le processus de transcription au site de dommage en activant le complexe de remodelage de la chromatine PBAF, empêchant ainsi l'élongation de l'ARN polymérase II (Kakarougkas et al., 2014). Enfin comme évoqué précédemment, ATM peut également conduire à la production d'IFN par la cellule et stimuler l'inflammation (Brzostek-Racine et al., 2011; Yu et al., 2015).

Les DSBs peuvent également induire une réponse inflammatoire *via* la reconnaissance d'ADN cytoplasmique par la voie cGAS-STING (***Figure 28***) (Harding et al., 2017; Mackenzie et al., 2017). En effet, un défaut d'arrêt du cycle cellulaire après un dommage conduit à la formation de micro-noyaux, reconnus par la protéine cGAS cytoplasmique. Cette dernière promeut l'activation de la voie STING, évoquée dans la partie *III.2.i*, et la sécrétion d'IFN de type I.

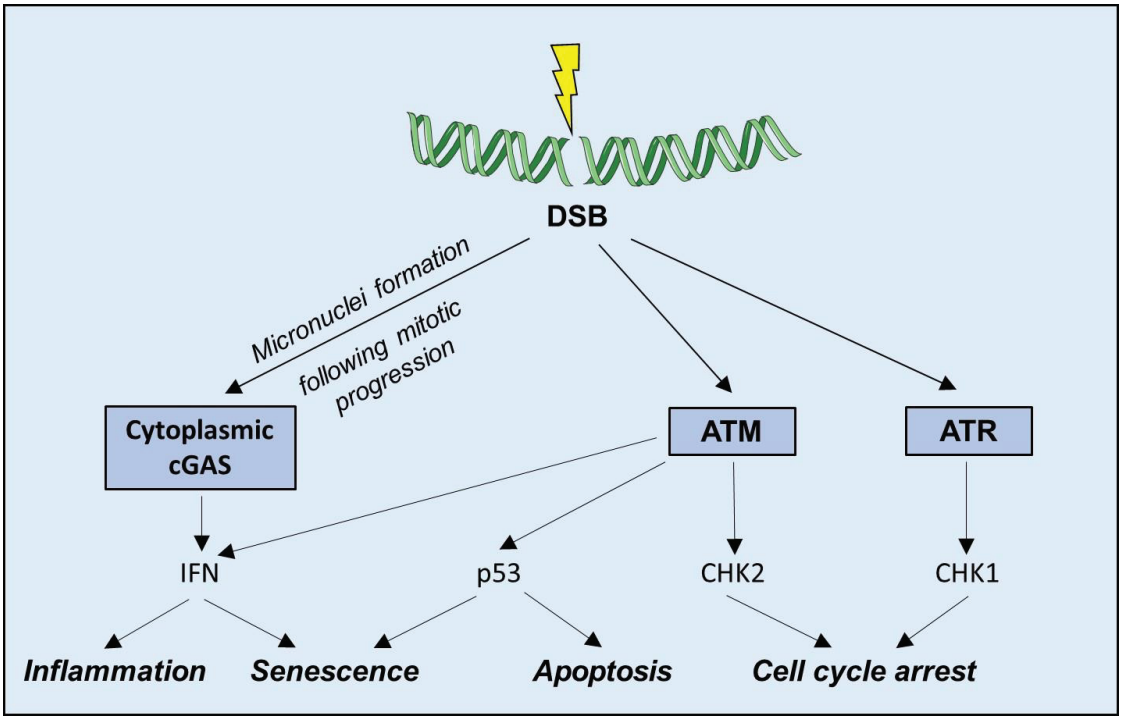


**Figure 28. Les différentes voies de signalisation induites par les cassures double brin.** L'induction de DSBs induit l'activation des kinases ATM et ATR. Ces dernières phosphorylent respectivement CHK2 et CHK1, qui promeuvent l'arrêt du cycle cellulaire. L'activation d'ATM induit également la phosphorylation et l'activation de p53, impliquée dans l'induction de la sénescence et de l'apoptose. Enfin, il a été montré que l'activation d'ATM pouvait conduire à l'expression d'IFN de type I. De plus, si la mitose a lieu après l'induction de DSBs, cela conduit à la formation de micro-noyaux, reconnus par la protéine cGAS cytoplasmique. Cette dernière synthétise du cGAMP et active la voie STING, induisant l'expression d'IFN de type I.

## IV.2. La réparation de l'ADN et la chromatine

La structure de la chromatine a une influence sur le processus de réparation (pour revue, voir Aleksandrov et al., 2020; Ferrand et al., 2021; Soria et al., 2012). En effet, pour faciliter le processus de réparation, la chromatine doit être 'préparée'. Elle est ensuite 'réparée' et sa structure initiale doit être 'restaurée' afin d'assurer l'intégrité de la chromatine et permettre le bon déroulement des processus cellulaire de réplication et de transcription (concept de 'Access/prime, repair, restore' introduit par Smerdon, 1991). Dans cette partie, je m'intéresserai aux processus impliqués dans la réparation des dommages chez les mammifères mais beaucoup d'études sur le lien entre la chromatine et la réparation ont été conduites chez la levure et la drosophile, certains mécanismes étant conservés chez les mammifères et d'autres pouvant différer.

### *IV.2.i. Les caractéristiques épigénétiques du processus de réparation : la 'préparation' et la 'réparation' de la chromatine*

Pour préparer la chromatine au processus de réparation, la chromatine subit une décompaction facilitant l'accès au site de lésion par la machinerie de réparation (Ferrand et al., 2021; Soria et al., 2012). Plusieurs mécanismes sont impliqués dans le relâchement de la chromatine associée à la réparation. Premièrement, certaines marques d'histones

favorisent la décompaction de la structure chromatinienne. Ainsi, les acétyltransférases d'histones p300 et TIP60 favorisent la relaxation de la chromatine respectivement après des dommages aux UV ou des DSBs (Murr et al., 2006; Rubbi and Milner, 2003). La marque H2BK120ub (établie par les ubiquitine ligases RNF20 et RNF40) semble également jouer un rôle dans la décompaction de la chromatine induite par DSBs (Oliveira et al., 2014). En effet, les cellules déficientes pour la RNF20 recrutent difficilement les facteurs de réparation des DSBs. Ce recrutement est rétabli lorsque les cellules sont traitées à la chloroquine, un agent induisant le relâchement de la chromatine. L'addition de chaînes de poly(ADP-ribose) (PAR) par la protéine PARP1 induit également une décompaction de la chromatine en promouvant l'éviction des histones (Luijsterburg et al., 2016; Sellou et al., 2016; Smith et al., 2018; Yang et al., 2020). Les histones peuvent être également évincées de la chromatine par l'action de protéines de remodelage (par ex. p400, INO80) (van Attikum et al., 2007; Courilleau et al., 2012; Li and Tyler, 2016) et de protéines chaperons d'histones (par ex. ANP32E, FACT, nucléoline) (Goldstein et al., 2013; Gursoy-Yuzugullu et al., 2015; Yang et al., 2020). Enfin, les histones peuvent être également dégradées par le protéasome en réponse aux dommages de l'ADN (Hauer et al., 2017).

Afin d'assurer une bonne réparation des dommages, le processus de transcription doit être stoppé. Cela permet également d'éviter la production de transcrits mutés. Plusieurs marques d'histones permettent de contrôler l'arrêt de la transcription au niveau du site de lésion. On peut ainsi citer les marques H2AK119ub pour les dommages UV et DSBs (Bergink et al., 2006; Ismail et al., 2010; Kakarougkas et al., 2014; Sanchez et al., 2016; Shanbhag et al., 2010; Ui et al., 2015) et H3K27me3 pour les DSBs (Abu-Zhayia et al., 2018; Chou et al., 2010; O'Hagan et al., 2008, 2011). L'ubiquitine ligase RNF8 permet également une polyubiquitination sur une lysine non définie de H2A à la suite de DSB, réduisant l'activité transcriptionnelle (Paul and Wang, 2017). Enfin, au niveau des DSBs, le complexe répressif NuRD est recruté à la suite de la déméthylation de H3K4 et l'acétylation de H4 (Gong et al., 2015, 2017).

Le paysage épigénétique au niveau de la lésion participe au processus de réparation (***Figure 29***). Dans le cas de cassures double-brin, la phosphorylation de la sérine 139 de H2AX est la plus décrite (H2AXS139P ou γH2AX) (Rogakou et al., 1998). Cette marque est majoritairement établie par la kinase ATM mais peut également être médiée par ATR ou DNA-PK (Blackford and Jackson, 2017). La marque γH2AX s'étend tout le long du TAD dans lequel la cassure à lieu (Arnould et al., 2021) et permet d'établir un environnement favorable au mécanisme de réparation. En effet, elle permet le recrutement de facteurs impliqués dans la signalisation des dommages et leur réparation. La marque γH2AX sert

notamment de plateforme de liaison pour la protéine MDC1 (Mediator of DNA damage Checkpoint protein 1) (Stucki et al., 2005). La protéine MDC1 se lie avec la protéine NBS1 du complexe MRN (Chapman and Jackson, 2008; Melander et al., 2008; Spycher et al., 2008). Cela pourrait conduire à une accentuation du recrutement de ATM et une augmentation de la signalisation associée aux DSBs (Blackford and Jackson, 2017). La protéine MDC1 liée à γH2AX permet aussi le recrutement de l'ubiquitine ligase RNF8 (Huen et al., 2007; Kolas et al., 2007; Mailand et al., 2007). RNF8, en plus de la polyubiquitination de H2A décrite plus haut, stimule également l'ubiquitination de l'histone

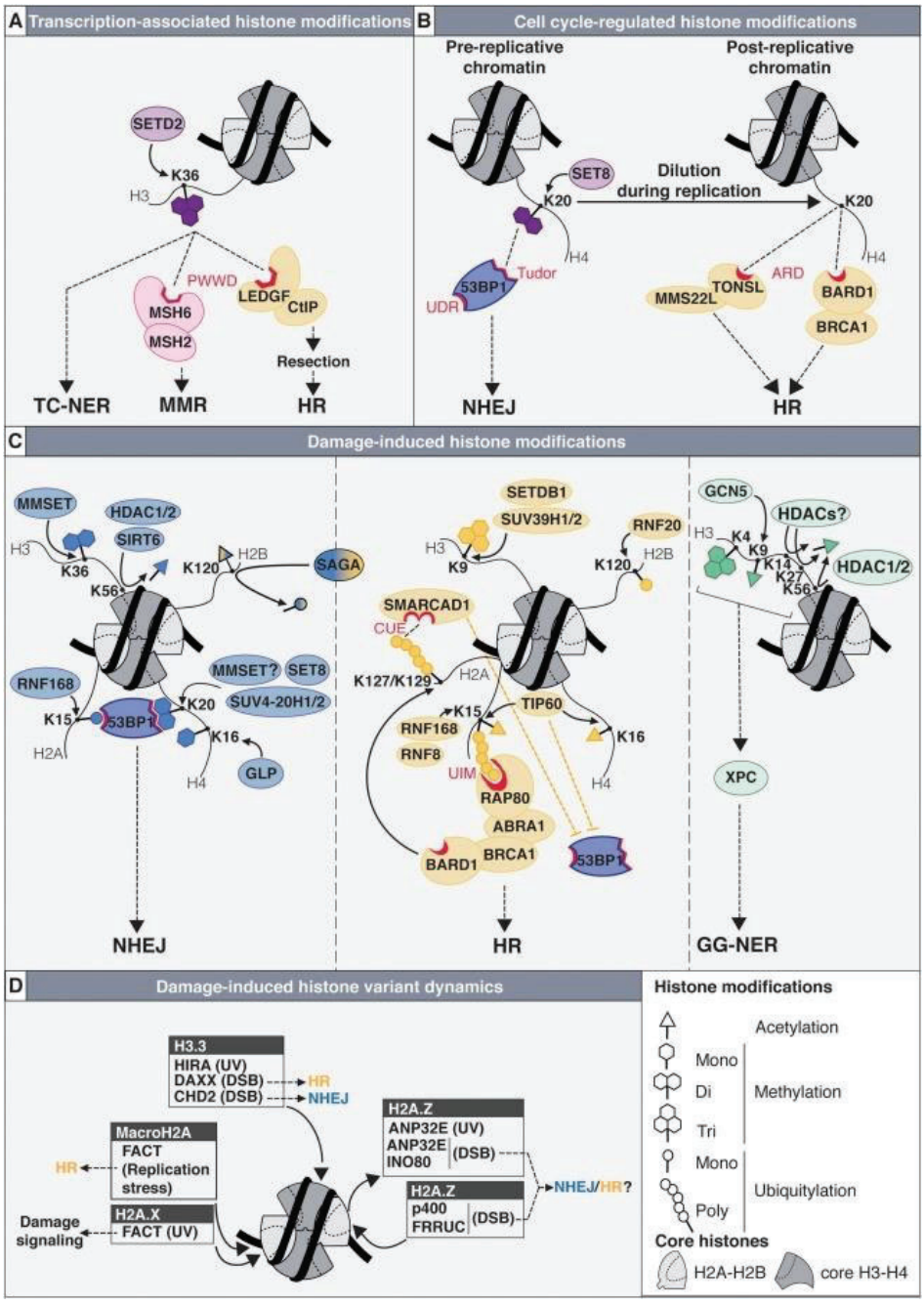


**Figure 29. Les marques épigénétiques associées aux dommages à l'ADN.** (*Ferrand et al., 2021*) Cette figure illustre les différentes marques épigénétiques associées avec la réparation de l'ADN et détaillées dans le texte principal.

de liaison H1 et le recrutement d'une autre ubiquitine ligase, RNF168 (Thorslund et al., 2015). Cette dernière ubiquitine à son tour l'histone H2A sur la lysine 13 ou 15 (H2AK13/15ub) qui permet le recrutement de 53BP1 et favorise la réparation de la lésion par NHEJ (Fradet-Turcotte et al., 2013; Mattiroli et al., 2012; Thorslund et al., 2015). L'ubiquitination de H2A peut être étendue par RNF8 et RNF168 afin de recruter le complexe BRCA1-BARD1 qui favorise la réparation par HR (Gatti et al., 2015; Kim et al., 2007; Sobhian et al., 2007; Yan et al., 2007). Les DSBs induisent également l'établissement de la marque H2BK120ub. Cette dernière favorise la réparation par HR mais le mécanisme moléculaire n'est pas encore connu (Evangelista et al., 2018; Moyal et al., 2011; Nakamura et al., 2011; Zheng et al., 2018). H2BK120 peut également être déubiquitinylée puis acétylée par le complexe SAGA, favorisant la réparation par HR et NHEJ (Clouaire et al., 2018; Kim et al., 2019; Ramachandran et al., 2016). La marque H3K36me3, enrichie dans les régions transcriptionnellement actives, favorise la réparation des DSBs par HR (Aymard et al., 2014; Carvalho et al., 2014; Daugaard et al., 2012; Pfister et al., 2014). En effet, elle est reconnue par la protéine LEDGF (Lens Epithelial Derived Growth Factor) qui interagit avec le facteur de résection CtIP (Aymard et al., 2014; Daugaard et al., 2012). La marque H3K36me3 favorise également la réparation de dommages par les voies de réparations TC-NER et MMR (Li et al., 2013; Lim et al., 2017). H3K36me3 peut être convertie en H3K36me2 par la protéine MMSET et favoriser la réparation par NHEJ (Fnu et al., 2011). La marque H4K20me2 (marque régulée par le cycle cellulaire) participe au choix de la voie de réparation pour les DSBs ; en effet, la marque est reconnue par 53BP1 favorisant la réparation par NHEJ (Botuyan et al., 2006; Clouaire et al., 2018; Hsiao and Mizzen, 2013; Pei et al., 2011; Tuzon et al., 2014) mais au cours de la réplication, elle est diluée et la lysine non méthylée est reconnue par des complexes promouvant la HR (càd. TONSL-MMS22L et BRCA1-BARD1) (Nakamura et al., 2019; Saredi et al., 2016). La marque H3K9me3, enrichie dans les régions d'hétérochromatine, favorise le recrutement de l'acétyltransférase TIP60, favorisant la réparation des DSBs par HR (Sun et al., 2009; Tang et al., 2013). Enfin, la lysine H3K56, marquant l'ADN nouvellement répliqué, est désacétylée par les protéines HDAC1/2 ou SIRT6 en réponse aux DSBs (Miller et al., 2010; Toiber et al., 2013). HDAC1/2 stimule la réparation par NHEJ quand SIRT6 favorise la réparation par NHEJ et HR.

Le processus de réparation des lésions induites par UV, la NER, est également stimulée par l'établissement ou l'enlèvement de marques épigénétiques particulières. Ainsi, comme pour les DSBs, la marque H3K56ac est enlevée (Battu et al., 2011). Cela participe à l'arrêt du cycle cellulaire associé à la réparation. Les marques H3K14 et K27 sont également désacétylées pour favoriser le recrutement du senseur XPC (Kakumu et al., 2017). En

revanche, l'acétylation de H3K9 est favorisée au niveau des lésions UV, stimulant la réparation par NER (Guo et al., 2011). La triméthylation de H3K4 participe également à la réparation par NER en favorisant le recrutement de XPC (Balbo Pogliano et al., 2017).

Les variants d'histones jouent également un rôle dans la réparation des dommages. Ainsi, le variant H3.3 est important pour la réparation des DSBs par NHEJ et HR (Juhász et al., 2018; Luijsterburg et al., 2016), mais pas pour la réparation des dommages UV (Adam et al., 2013). Le variant H2AZ pourrait également jouer un rôle dans le choix de réparation des DSBs mais sa contribution est encore discutée (Clouaire et al., 2018; Ferrand et al., 2021). Le variant MacroH2A s'accumule aussi au niveau de la chromatine en réponse à l'induction de DSBs où il favorise le recrutement de BRCA1 et la réparation par HR (Clouaire et al., 2018; Khurana et al., 2014; Kim et al., 2018; Timinszky et al., 2009; Xu et al., 2012).

#### *IV.2.ii. Le rétablissement de la structure chromatinienne après la réparation : la 'restauration'*

Une fois le processus de réparation de l'ADN effectué, il est important de rétablir une structure chromatinienne correcte (Ferrand et al., 2021; Soria et al., 2012). Au niveau des DSBs réparés par NHEJ, les chaperons d'histones CAF-1 et HIRA incorporent H3.1/2 ou H3.3 (Li and Tyler, 2016). Cette étude ne fait cependant pas la distinction entre les histones préexistantes et les histones nouvellement synthétisées. La technologie SNAP-tag permet d'observer l'incorporation d'histones nouvellement synthétisées. Cette technologie a permis de montrer une incorporation d'histones H3.1/2 nouvellement synthétisées au niveau des DSBs (Luijsterburg et al., 2016; Polo et al., 2006) ; elle a également permis de montrer une incorporation d'histones H3.3 nouvellement synthétisées au niveau des DSBs médiée par la protéine de remodelage CHD2 et par le complexe DAXX/ATRX (Juhász et al., 2018; Luijsterburg et al., 2016). En plus de l'incorporation d'histone, les marques associées à la réparation doivent être retirées. Ainsi, les phosphatases PP1, PP2A, PP4, PP6 et WIP1 permettent la déphosphorylation de γH2AX (Chowdhury et al., 2005, 2008; Nakada et al., 2008; Nazarov et al., 2003) tandis que la déubiquitinase USP16 permet de retirer la marque H2AK119ub et favorise la reprise de la transcription (Shanbhag et al., 2010).

Au niveau des lésions UV, les chaperons CAF-1 et HIRA sont impliqués dans le dépôt d'histones H3.1/2 ou H3.3 nouvellement synthétisées (Adam et al., 2013; Fortuny et al., 2021; Polo et al., 2006). Le chaperon d'histone FACT favorise lui l'incorporation de nouvelles histones H2A et H2AX (Dinant et al., 2013; Piquet et al., 2018).

Plusieurs questions restent encore à résoudre concernant le rétablissement de la chromatine après la réparation de l'ADN et en particulier le maintien ou non du paysage épigénétique d'origine. En effet, les histones nouvellement synthétisées ne portent pas forcément les marques présentent sur les histones parentales. Ces nouvelles histones pourraient éventuellement marquées la chromatine réparée et servir d'empreinte dans les régions facilement dommageables et permettre une réparation plus rapide en cas de nouvelle lésion (Ferrand et al., 2021; Soria et al., 2012).

# Questions biologiques

# I. Les trois grandes questions biologiques investiguées

Mon projet de thèse visait à mieux comprendre la relation entre le complexe chaperon d'histone HIRA et les PML NB ainsi que l'impact de sa relocalisation sur la dynamique de la chromatine dans un contexte inflammatoire et de cassures de l'ADN. En particulier, j'ai focalisé mes recherches sur 3 questions principales : (1) quelle(s) voie(s) de signalisation est (sont) impliquée(s) dans la relocalisation de HIRA dans les PML NBs ? ; (2) quel est le mécanisme moléculaire associé au recrutement de HIRA au sein des PML NBs ? ; (3) quel est l'impact de la relocalisation de HIRA dans les PML NB sur la dynamique de la chromatine ? (***Figure 30***).

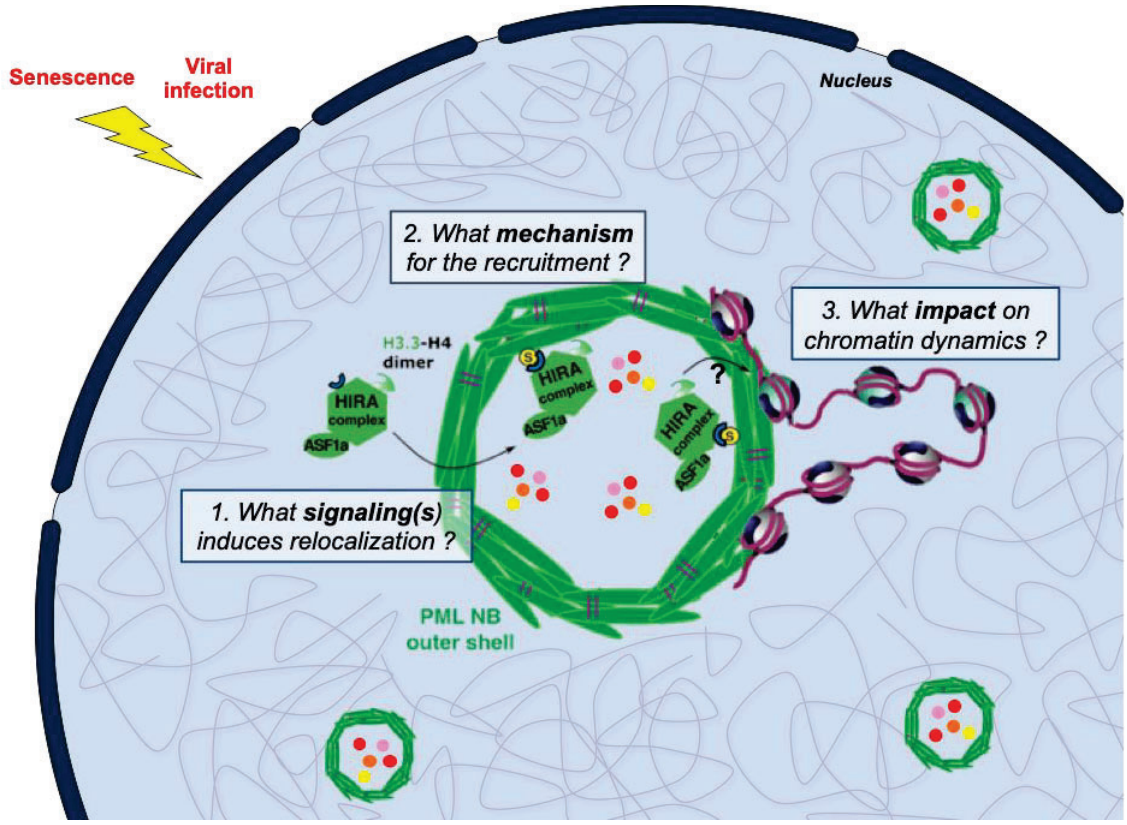


**Figure 30. Schéma des 3 principales questions investiguées au cours de ma thèse.** Lorsque des cellules primaires sont soumises à un stress tel qu'une infection virale ou l'induction de la sénescence, le complexe chaperon d'histones HIRA relocalise dans les PML NBs. Peu de choses sont jusqu'à présent connu sur le mécanisme derrière cette relocalisation et son rôle. Ce schéma résume les 3 questions biologiques investiguées au cours de ma thèse concernant la signalisation, le mécanisme moléculaire et l'impact de la relocalisation du complexe HIRA dans les PML NBs.

### (1) Quelles voies de signalisation sont impliquées dans la relocalisation du complexe HIRA dans les PML NBs ?

Deux études sont sorties au cours de ma thèse décrivant l'implication de la voie IFN dans la relocalisation du complexe HIRA dans les PML NBs (McFarlane et al., 2019; Rai et al., 2017) (observation également faite dans mes travaux). Cependant, comme décrit en introduction, plusieurs molécules sont sécrétées lors d'une infection virale et plus

largement dans un contexte inflammatoire, comme les cytokines IL-6, IL-8 ou encore le TNF$\alpha$. De plus, comme évoqué en introduction, la sécrétion d'IFN de type I par les cellules sénescentes est un évènement plutôt tardif alors que la relocalisation du complexe HIRA en sénescence est observée très précocement (Cecco et al., 2019; Zhang et al., 2005). Ainsi, au cours de ma thèse, j'ai cherché à regarder si d'autres voies de signalisation, en plus de la voie IFN, pouvaient être impliquées dans la relocalisation d'HIRA au sein des PML NBs.

**(2) Quel est le mécanisme moléculaire impliqué dans le recrutement du complexe HIRA dans les PML NBs ?**

Les protéines clientes des PML NBs sont couramment recrutées au sein de ces structures *via* des interactions entre des motifs SIMs sur les protéines partenaires et la protéine PML SUMOylée (Sahin et al., 2014a). En revanche, aucun mécanisme moléculaire n'a pour le moment été décrit pour le recrutement de HIRA au sein des PML NBs. L'hypothèse la plus évidente repose sur un recrutement *via* des interactions SIM-SUMO. Ainsi, à travers différentes stratégies, j'ai cherché à valider ou infirmer cette hypothèse et à décrypter le mécanisme moléculaire impliqué dans le recrutement de HIRA dans les PML NBs.

**(3) Quel est l'impact fonctionnel de la relocalisation du complexe HIRA au sein des PML NBs, en particulier sur la dynamique de la chromatine ?**

L'impact fonctionnel de la relocalisation du complexe HIRA au sein des PML NBs est encore mal compris. Les PML NBs ont été proposé comme facilitant l'acheminement du variant H3.3 et de ses chaperons du nucléoplasme vers la chromatine (Corpet et al., 2014; Delbarre et al., 2013). De plus, les PML NBs sont juxtaposés à certaines régions chromatiniennes, le plus souvent des régions transcriptionnellement actives. Sous condition de stress, le complexe HIRA pourrait ainsi être recruté au sein des PML NBs pour agir sur des régions chromatiniennes où son action est requise. J'ai donc cherché à visualiser si des régions cibles pouvaient se trouver à proximité des PML NBs après l'induction de la relocalisation du complexe HIRA (par exemple, les gènes induits par l'IFN (ISGs) dans le cas de la relocalisation induite par l'inflammation). J'ai également cherché à savoir si ces régions pouvaient être associées avec le variant H3.3 déposé par le complexe HIRA.

## II. Modèle cellulaire utilisé

Dans le cadre de ma thèse, l'utilisation de cellules primaires est requise car la relocalisation du complexe HIRA dans les PML NBs n'est pas observée dans des lignées cancéreuses. Ainsi, j'ai utilisé principalement comme modèle cellulaire des fibroblastes primaires humains de type BJ (***Figure 31***), prélevés sur des prépuces de nouveau-nés. Les fibroblastes sont des cellules adhérentes du tissu conjonctif, couramment utilisées dans les études de sénescence. En effet, ce type cellulaire fût utilisé dans les années 1960 par Leonard Hayflick pour la première description de la sénescence réplicative (Hayflick, 1965; Hayflick and Moorhead, 1961), démocratisant le modèle pour les études suivantes.

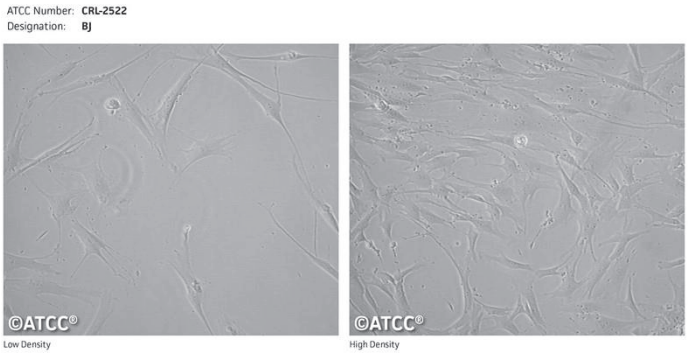


**Figure 31. Fibroblastes BJ en culture.** *(Images issues de la fiche technique d'ATCC (ref CRL-2522))* Les cellules BJ sont fusiformes. A confluence, les cellules forment des faisceaux.

Les BJ sont des fibroblastes relativement faciles à cultiver car ils ne nécessitent pas d'être mis en présence de facteurs particuliers ou de pousser sur un revêtement spécial. En comparaison aux autres fibroblastes, les BJ présentent une longue durée de vie et peuvent proliférer jusqu'à un maximum de 72 doublements de population (données issues de la fiche technique d'ATCC (CRL-2522)). Ces cellules sont couramment utilisées dans le laboratoire et bien maîtrisées (Cohen et al., 2018; Maroui et al., 2016). Elles ont donc été naturellement choisies pour mes travaux de thèse. Néanmoins, il est important de noter que, comparées à d'autres fibroblastes, les cellules BJ expriment des niveaux très faibles de la protéine p16 (un inducteur de la sénescence), pouvant apporter un biais sur certaines expériences, notamment sur les expériences de sénescence.

# Résultats

# I. Article scientifique (manuscrit en préparation en anglais)

## Interplay between PML NBs and HIRA for H3.3 deposition on transcriptionally active interferon-stimulated genes

Kleijwegt C.[1], Bressac F.[1], Kimenyi-Ishimwe AB.[1,2], Cohen C.[1,3], Texier P.[1], Simonet T.[4], Schaeffer L.[4], Lomonte P.[1] and Corpet A.[1]

1. Univ Lyon, Université Claude Bernard Lyon 1, CNRS UMR5310, INSERM U1217, LabEx DEVweCAN, Institut NeuromyoGène (INMG), Team Chromatin Dynamics, Nuclear Domains, Virus F-69008, Lyon, France.
2. Current address: Centre de recherche de l'Hôpital Maisonneuve-Rochemont, 5415 boulevard de l'Assomption, Montréal, H1T 2M4, Canada.
3. Current address: Univ Montpellier, CNRS UMR 5235, Laboratory of Pathogen Host Interactions, F-34095, Montpellier, France.
4. Univ Lyon, Université Claude Bernard Lyon 1, CNRS UMR 5310, INSERM U 1217, Institut NeuroMyoGène (INMG), team Nerve-Muscle interactions. F-69008, Lyon, France

**Résumé**

Les corps nucléaires PML (PML NBs) sont des organelles sans membrane physiquement associé avec la chromatine soulignant leur rôle crucial dans la fonction du génome. Le complexe chaperon d'histones HIRA localise dans les PML NBs dans les cellules sénescentes ou sous infection virale. Cependant, les mécanismes moléculaires de cette accumulation et sa fonction dans la régulation de la dynamique des histones restent peu compris. Ici, nous montrons que deux voies indépendantes, les réponses inflammatoires et aux dommages à l'ADN, induisent la relocalisation d'HIRA dans les PML NBs. En utilisant des siRNAs spécifiques et des protéines Affimers, nous identifions les interactions intermoléculaires SUMO-SIM comme un mécanisme essentiel pour le recrutement de HIRA dans les corps nucléaires. Sous stimulation IFN-I, PML est requise pour la régulation positive immédiate des gènes stimulés par l'interféron (ISGs), ce qui corrèle avec la juxtaposition des loci ISGs avec les PML NBs. HIRA et PML sont nécessaires pour le dépôt prolongé d'H3.3 dans la région distale des ISGs, bien après le pic de transcription. Enfin, la perte d'H3.3 empêche l'arrêt de la transcription des ISGs. Nous proposons que l'accumulation d'HIRA dans les PML NBs régule le dépôt d'H3.3 au niveau des ISGs juxtaposant les PML NBs pour contrôler leur transcription et la réponse inflammatoire.

**Abstract**

Promyelocytic Leukemia Nuclear Bodies (PML NBs) are nuclear membrane-less organelles physically associated with chromatin underscoring their crucial role in genome function. The H3.3 histone chaperone complex HIRA localizes in PML NBs upon senescence or viral infection. Yet, the molecular mechanisms of this partitioning and its function in regulating histone dynamics have remained elusive. Here we show that two independent pathways, including the DNA damage and inflammatory responses, trigger HIRA relocalization in PML NBs. Using specific siRNAs and protein Affimers, we identify intermolecular SUMO-SIM interactions as an essential mechanism for HIRA recruitment in the nuclear bodies. Upon IFN-I stimulation, PML is required for the immediate transcriptional upregulation of interferon-stimulated genes (ISGs), which correlates with the juxtaposition of ISGs loci with PML NBs. HIRA and PML are necessary for the prolonged H3.3 deposition in the distal region of ISGs, well beyond the peak of transcription. Finally, abrogation of H3.3 prevents ISGs transcriptional shut-off. We propose that HIRA partitioning in PML NBs regulates H3.3 deposition on ISGs juxtaposed to PML NBs to control their transcription, which has physiological implications for inflammatory responses.

**Interplay between PML NBs and HIRA for H3.3 deposition on transcriptionally active interferon-stimulated genes**

Constance Kleijwegt[1], Florent Bressac[1], Aimé-Boris Kimenyi-Ishimwe[1,2], Camille Cohen[1,3], Pascale Texier[1], Thomas Simonet[4], Laurent Schaeffer[4], Patrick Lomonte[1,*] and Armelle Corpet[1,*]

1. Univ Lyon, Université Claude Bernard Lyon 1, CNRS UMR 5310, INSERM U 1217, LabEx DEVweCAN, Institut NeuroMyoGène (INMG), team Chromatin Dynamics, Nuclear Domains, Virus. F-69008, Lyon, France
2. Current address: Centre de recherche de l'Hôpital Maisonneuve-Rochemont, 5415 boulevard de l'Assomption, Montréal, H1T 2M4, Canada
3. Current address: Univ Montpellier, CNRS UMR 5235, Laboratory of Pathogen Host Interactions, F-34095, Montpellier, France.
4. Univ Lyon, Université Claude Bernard Lyon 1, CNRS UMR 5310, INSERM U 1217, Institut NeuroMyoGène (INMG), team Nerve-Muscle interactions. F-69008, Lyon, France

* To whom correspondence should be addressed.
Email : armelle.corpet@univ-lyon1.fr; patrick.lomonte@univ-lyon1.fr

**Abstract**

Promyelocytic Leukemia Nuclear Bodies (PML NBs) are nuclear membrane-less organelles physically associated with chromatin underscoring their crucial role in genome function. The H3.3 histone chaperone complex HIRA localizes in PML NBs upon senescence or viral infection. Yet, the molecular mechanisms of this partitioning and its function in regulating histone dynamics have remained elusive. Here we show that two independent pathways, including the DNA damage and inflammatory responses, trigger HIRA relocalization in PML NBs. Using specific siRNAs and protein Affimers, we identify intermolecular SUMO-SIM interactions as an essential mechanism for HIRA recruitment in the nuclear bodies. Upon IFN-I stimulation, PML

is required for the immediate transcriptional upregulation of interferon-stimulated genes (ISGs), which correlates with the juxtaposition of ISGs loci with PML NBs. HIRA and PML are necessary for the prolonged H3.3 deposition in the distal region of ISGs, well beyond the peak of transcription. Finally, abrogation of H3.3 prevents ISGs transcriptional shut-off. We propose that HIRA partitioning in PML NBs regulates H3.3 deposition on ISGs juxtaposed to PML NBs to control their transcription, which has physiological implications for inflammatory responses.

## Introduction

Eukaryotic nuclei constitute a crowded environment containing the densely packed genetic material together with all the biological macromolecules required to organize, replicate and interpret this genetic information. Promyelocytic Leukemia Nuclear Bodies (PML NBs) are membrane-less organelles, also called biomolecular condensates (Banani et al., 2017), that concentrate proteins at discrete sites within the nucleoplasm thus participating in the spatio-temporal control of biochemical reactions (Corpet et al., 2020; Lallemand-Breitenbach and de Thé, 2018; Li et al., 2020). In the majority of mammalian cell nuclei, PML NBs are found as 0.1-1μm diameter doughnut-shaped structures that vary in size and number depending on cell type, cell-cycle phase, or physiological state, highlighting their stress-responsive nature. The tumor-suppressor PML protein is the primary scaffold of PML NBs and forms an outer shell surrounding an inner core of dozens of proteins that localize constitutively or transiently in PML NBs (Van Damme et al., 2010). The *PML* gene was identified at the breakpoint of a common translocation t(15,17) resulting in a PML-retinoic acid receptor alpha (RARα) fusion protein which disrupts PML NBs and drives acute promyelocytic leukemia (APL) (de Thé et al., 2012).

PML (also known as TRIM19) is a member of the tripartite motif (TRIM)-containing protein superfamily characterized by a conserved RBCC motif. While several isoforms of PML exist, they all contain the N-terminal RBCC motif which is essential for PML polymerization and for recruitment of UBC9, the only SUMO E2-conjugating enzyme, driving NB formation. All PML isoforms contain three well-characterized small-ubiquitin-related modifier (SUMO) modification sites at lysines K65, K160 and K490 of the PML primary sequence as well as a SUMO interacting motif (SIM) enabling it to interact with SUMOylated proteins (Corpet et al., 2020; Kamitani et al., 1998). UBC9-

mediated SUMOylation of PML enforces PML-PML interactions via intermolecular SUMO-SIM interactions and drives the multivalent recruitment of inner core protein clients through their SIM possibly via liquid-liquid phase separation (LLPS) mechanisms (Corpet et al., 2020; Li et al., 2020; Sahin et al., 2014).

PML NBs have been involved in a wide variety of biological processes such as senescence, antiviral response, DNA damage response, or stemness suggesting that they are fully significant structures. However, the molecular mechanisms through which they exert their broad physiological impact are not fully elucidated yet. While PML NBs are mostly devoid of DNA, except in specific cases (for review (Corpet et al., 2020)), they reside in the interchromatin nuclear space (Boisvert et al., 2000) and can associate with specific genomic loci (Chang et al., 2013; Ching et al., 2013; Delbarre et al., 2017; Kumar et al., 2007; Kurihara et al., 2020; Shiels et al., 2001; Wang, 2004). In particular, PML NBs have been found associated with both transcriptionally-permissive domains, as well as heterochromatin regions such as telomeres suggesting an important function in chromatin domain organization and regulation of their transcriptional state.

Targeted deposition of histones variants is crucial for chromatin homeostasis and the maintenance of cell identity (Allis and Jenuwein, 2016). Among histone H3 variants, H3.3 is expressed throughout the cell cycle and is incorporated onto DNA in a DNA-synthesis independent manner by dedicated histone chaperone complexes (Martire and Banaszynski, 2020). Histone cell cycle regulator A (HIRA) chaperone complex, composed of HIRA, ubinuclein 1 or ubinuclein 2 (UBN1 or UBN2) and calcineurin-binding protein CABIN1 is responsible for H3.3 deposition in transcriptionally active regions including enhancers, promoters and gene bodies, as well as in nucleosome-free regions and DNA damage sites (Goldberg et al., 2010; Ray-Gallet et al., 2002; 2011; Zhang et al., 2017) (for review (Martire and Banaszynski, 2020; Ricketts and Marmorstein, 2016)). Anti-silencing function 1A (ASF1A) is considered as an auxiliary component and delivers H3.3-H4 dimers to the HIRA complex (Tang et al., 2006)(for review (Ricketts and Marmorstein, 2016)). In contrast, the histone chaperone complex comprising death-domain associated protein (DAXX) and α-thalassemia mental retardation syndrome X-linked (ATRX) targets H3.3 in specific heterochromatin regions such as telomeres, pericentromeric heterochromatin or endogenous retroviral sequences, and is required for H3.3-mediated deposition of H3

lysine 9 trimethylation (H3K9me3) to regulate transcriptional silencing (Chang et al., 2013; Drane et al., 2010; Elsässer et al., 2015; Goldberg et al., 2010; Sadic et al., 2015; Voon et al., 2015). In human somatic cells, a pool of neo-synthesized non-nucleosomal H3.3 is recruited to PML NBs by DAXX, which localizes constitutively in PML NBs together with ATRX, before deposition onto chromatin (Corpet et al., 2014; Delbarre et al., 2013), highlighting a key role of PML NBs in regulating the H3.3 chromatin assembly pathways (Corpet et al., 2014; Delbarre et al., 2013; 2017; Ivanauskiene et al., 2014). While HIRA complex is diffusively distributed in the nuclei of proliferating somatic cells, it relocalizes in PML NBs upon various stresses such as senescence entry (Banumathy et al., 2009; Rai et al., 2011; Zhang et al., 2005), a stable cell-cycle arrest playing an essential anti-tumoral role, viral infection (Cohen et al., 2018; Rai et al., 2017), or interferon type I (IFN-I) treatment (McFarlane et al., 2019; Rai et al., 2017). These latter events underscore a role of HIRA in intrinsic anti-viral defense via chromatinization of incoming viral genomes (Cohen et al., 2018; Rai et al., 2017) as well as stimulation of innate immune defenses in the case of viral infection (McFarlane et al., 2019).

However, the exact significance of HIRA localization in PML NBs upon stress response, as well as the role of the PML NBs themselves, remain unclear. PML NBs may both act as buffering/sequestration/degradation structures for various chromatin-related proteins, or may be a means to target them to specific chromatin regions juxtaposed to PML NBs. Here we investigated the signaling pathways as well as the mechanisms of HIRA relocalization in PML NBs. We show that HIRA relocalizes in PML NBs upon various independent signaling pathways, including pro-inflammatory and DNA damage responses, in a SIM-SUMO-dependent manner. In response to inflammation, we provide evidence that PML is required for interferon-stimulated genes (ISGs) expression, and that ISGs loci are juxtaposed to PML NBs. ChIP-Seq analysis reveals a long-lasting H3.3 deposition on the distal part of interferon-stimulated genes (ISGs), which is dependent on HIRA and PML. Finally, H3.3 depletion prevents ISGs transcriptional shut-down. Thus, our results shed light on how a PML NBs-HIRA-H3.3 axis finely tunes ISGs expression in inflammatory contexts.

## Results

### Independent signaling pathways trigger relocalization of HIRA in PML NBs

We first decided to extend the analysis of the various signaling pathways involved in HIRA's recruitment in PML NBs. In the majority of proliferating somatic cells, HIRA complex is diffusively distributed throughout the nucleus. While HIRA's relocalization in PML NBs has historically been linked to senescence entry (Banumathy et al., 2009; Jiang et al., 2011; Rai et al., 2011; Zhang et al., 2005), recent studies have underscored the importance of a viral infection with Herpes simplex virus 1 (HSV-1), a dsDNA containing virus, or transfection of a naked DNA, in triggering the recruitment of HIRA in PML NBs (Cohen et al., 2018; McFarlane et al., 2019; Rai et al., 2017). Recognition of microbial and viral products by Pattern Recognition Receptors (PRRs) can trigger secretion of pro-inflammatory cytokines and activation of the IFN-I signaling pathway is responsible for HIRA relocalization in PML NBs (Cohen et al., 2018; McFarlane et al., 2019; Rai et al., 2017). Of note, treatment of human primary foreskin diploïd fibroblast BJ cells with poly(I:C), a synthetic analog of double-stranded RNA simulating infection with RNA viruses, also triggered a strong relocalization of HIRA in PML NBs (Figure 1A). This relocalization was abrogated with ruxolitinib, an inhibitor of the JAK-STAT pathway downstream of the IFN-I receptor, extending the importance of the IFN-I response for triggering HIRA relocalization in PML NBs in a viral context (Figure 1A).

Senescent cells display hallmark features such as activation of an early DNA damage response (DDR), followed by the secretion of a complex mixture of cytokines and chemokines collectively known as the senescence-associated secretory phenotype (SASP) (Coppe et al., 2008). Interestingly, in addition to the proinflammatory IL-6 and Tumor necrosis factor $\alpha$ (TNF$\alpha$) cytokines and IL-8 chemokine (Coppe et al., 2008), IFN-I was also found in the SASP (Baz-Martínez et al., 2016; Cecco et al., 2019; Novakova et al., 2009), although its level only rises as a late-response phenotype that contributes to the SASP and ultimately to age-associated inflammation (Cecco et al., 2019). Upon replicative senescence, relocalization of HIRA increases progressively and appears as an early process concomitant with activation of the DDR and the SASP, but preceding the late IFN-I response (Cecco et al., 2019; Zhang et al., 2005). We thus hypothesized that alternative signaling pathways could be involved in the

relocalization of HIRA in PML NBs, and decided to clarify which cytokines/stresses may trigger its partitioning upon senescence entry.

We first tested whether IFN-I response was essential for HIRA relocalization in PML NBs upon senescence entry. We made use of IMR90 primary human fibroblasts stably expressing a 4-hydroxytamoxifen (4-OHT) inducible ER:Ras fusion protein (Young et al., 2009). After 3 days of 4-OHT treatment, we could observe HIRA relocalization in PML NBs concomitant with the activation of a DNA damage response marked by γH2A.X foci in immunofluorescence (Sup. Figures 1A-B). However, addition of ruxolitinib did not blunt the relocalization of HIRA in PML NBs (Sup. Figure 1A). These data suggest that IFN-I signaling is not sole responsible for the relocalization of HIRA in PML NBs in senescent cells. We investigated whether the pro-inflammatory SASP cytokines such as IL-6, IL-8, TNFα or activation of the DNA damage response, two hallmarks of senescent cells, could also be involved. Treatment of BJ cells with IL-6 or IL-8 for 24h did not alter HIRA pan-nuclear localization (Sup. Figure 1C). In contrast, the pro-inflammatory TNFα cytokine triggered a significant relocalization of HIRA in a dose- and IFN-I dependent manners (Figure 1B, Sup. Figure 1D). Transcription of the PML gene is known to be stimulated by IFN-I (Stadler et al., 1995) as well as by TNFα (Gao et al., 2008). Both IFNβ and TNFα increased the levels of the PML protein as seen by western blot analysis (Sup. Figure 1E), suggesting a related mechanism dependent on the IFN-I signaling pathway for triggering HIRA recruitment in PML NBs.

We then treated cells with the topoisomerase II inhibitor etoposide, a potent inducer of double-strand breaks (DSBs) at regions of topological problems arising during transcription or replication. This triggered a significant increase in the relocalization of all subunits of the HIRA complex in PML NBs, with in average 65.2% (±SD) of cells showing HIRA in PML NBs (Figure 1C and Sup. Figure 2A). In comparison, 80.5% (±SD) of cells treated with IFNβ, an IFN-I cytokine, showed HIRA in PML NBs (Figure 1C). DNA damage can lead to formation of micronuclei that can induce pro-inflammatory type I IFNs through activation of the cGAS-STING pathway (Harding et al., 2017; Mackenzie et al., 2017). Addition of ruxolitinib, which inhibits the IFN-I signaling pathway, did not affect HIRA relocalization in PML NBs upon etoposide treatment, unlike upon IFNβ treatment as expected (Figure 1C). In contrast, ATM inhibition strongly reduced the ability of the DNA damage to stimulate HIRA

relocalization in PML NBs (Sup. Figure 2B). Of note, PML protein level remained stable upon etoposide treatment in contrast to the increase observed upon IFNβ or TNFα stimulation (Sup. Figure 2C) comforting an IFN-I independent mechanism for HIRA relocalization in PML NBs. In addition, cells treated for a short time before recovery, with the DNA-damage drug neocarzinostatin (NCS) that triggers DSBs in a rapid manner, displayed HIRA at PML NBs in a time-scale that was faster than with etoposide treatment. Relocalization of HIRA was maximal at 3-6 hours of recovery post NCS treatment, reaching 51% of cells with HIRA in PML NBs at 6 hours of recovery, and then decreased at 24 hours of recovery (Figure 1D).

Thus, our data extend the signaling pathways involved in HIRA complex's relocalization in PML NBs, and define it as a broad stress response independently triggered by different mechanisms. We uncover two independent pathways triggering HIRA recruitment in PML NBs: an IFN-I pathway triggered by various stresses (DNA or RNA viruses, TNFα inflammatory cytokine) and a novel IFN-I-independent DNA damage response pathway.

**Relocalization of HIRA in PML NBs is dependent on SUMOylated PML**

Little is known about HIRA's targeting mechanisms to PML NBs. These nuclear bodies contain multiple chromatin-associated factors whose localization is regulated via a switch-like partitioning between the diffuse nucleoplasmic phase and the condensed PML NB phase (Banani et al., 2016; Corpet et al., 2020). Previous studies suggest that a valency-dependent partitioning of a given client protein is controlled by the multivalent interactions between its SIM motifs and SUMOylated lysines on the PML protein, as shown for DAXX (Banani et al., 2016; Sahin et al., 2014). We thus hypothesize that HIRA's recruitment in PML NBs may be regulated by a switch-like partitioning involving SUMO-SIM interactions. We first investigated whether HIRA and PML/SUMO could interact together *in cellulo*. We used Proximity Labelling Assay (PLA) which allows the detection of closely interacting protein partners *in situ* at distances below 40nm (Sahin et al., 2016). Using PLA, we detected interaction foci between PML and SUMO2/3 as expected (Sahin et al., 2016), and the number of interaction foci increased significantly upon IFNβ treatment (Figures 2A-B), which is known to stimulate PML SUMOylation (Stadler et al., 1995). We then applied PLA to assess interactions between HIRA and PML or HIRA and SUMO2/3. In presence of

IFNβ, we could detect a significant interaction between these proteins (Figures 2A-B), a condition under which HIRA relocalizes in PML NBs. Positive PLA signal between HIRA and SUMO2/3 could either mean that HIRA is SUMOylated or that HIRA interacts with other SUMOylated proteins. However, the molecular mass of HIRA remained unchanged upon IFNβ treatment of BJ cells (Sup. Figure 2C), as previously described (McFarlane et al., 2019), arguing against a post-translational modification of HIRA with SUMO groups. We thus conclude that HIRA interacts with SUMOylated PML *in situ*.

To confirm that SUMOylation of cellular proteins, including PML, is required for HIRA partitioning in PML NBs, we depleted the pool of SUMO1/2/3 by siRNA treatment, which led to the disappearance of most SUMOylated proteins in cells (Figure 2C). Depletion of SUMO1/2/3 led to a significant decrease of HIRA relocalization in PML NBs both upon IFNβ or etoposide treatment (Figure 2D). Of note, in absence of SUMO, PML NBs appear as large aggregates devoid of DAXX (Sup. Figure 3A), reminiscent of the alternative PML NBs structures observed during mitosis, in human embryonic stem cells or sensory neurons (Corpet et al., 2020). Thus, presence of SUMO proteins, that can undergo LLPS *in vitro*, seems key to promote partitioning of HIRA. Depletion of UBC9, the only known E2 SUMO conjugating enzyme in mammalian cells did not impair HIRA relocalization (Sup. Figure 3B-C) and (McFarlane et al., 2019)) nor DAXX localization in PML NBs (Sup. Figure 3A) underscoring the importance of removing the whole pool of SUMO proteins to impact on client recruitment and suggesting that the steady state SUMOylation levels are not sufficiently impacted by UBC9 depletion. On the contrary, overexpression of free SUMO proteins did not trigger HIRA accumulation in PML NBs (Sup. Figure 3D) suggesting that SUMO proteins need to be conjugated to specific proteins to trigger HIRA relocalization in PML NBs.

To further substantiate the requirements for non-covalent SUMO/SIM interactions in mediating HIRA relocalization in PML NBs, we used the Affimer technology, previously known as Adhiron. Affimers are artificial protein aptamers consisting of a scaffold with two variable peptide presentation loops that can specifically bind with high affinity and high specificity to their binding partners. A recent screen identified several Affimers that inhibit SUMO-dependent protein-protein interactions mediated by SIM motifs (Hughes et al., 2017). We selected the S1S2D5 Affimer that specifically targets both SUMO1 and SUMO2/3-mediated interactions and possesses a consensus

SIM motif (Hughes et al., 2017). We first verified the expression of the S1S2D5 Affimer from inducible 6xHis-tagged S1S2D5 Affimer-expressing BJ cells. S1S2D5-His Affimer showed a nuclear staining with accumulation of the Affimer in PML NBs as expected for a synthetic peptide that exhibits a SIM domain (Banani et al., 2016; Hughes et al., 2017) (Figure 3A). In conditions where the S1S2D5-His Affimer was expressed, we found that the relocalization of HIRA in PML NBs upon IFNβ stimulation or etoposide treatment was greatly impaired (Figures 3B and 3C). Immunofluorescence quantification revealed a significant decrease in the number of cells showing colocalization of HIRA within PML NBs in both conditions (Figure 3D). Importantly, SUMO-specific Affimers did not affect HIRA nor PML levels as verified by western Blot (Sup. Figure 3E). In addition, they do not prevent *in vivo* conjugation of SUMO by UBC9 (Hughes et al., 2017) corroborating our results (Sup. Figures 3A-C) and those of McFarlane (McFarlane et al., 2019) in the non-essential role of UBC9 in regulating HIRA partitioning. Instead our results demonstrate that SUMO/SIM interactions play a crucial role in the targeting of HIRA in PML NBs.

PML is known to be mainly SUMOylated on three major lysines K65, K160 and K490 (Kamitani et al., 1998). We took advantage of immortalized *pml-/-* mouse embryonic fibroblasts (MEFs) reconstituted with a doxycyclin-inducible wild-type Myc-tagged version of human PML (Myc-PML WT) or a PML mutated on its three main SUMOylation sites (Myc-PML 3K) to investigate the specific requirements for PML SUMOylation in HIRA partitioning (Figure 3E). Of note, super resolution microscopy analyses of these MEFs reveal that PML 3K form spherical structures exactly like WT PML (Sahin et al., 2014). In addition, we also verified that HIRA localization in PML NBs was conserved in wild-type MEFs upon treatment with a mouse IFNα and is lost in *pml-/-* MEFs (Sup. Figure 3F). Upon doxycyclin induction, Myc-PML WT or its mutated form were expressed at high levels in *pml-/-* MEFs, although addition of mouse IFNα lowered the expression levels of the tagged PML proteins (Figure 3E). Nevertheless, presence of the wild type exogenous tagged PML protein rescued HIRA localization in PML NBs upon IFNα addition while presence of the 3K mutated form of PML prevented it (Figure 3F). These data demonstrate that PML SUMOylation on K65, K160 and K490 is required for HIRA recruitment in PML NBs. Multivalent interactions between client SIM motifs and SUMOylated lysines on the PML protein are implicated in client recruitment in PML NBs, as shown for DAXX (Banani et al.,

2016; Sahin et al., 2014). Using JASSA (Beauclair et al., 2015) and GPS-SUMO (Zhao et al., 2014), we selected a set of 5 putative SIM motifs in HIRA protein sequence and tested whether they were involved in HIRA recruitment in PML NBs. BJ cells expressing the wild-type (WT) tagged version of HIRA (HIRA-HA WT) displayed ectopic HIRA localization in PML NBs upon IFNβ treatment (Figure 3G). While mSIM1 and mSIM3 mutants did not show sufficient expression to allow interpretation of their localization, none of the mSIM4 and 5 HIRA-HA mutants showed any defects in the localization in PML NBs (Sup. Figure 3G). In contrast, the HIRA-HA mSIM2 showed an impaired localization in PML NBs upon IFNβ treatment (Figure 3G). Although the number of cells expressing HIRA-HA mSIM2 remained rather low, we could observe in a significant number of individual cells a strong decrease of HIRA-HA mSIM2 mutant in PML NBs upon IFNβ stimulation (Figure 3G), suggesting the importance of this putative SIM in HIRA recruitment within PML NBs.

Having demonstrated that HIRA relocalizes by two independent pathways in PML NBs via a similar mechanism implicating SUMO/SIM interactions, we decided to focus on the functional role of this relocalization in the context of the inflammatory response, which has a crucial role in various physiological or pathological processes. In particular, IFN-I is responsible for the upregulation of hundreds of genes, collectively known as IFN-stimulated genes (ISGs) that interfere with virus replication (Schoggins and Rice, 2011). We therefore decided to further investigate the role of PML NBs and HIRA in the inflammatory transcriptional response.

**Transcription inhibition prevents HIRA relocalization in PML NBs**

PML NBs have been extensively linked with transcription: they are found in regions of high transcriptional activity (Boisvert et al., 2000; Kurihara et al., 2020; Wang, 2004) with accumulation of nascent RNA in their vicinity (Boisvert et al., 2000). CREB-binding protein (CBP), an histone acetyltransferase involved in positive transcriptional regulation, also localizes within PML NBs (LaMorte et al., 1998). We hypothesize that HIRA recruitment into PML NBs might be related to transcriptional activation of ISGs upon IFN-I treatment. We therefore assessed HIRA localization relative to PML NBs with various transcriptional inhibitors. Treatment of cells with DRB, a general transcription inhibitor that inhibits CDK9, the kinase subunit of P-TEFb required for productive elongation, for 6 hours significantly decreased

relocalization of HIRA. Frequency of cells showing HIRA in PML NBs decreased from 59% (±SD) in IFNβ-treated cells to 22.7% (±SD) in IFNβ+DRB-treated cells as shown by quantification (Sup. Figure 4A). We verified that treatment with DRB did not affect HIRA or PML levels by western blot analysis (Sup. Figure 4B). In addition, DAXX presence in PML NBs was not affected by DRB (Sup. Figure 4C) underscoring the fact that PML NBs are still able to recruit client proteins under this treatment. Identical results were obtained with other CDK9 inhibitors such as LDC067 (simplified as CDK9i) or flavopiridol, which decreased the number of cells showing HIRA localization in PML NBs (Sup. Figure 4D).

To corroborate our findings, we used alternative transcriptional inhibitors such α-amanitin, which triggers degradation of RNA polymerase II (Bensaude, 2014) or JQ1, a specific inhibitor for the bromodomains of the BET family proteins that inhibits Bromodomain protein 4 (BRD4) binding to acetylated histones (Qi, 2014). Bromodomain protein 4 (BRD4) is a BET family protein that binds to acetylated histones and recruits the positive elongation factor b (P-TEFb) to stimulate transcriptional elongation of many genes. In the context of IFN stimulation, recruitment of BRD4 to ISGs is inhibited by JQ1 which then blocks recruitment of P-TEFb to the ISGs, leading to the inhibition of their transcription (Patel et al., 2013). Inhibitors were added 1 hour before treatment with IFNβ for 24h. Immunofluorescence analysis followed by quantification showed a strong significant decrease of HIRA localization in PML NBs in presence of α-amanitin (Sup. Figure 4E), that did not impact HIRA nor PML protein levels, as seen by western blot analysis (Sup. Figure 4F). This suggests that it is the transcriptional inhibition *per se* that is responsible for loss of HIRA in PML NBs. Treatment of cells with JQ1 1 hour prior to IFNβ treatment also led to a significant decrease of HIRA relocalization in PML NBs (Sup. Figure 4G), while it did not impact DAXX presence in PML NBs (Sup. Figure 4C), nor impacted HIRA/PML levels (Sup. Figure 4H). Thus, the IFNβ-stimulated recruitment of HIRA in PML NBs is dependent on active transcription by RNA polymerase II.

**ISGs expression is impaired in PML depleted cells**

PML NBs as well as well as the PML protein itself and the HIRA complex have been associated with transcriptional regulation of specific genes (Corpet et al., 2020;

Kurihara et al., 2020; Martire and Banaszynski, 2020). We therefore assessed whether HIRA or PML could contribute to the transcriptional regulation of ISGs. We first analyzed the expression of a selected set of ISGs, *MX1*, *OAS1*, *ISG15* or *ISG54* (*IFIT2*), in cells treated with 100U/mL of IFNβ for 6 hours or 24 hours by RT-QPCR. mRNA levels of these ISGs increased strongly after IFNβ treatment, peaking at 6 hours of treatment. Transcripts levels then gradually decreased over time, although remained highly expressed at 24 hours of IFNβ treatment (Figure 4A). Of note, HIRA relocalization in PML NBs increased gradually over time but was only observed in more than 50% of the cells after 15h of IFNβ suggesting that it is a late event as compared to ISGs upregulation and that it might not be directly involved in their transcriptional upregulation (Figure 4B). We then analyzed mRNA levels of these ISGs in cells depleted of HIRA or PML. RT-QPCR and WB analysis confirmed a robust and specific depletion of each of these proteins by siRNA (Figure 4C). IFNβ stimulation did not significantly alter HIRA mRNA or protein levels, as shown previously (McFarlane et al., 2019; Rai et al., 2017), while it triggered moderate upregulation of PML (Sup. Figure 5A) (Stadler et al., 1995), as compared to the other ISGs studied (Figure 5A). Depletion of HIRA had no major impact on ISGs expression at 6 hours of IFNβ stimulation (Figure 4D), consistent with previous reports (McFarlane et al., 2019; Rai et al., 2017), while a slight but not significant increase of ISGs in the absence of HIRA was observed after 24h of IFNβ. In contrast, PML depletion led to a dramatic reduction in ISGs expression both at 6 hours and 24 hours after IFNβ stimulation (Figure 4D). *MX1*, *OAS1*, *ISG15* or *ISG54* mRNA levels were only 27%, 16%, 28% or 35 % of the levels observed in IFN 6h-treated cells respectively. The effect of PML depletion was slightly less dramatic in cells treated with IFN for 24 hours in which ISGs expression tends to decrease. Thus, the results suggest an essential role of PML in the IFN-dependent transcriptional upregulation of ISGs, that is independent of HIRA.

**Interferon-stimulated gene loci are juxtaposed to PML NBs after IFN-I stimulation**

PML NBs make direct physical contacts with surrounding chromatin regions and these associations may serve to modulate genome functions (Corpet et al., 2020). In particular, PML depletion led to a marked reduction in the expression of a subset of Y-linked genes that are closely associated with PML NBs suggesting a crucial role of

PML NBs in transcriptional regulation of specific genes (Kurihara et al., 2020). In the context of the inflammatory response, it was previously shown that the nuclear DNA helicase II (NDH II), which is essential for gene activation, relocalizes in PML NBs in a transcription-dependent manner and could play a role in the transcriptional regulation of ISGs attached to PML NBs, although this later point was not investigated (Fuchsová et al., 2002). In addition, in response to IFNγ, genes within the MHCII locus are located closer to PML NBs (Gialitakis et al., 2010). Given the role of PML in ISGs upregulation upon IFNβ stimulation (Figure 4D), we thus decided to examine the spatial relationship between PML NBs and specific ISG loci. We performed immunostaining of the PML protein, together with fluorescence *in situ* hybridization (immuno-FISH) to DNA of the *PML*, *MX1*, *OAS1* gene loci in BJ cells treated with IFNβ. PML was used as a positive ISG control since previous immuno-trap analyses found a specific interaction between PML NBs and the *PML* gene locus, that is increased upon IFNα treatment (Ching et al., 2013). *MX1* and *OAS1* are well-known ISGs (Schoggins and Rice, 2011). To evaluate the specificity of potential spatial changes, we also scored localization of the Grehlin and Obestatin Prepropeptide (*GHRL)* locus. *GHRL* is not induced by IFNβ in BJ cells (Eggenberger et al., 2019) and its locus is found in heterochromatin regions (Becker et al., 2017). Visual inspection showed an overall closer locus-PML NB association of *PML*, *MX1* and *OAS1* in IFNβ-treated cells relative to untreated cells, which was not observed for *GHRL* (Figure 5A). In addition, by performing a three-color immuno-FISH, we verified that HIRA effectively localizes in the PML NB juxtaposed to the ISG loci (Sup. Figure 5B). To quantify the association of PML NB with ISG loci, we calculated the minimal distance between each locus and the closest PML NB per nucleus in untreated and treated cells. Median minimal distance (mmd) decreased to 1.1µm after 24h of IFNβ for the *GHRL* locus, as compared to a decrease to 0.91µm, 0.93µm and 0.96µm for the *PML*, *MX1* or *OAS1* loci, respectively (Figure 5B). Of note, the decrease in mmd was stronger for *MX1* and *PML* loci after 48h of IFNβ stimulation, reaching a calculated mmd of respectively 0.67µm and 0.72µm while it remained stable for the *GHRL* locus (1.06µm) (Figure 5B). Since PML NBs are known to increase in size and number upon IFNβ treatment (Figure 5C), we reasoned that the decreased distance observed might be a consequence of the higher number of PML NBs. We thus normalized the mmd for the ISGs to the mmd calculated

for the *GHRL* locus. A marked decrease in the association of PML NBs with the *PML*, *MXI* and *OAS1* loci was still scored, although it was only statistically significant for the *PML* and *MX1* loci (Figure 5D). While the nucleoplasmic pool of PML is required for transcription of ISGs which peaks at 6h (Figures 4A and D), juxtaposition of PML NBs with ISG loci was observed at late time-points after 24h and 48h of IFNβ stimulation, suggesting *de novo* formation of PML NBs at ISGs loci mediated by nucleation of PML proteins involved in ISGs transcription. Thus, the immuno-FISH analysis demonstrates that loci-PML NBs associations are not random, and that new associations between ISGs and PML NBs are found upon IFN-I stimulation.

**IFN-I stimulation triggers accumulation of endogenous H3.3 in the distal region of ISGs**

Using a tagged version of H3.3 in MEF cells, previous studies showed an increased and prolonged deposition of ectopic H3.3 in the transcription end sites (TES) region of ISGs upon IFN-I stimulation (Sarai et al., 2013; Tamura et al., 2009). Since the H3.3 histone chaperone complex HIRA localizes in PML NBs which are juxtaposed to ISGs (Figures 5A and D), we wondered if this would impact H3.3 deposition patterns on ISGs. To investigate this matter, we took advantage of an H3.3-specific antibody, that was previously validated in ChIP (Lee et al., 2019), to monitor the endogenous H3.3 occupancy on specific ISGs following IFNβ-induced transcription. Levels of H3.3 were unaffected by 24 hours of IFNβ stimulation as seen by RT-QPCR or WB treatment (Sup. Figure 6A). We first investigated H3.3 incorporation on *MX1*, *OAS1* and *ISG54* (*IFIT2*) which are representative ISGs induced upon IFNβ stimulation. ChIP assays with the H3.3-specific antibodies were performed over three distinct regions of the selected ISGs: the promoter region, located just upstream (-120pb) of the transcriptional start site (TSS), the middle of the coding region (mid), and a distal site in the coding region near the transcriptional end site (TES) (see map in Figure 6A). IFNβ treatment for 24 hours did not increase H3.3 occupancy at promoter regions, but rather slightly decreased it (Figure 6A). This reduction following IFN stimulation likely reflects transcription-induced nucleosome depletion known to happen for many genes (Workman, 2006). Remarkably, IFNβ stimulation induced H3.3 incorporation most noticeably over the distal site of the coding region (Figure 6A). Use of a non-targeting IgG antibody did not lead to any significant amount of

immunoprecipitated DNA (% input) in any of the conditions highlighting the specificity of our ChIP experiment (Sup. Figure 6B). In addition, no change in H3.3 occupancy was observed at an enhancer region known to be enriched with H3.3 (Pchelintsev et al., 2013), underscoring the specificity of H3.3 incorporation in ISGs (Figure 6A). To investigate the relationship between IFN-induced H3.3 deposition and ISGs expression, we performed ChIP-QPCR in a time-course after IFNβ stimulation. When looking at H3.3 deposition, no significant increase was observed at representative mid or TES regions at 6 or 12 hours of IFNβ treatment (Sup. Figure 6C). This suggests that the induced H3.3-deposition is taking place after the peak of transcription, and corroborates our previous data on the unlikely contribution of HIRA in ISGs transcription. Importantly, the induced H3.3 deposition seen at 24h of IFNβ continued for an extended period of time and was even higher after 48 hours of IFNβ suggesting that it may leave a long-lasting chromatin mark on ISGs (Sup. Figure 6C).

To get a more comprehensive picture of endogenous H3.3 deposition, we performed ChIP-Seq analyses on cells treated with IFNβ for 24 hours. We first examined H3.3 enrichment over the gene bodies of a published panel of equivalent sized ISGs or non-interferon stimulated genes (non-ISGs) (McFarlane et al., 2019). The levels of H3.3 significantly increased on ISGs in IFNβ-treated cells with a clear bias towards the TES region of the genes (Figure 6B). The drop of H3.3 at the TSS region was higher in IFNβ-stimulated cells reflecting transcription-induced nucleosome depletion as observed by QPCR. In contrast, no significant difference of H3.3 enrichment could be observed across the non-ISGs (Figure 6C). We selected genes for which the difference in H3.3 enrichment at the TES region between IFNβ treated and non treated cells was the highest and perform Gene Ontology (GO) analysis to get a view of their nature. GO analysis showed an enrichment in genes involved in IFNα and IFNγ response comforting the specific enrichment of H3.3 on the TES region of ISGs as a prolonged response after IFNβ stimulation (Figure 6D). In addition, to evaluate the identity of H3.3-enriched genes in an unbiased manner, we performed an independent GO analysis on all genes found in our ChIP peak calls. This yielded similar results with IFNα and IFNγ responses being the most highly significant GO terms (Sup. Figure 6D), thus reflecting a specific H3.3 deposition on genes linked to IFN response.

**H3.3 deposition on ISGs is impaired upon HIRA or PML depletion**

HIRA is involved in deposition of H3.3 in genic regions, including enhancers and promoters (Goldberg et al., 2010; Martire and Banaszynski, 2020; Zhang et al., 2017). As shown above, following IFNβ stimulation, HIRA and ISGs concomitantly relocalize in, and juxtapose with PML NBs, respectively. While HIRA is not directly implicated in the transcriptional upregulation of ISGs (Figure 4), we wondered whether HIRA was still essential for H3.3 deposition at ISGs observed mainly in the TES region. In addition, PML NBs have been proposed to facilitate the routing of H3.3 histones and their histone chaperones from the nucleoplasm to chromatin (Corpet et al., 2014; Delbarre et al., 2013). PML may both promote or prevent H3.3 deposition depending on the level of differentiation, the cell-cycle stage or the loci considered (Chang et al., 2013; Delbarre et al., 2017; Shastrula et al., 2019; Spirkoski et al., 2019). We thus performed ChIP-QPCR analysis in cells depleted of HIRA or PML and treated with IFNβ for 24 hours. Knock-down efficiency was verified by western blot analysis and showed a strong depletion of both proteins (Figure 6E). When looking at mid or TES regions of selected ISGs, we observed a moderate but consistent decrease in H3.3 deposition in absence of HIRA or PML (Figure 6E), suggesting the importance of these two proteins for the long-lasting H3.3 deposition on ISGs. ChIP-Seq analysis of HIRA-depleted or PML-depleted cells showed a significant decrease (p-value = 4,76e-03 or 1.262e-03 respectively, as assessed by a paired Student's t-test) in the loading of H3.3 on the panel of ISGs (Figure 6F), with two representative examples shown in Figure 6G. We thus conclude that HIRA and PML both contribute to the increased long-lasting H3.3 deposition in the TES region of ISGs.

**H3.3 depletion leads to an increase in ISGs expression**

We wondered what could be the role of the significant increase in H3.3 deposition in the TES region of ISGs. We used previously published siRNA to target both *H3F3A* and *H3F3B* gene products (Adam et al., 2016; Cohen et al., 2018; Zhang et al., 2007) to investigate this manner. Knock-down efficiency was verified by RT-QPCR and showed a strong depletion of H3.3 (Figure 7A). We then analyzed mRNA levels of selected ISGs in cells depleted of H3.3 for 48h prior to addition of IFNβ in the last 6h or 24h. Strikingly, H3.3 depletion led to a significant upregulation of all 4 ISGs after 6 hours

of IFNβ (Figure 7B), which could indicate facilitation of the ISGs transcriptional induction with a low nucleosome occupancy at promoter regions. Upregulation of ISGs in H3.3-depleted cells was even stronger after 24h for 3 ISGs as compared to siLuc-treated cells (Figure 7B), in a situation where ISGs expression is normally decreasing (Figure 4A). This suggests that H3.3 depletion impairs the shut-down of transcription of ISGs after 24h of IFN-I stimulation, and comforts the essential role of HIRA and PML-dependent long-lasting deposition of H3.3 at the distal regions of ISGs to regulate their expression.

**Discussion**

There has been considerable efforts in defining the multiple roles of PML NBs in the recent years including in chromatin dynamics. Our work underscores the role of PML NBs structure in regulating both the transcriptional status of ISGs and the HIRA-mediated H3.3-deposition at these transcriptionally active ISGs, thus strongly supporting a role of PML NBs in transcriptional regulation (Corpet et al., 2020). We discuss how the PML NBs-HIRA chaperone axis may help to fine-tune stress-responsive responses, including the IFN-I response, as both overactivation and underactivation can be deleterious to the host.

**Various signaling pathways are implicated in HIRA partitioning in PML NBs**

First, we show that HIRA partitioning in PML NBs occurs in a specific stress-responsive manner. While IFN-I signaling pathway was recently shown to be responsible for the relocalization of HIRA after a viral infection (Cohen et al., 2018; McFarlane et al., 2019; Rai et al., 2017), we have now extended and corroborated these findings by showing that various inflammatory stresses, including TNFα, or a synthetic dsRNA (PolyI:C), which triggers IFN-I signaling pathway through PRRs, can also mediate HIRA recruitment in PML NBs. Inflammatory responses play an essential role in a wide range of physiological and pathological biological phenomena such as viral infection, DNA damage, or aging (Medzhitov, 2008). In particular, the recent SARS-CoV2 pandemic, causing COVID-19, has underlined importance of the innate immune that triggers transcription of IFN-I, as well as of TNFα, followed by induction of numerous ISGs with various anti-viral functions (for review (Schultze and Aschenbrenner, 2021)). Impaired IFN-I response was recently associated with

COVID-19 severity (Hadjadj et al., 2020; Trouillet-Assant et al., 2020)(for review (Schultze and Aschenbrenner, 2021)). Interestingly, members of the HIRA chaperone complex as well as PML have been identified as anti-viral factors in a genome-wide CRISPR screen (Wei et al., 2021). Whether this anti-viral role may relate to their function in ISG transcriptional induction and H3.3 deposition remains to be investigated.

Senescence was the first stress shown to induce relocalization of HIRA complex in PML NBs (Banumathy et al., 2009; Jiang et al., 2011; Rai et al., 2011; Zhang et al., 2005). Recruitment of HIRA to PML NBs in this context does not require functional pRB or p53 tumor suppressor pathways (Ye et al., 2007a). We now show that HIRA relocalization in PML NBs in oncogene-induced senescent cells does not rely on IFN-I signaling pathway, which is activated in the late senescence cells (Cecco et al., 2019), but likely relies on the DNA damage pathway. The HIRA histone chaperone has a well-described role in UV damage repair. It accumulates at sites of UVC damage, promoting deposition of newly synthesized H3.3 after completion of repair (Adam et al., 2013). While we did not observe HIRA relocalization in PML NBs upon UV radiation (data not shown and (Rai et al., 2017)), our results put forward a specific and novel role of DSBs induced by etoposide or NCS for HIRA recruitment in PML NBs, that is independent of the IFN-I signaling pathway. These results are not matching previous findings by Rai et al showing that etoposide or ionizing radiations failed to recruit HIRA in PML NBs (Rai et al., 2017). This seemingly discrepancy could probably be attributed to different doses, time recovery after damage, or cell lines. Further studies will evaluate the exact contribution of the relocalization of HIRA in PML NBs in the DSB repair pathways. Interestingly, PML NBs are juxtaposed to persistent DSBs (Vancurova et al., 2019). These nuclear bodies contain many DDR related proteins and have been implicated in HR-mediated DNA repair (Carbone et al., 2002; Dellaire et al., 2006; Vancurova et al., 2019) (for review (Chang et al., 2018)). In addition, newly synthesized H3.3 is incorporated at local DSB sites, likely contributing to the re-establishment of chromatin structure after DNA damage (Juhász et al., 2018; Luijsterburg et al., 2016). We found that HIRA relocalization in PML NBs is dependent on ATM, the main kinase involved in the HR repair pathway. We thus hypothesize that HIRA's targeting in PML NBs upon DNA damage may help to manage H3.3 histone dynamics at HR-mediated DSB repair sites, which are juxtaposed to PML NBs. Studies,

in progress in our laboratory, will help to decipher the interplay between HIRA and PML NBs in the chromatin dynamics in response to DSB induction.

**HIRA recruitment in PML NBs is dependent on functional SUMO/SIM interactions**

Control of the composition of membrane-less organelles such as PML NBs have recently been revisited through the prism of LLPS (for reviews (Alberti et al., 2019; Banani et al., 2017; Corpet et al., 2020). Regulation of the composition of PML NBs is crucial for their function and implies SUMO/SIM interaction modules whose valency and affinity regulate interactions between the PML scaffold protein and client proteins (Corpet et al., 2020). Here, we show that HIRA partitioning in PML NBs is indeed mediated by SUMO/SIM interactions, that can be inhibited with specific Affimers (Figure 3). Interestingly, HIRA and/or UBN1 were identified as SUMOylated proteins on K809 and K530 respectively in various SUMO screens (Hendriks et al., 2014; Schimmel et al., 2014). However, our western blot analysis as well as results from McFarlane et al. do not support modification of HIRA with SUMO groups upon IFNβ stimulation. In addition, ectopic HIRA mutated on a K809 was still recruited in PML NBs similar to the wild-type protein (Sup. Figure 7A), suggesting that lysine K809 is dispensable for HIRA recruitment in PML NBs. Remarkably, SIM-containing clients, as exemplified with DAXX (Sahin et al., 2014), are favored for partitioning in endogenous PML NBs containing a higher valency of SUMO sites compared to SIM sites (Banani et al., 2016). Increase in PML SUMOylation upon IFNβ stimulation (Sup. Figure 1E) (Stadler et al., 1995) could thus trigger the switch-like partitioning of HIRA in PML NBs thanks to an increase in free SUMO sites. Our data using *Pml*$^{-/-}$ MEFs reconstituted with PML WT or PML 3K confirm the importance of PML main SUMOylation sites in recruiting HIRA complex. In addition, we identified a putative SIM motif on HIRA sequence that may participate in HIRA complex recruitment in PML NBs. Interestingly, the VLRL SIM motif identified is followed by a Serine. Phosphorylation adjacent to SIM motifs could lead to an increased affinity towards SUMO1 lysine residues (Cappadocia et al., 2015). One could hypothesize that other post-translational modifications such as phosphorylation could thus be important in regulating HIRA partitioning by changing the affinity between HIRA and SUMOylated PML proteins/partners. Of note, glycogen synthase kinase 3 β (GSK-3β) mediated-

phosphorylation of HIRA on S697 was suggested to drive HIRA relocalization to PML NBs upon senescence entry (Ye et al., 2007b). However, we did not observe any defects in the localization of an ectopic form of HIRA mutated on S697 (HIRA-HA S697A) upon IFNβ stimulation (Sup. Figure 7B), and GSK-3β inhibitors did not alleviate the localization of HIRA in PML NBs in response to IFNβ stimulation similarly to observations by McFarlane et al (McFarlane et al., 2019). Thus, HIRA partitioning in PML NBs relies on SUMO/SIM interactions after IFN-I stimulation or DSB induction. The use of SUMO-specific Affimers opens up interesting avenues to interfere with client recruitments in PML NBs including HIRA, but caution should be taken with their use since they inhibit all SUMO/SIM interactions.

**PML NBs associate with ISG loci**

Numerous studies have underscored a close connection between PML NBs and specific chromatin regions (Chang et al., 2013; Ching et al., 2013; Delbarre et al., 2017; Kumar et al., 2007; Kurihara et al., 2020; Shiels et al., 2001; Wang, 2004). Here, using immuno-FISH, we demonstrate a closer association of a subset of ISG loci with PML NBs after IFNβ stimulation underscoring the probable importance of PML NBs-gene loci association as a marker of the physiological state of the cell. Yet, the mechanisms regarding this increased association upon IFNβ stimulation remains to be investigated. PML targeting at specific gene loci is sufficient to induce *de novo* formation of PML NBs (Brouwer et al., 2009; Chung et al., 2011; Erdel et al., 2020; Kaiser et al., 2008; Wang et al., 2018). Our expression analysis underscores the importance of the PML protein for the initial burst of transcription of ISGs after 6 hours of IFNβ stimulation, consistent with the association of PML NBs with transcriptional sites after IFNα stimulation, as shown by visualization of nascent transcripts (Fuchsová et al., 2002) and consistent with the role of PML in ISGs induction following viral infection (Alandijany et al., 2018). PML proteins could be recruited to transcriptionally active ISGs by a specific, yet to be defined, protein-protein interaction, and these chromatin-bound PML proteins could then act as seeds to mediate nucleation of new PML NBs close to ISG loci (Corpet et al., 2020) (see model in Figure 7C). This would explain why juxtaposition of PML NBs with ISGs is monitored at late time-points of IFNβ stimulation (Figure 5). One of these proteins could be STAT2, a protein member of the Interferon Simulated Gene factor 3 (ISGF3)

complex that is required to activate transcription of ISGs. STAT2 binds to CBP (Bhattacharya et al., 1996) that localizes in PML NBs (Doucas et al., 1999; LaMorte et al., 1998; Mikecz et al., 2000) and could thus mediate recruitment of PML to ISGs. In addition, BRD4 recruitment to ISGs is concomitant to STAT2 (Patel et al., 2013) suggesting an interplay between the ISGF3 complex and the BRD4-CBP-PolII machinery to recruit PML/PML NBs to ISGs. Using various transcriptional inhibitors, including CDK9 inhibitors or the BET inhibitor JQ1, we show that HIRA recruitment in PML NBs is dependent on transcription (Sup. Figure 4). Interestingly, PML was recently shown to be essential for HIRA recruitment to ISGs loci (McFarlane et al., 2019). Thus, PML role in ISGs transcription could both mediate PML NBs formation close to ISGs as well as HIRA recruitment on these ISGs. Alternatively, movement of ISGs and/or of a preexisting PML NB toward each other could explain this closer association.

Recently, the use of an APEX2 peroxidase fused to PML in mouse ESCs to mediate chromatin labeling and purification combined with deep-sequencing (ALaP-Seq) allowed the identification of chromatin regions proximal to PML NBs. PML NBs were shown to associate with active genes located in an open chromatin environment and were required to maintain specific Y-linked genes expression through exclusion of DNMT3A (Kurihara et al., 2020). Use of this method could nicely complement our immuno-FISH analysis to identify genome-wide changes in PML-NBs-chromatin associations upon IFN stimulation.

**H3.3-induced deposition in the TES region of ISGs is mediated by HIRA and PML**

Several studies have demonstrated a HIRA-dependent enrichment of H3.3 at active genes. HIRA is enriched at specific promoters and enhancers regions and is required for deposition at these sites. In addition, HIRA can interact with both RNA pol II and naked DNA providing means for H3.3 deposition coupled to transcription (Pchelintsev et al., 2013; Ray-Gallet et al., 2011; Zhang et al., 2017). Here, we investigated the role of HIRA in the H3.3-mediated deposition on ISGs. We first show that endogenous H3.3 displays a long-lasting deposition, increasing after the peak of transcription of the ISGs up to 48h after IFN-I stimulation, and with a strong preference for the TES region, consistent with previous reports obtained in MEF cells (Sarai et al., 2013; Tamura et al., 2009). Deposition of endogenous H3.3 was reduced

in the absence of PML consistent with the role of PML NBs in targeting H3.3 to chromatin (Delbarre et al., 2013). Alternatively, since PML depletion impairs transcription of ISGs, it could affect H3.3 deposition at TES regions, which is linked to transcriptional activity *per se* of ISGs (Sarai et al., 2013). HIRA depletion also impaired H3.3 deposition consistent with its known function in H3.3-nucleosome assembly. HIRA interacts with RNA pol II and also with H3K36me3 (Ray-Gallet et al., 2011; Torné et al., 2020), a histone mark added by the methyltransferase SETD2, which moves with RNA pol II during transcription (Yoh, G&D 2008). In MEFs, HIRA also interacts with WHSC1, an H3K36me3 methylase that recruits HIRA for prolonged H3.3 deposition on ISGs (Sarai et al., 2013). Since H3K36me3 was also found to be enriched in the distal part of ISGs in our IFNβ treated cells (Sup. Figure 6E), one could thus hypothesize that similar recruitment of HIRA via the H3K36methylase/H3K36me3 mark might be at play.

The role of the prolonged H3.3 deposition on ISGs can be multiple. First, this long-lasting mark could contribute to the acquisition of a functional IFN memory. Indeed, H3.3 was shown to mediate memory of an active state upon nuclear transfer in *Xenopus laevis* (Ng and Gurdon, 2007). In addition, in mouse embryonic fibroblasts, IFNβ stimulation creates a transcriptional memory of a subset of ISGs, which coincides with acquisition of H3.3 and H3K36me3 on chromatin (Kamada et al., 2018). Second stimulation with IFNβ allows a faster and greater transcription of memory ISGs, which is dependent on H3.3 deposition in the first stimulation phase (Kamada et al., 2018). However, H3.3 mark could only mediate a short-term memory as shown recently in IFNγ memory in HeLa cells (Siwek et al., 2020). In HeLa cells, PML was required for the stronger reexpression of HLA-DRA after IFNγ restimulation, a locus that remained juxtaposed to PML NBs after transcription shut-off (Gialitakis et al., 2010). Here, we found a juxtaposition of PML NBs with ISGs that is posterior to the peak of ISGs transcription and that increases over IFNβ treatment. Whether this juxtaposition is kept after IFNβ removal remains to be investigated. Nevertheless, the close association of PML NBs with ISGs can mediate the HIRA/PML-dependent H3.3 long-lasting deposition in the distal region of ISGs (Figure 7C), which could contribute to the acquisition of a functional short-term IFN memory.

Alternatively, H3.3 deposition may also serve to directly regulate ISGs expression. In mouse cells, H3.3 was found to be phosphorylated on Serine 31 on stimulation-

induced genes, a mark that could serve as an ejection switch of the ZMYND11 transcriptional repressor thus amplifying the transcription of these genes (Armache et al., 2020). While we have not investigated H3.3S31P deposition on ISGs, our data rather suggest a repressive role of H3.3 in ISGs transcription. Indeed, we show that siRNA depletion of H3.3 increased ISGs transcription and sustained ISGs transcription at 24 hours of IFNβ stimulation underscoring the importance of H3.3 incorporation to shut-down the inflammatory response. Of note, siRNA depletion of HIRA led to a slight increase of ISGs after 24h of IFNβ as compared to NT (Figure 4D), but it remained non significant as compared to the strong increase seen upon total H3.3 depletion. Together with our ChIP data showing a moderate reduction in H3.3 incorporation upon HIRA depletion, this suggests that other histone chaperones such as the DAXX/ATRX complex which localizes in PML NBs, could potentially compensate for the loss of HIRA and deposit H3.3 on ISGs. Enrichment of H3K36me3 was observed concomitantly to H3.3 in the TES region of ISGs, consistent with previous studies (Sarai et al., 2013; Tamura et al., 2009). This mark is linked to histone deacetylation and transcription repression (Workman, 2006) and could thus explain in part the inhibitory effect of H3.3 deposition on ISGs transcription.

Of note, our data do not exclude that HIRA complexes present in PML NBs are sequestered and prevented to exert their histone chaperone function in the rest of the nucleus. Indeed, no major changes were observed for HIRA levels after IFN-I treatment, with a non significant increase in RNA levels (Sup. Figure 5A) and no detectable changes at the protein level (Sup. Figure 4) (McFarlane et al., 2019; Rai et al., 2017) anticipating a decrease of HIRA complexes in the nucleoplasm. In particular, a specific role for HIRA in recycling old evicted histones during transcription has recently been put forward (Torné et al., 2020). Improper recycling of old histones during transcription of house-keeping genes could potentially put the maintenance of chromatin organization and the epigenome at risk.

In conclusion, we propose the following model for the role of PML NBs during inflammatory response (Figure 7C). PML would be recruited to ISGs upon stimulation and is required to mediate their transcription upregulation as observed at 6h of IFN-I. Accumulation of PML proteins on ISGs would serve as a seed to mediate nucleation of PML NBs juxtaposed to ISGs at later time-points after transcriptional peak. HIRA would be recruited to ISGs in a PML-dependent manner (McFarlane et al., 2019) and

would mediate prolonged deposition of H3.3 on ISGs. HIRA would accumulate in pre-existing but also neo-nucleated PML NBs in a SIM/SUMO-dependent manner and remain juxtaposed to ISGs at late timepoints. While PML- and HIRA-dependent H3.3 deposition seems required for the shut-down of ISGs expression, it could also potentially serve to mediate a short-term epigenetic memory of the transcriptional status. Thus, our findings highlight the importance of the interplay between PML NBs and H3.3 chromatin dynamics to maintain gene expression patterns and chromatin homeostasis.

## Materials and Methods

### *Cell lines and lentiviruses production*

Human BJ primary foreskin fibroblasts (ATCC, CRL-2522), Human IMR90 fetal lung fibroblasts (ATCC, CCL-186), human HEK 293T embryonic kidney cells (Intercell, AG) and mouse MEFs embryonic fibroblasts $PML^{-/-}$ (from Dr. Lallemand-Breitenbach) were cultivated in DMEM medium (Sigma-Aldrich, D6429) containing 10% of fetal calf serum (FCS) (Sigma-Aldrich, F7524), 1% of penicillin/streptomycin (Sigma-Aldrich, P4458), at 37°C under 5% CO2 and humid atmosphere.

Drugs and molecules used for cell treatments are described in **Table 1** (duration is mentioned in the main text).

**Table 1: Lists of drugs and molecules used in this study**

| Name | Reference | Final concentration |
|---|---|---|
| 4-Hydoxytamoxifen (4-OHT) | Sigma-Aldrich, H7904 | 100ng/mL |
| α-amanitin | Sigma-Aldrich, A2263 | 2µg/mL |
| ATMi KU-55933 | Sigma-Aldrich, SML1109 | 5µg/mL |
| CDK9i (LDC067) | Sigma-Aldrich, SML2179 | 10µM |
| Doxycycline | Sigma-Aldrich, D9891 | 100ng/mL |
| DRB | Sigma-Aldrich, D1916 | 50µM |
| Etoposide | Alexis, 270-209-M100 | 10µM |
| Flavopiridol | Euromedec, SE-S1230 | 50nM |
| IFNβ (human, recombinant) | Peprotech, 300-02BC | 100 or 1000U/mL |
| IFNα (mouse, recombibnant) | PBL assay science 12105-1 | 1000U/mL |
| IL-6 (human, recombinant) | Peprotech, 200-06 | 200ng/mL |
| IL-8 (human, recombinant) | Peprotech, 200-08 | 200ng/mL |
| JQ1 | Sigma-Aldrich, SML1524 | 100-1000nM |
| Neocarzinostatin | Sigma-Aldrich, N9162 | 100ng/mL |
| PolyI:C | Invivogen, tlrl-pic | 10µg/mL |
| Ruxolitinib | Invivogen, tlrl-rux | 2µM |

BJ, MEFs or IMR90 cells stably expressing transgenes were obtained by lentiviral transduction. Briefly, lentiviruses were produced in HEK 293T cells transfected by calcium-phosphate method with lentiviral plasmid containing the construct of interest, as well as psPAX.2 and pMD2.G packaging vectors in a 3:2:1 ratio. After 48h, the medium containing lentiviruses was filtered and applied on cells for transduction in complete medium containing polybrene at 8μg/mL final concentration. Transduced cells were then selected 24h later by adding the appropriate selective drug (puromycin (Invivogen, ant-pr) at 1μg/mL or blasticidin (Invivogen, ant-bl) at 5μg/mL)

***Plasmids***

Tat-S1S2D5-Flag-His Affimer (Tat: nuclear localization sequence), obtained by PCR using pcDNA5-Tat-S1S2D5-Flag-His as template (graciously sent by Dr. David J. Hughes (Hughes et al., 2017)), was cloned in puromycin resistant pLVX-TetOne plasmid with BamHI and BstZ17I restriction enzymes.

HIRA-HA WT, obtained by RT-PCR from HeLa cells, was cloned in blasticidin resistant pLentiN plasmid with EcoRI and XhoI restriction enzymes. HIRA-HA mSIM and K809G mutants were obtained by site-directed mutagenesis using QuickChange Lightning Site-directed Mutagenesis kit (Agilent Technologies, #210518). mSIM mutant sequences are the following: mSIM1: aa $^{124}$VSIL$^{127}$ mutated in $^{124}$GGIL$^{127}$, mSIM2: aa $^{225}$VLRL$^{228}$ mutated in $^{225}$GGRL$^{228}$, mSIM3: aa $^{320}$LLVI$^{323}$ mutated in $^{320}$GGVI$^{323}$, mSIM4: aa $^{805}$VVVV$^{808}$ mutated in $^{805}$GGVV$^{808}$, mSIM5: aa $^{978}$VVGL$^{981}$ mutated in $^{978}$GGGL$^{981}$.

Myc-PML1 WT and 3K mutant, obtained by PCR using pLNGY-PML1 and pLNGY-PML1.KKK as template (graciously sent by Dr. Roger Everett), were cloned in puromycin resistant pLVX-TetOne plasmid with AgeI and BamHI restriction enzymes. pLNCX2 ER:RASV12 plasmid was a gift from Masashi Narita (Addgene plasmid # 67844 ; http://n2t.net/addgene:67844 ; RRID:Addgene_67844).

***siRNAs***

BJ cells were transfected with 60nM of human siRNA for different timings (indicated in the main text for each experiment) using Lipofectamine RNAiMax reagent (Invitrogen, 13778-075) and Opti-MEM medium (Gibco, 31-985-070). siRNAs used

and their sequences are summarized in **Table 2**. siH3.3A and siH3.3B, siSUMO-1 and siSUMO-2, were co-transfected into BJ cells at 30nM each.

**Table 2: List of siRNAs and their sequences**

| siRNA | Sequence | Reference |
|---|---|---|
| siH3.3A | 5'CUACAAAAGCCGCUCGCAAdTdT | (Adam et al., 2016) |
| siH3.3B | 5'GCUAAGAGAGUCACCAUCAdTdT | (Adam et al., 2016) |
| siHIRA | 5'GGAUAACACUGUCGUCAUCdTdT | (Ray-Gallet et al., 2011) |
| siLuc | 5'CGUACGCGGAAUACUUCGAdTdT | (Adam et al., 2013) |
| siPML | 5'AGATGCAGCTGTATCCAAGdTdT | (Everett et al., 2006) |
| siSUMO-1 | 5'GGACAGGAUAGCAGUGAGAdTdT | (Lallemand-Breitenbach et al., 2008) |
| siSUMO-2/3 | 5'GUCAAUGAGGCAGAUCAGAdTdT | (Yao et al., 2011) |
| siUBC9 | 5'GAAGUUUGCGCCCUCAUAAdTdT | (Rojas-Fernandez et al., 2014) |

***Antibodies***

All the primary antibodies used in this study, together with the species, the reference and the dilutions for immunofluorescence and western blotting, are summarized in **Table 3**.

**Table 3: List of primary antibodies**

| Antibody | Species | Reference | Dilution | |
|---|---|---|---|---|
| | | | IF | WB |
| Actin | Rabbit polyclonal | Sigma-Aldrich A2066 | | 1:1000 |
| ASF1a | Rabbit polyclonal | Genevieve Almouzni (Corpet et al., 2011) | 1:1000 | |
| CABIN1 | Rabbit polyclonal | Sigma-Aldrich HPA043296 | 1:100 | |
| γH2AX #01 | Mouse monoclonal (clone 6L16) | Millipore 05-636 | 1:500 | 1:1000 |
| γH2AX #02 | Rabbit polyclonal | Abcam ab2893 | 1:500 | 1:1000 |
| panH3 | Rabbit polyclonal | Abcam ab1791 | | 1:5000 |
| H3.3 | Rabbit monoclonal | Diagenode C15210011 | | 1:1000 |
| HA #01 | Rabbit polyclonal | Abcam Ab9110 | 1:1000 | 1:1000 |
| HIRA #01 | Mouse monoclonal | Active Motif 3558 | 1:500 | 1:1000 |

| | | | | |
|---|---|---|---|---|
| | (clone WC119) | | | |
| HIRA #02 | Mouse monoclonal (clone WC119) | Millipore 04-1488 | 1:500 | 1:1000 |
| HIRA #03 (for mouse) | Rabbit polyclonal | Abcam ab20655 | 1:100 | |
| 6xHis #01 | Mouse monoclonal (clone 3D5) | Clontech 631212 | 1:1000 | |
| 6xHis #02 | Rabbit polyclonal | Bethyl A190-114A | 1:10000 | |
| c-Myc #01 | Mouse monoclonal (clone 9E10) | Santa Cruz sc-40 | | 1:1000 |
| c-Myc #02 | Rabbit polyclonal | Abcam ab9106 | 1:1000 | |
| PML #01 | Mouse monoclonal (clone PG-M3) | Santa Cruz sc-966 | 1:200 | |
| PML #02 | Rabbit polyclonal | Santa Cruz sc-5621 | 1:200 | 1:1000 |
| PML #03 | Rabbit polyclonal | Sigma PLA0172 | 1:5000 | 1:1000 |
| PML #04 (for mouse) | Mouse monoclonal (clone 36.1-104) | Millipore MAB3738 | 1:100 | |
| SUMO-1 | Rabbit monoclonal (clone Y299) | Abcam ab32058 | | 1:1000 |
| SUMO-2/3 | Rabbit polyclonal | Abcam ab3742 | | 1:1000 |
| αTubulin | Mouse monoclonal (clone DM1A) | Sigma T6199 | | 1:10000 |
| UBC9 | Rabbit polyclonal | Abcam ab33044 | | 1:1000 |
| UBN1 | Mouse monoclonal (clone ZAP1) | Henri Gruffat (Aho et al., 2000) | 1:100 | |

***Immunofluorescence (IF)***

Cells were grown on glass coverslips. After treatments, cells were fixed in 2% paraformaldehyde (PFA) for 12 minutes at room temperature (RT°C). The cells were then permeabilized in PBS 0,2% Triton X-100 for 5 minutes at RT°C and blocked in

PBS 0,1% Tween (PBST) 5% Bovine Serum Albumin (BSA) for 20 minutes at RT°C. Cells were incubated in humid chamber with primary antibodies diluted in PBST 5% BSA for 1 hour at RT°C or O/N at 4°C (see **Table 3** for antibodies dilution). After washing in PBST, cells were incubated with goat anti-mouse or anti-rabbit (H+L) cross-absorbed secondary antibodies Alexa-488, Alexa-555 or Alexa-647 (Invitrogen) diluted in PBST 5% BSA in dark and humid chamber for 30 minutes at RT°C. Cells were then incubated in DAPI (Invitrogen Life Technologies, D1306) diluted in PBS at 0,1µg/mL for 5 minutes at RT°C. Coverslips were mounted in Fluoromount-G (SouthernBiotech, 0100-01) and stored at 4°C before observation.

***Immunofluorescence - Fluorescence in situ hybridization (IF-FISH)***

FISH probes were generated from different BAC : RP11-438J1 BAC Clone for *GHRL*, RP11-185E17 BAC clone for *PML*, RP11-120C17 BAC clone for *MX1* and RP11-134B23 BAC clone for *OAS1*. Briefly, 1µg of BAC were incubated for nick-translation with 4.3 ng of DNAse I (Roche, 104159), 7U of DNA polymerase (Promega, M2051), dithiothreitol (DTT) at 10µM, dATP, dTTP and dGTP at 40µM each (Thermo Scientific, R0141/R0161/R0171), dCTP at 10µM (Thermo Scientific, R0151) and Cy3 labelled dCTP at 10µM (Cytiva, PA53021). Nick-translation was performed for 3 hours at 15°C and stopped by an incubation at 72°C for 10 minutes. Size of generated probes were verified on agarose gel. Probes were then mixed with 20µg of COT Human DNA (Roche, 11 581 074 001) and 79µg of Salmon sperm DNA (Invitrogen, 15632-011). Volume was completed with TE buffer (10mM Tris-HCl pH8, 1mM EDTA). DNA was precipitated with 300mM of sodium acetate and 70% of chilled EtOH for 2 hours at -20°C. DNA pellets were resuspended in formamide at 20ng/µL final concentration.

After performing classic immunofluorescence as described above (without the DAPI staining step), cells were post-fixed in 2% PFA for 12 minutes at RT°C and then permeabilized and deproteinized in PBS 0,5% Triton X-100 0,1M HCl for 10 minutes at RT°C. Samples were dehydrated in successive EtOH baths, 2 times in 70% EtOH, 2 times in 85% EtOH and 2 times in 100% EtOH. After co-denaturation at 80°C for 5 minutes, cells' DNA was hybridized with FISH probes diluted at 1/5 O/N at 37°C in dark and humid chamber. Cells were then washed 5 minutes in Saline-Sodium Citrate (SSC) 0,5X at 68°C, 2 minutes in SSC 1X at RT°C and incubated in DAPI diluted in SSC

2X for 5 minutes at RT°C. Coverslips were mounted in Fluoromount-G and stored at 4°C before observation.

***Proximity Ligation Assay (PLA)***

Proximity Ligation Assays were performed with the Duolink In Situ Red Starter Kit Mouse/Rabbit (Sigma-Aldrich, DUO92101). Cells on coverslips were fixed in 2% PFA for 12 minutes at RT°C and then permeabilized in PBS 0,2 % Triton X-100 for 5 minutes at RT°C. Cells were incubated in Duolink Blocking Solution for 1 hour at 37°C in humid chamber. Cells were then incubated in humid chamber with primary antibodies diluted in PBST 0,1% BSA for 1 hour at RT°C (see **Table 3** for antibodies dilution). Cells were washed twice for 5 minutes in 1X Duolink Wash Buffer A at RT°C and then incubated in humid chamber for 1 hour at 37°C with PLUS and MINUS PLA probes diluted at 1:5 in the Duolink Antibody Diluent solution. After incubation, cells were washed twice for 5 minutes in 1X Duolink Wash Buffer A at RT°C. Ligation step were then processed by incubating cells with the ligase diluted at 1:40 in 1X Duolink Ligation Buffer in humid chamber for 30 minutes at 37°C. Cells were washed twice for 5 minutes in 1X Duolink Wash Buffer A ar RT°C before the amplification step where cells were incubated in a polymerase diluted at 1:80 in 1X Duolink Amplification Buffer in dark and humid chamber O/N at 37°C. Finally, cells were washed twice for 10 minutes in 1X Duolink Wash Buffer B and once for 1 minute in 0,01X Duolink Wash Buffer B at RT°C. Coverslips were mounted in Duolink In Situ Mounting Medium with DAPI and stored at 4°C before observation.

***Microscopy, imaging, and quantification***

Images were acquired with the Axio Observer Z1 inverted wide-field epifluorescence microscope (100X or 63X objectives/N.A. 1.46 or 1.4) (Zeiss) and a CoolSnap HQ2 camera from Photometrics or with the LSM 880 confocal microscope (63X objective/N.A. 1.4) (Zeiss). Identical settings and contrast were applied for all images of the same experiment to allow data comparison. Raw images were treated with Fiji software.

HIRA complex relocalization was attested by counting of a minimum of 100 cells for each condition.

PML-NBs and genes loci proximity was attested using the Fiji RenyiEntropy mask on PML and FISH staining. X and Y positions were recovered and all distances between

each PML NBs and gene loci were calculated using the formula $d = \sqrt{(x1 - x2)^2 + (y1 - y2)^2}$ to find the minimal distance in each nucleus.

***Western blotting (WB)***

Total cellular extracts were obtained by directly lysing the cells in 2X Laemmli sample buffer (LSB) (125 mM Tris-HCl pH 6.8, 20% glycerol, 4% SDS, bromophenol blue) containing 100mM DTT. RIPA extracts were obtained by lysing the cells in RIPA buffer (50mM Tris-HCl pH 7.5, 150mM NaCl, 0,5% Na-Deoxycholate, 1% NP-40, 0,1% SDS, 5mM EDTA) supplemented with 1X protease inhibitor cocktail (PIC) for 20min on ice. After incubation, RIPA extracts were centrifugated for 10min at 16000g at 4°C and supernatants were recovered and diluted with 4X LSB (250mM Tris-HCl pH 6.8, 40% glycerol, 8% SDS, bromophenol blue).

Protein extracts were boiled for 10 minutes and then loaded on polyacrylamide gels (TGX Stain-Free FastCast gels (Bio-Rad, 1610181/1610183) or home-made gels) for electrophoresis. Stain-free technology or Ponceau 0,1% (Sigma-Aldrich, P7170) were used to reveal proteins transferred on nitrocellulose membrane with the Trans-Blot Turbo Transfer System (Bio-Rad, 1704150). Membranes were blocked in PBST 5% milk for 30 minutes at RT°C and incubated with primary antibodies diluted in PBST or PBST 5% BSA O/N at 4°C (see **Table 3** for antibodies dilution). After washing the membranes thrice in PBST, they were incubated in secondary antibodies conjugated with horseradish peroxidase (HRP) (Dako, P0399, P0447 and P0450) diluted according to supplier recommendations in PBST for 1 hour at RT°C. Signal was revealed on ChemiDoc Imaging System (Bio-Rad) by using Amersham ECL Prime Western Blotting Detection Reagent (GE Healthcare Life Sciences, RPN2236) or Clarity Max Western ECL Blotting Substrate (Bio-Rad, 1705062).

***Chromatin immunoprecipitation (ChIP)***

Cells were crosslinked directly in the culture dishes by adding fixing solution (11% formaldehyde, 50mM HEPES-KOH pH 7.5, 100mM NaCl, 1mM EDTA, 0,5mM EGTA) to the medium to have 1% formaldehyde final concentration and incubated with agitation for 5 minutes at RT°C. Crosslinking was quenched by adding 125mM glycine and cells were incubated with agitation for 5 minutes at RT°C. Cells were washed with ice-cold PBS, scraped and collected in 15mL tubes. They were washed twice with ice-

cold PBS and pelleted at 200g for 4 minutes at 4°C. Cell pellets were snap-frozen in liquid nitrogen and stored at -80°C before immunoprecipitation.

Cells were de-frozen on ice and lysed in 1X Lysis buffer (50mM HEPES-KOH pH 7.5, 140mM NaCl, 10% Glycerol, 1mM EDTA, 0,5% NP-40, 0,25% Triton X-100) supplemented with protease inhibitors (0,2mM PMSF and 1X PIC) for 10 minutes on a rotating wheel at 4°C. Intact nuclei were pelleted by centrifugation at 1700g for 5 minutes at 4°C. Nuclei were washed with 1X Wash buffer (10mM Tris-HCl pH 8.0, 200mM NaCl, 1mM EDTA, 0,5mM EGTA) supplemented with protease inhibitors for 10 minutes on a rotating wheel at 4°C. Intact nuclei were pelleted by centrifugation at 1700g for 5 minutes at 4°C. Nuclei were washed twice in 1X Shearing buffer (10mM Tris-HCl pH 8.0, 1mM EDTA, 0,1% SDS) supplemented with protease inhibitors, pelleted by centrifugation at 1700g for 5 minutes at 4°C and resuspended in 1X Shearing buffer with inhibitors for sonication. We used the Covaris M220 Focused-ultrasonicator to shear through chromatin (7 minutes at 140W, Duty off 10%, Burst cycles 200). After shearing, samples were supplemented with 1% Triton X-100 and 150mM NaCl. Samples were centrifuged at maximal speed for 10 minutes at 4°C to get rid of nuclear debris. The desired mass of chromatin was aliquoted into low-retention 1,5mL tubes (Axygen, MCT-150-L-C) and volume was completed to 1mL with IP buffer (10mM Tris-HCl pH 8.0, 150mM NaCl, 1mM EDTA, 0,1% SDS, 1% Triton X-100) with protease inhibitors. A separate aliquot of chromatin was reserved as the input sample and store at -20°C.

Dynabeads protein A magnetic beads (Invitrogen, 10001D) were used for immunoprecipitation with rabbit primary antibodies. Dynabeads were washed twice with ice-cold PBS and resuspended in PBS 0,5% BSA supplemented with primary antibodies (anti-H3.3 (Diagenode, C15210011), anti-panH3 (Abcam, ab1791), rabbit IgG (Diagenode, C15410206)). We used 2µg of antibody for 20µL of dynabeads. Dynabeads and antibodies were incubated on a rotating wheel for 6 hours at 4°C to allow antibody conjugation. Antibody-conjugated dynabeads were then washed twice with IP buffer and resuspended in the 1mL of chromatin. ChIP samples were incubated on a rotating wheel O/N at 4°C.

Using a magnetic rack, the unbound lysates were aspirated and dynabeads were washed five times with ice-cold ChIP RIPA Buffer (50mM HEPES pH 7.5, 500mM LiCl, 1mM EDTA, 1% NP-40, 0,7% Na-deoxycholate) and once with ice-cold TE buffer

(10mM Tris-HCl pH 8.0, 1mM EDTA). Chromatin was then eluted in 200uL of ChIP Elution buffer (Tris-HCl pH 8.0, 10mM EDTA, 1% SDS) for 30 minutes at 65°C with shaking and the eluates were transferred to a new tube. Reserved input samples were diluted at least 3-fold in ChIP Elution buffer. To purify DNA, ChIP eluates and input samples were decrosslinked by heating O/N at 65°C. Samples were diluted with 200µL of TE buffer and treated for 2 hours with RNase A (200µg/mL) (SIGMA R6513) at 37°C followed by 2 hours with recombinant Proteinase K (200µg/mL) (Thermo Scientific, 10181030) at 55°C. DNA was purified by phenol-chloroform-isoamyl alcohol extraction. The extracted aqueous phase was supplemented with 200mM of NaCl and 20µg of glycogen. DNA was precipitated with EtOH for 2 hours at -20°C and pelleted at 20 000g for 20 minutes at 4°C. DNA pellets were resuspended in ddH20 and stored at -20°C before qPCR analysis.

***Reverse Transcription (RT)***

TRIzol reagent protocol (Invitrogen, 15596026) was used to isolate total RNAs, resuspended in ddH2O according to the manufacturer instructions. Contaminant DNA was removed with the DNA-free DNA Removal Kit (Invitrogen, AM1906). We used 1µg of RNA for reverse transcription (RT). RNAs were annealed with Random Primers (Promega, C118A) and RT was performed with the RevertAid H Minus Reverse Transcriptase (Thermo Scientific, EP0452) according to the manufacturer instructions. cDNAs were stored at -20°C before qPCR analysis.

***Quantitative PCR (qPCR)***

qPCRs were performed using the KAPA SYBR qPCR Master Mix (SYBR Green I dye chemistry) (KAPA BIOSYSTEMS, KK4618). Primers used for qPCR are described in **Table 4**.

**Table 4: List of primers used for qPCR**

| Name | Forward primers (5'→3') | Reverse primers (5'→3') | Ref |
|---|---|---|---|
| **ChIP qPCR** | | | |
| H3.3-ChIP-cluster3-Chr1 | GCC-ACT-TGC-CAA-TGT-TTC-TC | TGG-CCC-CAT-GTA-GTG-AAA-AG | (Pchelintsev et al., 2013) |
| ChIP-MX1-TSS | GGG-ACA-GGC-ATC-AAC-AAA-GCC | GCC-CTC-TCT-TCT-TCC-AGG-CAA-C | (Cheon et al., 2013) |
| ChIP-MX1-mid | TCT-ACG-CTC-TGG-GGA-CAT-CA | GAA-CCA-AAC-CCA-CCA-CCA-GA | |

| | | | |
|---|---|---|---|
| ChIP-MX1-TES | CTC-CCG-TGA-ACT-GTT-CTT-TCC-T | GCT-GTA-GGT-GTC-CTT-GTC-CT | |
| ChIP-OAS1-TSS | ACC-ACA-GAC-AAC-TGT-GAA-AGG | GTC-CTT-TAG-CCA-GCA-ACA-AGC | |
| ChIP-OAS1-mid | GCA-GCA-CGT-TGG-GAG-ATA-GA | TTC-TCC-TGA-TGT-GGC-AAG-GG | |
| ChIP-OAS1-TES | CTT-GTC-ACA-TCC-CCA-CCT-CTC | GTC-CTT-TGC-CCC-TGT-TTA-GC | |
| ChIP-ISG54-TSS | GCA-GGA-AGT-GGG-GTT-TGC-TA | GAG-GGA-TGT-TTC-ATC-GGC-CT | |
| ChIP-ISG54-mid | ATG-TAA-CTA-ACC-CCA-GGT-GCG | TGC-TTC-CCA-CTC-CCA-TTT-TGA | |
| ChIP-ISG54-TES | AGT-CTG-GAA-GCC-TCA-TCC-CT | CCT-AGT-GGG-CAC-CAC-ATC-TC | |
| **RT qPCR** | | | |
| *GAPDH* | GAG-TCA-ACG-GAT-TTG-GTC-GT | TTG-ATT-TTG-GAG-GGA-TCT-CG | |
| *H3F3A* | CCA-GGA-AGC-AAC-TGG-CTA-CA | ACC-AGG-CCT-GTA-ACG-ATG-AG | |
| *H3F3B* | GGA-TTT-CAA-AAC-CGA-CCT-GA | AGC-CAA-CTG-GAT-GTC-TTT-GG | |
| *HIRA* | AGG-ACT-CTC-GTC-TCA-TGC-CT | CAG-CTT-CAG-TGC-AAG-TGC-TG | |
| *ISG15* | GGT-GGA-CAA-ATG-CGA-CGA-AC | TCG-AAG-GTC-AGC-CAG-AAC-AG | |
| *ISG54* | TGA-AAG-AGC-GAA-GGT-GTG-CT | CTC-AGA-GGG-TCA-ATG-GCG-TT | |
| *MX1* | GGA-GGC-ACT-GTC-AGG-AGT-TG | TCC-TGG-TAA-CTG-ACC-TTG-CC | |
| *OAS1* | AGC-TGG-AAG-CCT-GTC-AAA-GA | AGG-TTT-ATA-GCC-GCC-AGT-CAA | |
| *PML* | CAG-GGA-CCC-TAT-TGA-CGT-TG | ATG-GAG-AAG-GCG-TAC-ACT-GG | |

***ChIP-Seq analysis***

After ChIP, libraries were made in BGI and sequenced on a BGISEQ-500 sequencing platform (https://www.bgi.com). An average of 34 Million single-end 50bp reads was obtained for each library. Reads were trimmed using Trimmomatic and quality assessed with FastQC. Reads were aligned to the human genome hg38 using the BWA alignment software. Duplicate reads were identified using the picard tools script and only non-duplicate reads were retained. Broad peaks calling was performed with MACS2 (Zhang et al., 2008) ("--extsize 250 -q 0.01 --broad --broad-cutoff 0.05"), using input DNA as control. We defined all possible locations of H3.3 by merging broad

peaks identified in our four conditions (n=190295), and annotated them with Homer (http://homer.ucsd.edu/homer/download.html). We counted reads extended to 250bp falling into these possible locations, in the four ChIP and their corresponding inputs, using bedtools-intersect. CPMs were obtained by dividing raw counts by the total number of mapped reads normalized to 1e6, and RPKMs by dividing CPMs by the peak length normalized to 1e3. Input RPKMs, used as background, was substracted from the respective ChIP RPKMs. We focused on 0,5% of the peaks with highest RPKM difference (n=951) between IFNβ treated and not treated conditions, of which 711 were intragenic. These peaks allowed us to defined a set of 654 genes, on which we performed GO analysis, with MsigDB, using enrichR plaform (Kuleshov et al., 2016).

As a complementary approach, we measured the ChIP enrichment within the 1000bp regions spanning the TESs (–500 +500), extending all unique reads into 250bp fragments, and counting those falling within TES using bedtools-intersect. CPMs were obtained similarly, and input DNA CPMs, used as background, was substracted from ChIP CPMs. Genes with the log2 of differential TES enrichment between IFNβ treated and not treated conditions being higher than 5 (log2(Fold Change)>5) were retained for GO analysis, as described above.

PlotProfile were generated using the DeepTools suite, starting from the MACS2 fold enrichment bigwig files, which take into account the read extension, the input DNA background and the library size normalization. The list of 48 core ISGs and 48 non-ISGs equal in size to the core ISGs was taken from (McFarlane et al., 2019). In order to reduce the noise on the profiles, we selected for each gene the transcript with the highest H3.3 enrichment at the TES in the IFNβ treated condition. Genome browser snapshots of H3.3 enrichment were generated using Integrative Genomics viewer (IGV : https://software.broadinstitute.org/software/igv/).

### *Statistical analyses*

Statistical analyses were performed using GraphPad Prism 6. To perform Student t test, we verified normal distribution of samples using Shapiro test and variance equality with Fisher test. Mann-Whitney u-test was applied in absence of normality for the sample distribution. p-values are depicted on graphs as follows : *<0,05; **<0,01; ***<0,001; ****<0,0001.

**Figure Legends**

**Figure 1. HIRA relocalization in PML NBs is induced by different signaling pathways**.

**A-D**. Fluorescence microscopy visualization of HIRA (green) and PML (red) in BJ cells with different treatments. Cell nuclei are visualized by DAPI staining (grey). Scale bars represent 10µm. Histograms show quantitative analysis of cells with HIRA localization at PML NBs. p-values (Student t-test): *<0,05; **<0,01; ****<0,0001; ns: non significant. Numbers on all histograms represent the mean of 3 independent experiments (±SD). **A.** Images (left) and histogram (right) for BJ cells treated with PolyIC at 10µg/mL for 24h and with Ruxo at 2µM for 24h. **B.** Images (left) and histogram (right) for BJ cells treated with TNFα at 100ng/mL for 24h and with Ruxo at 2µM one hour before TNFα treatment and for 25h. **C.** Images (top) and histogram (bottom) for BJ cells treated with IFNβ at 1000U/mL or Etoposide (Etop) at 10µM for 24h. Ruxolitinib (Ruxo) was added at 2µM one hour before IFNβ treatment and left for 25h. **D.** Images (top) and histogram (bottom) for BJ cells treated with neocarzinostatin (NCS) at 100ng/mL for 15min followed by a recovery time of 3, 6 or 24h.

**Figure 2. HIRA recruitment to PML NBs is dependent on SUMO proteins**.

**A.** Fluorescence microscopy visualization of Proximity Ligation Assays (PLA) signals (red) obtained after incubation of anti-PML+anti-SUMO, anti-HIRA+anti-PML or anti-HIRA+anti-SUMO antibodies on BJ cells treated or not with IFNβ at 1000U/mL for 24h. Cell nuclei are visualized by DAPI staining (grey or blue on the merge). Scale bar represents 10µm. **B.** Box-and-whisker plot shows the number of PLA spots detected in cells described in A. In average, 200 nuclei/condition were analyzed from 3 independent experiments. The line inside the box represents the median of all observations. p-values (Mann-Whitney u-test): ****<0,0001. **C.** Western-blot visualization of SUMO-1 and SUMO-2/3 from total cellular extracts of BJ cells treated with 60nM of siRNAs against luciferase or SUMO-1+SUMO-2/3 for 48h and with IFNβ at 1000U/mL during the last 24h. Actin is a loading control. **D.** (left) Fluorescence microscopy visualization of HIRA (green) and PML (red) in BJ cells treated with siRNAs as described in C and with IFNβ at 1000U/mL or with etoposide (Etop) at

10μM for the last 24h of siRNAs treatment. (right) Histograms show quantitative analysis of cells with HIRA localization at PML NBs. Numbers represent the mean of 3 independent experiments (±SD). p-values (Student t-test): *<0,05.

**Figure 3. HIRA recruitment to PML NBs relies on SIM-SUMO interactions.**

**A.** Experimental design to assess SUMO-specific Affimers impact on HIRA relocalization to PML NBs. BJ cells were transduced with a Dox-inducible lentiviral vector encoding for an 6xHis-tagged SUMO-specific S1S2D5 Affimer ($BJ_{aff}$ cells). When expressed, S1S2D5-His Affimers localize at PML NBs through their interactions with SUMOylated PML. The fluorescence image shows the colocalization of the S1S2D5-His Affimer (red) and PML NBs (cyan). Cells are then treated with type I IFN or etoposide (Etop) and HIRA localization is observed by fluorescence microscopy. **B-C.** Fluorescence microscopy visualization HIRA (green) and S1S2D5-His Affimer (red) in $BJ_{aff}$ cells induced or not with doxycycline at 100nM for 30h and treated with IFNβ at 1000U/mL (B) or Etop at 10μM (C) for the last 24h. Cell nuclei are visualized by DAPI staining (grey). Scale bars represent 10μm. **D.** Histograms show quantitative analysis of cells with HIRA localization at PML NBs for cells described in B (left histogram) and C (right histogram). Numbers represent the mean of 4 independent experiments for the left histogram and 3 independent experiments for the right histogram (±SD). p-values (Student t-test): *<0,05; **<0,01; ***<0,001. **E.** Experimental design to assess SUMOylated PML requirement for HIRA relocalization to PML NBs (top). MEFs *Pml*$^{-/-}$ cells were transduced with Dox-inducible lentiviral vectors encoding for Myc-tagged WT or 3K non-SUMOylable PML proteins. Cells were then treated with murine type I IFNα and HIRA localization was observed by fluorescence microscopy. Myc-PML proteins expression was verified by western blot analysis (bottom) of PML from total cellular extracts of MEFs cells describe above. HIRA proteins level was also verified. Actin is a loading control. **F.** (left) Fluorescence microscopy visualization of HIRA (green) and Myc-PML (red) on MEFs *Pml*$^{-/-}$ cells rescued with Myc-tagged WT (top) or 3K (bottom) PML proteins through doxycycline treatment at 100nM for 24h. Cells were at the same time treated with murine IFNα at 1000U/mL. Cell nuclei are visualized by DAPI staining (grey). Scale bars represent 10μm. (right) Histogram shows quantitative analysis of cells with HIRA localization at rescued WT or 3K PML NBs. Numbers represent the mean of 3 independent experiments (±SD). p-value

(Student t-test): ****<0,0001. **G.** (left) Schematic representation of the localization of the mutations on putative SIM motifs on HIRA protein. Fluorescence microscopy visualization of HIRA-HA (green) and PML (red) in BJ cells stably transduced with HIRA-HA WT or HIRA-HA mSIM2 mutant and treated with IFNβ at 1000U/mL for 24h. (right) Graphics show HA signal intensity of each pixel delimitated within the nuclei in a 3D-surface plot. Higher expression signal appears in yellow to white colors. Histogram shows quantitative analysis of cells with HIRA-HA localization in PML NBs. Numbers represent the mean of 3 independent experiments (±SD). p-value (Student t-test): **<0,01.

**Figure 4. PML depletion, but not HIRA depletion, impairs ISGs transcription under IFN-I.**

**A.** Histogram shows ISGs (*MX1*, *OAS1*, *ISG15* and *ISG54*) mRNA relative levels (normalized on *GAPDH* mRNA levels) of BJ cells treated with IFNβ at 100U/mL for 6h and 24h. Rationalization was performed on ISGs mRNA levels of untreated cells (NT). Numbers represent the mean of 2 independent experiments (±SD). **B.** (left) Fluorescence microscopy visualization of HIRA (green) and PML (red) in BJ cells treated with IFNβ at 1000U/mL for 2h, 6h, 15h or 24h. Cell nuclei are visualized by DAPI staining (grey). Scale bar represents 10µm. (right) Histogram shows quantitative analysis of cells with HIRA localization at PML NBs. Numbers represent the mean of 3 independent experiments (±SD). p-value (Student t-test): *<0,05; **<0,01; ns: non significant. **C.** Histogram shows HIRA (left) and PML (middle) mRNA relative levels (normalized on GAPDH mRNA levels) of BJ cells treated with siRNAs against luciferase, HIRA or PML for 72h and with IFNβ at 100U/mL for the last 24h or 6h of siRNAs treatment. Rationalization was performed on mRNA levels of siLuc NT cells. Numbers represent the mean of 3-5 independent experiments (±SD). p-value (Student t-test): ***<0,001; ns: non significant. (right) Western blot visualization of PML and HIRA from total cellular extracts of BJ cells treated as in the right panel. Tubulin is a loading control. **D.** Histograms show ISGs mRNA relative levels of *MX1*, *OAS1*, *ISG15* and *ISG54* normalized on GAPDH mRNA levels of BJ cells treated as in C. Rationalization was performed on mRNA levels of siLuc+IFN cells. Numbers represent the mean of 3-5 independent experiments (±SD). p-value (Student t-test): *<0,05; **<0,01; ***<0,001; ns: non significant.

**Figure 5. ISGs loci and PML NBs become spatially closer with IFN-I treatment.**

**A.** Confocal fluorescence microscopy visualization of IF-FISH against PML proteins (green) and *GHRL* control gene locus (red) or *PML*, *MX1* or *OAS1* ISGs loci (red) in BJ cells treated with IFNβ at 1000U/mL for 48h. Insets represent enlarged images (3X) of selected areas and show the relative distance between one PML NB and one gene locus. Scale bar represents 10μm. **B.** Scatter plot shows the minimal distance in μm (see Materials and Methods) between PML NBs and indicated gene loci in nuclei from BJ cells treated or not with IFNβ at 1000U/mL for 24h or 48h. The line in the middle represents the median distance of all observations. **C.** Scatter plot shows the number of PML NBs per nucleus. The line in the middle represents the median of all observations. Nuclei used for the analysis are the same as described in B. **D.** Scatter plot shows the ratio of the minimal distance between PML NBs and ISGs loci on the mean minimal distance between PML NBs and *GHRL* control gene locus. Nuclei used for the analysis are the same described in B and C. The line in the middle represents the median of all observations. **B-D** Results are from one representative experiment out of two experiments and are calculated on an average of 40 nuclei/condition. p-value (Mann-Whitney u-test): *<0,05; **<0,01; ***<0,001; ****<0,0001; ns: non significant.

**Figure 6. HIRA and PML depletions impair H3.3 enrichment at distal regions of ISGs.**

**A.** (top) Schematic representation of *MX1*, *OAS1* and *ISG54* gene loci. Localization of primers is marked in color: red, green and blue for primers localized in the Transcription Start Site (TSS-, mid or Transcription End Site (TES) region respectively. Black boxes represent exons and lines represent introns. (bottom) Histogram shows H3.3 enrichment fold change obtained through ChIP experiments on BJ cells treated or not with IFNβ at 1000U/mL for 24h. Rationalization was performed on H3.3 enrichment in untreated cells. qPCR was performed on *MX1*, *OAS1* and *ISG54* ISGs TSS, mid and TES regions and on one enhancer region on chromosome 1 (Enh1). Numbers represent the mean of 3 independent experiments (±SD). p-value (Student t-test): **<0,01; ***<0,001; ****<0,0001. **B.** ChIP-Seq profile of H3.3 enrichment over 49 core ISGs (McFarlane et al., 2019) ranging from -2.0kb to 2.0 kb

downstream and upstream of the gene bodies in BJ cells treated as in A. **C.** ChIP-Seq profile of H3.3 enrichment over 49 coding non-ISGs equal in size to core ISGs (McFarlane et al., 2019), ranging from -2.0kb to 2.0 kb downstream and upstream of the gene bodies (regions from TSS to +1000bp and from -1000 to TES being kept unscaled) in BJ cells treated as in A. **D.** Gene Ontology analysis on genes showing the highest differential H3.3 enrichment (log2(Fold Change)>5) in the TES +/- 0.5kb region between IFNβ treated and not treated conditions. **E.** (left) Western blot analysis of HIRA and PML from total cellular extracts of BJ cells treated with the indicated siRNAs for 72h and with IFNβ at 1000U/mL for the last 24h of siRNAs treatment. Tubulin is a loading control. (right) Histogram shows H3.3 enrichment obtained through ChIP experiments on BJ cells treated as on the left panel. Rationalization was performed on H3.3 enrichment in siLuc +IFN treated cells. qPCR was performed on *MX1* mid and TES regions, *OAS1* TES region and *ISG54* mid region. Numbers represent the mean of 4 independent experiments (±SD). p-value (Student t-test): *<0,05; **<0,01; ****<0,0001; ns: non significant. **F.** ChIP-Seq profile of H3.3 enrichment over 49 core ISGs (McFarlane et al., 2019) ranging from -0.5kb to 0.5kb downstream and upstream of the TES in BJ cells treated as in E. **G.** Representative genome browser snapshots of the H3.3 enrichment across the TES region of 2 ISGS : *STAT1* and GTP cyclohydrolase 1 (*GCH1*). Shown are the log2 fold changes of H3.3 enrichment in siLuc + IFN/siLuc NT cells (blue), siHIRA+IFN/siLuc+IFN treated cells (green) and siPML+IFN/siLuc+IFN treated cells (orange).

**Figure 7. H3.3 depletion increases ISGs expression upon IFN-I treatment.**

**A.** Histogram shows *H3F3A* (top) or *H3F3B* (bottom) mRNA relative levels (normalized on *GAPDH* mRNA levels) of BJ cells treated with the indicated siRNAs for 72h and with IFNβ at 100U/mL for the last 6h or 24h of siRNAs treatment. Rationalization was performed on mRNA levels of siLuc NT cells. Numbers represent the mean of 1-2 independent experiments (±SD). **B.** Histograms show ISGs mRNA relative levels of *MX1*, *OAS1*, *ISG15* and *ISG54* (normalized on *GAPDH* mRNA levels of BJ cells treated as in A. Rationalization was performed on mRNA levels of siLuc+IFN cells. Numbers represent the mean of 2-3 independent experiments (±SD). **C.** Hypothetical model describing the interplay between PML NBs and HIRA in the regulation of ISGs transcription and H3.3 deposition. See main text for description.

**Supplementary Figure 1. Impact of senescence and SASP cytokines on HIRA relocalization in PML NBs.**

**A.** (left) Fluorescence microscopy visualization (left) of HIRA (green) and PML (red) in BJ cells transduced with 4-OHT-inducible Ras. Cells were treated with 4-OHT at 100nM for 3 days for Ras induction together with ruxolitinib (Ruxo) at 2µM. DAPI stains nuclei. (right) Histogram shows quantitative analysis of cells with HIRA localization at PML NBs. Numbers represent the mean of 3 independent experiments (±SD). p-value (Student t-test): **<0,01; ns: non significant **B.** Fluorescence microscopy visualization of Ras (green) and γH2AX (red) in BJ cells described in A. DAPI stains nuclei. **C.** (left) Fluorescence microscopy visualization (left) of HIRA (green) and PML (red) in BJ cells treated with IL-6 or IL-8 at 200ng/mL for 24h. DAPI stains nuclei. (right) Histogram shows quantitative analysis of cells with HIRA localization at PML NBs. Numbers represent the mean of 3 independent experiments (±SD). p-value (Student t-test): ns: non significant. **D.** (left) Fluorescence microscopy visualization of HIRA (green) and PML (red) in BJ cells treated with TNFα at 50ng/mL or 100ng/mL for 24h. (right) Histogram shows quantitative analysis of cells with HIRA localization at PML NBs. Numbers represent the mean of 3 independent experiments (±SD). p-value (Student t-test): *<0,05. **A-D.** Scale bar represents 10µm.

**Supplementary Figure 2. HIRA complex relocalizes in PML NBs upon DNA damage in an ATM-dependent manner.**

**A.** Fluorescence microscopy visualization of HIRA, UBN1, CABIN1 or ASF1a (green) and PML (red) in BJ cells treated or not with etoposide (Etop) at 10µM for 24h. **B.** (left) Fluorescence microscopy visualization of HIRA (green) and PML (red) in BJ cells treated with Etop at 10µM for 24h and with ATM inhibitor (ATMi) at 5mM for 25h. (right) Histogram shows quantitative analysis of cells with HIRA localization at PML NBs. Numbers represent the mean of 3 independent experiments (±SD). p-value (Student t-test): *<0,05; **<0,01; ns: non significant. **C.** Western blot visualization of PML, γH2AX and HIRA from RIPA extracts of BJ cells treated with IFNβ at 1000U/mL, Etop at 10µM or TNFα at 100ng/mL for 24h and with ruxolitinib (Ruxo) at 2µM one hour before IFNβ, Etop TNFα treatments and for 25h. Tubulin is a loading control.

**Supplementary Figure 3. HIRA relocalization in PML NBs does not depend on UBC9 nor overexpression of SUMO proteins.**

**A.** Fluorescence microscopy visualization of DAXX (green) and PML (red) in BJ cells treated with the indicated siRNAs for 48h. **B.** (left) Western blot visualization (left) of UBC9 from total cellular extracts of BJ cells treated with the indicated siRNAs for 48h and with IFNβ for the last 24h of siRNA treatment. Actin is a loading control. (right) Histogram shows quantitative analysis of cells with HIRA localization at PML NBs in cells treated as on the left panel. Numbers represent the mean of 3 independent experiments (±SD). p-value (Student t-test): ns: non significant. **C.** Fluorescence microscopy visualization of HIRA (green) and PML (red) in BJ cells treated as in B. **D.** Fluorescence microscopy visualization of HIRA (green) and 6xHis-SUMO (red) in BJ cells transduced with lentiviral vectors 6xHis-tagged SUMO-1 or SUMO-2 proteins. Cells were fixed 48h after the transduction. **E.** Western blot visualization of HIRA and PML from total cellular extracts of $BJ_{aff}$ cells treated as in Figure 3B. Tubulin is a loading control. **F.** Fluorescence microscopy analysis of HIRA (green) and PML (red) in WT MEFs and in MEFs *Pml*$^{-/-}$. **G.** Fluorescence microscopy analysis of HIRA-HA (green) and PML (red) in BJ cells transduced with HIRA-HA WT, or mSIM4/5 mutants and treated with IFNβ for 24h. **A,C,D,F, G**. Cell nuclei are visualized in fluorescence microscopy by DAPI staining (grey). Scale bars represent 10µm.

**Supplementary Figure 4. Transcription inhibition impairs IFN-induced HIRA relocalization to PML NBs.**

**A,C,E.** Fluorescence microscopy visualization of HIRA (green) and PML (red) in BJ cells with different treatments. Cell nuclei are visualized by DAPI staining (grey). Scale bars represent 10µm. Histograms show quantitative analysis of cells with HIRA localization at PML NBs. p-values (Student t-test): * < 0,05; **<0,01; ***<0,001; ns: non significant. **A.** Images (left) and histogram (right) for BJ cells treated with IFNβ at 1000U/mL for 24h and DRB at 50mM for the last 6 hours. Numbers on the histogram represent the mean of 3 independent experiments (±SD). **B.** Western blot visualization of PML and HIRA from total cellular extracts of BJ cells treated as in A. Tubulin is a loading control. **C.** Fluorescence microscopy visualization of DAXX (green) and PML (red) in BJ cells treated with IFNβ at 1000U/mL for 24h and DRB at 50mM for the last 6h or JQ1 at 500nM for 25h. Cell nuclei are visualized by DAPI

staining (grey). Scale bar represents 10µm. **D.** Histograms show quantitative analysis of HIRA localization at PML NBs in BJ cells treated with IFNβ at 1000U/mL for 24h and with CDK9i at 10mM for 25h (top) or Flavopiridol (Flavo) at 50nM for 25h (bottom). Numbers represent the mean of 2 independent experiments for the left histogram and 3 independent experiments for the right histogram (±SD). **E.** Images (left) and histogram (right) for BJ cells treated with IFNβ at 1000U/mL for 24h. α-amanitin (α-Ama) was added one hour before IFNβ treatment and left for 25h. Numbers on the histogram represent the mean of 3 independent experiments (±SD). **F.** Western blot visualization of PML and HIRA from total cellular extracts of BJ cells treated as in C. Tubulin is a loading control. **G.** Images (left) and histogram (right) for BJ cells treated with IFNβ at 1000U/mL for 24h. JQ1 was added at 500nM one hour before IFNβ treatment and left for 25h. Numbers on the histogram represent the mean of 3 independent experiments (±SD). **H.** Western blot visualization of PML and HIRA from total cellular extracts of BJ cells treated as in C. Tubulin is a loading control.

**Supplementary Figure 5. HIRA mRNA levels are not impacted upon IFN-I treatment and HIRA juxtaposes to ISGs following IFN-I treatment**

**A.** Histogram shows *HIRA* (left) and *PML* (right) mRNA relative levels (normalized on *GAPDH* mRNA levels) of BJ cells treated with the indicated siRNAs for 72h and with IFNβ at 100U/mL for the last 6h or 24h of siRNAs treatment. Rationalization was performed on mRNA levels of siLuc NT cells. Numbers represent the mean of 3-4 independent experiments (±SD). **B.** Confocal fluorescence microscopy visualization of IF-FISH against HIRA (green) and PML (red) proteins and *GHRL* control gene locus (cyan) or *PML*, *MX1* or *OAS1* ISGs loci (cyan) in BJ cells treated with IFNβ at 1000U/mL for 48h. Insets represent enlarged images (2X) of selected areas and show the relative distance between one PML NB and one gene locus. Scale bar represents 10µm.

**Supplementary Figure 6. H3.3 and H3K36m3 increase on ISGs upon IFN-I**

**A.** (left) Histogram shows relative *H3F3A* mRNA levels (normalized on *GAPDH* mRNA levels) of BJ cells treated or not with IFNβ at 1000U/mL. Rationalization was performed on the untreated condition. (right) Western blot visualization of H3.3 from total cellular extracts of BJ cells treated as in A. Tubulin is used here as a loading control. **B.** Histogram shows H3.3 and IgG enrichment (% of input) obtained through

ChIP experiments on BJ cells treated or not with IFNβ at 1000U/mL for 24h. qPCR was performed on *MX1*, *OAS1* and *ISG54* ISGs TSS, mid and TES regions and on one enhancer region on chromosome 1 (Enh1). Numbers represent the mean of 3 independent experiments (±SD). **C**. Histogram shows H3.3 enrichment fold change obtained through ChIP experiments on BJ cells treated or not with IFNβ at 1000U/mL for the indicated times. Rationalization was performed on H3.3 enrichment in untreated cells. qPCR was performed on *MX1* TES and *ISG54* Mid. Numbers represent one experiment. **D.** Gene Ontology analysis on a set of 654 genes having with the highest RPKM difference between IFNβ treated and not treated conditions (see Materials and Methods). **E.** Histogram shows H3K36me3 enrichment (% of input) obtained through ChIP experiments on BJ cells treated with IFNβ at 1000U/mL for 24h. qPCR was performed on *MX1* and *OAS1* TSS or TES regions. Numbers represent the mean of two independent experiments.

**Supplementary Figure 7. HIRA SUMO site K809 and phosphorylation site S697 mutations do not impact its localization in PML NBs**

**A.** Fluorescence microscopy visualization of HIRA-HA (green) and PML (red) in IMR90 cells transduced with a lentiviral vector encoding WT or K809G HIRA-HA proteins. Cell nuclei are visualized by DAPI staining (grey). Scale bar represents 10μm. **B.** Fluorescence microscopy visualization of HIRA-HA (green) and PML (red) in BJ cells transduced with a lentiviral vector encoding WT or S697A HIRA-HA proteins. Cell nuclei are visualized by DAPI staining (grey). Scale bar represents 10μm.

**Acknowledgments**

We thank Dr. Valérie Lallemand-Breitenbach for the *Pml* WT and *Pml-/-* MEFs. We thank Dr. David J. Hughes for the SUMO-specific Affimers plasmids. We thank Dr. Roger Everett for the PML-containing plasmids. We thank Dr. Chris Boutell for the pLVX-His-SUMO1/2/3 plasmids. We thank Masahi Narita for the pLNCX2 ER:RASV12 plasmid (Addgene plasmid # 67844 ; http://n2t.net/addgene:67844 ; RRID:Addgene_67844). We thank Dr. Henri Gruffat for the gift of UBN1 antibody. We thank Dr. Caroline Schluth-Bolard for her kind help with the FISH on ISGs and for the GHRL BAC. P.L. laboratory is funded by grants from the Centre National de la Recherche Scientifique (CNRS), Institut National de la Santé et de la Recherche

Médicale (INSERM), University Claude Bernard Lyon 1, French National Agency for Research-ANR [EPIPRO ANR-18-CE15-0014-01, CHROMACoV ANR-20-COV9-0004]; LabEX DEVweCAN and DEV2CAN [ANR-10-LABX-61]; AFM MyoNeurALP, the Comité départemental du Rhône de La Ligue contre le Cancer and the Fondation pour la Recherche Médicale (FRM). P.L. is a CNRS Research Director and AC is assistant professor in the University Claude Bernard Lyon 1.

*Conflict of interest statement.* None declared.

## Bibliography

Adam, S., Dabin, J., Chevallier, O., Leroy, O., Baldeyron, C., Corpet, A., Lomonte, P., Renaud, O., Almouzni, G., and Polo, S.E. (2016). Real-Time Tracking of Parental Histones Reveals Their Contribution to Chromatin Integrity Following DNA Damage. Molecular Cell 1–15.

Adam, S., Polo, S.E., and Almouzni, G. (2013). Transcription Recovery after DNA Damage Requires Chromatin Priming by the H3.3 Histone Chaperone HIRA. Cell *155*, 94–106.

Aho, S., Buisson, M., Pajunen, T., Ryoo, Y.W., Giot, J.F., Gruffat, H., Sergeant, A., and Uitto, J. (2000). Ubinuclein, a novel nuclear protein interacting with cellular and viral transcription factors. J Cell Biol *148*, 1165–1176.

Alandijany, T., Roberts, A.P.E., Conn, K.L., Loney, C., McFarlane, S., Orr, A., and Boutell, C. (2018). Distinct temporal roles for the promyelocytic leukaemia (PML) protein in the sequential regulation of intracellular host immunity to HSV-1 infection. PLoS Pathogens *14*, e1006769.

Alberti, S., Gladfelter, A., and Mittag, T. (2019). Considerations and Challengesin Studying Liquid-Liquid Phase Separation and Biomolecular Condensates. Cell *176*, 419–434.

Allis, C.D., and Jenuwein, T. (2016). The molecular hallmarks of epigenetic control. Nature Reviews Genetics *17*, 487–500.

Armache, A., Yang, S., de Paz, A.M.X.N., Robbins, L.E., Durmaz, C., Cheong, J.Q., Ravishankar, A., Daman, A.W., Ahimovic, D.J., Klevorn, T.X.S., et al. (2020). Histone H3.3 phosphorylation amplifies stimulation-induced transcription. Nature 1–26.

Banani, S.F., Lee, H.O., Hyman, A.A., and Rosen, M.K. (2017). Biomolecular condensates: organizers of cellular biochemistry. Nature Publishing Group *18*, 285–298.

Banani, S.F., Rice, A.M., Peeples, W.B., Lin, Y., Jain, S., Parker, R., and Rosen, M.K. (2016). Compositional Control of Phase-Separated Cellular Bodies. Cell *166*, 651–663.

Banumathy, G., Somaiah, N., Zhang, R., Tang, Y., Hoffmann, J., Andrake, M., Ceulemans, H., Schultz, D., Marmorstein, R., and Adams, P.D. (2009). Human UBN1 Is an Ortholog of Yeast Hpc2p and Has an Essential Role in the HIRA/ASF1a Chromatin-Remodeling Pathway in Senescent Cells. Molecular and Cellular Biology *29*, 758–770.

Baz-Martínez, M., Da Silva-Álvarez, S., Rodríguez, E., Guerra, J., Motiam, El, A., Vidal, A., García-Caballero, T., González-Barcia, M., Sánchez, L., Muñoz-Fontela, C., et al. (2016). Cell senescence is an antiviraldefense mechanism. Sci. Rep. 1–11.

Beauclair, G., Bridier-Nahmias, A., Zagury, J.-F., Saïb, A., and Zamborlini, A. (2015). JASSA: a comprehensive tool for prediction of SUMOylation sites and SIMs. Bioinformatics *31*, 3483–3491.

Becker, J.S., McCarthy, R.L., Sidoli, S., Donahue, G., Kaeding, K.E., He, Z., Lin, S., Garcia, B.A., and Zaret, K.S. (2017). Genomic and Proteomic Resolution of Heterochromatin and Its Restriction of Alternate Fate Genes. Molecular Cell *68*, 1023–1037.e15.

Bensaude, O. (2014). Inhibiting eukaryotic transcription. Which compound to choose? How to evaluate its activity? Transcription *2*, 103–108.

Bhattacharya, S., Eckner, R., Grossman, S., Oldread, E., Arany, Z., D'Andrea, A., and Livingston, D.M. (1996). Cooperation of Stat2 and p300/CBP in signalling induced by interferon-alpha. Nature *383*, 344–347.

Boisvert, F.-M., Hendzel, M.J., and Bazett-Jones, D.P. (2000). Promyelocytic leukemia (PML) nuclear bodies are protein structures that do not accumulate RNA. J Cell Biol *148*, 283–292.

Brouwer, A.K., Schimmel, J., Wiegant, J.C.A.G., Vertegaal, A.C.O., Tanke, H.J., and Dirks, R.W. (2009). Telomeric DNA mediates de novo PML body formation. Molecular Biology of the Cell *20*, 4804–4815.

Cappadocia, L., Mascle, X.H., Bourdeau, V., Tremblay-Belzile, S., Chaker-Margot, M., Lussier-Price, M., Wada, J., Sakaguchi, K., Aubry, M., Ferbeyre, G., et al. (2015). Structural and Functional Characterizationof the Phosphorylation-Dependent Interaction between PML and SUMO1. Structure/Folding and Design *23*, 126–138.

Carbone, R., Pearson, M., Minucci, S., and Pelicci, P.G. (2002). PML NBs associate with the hMre11 complex and p53 at sites of irradiation induced DNA damage. Oncogene *21*, 1633–1640.

Cecco, M., Ito, T., Petrashen, A.P., Elias, A.E., Skvir, N.J., Criscione, S.W., Caligiana, A., Brocculi, G., Adney, E.M., Boeke, J.D., et al. (2019). L1 drives IFN in senescent cells and promotes age-associated inflammation. Nature 1–33.

Chang, F.T.M., McGhie, J.D., Chan, F.L., Tang, M.C., Anderson, M.A., Mann, J.R., Andy Choo, K.H., and Wong, L.H. (2013). PML bodies provide an important platform for the maintenance of telomeric chromatin integrity in embryonic stem cells. Nucleic Acids Research *41*, 4447–4458.

Chang, H.R., Munkhjargal, A., Kim, M.-J., Park, S.Y., Jung, E., Ryu, J.-H., Yang, Y., Lim, J.-S., and Kim, Y. (2018). The functional roles of PML nuclear bodies in genome maintenance. Mutation Research/Fundamental and Molecular Mechanisms of Mutagenesis *809*, 99–107.

Cheon, H., Holvey-Bates, E.G., Schoggins, J.W., Forster, S., Hertzog, P., Imanaka, N., Rice, C.M., Jackson, M.W., Junk, D.J., and Stark, G.R. (2013). IFN-dependent increases in STAT1, STAT2, and IRF9 mediate resistance to viruses and DNA damage. The EMBO Journal *32*, 2751–2763.

Ching, R.W., Ahmed, K., Boutros, P.C., Penn, L.Z., and Bazett-Jones, D.P. (2013). Identifying gene locus associations with promyelocytic leukemia nuclear bodies using immuno-TRAP. J Cell Biol *201*, 325–335.

Chung, I., Leonhardt, H., and Rippe, K. (2011). De novo assembly of a PML nuclear subcompartment occurs through multiple pathways and induces telomere elongation. Journal of Cell Science *124*, 3603–3618.

Cohen, C., Corpet, A., Roubille, S., Maroui, M.A., Poccardi, N., Rousseau, A., Kleijwegt, C., Binda, O., Texier, P., Sawtell, N., et al. (2018). Promyelocytic leukemia (PML) nuclear bodies (NBs) induce latent/quiescent HSV-1 genomes chromatinization through a PML NB/Histone H3.3/H3.3 Chaperone Axis. PLoS Pathogens *14*, e1007313.

Coppe, J.-P., Patil, C.K., Rodier, F., Sun, Y., Muñoz, D.P., Goldstein, J., Nelson, P.S., Desprez, P.-Y., and Campisi, J. (2008). Senescence-Associated Secretory Phenotypes Reveal Cell-Nonautonomous Functions of Oncogenic RAS and the p53 Tumor Suppressor. Plos Biol *6*, e301.

Corpet, A., De Koning, L., Toedling, J., Savignoni, A., Berger, F., Lemaître, C., O'Sullivan, R.J., Karlseder, J., Barillot, E., Asselain, B., et al. (2011). Asf1b, the necessary Asf1 isoform for proliferation, is predictive of outcome in breast cancer. The EMBO Journal *30*, 480–493.

Corpet, A., Kleijwegt, C., Roubille, S., Juillard, F., Jacquet, K., Texier, P., and Lomonte, P. (2020). PML nuclear bodies and chromatin dynamics: catch me if you can! Nucleic Acids Research *389*, 251–23.

Corpet, A., Olbrich, T., Gwerder, M., Fink, D., and Stucki, M. (2014). Dynamics of histone H3.3 deposition in proliferating and senescent cells reveals a DAXX-dependent targeting to PML-NBs important for pericentromeric heterochromatin organization. Cell Cycle *113*, E3213–E3220.

de Thé, H., Le Bras, M., and Lallemand-Breitenbach, V. (2012). The cell biology of disease: Acute promyelocytic leukemia, arsenic, and PML bodies. Journal of Cell Biology *198*, 11–21.

Delbarre, E., Ivanauskiene, K., Küntziger, T., and Collas, P. (2013). DAXX-dependent supply of soluble (H3.3-H4) dimers to PML bodies pending deposition into chromatin. Genome Research.

Delbarre, E., Ivanauskiene, K., Spirkoski, J., Shah, A., Vekterud, K., Moskaug, J.Ø., Bøe, S.O., Wong, L.H., Küntziger, T., and Collas, P. (2017). PML protein organizes heterochromatin domains where it regulates histone H3.3 deposition by ATRX/DAXX. Genome Research *27*, 913–921.

Dellaire, G., Ching, R.W., Ahmed, K., Jalali, F., Tse, K.C.K., Bristow, R.G., and Bazett-Jones, D.P. (2006). Promyelocytic leukemia nuclear bodies behave as DNA damage sensors whose response to DNA double-strand breaks is regulated by NBS1 and the kinases ATM, Chk2, and ATR. Journal of Cell Biology *175*, 55–66.

Doucas, V., Tini, M., Egan, D.A., and Evans, R.M. (1999). Modulation of CREB binding protein function by the promyelocytic (PML) oncoprotein suggests a role for nuclear bodies in hormone signaling. Proc Natl Acad Sci USA *96*, 2627–2632.

Drane, P., Ouararhni, K., Depaux, A., Shuaib, M., and Hamiche, A. (2010). The death-associated protein DAXX is a novel histone chaperone involved in the replication-independent deposition of H3.3. Genes & Development *24*, 1253–1265.

Eggenberger, J., Blanco-Melo, D., Panis, M., Brennand, K.J., and tenOever, B.R. (2019). Type I interferon response impairs differentiation potential of pluripotent stem cells. Proceedings of the National Academy of Sciences *116*, 1384–1393.

Elsässer, S.J., Noh, K.-M., Diaz, N., Allis, C.D., and Banaszynski, L.A. (2015). Histone H3.3 is required for endogenous retroviral element silencing in embryonic stem cells. Nature.

Erdel, F., Rademacher, A., Vlijm, R., Tünnermann, J., Frank, L., Weinmann, R., Schweigert, E., Yserentant, K., Hummert, J., Bauer, C., et al. (2020). Mouse Heterochromatin Adopts Digital Compaction States without Showing Hallmarks of HP1-Driven Liquid-Liquid Phase Separation. Molecular Cell *78*, 236–249.e237.

Everett, R.D., Rechter, S., Papior, P., Tavalai, N., Stamminger, T., and Orr, A. (2006). PML Contributes to a Cellular Mechanism of Repression of Herpes Simplex Virus Type 1 Infection That Is Inactivated by ICP0. Journal of Virology *80*, 7995–8005.

Fuchsová, B., Novák, P., Kafková, J., and Hozák, P. (2002). Nuclear DNA helicase II is recruited to IFN-α–activated transcription sites at PML nuclear bodies. Journal of Cell Biology *158*, 463–473.

Gao, C., Cheng, X., Lam, M., Liu, Y., Liu, Q., Chang, K.-S., and Kao, H.-Y. (2008). Signal-dependent Regulation of Transcription by Histone Deacetylase 7 Involves Recruitment to Promyelocytic Leukemia Protein Nuclear Bodies. Molecular Biology of the Cell *19*, 3020–3027.

Gialitakis, M., Arampatzi, P., Makatounakis, T., and Papamatheakis, J. (2010). Gamma Interferon-Dependent Transcriptional Memory via Relocalization of a Gene Locus to PML Nuclear Bodies. Molecular and Cellular Biology *30*, 2046–2056.

Goldberg, A.D., Banaszynski, L.A., Noh, K.-M., Lewis, P.W., Elsaesser, S.J., Stadler, S., Dewell, S., Law, M., Guo, X., Li, X., et al. (2010). Distinct factors control histone variant H3.3 localization at specific genomic regions. Cell *140*, 678–691.

Hadjadj, J., Yatim, N., Barnabei, L., Corneau, A., Boussier, J., Smith, N., Péré, H., Charbit, B., Bondet, V., Chenevier-Gobeaux, C., et al. (2020). Impaired type I interferon activity and inflammatory responses in severe COVID-19 patients. Science *31*, eabc6027–15.

Harding, S.M., Benci, J.L., Irianto, J., Discher, D.E., Minn, A.J., and Greenberg, R.A. (2017). Mitotic progression following DNA damage enables pattern recognition within micronuclei. Nature 1–15.

Hendriks, I.A., D'Souza, R.C.J., Yang, B., Vries, M.V.-D., Mann, M., and Vertegaal, A.C.O. (2014). Uncovering global SUMOylation signaling networks in a site-specific manner. Nat Struct Mol Biol *21*, 927–936.

Hughes, D.J., Tiede, C., Penswick, N., Tang, A.A.-S., Trinh, C.H., Mandal, U., Zajac, K.Z., Gaule, T., Howell, G., Edwards, T.A., et al. (2017). Generation of specific inhibitors of SUMO-1- and SUMO-2/3-mediated protein-protein interactions using Affimer (Adhiron) technology. Sci Signal *10*.

Ivanauskiene, K., Delbarre, E., McGhie, J.D., Kuntziger, T., Wong, L.H., and Collas, P. (2014). The PML-associated protein DEK regulates the balance of H3.3 loading on chromatin and is important for telomere integrity. Genome Research.

Jiang, W.-Q., Nguyen, A., Cao, Y., Chang, A.C.-M., and Reddel, R.R. (2011). HP1-Mediated Formation of Alternative Lengthening of Telomeres-Associated PML Bodies Requires HIRA but Not ASF1a. PLoS ONE *6*, e17036.

Juhász, S., Elbakry, A., Mathes, A., and Löbrich, M. (2018). ATRX Promotes DNA Repair Synthesis and Sister Chromatid Exchange during Homologous Recombination. Molecular Cell *71*, 11–24.e17.

Kaiser, T.E., Intine, R.V., and Dundr, M. (2008). De novo formation of a subnuclear body. Science *322*, 1713–1717.

Kamada, R., Yang, W., Zhang, Y., Patel, M.C., Yang, Y., Ouda, R., Dey, A., Wakabayashi, Y., Sakaguchi, K., Fujita, T., et al. (2018). Interferon stimulation creates chromatin marks and establishes transcriptional memory. Proceedings of the National Academy of Sciences *115*, E9162–E9171.

Kamitani, T., Kito, K., Nguyen, H.P., Wada, H., Fukuda-Kamitani, T., and Yeh, E.T. (1998). Identification of three major sentrinization sites in PML. J Biol Chem *273*, 26675–26682.

Kuleshov, M.V., Jones, M.R., Rouillard, A.D., Fernandez, N.F., Duan, Q., Wang, Z., Koplev, S., Jenkins, S.L., Jagodnik, K.M., Lachmann, A., et al. (2016). Enrichr: a comprehensive gene set enrichment analysis web server 2016 update. Nucleic Acids Research *44*, W90–W97.

Kumar, P.P., Bischof, O., Purbey, P.K., Notani, D., Urlaub, H., Dejean, A., and Galande, S. (2007). Functional interaction between PML and SATB1 regulates chromatin-loop architecture and transcription of the MHC class I locus. Nat Cell Biol *9*, 45–56.

Kurihara, M., Kato, K., Sanbo, C., Shigenobu, S., Ohkawa, Y., Fuchigami, T., and Miyanari, Y. (2020). Genomic Profiling by ALaP-Seq Reveals Transcriptional Regulation by PML Bodies through DNMT3A Exclusion. Molecular Cell *78*, 493–505.e498.

Lallemand-Breitenbach, V., and de Thé, H. (2018). ScienceDirectPML nuclear bodies: from architecture to function. Current Opinion in Cell Biology *52*, 154–161.

Lallemand-Breitenbach, V., Jeanne, M., Benhenda, S., Nasr, R., Lei, M., Peres, L., Zhou, J., Zhu, J., Raught, B., and de Thé, H. (2008). Arsenic degrades PML or PML–RARα through a SUMO-triggered RNF4/ubiquitin-mediated pathway. Nat Cell Biol *10*, 547–555.

LaMorte, V.J., Dyck, J.A., Ochs, R.L., and Evans, R.M. (1998). Localization of nascent RNA and CREB binding protein with the PML-containing nuclear body. Proc Natl Acad Sci USA *95*, 4991–4996.

Lee, J.-S., Mo, Y., Gan, H., Burgess, R.J., Baker, D.J., van Deursen, J.M., and Zhang, Z. (2019). Pak2 kinase promotes cellular senescence and organismal aging. Proceedings of the National Academy of Sciences *1*, 201903847.

Li, Y., Ma, X., Wu, W., Chen, Z., and Meng, G. (2020). PML Nuclear Body Biogenesis, Carcinogenesis, and Targeted Therapy. Trends Cancer.

Luijsterburg, M.S., de Krijger, I., Wiegant, W.W., Shah, R.G., Smeenk, G., de Groot, A.J.L., Pines, A., Vertegaal, A.C.O., Jacobs, J.J.L., Shah, G.M., et al. (2016). PARP1 Links CHD2-Mediated Chromatin Expansion and H3.3 Deposition to DNA Repair by Non- homologous End-Joining. Molecular Cell *61*, 547–562.

Mackenzie, K.J., Carroll, P., Martin, C.-A., Murina, O., Fluteau, A., Simpson, D.J., Olova, N., Sutcliffe, H., Rainger, J.K., Leitch, A., et al. (2017). cGAS surveillance of micronuclei links genome instability to innate immunity. Nature *548*, 461–465.

Martire, S., and Banaszynski, L.A. (2020). The roles of histone variants in fine-tuning chromatin organization and function. Nature Reviews Molecular Cell Biology 1–20.

McFarlane, S., Orr, A., Roberts, A.P.E., Conn, K.L., Iliev, V., Loney, C., da Silva Filipe, A., Smollett, K., Gu, Q., Robertson, N., et al. (2019). The histone chaperone HIRA promotes the induction of host innate immune defences in response to HSV-1 infection. PLoS Pathogens *15*, e1007667.

Medzhitov, R. (2008). Origin and physiological roles of inflammation. Nature *454*, 428–435.

Mikecz, von, A., Zhang, S., Montminy, M., Tan, E.M., and Hemmerich, P. (2000). CREB-binding protein (CBP)/p300 and RNA polymerase II colocalize in transcriptionally active domains in the nucleus. J Cell Biol *150*, 265–273.

Ng, R.K., and Gurdon, J.B. (2007). Epigenetic memory of an active gene state depends on histone H3.3 incorporation into chromatin in the absence of transcription. Nat Cell Biol *10*, 102–109.

Novakova, Z., Hubackova, S., Kosar, M., Janderova-Rossmeislova, L., Dobrovolna, J., Vasicova, P., Vancurova, M., Horejsi, Z., Hozak, P., Bartek, J., et al. (2009). Cytokine expression and signaling in drug-induced cellular senescence. Oncogene *29*, 273–284.

Patel, M.C., Debrosse, M., Smith, M., Dey, A., Huynh, W., Sarai, N., Heightman, T.D., Tamura, T., and Ozato, K. (2013). BRD4 coordinates recruitment of pause release factor P-TEFb and the pausing complex NELF/DSIF to regulate transcription elongation of interferon-stimulated genes. Molecular and Cellular Biology *33*, 2497–2507.

Pchelintsev, N.A., McBryan, T., Rai, T.S., van Tuyn, J., Ray-Gallet, D., Almouzni, G., and Adams, P.D. (2013). Placing the HIRA Histone Chaperone Complex in the Chromatin Landscape. CellReports *3*, 1012–1019.

Qi, J. (2014). Bromodomain and Extraterminal Domain Inhibitors (BETi) for Cancer Therapy: Chemical Modulation of Chromatin Structure. Cold Spring Harbor Perspectives in Biology *6*, a018663–a018663.

Rai, T.S., Puri, A., McBryan, T., Hoffman, J., Tang, Y., Pchelintsev, N.A., van Tuyn, J., Marmorstein, R., Schultz, D.C., and Adams, P.D. (2011). Human CABIN1 Is a Functional Member of the Human HIRA/UBN1/ASF1a Histone H3.3 Chaperone Complex. Molecular and Cellular Biology *31*, 4107–4118.

Rai, T.S., Glass, M., Cole, J.J., Rather, M.I., Marsden, M., Neilson, M., Brock, C., Humphreys, I.R., Everett, R.D., and Adams, P.D. (2017). Histone chaperone HIRA deposits histone H3.3 onto foreign viral DNA and contributes to anti-viral intrinsic immunity. Nucleic Acids Research.

Ray-Gallet, D., Quivy, J.-P., Scamps, C., Martini, E.M.-D., Lipinski, M., and Almouzni, G. (2002). HIRA is critical for a nucleosome assembly pathway independent of DNA synthesis. Molecular Cell *9*, 1091–1100.

Ray-Gallet, D., Woolfe, A., Vassias, I., Pellentz, C., Lacoste, N., Puri, A., Schultz, D.C., Pchelintsev, N.A., Adams, P.D., Jansen, L.E.T., et al. (2011). Dynamics of Histone H3 Deposition In Vivo Reveal a Nucleosome Gap-Filling Mechanism for H3.3 to Maintain Chromatin Integrity. Molecular Cell *44*, 928–941.

Ricketts, M.D., and Marmorstein, R. (2016). A Molecular Prospective for HIRA Complex Assembly and H3.3-Specific Histone Chaperone Function. J. Mol. Biol. 1–10.

Rojas-Fernandez, A., Plechanovova, A., Hattersley, N., Jaffray, E., Tatham, M.H., and Hay, R.T. (2014). SUMO Chain-Induced Dimerization Activates RNF4. Molecular Cell *53*, 880–892.

Sadic, D., Schmidt, K., Groh, S., Kondofersky, I., Ellwart, J., Fuchs, C., Theis, F.J., and Schotta, G. (2015). Atrx promotes heterochromatin formation at retrotransposons. EMBO Rep *16*, 836–850.

Sahin, U., Ferhi, O., Jeanne, M., Benhenda, S., Berthier, C., Jollivet, F., Niwa-Kawakita, M., Faklaris, O., Setterblad, N., de The, H., et al. (2014). Oxidative stress-induced assembly of PML nuclear bodies controls sumoylation of partner proteins. J Cell Biol *204*, 931–945.

Sahin, U., Jollivet, F., Berthier, C., de Thé, H., and Lallemand-Breitenbach, V. (2016). Detection of Protein SUMOylation In Situ by Proximity Ligation Assays. Methods Mol. Biol. *1475*, 139–150.

Sarai, N., Nimura, K., Tamura, T., Kanno, T., Patel, M.C., Heightman, T.D., Ura, K., and Ozato, K. (2013). WHSC1 links transcription elongation to HIRA-mediated histone H3.3 deposition. The EMBO Journal *32*, 2392–2406.

Schimmel, J., Eifler, K., Sigurðsson, J.O., Cuijpers, S.A.G., Hendriks, I.A., Vries, M.V.-D., Kelstrup, C.D., Francavilla, C., Medema, R.H., Olsen, J.V., et al. (2014). Uncovering SUMOylation Dynamicsduring Cell-Cycle Progression Reveals FoxM1 as a Key Mitotic SUMO Target Protein. Molecular Cell *53*, 1053–1066.

Schoggins, J.W., and Rice, C.M. (2011). Interferon-stimulated genes and their antiviral effector functions. Current Opinion in Virology *1*, 519–525.

Schultze, J.L., and Aschenbrenner, A.C. (2021). COVID-19 and the human innate immune system. Cell *184*, 1671–1692.

Shastrula, P.K., Sierra, I., Deng, Z., Keeney, F., Hayden, J.E., Lieberman, P.M., and Janicki, S.M. (2019). PML is recruited to heterochromatin during S phase and represses DAXX-mediated histone H3.3 chromatin assembly. Journal of Cell Science *132*.

Shiels, C., Islam, S.A., Vatcheva, R., Sasieni, P., Sternberg, M.J., Freemont, P.S., and Sheer, D. (2001). PML bodies associate specifically with the MHC gene cluster in interphase nuclei. Journal of Cell Science *114*, 3705–3716.

Siwek, W., Tehrani, S.S.H., Mata, J.F., and Jansen, L.E.T. (2020). Activation of Clustered IFNgamma Target Genes Drives Cohesin-Controlled Transcriptional Memory. Molecular Cell *80*, 396–409.e396.

Spirkoski, J., Shah, A., Reiner, A.H., Collas, P., and Delbarre, E. (2019). PML modulates H3.3 targeting to telomeric and centromeric repeats in mouse fibroblasts. Biochemical and Biophysical Research Communications *511*, 882–888.

Stadler, M., Chelbi-Alix, M.K., Koken, M.H., Venturini, L., Lee, C., Saïb, A., Quignon, F., Pelicano, L., Guillemin, M.C., and Schindler, C. (1995). Transcriptional induction of the PML growth suppressor gene by interferons is mediated through an ISRE and a GAS element. Oncogene *11*, 2565–2573.

Tamura, T., Smith, M., Kanno, T., Dasenbrock, H., Nishiyama, A., and Ozato, K. (2009). Inducible deposition of the histone variant H3.3 in interferon-stimulated genes. J Biol Chem *284*, 12217–12225.

Tang, Y., Poustovoitov, M.V., Zhao, K., Garfinkel, M., Canutescu, A., Dunbrack, R., Adams, P.D., and Marmorstein, R. (2006). Structure of a human ASF1a–HIRA complex and insights into specificity of histone chaperone complex assembly. Nat Struct Mol Biol *13*, 921–929.

Torné, J., Ray-Gallet, D., Boyarchuk, E., Garnier, M., Le Baccon, P., Coulon, A., Orsi, G.A., and Almouzni, G. (2020). Two HIRA-dependent pathways mediate H3.3 de novo deposition and recycling during transcription. Nat Struct Mol Biol *389*, 251–12.

Trouillet-Assant, S., Viel, S., Gaymard, A., Pons, S., Richard, J.-C., Perret, M., Villard, M., Brengel-Pesce, K., Lina, B., Mezidi, M., et al. (2020). Type I IFN immunoprofiling in COVID-19 patients. J. Allergy Clin. Immunol. *146*, 206–208.e2.

Van Damme, E., Laukens, K., Dang, T.H., and Van Ostade, X. (2010). A manually curated network of the PML nuclear body interactome reveals an important role for PML-NBs in SUMOylation dynamics. Int. J. Biol. Sci. *6*, 51–67.

Vancurova, M., Hanzlikova, H., Knoblochova, L., Kosla, J., Majera, D., Mistrik, M., Burdova, K., Hodny, Z., and Bartek, J. (2019). PML nuclear bodies are recruited to persistent DNA damage lesions in an RNF168-53BP1 dependent manner and contribute to DNA repair. DNA Repair (Amst) *78*, 114–127.

Voon, H.P.J., Hughes, J.R., Rode, C., La Rosa-Velázquez, De, I.A., Jenuwein, T., Feil, R., Higgs, D.R., and Gibbons, R.J. (2015). ATRX Plays a Key Role in Maintaining Silencing at Interstitial Heterochromatic Loci and Imprinted Genes. CellReports 1–32.

Wang, H., Xu, X., Nguyen, C.M., Liu, Y., Gao, Y., Lin, X., Daley, T., Kipniss, N.H., La Russa, M., and Qi, L.S. (2018). CRISPR-Mediated Programmable 3D Genome Positioning and Nuclear Organization. Cell *175*, 1405–1417.e1414.

Wang, J. (2004). Promyelocytic leukemia nuclear bodies associate with transcriptionally active genomic regions. J Cell Biol *164*, 515–526.

Wei, J., Alfajaro, M.M., DeWeirdt, P.C., Hanna, R.E., Lu-Culligan, W.J., Cai, W.L., Strine, M.S., Zhang, S.-M., Graziano, V.R., Schmitz, C.O., et al. (2021). Genome-wide CRISPR Screens Reveal Host Factors Critical for SARS-CoV-2 Infection. Cell *184*, 76–91.e13.

Workman, J.L. (2006). Nucleosome displacement in transcription. Genes & Development *20*, 2009–2017.

Yao, Q., Li, H., Liu, B.-Q., Huang, X.-Y., and Guo, L. (2011). SUMOylation-regulated protein phosphorylation, evidence from quantitative phosphoproteomics analyses. Journal of Biological Chemistry *286*, 27342–27349.

Ye, X., Zerlanko, B., Zhang, R., Somaiah, N., Lipinski, M., Salomoni, P., and Adams, P.D. (2007a). Definition of pRB- and p53-Dependent and -Independent Steps in HIRA/ASF1a-Mediated Formation of Senescence-Associated Heterochromatin Foci. Molecular and Cellular Biology *27*, 2452–2465.

Ye, X., Zerlanko, B., Kennedy, A., Banumathy, G., Zhang, R., and Adams, P.D. (2007b). Downregulation of Wnt Signaling Is a Trigger for Formation of Facultative Heterochromatin and Onset of Cell Senescence in Primary Human Cells. Molecular Cell *27*, 183–196.

Young, A.R.J., Narita, M., Ferreira, M., Kirschner, K., Sadaie, M., Darot, J.F.J., Tavare, S., Arakawa, S., Shimizu, S., and Watt, F.M. (2009). Autophagy mediates the mitotic senescence transition. Genes & Development *23*, 798–803.

Zhang, H., Gan, H., Wang, Z., Lee, J.-H., Zhou, H., Ordog, T., Wold, M.S., Ljungman, M., and Zhang, Z. (2017). RPA Interacts with HIRA and Regulates H3.3 Deposition at Gene Regulatory Elements in Mammalian Cells. Molecular Cell *65*, 272–284.

Zhang, R., Liu, S.-T., Chen, W., Bonner, M., Pehrson, J., Yen, T.J., and Adams, P.D. (2007). HP1 Proteins Are Essential for a Dynamic Nuclear Response That Rescues the Function of Perturbed Heterochromatin in Primary Human Cells. Molecular and Cellular Biology *27*, 949–962.

Zhang, R., Poustovoitov, M.V., Ye, X., Santos, H.A., Chen, W., Daganzo, S.M., Erzberger, J.P., Serebriiskii, I.G., Canutescu, A.A., Dunbrack, R.L., et al. (2005). Formation of MacroH2A-containing senescence-associated heterochromatin foci and senescence driven by ASF1a and HIRA. Developmental Cell *8*, 19–30.

Zhang, Y., Liu, T., Meyer, C.A., Eeckhoute, J., Johnson, D.S., Bernstein, B.E., Nusbaum, C., Myers, R.M., Brown, M., Li, W., et al. (2008). Model-based analysis of ChIP-Seq (MACS). Genome Biol *9*, R137–R139.

Zhao, Q., Xie, Y., Zheng, Y., Jiang, S., Liu, W., Mu, W., Liu, Z., Zhao, Y., Xue, Y., and Ren, J. (2014). GPS-SUMO: a tool for the prediction of sumoylation sites and SUMO-interaction motifs. Nucleic Acids Research *42*, W325–W330.

# Figure 1

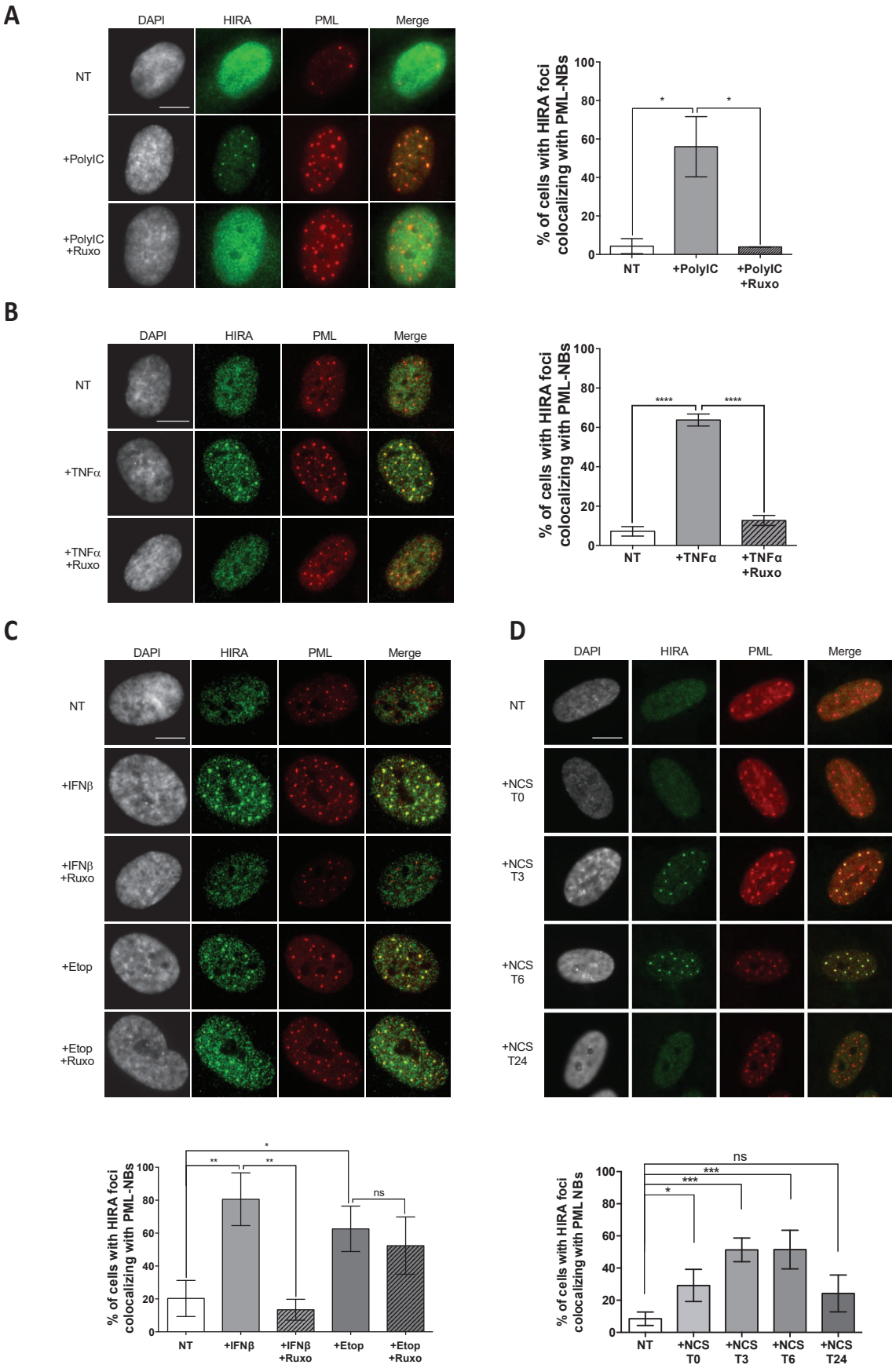
A
DAPI
HIRA
PML
Merge
NT
+PolyIC
+PolyIC +Ruxo
% of cells with HIRA foci colocalizing with PML-NBs
NT
+PolyIC
+PolyIC +Ruxo
B
+TNFα
+TNFα +Ruxo
C
+IFNβ
+IFNβ +Ruxo
+Etop
+Etop +Ruxo
D
+NCS T0
+NCS T3
+NCS T6
+NCS T24
% of cells with HIRA foci colocalizing with PML NBs

# Figure 2

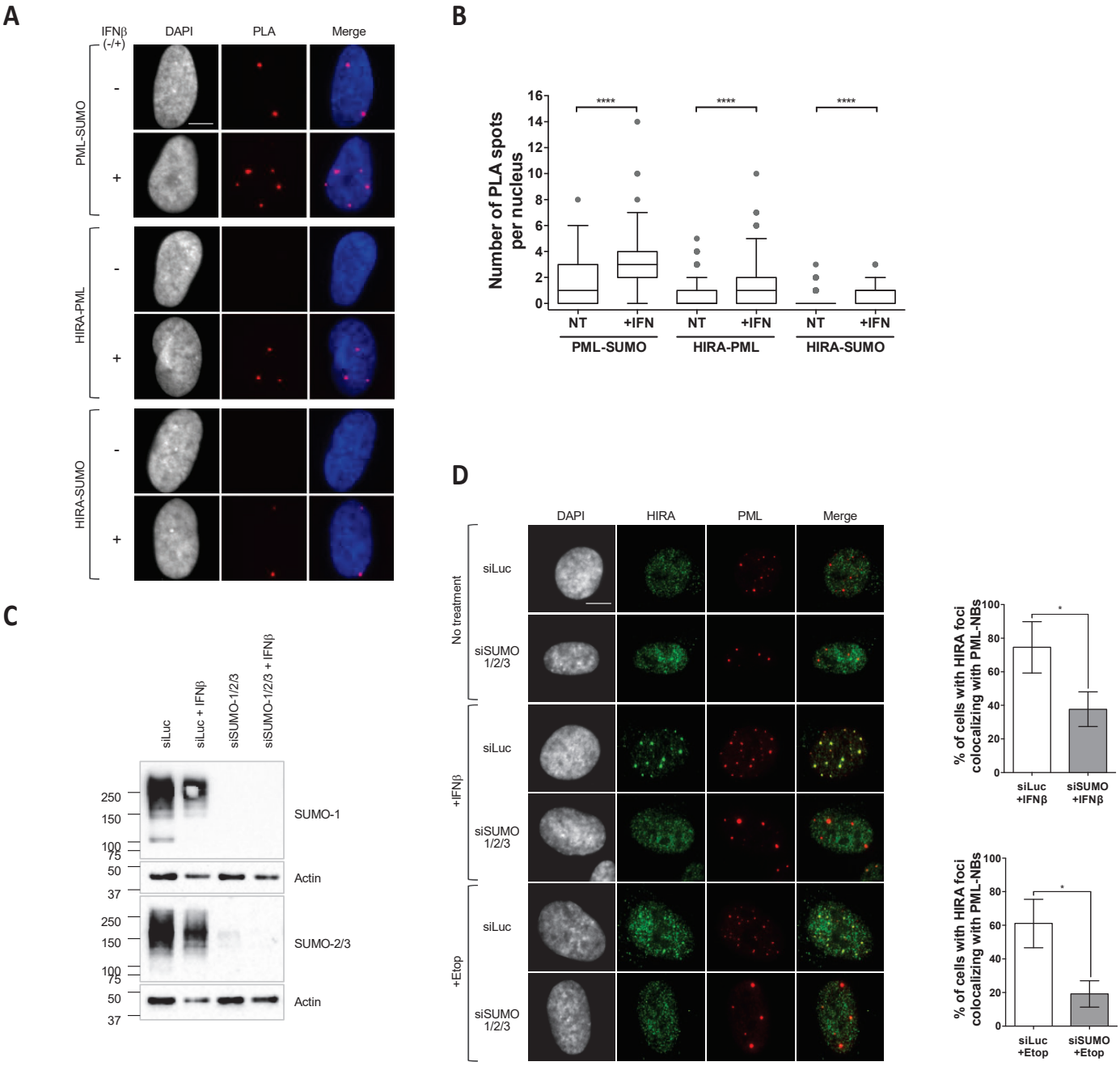
A
IFNβ (-/+)
DAPI
PLA
Merge
PML-SUMO
HIRA-PML
HIRA-SUMO
B
Number of PLA spots per nucleus
****
NT
+IFN
PML-SUMO
HIRA-PML
HIRA-SUMO
C
siLuc
siLuc + IFNβ
siSUMO-1/2/3
siSUMO-1/2/3 + IFNβ
SUMO-1
Actin
SUMO-2/3
D
DAPI
HIRA
PML
Merge
No treatment
+IFNβ
+Etop
siLuc
siSUMO 1/2/3
% of cells with HIRA foci colocalizing with PML-NBs
siLuc +IFNβ
siSUMO +IFNβ
siLuc +Etop
siSUMO +Etop

# Figure 3

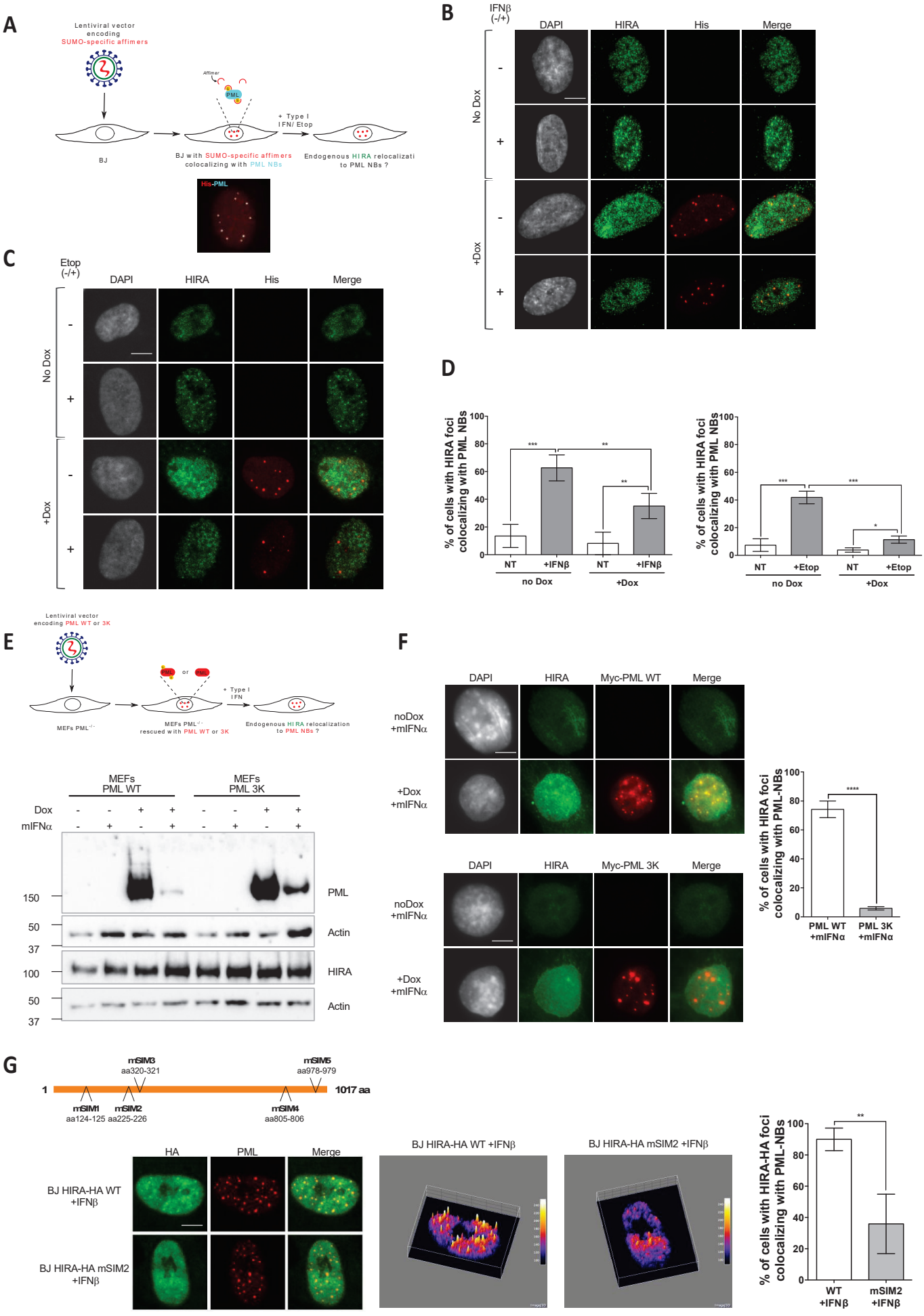
A
Lentiviral vector encoding SUMO-specific affimers
Affimer
PML
BJ
BJ with SUMO-specific affimers colocalizing with PML NBs
+ Type I IFN/ Etop
Endogenous HIRA relocalizati to PML NBs ?
His-PML
B
IFNβ (-/+)
DAPI
HIRA
His
Merge
No Dox
+Dox
C
Etop (-/+)
D
% of cells with HIRA foci colocalizing with PML NBs
NT
+IFNβ
no Dox
+Dox
+Etop
E
Lentiviral vector encoding PML WT or 3K
MEFs PML-/-
MEFs PML-/- rescued with PML WT or 3K
Endogenous HIRA relocalization to PML NBs ?
MEFs PML WT
MEFs PML 3K
Dox
mIFNα
150
50
37
100
PML
Actin
HIRA
F
Myc-PML WT
Myc-PML 3K
noDox +mIFNα
+Dox +mIFNα
PML WT +mIFNα
PML 3K +mIFNα
G
mSIM1 aa124-125
mSIM2 aa225-226
mSIM3 aa320-321
mSIM4 aa805-806
mSIM5 aa978-979
1
1017 aa
HA
PML
Merge
BJ HIRA-HA WT +IFNβ
BJ HIRA-HA mSIM2 +IFNβ
% of cells with HIRA-HA foci colocalizing with PML-NBs
WT +IFNβ
mSIM2 +IFNβ

Figure 4

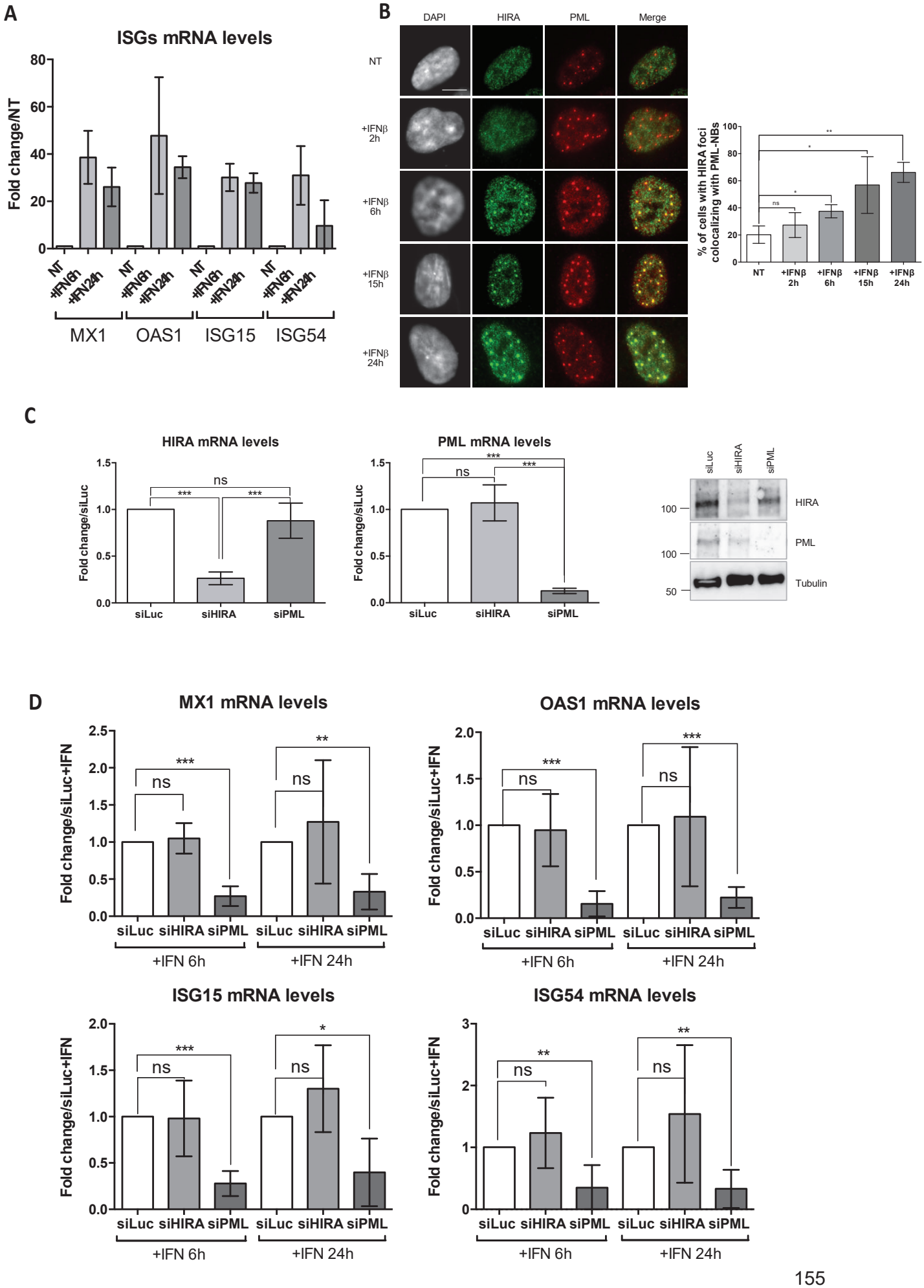
A
ISGs mRNA levels
Fold change/NT
NT
+IFNβ 6h
+IFNβ 24h
MX1
OAS1
ISG15
ISG54
B
DAPI
HIRA
PML
Merge
NT
+IFNβ 2h
+IFNβ 6h
+IFNβ 15h
+IFNβ 24h
% of cells with HIRA foci colocalizing with PML-NBs
C
HIRA mRNA levels
PML mRNA levels
Fold change/siLuc
siLuc
siHIRA
siPML
HIRA
PML
Tubulin
D
MX1 mRNA levels
OAS1 mRNA levels
ISG15 mRNA levels
ISG54 mRNA levels
Fold change/siLuc+IFN
+IFN 6h
+IFN 24h

# Figure 5

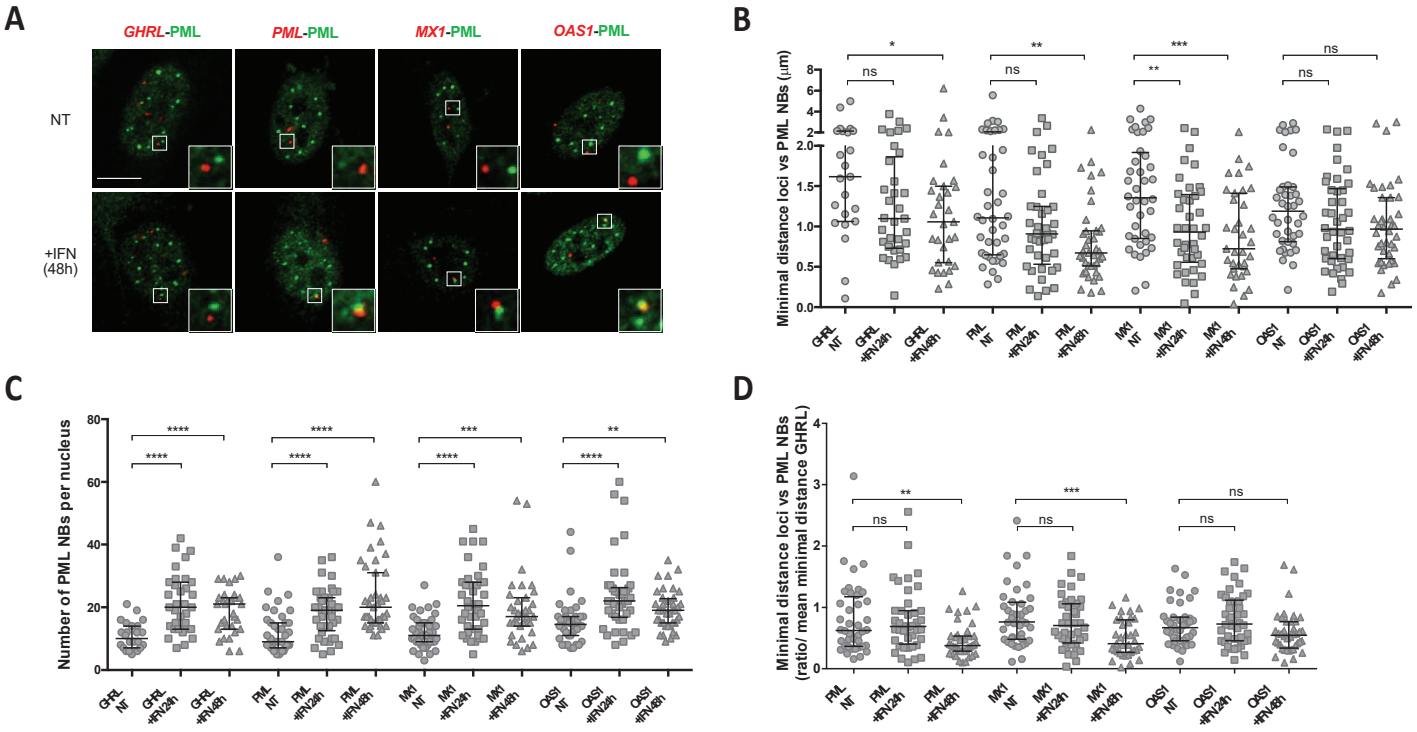
A
GHRL-PML
PML-PML
MX1-PML
OAS1-PML
NT
+IFN (48h)
B
Minimal distance loci vs PML NBs (µm)
C
Number of PML NBs per nucleus
D
Minimal distance loci vs PML NBs (ratio/ mean minimal distance GHRL)

# Figure 6

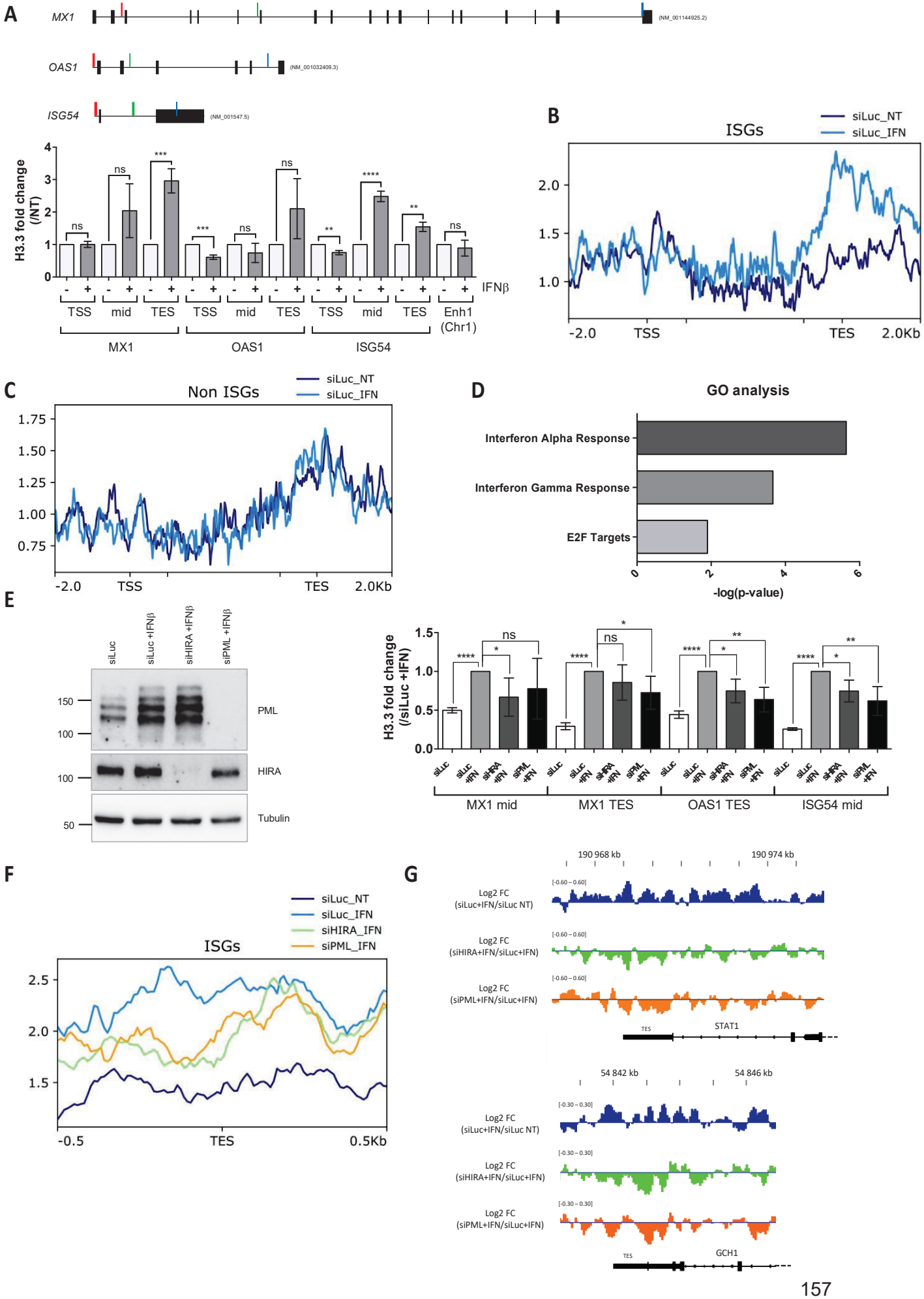
A
MX1
OAS1
ISG54
H3.3 fold change (/NT)
IFNβ
TSS
mid
TES
Enh1 (Chr1)
MX1
OAS1
ISG54
B
ISGs
siLuc_NT
siLuc_IFN
-2.0
TSS
TES
2.0Kb
C
Non ISGs
siLuc_NT
siLuc_IFN
D
GO analysis
Interferon Alpha Response
Interferon Gamma Response
E2F Targets
-log(p-value)
E
siLuc
siLuc +IFNβ
siHIRA +IFNβ
siPML +IFNβ
PML
HIRA
Tubulin
H3.3 fold change (/siLuc +IFN)
MX1 mid
MX1 TES
OAS1 TES
ISG54 mid
F
ISGs
siLuc_NT
siLuc_IFN
siHIRA_IFN
siPML_IFN
-0.5
TES
0.5Kb
G
190 968 kb
190 974 kb
Log2 FC (siLuc+IFN/siLuc NT)
Log2 FC (siHIRA+IFN/siLuc+IFN)
Log2 FC (siPML+IFN/siLuc+IFN)
STAT1
54 842 kb
54 846 kb
GCH1

Figure 7

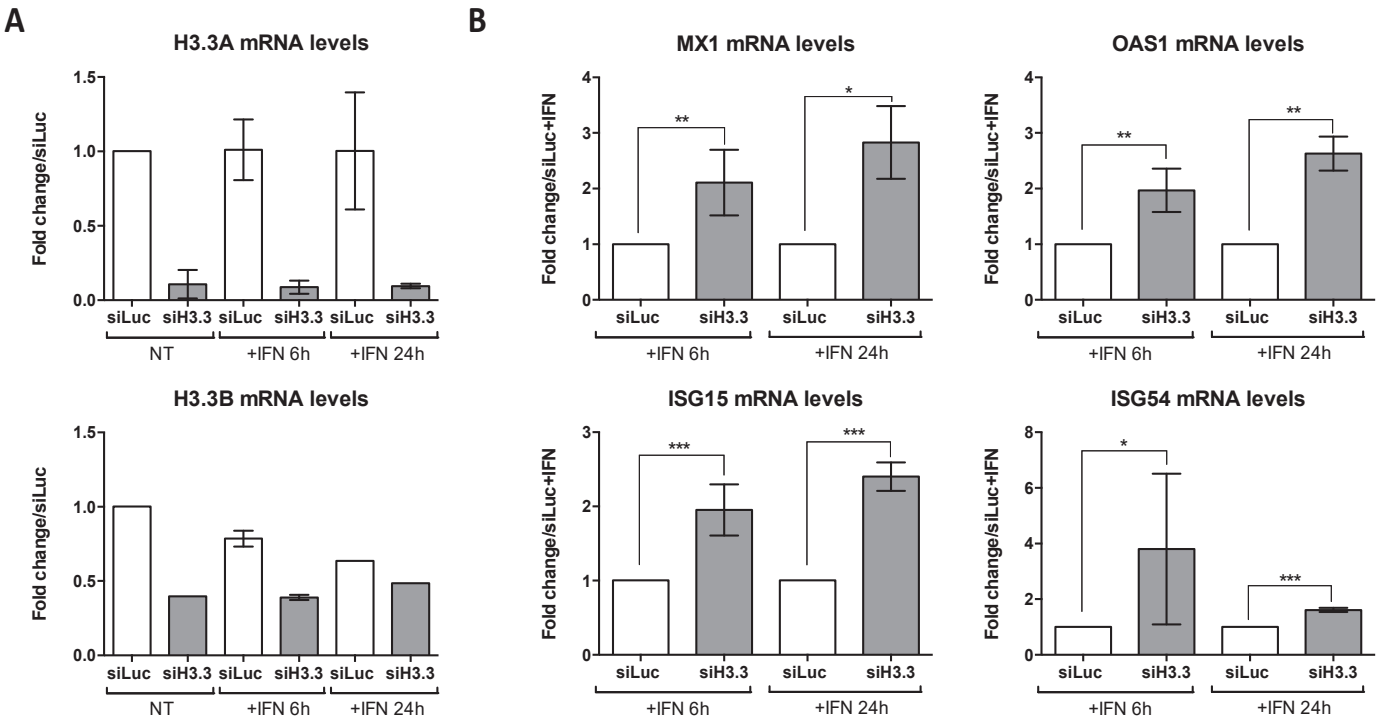
A
H3.3A mRNA levels
Fold change/siLuc
siLuc siH3.3 siLuc siH3.3 siLuc siH3.3
NT +IFN 6h +IFN 24h
H3.3B mRNA levels
B
MX1 mRNA levels
OAS1 mRNA levels
ISG15 mRNA levels
ISG54 mRNA levels
Fold change/siLuc+IFN
+IFN 6h +IFN 24h

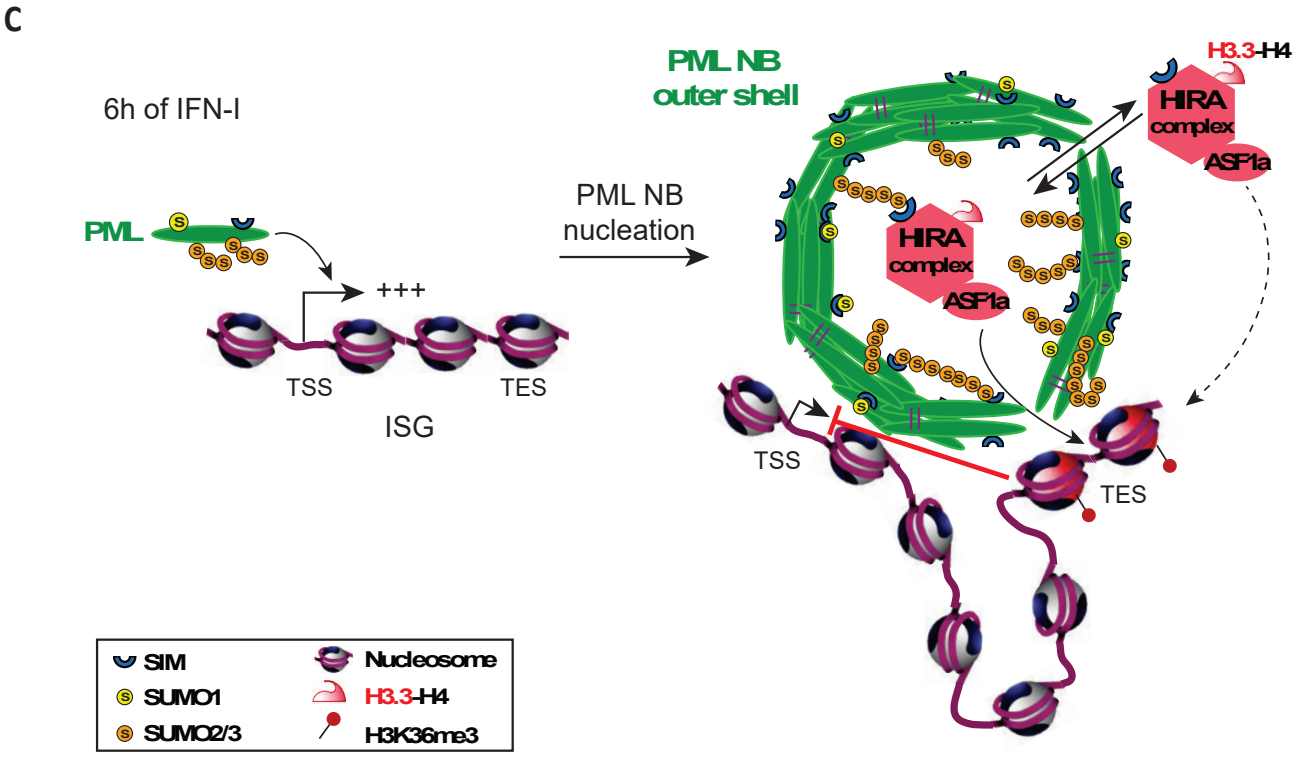
C
6h of IFN-I
PML
+++
TSS
TES
ISG
PML NB nucleation
PML NB outer shell
HIRA complex
ASF1a
H3.3-H4
SIM
SUMO1
SUMO2/3
Nucleosome
H3K36me3

# Supplementary Figure 1

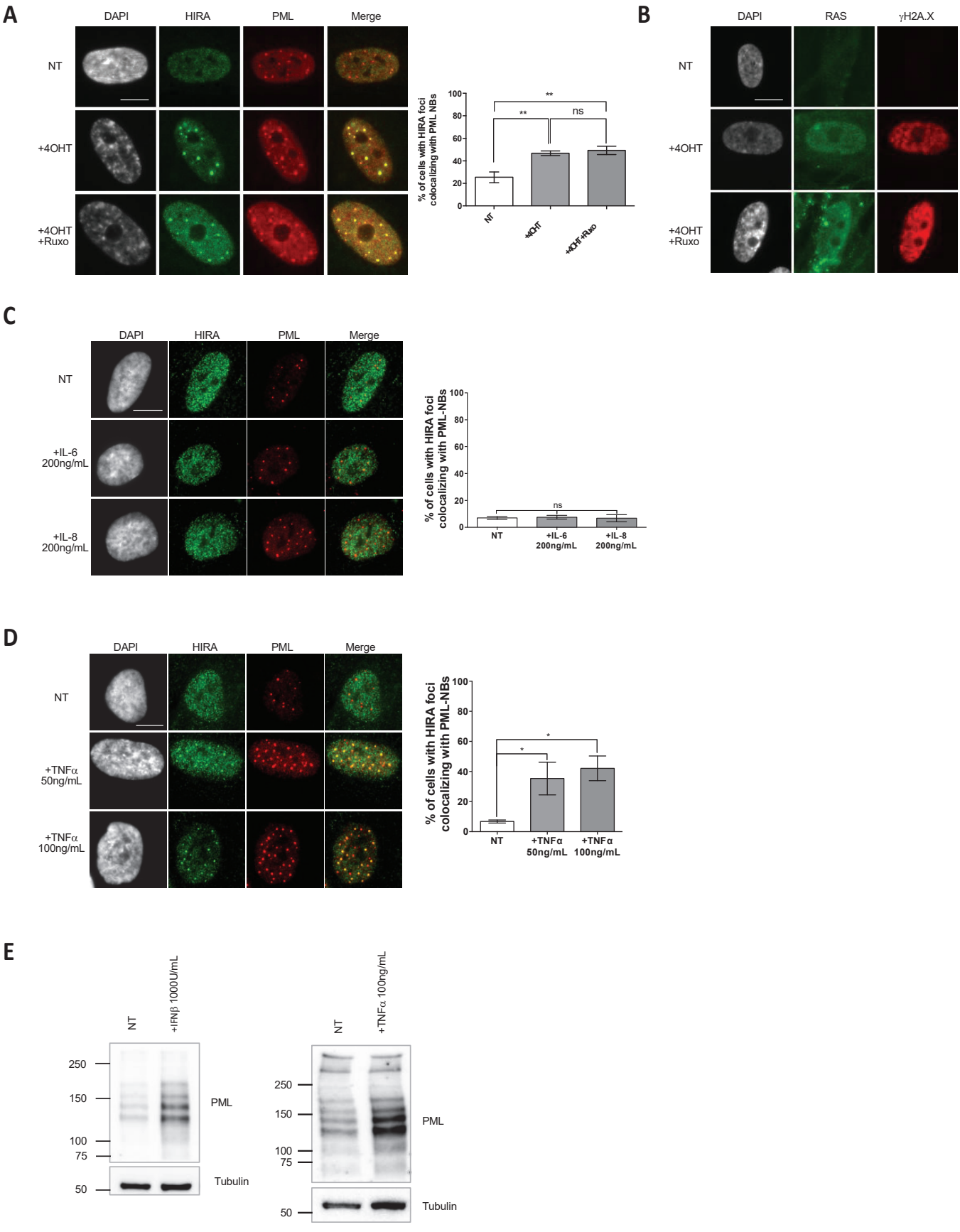

# Supplementary Figure 2

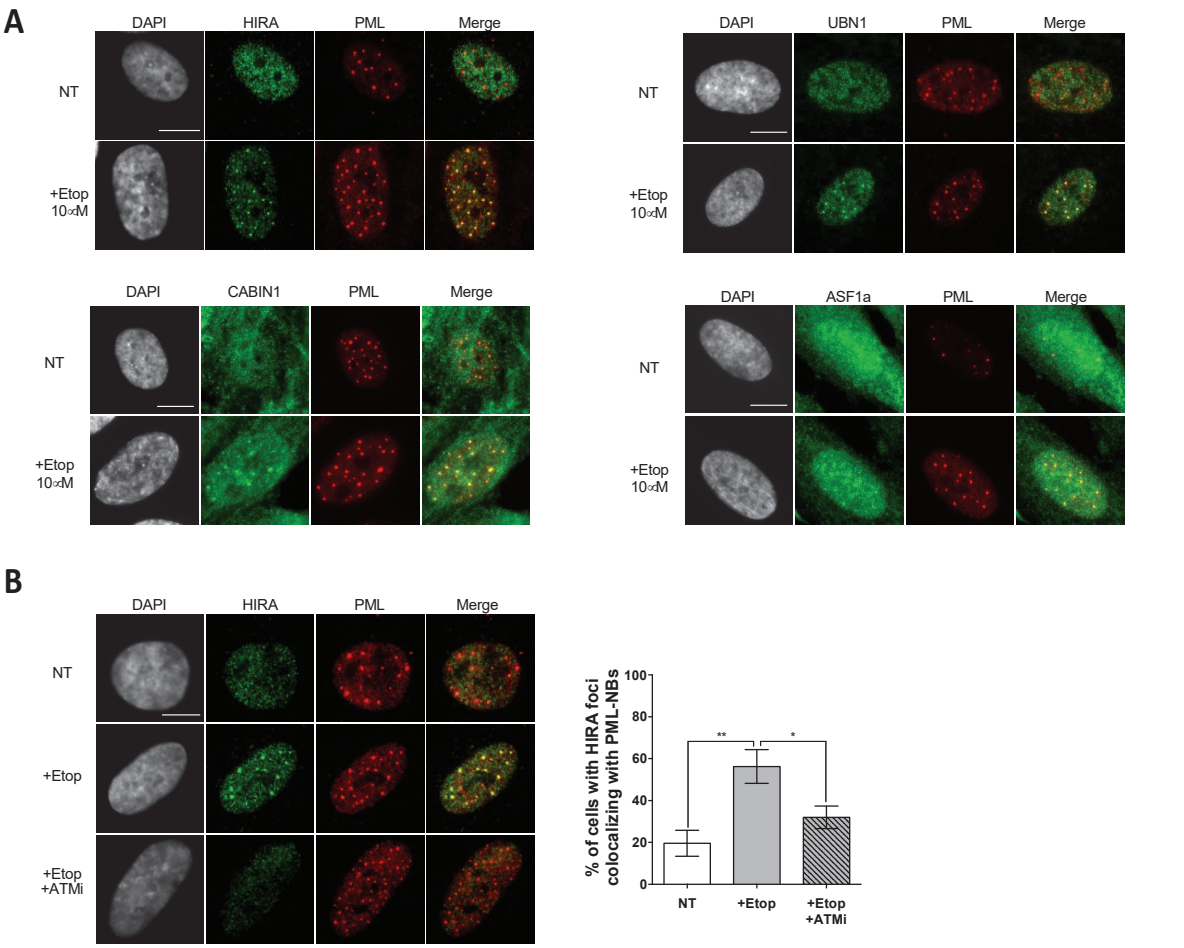

# Supplementary Figure 3

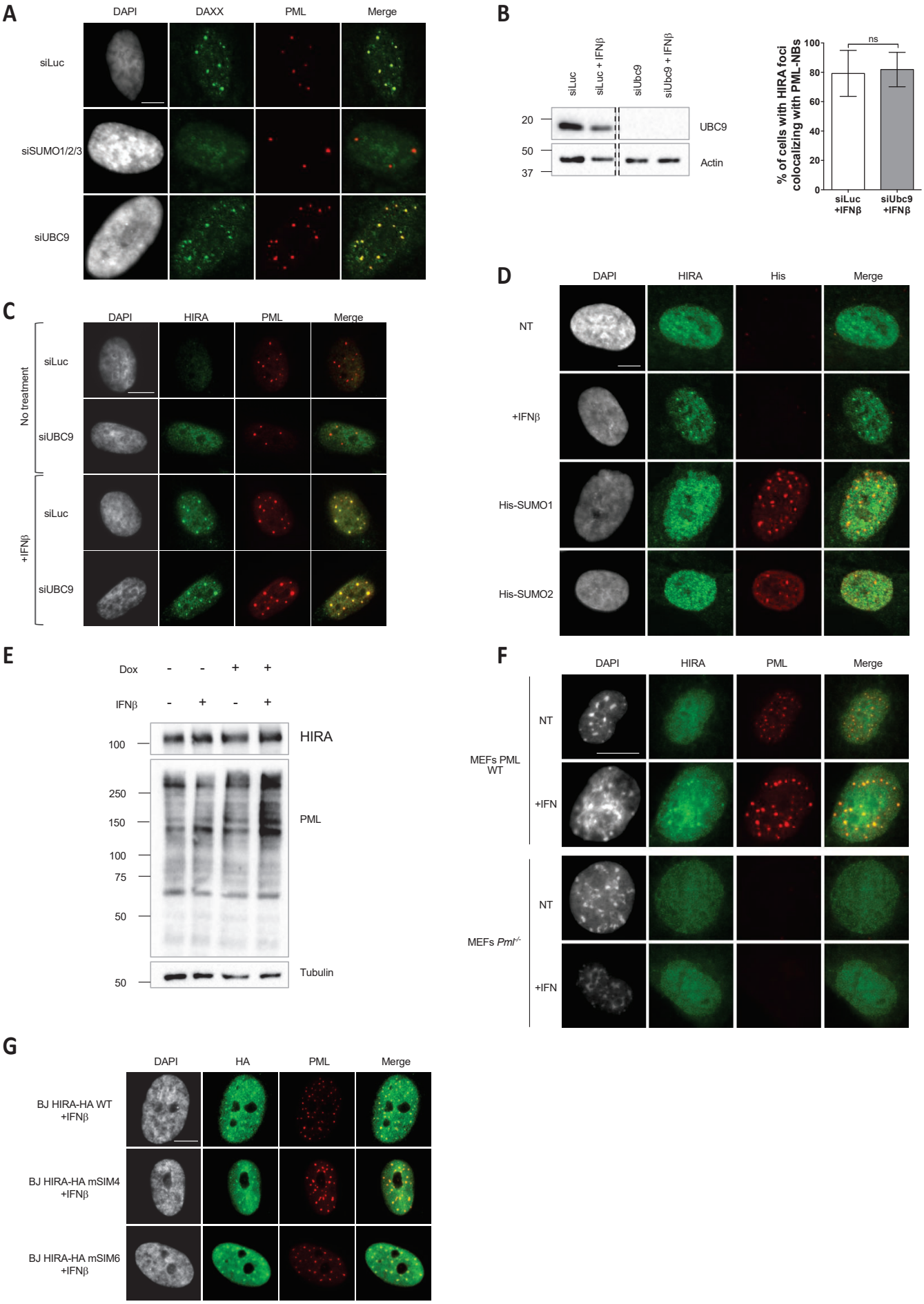

# Supplementary Figure 4

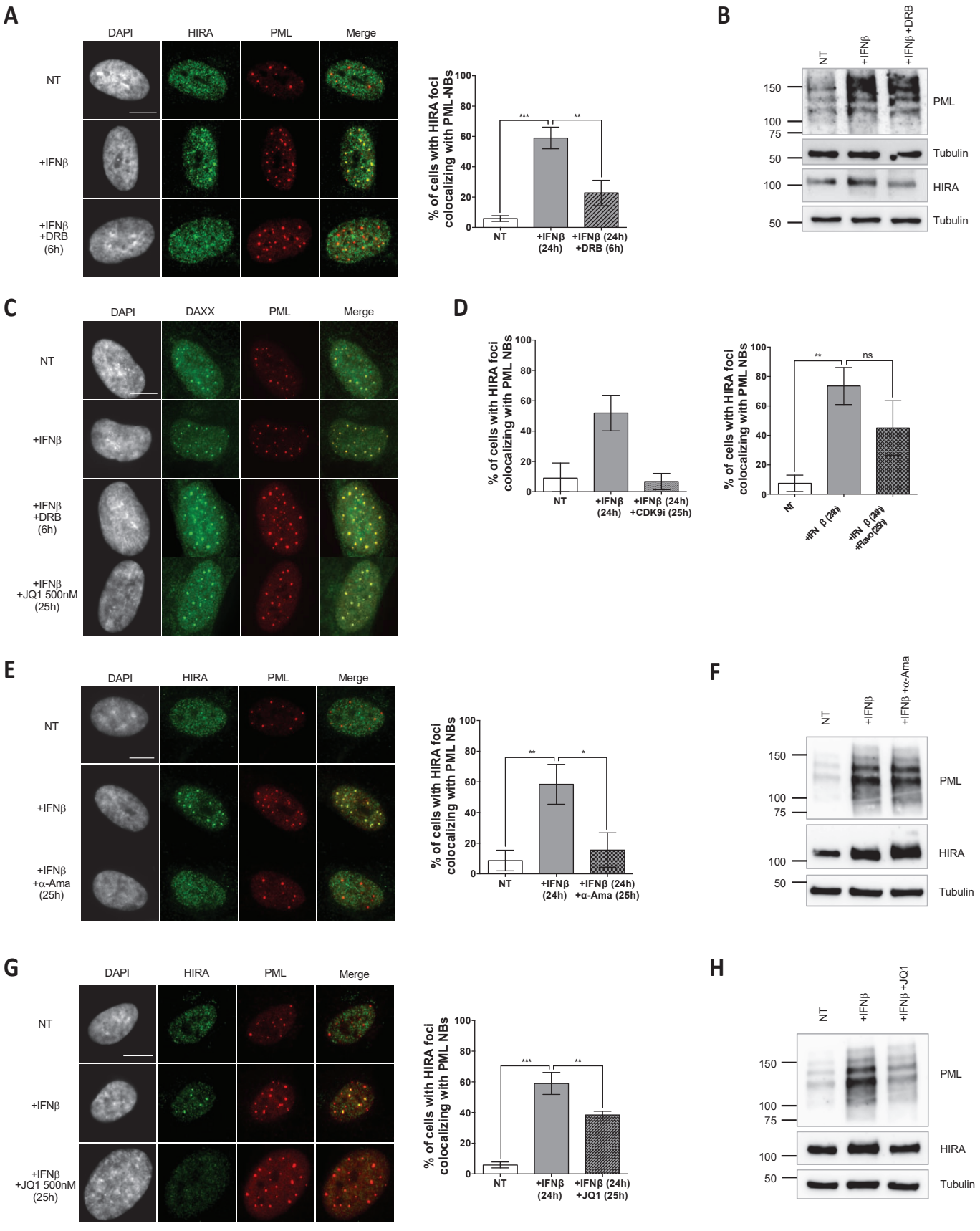

# Supplementary Figure 5

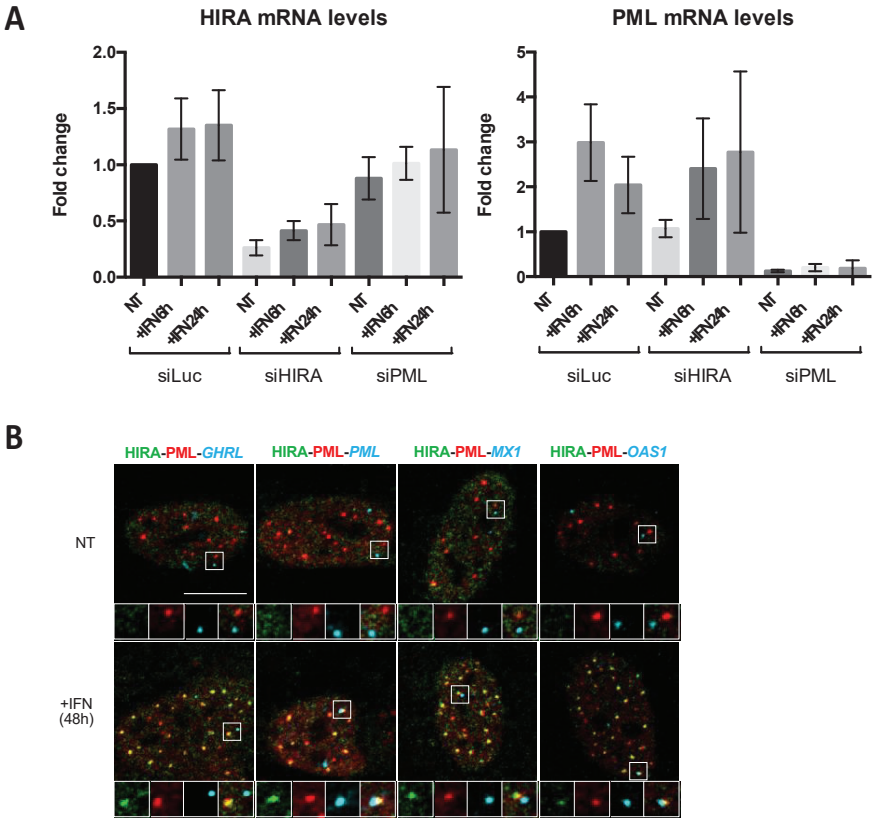

# Supplementary Figure 6

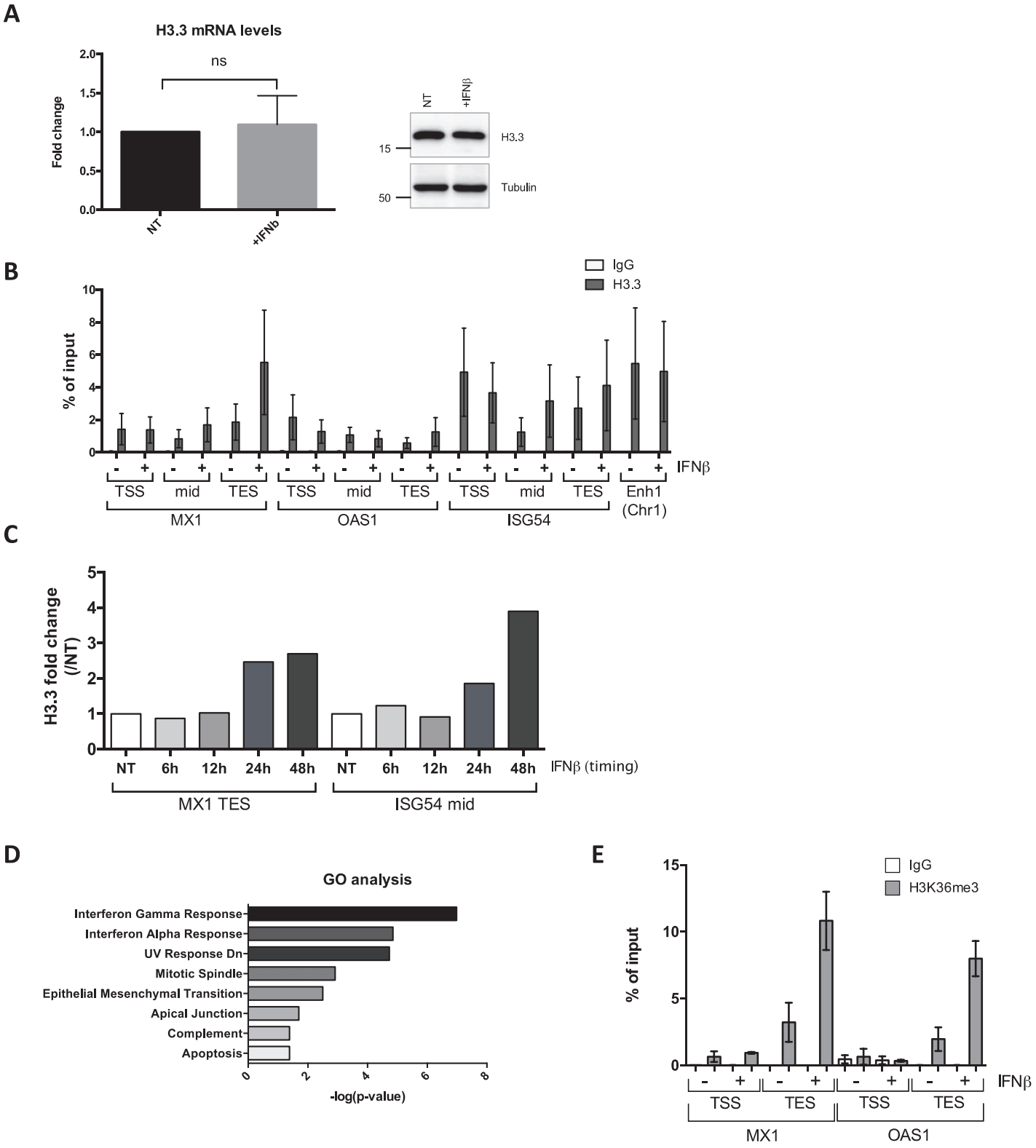

# Supplementary Figure 7

**A**

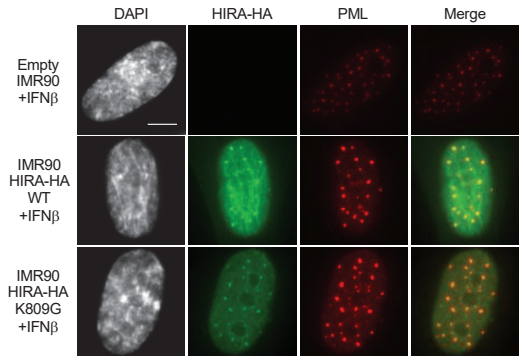


**B**

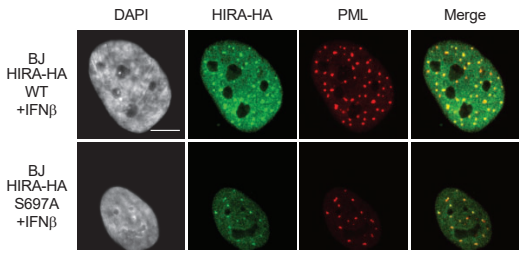

# II. Résultats supplémentaires

Outre les résultats présentés précédemment dans le manuscrit, mes travaux de thèse ont permis d'explorer d'autres questions, en particulier sur la relocalisation d'HIRA dans les PML NBs en réponse aux DSBs. Ces résultats supplémentaires sont présentés dans cette partie.

Nos résultats ont montré que le traitement de cellules avec des agents génotoxiques générateurs de DSBs induit la relocalisation du complexe HIRA dans les PML NBs de façon indépendante de la voie IFN. Le recrutement de HIRA dans les PML NBs sous étoposide est dépendant d'une interaction SIM-SUMO, comme pour la relocalisation induite par l'IFN. De façon intéressante, la relocalisation corrèle avec une juxtaposition des PML NBs et des sites de dommage à l'ADN, juxtaposition observée dans de nombreuses autres études (Carbone et al., 2002; Dellaire and Bazett-Jones, 2004; Dellaire et al., 2006a; Vancurova et al., 2019; Yeung et al., 2012). Nous avons donc voulu regarder plus en détail le mécanisme de relocalisation d'HIRA dans les PML NBs et de juxtaposition aux sites de dommages.

## Matériels et méthodes complémentaires

Une grande partie des matériels et méthodes est décrit dans le manuscrit d'article scientifique. Cependant, les résultats supplémentaires présentés ci-dessous m'amènent à préciser de nouveaux éléments.

*Plasmides supplémentaires*

Les transgènes GFP-Flag-cGAS WT et mCat (E225A D227A) ont été obtenus par PCR en utilisant le plasmide pTRIP-CMV-GFP-Flag-cGAS WT ou mCat (Addgene, #86675 et #86674) comme modèle et ont été clonés dans le plasmide pLVX-TetOne résistant à la puromycine, avec les enzymes de restriction BstZ17I et AgeI. Les mutations pour la résistance au sicGAS #01 et pour le transgène GFP-Flag-cGAS mDNA-BD (C396A C397A) ont été réalisées par mutagenèse dirigée comme décrit précédemment.

*Séquences siRNAs supplémentaires*

Le protocole de transfection avec un siRNA utilisé est décrit dans le matériel et méthode du manuscrit d'article. Les siRNAs utilisés pour les études supplémentaires et leurs séquences sont résumés dans le ***Tableau 5***.

**Tableau 5. Liste des siRNAs utilisés dans les résultats supplémentaires.**

| siRNA | Séquence |
|---|---|
| sicGAS #01 | 5'CGUGAAGAUUUCUGCACCUdTdT |
| sicGAS #02 | 5'GCAAAAGUUAGGAAGCAACdTdT |
| siLuc | 5'CGUACGCGGAAUACUUCGAdTdT |
| siSTING | 5'CCUCAUCAGUGGAAUGGAAdTdT |

*Anticorps supplémentaires*

La liste des anticorps supplémentaires utilisés ainsi que les espèces chez lesquelles ils ont été produit, les références et les dilutions sont résumées dans le ***Tableau 6***.

**Tableau 6. Liste des anticorps utilisés dans les résultats supplémentaires.**

| Antibody | Species | Reference | Dilution | |
|---|---|---|---|---|
| | | | IF | WB |
| Actin | Rabbit polyclonal | Sigma A2066 | | 1:1000 |
| cGAS | Rabbit monoclonal (clone D1D3G) | Cell Signaling 15102 | 1:100 | 1:500 |
| γH2AX #01 | Mouse monoclonal (clone 6L16) | Millipore 05-636 | 1:500 | 1:1000 |
| γH2AX #02 | Rabbit polyclonal | Abcam ab2893 | 1:500 | 1:1000 |
| HA #01 | Rabbit polyclonal | Abcam Ab9110 | 1:1000 | |
| HIRA #01 | Mouse monoclonal (clone WC119) | Active Motif 3558 | 1:500 | 1:1000 |
| HIRA #02 | Mouse monoclonal (clone WC119) | Millipore 04-1488 | 1:500 | 1:1000 |
| PML #01 | Mouse monoclonal (clone PG-M3) | Santa Cruz sc-966 | 1:200 | |
| PML #02 | Rabbit polyclonal | Santa Cruz sc-5621 | 1:200 | 1:1000 |
| PML #03 | Rabbit polyclonal | Sigma PLA0172 | 1:50000 | 1:1000 |
| STING | Mouse monoclonal (clone #723505) | R&D MAB7169 | | 1:1000 |
| αTubulin | Mouse monoclonal (clone DM1A) | Sigma T6199 | | 1:10000 |

*Analyses de microscopie*

Les images ont été acquises avec le microscope à épifluorescence Axio Observer Z1 inversé (100X ou 63X/N.A. 1.46 ou 1.4) (Zeiss) et une caméra CoolSnap HQ2 (Photometrics). Des réglages identiques ont été appliqués pour les images d'une même expérience pour permettre la comparaison des données. Les images ont été traitées avec le logiciel Fiji.

La relocalisation de HIRA a été attesté par le comptage d'un minimum de 100 cellules pour chaque condition.

Le chevauchement des PML NBs avec des foyers γH2AX a été mesuré en utilisant le masque RenyiEntropy de Fiji sur les marquages PML et γH2AX. Le chevauchement a été calculé avec le plugin Image Calculator en utilisant l'opération 'AND' (***Figure 32***).

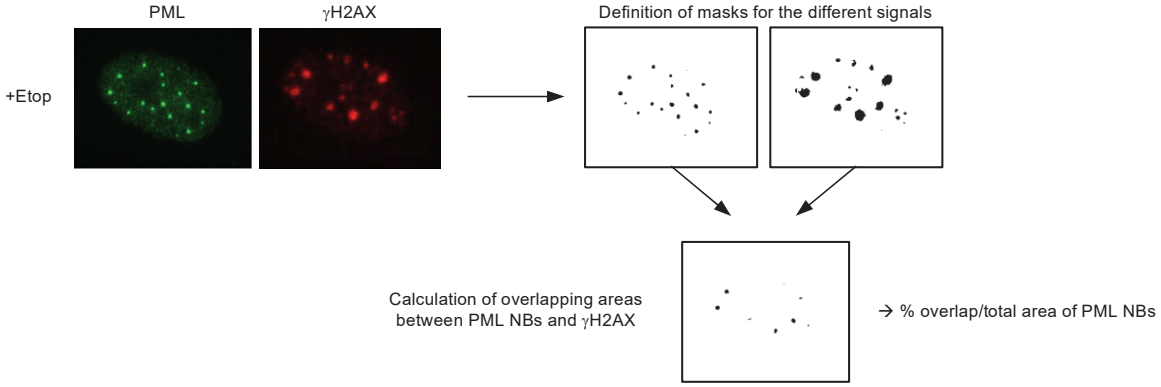


**Figure 32. Analyse de la juxtaposition entre les PML NBs et les foyers γH2AX.** Modèle pour la mesure de l'aire de chevauchement entre les PML NBs et les foyers γH2AX. L'aire de chevauchement est rapportée sur l'aire des PML NBs pour générer le % d'aire de PML NBs ch chevauchant du signal γH2AX.

## Résultats

*La protéine cGAS est impliquée dans la relocalisation d'HIRA aux PML NBs sous étoposide, indépendamment de l'activation de STING*

L'induction de DSBs et la poursuite du cycle cellulaire peut conduire à la formation de micronoyaux, l'activation de la voie cGAS-STING et la production d'IFN de type I par les cellules endommagées (Harding et al., 2017 ; Mackenzie et al., 2017). La liaison de l'IFN de type I à son récepteur pourrait ainsi induire la relocalisation du complexe HIRA observée après l'induction de dommages. Nos résultats avec le ruxolitinib suggèrent que la relocalisation induite par les DSBs est en fait indépendante de la voie de signalisation à l'IFN. Nous avons également voulu voir si l'inactivation des protéines cGAS et STING pouvait corroborer les résultats obtenus avec le ruxolitinib. De façon similaire au ruxolitinib, l'inactivation de la protéine STING n'impacte pas la relocalisation de HIRA sous étoposide (***Figure 33a et b***). En revanche, et de manière surprenante, l'inactivation de la protéine

cGAS diminue de façon significative le pourcentage de cellules présentant HIRA en foyer dans les PML NBs sous étoposide (***Figure 33a et b***). Ainsi, cela suggère un rôle spécifique de la protéine cGAS dans l'induction de la relocalisation, indépendant de la voie cGAS-

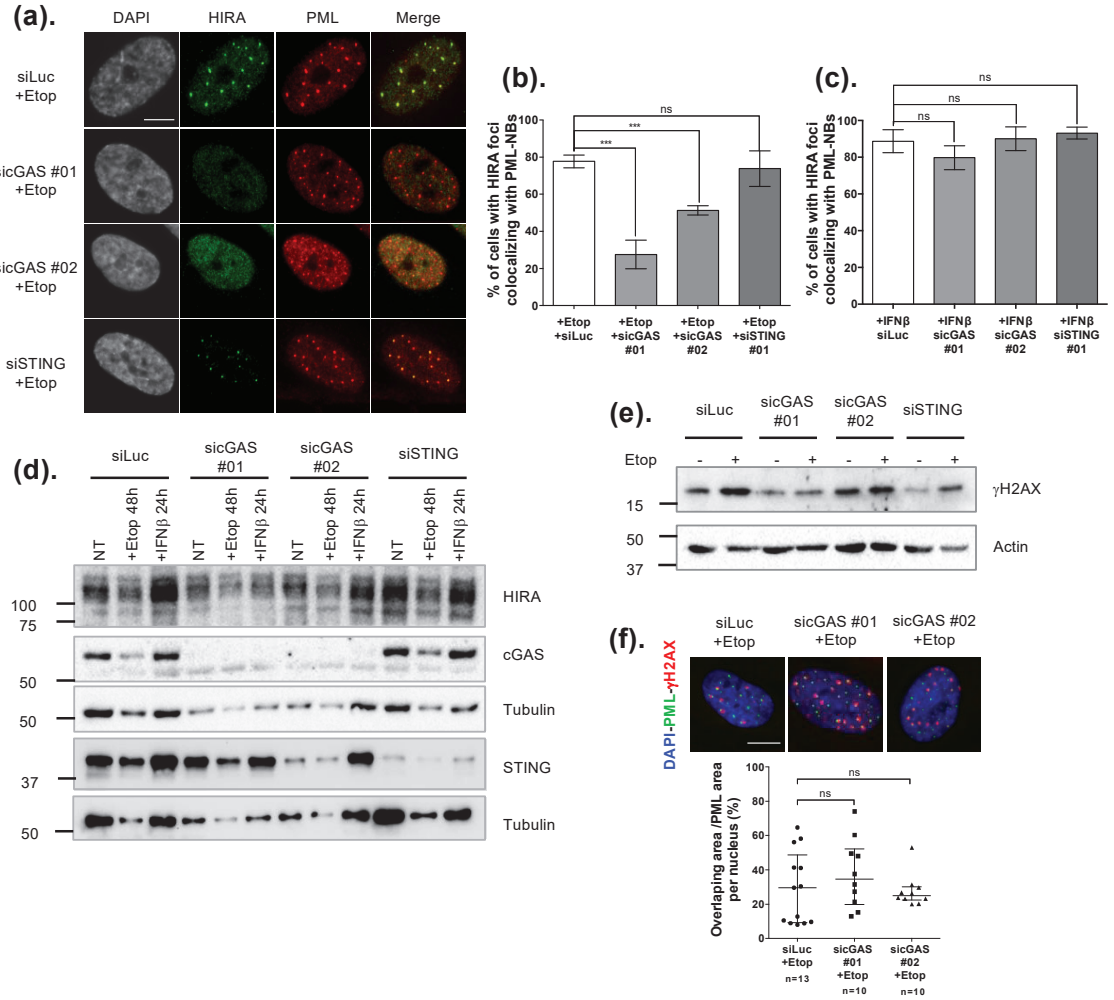


**Figure 33. L'inactivation de cGAS inhibe la relocalisation de HIRA dans les PML NBs**. **(a)**. Visualisation de HIRA (vert) et PML (rouge) par microscopie à fluorescence dans des cellules BJ traitées avec 60nM de siRNA contre la luciférase (Luc), cGAS ou STING pendant 72h et avec de l'étoposide (Etop) à 10μM pendant les 48 dernières heures. On observe une perte de foyers HIRA après l'inactivation de cGAS. Le noyau des cellules est visualisé par un marquage DAPI (gris). La barre d'échelle correspond à 10μm. **(b)**. Analyse quantitative du pourcentage de cellules présentant des foyers HIRA co-localisant avec les PML NBs. Les cellules sont traitées comme dans le panel **a**. Moyenne de 3 expériences indépendantes ±SD. p-value (Student t-test): ***<0,001 ; ns=non-significatif. **(c)**. Analyse quantitative du pourcentage de cellules présentant des foyers HIRA co-localisant avec les PML NBs. Les cellules sont traitées avec 60nM de siRNA contre Luc, cGAS ou STING pendant 72h et avec de l'IFNβ 1000U/mL pendant les 24 dernières heures. Moyenne de 3 expériences indépendantes ±SD. p- value (Student t-test): ns=non significatif. **(d)**. Visualisation par western blot de HIRA, cGAS et STING à partir d'extraits cellulaires totaux de BJ traitées comme dans **a** et **b** ou **c**. La tubuline sert ici de contrôle de dépôt. On observe notamment que la concentration en protéines déposées pour les différentes conditions n'est pas constante ; néanmoins, on peut visualiser la baisse de protéines cGAS ou STING induite par le traitement siRNA. **(e)**. Visualisation par western blot de γH2AX à partir d'extraits cellulaires totaux de BJ traitées comme dans **a** et **b**. L'actine sert ici de contrôle de dépôt. **(f)**. Visualisation de PML (vert) et γH2AX (rouge) par microscopie à fluorescence (en haut) dans des cellules BJ traitées comme dans a et b. Le noyau des cellules est visualisé par un marquage DAPI (bleu). La barre d'échelle correspond à 10μm. Mesure du pourcentage de chevauchement entre les PML NBs et les foyers γH2AX (en bas). Chaque point correspond à un noyau analysé. La barre du milieu correspond à la médiane des valeurs, les barres du bas et du haut correspondent respectivement au 1er et 3ème quartile. L'information n=x correspond au nombre de noyaux analysés. Les noyaux analysés sont issus d'une expérience. p-value (Mann-Whitney u-test): ns=non-significatif.

STING-IFN. Ce rôle est spécifique à la relocalisation induite par les DSBs puisque l'inactivation de cGAS dans des cellules traitées à l'IFNβ n'impacte pas la relocalisation de HIRA (***Figure 33c***). Nous avons voulu voir si l'inactivation de cGAS pouvait également impacter la juxtaposition des PML NBs avec les sites de dommages. Pour ce faire, nous avons défini des masques sur les différents signaux, puis nous avons généré un masque représentant les zones de chevauchement (***Figure 32).*** Nous avons ensuite calculé l'aire de chevauchement rapportée sur l'aire totale de PML NB. Dans la condition siLuc, en moyenne 30% de l'aire des PML NBs chevauche du signal γH2AX lors d'un traitement à l'étoposide de 48h. La perte de cGAS ne semble pas impacter le pourcentage de chevauchement (Figure 33f). Ainsi, la protéine cGAS, bien qu'elle soit impliquée dans la relocalisation d'HIRA dans les PML NBs sous étoposide, ne semble pas jouer un rôle dans la juxtaposition des PML NBs avec les sites de dommages.

Pour mieux comprendre le lien entre la protéine cGAS et la relocalisation du complexe HIRA sous étoposide, nous avons tout d'abord regardé la localisation cellulaire de cGAS. En conditions normales et sous IFNβ, la protéine cGAS endogène présente une localisation pan-nucléaire. Lorsque les cellules sont soumises à un traitement à l'étoposide pendant 24h, le marquage nucléaire de cGAS diminue fortement (***Figure 34a et b***). La protéine GFP-cGAS WT exogène présente également un marquage nucléaire dans les cellules non traitées. Sous étoposide, le marquage nucléaire de GFP-cGAS WT diminue et un marquage cytoplasmique apparaît (***Figure 34c***). Ainsi, lors de l'induction de DSBs, la protéine cGAS semble transloquer dans le cytoplasme. Cette translocation ne semble pas dépendre de la relocalisation de HIRA dans les PML NBs. En effet, l'accumulation de

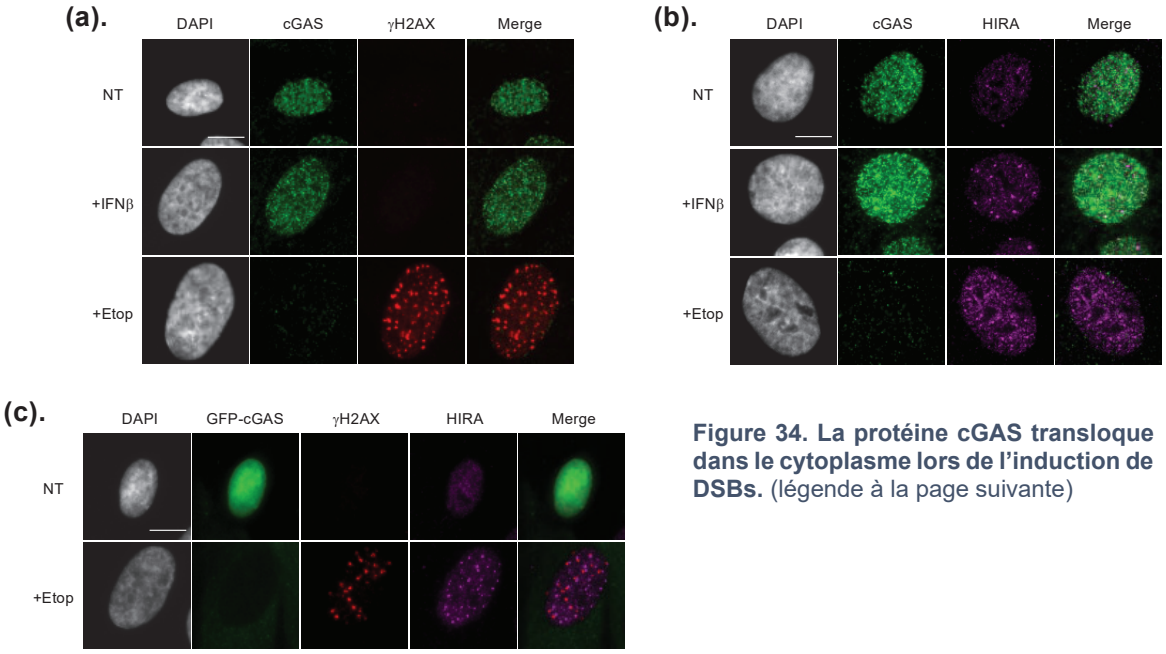


**Figure 34. La protéine cGAS transloque dans le cytoplasme lors de l'induction de DSBs.** (légende à la page suivante)

**Figure 34. La protéine cGAS transloque dans le cytoplasme lors de l'induction de DSBs.** (page précédente) **(a)**. Visualisation de cGAS endogène (vert) et de γH2AX (rouge) par microscopie à fluorescence dans des cellules BJ traitées avec de l'IFNβ à 1000U/mL ou de l'étoposide (Etop) à 10μM pendant 24h. On observe une disparition du signal cGAS sous étoposide. **(b)**. Visualisation de cGAS endogène (vert) et de HIRA (magenta) par microscopie à fluorescence dans des cellules BJ traitées comme pour **a**. **(c)**. Visualisation de GFP-cGAS WT (vert), de γH2AX (rouge) et de HIRA (magenta) par microscopie à fluorescence dans des cellules BJ transduites avec une construction GFP-cGAS WT inductible par la doxycycline (Dox) (induction à 100ng/mL pendant 26h) et traitées avec de l'étoposide (Etop) pendant 24h. On observe une translocation du signal GFP-cGAS dans le cytoplasme sous étoposide. **(a-c)**. Le noyau des cellules est visualisé par un marquage DAPI (gris). La barre d'échelle correspond à 10μm.

HIRA en foyers induite par un traitement à l'IFNβ coïncide avec un marquage cGAS nucléaire. En revanche, il serait intéressant de voir si à l'inverse, la relocalisation du complexe HIRA à la suite de DSBs dépend de la translocation de cGAS dans le cytoplasme.

Afin de confirmer que la localisation de HIRA au sein des PML NBs est dépendante de cGAS, nous avons réintroduit la protéine GFP-cGAS WT dans des cellules préalablement inactivées pour cGAS endogène. La protéine exogène est résistante à l'inactivation par le siRNA cGAS #01 grâce à des mutations silencieuses G>A aux positions 654 et 657 du cDNA. Comme démontré précédemment, l'inactivation de cGAS dans les BJ GFP-cGAS WT non induites diminue de façon importante le pourcentage de cellules présentant des foyers de protéines HIRA (***Figure 35d et e***). L'expression de la protéine GFP cGAS WT restaure le phénomène de relocalisation de HIRA sous étoposide, démontrant que la protéine cGAS sauvage est importante pour le recrutement de HIRA dans les PML NBs après l'induction de DSBs. Nous avons ensuite ré-introduit différents mutants de cGAS dans des cellules inactivées pour cGAS endogène. Les mutants sélectionnés ont été identifiés dans la littérature (Jiang et al., 2019; Raab et al., 2016) : un mutant catalytique (noté mCat) portant les mutations E225A et D227A et un mutant de liaison à l'ADN (noté mDNA-BD) présentant les mutations C396A C397A (***Figure 35a***). Les mutants mCat et mDNA-BD s'expriment correctement après induction pendant 26h (***Figure 35b et c***) et présentent un marquage nucléaire en conditions normales et un marquage cytoplasmique après un traitement à l'étoposide (***Figure 35b***). Certaines cellules présentent également un marquage nucléaire après le traitement à l'étoposide mais ce phénomène reste minoritaire. L'expression des mutants mCat et mDNA-BD, contrairement à la forme WT, ne restaurent que partiellement la relocalisation (***Figure 35d et e***). Ce sauvetage partiel pourrait être dû à un requis de ces domaines pour la relocalisation mais on ne peut pas exclure qu'une expression plus faible de ces mutants explique ce résultat. Concernant le domaine catalytique, dans la mesure où la relocalisation de HIRA sous étoposide n'est pas dépendante de la voie IFN, il semble peu probable qu'il joue un rôle essentiel dans la relocalisation de HIRA et nous faisons l'hypothèse que le sauvetage pourra être amélioré.

Cette expérience préliminaire devra donc être reproduite et d'autres mutants de cGAS pourront être investigués.

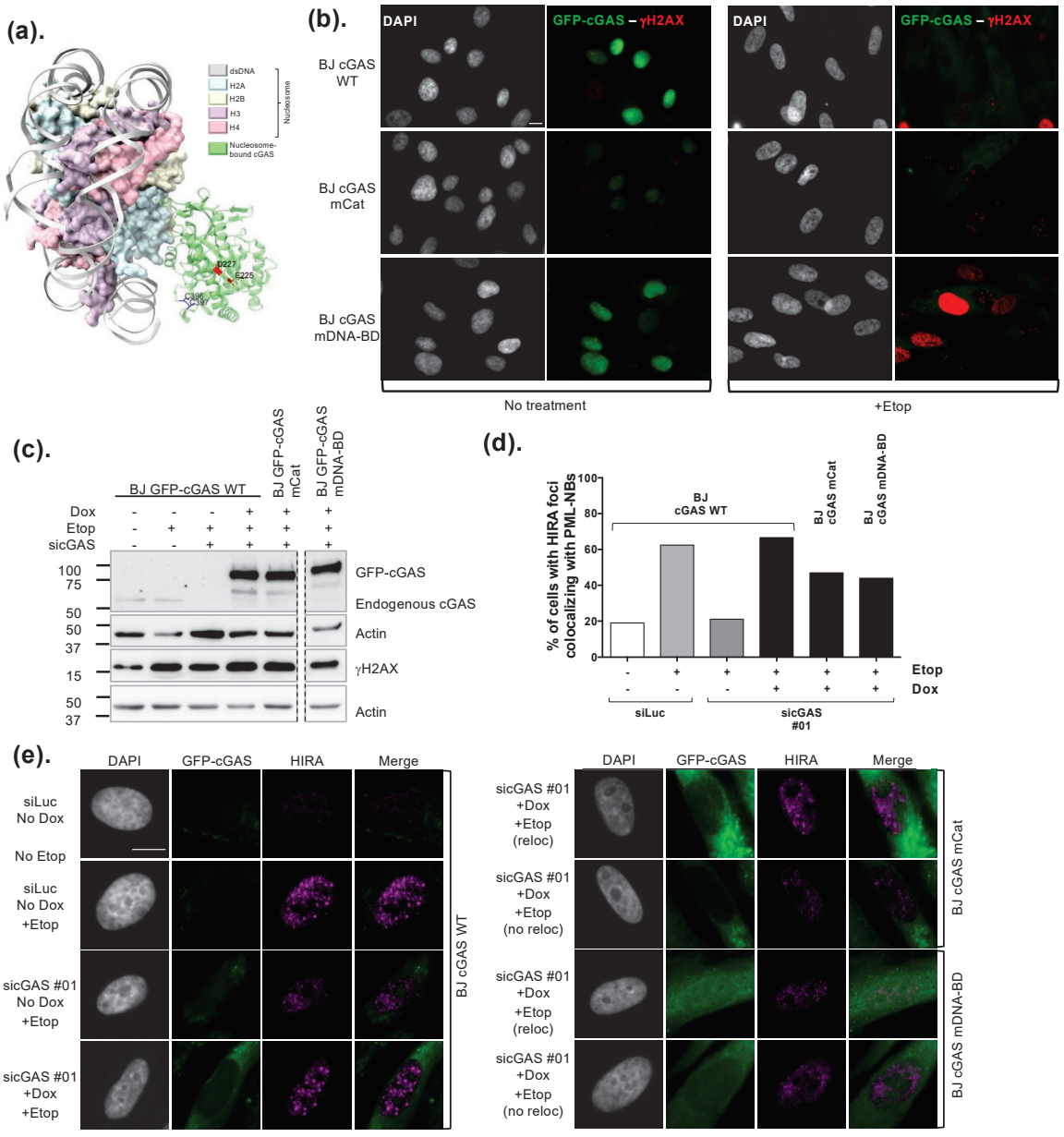


**Figure 35. Réintroduction de différents mutants de la protéine cGAS et visualisation de leur impact sur la relocalisation de HIRA dans les PML NBs. (a)**. Représentation 3D de la protéine cGAS monomérique (vert) liée à un nucléosome, réalisée avec le logiciel UCSF ChimeraX à partir des données publiées par Pathare et al., 2020 (PDB : 6y5e). Les résidus E225 et D227 (rouge) sont remplacés par des alanines dans le mutant mCat. Les résidus C396 et C397 (bleu foncé) sont remplacés par des alanines dans le mutant mDNA-BD. **(b)**. Visualisation de GFP-cGAS WT, mCat et mDNA-BD (vert) et γH2AX (rouge) par microscopie à fluorescence. Le noyau des cellules est visualisé par un marquage DAPI (gris). La barre d'échelle représente 10μm. Les différentes protéines GFP-cGAS exogènes ont été induite avec 100ng/mL de doxycycline pendant 26h et traitées ou non avec 10μM d'étoposide (Etop) pendant 24h. **(c)**. Visualisation par western blot de cGAS et γH2AX à partir d'extraits cellulaires de BJ transduites avec des constructions GFP-cGAS inductibles par la doxycycline (Dox). Les cellules ont été traitées avec 60nM de siRNA contre la luciférase (Luc) ou cGAS endogène (sicGAS #01) pendant 48h. Les différentes protéines GFP-cGAS exogènes ont été induites comme dans **b** et traitées avec 10μM d'étoposide (Etop) pendant 24h. L'actine sert ici de contrôle de dépôt. **(d)**. Analyse quantitative du pourcentage de cellules présentant des foyers HIRA co-localisant avec les PML NBs. Les cellules ont été traitées comme dans c. Un seul réplicat biologique pour cette expérience. **(e)**. Visualisation de GFP-cGAS WT, mCat et mDNA-BD (vert) et HIRA (magenta) par microscopie à fluorescence. Le noyau des cellules est visualisé par un marquage DAPI (gris). La barre d'échelle représente 10μm. Les cellules ont été traitées comme dans **c** et **d**.

*La relocalisation d'HIRA et la juxtaposition des PML NBs avec les sites de dommages pourraient dépendre du processus de transcription*

Les PML NBs ont été montrés comme impliqués dans la réparation des DSBs par HR. De façon intéressante, la HR est particulièrement employée pour la réparation de DSBs dans des régions transcriptionnellement actives (Aymard et al., 2014). Nos résultats sur la relocalisation induite par l'IFNβ semble indiquer que le processus de transcription joue un rôle pour le recrutement de HIRA dans les PML NB. Nous avons donc voulu regarder si l'inhibition de la transcription pouvait impacter la relocalisation induite par les DSBs. Nous avons inhibé la transcription avec différentes molécules : le DRB, le CDK9i, le flavopiridol et l'α-amanitine et avons regardé si ces dernières pouvaient avoir un effet sur la relocalisation induite par un traitement étoposide (***Figure 36a-d***). Les différents traitements impactent de façon importante le pourcentage de cellules présentant des foyers HIRA localisant dans les PML NBs. Cependant, le temps d'inhibition de la transcription (25h) n'est pas optimal car les niveaux protéiques de HIRA et de PML sont impactés (illustré par la ***Figure 36f*** avec un traitement DRB) et une inhibition plus courte devra être effectuée.

Nous avons également voulu voir si l'inhibition de la transcription pouvait impacter la juxtaposition des PML NBs et des foyers γH2AX (***Figure 36e)***. Dans des conditions normales, en moyenne 27% de l'aire des PML NBs chevauche du signal γH2AX. Lorsque les cellules sont traitées avec du DRB ou un inhibiteur de CDK9, on observe une baisse significative du pourcentage de chevauchement (Δmoyenne ≈ -16% ; Δmédiane ≈ -19%) suggérant un rôle du processus de transcription dans l'interaction entre les PML NBs et les sites de dommages.

Ces résultats supplémentaires apportent de nouveaux éléments dans la compréhension de la relocalisation induite par les DSBs qui dépend de la protéine cGAS et potentiellement du processus de transcription. Ces premiers résultats ouvrent des perspectives de recherche intéressantes exposées dans la prochaine partie.

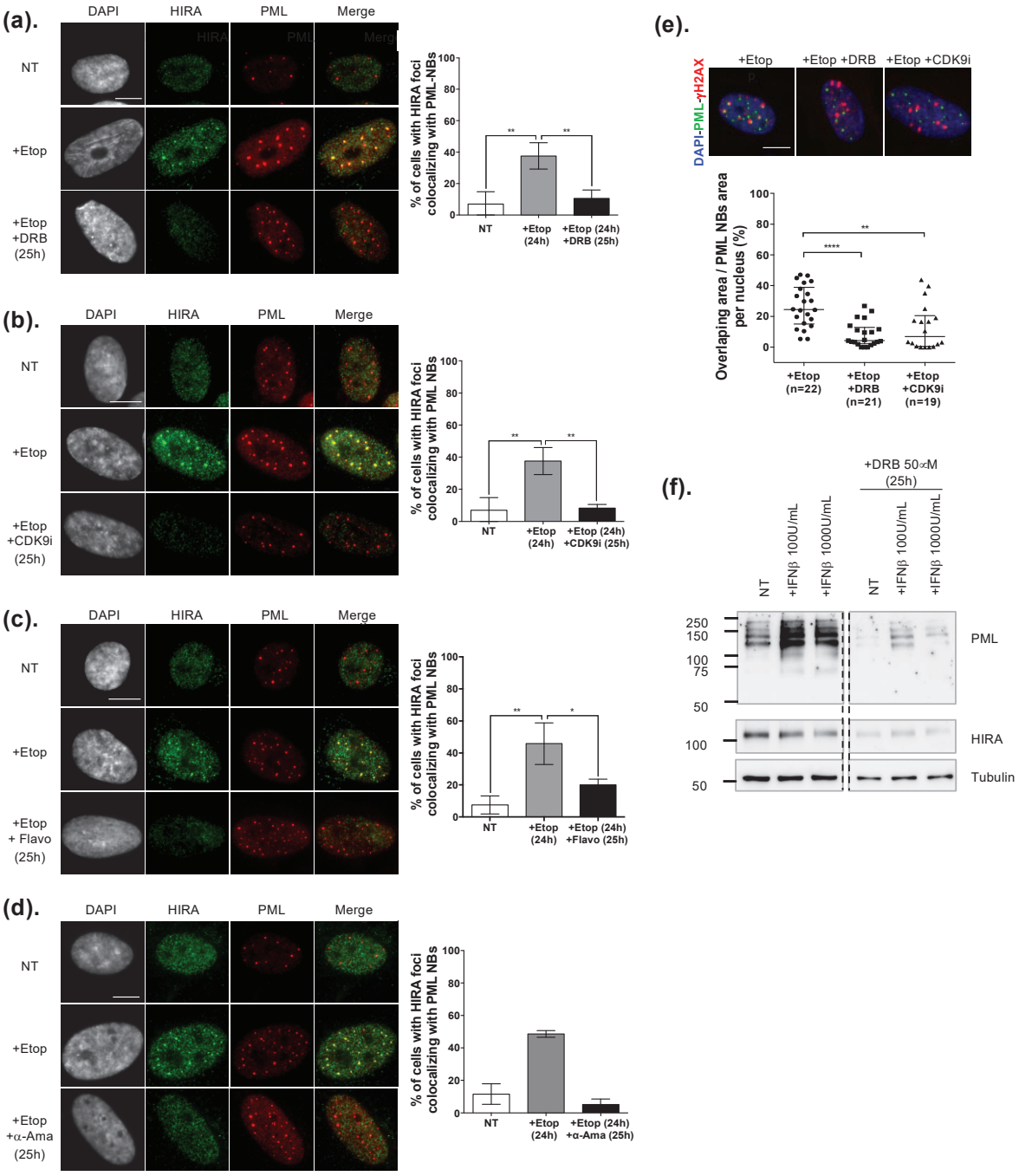


**Figure 36. Impact de l'inhibition de la transcription sur la relocalisation de HIRA et la juxtaposition des PML NBs aux sites de DSBs. (a-d)**. Visualisation de HIRA (vert) et PML (rouge) (gauche) par microscopie à fluorescence dans des cellules BJ traitées avec de l'étoposide (Etop) à 10μM pendant 24h et avec divers inhibiteurs de transcription 1h avant le traitement Etop et pendant 25h. Le noyau des cellules est visualisé par un marquage DAPI (gris). La barre d'échelle correspond à 10μm. Analyse quantitative du pourcentage de cellules présentant des foyers HIRA co-localisant avec les PML NBs (droite). p-value (Student t-test) : *<0,05 ; **<0,01. **(a)**. Immunofluorescence et quantification sur des cellules traitées avec du DRB à 50μM. Moyenne de 3 expériences indépendantes ±SD. **(b)**. Immunofluorescence et quantification sur des cellules traitées avec du CDK9i à 10μM. Moyenne de 3 expériences indépendantes ±SD. **(c)**. Immunofluorescence et quantification sur des cellules traitées avec du Flavopiridol à 50nM. Moyenne de 3 expériences indépendantes ±SD. **(d)**. Immunofluorescence et quantification sur des cellules traitées avec de l'α-amanitine à 2μg/mL. Moyenne de 2 expériences indépendantes ±SD. **(e)**. Mesure du pourcentage de chevauchement sur des cellules BJ traitées comme dans **a** ou **b**. Les aires des signaux ont été mesurées sur des images d'immunofluorescence (en haut) de PML (vert) et γH2AX (rouge). Le noyau est visualisé par un marquage au DAPI (bleu). Le graphique en nuage de points (en bas) représente le pourcentage d'aire de PML NB chevauchant le signal γH2AX. Chaque point correspond à un noyau analysé. La barre du milieu correspond à la médiane des valeurs, les barres du bas et du haut correspondent respectivement au 1er et 3ème quartile. L'information n=x correspond au nombre de noyaux analysés. Les noyaux analysés sont issus d'une expérience. p-value : **<0,01, ****<0,0001. **(f)**. Visualisation par western blot de PML et HIRA à partir d'extraits cellulaires totaux de BJ traitées avec de l'IFNβ à 100 ou 1000U/mL pendant 24h et avec du DRB à 50μM 1h avant le traitement IFN et pendant 25h. La tubuline sert ici de contrôle de dépôt. Un western blot devra être effectuée avec des extraits cellulaires totaux de BJ traitées comme dans **a**.

# Discussion et perspectives

Mes travaux de thèse ont permis d'apporter plusieurs éléments pour la compréhension des mécanismes moléculaires impliqués dans la relocalisation du complexe HIRA dans les PML NBs ainsi que de premières informations sur le rôle fonctionnel de cette localisation spécifique. Ces résultats ouvrent de nouvelles perspectives de travail que je souhaite discuter dans cette partie.

## I. La relocalisation du complexe HIRA induite dans un contexte inflammatoire

**La relocalisation observée en inflammation est dépendante de la voie de signalisation aux IFNs de type I**

La relocalisation du complexe HIRA induites par la reconnaissance d'ADN double-brin nu étranger (ADN virale ou plasmide) observée par notre équipe et d'autres (Cohen et al., 2018; Rai et al., 2017), ainsi que la relocalisation observée par le traitement au poly(I:C) (reproduisant l'introduction d'ARN double-brin étranger), nous ont amenés à investiguer l'impact plus global de l'inflammation sur la relocalisation. Le traitement de cellules avec différentes cytokines de l'inflammation, nous a montré que seuls les traitements au TNF$\alpha$ et l'IFN de type I étaient capables d'induire la relocalisation du complexe HIRA dans les PML NBs, de façon dépendante à la voie de signalisation à l'IFN de type I. Ces résultats sont en concordance avec les résultats de McFarlane et al. impliquant la voie IFN dans la relocalisation du complexe HIRA induite par le virus HSV-1 (McFarlane et al., 2019). Cette relocalisation semble dépendante du processus de transcription car son inhibition prévient l'accumulation de HIRA dans les PML NBs.
D'autres cytokines pro-inflammatoires restent encore à tester pour leur habilité potentielle à induire la relocalisation du complexe HIRA dans les PML NBs, par exemple les cytokines de la famille des IL-1 (IL-1$\alpha$ et $\beta$, IL-36$\alpha$, $\beta$ and $\gamma$). Il serait aussi intéressant de regarder si d'autres médiateurs de l'inflammation comme les médiateurs lipidiques pourraient être impliqués dans la relocalisation induite dans un contexte inflammatoire.

**Le recrutement de HIRA dans les PML NBs est dépendant des interactions SIM-SUMO**

L'utilisation du mutant PML 3K ainsi que l'expression d'Affimers SUMO-spécifiques ont permis de montrer que le recrutement de HIRA dans les PML NBs dépendait d'interactions SIM-SUMO. De plus, une analyse des motifs SIM putatifs sur la protéine HIRA a permis d'identifier le motif SIM2 comme important pour le recrutement d'HIRA dans les PML NB, potentiellement grâce à la reconnaissance de PML SUMOylée. La signalisation IFN est connue comme capable de stimuler la transcription de PML (Chelbi-Alix et al., 1995; Lavau

et al., 1995; Stadler et al., 1995). De plus, l'IFN permet de lever l'inhibition qu'exerce les micro ARNs let-7 sur les gènes *SUMO1*, *SUMO2* et *SUMO3* en stimulant l'expression de la protéine Lin28B (Sahin et al., 2014b). Le recrutement des protéines clientes des PML NBs est favorisé par l'augmentation de la valence des sites SUMOylés par rapport aux motifs SIM (Banani et al., 2016). Dans le cas de HIRA, l'augmentation de protéines PML SUMOylées au niveau des PML NBs lors d'une stimulation à l'IFNβ pourrait induire le recrutement de HIRA par un phénomène de séparation de phase liquide-liquide. Cependant, les résultats obtenus avec l'étoposide (discutés plus bas) montrent que le niveau d'expression de PML reste inchangé après l'induction de DSBs alors que le recrutement de HIRA est également dépendant des interactions SIM-SUMO. Ainsi, des facteurs autres que l'augmentation de la valence des sites SUMOylés pourraient être impliqués dans le recrutement. De façon intéressante, le motif SIM2 sur la protéine HIRA est suivi d'une sérine en position 229. L'étude des motifs SIM suggère que la phosphorylation d'un résidus sérine ou thréonine (souvent retrouvés au niveau des motifs SIM) permettrait d'introduire des charges négatives au niveau du SIM et favoriserait l'interaction avec les protéines SUMO (Hecker et al., 2006; Kerscher, 2007). C'est le cas pour les protéines PML et DAXX dont la phosphorylation des sérines à proximité de leur motifs SIM augmentent leur affinité de liaison avec SUMO-1 (Cappadocia et al., 2015; Chang et al., 2011). Ainsi, il serait intéressant de regarder si la sérine S229 d'HIRA peut être phosphorylée en condition de stress et si cette phosphorylation est importante pour le recrutement du complexe dans les PML NBs. Comme mentionné en introduction, la phosphorylation de la sérine S697 d'une version tronquée de la protéine HIRA a été montrée comme importante pour son recrutement dans les PML NBs lors de l'entrée en sénescence (Ye et al., 2007b). Cependant, l'introduction de la mutation dans une forme ectopique entière de HIRA réalisée au cours de ma thèse n'a pas eu d'impact sur sa relocalisation dans les PML NBs sous IFNβ. De plus, le traitement de cellules avec un inhibiteur de GSK3β n'a pas ou peu d'effet sur la relocalisation d'HIRA induite par l'IFNβ (McFarlane et al., 2019). L'impact de la mutation de S697 ou de l'inhibition de GSK3β n'a cependant pas été investigué pour la relocalisation induite par des DSBs et reste envisageable.

**Un traitement à l'IFN de type I induit une juxtaposition des loci ISGs et des PML NBs ainsi que l'incorporation de l'histone H3.3 dans les régions distales de ces gènes**

La production de sondes spécifiques aux ISGs pour le FISH nous a permis d'observer une juxtaposition entre les locis ISGs et les PML NBs lors d'un traitement à l'IFNβ comparé à un locus non-ISG (ici *GHRL*). Cette observation concorde avec les résultats de Gialitakis

*et al.*, montrant une association entre le locus *DRA* et un PML NBs lors d'une stimulation à l'IFNγ (Gialitakis et al., 2010). Cette juxtaposition pourrait être liée au processus de transcription. En effet, nos données montrent que la suppression de la protéine PML impacte fortement l'expression des ISGs 6h et 24h après la stimulation à l'IFNβ. De plus, les PML NBs ont été montrés comme proches de régions transcriptionnellement actives (Kurihara et al., 2020; Wang et al., 2004). Cependant, la juxtaposition entre les ISGs et les PML NBs n'est réellement observable qu'à un temps tardif (48h après l'induction à l'IFNβ). Une hypothèse est que la protéine PML libre participerait au processus de transcription des ISGs en se liant au locus et entraînerait la nucléation d'un PML NB à proximité. En effet, il a été démontré que la liaison forcée de protéines PML à la chromatine entraine la formation d'un PML NBs au locus ciblé (Chung et al., 2011; Erdel et al., 2020; Kaiser et al., 2008; Wang et al., 2018a). L'utilisation d'inhibiteurs tels que le DRB pourrait nous apporter des réponses sur le lien entre la transcription et la juxtaposition des gènes induits par l'IFN et les PML NBs sous IFN. De plus, la juxtaposition observée en microscopie pourra être complétée par des approches biochimiques. En effet, la technologie de marquage de la chromatine par la peroxydase APEX2 couplée à la protéine PML (ALaP) (Kurihara et al., 2020) pourrait nous permettre de précipiter la chromatine marquée après un traitement à l'IFN pour confirmer et compléter nos résultats de FISH.

Nos études de ChIP ont permis de montrer un enrichissement du variant d'histone H3.3 au niveau des régions distales des ISGs. Ces résultats corroborent ceux obtenus par l'équipe du Dr. Ozato, qui montrent une accumulation de l'histone H3.3 ectopique au niveau des TES des ISGs chez la souris (Sarai et al., 2013). Nos données ont aussi montré que ce dépôt était modérément impacté par la perte de HIRA et un peu plus fortement par la perte de PML suggérant que ces protéines pourraient être impliquées dans le dépôt d'H3.3 au niveau des ISGs. La protéine HIRA est d'ailleurs retrouvée enrichie au niveau des ISGs lors d'une stimulation à l'IFNβ de façon dépendante de PML (McFarlane et al., 2019). La baisse modérée observée par la perte d'HIRA pourrait s'expliquer par une compensation par les autres chaperons de l'histone H3.3. L'autre complexe chaperon d'H3.3, DAXX/ATRX, localise de manière constitutive dans les PML NBs et pourrait notamment être impliqué dans cette compensation. De plus, la protéine de remodelage CHD2 est recrutée aux sites de transcription où elle incorpore H3.3 (Harada et al., 2012; Siggens et al., 2015). Il serait ainsi intéressant de voir si CHD2 localise dans les PML NBs et si sa perte pourrait impacter le dépôt d'H3.3 au niveau des ISGs après l'induction de leur transcription par un traitement IFN.

De façon intéressante, et *a priori* en contradiction avec nos résultats, la protéine PML associée à la chromatine (au niveau des domaines PADs) a été montrée comme restreignant l'enrichissement d'H3.3 dans ces régions. Cette différence pourrait s'expliquer par une différence de fonction entre la protéine PML nucléoplasmique et la protéine PML associée aux PML NBs. Les PADs sont d'ailleurs spatialement éloignés des PML NBs et représentent des régions d'hétérochromatine à la différence des ISGs qui sont dans des régions transcriptionnellement actives. Ainsi, l'incorporation d'H3.3 au niveau des ISGs pourrait être médiée par la protéine PML associée aux PML NBs, probablement à travers le recrutement du complexe chaperon HIRA.

**Quel pourrait-être le rôle de l'incorporation d'H3.3 au niveau des ISGs ?**

L'expression des ISGs atteint son pic après 6h d'induction à l'IFN avant de diminuer après 24h de traitement. De façon intéressante, nos résultats montrent que la perte d'H3.3 induit une augmentation de la transcription des ISGs à 24h de traitement à l'IFNβ. Ces résultats suggèrent que l'incorporation d'H3.3 pourrait permettre de réguler l'expression des ISGs et moduler la réponse inflammatoire. La perte d'HIRA induit quant à elle seulement une légère augmentation du taux d'expression des ISGs. Ce résultat est cohérent avec nos données de ChIP montrant un impact modéré de la perte d'HIRA sur l'enrichissement d'H3.3 aux TES des ISGs. Comme évoqué précédemment, une compensation par d'autres chaperons d'H3.3 est envisageable et devra être investiguée (par ex. le complexe DAXX/ATRX ou la protéine CHD2).

L'incorporation d'H3.3 pourrait également servir comme marque épigénétique de la mémoire transcriptionnelle des ISGs. En effet, en 2018, Kamada *et al*. ont montré que l'accumulation du variant H3.3 et de la marque H3K36me3 au niveau des TES des ISGs mémoires lors d'une première stimulation à l'IFNβ permet une transcription plus importante et plus rapide de ces gènes lors d'une seconde stimulation (Kamada et al., 2018). De plus, PML est importante pour l'établissement d'une mémoire transcriptionnelle au niveau du gène *DRA* après une stimulation à l'IFNγ (Gialitakis et al., 2010). Il serait intéressant de voir si l'absence d'HIRA au moment d'une première stimulation à l'IFN impacte la transcription des ISGs mémoires lors d'une seconde stimulation afin de voir si HIRA contribue à l'établissement d'un environnement chromatinien permettant la mémoire transcriptionnelle. Il serait également intéressant de regarder l'enrichissement pour la marque H3.3S31ph au niveau des ISGs mémoires. En effet, cette marque est mise en place au niveau des gènes induit par stimulation de macrophages murins et participe à l'établissement d'un environnement chromatinien transcriptionnellement actif. Cette marque, spécifique du variant H3.3, pourrait donc jouer un rôle dans la mémoire

transcriptionnelle des ISGs (Armache et al., 2020). L'importance de H3.3 pour la mémoire transcriptionnelle est cependant débattue. En effet, Siwek *et al.* ont récemment montré que le variant n'était retrouvé enrichi que sur une courte période au niveau des ISGs *GBP4* et *GBP5* dans des cellules HeLa stimulées à l'IFNγ (càd. jusqu'à 2 jours après le traitement), tandis que la mémoire transcriptionnelle de *GBP5* est maintenue jusqu'à 14 jours après la première stimulation (Siwek et al., 2020).

Ces premiers travaux ont mené au développement de deux projets en collaboration avec d'autres équipes de recherche. Le premier, en collaboration avec le Dr. Olivier Terrier au Centre International de Recherche en Infectiologie à Lyon et le Dr. Vincent Maréchal au Centre de Recherche Saint-Antoine à Paris, vise à étudier l'impact de l'infection par le virus du SARS-Cov2 et de l'orage cytokinique dont il est responsable en relation avec l'activité du complexe HIRA et des PML NBs sur le contrôle transcriptionnel des ISGs. De façon intéressante, dans une étude récente sur les facteurs cellulaires impliqués dans l'infection au SARS-Cov2, les protéines HIRA et PML semble présenter un rôle anti-viral qu'il serait donc intéressant d'investiguer (Wei et al., 2021). Le projet, appelé projet CHROMACov et lauréat de l'appel d'offre ANR « Recherche- Action Covid19 », est actuellement mené par le Dr. Clément Droillard actuellement post-doctorant dans l'équipe. Il permettra d'apporter des éléments de compréhension de la maladie Covid-19 par le prise de la régulation des ISGs et du processus inflammatoire et pourra potentiellement déboucher sur d'intéressantes stratégies thérapeutiques. Le deuxième projet est né d'une collaboration avec l'équipe du Dr. Bénédicte Chazaud à l'Institut Neuromyogène à Lyon et le Dr. Olivier Benveniste au Centre de Recherche en Myologie à Paris. Il s'intéresse au rôle d'HIRA dans les myopathies idiopathiques inflammatoires, où la surproduction d'IFN de type I perturbe le processus de myogenèse. Des études préliminaires sur des cellules précurseurs myogéniques de patients menées par le Dr. Laure Gallay, docteure récemment diplômée de l'équipe Chazaud, et par le Dr. Armelle Corpet, ont montré que la protéine HIRA localise dans les PML NBs chez les patients atteints de myopathies inflammatoires. Notre hypothèse est que les niveaux anormaux d'IFN dans ces pathologies mènent à une dérégulation épigénétique dans les cellules souches musculaires, en partie responsable du défaut de myogenèse observé.

## II. La relocalisation du complexe HIRA induite par les cassures double-brin

**La relocalisation induite par les cassures double-brin est indépendante de la voie IFN et dépendante de la protéine cGAS**

La relocalisation du complexe HIRA est observée dans les cellules sénescentes (Banumathy et al., 2009; Rai et al., 2011; Zhang et al., 2005). Ces dernières ont la particularité de produire un cocktail de cytokines, le SASP, créant un environnement inflammatoire autour des cellules sénescentes (Coppé et al., 2008; Novakova et al., 2010). Nos résultats ont montré que les cytokines IL-6 et IL-8 n'entraînent pas la relocalisation. En revanche, les cellules sénescentes produisent également du TNF$\alpha$ et de l'IFN de type I, des cytokines induisant la relocalisation de HIRA par la voie IFN. Cependant, nos résultats ont montré que l'inhibition de la voie IFN par le ruxolitinib ne prévient pas la relocalisation observée dans les cellules sénescentes. De plus, comme évoqué en introduction, la relocalisation du complexe HIRA apparaît dans les étapes précoces de la sénescence (Zhang et al., 2005) quand la sécrétion d'IFN de type I est plus tardive (Cecco et al., 2019). Nous avons donc investigué l'effet de la réponse aux cassures double-brin (DSBs), particulièrement mobilisées dans les cellules sénescentes (Bartkova et al., 2006; Micco et al., 2006). L'induction de DSBs par un traitement à l'étoposide induit la relocalisation du complexe HIRA dans les PML NBs et ce de manière indépendante de la voie IFN mais de façon dépendante de la kinase ATM, impliquée dans la signalisation induite par les cassures double-brin et en particulier la réparation par HR. De manière similaire, les DSBs induites par la NCS induisent également l'accumulation d'HIRA dans les PML NBs. Ainsi, l'apparition de cassures double-brin dans les cellules sénescentes pourraient être à l'origine de la relocalisation du complexe HIRA observée dans ces cellules et il serait intéressant de regarder si l'inhibition de la kinase ATM dans les cellules sénescentes prévient ce phénomène. Il serait également intéressant de regarder l'importance d'autres acteurs de la réparation par HR dans le recrutement d'HIRA dans les PML NBs (par ex. les protéines RPA, RAD51, RNF168, 53BP1).

Comme observé pour la relocalisation induite par l'IFN$\beta$, l'inhibition de la transcription par différentes molécules (DRB, CDK9i, Flavopiridol et $\alpha$-amanitine) impacte de manière significative la relocalisation induite par un traitement à l'étoposide. Cependant, seules des inhibitions de 25h ont été réalisées, diminuant les niveaux protéiques de HIRA et PML et introduisant un biais important dans ces expériences. Ces résultats devront donc être reproduits en effectuant des traitements plus courts avec les différents inhibiteurs et en vérifiant les niveaux protéiques de HIRA, de PML et de SUMO afin de déterminer le lien

potentiel entre le processus de transcription et la relocalisation du complexe HIRA dans les PML NBs.

Nos expériences d'inactivation ont permis de montrer que la protéine cGAS était impliquée dans la relocalisation de HIRA induite par les DSBs. Lorsque nous analysons sa localisation cellulaire, nous observons de manière surprenante une translocation de la protéine cGAS du noyau vers le cytoplasme lors de l'induction de DSBs. Ces résultats sont en contradiction avec l'étude de Jiang *et al*., de 2019 qui montrent que la protéine cGAS localise continuellement dans le noyau, y compris lorsque les cellules sont soumises à une irradiation de type gamma (Jiang et al., 2019) et avec ceux de Liu *et al*. de 2018 qui montrent une translocation de cGAS exogène du cytoplasme vers le noyau dans différentes lignées cellulaires traités avec différents agents génotoxiques (étoposide, camptothécine et $H_2O_2$) (Liu et al., 2018). Les différences observées avec les résultats de Jiang *et al*. peuvent s'expliquer par le modèle cellulaire employé ; en effet, leurs investigations ont été faites sur une lignée de cellules HEK293, cellules dans lesquelles HIRA ne relocalise pas dans les PML NBs. Concernant l'étude de Liu *et al*., la localisation cytoplasmique de la protéine cGAS dans les cellules non traitées va à l'encontre des études montrant une localisation de cGAS majoritairement nucléaire (Jiang et al., 2019; Sun et al., 2021; Volkman et al., 2019), y compris dans nos expériences ; il est donc difficile de comparer nos données avec les leurs. La protéine cGAS nucléaire, en se liant à la chromatine, inhibe la réparation par HR dans des cellules cancéreuses et favorise la tumorigenèse. Dans des cellules primaires, l'induction de dommages pourrait provoquer son détachement de la chromatine afin de permettre la réparation des dommages, pouvant expliquer la translocation cytoplasmique que nous observons. Cependant, il est difficile d'établir un lien entre la localisation cytoplasmique de cGAS sous étoposide et la relocalisation d'HIRA dans les PML NBs au niveau du noyau. La protéine cGAS cytoplasmique est associée à la signalisation STING et la production d'IFN de type I, qui ne semblent pas être impliqués dans la relocalisation induite par les dommages. Cependant, la description de la protéine cGAS reste relativement récente et il est envisageable qu'elle puisse activer d'autres voies de signalisation dans le cytoplasme. La cinétique de la translocation devra aussi être investiguée. En effet, nos observations sont faites après 24h de traitement à l'étoposide. Il est envisageable que cGAS puisse agir dans le noyau au moment de l'induction de cassures et avant sa translocation dans le cytoplasme. Les questions sur l'importance de la localisation nucléaire de cGAS ou de sa translocation cytoplasmique pourront être investiguées en supprimant la séquence d'export nucléaire sur la protéine cGAS, récemment décrite par Sun *et al*., ou bien en

inhibant la protéine d'export CRM1 responsable de son export en présence d'ADN cytoplasmique (Sun et al., 2021).

Nos premiers résultats sur l'implication des domaines catalytiques et de liaison à l'ADN de cGAS dans la relocalisation d'HIRA nous montrent que ces domaines pourraient être partiellement impliqués mais des expériences complémentaires devront être effectuées pour valider ou infirmer ces premiers résultats. De plus, la caractérisation récente de la structure de cGAS lié à la chromatine nous ouvre de nouvelles perspectives d'investigations (Boyer et al., 2020; Kujirai et al., 2020; Michalski et al., 2020; Pathare et al., 2020). Ainsi, les différentes études identifient les résidus R236 et R255 comme essentiels pour l'interaction de cGAS avec le patch acide de H2A-H2B au niveau des nucléosomes et il pourrait être intéressant de regarder l'importance de ces résidus pour la relocalisation de HIRA à la suite de dommages.

**La relocalisation d'HIRA dans les PML NBs pourrait-elle jouer un rôle fonctionnel dans la réparation des DSBs ?**

Aucune donnée dans la littérature actuelle ne montre l'effet des DSBs sur l'accumulation du complexe HIRA dans les PML NBs et nos données offrent de nouvelles perspectives dans l'étude du rôle des PML NBs dans la réparation des cassures double-brin. En effet, comme mentionné en introduction, les PML NBs juxtaposent les foyers γH2AX (Carbone et al., 2002; Dellaire et al., 2006a) et sont impliqués dans la réparation des dommages par recombinaison homologue (HR) (Vancurova et al., 2019; Yeung et al., 2012). De plus, de nombreux facteurs de réparation sont retrouvés dans les PML NBs (Chang et al., 2018; Dellaire and Bazett-Jones, 2004) et la protéine PML a été identifié dans des cribles utilisant les protéines fusionnées APEX2-53BP1, APEX2-BRCA1 ou APEX2-MDC1 (Gupta et al., 2018). L'incorporation du variant H3.3 nouvellement synthétisé au niveau des DSBs est importante pour le bon déroulement des processus de réparation par NHEJ et par HR, grâce aux actions respectives de la protéine CHD2 ou du complexe DAXX/ATRX (Juhász et al., 2018; Luijsterburg et al., 2016). Le complexe HIRA a quant à lui été montré comme impliqué dans l'incorporation d'histones au niveau des DSBs réparées par NHEJ pour le rétablissement de la structure chromatinienne (Li and Tyler, 2016). Notre hypothèse est que le complexe chaperon HIRA est dirigé dans les PML NBs afin de cibler les régions endommagées, où son action est requise. De manière intéressante, des résultats non publiés de l'équipe montrent que l'inhibition de la relocalisation d'HIRA par l'expression d'un Affimer SUMO-spécifiques semble prévenir l'association des PML NBs avec les foyers γH2AX. Il serait intéressant de voir si l'absence de recrutement impacte le

rétablissement de la structure chromatinienne, et plus particulièrement l'incorporation d'H3.3 au site de DSBs.

La technologie de DSBs ciblées avec l'enzyme ER-AsiSI, développée par l'équipe du Dr. Gaëlle Legube (Iacovoni et al., 2010; Massip et al., 2010) et désormais mise en place dans notre équipe dans des cellules pirmaires, nous permettra de mieux investiguer la relation entre la relocalisation d'HIRA aux PML NBs et la réparation des DSBs. Cette technique permet la translocation nucléaire de l'enzyme AsiSI contrôlée par l'ajout de 4-hydroxytamoxifène dans le milieu. L'enzyme génère ensuite environ 100 cassures double-brin au niveau de la séquence consensus GCGATCGC. L'équipe du Dr. Legube a pu distinguer les DSBs réparées par HR de celles réparées par NHEJ (Aymard et al., 2014). Les cassures ont déjà été annotées pour plusieurs marques épigénétique (Clouaire et al., 2018); cependant l'enrichissement pour H3.3 n'a pas été testé. Cette technologie nous permettra de suivre premièrement par ChIP la liaison des protéines HIRA et PML au niveau des DSBs à différents temps après l'induction de cassures pour pouvoir analyser la dynamique de leur recrutement aux sites de dommages. Elle permettra également d'observer l'incorporation du variant H3.3 aux sites de cassures. L'utilisation de la technologie SNAP-tag nous permettra de distinguer les histones préexistantes des histones nouvellement synthétisées. L'utilisation de mutants et d'Affimers SUMO-spécifiques nous permettra de mesurer l'importance du recrutement de HIRA dans les PML NBs pour leur recrutement au site de dommage et pour le rétablissement de la structure chromatinienne après la réparation.

De façon intéressante, la juxtaposition des PML NBs et des foyers γH2AX semble impactée par l'inhibition de la transcription par un traitement au DRB ou au CDK9i. Cette analyse n'a été effectuée que sur une seule expérience et nécessite d'être reproduite. Cependant, la littérature semble montrer un lien entre la réparation des DSBs par HR et le processus de transcription. En effet, dans leur étude de 2014, Aymard *et al*. ont montré une préférence pour la réparation des DSB par HR au niveau de loci transcrits, à l'inverse de la réparation par NHEJ ayant lieu principalement sur des loci non transcrits, au niveau de gènes inactifs ou dans des régions intergéniques (Aymard et al., 2014). Comme supposé pour la régulation de la transcription des ISGs, la machinerie transcriptionnelle au niveau du site de cassure pourrait participer au recrutement des PML NBs, importants pour la réparation par HR. L'importance du processus de transcription pour le recrutement des PML NBs et de HIRA aux sites de lésions pourra être investiguée par des études biochimiques de ChIP avec l'utilisation de l'enzyme ER-AsiSI.

**La relocalisation d'HIRA dans les PML NBs pourrait-elle être impliquée dans la réparation d'autres types de dommages à l'ADN ?**

Nos résultats sur la relocalisation d'HIRA dans les PML NBs après l'induction de DSBs et son implication potentielle dans le rétablissement de la structure chromatinienne après la réparation, soulèvent évidemment la question d'une implication plus globale de ce processus en réponse à d'autres types de dommages à l'ADN. L'étude de Adam *et al*. en 2013 a par exemple montré que le complexe HIRA s'accumule au niveau des lésions causées par les UVC et est impliqué dans le dépôt d'H3.3 au site de dommage (Adam et al., 2013). De plus, l'exposition de cellules aux UVC montre une localisation des PML NBs aux sites de dommages (Seker et al., 2003). Ainsi, il serait envisageable de penser que le complexe HIRA puisse relocaliser dans les PML NBs en réponse à un stress UV pour cibler les sites de dommages et participer au rétablissement de la structure chromatinienne après la réparation par NER. Cependant, une exposition globale aux UV de cellules BJ réalisée au cours de ma thèse n'a pas permis d'observer une relocalisation de HIRA dans les PML NBs. Ces résultats sont en cohérence avec les résultats de Rai *et al*. (Rai et al., 2017), suggérant un mécanisme distinct pour la réparation de ce type de lésion. L'induction d'autres types de dommages à l'ADN pourra être testée et permettra de voir si la relocalisation aux PML NBs observée à la suite des DSBs est spécifique à ce type de stress ou se révèle plus globale et participe au maintien de l'intégrité génomique.

Les travaux sur l'implication du recrutement d'HIRA dans les PML NBs pour la réparation des dommages à l'ADN seront poursuivis par Florent Bressac, nouveau doctorant au sein de l'équipe.

En conclusion, mon travail de thèse a permis d'affiner les connaissances actuelles sur le rôle des PML NBs dans la dynamique de la chromatine au cours de la réponse inflammatoire, en agissant de concert avec le complexe chaperon d'histone HIRA pour l'incorporation du variant H3.3 au niveau des gènes induits par l'IFN de type I. Ces travaux offrent des perspectives intéressantes dans la compréhension de pathologies inflammatoires.

Mon travail ouvre également la voie pour comprendre plus en détail le rôle des PML NBs dans la réparation de l'ADN en cas de cassures double-brin. En particulier, j'ai mis pour la première fois en évidence l'accumulation du complexe HIRA dans les PML NBs juxtaposant les sites de dommages. La compréhension du rôle de cette relocalisation pourrait offrir de nouvelles stratégies thérapeutiques pour le traitement de cancers et prévenir l'instabilité génomique qui y est associée. De même, ces travaux pourraient permettre de mieux comprendre l'impact des mutations d'H3.3 dans le développement de

glioblastomes pédiatriques et de tumeurs osseuses (Lowe et al., 2019; Qiu et al., 2018; Shi et al., 2017).

# Annexes

# Annexe 1: Article de revue

Nucleic Acids Research, 2020 Dec 2
doi: 10.1093/nar/gkaa828; PMID: 33068408; PMCID: PMC7708061

## PML nuclear bodies and chromatin dynamics: catch me if you can!

Corpet A[1], Kleijwegt C.[1], Roubille S.[1], Juillard F.[1], Jacquet K.[1], Texier P.[1], Lomonte P.[1]

1. Univ Lyon, Université Claude Bernard Lyon 1, CNRS UMR5310, INSERM U1217, LabEx DEVweCAN, Institut NeuromyoGène (INMG), Team Chromatin Dynamics, Nuclear Domains, Virus F-69008, Lyon, France.

### Abstract

Eukaryotic cells compartmentalize their internal milieu in order to achieve specific reactions in time and space. This organization in distinct compartments is essential to allow subcellular processing of regulatory signals and generate specific cellular responses. In the nucleus, genetic information is packaged in the form of chromatin, an organized and repeated nucleoprotein structure that is a source of epigenetic information. In addition, cells organize the distribution of macromolecules via various membrane-less nuclear organelles, which have gathered considerable attention in the last few years. The macromolecular multiprotein complexes known as Promyelocytic Leukemia Nuclear Bodies (PML NBs) are an archetype for nuclear membrane-less organelles. Chromatin interactions with nuclear bodies are important to regulate genome function. In this review, we will focus on the dynamic interplay between PML NBs and chromatin. We report how the structure and formation of PML NBs, which may involve phase separation mechanisms, might impact their functions in the regulation of chromatin dynamics. In particular, we will discuss how PML NBs participate in the chromatinization of viral genomes, as well as in the control of specific cellular chromatin assembly pathways which govern physiological mechanisms such as senescence or telomere maintenance.

*11890–11912* *Nucleic Acids Research, 2020, Vol. 48, No. 21* *Published online 17 October 2020*
*doi: 10.1093/nar/gkaa828*

# SURVEY AND SUMMARY

# PML nuclear bodies and chromatin dynamics: catch me if you can!

**Armelle Corpet*, Constance Kleijwegt, Simon Roubille, Franceline Juillard, Karine Jacquet, Pascale Texier and Patrick Lomonte***

Univ Lyon, Université Claude Bernard Lyon 1, CNRS UMR 5310, INSERM U 1217, LabEx DEVweCAN, Institut NeuroMyoGène (INMG), team Chromatin Dynamics, Nuclear Domains, Virus F-69008, Lyon, France

Received June 11, 2020; Revised September 15, 2020; Editorial Decision September 16, 2020; Accepted September 18, 2020

## ABSTRACT

**Eukaryotic cells compartmentalize their internal milieu in order to achieve specific reactions in time and space. This organization in distinct compartments is essential to allow subcellular processing of regulatory signals and generate specific cellular responses. In the nucleus, genetic information is packaged in the form of chromatin, an organized and repeated nucleoprotein structure that is a source of epigenetic information. In addition, cells organize the distribution of macromolecules via various membrane-less nuclear organelles, which have gathered considerable attention in the last few years. The macromolecular multiprotein complexes known as Promyelocytic Leukemia Nuclear Bodies (PML NBs) are an archetype for nuclear membrane-less organelles. Chromatin interactions with nuclear bodies are important to regulate genome function. In this review, we will focus on the dynamic interplay between PML NBs and chromatin. We report how the structure and formation of PML NBs, which may involve phase separation mechanisms, might impact their functions in the regulation of chromatin dynamics. In particular, we will discuss how PML NBs participate in the chromatinization of viral genomes, as well as in the control of specific cellular chromatin assembly pathways which govern physiological mechanisms such as senescence or telomere maintenance.**

## INTRODUCTION

Eukaryotic cells package ∼2 m of DNA into a nucleus of a few micrometers diameter together with all the biological macromolecules required to organize, replicate, and interpret this genetic information. Mechanisms have thus evolved to organize this crowded environment. Our genetic material is packaged in a complex nucleoprotein structure called chromatin, whose basic unit, the nucleosome is composed of an octamer of histones comprising two copies of each core histone H2A, H2B, H3 and H4, around which is wrapped 147 bp of DNA (1). Targeted deposition of histone variants, or addition of specific post-translational modifications to histones and DNA provide a large repertoire of epigenetic information that can modulate chromatin accessibility and gene expression, and thus regulate cell identity (2). On the other hand, spatial and temporal distribution of macromolecules is organized through membrane-bound and membrane-less organelles which participate in the compartmentalization of biochemical reactions in the nucleus. Liquid–liquid phase separation (LLPS) has recently emerged as a new biophysical paradigm providing a mechanistical basis for membrane-less organelles assembly in a spontaneous manner (3–8). Upon specific biophysical conditions (pH, temperature, concentration, nature of the macromolecule, etc.), biological macromolecules concentrate in phase-separated liquid-like droplets, which coexist with a dilute phase, like oil drops in water. This process is energetically favorable and allows the formation of membrane-less compartments, called biomolecular condensates (3, 4).

Promyelocytic leukemia (PML) nuclear bodies (NBs) (also known as ND10) are an archetype of membrane-less organelles, that concentrate proteins at discrete sites within the nucleoplasm (9,10). They form a sphere of ∼0.1–1 μm in diameter and are present in the majority of mammalian cell nuclei (9). PML NBs were discovered through their disorganization in acute promyelocytic leukemia (APL). The *PML* gene was identified at the breakpoint of a common translo-

*To whom correspondence should be addressed. Tel: +33 4 26 68 82 58; Fax: +33 4 26 68 82 92; Email: armelle.corpet@univ-lyon1.fr
Correspondence may also be addressed to Patrick Lomonte. Tel: +33 4 26 68 82 57; Fax: +33 4 26 68 82 92; Email: patrick.lomonte@univ-lyon1.fr

cation t(15,17) resulting in a fusion protein with retinoic acid receptor alpha (RARα) that drives APL (11). The tumor-suppressor PML protein is the main organizer of PML NBs and forms a shell surrounding an inner core of dozens of proteins (12). PML NBs have been implicated in a wide range of biological processes such as senescence, antiviral defense or stemness. They may act both to concentrate components to facilitate biochemical reactions such as sumoylation or as storage compartments regulating protein availability in the nucleus.

In this review, we will discuss how the biophysical process of LLPS may participate in the multi-step biogenesis of PML NBs (3,6). We will consider the interplay between PML NBs and the regulation of chromatin dynamics in light of this new paradigm of phase separation and explore its various functional implications. We will provide some perspective on how the partitioning of various chromatin-related factors in the PML NBs might provide a means to fine-tune gene expression and chromatin plasticity.

## STRUCTURE AND FORMATION OF PML NBs

### Structure of PML and PML NBs

The structure of PML NBs has been extensively studied using both light and electron microscopy. There are typically 5–30 PML nuclear bodies per nucleus depending on the cell type, cell-cycle phase or physiological state (13). In immunofluorescence, they appear as nuclear dot-shaped spherical structures that reside in the interchromatin nuclear space (14). By electron or super-resolution light microscopy, it was observed that PML protein is concentrated in a ≈100 nm thick shell at the periphery of nuclear bodies, surrounding an inner core filled with dozens of factors (15,16). More than 170 proteins have been found to reside either constitutively or transiently in PML NBs (12). Among them, the nuclear antigen Sp100 was the first characterized protein to localize in these nuclear bodies (17) and is found together with PML in the periphery (16).

The PML protein (also known as TRIM19) is an essential component of PML NBs (Figure 1A). PML belongs to the family of tripartite motif (TRIM)-containing proteins characterized by a conserved RBCC motif consisting of a RING finger domain (R) followed by two cysteine-histidine-rich B-box domains (B) and an alpha-helical coiled-coil domain (CC). While alternative splicing of C-terminal exons generates seven different isoforms of PML, they all contain the conserved RBCC motif in their N-terminal part (13). All PML isoforms, except PML-VII, show a predominantly nuclear pattern due to the conservation of the nuclear localization signal (NLS) present in exon 6, but may also display specific functions that will not be discussed in the present study (for review (18)). PML protein sustains multiple post-translational modifications including SUMOylation, the covalent attachment of a small ubiquitin-like modifier (SUMO) protein to a protein-specific lysine residue (19). PML main SUMOylation sites are lysines K65, K160 and K490 (20), although SUMOylation of other lysines, like K616 has also been reported (21). PML also contains a SUMO interacting motif (SIM) at position aa 556–562 enabling it to interact with SUMOylated proteins (22) (Figure 1A). PML's branched SUMO chains and SIM motifs may provide a 'molecular glue' to stabilize proteins within PML NBs (see below).

### Formation of PML NBs and LLPS

While early models put forward an interaction between PML-conjugated SUMO and PML-SIM to nucleate NBs (22–24), recent analyses brought new insights on the multi-step formation of PML NBs and the recruitment of their protein constituents possibly through phase separation mechanisms.

PML, which is the main organizer of PML NBs, is a multivalent protein with multiple modular domains and interaction motifs, a key feature that can enable polymerization-driven liquid-liquid phase separation. PML is essential for the structural integrity of PML NBs (25) and is therefore referred to as a *scaffold* protein. Other proteins that permanently or transiently reside in PML NBs are called *client* proteins (6). The first phase of PML NB formation relies on intermolecular covalent disulfide linkage of oxidized PML monomers, as well as non-covalent interactions between the RBCC domains to drive assembly of PML multimers forming the primary nuclear body outer shell (24,26,27). These PML multimers are absent in MEF *Pml*–/– cells reconstituted with a PML mutated in the RBCC domain, emphasizing the importance of this domain for nuclear body formation (27). Recent crystallographic studies of PML RING and B1 domains put forward a cooperative mechanism in which a RING tetramerization step is followed by B1 polymerization of PML to allow macromolecular scaffolding of PML (28,29). On the contrary, PML SUMO-mutants (e.g. PML 3KR), or devoid of their SIM (PMLΔSIM) allow the formation of PML multimers and the formation of spherical PML NBs exactly like the WT structures when introduced into MEFs *Pml*–/– (27). This underscores the non-essential role of the PML SUMO-SIM interactions for the initial steps of PML NB formation. Of note, studies also point out the importance of C-terminal regions of specific PML isoforms in the oligomerization process of PML (30,31). The next step involves the recruitment of UBC9, the only SUMO E2-conjugating enzyme known so far, which is dependent on the RBCC oligomerization of PML (28). UBC9-mediated SUMOylation of PML then regulates and enforces PML-PML interactions via intermolecular SUMO-SIM interactions consistent with their importance to form mature PML NBs (22–24,27) (Figure 1B). In addition, SUMOylated PML drives the multivalent recruitement of inner core client proteins through their SIM, to form mature PML NBs (see below).

Membrane-less organelles biogenesis has recently been revisited through the prism of LLPS which stipulates that above a concentration threshold some proteins may phase separate and form liquid-like droplets with a distinct composition from the surrounding environment (3,8,32). Beautiful *in vitro* experiments demonstrated that mixes of polySUMO-polySIM polymers allow droplet formation that can recruit SUMO/SIM clients depending on the number of free sites remaining on the polymer (6). When transfected into cells, these polymers trigger the formation of condensates, that can be induced specifically at telomeres, and regulate partitioning of SUMO/SIM-containing

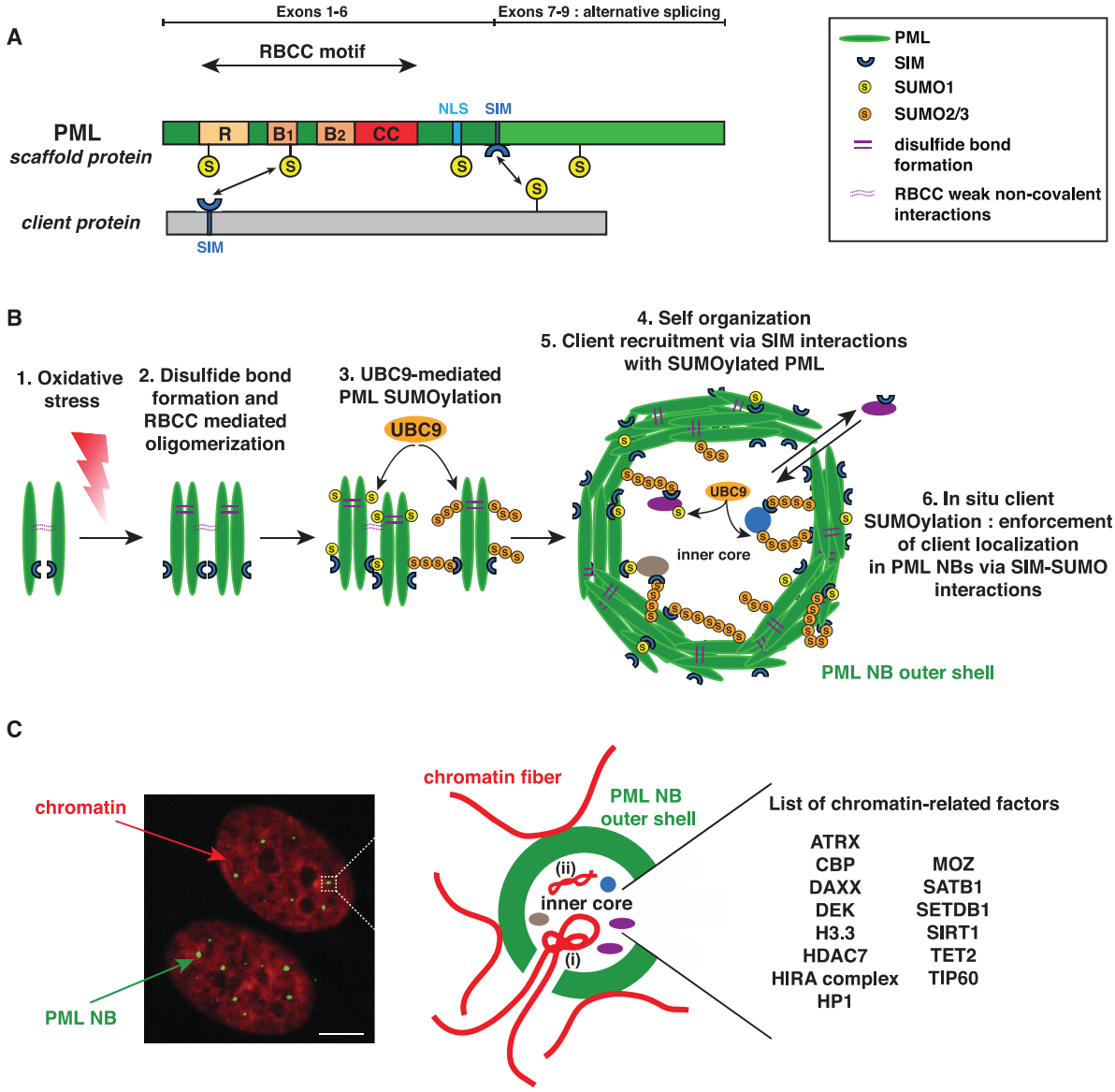


**Figure 1.** Structure of PML and organization of PML NBs. (**A**) Structure of the PML protein scaffold. All PML isoforms (I–VII), ranging from 882aa (PML-I) to 435aa (PML-VII), possess a conserved RBCC/TRIM motif in their N-terminal part. The different C-terminal parts of PML-I to VI are generated through alternative splicing of the 3′ exons 7 to 9 of the unique PML gene, while PML-VII only possesses exons (1–4 and 7b). SUMO modification sites (S) are indicated at lysine positions K65, K160, K490 and K616. The NLS (Nuclear Localisation Sequence) and the SIM (SUMO Interacting Motif) are indicated. NB: PML structure is not to scale. (**B**) Formation of canonical PML NBs. (1) Oxidative stress triggers PML cross-linking by disulfide bond formation. (2) Together with RBCC weak non-covalent interactions, this triggers oligomerization of non SUMOylated PML proteins. (3) UBC9-mediated (poly-)SUMOylation of PML then allows multiple SUMO-SIM interactions, (4) which stabilize the formation of the self-organized matrix-associated outer shell, possibly involving liquid-liquid phase separation mechanisms. Of note SUMO1 modification (yellow) is mostly present in the PML NB outer shell, while the poly-SUMO2/3 chains (orange) present in the shell also protrude to variable degrees in the interior of the PML NB. (5) Client proteins are recruited in the outer shell (eg Sp100 not shown) as well as in the inner core through specific interactions of their SIM with the SUMOylated-PML scaffold. (6) UBC9 SUMOylation of client proteins then enforces their sequestration in PML NBs. Turnover of client proteins is relatively rapid ranging from seconds to a few minutes. (**C**) PML NBs are interspersed in the chromatin. (left) Immunofluorescence analysis of human primary BJ fibroblasts stained by PML (green) and DAPI (red). Scale bar is 10μm. (right) Scheme showing PML NBs (green) surrounded by chromatin loops (red). Cellular loci, such as telomeres, can localize partly within PML NBs in specific cases (i) (see main text). Chromatin-related factors (histone modifiers, histone readers and histone chaperones) as well as viral genomes (ii) localize inside PML NBs.

clients (6,33,34). While PML is a multivalent protein with several identified SUMO/SIM interaction modules that could contribute to a possible phase separation of PML NBs, phase transition properties of the PML protein itself have yet to be demonstrated. In addition, this SUMO/SIM condensation process is not sufficient alone to explain the specific architecture of PML NBs, which exhibit a spherical shell formed by the oligomerized PML protein surrounding an inner core of client proteins (35). This dual phase architecture is rather unique among membrane-less organelles, and it remains to be determined to what extent the shell and the inner core present different solid-like versus liquid-like biophysical properties. Yet, the existence of multiphase biomolecular condensates, formed by LLPS such as the nucleolus (3,36) does not exclude the possible contribution of LLPS to PML NBs biogenesis. In particular, one hallmark feature of the LLPS model, ie, the concentration buffering/dependence, is validated by PML NBs (3,8,37). Size of the PML NBs scales up when increasing the concentration of PML as observed upon IFN-I treatment or senescence entry (38–42). On the contrary PML NBs are dissolved when artifically expanding the volume of the nucleus (43). In addition, PML NBs exhibit many other properties that meet the criteria defining LLPS-based structures, including a spherical shape, fusion/fission events in physiological or stress conditions, or high molecular mobility of internal components (Table 1). Nevertheless, many of this evidence remains qualitative and only provides indirect evidence for LLPS *in vivo* (32).

It is also important to discriminate between true LLPS and alternative mechanisms that could concentrate factors in a given place. In particular, it was recently shown that the transient non-specific binding of RNA polymerase II to the naked DNA of the herpes simplex virus 1 (HSV-1) genome during the lytic phase, leads to a viral DNA-mediated nuclear compartmentalization of replication foci through a mechanism distinct from LLPS (44), and rather driven by polymer-polymer phase separation (PPPS) (for review (37)). This chromatin bridging mechanism also explains the formation of heterochromatin foci that behave as collapsed chromatin globules (45), despite the fact that Heterochromatin Protein 1 (HP1) can undergo LLPS (46,47). As described above, several lines of evidence rather support a contribution of LLPS mechanisms for PML NBs biogenesis, independently of the chromatin polymer (Table 1). Yet, presence of DNA nucleation sites may help to recruit and concentrate PML proteins to reach the saturation concentration required for PML NBs droplet formation. PML NBs can be formed *de novo* at telomeric DNA and subsequently detach from them, suggesting that a nucleation site could mediate the formation of a subset of PML NBs (48). In addition, forced tethering of PML proteins to chromatin by the LacO/LacI or dCas9 systems induces PML NB formation at the targeted locus, suggesting that chromatin-bound PML proteins could be seeds for PML NB formation at specific loci by reaching the saturation concentration for condensate formation (45,49–51).

Many membrane-less organelles, such as nucleolus or Cajal bodies, are condensates that contain, in addition to proteins, RNA molecules which are critical for LLPS. PML NBs are found in regions of high transcriptional activity (14, 52) and early studies showed that nascent RNA could be found inside PML NBs in normal conditions (53) or upon interferon (IFN) α or IFNγ stimulation (54,55). In addition, it was recently shown that the long non-coding RNA (lncRNA) telomeric repeat-containing RNA (TERRA) is found within PML NBs of cells that activate a specific telomere maintenance pathway (56) (see below). Yet, it remains controversial to what extent bulk RNAs physically localize within PML NBs. Other publications showed that nascent RNAs are not enriched in PML NBs (57) but rather accumulate in their vicinity together with highly acetylated blocks of chromatin (14). In addition, brief transcriptional inhibition does not dramatically impact PML NBs structure (54,58), in contrast to nucleoli (59,60), and RNAs are not required *per se* for PML NBs biogenesis (6).

PML NBs thus appear as membrane-less organelles formed through a multi-step process that initially involves PML polymerization-driven shell formation followed by multivalent SUMO–SIM interactions of the PML scaffold and partners that could regulate liquid–liquid phase separation of PML NBs and their composition (see below), without any contributing RNA. We refer hereafter to these nuclear bodies as canonical PML NBs.

### Alternative PML-containing structures

Remarkably, a continuum of PML-containing structures has been observed, in which the liquid-like properties of canonical PML NBs seem to be lost. After entry into mitosis, PML NBs undergo dramatic rearrangements (61), and partition in distinct larger aggregates of PML proteins called MAPPs (Mitotic Accumulation of PML Protein) (62) (for review (63)). MAPPs neither undergo rapid exchange of the PML protein, nor fusion/fission processes (62), that are essential criteria for LLPS (Table 1). PML undergoes an extensive de-SUMOylation preventing it from recruiting SIM-containing proteins such as the regular components of PML NBs, Sp100 or Death Domain-Associated Protein (DAXX) (61,62) (see below). In early G1, PML NBs, in the form of the so-called CyPNs (Cytoplasmic assemblies of PML and Nucleoporins), become associated with karyopherin KPNB1 which recruits FG-repeat-containing nucleoporins. The latter have the ability to form an hydrogel that encapsulates PML aggregates, which could facilitate their re-solubilization and nuclear import (64,65). Sequential recruitment of PML NBs components then occurs allowing reformation of mature canonical PML NBs (62,66). Other atypical PML-containing structures associated with nuclear lipid droplets were observed in cells after fatty acid stress (67,68). These so-called lipid-associated PML structures (LAPS) differ from canonical PML NBs as they lack SUMO1, Sp100 and DAXX proteins (68). PML only occupies part of the surface of the nuclear lipid droplets and is not required for their formation but is necessary for their functional maturation (68). In human embryonic stem cells (hESCs), PML-containing structures, also devoid of SUMO1, Sp100 or DAXX, show particular morphological types in the forms of long-linear rods or rosettes (69), which may be used as an indicator of the pluripotent state of the cells (70). Finally, our data char-

**Table 1.** Summary of LLPS criteria that are matched or not by canonical PML NBs. In this table, we put forward the experimental evidence that sustains or not the involvement of LLPS in biogenesis of canonical PML NBs. Criteria listed here have been chosen based on the following reviews (4,8,32) and may not be all necessary/sufficient to prove LLPS. n.d. : non determined

| LLPS criterion | Criterion met by PML NBs | Experimental evidence | References |
|---|---|---|---|
| **Spherical shape (roundness)**: liquid droplets have a spherical shape driven by surface tension | Yes | Super-resolution microscopy or transmission electron microscopy of PML NBs show sphericity of these nuclear bodies | (15,16,27,35) |
| **Fusion/fission**: like oil droplets in water, biomolecular condensates have the ability to fuse or drip | Yes | Time-lapse observations of PML NBs confirms their ability to undergo fusion/fission events during DNA replication or upon various stress conditions such as DNA damage, heat shock or physical pressure | (15,171–172) |
| **Molecular mobility**[a]: liquid condensates are characterized by a high mobility of proteins within them which is essentially depending on diffusion | Partially | FRAP experiments underlined fast recovery times for client proteins such as DAXX, CBP or BLM in the range of seconds, while PML isoforms exhibit slightly slower recovery times in the range of a few minutes compatible with the liquid-like nature of PML NBs. However, long recovery rates have been observed for specific isoforms such as PML V which may contribute to the structural integrity of nuclear bodies and could act as a stable scaffold for the recruitment of faster-exchanging molecules such as DAXX or CBP | (14–15,115) |
| **Concentration buffering/dependence**: LLPS is a function of concentration: past the critical concentration required for droplet formation, production of more protein increases droplet size but does not change concentration in either phase | Yes | Increase in PML intracellular concentration, as observed upon IFN-I treatment or senescence entry, results in an increased PML NBs size, while a decrease in PML protein concentration dissolves PML NBs *in vivo* | (38–43) |
| **Interfacial boundary**[b]: phase-separated proteins should preferentially move within the droplet. Presence of a phase boundary should reduce diffusion across the boundary | Partially | Diffusion coefficient for NLS-GFP was determined in nucleoplasm or in PML NBs by FCS. This demonstrated a 3-fold reduction in the diffusion coefficient inside the PML NBs as well as reduced exchanges of NLS-GFP between PML NBs and the nucleoplasm | (16,115) |
| **Undergoes LLPS *in vitro/in vivo*** | Partially | Not demonstrated for the PML protein itself. Yet, polySUMO-polySIM polymers form droplets *in vitro* and *in vivo* and recruit SUMO/SIM containing protein clients *in vitro* and *in vivo* | (633–34) |
| **Temperature/ion strenght/pH dependance**: measure of droplet formation in vivo should show dependance on temperature, ion concentration or pH | n.d. | n.d. | - |
| **Sensitivity to 1,6-hexanediol**: this chemical compound perturbs weak hydrophobic interactions that are involved in LLPS. Yet, sensitivity to 1,6 hexanediol is neither necessary nor sufficient to demonstate that a structure is formed by LLPS | n.d. | n.d. | - |
| **Optodroplet assay**: investigate whether expression of a fusion protein (protein of interest fused to a photolyase domain that can self-associate upon blue light) facilitates droplet formation *in vivo* upon blue light stimulation. Results should be interpreted with caution since these experiments rely on an artificial fusion protein system and should thus be combined with other experiments to prove LLPS *in vivo* | n.d. | n.d. | - |

[a]Molecular mobility is traditionally measured by Fluorescence Recovery After Photobleaching (FRAP). However, it should be noted that the use of recovery time as a marker of LLPS is insufficient *per se* since rapid recovery can result from a variety of mechanisms (32). One critical point is to demonstrate that the recovery rate is truely dominated by diffusion (rather than binding), which can be assessed by performing FRAP with various sizes of the bleach spot (32), which has not been performed yet in PML NBs.
[b]Diffusion across the boundary can be measured by fluorescence correlation spectroscopy (FCS) or single-molecule tracking (SMT). Alternatively, FRAP performed on half of the condensate, as performed in (45) provides an original and quantitative measure for the presence of a impermeable boundary, which could potentially be applied to PML NBs.

acterizing PML NBs in sensory neurons within human trigeminal ganglia show the presence of large aggregates of PML, lacking SUMO1, Sp100 and DAXX (71) (and unpublished). Thus, self-association of the PML protein scaffold allows to form various alternative PML-containing structures that do not exhibit LLPS properties. We hypothesize that the presence of SUMO1, which can undergo LLPS *in vitro* (6), is key to promote formation of canonical PML NBs possibly via triggering LLPS and thus partitioning of regular client proteins such as DAXX or Sp100 in PML NBs.

While canonical PML NBs appear as discrete foci interspersed between chromatin (Figure 1C), we will now focus on understanding the physical and functional connection of PML NBs with chromatin and investigate how the compartmentalization activity of PML NBs through phase separation mechanisms provides multiple strategies to regulate chromatin-related factors partitioning and chromatin

dynamics. In particular, we can envisage three main non-exclusive processes that will be discussed: (1) PML NBs may be hotspots for modifications such as SUMOylation, potentially modulating the activity of chromatin-related factors; (2) PML NBs may store/sequestrate chromatin-related factors and control their dynamic release thereby fine-tuning the nucleoplasmic pool of a given factor and (3) PML NBs may help targeting chromatin-related factors to specific chromatin-associated regions by compartmentalizing them (Figure 2).

## A CONNECTION OF PML NBS WITH CHROMATIN

### PML NBs contain multiple chromatin associated proteins, including histones and histone chaperones

The idea of a role for PML NBs in the regulation of chromatin dynamics emerged via the identification of numerous chromatin-modifying factors within PML NBs, such as the CREB-Binding Protein (CBP), an histone acetyltransferase (HAT) involved in transcriptional regulation (53,72,73), or HP1 (74–77). HP1 is a key protein involved in heterochromatin formation, which interacts with Sp100, a constitutive component of PML NBs, and which localizes within these bodies in interphase as well as in senescent cells (74–78), suggesting very early on a connection of PML NBs with chromatin dynamics. Together with HP1, DAXX was identified as a constitutive PML NBs component (25,77) but it was not until its identification as a histone chaperone that the connection with chromatin dynamics was made (79). DAXX associates with the chromatin remodeler ATRX to form an H3.3-specific histone chaperone essential for H3.3 deposition at heterochromatin loci (79–81), and is required for ATRX localization in PML NBs (82–85) (Table 2).

Histone chaperones are dedicated proteins, which associate with non-nucleosomal histones and escort them throughout their cellular life in processes ranging from nuclear import, storage, assembly/disassembly onto chromatin during several DNA metabolic processes (86). Histone chaperones can be distinguished on the basis of their histone binding selectivity with a preference for H2A–H2B or H3–H4 histones and with additional selectivity towards specific histone variants. The replicative histone variants represent the bulk of histones and are expressed in S-phase, while replacement variants are expressed constitutively at lower levels. Among the H3-H4 histone chaperones, the CAF-1 complex is involved in the specific deposition of the H3.1 replicative histone variant in a DNA-synthesis dependent manner, while HIRA and DAXX-ATRX are H3.3 specific histone chaperones complexes implicated in H3.3–H4 deposition in a DNA-synthesis independent manner (for review (86)). H3.3 deposition was initially identified as characteristic of euchromatic transcriptionally active regions with high histone turnover (87–89). HIRA interacts with RNA polymerase II (90), specific transcription factors (TFs) (91) or replication protein A (RPA) found in nucleosome-free regions (92), thus mediating H3.3 deposition at active regulatory elements such as enhancers, promoters or gene bodies (80,92). Although unexpected, H3.3 was later found enriched in heterochromatin loci such as telomeres or pericentromeric chromatin where it is deposited by the DAXX-ATRX complex (79–81). This reflects the double face of H3.3 histone variant in gene regulation, which is context-dependent (for review (86,93,94)).

Interestingly, PML NBs seem to have a strong connection with the H3.3 chromatin assembly pathway. In addition to the constitutive localization of the DAXX–ATRX complex in PML NBs, the HIRA H3.3-specific histone chaperone complex, composed of HIRA, UBN1, CABIN-1 and transiently ASF1A, also localizes in PML NBs upon senescence entry (78,95–97) and upon viral infection-associated type I interferon (IFN-I) signaling (98–100) (see below). Furthermore, soluble newly-synthesized H3.3-H4 histone dimers are brought to PML NBs in a DAXX-dependent manner before deposition onto chromatin (84,85), thus suggesting that PML NBs may be important regulatory sites for the sorting of H3.3 among various histone chaperones complexes and further incorporation of H3.3 onto chromatin. Of note, another H3.3 specific chaperone called DEK also localizes in PML NBs in stem cells, and may participate in the maintenance of an H3.3 soluble pool available for association with other chaperones in PML NBs (101) (Table 2 and see below).

Finally, SETDB1, an histone H3 lysine 9 (H3K9) specific methyltransferase also localizes constitutively in PML NBs, which may be related to the transcriptional repression of specific genes (102). Given the connection of SETDB1 with DAXX–ATRX in the heterochromatinization of retroelements in mouse ES cells (103,104), further studies will be required to determine the function of the SETDB1 pool in PML NBs in regards to its function in heterochromatin maintenance. Other H3K9 methyltransferases, such as SUV39H1 and G9a, or EZH2, an H3K27 methyltransferase member of the Polycomb Repressive Complex 2 (PRC2), associate with PML but it remains to be shown whether they actually localize in PML NBs (105–107). Interestingly, other histone modifiers, such as TIP60 (KAT5) and MOZ (KAT6A) histone acetyltransferases, histone deacetylase 7 (HDAC7), or SIRT1, partition in PML NBs to regulate chromatin dynamics and transcriptional regulation (108–112). Finally, PML NBs are also associated with DNA demethylation activities through the recruitment of the ten-eleven translocation dioxygenase 2 enzyme (TET2) in response to chemotherapy and exclusion of DNA methyltransferase 3A (DNMT3A) (113,114) (Table 2).

### Regulation of the composition of PML NBs in chromatin-related factors

How do cells regulate the composition of PML NBs and what molecular mechanisms govern the recruitment of the chromatin-associated factors in PML NBs? Indeed, while PML NBs are macroscopically stable and persist for hours/days, photobleaching recovery experiments showed that they are highly dynamic at the molecular level, turning over their contents on time-scales from seconds to minutes (15,115). In light of the LLPS paradigm, we will now explore how the partitioning of various histone chaperones in the membrane-less PML NBs is regulated. The number of interaction modules (valency) and their affinity are key parameters controlling phase separation and could thus enable compositional control of PML NBs (6). In particular, changes in concentration or specific post-translational

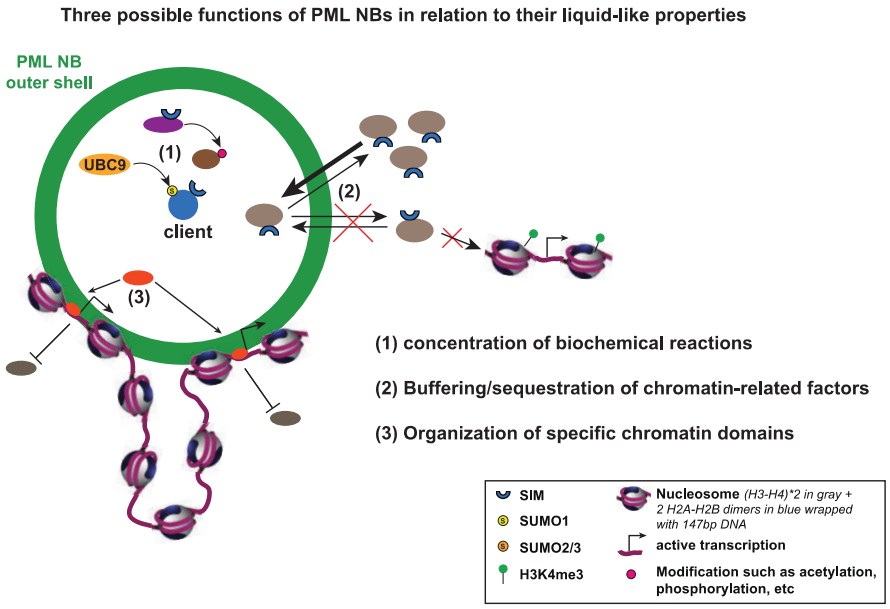


**Figure 2.** Three possible functions of PML NBs in relation to their liquid-like properties. Liquid properties are advantageous for the cells by providing the ability of fast and easy rearrangements of macromolecules. Yet, the separation of the "liquid" nucleoplasm in several membrane-less condensates including PML NBs is essential to allow the formation of small reaction volumes with a different composition from the outside. Description of PML NBs as biomolecular condensates can illuminate the understanding of their function. We can envisage three important functions which may explain their roles in chromatin dynamics: (1) PML NBs may concentrate biochemical reactions. The biochemical environment within phase-separated PML NBs is different from the nucleoplasm and could serve to regulate (i) the kinetics of enzymatic reactions or (ii) the specificity of the modifications catalyzed. This is consistent with the described role of PML NBs as sumoylation hotspots, but could also apply for other modifications such as phosphorylation, acetylation, ubiquitination, or protein degradation. An example of the SUMOylation of a given client by UBC9 or of another client modification by a specific enzyme is shown. (2) PML NBs may buffer/sequester proteins via liquid-liquid phase separation of these client proteins. Increase in PML/client concentration may trigger accumulation of a given protein in PML NBs as a means to buffer the amount of the free protein in the nucleoplasm (as observed early for CBP for example). In addition, protein sequestration in PML NBs might affect their known activity as observed for DAXX. (3) PML NBs may help to organize specific nuclear domains, such as chromatin domains. PML NBs are interspersed in the active chromatin compartment and could potentially help to organize this compartment by pulling together genomic loci with similar transcriptional regulation. Of note, these three functions are not mutually exclusive and may serve altogether to regulate chromatin dynamics. Concentration of various factors in PML NBs together with specific genomic loci may help to catalyse specific reactions at given loci, as in the case of the ALT pathway for example (see Figure 3).

modifications (e.g. SUMOylation) of the PML scaffold or of a client protein, modify the valency of free sites available, and thus the affinity between interacting modules regulating PML NB composition (6). SUMOylation of PML is not required for PML NB formation but is essential for the recruitment of partners containing one or several SIM motifs (23–25,27,116,117). Indeed, DAXX possesses 1 SIM motif, $I^{733}$IVLSDSD$^{740}$, at its C-terminus which is both critical for its localisation in PML NBs as shown by deletion experiments, and sufficient for the localization of a GFP-$DAXX^{SIM}$ fusion protein in PML NBs (27,118). Interestingly, DAXX can also be SUMOylated (118–121), but the forced fusion of SUMO1 or SUMO2 with DAXX is insufficient to rescue the DAXXΔSIM localization in PML condensates. Hence, in normal cell conditions, the presence of a SIM with affinity for SUMOylated PML is necessary and sufficient for a constitutive localization of DAXX in PML NBs. SUMOylation of DAXX by UBC9 present in the PML NBs then enforces its sequestration within the condensates by intermolecular interactions with PML SIM (27).

Interestingly, bioinformatics analysis of chromatin associated factors such as DEK or SETDB1, which can localize in PML NBs, identified putative SIM in these proteins with SETDB1's SIM being crucial for its interaction with SUMOylated proteins (101,122,123). It is tempting to speculate that these SIM motifs could be implicated in their recruitment to PML NBs, yet further studies will need to confirm the exact sequence requirements. Overexpression of the PML protein itself or increase in PML SUMOylation (eg following IFN treatment (38–40)) increases the number of available SUMO groups on PML (multivalency), which can trigger the switch-like recruitment of client proteins such as CBP (6,124). On the contrary, ectopic overexpression of client proteins, such as HIRA, UBN1 or CBP, leads to their recruitment to PML NBs, which may result from an increased valency of the client upon higher concentration and thus suggests a buffering mechanism for excess nucleoplasmic protein (95,124,125) (as represented in Figure 2 item (2)). Thus, caution should be taken when concluding on the localization of a given protein only based on the overexpression of an ectopic form. SETDB1 as well as HIRA also possess putative SUMO sites and have experimentally been found in screens for SUMOy-

**Table 2.** List of histone chaperones, histone modifiers or histone readers localizing within PML NBs. Only proteins with known localization in PML NBs are listed, those that interact with PML, but whose localization in PML NBs has not yet been proven, have been omitted. Presence of validated SUMOylation sites or SIM motifs is indicated, putative sites/motifs identified by bioinformatic analysis or in SUMO screens are not shown. Positions refers to human proteins unless stated otherwise. While HP1 has been shown to be SUMOylated (236), it remains to be determined whether this SUMOylation controls its localization in PML NBs. The function related to the localization in PML NBs is also depicted. n.d. : non determined. hMSCs : human mesenchymal stem cells. MARs : Matrix attachment regions

| Protein | Protein function | SUMO | SIM | Recruitment | Function related to localization in PML NBs | References for PML NB localization | References for SUMO/SIM |
|---|---|---|---|---|---|---|---|
| ATRX | H3.3 histone chaperone | n.d. | n.d. | Constitutive, DAXX-dependent | Heterochromatin establishment | (82–83) | - |
| CBP | Histone acetyltransferase | n.d. | n.d. | Constitutive | Transcriptional regulation via p53 acetylation | (53,72–73) | - |
| DAXX | H3.3 histone chaperone | Multiple lysine residues | SIM1 IIVL (aa 7-10) and SIM2 IIVLSDSD (aa 733–740) | Constitutive | Transcriptional regulation, heterochromatin establishment, H3.3 recruitment in PML NBs, H3.3-dependent chromatin assembly | (25,61) | (118) |
| DEK | H3.3 histone chaperone | n.d. | AKRE (aa 260–263) (not validated by mutation) | Constitutive (hMSCs) | Maintenance of an H3.3 soluble pool available for recruitment in PML NBs | (101) | (101) |
| H3.3 | Histone H3 variant found in transcriptionally active regions and specific heterochromatic regions | n.d. | n.d. | Constitutive as well in senescence, DAXX-dependent | H3.3 soluble pool available for triage between histone chaperones | (84–85) | - |
| HDAC7 | Class IIA histone deacetylase | n.d. | n.d. | Constitutive in a subset of PML NBs, increased upon TNF-α | Transcriptional regulation (sequestration in PML NBs to relieve gene repression) | (108) | - |
| HIRA complex | H3.3 histone chaperone complex composed of HIRA, UBN1, CABIN1 and transiently ASF1A | n.d. | n.d. | Stress-induced (senescence, IFN, viral infection) | H3.3-dependent chromatin assembly in transcriptionally active regions, sequestration mechanism ? | (78,95–100) | - |
| HP1 | Heterochromatin protein 1 | K84 + alternative usage of various lysines residues | n.d. | Constitutive as well as in senescence | Heterochromatin establishment, in particular at cell-cycle genes during senescence | (75–78) | (236) |
| MOZ (KAT6A) | Histone acetyltransferase | n.d. | n.d. | Stress-induced (DNA damage, senescence) | Transcriptional regulation via p53 acetylation | (112) | - |
| SATB1 | Chromatin organizer by anchoring of MARs to the nuclear matrix, transcriptional regulator | K744 | n.d. | Constitutive in a subset of PML NBs, SUMO-dependent | Transcriptional regulation in immune cells, regulation of SATB1 levels by caspase-induced cleavage | (143,182) | (182) |
| SETDB1 | Histone H3K9 trimethyltransferase | n.d. | IIEI (aa 125–129) | Constitutive | H3K9me3 heterochromatin establishment at specific loci (such as *Id2* gene) + maintenance of PML NBs | (102) | (122) |
| SIRT1 | NAD-dependent histone deacetylase | n.d. | n.d. | Stress-induced (PML-IV overexpression, senescence) | Deacetylation of p53 leading to repression of p53-mediated transactivation | (109) | - |
| TET2 | Oxidation of 5mC to promote DNA demethylation | n.d. | n.d. | Chemotherapy-induced, dependent on PML C-Terminus | Chemotherapy-induced demethylation of specific genes | (113) | - |
| TIP60 (KAT5) | Histone acetyltransferase | K430 and K451 | n.d. | UV-induced, SUMO-dependent, PML3-dependent | UV-induced DNA damage response (p53 recruitment in PML NBs and stabilization), SUMOylation promotes HAT activity, regulation of KAT5A stability | (110–111) | (110) |

lated proteins (119–121,126). Whether these sites are essential to enforce their localization in PML NBs or regulate their turnover as observed for Sp100 (115) remains to be tested.

Changes in affinity may also be regulated by post-translational modifications of the scaffold (PML) or of the client proteins. Phosphorylation adjacent to the SIM motifs, as observed for the phosphoSIMs of PML and DAXX, leads to an increased affinity towards SUMO1 via interaction with specific SUMO1 lysine residues (127–130). On the contrary, acetylation of SUMO1 decreases the affinity for SIM, as observed for DAXX which then looses its localization in PML NBs (131), and thus participates in the regulation of client partitioning into biomolecular condensates. Of note, acetylation of SUMO1 at key lysine residues alters binding to the phosphoSIMs of PML or DAXX showing the structural plasticity of SUMO-SIM interactions that can be controlled by residue-specific post-translational modifications (132). Phosphorylation of HIRA by glycogen synthase kinase 3β (GSK-3β) has been proposed to regulate its localization in PML NBs upon senescence (133), but does not seem to play a role in IFN-mediated relocalization of HIRA in PML NBs (100). Recently, a large RNAi screen also identified Homeodomain-Interacting Protein Kinases (HIPK1 & 2) as important regulators of PML NBs composition. Overexpression of these proteins led to a decreased accumulation of Sp100 in PML NBs, but not of PML itself. This suggests a role of HIPK1 & 2 in controlling the condensation of proteins in PML NBs by phosphorylation (134). The use of kinase-dead enzymes should rule out a possible titration effect where HIPK1 & 2 overexpression could saturate SUMO sites via binding of their SIM (135), hence displacing Sp100.

Thus, PML NBs contain multiple chromatin-associated factors whose localization is regulated by a switch-like partionning between the diffuse and the condensed phase controlled by the multivalency of PML and of the client protein itself. We will now discuss the possible physical contacts of PML NBs with chromatin.

### A physical connection of PML NBs with chromatin

The use of an analytic electron microscopic method called Electron Spectroscopic Imaging (ESI) was instrumental in precisely determining the nucleic acid-based regions and protein-based regions within and around PML NBs (14). Boisvert and colleagues demonstrated that the PML NB core is a protein-based structure and that PML NBs are devoid of nucleic acids in normal conditions. Yet, nascent RNA, as well as highly acetylated blocks of chromatin were found to accumulate in the vicinity of PML NBs suggesting an association of these nuclear bodies with transcriptionally active chromatin (14) (see below). Further ESI studies demonstrated that the protein cores of PML NBs are surrounded by chromatin fibers and make direct physical contact with them, allowing the positional stability of PML NBs (58). PML NBs are also found adjacent to replication foci labelled by BrdU in middle-late S-phase cells (57).

While PML NBs physically contact chromatin, additional studies explored their associations with specific regions of the genome. The use of immuno-DNA FISH to combine immunolocalization of PML NBs with localization of specific genomic loci provided convincing data to demonstrate the specific association of PML NBs with cellular chromosomal loci. Using this approach, Shiels *et al.* demonstrated for the first time a non-random association of a specific locus, the major histocompatibility complex (MHC) on chromosome 6, with PML NBs in human primary fibroblasts (136), which was consistent with the role of PML in the upregulation of MHC specific genes (137). The association of this gene-rich locus with PML NBs was neither dependent on transcription nor on cell cycle phase, and could be observed when the locus was placed on chromosome 18. Further immuno-DNA FISH studies showed a specific association of PML NBs with the *TP53* gene locus, but not *BCL2* in jurkat cells (138) as well as a more general association of PML NBs with regions of high transcriptional activity (52). Of note, the association of PML NBs with specific loci might be cell-cycle specific since association of the histone gene cluster was increased in S-phase when canonical histones genes are transcribed (52). Similarly, it was found that PML NBs are preferentially juxtaposed to centromeres during G2-phase (77). Juxtaposition of genomic loci to PML NBs may be a means to regulate specific gene expression (see below). PML NBs show significant association with the *Oct3/4* locus in ESCs, with a decrease upon differentiation in Neural Precursor Cells (NPCs), correlating with the decrease in Oct3/4 expression (139). In addition, Salsman *et al.* showed that PML NBs are not only juxtaposed to the *DDTI4* gene locus, but they are also closely associated with the *DDTI4* RNA transcriptional foci, as shown by immuno-RNA FISH, and consistent with the decreased expression of *DDIT4* upon PML loss (140).

Interestingly, IFNγ increases the spatial proximity between PML NBs and the MHC class II gene cluster and PML is required for the IFNγ-induced MHC class II gene transcription (141). In particular, the association of a gene from this locus, the *DRA* gene, with PML NBs is maintained after IFNγ shut-off and is required to keep a prolonged permissive chromatin state on the *DRA* promoter (142). This underlines the importance of the PML NBs spatial proximity with specific loci to mediate epigenetic memory of a stimulus through cell divisions to increase responsiveness of gene expression to future activation signals (142). The connection of PML with the MHC locus was further substantiated by genomic studies using ChIP showing that PML is directly associated with specific regions within the MHC class-I locus (143). Together with special AT-rich sequence binding protein 1 (SATB1), PML is involved in the chromatin-loop organization of the MHC class-I locus and regulates a distinct set of genes within this locus upon IFNγ treatment (143). Recent ChiP-Seq analysis of PML binding regions in MEFs also found PML enriched at heterochromatin gene-poor loci called PML-associated domains (PADs) (144). However, even if ChIP experiments overcome the *a priori* assumptions for selecting a genomic locus, ChIP cannot distinguish between the nucleoplasmic pool of PML and PML that is located within PML NBs. In particular, the recent ChIP-Seq analysis against PML in MEFs illustrates that most of the loci immunoprecipitated

with PML do not localize in PML NBs and PML association at these loci is required to preserve their H3K9me3 heterochromatic state (144). Immuno-FISH therefore remains an indispensable control to assess whether the association of PML with specific chromatin loci happens through PML NBs.

To overcome limitations of immuno-FISH and ChIP, the Bazett-Jones' team developped a method called immuno-TRAP which allows the deposition of biotin onto DNA in close proximity to PML NBs. DNA can then be purified with streptavidin agarose beads and analyzed in a unbiased manner (145). Using various FOSMIDS, the authors confirmed an interaction of PML NBs with *TP53* locus and uncover an association with the *PML* locus itself. The associations observed were cell-type specific and dependent on the cell's physiological state since IFNα treatment modified the loci association with PML NBs (145). Importantly, the use of an engineered APEX2 peroxidase fused to PML in mouse ESCs to mediate chromatin labeling and purification combined with deep-sequencing (ALaP-Seq) allowed the identification of chromatin regions proximal to PML NBs (114). The authors confirmed the association of PML NBs with regulatory regions of active genes in a genome-wide manner, as well as identified novel hotspots regions, such as the short arm of the Y chromosome, frequently associated with PML NBs (114). The use of a PML RING domain mutant, that is diffuse in the nucleoplasm, only gave very few peaks demonstrating that the majority of the ALaP-Seq peaks truely reflect chromatin interactions with PML NBs, but not with the nucleoplasmic pool of PML.

In parallel to the connection of PML NBs with cellular loci, it was early demonstrated that the genomes of specific viruses (HSV-1, Simian Virus 40 (SV40) and adenovirus) were also juxtaposed to PML NBs during the early stages of lytic virus infection (146,147). A role of PML NBs as potential docking sites for viruses favoring their replication and/or transcription was then confirmed for HSV-1 (148,149), human papilloma virus 11 (150), Epstein-Barr Virus (151), and bovine papillomavirus (152), suggesting that PML NBs could facilitate the infectious process under certain circumstances. In contrast, the presence of a foreign plasmid transgene or of latent human immunodeficiency virus (HIV) proviruses next to PML NBs was associated with transcriptional silencing (107,153). These examples suggest that cells could handle foreign genomes of viral origin in a non-random fashion, and that PML NBs are likely to show a Janus activity depending on the virus and the stage of the viral infection (see below).

### PML NBs can contain DNA/chromatin in specific cases

Specific cellular or viral loci can be juxtaposed to PML NBs. However, in certain cases, particular DNAs are located *inside* the nuclear bodies. The first example comes from telomerase-negative tumors and tumor-derived human cell lines that have been shown to maintain their telomeres length by a mechanism called alternative lengthening of telomeres (ALT) (154–156). ALT cells and tumors contain specific structures of PML NBs referred to as ALT-associated PML nuclear Bodies (APBs). High resolution microscopy images show that these APBs contain telomeric DNA in the interior of the structure, in addition to the PML protein and its partners (16,157,158) (Figure 3). In another specific pathology, the Immunodeficiency, Centromeric region instability, and Facial anomalies syndrome (ICF), enlarged ring-like PML structures, namely giant PML NBs, were observed in ICF G2 nuclei (159). ICF is a rare autosomal recessive disorder associated with mutations in the DNA-methyltransferase *DNMT3B* gene causing the hypomethylation and decondensation of the heterochromatic structure of satellite DNA mostly in pericentromeric regions of chromosomes 1 (1qh), 16 (16qh) and 9 (9qh) (160–162). Giant PML NBs contain the undercondensed 1qh or 16qh heterochromatin in the inner core with PML forming the outer shell (159) (Figure 3). Other PML NBs constituents, such as HP1, DAXX, ATRX, SP100, SUMO1, CBP and the DNA repair-associated factors BLM, TOP3A and BRCA1 were also found inside the structure adopting a specific multilayered organization (159).

In the case of viral infection with HSV-1, a dsDNA virus, the latent viral genome does not integrate in the host genome, and remains as a chromatinized episomal form in the nucleus of infected cells. We and others have shown by confocal microscopy that positioning of the latent HSV-1 genomes is not random and instead, the viral genome is encased in PML NBs forming structures called viral DNA-containing PML NBs (vDCP-NBs) or ND10-like (71,163–165). vDCP NBs contain, just like APBs and giant PML NBs, most of the PML partners, including the DAXX–ATRX complex, as well as all members of the H3.3 histone chaperone HIRA complex (98–100) (Figure 3). Interestingly, a physical and functional association of the genome of an RNA virus, the hepatitis delta virus was observed with PML NBs. The particular antigenomic RNA co-localizes with PML NBs but contrarily to the APBs, giant PML NBs and vDCP NBs, resides at the edge of a rim-like structure that shows in the inside the presence of the PML, SP100, DAXX and SUMO-1 proteins (166). This peculiar association plays a role in viral RNA synthesis mediated by host RNA polymerase II (167), but has not been studied further and remains so far the only example of a viral RNA product closely associated with PML NBs. Finally, an exogenous cytomegalovirus promoter-containing transgene array is found at the center of PML NBs, with PML and SUMOs forming a ring structure around it, as observed by confocal microscopy, supporting the evidence of DNA in the interior of PML NBs (168,169). Altogether these specific examples show that PML NBs have a strong physical connection with specific genomic loci and can entrap particular DNAs, supporting an important role in regulating DNA-metabolic processes (see below).

### Regulation of the physical connection of PML NBs with chromatin loci

PML NBs are very dynamic entities whose number and size varies depending on the cell cycle and on various stimuli (61,170). During interphase, nucleoplasm is separated from the cytoplasm by the nuclear envelope forming a selective barrier. PML NBs exhibit apparent stability in the nucleus of unperturbed healthy cells. Yet they are actively remodeled during S-phase due to chromatin topological changes with-

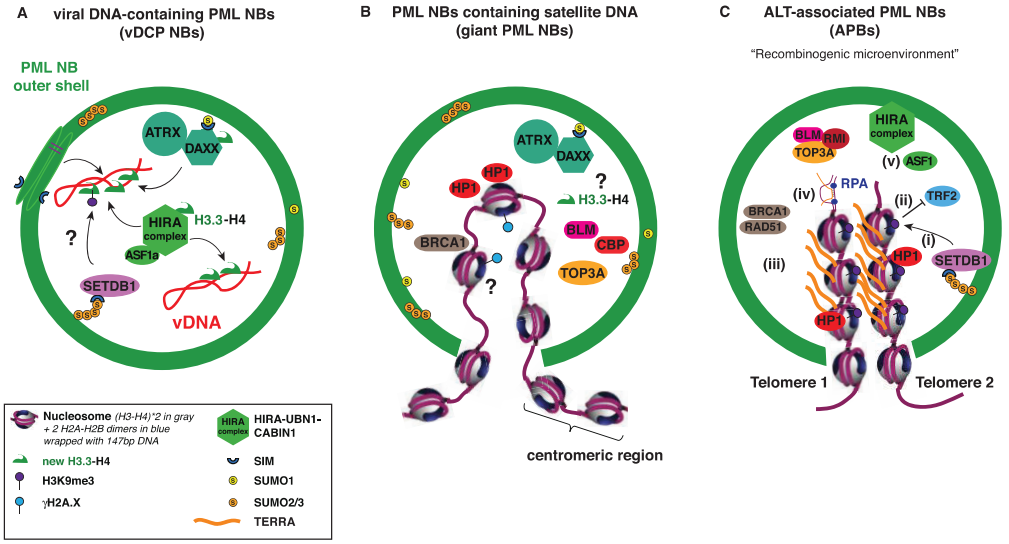


**Figure 3.** PML NBs directly regulate chromatin dynamics of DNA sequences found in the condensate. (**A**) Viral DNA-containing PML NBs (vDCP NBs) are specific PML NBs encasing the HSV-1 latent viral genome. Both H3.3 histone chaperone complexes (DAXX-ATRX and HIRA complexes) are found in these structures together with H3.3–H4. These complexes are essential for the H3.3 chromatinization of the virus, together with PML. H3.3 is decorated with the heterochromatin mark H3K9me3, which could be deposited by SETDB1 (question mark), a known client protein localizing constitutively in PML NBs. (**B**) PML NBs containing satellite DNA are found in the ICF syndrome in the form of giant PML NBs. These structures contain proteins organized in ordered concentric layers around the satellite DNA core, in the following order from the center: HP1 proteins, DAXX–ATRX complex, CBP/BLM/TOP3A, surrounded by a sphere of SUMO1/SP100 and then PML protein (concentric layers not shown). While the heterochromatin nature of the satellite DNA is atypical with absence of the constitutive H3K9me3 mark despite HP1 presence, the presence of γH2A.X in some giant PML NBs (25%) nevertheless suggests that satellite DNA is associated with chromatin inside PML NBs. Of note, normal PML NBs can also contain satellite DNA in G2 phase. PML NBs-containing satellite DNA may help remodelling and maintenance of the heterochromatin structure present at late-replicating satellite DNA. (**C**) ALT-associated PML NBs (APBs) are a hallmark of the ALT pathway. Here we only focus on the chromatin dynamics in APBs, and neither display the numerous repair factors present in APBs nor the mechanisms involved in ALT. Telomeric DNA localizes within PML NBs together with specific chromatin-related factors such as SETDB1, ASF1, or HIRA. Recent data suggest that telomeric DNA repeats are more compact, with higher levels of H3K9me3 deposited by SETDB1 (i), and bound less TRF2 in ABPs than regular telomeres (ii), which would cause telomeric deprotection and promote telomeric recombination. Increase in TERRA transcription (orange lines) is also observed (iii) and fuels the ALT process by increasing RNA:DNA hybrids (iv) and thus replicative stress. Depletion of the histone chaperone Asf1 promotes histone management dysfunction during telomeric replication and is sufficient to trigger ALT (v).

out major changes in PML protein levels or biochemical alterations. In S-phase, chromatin that undergoes replication retracts from PML NBs and actively pulls the PML NBs apart causing their fragmentation in smaller PML NBs by a fission mechanism (171). High rates of PML protein exchange between the nucleoplasmic pool and the PML NBs then ensures that the nascent PML microbodies increase in size by G2. Of note, fusion events can also contribute to the regulation of PML NBs size in S-phase (171).

Reduction of the physical contacts between PML NBs and chromatin can also be induced by specific stresses, such as heat shock, transcriptional repression, apoptosis induction, DNA damage or oxidative stress (58,114,172,173). This triggers the formation of newly formed microbodies by fission as well as in their increased mobility underscoring the importance of chromatin interactions for the structural and morphological integrity as well as the dynamics of PML NBs (58,174). Increase in PML NBs number may also be linked to chromatin decondensation mediated by an ATM-KAP1 axis during DNA damage, or as observed upon HDAC inhibition (172,173). Biomolecular condensates can fuse, coalesce and drip, which are typical properties of liquid assemblies (4). Fission and fusion events of PML NBs observed across the cell cycle or following various stresses thus appear as a convincing feature that would sustain the hypothesis of a liquid-like behavior for these nuclear bodies. Changes in the amount of PML NBs contacts with chromatin across the cell-cycle or following various stresses can thus provide many regulation opportunities for the cells that will need to be explored further.

## PML NBs ARE IMPORTANT FOR THE CHROMATINIZATION OF VIRAL GENOMES

The discovery of the association of PML NBs with the genomes of several viruses suggests that PML NBs and their chromatin-related factors mediate their antiviral activity partly through this physical interaction. Remarkably, viruses have evolved several strategies to counteract these antiviral effects by encoding specific anti-PML NBs viral proteins. This is the case for HSV-1 infected cell protein 0 (ICP0), which induces the proteasomal-dependent degradation of SUMOylated forms of PML, leading to PML NBs disappearance. Other viruses directly target the SUMO modification of PML (by preventing it or removing it), thus altering the multivalent potential of PML and the regula-

tion of their protein composition by phase separation (for reviews (175–177).

The packaging of viral DNA with cellular histones carrying specific post-translational modifications allows for a transcriptional control of viral expression (for review (178)). As mentioned above, latent HIV provirus juxtaposed to PML NBs is transcriptionally silent, while reactivation of the virus correlates with displacement of the provirus away from the nuclear bodies (107). Interestingly, the transcriptional repression activity of PML requires its binding to the latent chromatinized provirus, which allows the recruitment of the G9a methyltransferase responsible for H3K9 dimethylation (H3K9me2) on the provirus promoter. Knockdown of PML results in a decrease of provirus-bound G9a, a loss of H3K9me3 heterochromatin marks on the silent viral promoter and a concomitant gain in the transcriptionally-prone H3K4me3 marks (107). Another compelling example of the involvement of PML NBs in the chromatinization of a viral genome came from our lab with regards to the chromatinization of the nucleosome-free HSV-1 genome entering the nucleus of the infected cells, prior to the establishment of latency (99). PML NBs encase the latent viral genome together with the H3.3 chaperone complexes DAXX-ATRX and HIRA, thus allowing the concentration of histone chaperones together with the viral genome in a condensed phase (99) (Figures 2 and 3A). The two H3.3 histone chaperone complexes likely play redundant role in the chromatinization of latent HSV-1 genomes with H3.3-containing nucleosomes, together with the PML protein itself (99). Interestingly, H3.3 is modified with the repressive heterochromatin mark H3K9me3 on the HSV-1 latent genome and destabilization of PML NBs containing the viral genome by ICP0 results in the recovery of a lytic transcriptional program (99), underscoring the repressive function of the PML NB-H3.3 axis in virus latency (Figure 3A). However, HIRA mediated-deposition of H3.3 on HSV-1 genomes during the lytic phase is required for viral RNAs transcription (179), consistent with the double face of H3.3 which can thus be deposited in actively transcribed regions depending on the infectious context. Of note, the switch-like partitioning of HIRA in the PML-NBs following infection by HSV-1 (98–100), correlates with the transcriptional upregulation of host genes, including interferon stimulated genes (ISGs), and contributes to the intrinsic and innate immune defenses against HSV-1 infection (98,100). Therefore, the PML NBs antiviral activity could act both directly through the chromatinization-associated transcriptional regulation of the viral genomes, and indirectly through the regulation of ISGs. PML NBs thus play an essential role in the regulation of viral chromatinization with specific histones variants/marks and are essential for the epigenetic control of viral expression.

## PML NBs PARTICIPATE IN THE REGULATION OF CELLULAR CHROMATIN DYNAMICS

### PML NBs and the dynamics of chromatin during transcriptional regulation

PML NBs are present in regions of high transcriptional activity (14,52). The recent ALaP-Seq analysis of chromatin regions proximal to PML NBs confirms that PML NBs associate primarily with regulatory regions of active genes in a genome-wide manner (114). In addition to their role in the transcriptional regulation of viral genes, they also regulate transcription of cellular loci (for review (180)). While the PML protein itself can act as a transcriptional co-activator or co-repressor, we focus here specifically on the interplay between PML NBs and transcriptional regulation through the prism of chromatin dynamics and in light of their liquid-like properties (Figure 4).

First, PML NBs can regulate transcriptional activity through specific modifications of transcriptional factors as examplified for p53 acetylation and phosphorylation in senescence (see below) (Figure 4Ai). PML NBs are also known SUMOylation hotspots through concentration of the SUMO E2-conjugating enzyme UBC9 (12,27). SUMOylation could serve to regulate client activity as observed for TIP60-induced HAT activity upon UV damage (110) (Figure 4Ai). Poly-SUMOylation may initiate polyubiquitination by the SUMO-targeted Ubiquitin ligase (STUbl) RNF4 and subsequent proteasome-mediated degration, as observed for the degradation of the PML-RARα fusion protein (116,181) (Figure 4Aii). SUMOylation may also trigger caspase-dependent degradation of proteins within PML NBs as observed for SATB1, impairing its role in chromatin loop organization and transcriptional regulation (143,182) (Figure 4Aiii). However, the abundance of other chromatin related factors, such as HIRA, does not change upon relocalization in PML NBs (98,100) and it remains to be investigated whether SUMOylation could serve to regulate histone chaperone activity.

Second, PML NBs can regulate transcription by modulating the availability of chromatin associated factors within PML NBs. E2Fs transcription factors may be sequestered by pRb within PML NBs upon senescence preventing E2F target genes transcription (see below) (Figure 4Aiv). On the contrary, sequestration of the histone deacetylase HDAC7, a potent transcriptional repressor, in PML NBs could participate in upregulation of MEF2 target genes (108) (Figure 4Av). Dynamic changes in histone chaperone localization might also be a means to fine-tune gene expression. The H3.3 histone chaperone DAXX acts as a potent transcriptional repressor and is a well-studied PML NBs component. Sequestration of DAXX in PML NBs releases transcriptional repression on reporter genes or specific cellular genes, such as glucocorticoid receptor target genes, whereas disruption of DAXX localization in PML NBs by ICP0 or expression of SUMOylation-defective PML mutant fails to relieve DAXX-mediated transcriptional repression (183–185) (Figure 4Av). HIRA localizes in PML NBs upon specific stresses, such as IFN treatment, without any global change in the amount of HIRA RNA or protein levels (98,100). This anticipates a drop of HIRA concentration in the rest of the nucleoplasm through a sequestration mechanism in PML NBs. We can hypothesize that the depletion of HIRA from genomic loci could have a global impact on H3.3 dynamics at specific genes located at a distance from PML NBs, but this titration effect remains to be investigated (Figure 4Avi).

Third, PML NBs could participate in establishing chromatin domains that are either permissive or refractory to

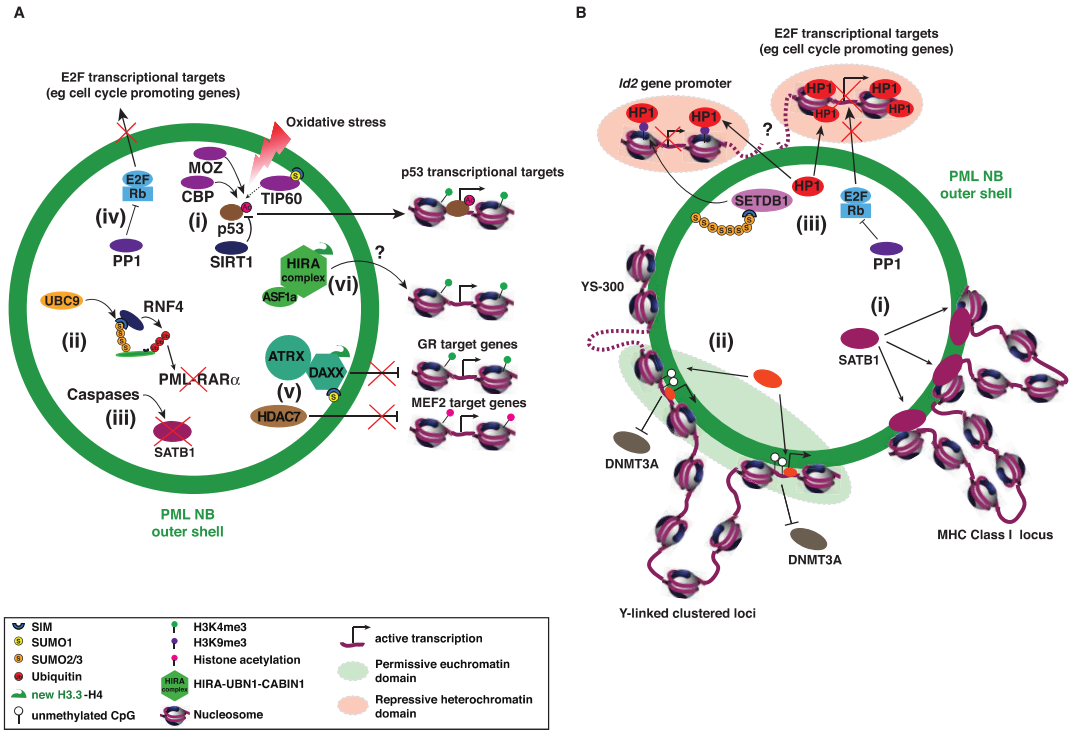


**Figure 4.** Role of PML NBs in transcriptional regulation. PML NBs has a dual effect on gene expression both facilitating or repressing expression of specific genes. (**A**) PML NBs regulates transcription through specific modifications of transcription factors or by modulating the availability of transcription factors or chromatin-related factors. (i) Upon Ras-induced senescence entry, p53 localizes in PML NBs which promotes its phosphorylation on serine 15 (not shown) as well as its acetylation on lysine 382 by CBP or MOZ, which may be counteracted by SIRT1. These PML-dependent modifications are required for p53 transactivation activity. TIP60 SUMO-dependent relocalization in PML NBs upon UV damage may also participate in p53 recruitment and stabilization (dashed arrow), thus favoring its transactivation activity. Oxidative stress can also trigger PML-dependent p53 activation conveying the ROS response (237). (ii) PML NBs can regulate proteins levels by SUMO-dependent poly-ubiquitination by RNF4 and subsequent proteasome-mediated degradation as observed for PML-RARα, or (iii) by caspase degradation as observed for SATB1. (iv) In senescence, PML NBs concentrate Protein Phosphatase 1 alpha (PP1α) together with Rb preventing its CDK-dependent phosphorylation and thus inhibiting E2F which remains sequestered in PML NBs and cannot activate cell-cycle promoting genes. (v) The DAXX histone chaperone brings new H3.3-H4 dimers within PML NBs but may then be sequestered preventing the transcriptional repression of its target genes such as Glucocorticoid receptor (GR) target genes. HDAC7 may also be sequestered to prevent repression of MEF2 target genes. (vi) The role for HIRA complex localization in PML NBs remains more enigmatic (question mark). (**B**) PML NBs could also participate in establishing chromatin domains that are either permissive or refractory to transcription. (i) Interaction between SATB1 and PML is essential to establish a specific chromatin-loop structure at the MHC class I locus and may serve to regulate transcriptional activity of genes within this locus. (ii) PML NBs can also provide a transcriptionally-permissive chromatin environment to neighboring loci (dashed green circle). In particular, binding to the short arm of the Y-chromosome (region YS300) to PML NBs allows anchoring of specific Y-linked gene promoters that are located away from this region (dashed line). PML NBs allow the maintenance of their transcriptional activity by excluding DNMT3A and preventing DNA methylation on these proximal promoters. Specific transcription factors or chromatin-related factors located in PML NBs (orange factor) could also contribute to gene expression in these chromatin domains. (iii) On the contrary, PML NBs may help to concentrate HP1 proteins on specific loci, possibly through phase separation of heterochromatin (dashed red circle), to promote repression of genes such as E2F target genes. SETDB1 may also participate in creating a repressing heterochromatin environment by depositing H3K9me3 on gene promoters such as for the *Id2* gene. However, it remains to be determined whether these repressed loci are found in vicinity of PML NBs (question mark).

transcription (Figure 4B). A recent paradigm shift in the field of transcriptional regulation has put forward a phase separation model for transcriptional control, in which multi-molecular assemblies would form by phase separation bridging enhancers and promoters allowing gene activation (186). As biomolecular condensates contacting specific chromatin loci, PML NBs could participate in forming specific transcriptional conditions on genomic loci. Using a novel CasDrop technology, a Crispr–Cas9-based optogenetic technology allowing local concentration of droplets at specific genomic loci, Shin et al. recently showed that condensates form preferentially in low-density chromatin regions (like PML NBs) and are able to mechanically pull together targeted genomic loci (187). Although CasDrop is an artificial system with the tethering of specific proteins able to phase separate onto genomic loci, the mechanical pulling of distal genomic loci may indeed occur *in vivo* for PML NBs. In particular, at the MHC locus, PML NBs might regulate transcription of specific genes through the formation of SATB1-associated specific chromatin loops, bringing closer some distal genes in the locus (143) (Figure 4Bi). In addition, using ALaP-Seq Kurihara et al. re-

cently showed that anchoring of PML NBs with the short arm of the Y chromosome (YS300) promotes the association of nearby Y-linked genes with PML NBs, which is required to maintain their expression through DNMT3A exclusion (114) (Figure 4Bii). Deletion of most of the YS300 sequence results in dissociation of Y-linked genes from the PML NBs and their downregulation. More generally, the authors showed that PML NBs associate significantly with regulatory regions, such as enhancers or promoters, that are located in an open chromatin environment (as confirmed by the ATAC-Seq, H3K27ac and H3K4me3 epigenetic signature), and correlates with the expression levels of the associated genes. PML NBs may thus play a novel role in the 3D organization of chromatin by providing a specific nuclear space protected from DNMT3A action and therefore create a transcriptionally-permissive chromatin environment with hypomethylated gene promoters (Figure 4Bii).

Alternatively, PML NBs might also help to organize repressive domains. As mentionned above, SETDB1 constitutively localizes within PML NBs and structural integrity of these nuclear bodies is essential for SETDB1 targeting to the *Id2* gene (102). SETDB1 deposits H3K9me3 mark on the *Id2* gene promoter, allowing its transcritional repression (102) (Figure 4Biii). In this case, concentration of SETDB1 in PML NBs together with HP1α, which is known to allow phase-separation formation of heterochromatin together with H3K9me3 (46,47,188) may help to organize a chromatin repressive structure around the *Id2* gene promoter (Figure 4Biii). Interestingly, the establishment of specific chromatin domains is not necessarily mutually exclusive with the buffering/sequestration role of PML NBs. Specific targeting of genomic loci to PML NBs could provide a way to regulate them by binding of a given client protein, while other loci remaining away from PML NBs could show a depletion of this same protein.

While some genomic loci localize within PML NBs or are juxtaposed to PML NBs, we could wonder about the order of events between PML NBs biogenesis and specific genomic loci targeting. Indeed, transcription factors and chromatin-related factors could help bring genomic loci in close proximity or even within PML NBs through interaction with chromatin, after the formation of PML NBs. Another alternative model suggests that transcription factors or other chromatin-bound proteins could first bind to genomic loci and then recruit PML. This could help the nucleation and possible phase separation of PML NBs at a given locus, aided by the fusion with pre-existing PML NBs to create a transcriptional specific environment. In the case of HSV-1 infection, it is interesting to note that chromatin-related factors, such as DAXX, are indeed recruited to HSV-1 genomes very early after infection, before the detection of PML (99,189). PML would then bind the viral genome and fuse with a pre-existing nearby PML NB (189).

Presence of numerous PML NBs client proteins that are associated with heterochromatin formation (e.g. DAXX, ATRX, HP1, SETDB1) hinted at the probable implication of PML NBs in heterochromatin dynamics. In the next sections, we will develop the various roles of PML NBs in heterochromatin formation and maintenance in specific cell states, such as senescence, as well as in specific regions, such as pericentromeres or telomeres.

**PML NBs and the regulation of chromatin dynamics in senescent cells**

Cell senescence is defined by a permanent arrest of the cell cycle that can be induced by various stresses, such as telomeres attrition (replicative senescence), oncogene activation or genotoxic insults. Senescence is therefore considered as a defense mechanism against tumoral transformation (190). Chromatin of senescent cells undergoes massive reorganization, with the condensation of each chromosome to form Senescence-Associated Heterochromatin Foci (SAHF) (191–193), which are enriched in heterochromatic markers such as H3K9me3, HP1 and histone macroH2A (for review (194)). This organization may contribute to the maintenance of a specific senescent gene expression profile, with the down-regulation of cell cycle promoting E2F target genes and the upregulation of genes coding for factors of the senescence-associated secretory phenotype (SASP), reinforcing the senescent state (194). The first evidence linking PML NBs with senescence came from the observation that PML NBs dramatically increase in size and number upon senescence entry (41,42). PML depleted cells are impaired in their ability to undergo senescence and conversely PML overexpression triggers senescence entry in a p53 and pRb/E2F pathways-dependent manner (41,42,195). SAHF formation is also tightly related to PML NBs, eventhough SAHF *per se* are not found inside PML NBs (78). Indeed, expression of the dominant negative PML-RARα fusion protein, which impairs PML NBs formation, eliminates SAHF formation in cells induced in senescence (196).

All three functions of PML NBs described in Figure 2 could be at play during senescence. First, these nuclear bodies could act as specific biochemical reactors to ensure p53 phosphorylation/acetylation and pRb hypophosphorylation, by concentrating them with modifying enzymes such as CBP, MOZ, TIP60 and Protein Phosphatase 1 alpha (PP1α), respectively (41,42,112,197) (Figure 4Ai and 4Aiv). Of note, SIRT1 localization in PML NBs upon senescence induction may counteract CBP-mediated p53 acetylation and thus repress p53 target genes (109) (Figure 4Ai). Second, PML NBs may also serve to sequestrate various client proteins such as the abundant E2Fs activators (E2F1-3), which localize in PML NBs in a pRb-dependent manner in oncogene-induced senescent cells. PML NBs prevent the CDK-dependent phosphorylation of pRb by concentrating it with PP1α, leading to E2Fs sequestration and obstruction of their cell-cycle promoting activity (197) (Figure 4Aiv). Moreover, all HP1 isoforms transiently accumulate within PML NBs in the early stages of senescence, before their stable incorporation into SAHF (78,196). This may be linked to a potential role of PML NBs in targeting HP1 to defined juxtaposed chromatin regions. In particular, in senescent cells, PML associates with promoters of E2F target genes and is required for their H3K9me3-mediated heterochromatinization in a pRb-dependent manner (Figure 4Biii). This silencing in turn is required to prevent DNA replication and cell cycle progression (197,198). As discussed above for the *Id2* gene, PML NBs could serve as concentration sites for HP1, enabling heterochromatin formation by liquid–liquid phase separation at E2F target genes. Finally, upon senescence entry, members of the HIRA chap-

erone complex relocalize within H3.3-containing PML NBs (78,95,97) and this specific accumulation is required for proper SAHF formation (78,196). However, since no enrichment of H3.3 is observed in SAHF structures (85), the exact role of HIRA complex in SAHF formation is still unclear and HIRA could play an indirect role in senescence via keeping the senescent expressed genes active (199).

### PML NBs and pericentromeric heterochromatin dynamics

First evidence of PML NBs association with pericentromeric chromatin arose from observation in cells derived from patients with the ICF syndrome (159,200) (see above). In those cells, decondensed pericentromeric regions are found within giant PML NBs together with DAXX, ATRX and HP1 (159,200). A subsequent study on normal cells also showed the localization of human pericentromeric DNA repeats within a subset of PML NBs in the G2 phase of the cell cycle, suggesting a general role of PML NBs in re-establishing condensed chromatin on these late-replicated regions (159). However, it remains to be shown if chromatin assembly can happen within PML NBs at these regions, since heterochromatin modifications, such as H3K9me3 or H4K20me3, are absent (Figure 3B). Interestingly, DAXX, which localizes in PML NBs, is required for H3.3 incorporation in the pericentromeric satellites repeats, as well as the PML protein itself (79,85). By modulating DAXX levels, it was shown that H3.3 deposition in pericentromeric regions is linked to the transcription of the repeats (79,85). This might promote further HP1 recruitment and heterochromatin condensation via a ncRNA-mediated mechanism, as observed during early development or in fission yeast (201–203). Of note, a recent study in MEF cells challenges the idea of a PML NB-dependent H3.3 incorporation in pericentromeric regions. PML depleted cells show an accumulation of H3.3 at pericentromeric repeats suggesting that the PML protein prevents H3.3 incorporation at these sites (204). Consistently, depletion of PML increases H3.3 incorporation at a repetitive heterochromatin transgene array which localizes in PML NBs in S phase (169). Explaining such discrepancies will require more investigations in a cell-cycle controlled manner in order to better characterize the roles of PML NBs in pericentromeric chromatin dynamics, and in particular the H3.3 chromatin assembly pathway.

### PML NBs and heterochromatin dynamics at telomeres

PML NBs association with telomeres was first suggested by the appearance of APBs in ALT tumors cells, where telomeres repeats are found within PML NBs (157) (see above). ALT is a telomerase-independent, but recombination-dependent, process involving replication stress as well as break-induced replication (BIR) mechanism in APBs to extend telomeres. APBs indeed contain numerous proteins involved in homologous recombination, such as Rad51, breast cancer susceptibility protein 1 (BRCA1), or RPA. While this review does not intend to provide an extensive description of the APBs structure and functions (for review (205,206)), we will nevertheless give a few highlights on the recent connections between PML NBs, chromatin dynamics and the ALT process. PML NBs may act to concentrate specific DNA repair and recombination factors, as well as chromatin modifiers, in a condensate organized around telomeric chromatin (Figures 2 and 3C). Interestingly, a series of recent studies provides evidence for this model. Formation of APB-like condensates by using a scaffold made of poly(SUMO)–poly(SIM) motifs tethered at telomeres or by using a chemically induced protein dimerization approach to tether SIM at telomeres, induced telomere clustering within the artificially engineered APBs *in vivo* (33,34). Overexpression of the helicase BLM triggered ALT-like phenotypes in presence of these reconstituted APB-like condensates suggesting that concentration of specific DNA repair factors, together with the clustering of telomeres to provide repair templates, are required for induction of the ALT phenotype (33). Stochiometry of the SUMO-SIM interactions controls recruitment of BLM or of the full BLM–TOP3A–RMI (BTR) complex at telomeric ends in APBs (33,207). The BTR complex is essential for telomere lengthening and its artificial tethering to telomeres can bypass the absence of PML to induce ALT (207). Moreover, by applying an assay to visualize telomeric DNA synthesis in human cells, it was shown that ALT DNA synthesis occurs exclusively in APBs and is dependent on PML (208), consistent with the essential role of PML NBs for ALT (209). Thus PML NBs cluster telomeric ends in a condensate together with all required factors to provide a 'recombinogenic microenvironment' in order to promote ALT.

APBs are also tightly linked to heterochromatin establishment/dynamics at telomeres. A strong correlation between ATRX/DAXX inactivation and the ALT phenotype has been observed in specific tumors, although loss of these chaperones is not sufficient to trigger ALT immediately, but may induce ALT via a gradual telomeric DNA replication dysfunction (210–213). Interestingly, depletion of the histone chaperone Asf1 enhances replicative stress posed at telomeres and provokes ALT appearance (214). The histone chaperone HIRA is also present in APBs of ALT cells and is required for the localization of HP1 in APBs (96). Since HIRA is in complex with UBN1, which is known to associate with an H3K9 histone methyltransferase activity (95), it could help the H3K9 trimethylation of telomeric DNA and ensure HP1 binding to telomeres in APBs. In this regard, it is interesting to note that SETDB1 is required for the H3K9me3 modification of telomeric chromatin in both mouse ES cells and human ALT cells (215). In contrast to the prevailing view of heterochromatin inhibiting the recombination process at telomeres in ALT cells (216), it was shown that increase in H3K9me3-heterochromatin mediated by SETDB1 at telomeres promotes ALT features and telomeric transcription of TERRA (215), which localizes in PML NBs (56) (Figure 3C). On the contrary, upon SETDB1 knockdown, decrease of H3K9me3 diminishes the number of APBs, as well as telomeric transcription and abrogates ALT (215). These results are consistent with a previous study showing that the knockdown of factors involved in heterochromatin formation, such as the histone H4K20 methyltransferase SUV4-20H2 (KMT5C), HP1γ or the histone H3K4 demethylase LSD1, reduces the number of APBs (209). The local compaction of chromatin could prevent TRF2 binding (209), a protein part of the shelterin complex protecting telomeres, thus facilitating recombination. Increased heterochromatin features at

telomeric DNA could also facilitate phase transitions, as observed for regular heterochromatin (46,47,188), to form the APB recombinogenic microenvironment. Interestingly, telomeric RNA present in ABPs generates RNA:DNA telomeric hybrids, which could promote replication stress and structures prone to engage into recombination (56) (Figure 3C). Reduction of TERRA transcription by a decrease of heterochromatin composition of telomeres within APBs or decrease in the amount of RNA:DNA hybrids by RNAseH1 or FANCM can impair the ALT process (56,217).

In addition to their role in the ALT pathway, further studies showed that PML NBs are also modulating chromatin structure at telomeres in non-neoplastic cells. Indeed, in mouse ES cells, FISH experiments showed that telomeres colocalize with PML NBs together with DAXX, ATRX and the histone variant H3.3, prominently in S phase (218). This is consistent with the known function of DAXX-ATRX complex for the incorporation of H3.3 at telomeric repeats in ES cells, associated with TERRA repression (80,219). ALaP-Seq survey showed that telomeric sequences were significantly enriched for PML, confirming telomeres association with PML NBs in mouse ESCs (114). PML depletion leads to a reduction of ATRX-dependent H3.3 incorporation at telomeres driving the appearance of damage in the form of telomere-induced dysfunctional foci (TIFs) (218). Interestingly, telomere-associated PML NBs are linked to the pluripotency and their near absence in somatic cell types coincides with a switch in the epigenetic signature of telomeric chromatin towards a more compact structure (218). Indeed, telomeres of somatic cells show a decrease of MNase accessibility, as well as higher levels of repressive chromatin marks including H3K9me3 and H4K20me3 (220), which can be reproduced in the absence of PML in ES cells (218). Therefore, PML NBs constitute an essential platform for the regulation of telomeric chromatin and seem important to maintain a 'less heterochromatic' structure of pluripotent cells telomeres, which could favor telomere-elongating activities by telomerase (highly expressed in human and mouse ES cells) and the capacity for continual telomere-renewal important for ES cells pluripotency (220).

Although telomere-associated PML NBs are mostly lost with differentiation, colocalization of PML NBs with telomeres was observed in cells with shortened or damaged telomeres (221). This suggests that PML NBs may participate in telomeres surveillance in somatic cells (221), which could be linked to their function in DNA repair (for review (222)) as well as in telomeric maintenance in ALT cells. While PML NBs no longer seem associated with telomeres in differentiated cells, it was recently shown by ChIP-Seq that PML protein prevents H3.3 incorporation at telomeres in MEFs and is required for maintenance of an H4K20me3-rich heterochromatin structure at the opposite of its role in embryonic cells (204). This 'guardian' function of PML in somatic cells is likely independent of PML NBs given that most PML immunoprecipitated comes from the nucleoplasmic pool (144) and will require further investigations.

## CONCLUSION AND FUTURE PERSPECTIVES

Phase separation as an organizing principle in biology allowed us to revisit the functional roles of PML NBs in chromatin dynamics under a new light. As discussed throughout the review, PML NBs exhibit remarkable plasticity, both in terms of composition, dynamic changes during the cell cycle and roles related to chromatin dynamics, which apply in different physiological contexts or at different times. The sensitivity of the phase separation mechanism to environmental changes makes PML NBs ideal nuclear bodies to process external stimuli towards specific chromatin responses.

PML NBs formation can be efficiently induced by known therapeutic drugs, such as Arsenic trioxide or IFN, thereby opening interesting therapeutic avenues. Drug-induced PML NB formation could favor senescence entry through p53 activation and HIRA localization in PML NBs, as well as promote specific client degradation of undesired proteins. In addition, the tight relationship between PML NBs and telomeric elongation in ALT cells is also of particular interest to target specific cancer cells. Targeting the replicative stress response of ALT cells by ATR inhibition or FANCM+BLM/BRCA1 depletion can prove useful to induce specific lethality of these cells (223–225). Others inhibitors against one or several of the DNA repair/recombination factors (TOP3A, POLD3, POLD4 etc.), or against the protein TSYPL5, a recently identified protein critical for ALT positive cells viability (226), could potentially provide additional therapeutic strategies for treating ALT tumors. Physiological relevance of this approach was confirmed in colorectal cancer (CRC) tissues with short telomeres, correlating with increased PML levels, APB formation and proliferation rate (227). Inhibition of ATR in patient-derived colorectal cancer organoids reduced APB formation, shortened telomeres and reduced proliferation (227).

Important questions remain opened for future studies on PML NBs and chromatin dynamics. In particular, the following challenges should be addressed in the next years to help decipher the many facets of PML NBs:

(1) What is the role of nucleoplasmic PML versus PML NBs? It will be important to distinguish the functions of the free PML protein, versus the one that is present in PML NBs. The use of APEX2-mediated chromatin labeling and purification in conjunction with PML WT or the nucleoplasmic diffused PML RING domain mutant has allowed to identify chromatin-PML NBs associations in a genome-wide fashion (114). This technique (or others related techniques such as BioID (228)) could be applied to investigate the PML NB proteome, and thus provide a more comprehensive picture of PML NBs functions.
(2) How heterogenous are PML NBs? To reconcile the divergent roles of PML NBs in both transcriptional activation and transcriptional repression, it can be envisaged that PML NBs could have a different composition relative to PML isoforms or client proteins, or a different localization by being targeted to various genomic loci throughout the nucleus. Alternatively, PML NBs could be subdivided in several functional subdomains with varying PML isoforms or client proteins concentrations within the subparts of the same nuclear body. Interestingly, subcompartmentalization of phase-separated condensates has recently been observed with co-existing liquid phases within a con-

densate regulated by different phosphorylation patterns. This subcompartmentalization allows the spatial coupling of translation regulation with mRNA deadenylation rates (229). Whether changing composition of PML NBs does actually matter for the regulation of chromatin dynamics should be explored in the future.

(3) Are PML NBs implicated in chromatin dynamics during DNA repair? PML NBs accumulate various proteins involved in DNA repair pathways and their role in the maintenance of genome integrity has been extensively studied (for review (222)). Whether they actually regulate histone disassembly/assembly processes that are known to occur during DNA repair remains unknown. Given the accumulation of various H3.3 histone chaperones in PML NBs, and their connection with DNA repair (230), as well as the localization of damaged foci juxtaposed to PML NBs (172,222,231,232), it is tempting to speculate that they could also potentially regulate chromatin dynamics at DNA repair foci, from within PML NBs.

(4) What is the actual role of PML NBs in diseases with strong inflammatory signature? Idiopathic inflammatory myopathies are characterized by muscle impairment associated with a strong IFN-signature (233). Since PML NBs number and size are controlled by IFN (38–40), we could speculate that their role in transcriptional regulation and chromatin dynamics could participate in the phenotypical alterations observed in these myopathies. Moreover, the recent SARS-CoV-2 pandemic has underlined the importance of IFN-I to activate ISGs and mediate antiviral reponse. Defects in IFNα/β production in patients correlated with the severity of the disease (234,235), but whether this depends on PML NBs functions remains to be investigated.

To conclude, many challenges still lie ahead to understand the complex functions of these fascinating nuclear bodies.

## ACKNOWLEDGEMENTS

We apologize to the authors whose work has not been cited due to length restrictions. We thank all our collaborators who contributed to the studies from our laboratory in connection with the present review. We thank Olivier Binda and Faouzi Baklouti for their comments on the manuscript and Fabian Erdel for helpful discussion on LLPS.

## FUNDING

P.L. laboratory is funded by grants from the Centre National de la Recherche Scientifique (CNRS) (http://www.cnrs.fr), Institut National de la Santé et de la Recherche Médicale (INSERM) (https://www.inserm.fr), University Claude Bernard Lyon 1 (https://www.univ-lyon1.fr), French National Agency for Research-ANR [CENTROLAT ANR-05-MIIM-008-01/02; VIRUCEPTION ANR-13-BSV3-0001-01; EPIPRO ANR-18-CE15-0014-01 http://www.agence-nationale-recherche.fr]; LabEX DEVweCAN and DEV2CAN [ANR-10-LABX-61, http://www.agence-nationale-recherche.fr]; Comité départemental du Rhône de La Ligue contre le cancer and the FINOVI foundation [142690]; P.L. is a CNRS Research Director and AC is assistant professor in the University Claude Bernard Lyon 1. Funding for open access charge: LabEX.

*Conflict of interest statement.* None declared.

## REFERENCES

1. Luger,K., Mäder,A.W., Richmond,R.K., Sargent,D.F. and Richmond,T.J. (1997) Crystal structure of the nucleosome core particle at 2.8 A resolution. *Nature*, **389**, 251–260.
2. Allis,C.D. and Jenuwein,T. (2016) The molecular hallmarks of epigenetic control. *Nat. Rev. Genet.*, **17**, 487–500.
3. Banani,S.F., Lee,H.O., Hyman,A.A. and Rosen,M.K. (2017) Biomolecular condensates: organizers of cellular biochemistry. *Nat. Rev. Mol. Cell. Biol.*, **18**, 285–298.
4. Alberti,S., Gladfelter,A. and Mittag,T. (2019) Considerations and challengesin studying liquid-liquid phase separation and biomolecular condensates. *Cell*, **176**, 419–434.
5. Mir,M., Bickmore,W., Furlong,E.E.M. and Narlikar,G. (2019) Chromatin topology, condensates and gene regulation: shifting paradigms or just a phase? *Development*, **146**, dev182766.
6. Banani,S.F., Rice,A.M., Peeples,W.B., Lin,Y., Jain,S., Parker,R. and Rosen,M.K. (2016) Compositional control of phase-separated cellular bodies. *Cell*, **166**, 651–663.
7. Hyman,A.A., Weber,C.A. and Jülicher,F. (2014) Liquid-liquid phase separation in biology. *Annu. Rev. Cell Dev. Biol.*, **30**, 39–58.
8. A,P. and Weber,S.C. (2019) Evidence for and against liquid-liquid phase separation in the nucleus. *ncRNA*, **5**, 50.
9. Lallemand-Breitenbach,V. and de Thé,H. (2018) ScienceDirectPML nuclear bodies: from architecture to function. *Curr. Opin. Cell Biol.*, **52**, 154–161.
10. Li,Y., Ma,X., Wu,W., Chen,Z. and Meng,G. (2020) PML nuclear body biogenesis, carcinogenesis, and targeted therapy. *Trends Cancer*, doi:10.1016/j.trecan.2020.05.005.
11. de Thé,H., Le Bras,M. and Lallemand-Breitenbach,V. (2012) The cell biology of disease: acute promyelocytic leukemia, arsenic, and PML bodies. *J. Cell Biol.*, **198**, 11–21.
12. Van Damme,E., Laukens,K., Dang,T.H. and Van Ostade,X. (2010) A manually curated network of the PML nuclear body interactome reveals an important role for PML-NBs in SUMOylation dynamics. *Int. J. Biol. Sci.*, **6**, 51–67.
13. Bernardi,R. and Pandolfi,P.P. (2007) Structure, dynamics and functions of promyelocytic leukaemia nuclear bodies. *Nat. Rev. Mol. Cell Biol.*, **8**, 1006–1016.
14. Boisvert,F.-M., Hendzel,M.J. and Bazett-Jones,D.P. (2000) Promyelocytic leukemia (PML) nuclear bodies are protein structures that do not accumulate RNA. *J. Cell Biol.*, **148**, 283–292.
15. Hoischen,C., Monajembashi,S., Weisshart,K. and Hemmerich,P. (2018) Multimodal light microscopy approaches to reveal structural and functional properties of promyelocytic leukemia nuclear bodies. *Front. Oncol.*, **8**, 3167.
16. Lang,M., Jegou,T., Chung,I., Richter,K., Munch,S., Udvarhelyi,A., Cremer,C., Hemmerich,P., Engelhardt,J., Hell,S.W. *et al.* (2010) Three-dimensional organization of promyelocytic leukemia nuclear bodies. *J. Cell Sci.*, **123**, 392–400.
17. Szostecki,C., Guldner,H.H., Netter,H.J. and Will,H. (1990) Isolation and characterization of cDNA encoding a human nuclear antigen predominantly recognized by autoantibodies from patients with primary biliary cirrhosis. *J. Immunol.*, **145**, 4338–4347.
18. Nisole,S., Maroui,M.A., Mascle,X.H., Aubry,M. and Chelbi-Alix,M.K. (2013) Differential roles of PML isoforms. *Front. Oncol.*, **3**, 125.
19. Seeler,J.-S. and Dejean,A. (2017) SUMO and the robustness of cancer. *Nat. Rev. Cancer*, **17**, 184–197.
20. Kamitani,T., Kito,K., Nguyen,H.P., Wada,H., Fukuda-Kamitani,T. and Yeh,E.T. (1998) Identification of three major sentrinization sites in PML. *J. Biol. Chem.*, **273**, 26675–26682.

21. Cuchet-Lourenço,D., Boutell,C., Lukashchuk,V., Grant,K., Sykes,A., Murray,J., Orr,A. and Everett,R.D. (2011) SUMO pathway dependent recruitment of cellular repressors to herpes simplex virus type 1 genomes. *PLoS Pathog.*, **7**, e1002123.
22. Shen,T.H., Lin,H.-K., Scaglioni,P.P., Yung,T.M. and Pandolfi,P.P. (2006) The mechanisms of PML-nuclear body formation. *Mol. Cell*, **24**, 331–339.
23. Zhong,S., Müller,S., Ronchetti,S., Freemont,P.S., Dejean,A. and Pandolfi,P.P. (2000) Role of SUMO-1-modified PML in nuclear body formation. *Blood*, **95**, 2748–2752.
24. Lallemand-Breitenbach,V., Zhu,J., Puvion,F., Koken,M., Honoré,N., Doubeikovsky,A., Duprez,E., Pandolfi,P.P., Puvion,E., Freemont,P. *et al.* (2001) Role of promyelocytic leukemia (PML) sumolation in nuclear body formation, 11S proteasome recruitment, and As2O3-induced PML or PML/retinoic acid receptor alpha degradation. *J. Exp. Med.*, **193**, 1361–1371.
25. Ishov,A.M., Sotnikov,A.G., Negorev,D., Vladimirova,O.V., Neff,N., Kamitani,T., Yeh,E.T., Strauss,J.F. and Maul,G.G. (1999) PML is critical for ND10 formation and recruits the PML-interacting protein daxx to this nuclear structure when modified by SUMO-1. *J. Cell Biol.*, **147**, 221–234.
26. Jeanne,M., Lallemand-Breitenbach,V., Ferhi,O., Koken,M., Le Bras,M., Duffort,S., Peres,L., Berthier,C., Soilihi,H., Raught,B. *et al.* (2010) PML/RARA oxidation and arsenic binding initiate the antileukemia response of As. *Cancer Cell*, **18**, 88–98.
27. Sahin,U., Ferhi,O., Jeanne,M., Benhenda,S., Berthier,C., Jollivet,F., Niwa-Kawakita,M., Faklaris,O., Setterblad,N., de The,H. *et al.* (2014) Oxidative stress-induced assembly of PML nuclear bodies controls sumoylation of partner proteins. *J. Cell Biol.*, **204**, 931–945.
28. Wang,P., Benhenda,S., Wu,H., Lallemand-Breitenbach,V., Zhen,T., Jollivet,F., Peres,L., Li,Y., Chen,S.-J., Chen,Z. *et al.* (2018) RING tetramerization is required for nuclear body biogenesis and PML sumoylation. *Nat. Commun.*, **9**, 1277.
29. Li,Y., Ma,X., Chen,Z., Wu,H., Wang,P., Wu,W., Cheng,N., Zeng,L., Zhang,H., Cai,X. *et al.* (2019) B1 oligomerization regulates PML nuclear body biogenesis and leukemogenesis. *Nat. Commun.*, **10**, 3789.
30. Geng,Y., Monajembashi,S., Shao,A., Cui,D., He,W., Chen,Z., Hemmerich,P. and Tang,J. (2012) Contribution of the C-terminal regions of promyelocytic leukemia protein (PML) isoforms II and V to PML nuclear body formation. *J. Biol. Chem.*, **287**, 30729–30742.
31. Li,C., Peng,Q., Wan,X., Sun,H. and Tang,J. (2017) C-terminal motifs in promyelocytic leukemia protein isoforms critically regulate PML nuclear body formation. *J. Cell Sci.*, **130**, 3496–3506.
32. McSwiggen,D.T., Mir,M., Darzacq,X. and Tjian,R. (2019) Evaluating phase separation in live cells: diagnosis, caveats, and functional consequences. *Genes Dev.*, **33**, 1619–1634.
33. Min,J., Wright,W.E. and Shay,J.W. (2019) Clustered telomeres in phase-separated nuclear condensates engage mitotic DNA synthesis through BLM and RAD52. *Genes Dev.*, **33**, 814–827.
34. Zhang,H., Zhao,R., Tones,J., Liu,M., Dilley,R.L., Chenoweth,D.M., Greenberg,R.A. and Lampson,M.A. (2020) Nuclear body phase separation drives telomere clustering in ALT cancer cells. *Mol. Biol. Cell*, **31**, 2048–2056.
35. Lallemand-Breitenbach,V. and de The,H. (2010) PML nuclear bodies. *Cold Spring Harb. Perspect. Biol.*, **2**, a000661.
36. Feric,M., Vaidya,N., Harmon,T.S., Mitrea,D.M., Zhu,L., Richardson,T.M., Kriwacki,R.W., Pappu,R.V. and Brangwynne,C.P. (2016) Coexisting liquid phases underlie nucleolar subcompartments. *Cell*, **165**, 1686–1697.
37. Erdel,F. and Rippe,K. (2018) Formation of chromatin subcompartments by phase separation. *Biophys. J.*, **114**, 2262–2270.
38. Lavau,C., Marchio,A., Fagioli,M., Jansen,J., Falini,B., Lebon,P., Grosveld,F., Pandolfi,P.P., Pelicci,P.G. and Dejean,A. (1995) The acute promyelocytic leukaemia-associated PML gene is induced by interferon. *Oncogene*, **11**, 871–876.
39. Stadler,M., Chelbi-Alix,M.K., Koken,M.H., Venturini,L., Lee,C., Saïb,A., Quignon,F., Pelicano,L., Guillemin,M.C. and Schindler,C. (1995) Transcriptional induction of the PML growth suppressor gene by interferons is mediated through an ISRE and a GAS element. *Oncogene*, **11**, 2565–2573.
40. Chelbi-Alix,M.K., Pelicano,L., Quignon,F., Koken,M.H., Venturini,L., Stadler,M., Pavlovic,J., Degos,L. and de The,H. (1995) Induction of the PML protein by interferons in normal and APL cells. *Leukemia*, **9**, 2027–2033.
41. Ferbeyre,G., de Stanchina,E., Querido,E., Baptiste,N., Prives,C. and Lowe,S.W. (2000) PML is induced by oncogenic ras and promotes premature senescence. *Genes Dev.*, **14**, 2015–2027.
42. Pearson,M., Carbone,R., Sebastiani,C., Cioce,M., Fagioli,M., Saito,S., Higashimoto,Y., Appella,E., Minucci,S., Pandolfi,P.P. *et al.* (2000) PML regulates p53 acetylation and premature senescence induced by oncogenic Ras. *Nature*, **406**, 207–210.
43. Hancock,R. (2004) A role for macromolecular crowding effects in the assembly and function of compartments in the nucleus. *J. Struct. Biol.*, **146**, 281–290.
44. McSwiggen,D.T., Hansen,A.S., Teves,S.S., Marie-Nelly,H., Hao,Y., Heckert,A.B., Umemoto,K.K., Dugast-Darzacq,C., Tjian,R. and Darzacq,X. (2019) Evidence for DNA-mediated nuclear compartmentalization distinct from phase separation. *Elife*, **8**, e47098.
45. Erdel,F., Rademacher,A., Vlijm,R., Tünnermann,J., Frank,L., Weinmann,R., Schweigert,E., Yserentant,K., Hummert,J., Bauer,C. *et al.* (2020) Mouse heterochromatin adopts digital compaction states without showing hallmarks of HP1-driven liquid-liquid phase separation. *Mol. Cell*, **78**, 236–249.
46. Strom,A.R., Emelyanov,A.V., Mir,M., Fyodorov,D.V., Darzacq,X. and Karpen,G.H. (2017) Phase separation drives heterochromatin domainformation. *Nature*, **547**, 241–245.
47. Larson,A.G., Elnatan,D., Keenen,M.M., Trnka,M.J., Johnston,J.B., Burlingame,A.L., Agard,D.A., Redding,S. and Narlikar,G.J. (2017) Liquid droplet formation by HP1. *Nature*, **547**, 236–240.
48. Brouwer,A.K., Schimmel,J., Wiegant,J.C.A.G., Vertegaal,A.C.O., Tanke,H.J. and Dirks,R.W. (2009) Telomeric DNA mediates de novo PML body formation. *Mol. Biol. Cell*, **20**, 4804–4815.
49. Kaiser,T.E., Intine,R.V. and Dundr,M. (2008) De novo formation of a subnuclear body. *Science*, **322**, 1713–1717.
50. Chung,I., Leonhardt,H. and Rippe,K. (2011) De novo assembly of a PML nuclear subcompartment occurs through multiple pathways and induces telomere elongation. *J. Cell Sci.*, **124**, 3603–3618.
51. Wang,H., Xu,X., Nguyen,C.M., Liu,Y., Gao,Y., Lin,X., Daley,T., Kipniss,N.H., La Russa,M. and Qi,L.S. (2018) CRISPR-mediated programmable 3D genome positioning and nuclear organization. *Cell*, **175**, 1405–1417.
52. Wang,J. (2004) Promyelocytic leukemia nuclear bodies associate with transcriptionally active genomic regions. *J. Cell Biol.*, **164**, 515–526.
53. LaMorte,V.J., Dyck,J.A., Ochs,R.L. and Evans,R.M. (1998) Localization of nascent RNA and CREB binding protein with the PML-containing nuclear body. *Proc. Natl Acad. Sci. U.S.A.*, **95**, 4991–4996.
54. Fuchsová,B., Novák,P., Kafková,J. and Hozák,P. (2002) Nuclear DNA helicase II is recruited to IFN-α–activated transcription sites at PML nuclear bodies. *J. Cell Biol.*, **158**, 463–473.
55. Kiesslich,A., Mikecz von,A. and Hemmerich,P. (2002) Cell cycle-dependent association of PML bodies with sites of active transcription in nuclei of mammalian cells. *J. Struct. Biol.*, **140**, 167–179.
56. Arora,R., Lee,Y., Wischnewski,H., Brun,C.M., Schwarz,T. and Azzalin,C.M. (2014) RNaseH1 regulates TERRA-telomeric DNA hybrids and telomere maintenance in ALT tumour cells. *Nat. Commun.*, **5**, 5220.
57. Grande,M.A., van der Kraan,I., van Steensel,B., Schul,W., de The,H., van der Voort,H.T., de Jong,L. and van Driel,R. (1996) PML-containing nuclear bodies: their spatial distribution in relation to other nuclear components. *J. Cell. Biochem.*, **63**, 280–291.
58. Eskiw,C.H., Dellaire,G. and Bazett-Jones,D.P. (2004) Chromatin contributes to structural integrity of promyelocytic leukemia bodies through a SUMO-1-independent mechanism. *J. Biol. Chem.*, **279**, 9577–9585.
59. Berry,J., Weber,S.C., Vaidya,N., Haataja,M. and Brangwynne,C.P. (2015) RNA transcription modulates phase transition-driven nuclear body assembly. *Proc. Natl. Acad. Sci U.S.A.*, **112**, E5237–E5245.
60. Falahati,H., Pelham-Webb,B., Blythe,S. and Wieschaus,E. (2016) Nucleation by rRNA dictates the precision of nucleolus assembly. *Curr. Biol.*, **26**, 277–285.
61. Everett,R.D., Lomonte,P., Sternsdorf,T., van Driel,R. and Orr,A. (1999) Cell cycle regulation of PML modification and ND10 composition. *J. Cell Sci.*, **112**, 4581–4588.

62. Dellaire,G. (2006) Mitotic accumulations of PML protein contribute to the re-establishment of PML nuclear bodies in G1. *J. Cell Sci.*, **119**, 1034–1042.
63. Lång,A., Lång,E. and Bøe,S.O. (2019) PML bodies in mitosis. *Cells*, **8**, 893.
64. Jul-Larsen,A., Grudic,A., Bjerkvig,R. and Ove Boe,S. (2009) Cell-cycle regulation and dynamics of cytoplasmic compartments containing the promyelocytic leukemia protein and nucleoporins. *J. Cell Sci.*, **122**, 1201–1210.
65. Lång,A., Eriksson,J., Schink,K.O., Lång,E., Blicher,P., Połeć,A., Brech,A., Dalhus,B. and Bøe,S.O. (2017) Visualization of PML nuclear import complexes reveals FG-repeat nucleoporins at cargo retrieval sites. *nucleus*, **8**, 404–420.
66. Chen,Y.-C.M., Kappel,C., Beaudouin,J., Eils,R. and Spector,D.L. (2008) Live cell dynamics of promyelocytic leukemia nuclear bodies upon entry into and exit from mitosis. *Mol. Biol. Cell*, **19**, 3147–3162.
67. Ohsaki,Y., Kawai,T., Yoshikawa,Y., Cheng,J., Jokitalo,E. and Fujimoto,T. (2016) PML isoform II plays a critical role in nuclear lipid droplet formation. *J. Cell Biol.*, **212**, 29–38.
68. Lee,J., Salsman,J., Foster,J., Dellaire,G. and Ridgway,N.D. (2020) Lipid-associated PML structures assemble nuclear lipid droplets containing CCTα and Lipin1. *Life Sci. Alliance*, **3**, e202000751-13.
69. Butler,J.T., Hall,L.L., Smith,K.P. and Lawrence,J.B. (2009) Changing nuclear landscape and unique PML structures during early epigenetic transitions of human embryonic stem cells. *J. Cell. Biochem.*, **107**, 609–621.
70. Tokunaga,K., Saitoh,N., Goldberg,I.G., Sakamoto,C., Yasuda,Y., Yoshida,Y., Yamanaka,S. and Nakao,M. (2014) Computational image analysis of colony and nuclear morphology to evaluate human induced pluripotent stem cells. *Sci. Rep.*, **4**, 704–707.
71. Maroui,M.A., Calle,A., Cohen,C., Streichenberger,N., Texier,P., Takissian,J., Rousseau,A., Poccardi,N., Welsch,J., Corpet,A. *et al.* (2016) Latency entry of herpes simplex virus 1 is determined by the interaction of its genome with the nuclear environment. *PLoS Pathog.*, **12**, e1005834.
72. Doucas,V., Tini,M., Egan,D.A. and Evans,R.M. (1999) Modulation of CREB binding protein function by the promyelocytic (PML) oncoprotein suggests a role for nuclear bodies in hormone signaling. *Proc. Natl Acad. Sci. U.S.A.*, **96**, 2627–2632.
73. Mikecz von,A., Zhang,S., Montminy,M., Tan,E.M. and Hemmerich,P. (2000) CREB-binding protein (CBP)/p300 and RNA polymerase II colocalize in transcriptionally active domains in the nucleus. *J. Cell Biol.*, **150**, 265–273.
74. Lehming,N., Le Saux,A., Schüller,J. and Ptashne,M. (1998) Chromatin components as part of a putative transcriptional repressing complex. *Proc. Natl Acad. Sci. U..S.A.*, **95**, 7322–7326.
75. Seeler,J.S., Marchio,A., Sitterlin,D., Transy,C. and Dejean,A. (1998) Interaction of SP100 with HP1 proteins: a link between the promyelocytic leukemia-associated nuclear bodies and the chromatin compartment. *Proc. Natl Acad. Sci. U.S.A.*, **95**, 7316–7321.
76. Hayakawa,T. (2003) Cell cycle behavior of human HP1 subtypes: distinct molecular domains of HP1 are required for their centromeric localization during interphase and metaphase. *J. Cell Sci.*, **116**, 3327–3338.
77. Everett,R.D., Earnshaw,W.C., Pluta,A.F., Sternsdorf,T., Ainsztein,A.M., Carmena,M., Ruchaud,S., Hsu,W.L. and Orr,A. (1999) A dynamic connection between centromeres and ND10 proteins. *J. Cell Sci.*, **112**, 3443–3454.
78. Zhang,R., Poustovoitov,M.V., Ye,X., Santos,H.A., Chen,W., Daganzo,S.M., Erzberger,J.P., Serebriiskii,I.G., Canutescu,A.A., Dunbrack,R.L. *et al.* (2005) Formation of MacroH2A-containing senescence-associated heterochromatin foci and senescence driven by ASF1a and HIRA. *Dev. Cell*, **8**, 19–30.
79. Drane,P., Ouararhni,K., Depaux,A., Shuaib,M. and Hamiche,A. (2010) The death-associated protein DAXX is a novel histone chaperone involved in the replication-independent deposition of H3.3. *Genes Dev.*, **24**, 1253–1265.
80. Goldberg,A.D., Banaszynski,L.A., Noh,K.-M., Lewis,P.W., Elsaesser,S.J., Stadler,S., Dewell,S., Law,M., Guo,X., Li,X. *et al.* (2010) Distinct factors control histone variant H3.3 localization at specific genomic regions. *Cell*, **140**, 678–691.
81. Lewis,P.W., Elsaesser,S.J., Noh,K.-M., Stadler,S.C. and Allis,C.D. (2010) Daxx is an H3.3-specific histone chaperone and cooperates with ATRX in replication-independent chromatin assembly at telomeres. *Proc. Natl. Acad. Sci. U.S.A.*, **107**, 14075–14080.
82. Xue,Y., Gibbons,R., Yan,Z., Yang,D., McDowell,T.L., Sechi,S., Qin,J., Zhou,S., Higgs,D. and Wang,W. (2003) The ATRX syndrome protein forms a chromatin-remodeling complex with Daxx and localizes in promyelocytic leukemia nuclear bodies. *Proc. Natl Acad. Sci. U.S.A.*, **100**, 10635–10640.
83. Ishov,A.M. (2004) Heterochromatin and ND10 are cell-cycle regulated and phosphorylation-dependent alternate nuclear sites of the transcription repressor Daxx and SWI/SNF protein ATRX. *J. Cell Sci.*, **117**, 3807–3820.
84. Delbarre,E., Ivanauskiene,K., Küntziger,T. and Collas,P. (2013) DAXX-dependent supply of soluble (H3.3-H4) dimers to PML bodies pending deposition into chromatin. *Genome Res.*, **23**, 440–451.
85. Corpet,A., Olbrich,T., Gwerder,M., Fink,D. and Stucki,M. (2014) Dynamics of histone H3.3 deposition in proliferating and senescent cells reveals a DAXX-dependent targeting to PML-NBs important for pericentromeric heterochromatin organization. *Cell Cycle*, **113**, E3213–E3220.
86. Gurard-Levin,Z.A., Quivy,J.-P. and Almouzni,G. (2014) Histone chaperones: assisting histone traffic and nucleosome dynamics. *Annu. Rev. Biochem.*, **83**, 487–517.
87. Ahmad,K. and Henikoff,S. (2002) The histone variant H3.3 marks active chromatin by replication-independent nucleosome assembly. *Mol. Cell*, **9**, 1191–1200.
88. Mito,Y., Henikoff,J.G. and Henikoff,S. (2005) Genome-scale profiling of histone H3.3 replacement patterns. *Nat. Genet.*, **37**, 1090–1097.
89. Deaton,A.M., Gómez-Rodríguez,M., Mieczkowski,J., Tolstorukov,M.Y., Kundu,S., Sadreyev,R.I., Jansen,L.E. and Kingston,R.E. (2016) Enhancer regions show high histone H3.3 turnover that changes during differentiation. *Elife*, **5**, e15316.
90. Ray-Gallet,D., Woolfe,A., Vassias,I., Pellentz,C., Lacoste,N., Puri,A., Schultz,D.C., Pchelintsev,N.A., Adams,P.D., Jansen,L.E.T. *et al.* (2011) Dynamics of histone H3 deposition in vivo reveal a nucleosome gap-filling mechanism for H3.3 to maintain chromatin integrity. *Mol. Cell*, **44**, 928–941.
91. Soni,S., Pchelintsev,N., Adams,P.D. and Bieker,J.J. (2014) Transcription factor EKLF (KLF1) recruitment of the histone chaperone HIRA is essential for β-globin gene expression. *Proc. Natl. Acad. Sci. U.S.A.*, **111**, 13337–13342.
92. Zhang,H., Gan,H., Wang,Z., Lee,J.-H., Zhou,H., Ordog,T., Wold,M.S., Ljungman,M. and Zhang,Z. (2017) RPA Interacts with HIRA and Regulates H3.3 Deposition at Gene Regulatory Elements in Mammalian Cells. *Mol. Cell*, **65**, 272–284.
93. Szenker,E., Ray-Gallet,D. and Almouzni,G. (2011) The double face of the histone variant H3.3. *Cell Res.*, **21**, 421–434.
94. Martire,S. and Banaszynski,L.A. (2020) The roles of histone variants in fine-tuning chromatin organization and function. *Nat. Rev. Mol. Cell Biol.*, **21**, 522–541.
95. Banumathy,G., Somaiah,N., Zhang,R., Tang,Y., Hoffmann,J., Andrake,M., Ceulemans,H., Schultz,D., Marmorstein,R. and Adams,P.D. (2009) Human UBN1 is an ortholog of yeast Hpc2p and Has an essential role in the HIRA/ASF1a chromatin-remodeling pathway in senescent cells. *Mol. Cell. Biol.*, **29**, 758–770.
96. Jiang,W.-Q., Nguyen,A., Cao,Y., Chang,A.C.-M. and Reddel,R.R. (2011) HP1-mediated formation of alternative lengthening of telomeres-associated PML bodies requires HIRA but not ASF1a. *PLoS One*, **6**, e17036.
97. Rai,T.S., Puri,A., McBryan,T., Hoffman,J., Tang,Y., Pchelintsev,N.A., van Tuyn,J., Marmorstein,R., Schultz,D.C. and Adams,P.D. (2011) Human CABIN1 Is a Functional Member of the Human HIRA/UBN1/ASF1a Histone H3.3 Chaperone Complex. *Mol. Cell. Biol.*, **31**, 4107–4118.
98. Rai,T.S., Glass,M., Cole,J.J., Rather,M.I., Marsden,M., Neilson,M., Brock,C., Humphreys,I.R., Everett,R.D. and Adams,P.D. (2017) Histone chaperone HIRA deposits histone H3.3 onto foreign viral DNA and contributes to anti-viral intrinsic immunity. *Nucleic Acids Res.*, **45**, 11673–11683.
99. Cohen,C., Corpet,A., Roubille,S., Maroui,M.A., Poccardi,N., Rousseau,A., Kleijwegt,C., Binda,O., Texier,P., Sawtell,N. *et al.* (2018) Promyelocytic leukemia (PML) nuclear bodies (NBs) induce latent/quiescent HSV-1 genomes chromatinization through a PML

NB/Histone H3.3/H3.3 Chaperone Axis. *PLoS Pathog.*, **14**, e1007313.
100. McFarlane,S., Orr,A., Roberts,A.P.E., Conn,K.L., Iliev,V., Loney,C., da Silva Filipe,A., Smollett,K., Gu,Q., Robertson,N. *et al.* (2019) The histone chaperone HIRA promotes the induction of host innate immune defences in response to HSV-1 infection. *PLoS Pathog.*, **15**, e1007667.
101. Ivanauskiene,K., Delbarre,E., McGhie,J.D., Kuntziger,T., Wong,L.H. and Collas,P. (2014) The PML-associated protein DEK regulates the balance of H3.3 loading on chromatin and is important for telomere integrity. *Genome Res.*, **24**, 1584–1594.
102. Cho,S., Park,J.S. and Kang,Y.-K. (2011) Dual functions of histone-lysine N-methyltransferase Setdb1 protein at promyelocytic leukemia-nuclear body (PML-NB): maintaining PML-NB structure and regulating the expression of its associated genes. *J. Biol. Chem.*, **286**, 41115–41124.
103. Matsui,T., Leung,D., Miyashita,H., Maksakova,I.A., Miyachi,H., Kimura,H., Tachibana,M., Lorincz,M.C. and Shinkai,Y. (2010) Proviral silencing in embryonic stem cells requires the histone methyltransferase ESET. *Nature*, **464**, 927–931.
104. Elsässer,S.J., Noh,K.-M., Diaz,N., Allis,C.D. and Banaszynski,L.A. (2015) Histone H3.3 is required for endogenous retroviral element silencing in embryonic stem cells. *Nature*, **522**, 240–244.
105. Carbone,R., Botrugno,O.A., Ronzoni,S., Insinga,A., Di Croce,L., Pelicci,P.G. and Minucci,S. (2006) Recruitment of the histone methyltransferase SUV39H1 and its role in the oncogenic properties of the leukemia-associated PML-retinoic acid receptor fusion protein. *Mol. Cell. Biol.*, **26**, 1288–1296.
106. Villa,R., Pasini,D., Gutierrez,A., Morey,L., Occhionorelli,M., Viré,E., Nomdedeu,J.F., Jenuwein,T., Pelicci,P.G., Minucci,S. *et al.* (2007) Role of the polycomb repressive complex 2 in acute promyelocytic leukemia. *Cancer Cell*, **11**, 513–525.
107. Lusic,M., Marini,B., Ali,H., Lucic,B., Luzzati,R. and Giacca,M. (2013) Proximity to PML nuclear bodies regulates HIV-1 latency in CD4+ T cells. *Cell Host Microbe*, **13**, 665–677.
108. Gao,C., Cheng,X., Lam,M., Liu,Y., Liu,Q., Chang,K.-S. and Kao,H.-Y. (2008) Signal-dependent regulation of transcription by histone deacetylase 7 involves recruitment to promyelocytic leukemia protein nuclear bodies. *Mol. Biol. Cell*, **19**, 3020–3027.
109. Langley,E., Pearson,M., Faretta,M., Bauer,U.-M., Frye,R.A., Minucci,S., Pelicci,P.G. and Kouzarides,T. (2002) Human SIR2 deacetylates p53 and antagonizes PML/p53-induced cellular senescence. *EMBO J.*, **21**, 2383–2396.
110. Cheng,Z., Ke,Y., Ding,X., Wang,F., Wang,H., Ahmed,K., Liu,Z., Xu,Y., Aikhionbare,F., Yan,H. *et al.* (2007) Functional characterization of TIP60 sumoylation in UV-irradiated DNA damage response. *Oncogene*, **27**, 931–941.
111. Wu,Q., Hu,H., Lan,J., Emenari,C., Wang,Z., Chang,K.-S., Huang,H. and Yao,X. (2009) PML3 orchestrates the nuclear dynamics and function of TIP60. *J. Biol. Chem.*, **284**, 8747–8759.
112. Rokudai,S., Laptenko,O., Arnal,S.M., Taya,Y., Kitabayashi,I. and Prives,C. (2013) MOZ increases p53 acetylation and premature senescence through its complex formation with PML. *Proc. Natl. Acad. Sci. U.S.A.*, **110**, 3895–3900.
113. Song,C., Wang,L., Wu,X., Wang,K., Xie,D., Xiao,Q., Li,S., Jiang,K., Liao,L., Yates,J.R. *et al.* (2018) PML Recruits TET2 to Regulate DNA Modification and Cell Proliferation in Response to Chemotherapeutic Agent. *Cancer Res.*, **78**, 2475–2489.
114. Kurihara,M., Kato,K., Sanbo,C., Shigenobu,S., Ohkawa,Y., Fuchigami,T. and Miyanari,Y. (2020) Genomic profiling by ALaP-Seq reveals transcriptional regulation by PML bodies through DNMT3A exclusion. *Mol. Cell*, **78**, 493–505.
115. Weidtkamp-Peters,S., Lenser,T., Negorev,D., Gerstner,N., Hofmann,T.G., Schwanitz,G., Hoischen,C., Maul,G., Dittrich,P. and Hemmerich,P. (2008) Dynamics of component exchange at PML nuclear bodies. *J. Cell Sci.*, **121**, 2731–2743.
116. Lallemand-Breitenbach,V., Jeanne,M., Benhenda,S., Nasr,R., Lei,M., Peres,L., Zhou,J., Zhu,J., Raught,B. and de Thé,H. (2008) Arsenic degrades PML or PML–RARα through a SUMO-triggered RNF4/ubiquitin-mediated pathway. *Nat. Cell Biol.*, **10**, 547–555.
117. Zhu,J., Zhou,J., Peres,L., Riaucoux,F., Honoré,N., Kogan,S. and de Thé,H. (2005) A sumoylation site in PML/RARA is essential for leukemic transformation. *Cancer Cell*, **7**, 143–153.
118. Lin,D.-Y., Huang,Y.-S., Jeng,J.-C., Kuo,H.-Y., Chang,C.-C., Chao,T.-T., Ho,C.-C., Chen,Y.-C., Lin,T.-P., Fang,H.-I. *et al.* (2006) Role of SUMO-interacting motif in Daxx SUMO modification, subnuclear localization, and repression of sumoylated transcription factors. *Mol. Cell*, **24**, 341–354.
119. Lamoliatte,F., Caron,D., Durette,C., Mahrouche,L., Maroui,M.A., Caron-Lizotte,O., Bonneil,E., Chelbi-Alix,M.K. and Thibault,P. (2014) Large-scale analysis of lysine SUMOylation by SUMO remnant immunoaffinity profiling. *Nat. Commun.*, **5**, 5409.
120. Hendriks,I.A., D'Souza,R.C.J., Yang,B., Vries,M.V.-D., Mann,M. and Vertegaal,A.C.O. (2014) Uncovering global SUMOylation signaling networks in a site-specific manner. *Nat. Struct. Mol. Biol.*, **21**, 927–936.
121. Schimmel,J., Eifler,K., Sigurðsson,J.O., Cuijpers,S.A.G., Hendriks,I.A., Vries,M.V.-D., Kelstrup,C.D., Francavilla,C., Medema,R.H., Olsen,J.V. *et al.* (2014) Uncovering SUMOylation dynamicsduring cell-cycle progression reveals FoxM1 as a key mitotic SUMO target protein. *Mol. Cell*, **53**, 1053–1066.
122. Ivanov,A.V., Peng,H., Yurchenko,V., Yap,K.L., Negorev,D.G., Schultz,D.C., Psulkowski,E., Fredericks,W.J., White,D.E., Maul,G.G. *et al.* (2007) PHD domain-mediated E3 ligase activity directs intramolecular sumoylation of an adjacent bromodomain required for gene silencing. *Mol. Cell*, **28**, 823–837.
123. Ninova,M., Chen,Y.-C.A., Godneeva,B., Rogers,A.K., Luo,Y., Fejes Tóth,K. and Aravin,A.A. (2020) Su(var)2-10 and the SUMO pathway link piRNA-guided target recognition to chromatin silencing. *Mol. Cell*, **77**, 556–570.
124. Boisvert,F.M., Kruhlak,M.J., Box,A.K., Hendzel,M.J. and Bazett-Jones,D.P. (2001) The transcription coactivator CBP is a dynamic component of the promyelocytic leukemia nuclear body. *J. Cell Biol.*, **152**, 1099–1106.
125. Tang,Y., Puri,A., Ricketts,M.D., Rai,T.S., Hoffmann,J., Hoi,E., Adams,P.D., Schultz,D.C. and Marmorstein,R. (2012) Identification of an ubinuclein 1 region required for stability and function of the human HIRA/UBN1/CABIN1/ASF1a histone H3.3 chaperone complex. *Biochemistry*, **51**, 2366–2377.
126. Tammsalu,T., Matic,I., Jaffray,E.G., Ibrahim,A.F.M., Tatham,M.H. and Hay,R.T. (2014) Proteome-wide identification of SUMO2 modification sites. *Sci. Signal*, **7**, rs2.
127. Chang,C.-C., Naik,M.T., Huang,Y.-S., Jeng,J.-C., Liao,P.-H., Kuo,H.-Y., Ho,C.-C., Hsieh,Y.-L., Lin,C.-H., Huang,N.-J. *et al.* (2011) Structural and functional roles of Daxx SIM phosphorylation in SUMO paralog-selective binding and apoptosis modulation. *Mol. Cell*, **42**, 62–74.
128. Percherancier,Y., Germain-Desprez,D., Galisson,F., Mascle,X.H., Dianoux,L., Estephan,P., Chelbi-Alix,M.K. and Aubry,M. (2009) Role of SUMO in RNF4-mediated promyelocytic leukemia protein (PML) degradation: sumoylation of PML and phospho-switch control of its SUMO binding domain dissected in living cells. *J. Biol. Chem.*, **284**, 16595–16608.
129. Cappadocia,L., Mascle,X.H., Bourdeau,V., Tremblay-Belzile,S., Chaker-Margot,M., Lussier-Price,M., Wada,J., Sakaguchi,K., Aubry,M., Ferbeyre,G. *et al.* (2015) Structural and functional characterizationof the phosphorylation-dependent interaction between PML and SUMO1. *Structure/Folding Des.*, **23**, 126–138.
130. Stehmeier,P. and Müller,S. (2009) Phospho-regulated SUMO interaction modules connect the SUMO system to CK2 signaling. *Mol. Cell*, **33**, 400–409.
131. Ullmann,R., Chien,C.D., Avantaggiati,M.L. and Müller,S. (2012) An acetylation switch regulates SUMO-dependent protein interaction networks. *Mol. Cell*, **46**, 759–770.
132. Mascle,X.H., Gagnon,C., Wahba,H.M., Lussier-Price,M., Cappadocia,L., Sakaguchi,K. and Omichinski,J.G. (2020) Acetylation of SUMO1 alters interactions with the SIMs of PML and Daxx in a protein-specific manner. *Structure*, **28**, 157–168.
133. Ye,X., Zerlanko,B., Kennedy,A., Banumathy,G., Zhang,R. and Adams,P.D. (2007) Downregulation of Wnt signaling is a trigger for formation of facultative heterochromatin and onset of cell senescence in primary human cells. *Mol. Cell*, **27**, 183–196.
134. Berchtold,D., Battich,N. and Pelkmans,L. (2018) A systems-level study reveals regulators of membrane-less organelles in human cells. *Mol. Cell*, **72**, 1035–1049.
135. la Vega de,L., Fröbius,K., Moreno,R., Calzado,M.A., Geng,H. and Schmitz,M.L. (2011) Control of nuclear HIPK2 localization and

function by a SUMO interaction motif. *BBA - Mol. Cell Res.*, **1813**, 283–297.
136. Shiels,C., Islam,S.A., Vatcheva,R., Sasieni,P., Sternberg,M.J., Freemont,P.S. and Sheer,D. (2001) PML bodies associate specifically with the MHC gene cluster in interphase nuclei. *J. Cell Sci.*, **114**, 3705–3716.
137. Zheng,P., Guo,Y., Niu,Q., Levy,D.E., Dyck,J.A., Lu,S., Sheiman,L.A. and Liu,Y. (1998) Proto-oncogene PML controls genes devoted to MHC class I antigen presentation. *Nature*, **396**, 373–376.
138. Sun,Y., Durrin,L.K. and Krontiris,T.G. (2003) Specific interaction of PML bodies with the TP53 locus in Jurkat interphase nuclei. *Genomics*, **82**, 250–252.
139. Aoto,T., Saitoh,N., Ichimura,T., Niwa,H. and Nakao,M. (2006) Nuclear and chromatin reorganization in the MHC-Oct3/4 locus at developmental phases of embryonic stem cell differentiation. *Dev. Biol.*, **298**, 354–367.
140. Salsman,J., Stathakis,A., Parker,E., Chung,D., Anthes,L.E., Koskowich,K.L., Lahsaee,S., Gaston,D., Kukurba,K.R., Smith,K.S. *et al.* (2017) PML nuclear bodies contribute to the basal expression of the mTOR inhibitor DDIT4. *Sci. Rep.*, **7**, 45038.
141. Ulbricht,T., Alzrigat,M., Horch,A., Reuter,N., Mikecz von,A., Steimle,V., Schmitt,E., Krämer,O.H., Stamminger,T. and Hemmerich,P. (2012) PML promotes MHC class II gene expression by stabilizing the class II transactivator. *J. Cell Biol.*, **199**, 49–63.
142. Gialitakis,M., Arampatzi,P., Makatounakis,T. and Papamatheakis,J. (2010) Gamma interferon-dependent transcriptional memory via relocalization of a gene locus to PML nuclear bodies. *Mol. Cell. Biol.*, **30**, 2046–2056.
143. Kumar,P.P., Bischof,O., Purbey,P.K., Notani,D., Urlaub,H., Dejean,A. and Galande,S. (2007) Functional interaction between PML and SATB1 regulates chromatin-loop architecture and transcription of the MHC class I locus. *Nat. Cell Biol.*, **9**, 45–56.
144. Delbarre,E., Ivanauskiene,K., Spirkoski,J., Shah,A., Vekterud,K., Moskaug,J.Ø., Bøe,S.O., Wong,L.H., Küntziger,T. and Collas,P. (2017) PML protein organizes heterochromatin domains where it regulates histone H3.3 deposition by ATRX/DAXX. *Genome Res.*, **27**, 913–921.
145. Ching,R.W., Ahmed,K., Boutros,P.C., Penn,L.Z. and Bazett-Jones,D.P. (2013) Identifying gene locus associations with promyelocytic leukemia nuclear bodies using immuno-TRAP. *J. Cell Biol.*, **201**, 325–335.
146. Ishov,A.M. and Maul,G.G. (1996) The periphery of nuclear domain 10 (ND10) as site of DNA virus deposition. *J. Cell Biol.*, **134**, 815–826.
147. Maul,G.G., Ishov,A.M. and Everett,R.D. (1996) Nuclear domain 10 as preexisting potential replication start sites of herpes simplex virus type-1. *Virology*, **217**, 67–75.
148. Sourvinos,G. and Everett,R.D. (2002) Visualization of parental HSV-1 genomes and replication compartments in association with ND10 in live infected cells. *EMBO J.*, **21**, 4989–4997.
149. Tang,Q., Li,L., Ishov,A.M., Revol,V., Epstein,A.L. and Maul,G.G. (2003) Determination of minimum herpes simplex virus type 1 components necessary to localize transcriptionally active DNA to ND10. *J. Virol.*, **77**, 5821–5828.
150. Swindle,C.S., Zou,N., Van Tine,B.A., Shaw,G.M., Engler,J.A. and Chow,L.T. (1999) Human papillomavirus DNA replication compartments in a transient DNA replication system. *J. Virol.*, **73**, 1001–1009.
151. Bell,P., Lieberman,P.M. and Maul,G.G. (2000) Lytic but not latent replication of epstein-barr virus is associated with PML and induces sequential release of nuclear domain 10 proteins. *J. Virol.*, **74**, 11800–11810.
152. Day,P.M., Baker,C.C., Lowy,D.R. and Schiller,J.T. (2004) Establishment of papillomavirus infection is enhanced by promyelocytic leukemia protein (PML) expression. *Proc. Natl Acad. Sci. U.S.A.*, **101**, 14252–14257.
153. Bishop,C.L., Ramalho,M., Nadkarni,N., May Kong,W., Higgins,C.F. and Krauzewicz,N. (2006) Role for centromeric heterochromatin and PML nuclear bodies in the cellular response to foreign DNA. *Mol. Cell. Biol.*, **26**, 2583–2594.
154. Bryan,T.M., Englezou,A., Gupta,J., Bacchetti,S. and Reddel,R.R. (1995) Telomere elongation in immortal human cells without detectable telomerase activity. *EMBO J.*, **14**, 4240–4248.
155. Bryan,T.M., Englezou,A., Dalla-Pozza,L., Dunham,M.A. and Reddel,R.R. (1997) Evidence for an alternative mechanism for maintaining telomere length in human tumors and tumor-derived cell lines. *Nat. Med.*, **3**, 1271–1274.
156. Cesare,A.J. and Reddel,R.R. (2010) Alternative lengthening of telomeres: models, mechanisms and implications. *Nat. Rev. Genet.*, **11**, 319–330.
157. Yeager,T.R., Neumann,A.A., Englezou,A., Huschtscha,L.I., Noble,J.R. and Reddel,R.R. (1999) Telomerase-negative immortalized human cells contain a novel type of promyelocytic leukemia (PML) body. *Cancer Res.*, **59**, 4175–4179.
158. Draskovic,I., Arnoult,N., Steiner,V., Bacchetti,S., Lomonte,P. and Londoño-Vallejo,A. (2009) Probing PML body function in ALT cells reveals spatiotemporal requirements for telomere recombination. *Proc. Natl. Acad. Sci. U.S.A.*, **106**, 15726–15731.
159. Luciani,J.J., Depetris,D., Usson,Y., Metzler-Guillemain,C., Mignon-Ravix,C., Mitchell,M.J., Megarbane,A., Sarda,P., Sirma,H., Moncla,A. *et al.* (2006) PML nuclear bodies are highly organised DNA-protein structures with a function in heterochromatin remodelling at the G2 phase. *J. Cell Sci.*, **119**, 2518–2531.
160. Smeets,D.F., Moog,U., Weemaes,C.M., Vaes-Peeters,G., Merkx,G.F., Niehof,J.P. and Hamers,G. (1994) ICF syndrome: a new case and review of the literature. *Hum. Genet.*, **94**, 240–246.
161. Jeanpierre,M., Turleau,C., Aurias,A., Prieur,M., Ledeist,F., Fischer,A. and Viegas-Péquignot,E. (1993) An embryonic-like methylation pattern of classical satellite DNA is observed in ICF syndrome. *Hum. Mol. Genet.*, **2**, 731–735.
162. Xu,G.L., Bestor,T.H., Bourc'his,D., Hsieh,C.L., Tommerup,N., Bugge,M., Hulten,M., Qu,X., Russo,J.J. and Viegas-Péquignot,E. (1999) Chromosome instability and immunodeficiency syndrome caused by mutations in a DNA methyltransferase gene. *Nature*, **402**, 187–191.
163. Catez,F., Picard,C., Held,K., Gross,S., Rousseau,A., Theil,D., Sawtell,N., Labetoulle,M. and Lomonte,P. (2012) HSV-1 genome subnuclear positioning and associations with host-cell PML-NBs and centromeres regulate LAT locus transcription during latency in neurons. *PLoS Pathog.*, **8**, e1002852.
164. Everett,R.D., Murray,J., Orr,A. and Preston,C.M. (2007) Herpes simplex virus type 1 genomes are associated with ND10 nuclear substructures in quiescently infected human fibroblasts. *J. Virol.*, **81**, 10991–11004.
165. Alandijany,T., Roberts,A.P.E., Conn,K.L., Loney,C., McFarlane,S., Orr,A. and Boutell,C. (2018) Distinct temporal roles for the promyelocytic leukaemia (PML) protein in the sequential regulation of intracellular host immunity to HSV-1 infection. *PLoS Pathog.*, **14**, e1006769.
166. Bell,P., Brazas,R., Ganem,D. and Maul,G.G. (2000) Hepatitis delta virus replication generates complexes of large hepatitis delta antigen and antigenomic RNA that affiliate with and alter nuclear domain 10. *J. Virol.*, **74**, 5329–5336.
167. Li,Y.-J., Macnaughton,T., Gao,L. and Lai,M.M.C. (2006) RNA-templated replication of hepatitis delta virus: genomic and antigenomic RNAs associate with different nuclear bodies. *J. Virol.*, **80**, 6478–6486.
168. Newhart,A., Rafalska-Metcalf,I.U., Yang,T., Negorev,D.G. and Janicki,S.M. (2012) Single-cell analysis of Daxx and ATRX-dependent transcriptional repression. *J. Cell Sci.*, **125**, 5489–5501.
169. Shastrula,P.K., Sierra,I., Deng,Z., Keeney,F., Hayden,J.E., Lieberman,P.M. and Janicki,S.M. (2019) PML is recruited to heterochromatin during S phase and represses DAXX-mediated histone H3.3 chromatin assembly. *J. Cell Sci.*, **132**, jcs220970.
170. Dellaire,G. and Bazett-Jones,D.P. (2004) PML nuclear bodies: dynamic sensors of DNA damage and cellular stress. *Bioessays*, **26**, 963–977.
171. Dellaire,G., Ching,R.W., Dehghani,H., Ren,Y. and Bazett-Jones,D.P. (2006) The number of PML nuclear bodies increases in early S phase by a fission mechanism. *J. Cell Sci.*, **119**, 1026–1033.
172. Dellaire,G., Ching,R.W., Ahmed,K., Jalali,F., Tse,K.C.K., Bristow,R.G. and Bazett-Jones,D.P. (2006) Promyelocytic leukemia nuclear bodies behave as DNA damage sensors whose response to DNA double-strand breaks is regulated by NBS1 and the kinases ATM, Chk2, and ATR. *J. Cell Biol.*, **175**, 55–66.

173. Kepkay,R., Attwood,K.M., Ziv,Y., Shiloh,Y. and Dellaire,G. (2011) KAP1 depletion increases PML nuclear body number in concert with ultrastructural changes in chromatin. *Cell Cycle*, **10**, 308–322.
174. Eskiw,C.H., Dellaire,G., Mymryk,J.S. and Bazett-Jones,D.P. (2003) Size, position and dynamic behavior of PML nuclear bodies following cell stress as a paradigm for supramolecular trafficking and assembly. *J. Cell Sci.*, **116**, 4455–4466.
175. Everett,R.D. and Chelbi-Alix,M.K. (2007) PML and PML nuclear bodies: implications in antiviral defence. *Biochimie*, **89**, 819–830.
176. Everett,R.D., Boutell,C. and Hale,B.G. (2013) Interplay between viruses and hostsumoylation pathways. *Nat Rev Micro*, **11**, 400–411.
177. Lomonte,P. (2016) The interaction between herpes simplex virus 1 genome and promyelocytic leukemia nuclear bodies (PML-NBs) as a hallmark of the entry in latency. *Microb Cell*, **3**, 569–572.
178. Knipe,D.M. (2015) Nuclear sensing of viral DNA, epigenetic regulation of herpes simplex virus infection, and innate immunity. *Virology*, **479–480**, 153–159.
179. Placek,B.J., Huang,J., Kent,J.R., Dorsey,J., Rice,L., Fraser,N.W. and Berger,S.L. (2009) The histone variant H3.3 regulates gene expression during lytic infection with herpes simplex virus type 1. *J. Virol.*, **83**, 1416–1421.
180. Zhong,S., Salomoni,P. and Pandolfi,P.P. (2000) The transcriptional role of PML and the nuclear body. *Nat. Cell Biol.*, **2**, E85–E90.
181. Tatham,M.H., Geoffroy,M.-C., Shen,L., Plechanovova,A., Hattersley,N., Jaffray,E.G., Palvimo,J.J. and Hay,R.T. (2008) RNF4 is a poly-SUMO-specific E3 ubiquitin ligase required for arsenic-induced PML degradation. *Nat. Cell Biol.*, **10**, 538–546.
182. Tan,J.-A.T., Sun,Y., Song,J., Chen,Y., Krontiris,T.G. and Durrin,L.K. (2008) SUMO conjugation to the matrix attachment region-binding protein, special AT-rich sequence-binding protein-1 (SATB1), targets SATB1 to promyelocytic nuclear bodies where it undergoes caspase cleavage. *J. Biol. Chem.*, **283**, 18124–18134.
183. Li,H., Leo,C., Zhu,J., Wu,X., O'Neil,J., Park,E.J. and Chen,J.D. (2000) Sequestration and inhibition of Daxx-mediated transcriptional repression by PML. *Mol. Cell. Biol.*, **20**, 1784–1796.
184. Lin,D.-Y., Lai,M.-Z., Ann,D.K. and Shih,H.-M. (2003) Promyelocytic leukemia protein (PML) functions as a glucocorticoid receptor co-activator by sequestering Daxx to the PML oncogenic domains (PODs) to enhance its transactivation potential. *J. Biol. Chem.*, **278**, 15958–15965.
185. Newhart,A., Rafalska-Metcalf,I.U., Yang,T., Joo,L.M., Powers,S.L., Kossenkov,A.V., Lopez-Jones,M., Singer,R.H., Showe,L.C., Skordalakes,E. *et al.* (2013) Single cell analysis of RNA-mediated histone H3.3 recruitment to a cytomegalovirus promoter-regulated transcription site. *J. Biol. Chem.*, **288**, 19882–19899.
186. Hnisz,D., Shrinivas,K., Young,R.A., Chakraborty,A.K. and Sharp,P.A. (2017) A phase separation model for transcriptional control. *Cell*, **169**, 13–23.
187. Shin,Y., Chang,Y.-C., Lee,D.S.W., Berry,J., Sanders,D.W., Ronceray,P., Wingreen,N.S., Haataja,M. and Brangwynne,C.P. (2018) Liquid nuclear condensates mechanically sense and restructure the genome. *Cell*, **175**, 1481–1491.
188. Wang,L., Gao,Y., Zheng,X., Liu,C., Dong,S., Li,R., Zhang,G., Wei,Y., Qu,H., Li,Y. *et al.* (2019) Histone modifications regulate chromatin compartmentalization by contributing to a phase separation mechanism. *Mol. Cell*, **76**, 646–659.
189. Everett,R.D. (2016) Dynamic response of IFI16 and promyelocytic leukemia nuclear body components to herpes simplex virus 1 infection. *J. Virol.*, **90**, 167–179.
190. Criscione,S.W., Teo,Y.V. and Neretti,N. (2016) The chromatin landscape of cellular senescence. *Trends Genet.*, **32**, 751–761.
191. Zhang,R., Chen,W. and Adams,P.D. (2007) Molecular dissection of formation of senescence-associated heterochromatin foci. *Mol. Cell. Biol.*, **27**, 2343–2358.
192. Narita,M., Nũnez,S., Heard,E., Narita,M., Lin,A.W., Hearn,S.A., Spector,D.L., Hannon,G.J. and Lowe,S.W. (2003) Rb-mediated heterochromatin formation and silencing of E2F target genes during cellular senescence. *Cell*, **113**, 703–716.
193. Funayama,R., Saito,M., Tanobe,H. and Ishikawa,F. (2006) Loss of linker histone H1 in cellular senescence. *J. Cell Biol.*, **175**, 869–880.
194. Corpet,A. and Stucki,M. (2014) Chromatin maintenance and dynamics in senescence: a spotlight on SAHF formation and the epigenome of senescent cells. *Chromosoma*, **123**, 423–436.
195. de Stanchina,E., Querido,E., Narita,M., Davuluri,R.V., Pandolfi,P.P., Ferbeyre,G. and Lowe,S.W. (2004) PML is a direct p53 target that modulates p53 effector functions. *Mol. Cell*, **13**, 523–535.
196. Ye,X., Zerlanko,B., Zhang,R., Somaiah,N., Lipinski,M., Salomoni,P. and Adams,P.D. (2007) Definition of pRB- and p53-dependent and -independent steps in HIRA/ASF1a-mediated formation of senescence-associated heterochromatin foci. *Mol. Cell. Biol.*, **27**, 2452–2465.
197. Vernier,M., Bourdeau,V., Gaumont-Leclerc,M.-F., Moiseeva,O., Begin,V., Saad,F., Mes-Masson,A.-M. and Ferbeyre,G. (2011) Regulation of E2Fs and senescence by PML nuclear bodies. *Genes Dev.*, **25**, 41–50.
198. Talluri,S. and Dick,F.A. (2014) The retinoblastoma protein and PML collaborate to organize heterochromatin and silence E2F-responsive genes during senescence. *Cell Cycle*, **13**, 641–651.
199. Rai,T.S., Cole,J.J., Nelson,D.M., Dikovskaya,D., Faller,W.J., Vizioli,M.G., Hewitt,R.N., Anannya,O., McBryan,T., Manoharan,I. *et al.* (2014) HIRA orchestrates a dynamic chromatin landscape in senescence and is required for suppression of neoplasia. *Genes Dev.*, **28**, 2712–2725.
200. Luciani,J.J., Depetris,D., Missirian,C., Mignon-Ravix,C., Metzler-Guillemain,C., Megarbane,A., Moncla,A. and Mattei,M.-G. (2004) Subcellular distribution of HP1 proteins is altered in ICF syndrome. *Eur. J. Hum. Genet.*, **13**, 41–51.
201. Santenard,A., Ziegler-Birling,C., Koch,M., Tora,L., Bannister,A.J. and Torres-Padilla,M.-E. (2010) Heterochromatin formation in the mouse embryo requires critical residues of the histone variant H3.3. *Nat. Cell Biol.*, **12**,853–862.
202. Nishibuchi,G. and Dejardin,J. (2017) The molecular basis of the organization of repetitive DNA-containing constitutive heterochromatin in mammals. **25**, 77-87.
203. Probst,A.V., Okamoto,I., Casanova,M., Marjou,El, LeBaccon,F. and Almouzni,G. (2010) A strand-specific burst in transcriptionof pericentric satellites is required for chromocenter formation and early mouse development. *Dev. Cell*, **19**, 625–638.
204. Spirkoski,J., Shah,A., Reiner,A.H., Collas,P. and Delbarre,E. (2019) Biochemical and biophysical research communications. *Biochem. Biophys. Res. Commun.*, **511**, 882–888.
205. Chung,I., Osterwald,S., Deeg,K.I. and Rippe,K. (2012) PML body meets telomere. *nucleus*, **3**, 263–275.
206. Zhang,J.-M. and Zou,L. (2020) Alternative lengthening of telomeres: from molecular mechanisms to therapeutic outlooks. *Cell & Bioscience*, **10**, 30.
207. Loe,T.K., Li,J.S.Z., Zhang,Y., Azeroglu,B., Boddy,M.N. and Denchi,E.L. (2020) Telomere length heterogeneity in ALT cells is maintained by PML-dependent localization of the BTR complex to telomeres. *Genes Dev.*, **34**, 650–662.
208. Zhang,J.-M., Yadav,T., Ouyang,J., Lan,L. and Zou,L. (2019) Alternative lengthening of telomeres through two distinct break-induced replication pathways. *Cell Reports*, **26**, 955–968.
209. Osterwald,S., Deeg,K.I., Chung,I., Parisotto,D., Worz,S., Rohr,K., Erfle,H. and Rippe,K. (2015) PML induces compaction, TRF2 depletion and DNA damage signaling at telomeres and promotes their alternative lengthening. *J. Cell Sci.*, **128**, 1887–1900.
210. Heaphy,C.M., de Wilde,R.F., Jiao,Y., Klein,A.P., Edil,B.H., Shi,C., Bettegowda,C., Rodriguez,F.J., Eberhart,C.G., Hebbar,S. *et al.* (2011) Altered telomeres in tumors with ATRX and DAXX mutations. *Science*, **333**, 425.
211. Lovejoy,C.A., Li,W., Reisenweber,S., Thongthip,S., Bruno,J., de Lange,T., De,S., Petrini,J.H.J., Sung,P.A., Jasin,M. *et al.* (2012) Loss of ATRX, genome instability, and an altered DNA damage response are hallmarks of the alternative lengthening of telomeres pathway. *PLos Genet.*, **8**, e1002772.
212. Ceccarelli,M., Barthel,F.P., Malta,T.M., Sabedot,T.S., Salama,S.R., Murray,B.A., Morozova,O., Newton,Y., Radenbaugh,A., Pagnotta,S.M. *et al.* (2016) Molecular profiling reveals biologically discrete subsets and pathways of progression in diffuse glioma. *Cell*, **164**, 550–563.
213. Li,F., Deng,Z., Zhang,L., Wu,C., Jin,Y., Hwang,I., Vladimirova,O., Xu,L., Yang,L., Lu,B. *et al.* (2019) ATRX loss induces telomere dysfunction and necessitates induction of alternative lengthening of telomeres during human cell immortalization. *EMBO J.*, **38**, e96659.
214. O'Sullivan,R.J., Arnoult,N., Lackner,D.H., Oganesian,L., Haggblom,C., Corpet,A., Almouzni,G. and Karlseder,J. (2014)

Rapid induction of alternative lengthening of telomeres by depletion of the histone chaperone ASF1. *Nat. Struct. Mol. Biol.*, **21**, 167–174.
215. Gauchier,M., Kan,S., Barral,A., Sauzet,S., Agirre,E., Bonnell,E., Saksouk,N., Barth,T.K., Ide,S., Urbach,S. *et al.* (2019) SETDB1-dependent heterochromatin stimulates alternative lengthening of telomeres. *Sci. Adv.*, **5**, eaav3673.
216. Episkopou,H., Draskovic,I., Van Beneden,A., Tilman,G., Mattiussi,M., Gobin,M., Arnoult,N., Londoño-Vallejo,A. and Decottignies,A. (2014) Alternative lengthening of telomeres is characterized by reduced compaction of telomeric chromatin. *Nucleic Acids Res.*, **42**, 4391–4405.
217. Pan,X., Chen,Y., Biju,B., Ahmed,N., Kong,J., Goldenberg,M., Huang,J., Mohan,N., Klosek,S., Parsa,K. *et al.* (2019) FANCM suppresses DNA replication stress at ALT telomeres by disrupting TERRA R-loops. *Sci. Rep.*, **9**, 19110–19114.
218. Chang,F.T.M., McGhie,J.D., Chan,F.L., Tang,M.C., Anderson,M.A., Mann,J.R., Andy Choo,K.H. and Wong,L.H. (2013) PML bodies provide an important platform for the maintenance of telomeric chromatin integrity in embryonic stem cells. *Nucleic Acids Res.*, **41**, 4447–4458.
219. Wong,L.H., McGhie,J.D., Sim,M., Anderson,M.A., Ahn,S., Hannan,R.D., George,A.J., Morgan,K.A., Mann,J.R. and Choo,K.H.A. (2010) ATRX interacts with H3.3 in maintaining telomere structural integrity in pluripotent embryonic stem cells. *Genome Res.*, **20**, 351–360.
220. Wong,L.H., Ren,H., Williams,E., McGhie,J., Ahn,S., Sim,M., Tam,A., Earle,E., Anderson,M.A., Mann,J. *et al.* (2009) Histone H3.3 incorporation provides a unique and functionally essential telomeric chromatin in embryonic stem cells. *Genome Res.*, **19**, 404–414.
221. Marchesini,M., Matocci,R., Tasselli,L., Cambiaghi,V., Orleth,A., Furia,L., Marinelli,C., Lombardi,S., Sammarelli,G., Aversa,F. *et al.* (2016) PML is required for telomere stability in non-neoplastic human cells. *Oncogene*, **35**, 1811–1821.
222. Chang,H.R., Munkhjargal,A., Kim,M.-J., Park,S.Y., Jung,E., Ryu,J.-H., Yang,Y., Lim,J.-S. and Kim,Y. (2018) The functional roles of PML nuclear bodies in genome maintenance. *Mut. Res./Fundam. Mol. Mech. Mutagen.*, **809**, 99–107.
223. Pan,X., Ahmed,N., Kong,J. and Zhang,D. (2017) Breaking the end: Target the replication stress response at the ALT telomeres for cancer therapy. *Mol. Cell. Oncol.*, **4**, e1360978.
224. Pan,X., Drosopoulos,W.C., Sethi,L., Madireddy,A., Schildkraut,C.L. and Zhang,D. (2017) FANCM, BRCA1, and BLM cooperatively resolve the replication stress at the ALT telomeres. *Proc. Natl. Acad. Sci. U.S.A.*, **114**, E5940–E5949.
225. Flynn,R.L., Cox,K.E., Jeitany,M., Wakimoto,H., Bryll,A.R., Ganem,N.J., Bersani,F., Pineda,J.R., Suva,M.L., Benes,C.H. *et al.* (2015) Alternative lengthening of telomeres renders cancer cells hypersensitive to ATR inhibitors. *Science*, **347**, 273–277.
226. Episkopou,H., Diman,A., Claude,E., Viceconte,N. and Decottignies,A. (2019) TSPYL5 depletion induces specific death of ALT cells through USP7-dependent proteasomal degradation of POT1. *Mol. Cell*, **75**, 469–482.
227. Gong,P., Wang,H., Zhang,J., Fu,Y., Zhu,Z., Wang,J., Yin,Y., Wang,H., Zhou,Z., Yang,J. *et al.* (2019) Telomere maintenance-associated PML is a potential specific therapeutic target of human colorectal cancer. *Transl. Oncol.*, **12**, 1164–1176.
228. Roux,K.J., Kim,D.I., Raida,M. and Burke,B. (2012) A promiscuous biotin ligase fusion protein identifies proximal and interacting proteins in mammalian cells. *J. Cell Biol.*, **196**, 801–810.
229. Kim,T.H., Tsang,B., Vernon,R.M., Sonenberg,N., Kay,L.E. and Forman-Kay,J.D. (2019) Phospho-dependent phase separation of FMRP and CAPRIN1 recapitulates regulation of translation and deadenylation. *Science*, **365**, 825–829.
230. Dabin,J., Fortuny,A. and Polo,S.E. (2016) Epigenome maintenance in response to DNA damage. *Mol. Cell*, **62**, 712–727.
231. Vancurova,M., Hanzlikova,H., Knoblochova,L., Kosla,J., Majera,D., Mistrik,M., Burdova,K., Hodny,Z. and Bartek,J. (2019) PML nuclear bodies are recruited to persistent DNA damage lesions in an RNF168-53BP1 dependent manner and contribute to DNA repair. *DNA Repair (Amst.)*, **78**, 114–127.
232. Carbone,R., Pearson,M., Minucci,S. and Pelicci,P.G. (2002) PML NBs associate with the hMre11 complex and p53 at sites of irradiation induced DNA damage. *Oncogene*, **21**, 1633–1640.
233. Gallay,L., Mouchiroud,G. and Chazaud,B. (2019) Interferon-signature in idiopathic inflammatory myopathies. *Curr. Opin. Rheumatol.*, **31**, 634–642.
234. Sophie Trouillet-Assant,P., Sebastien Viel,P.P., Alexandre Gaymard,P.P., Sylvie Pons,M.S., Jean-Christophe Richard,M.P., Magali Perret,M.S., Marine Villard,P., Karen Brengel-Pesce,P., Bruno Lina,M.P., Mehdi Mezidi,M.D. *et al.* (2020) Type I IFN immunoprofiling in COVID-19 patients. *J. Allergy Clin. Immunol.*, **146**, 206–208.
235. Hadjadj,J., Yatim,N., Barnabei,L., Corneau,A., Boussier,J., Smith,N., Péré,H., Charbit,B., Bondet,V., Chenevier-Gobeaux,C. *et al.* (2020) Impaired type I interferon activity and inflammatory responses in severe COVID-19 patients. *Science*, **31**, eabc6027-15.
236. Maison,C., Bailly,D., Roche,D., de Oca,R.M., Probst,A.V., Vassias,I., Dingli,F., Lombard,B., Loew,D., Quivy,J.-P. *et al.* (2011) SUMOylation promotes de novo targeting of HP1α to pericentric heterochromatin. *Nat. Genet.*, **43**, 220–227.
237. Niwa-Kawakita,M., Ferhi,O., Soilihi,H., Le Bras,M., Lallemand-Breitenbach,V. and de Thé,H. (2017) PML is a ROS sensor activating p53 upon oxidative stress. *J. Exp. Med.*, **214**, 3197–3206.

# Annexe 2: Article de recherche

PLoS Pathogens, 2018 Sep 20
doi: 10.1371/journal.ppat.1007313; PMID: 30235352; PMCID: PMC6168178

## Promyelocytic leukemia (PML) nuclear bodies (NBs) induce latent/quiescent HSV-1 genomes chromatinization through a PML NB/Histone H3.3/H3.3 Chaperone Axis

Cohen C. [1], Corpet A.[1], Roubille S. [1], Maroui M. [1], Poccardi N.[2], Rousseau A.[2,3], Kleijwegt C. [1], Binda O.[1], Texier P. [1], Sawtell N.[4], Labetoulle M.[2,3], Lomonte P. [1]

1. Univ Lyon, Université Claude Bernard Lyon 1, CNRS UMR5310, INSERM U1217, LabEx
2. Virus, Lyon, France.
3. Institut de Biologie Intégrative de la Cellule (I2BC), Département de Virologie, Gif-sur-Yvette, France.
4. Université Paris Sud, Centre Hospitalier Universiaire de Bicêtre, Service d'Ophtalmologie, Le Kremlin-Bicêtre, France.
5. Division of infectious Diseases, Cincinnati Children's Hospital Medical Center, Cincinnati, Ohio, United States of America

**Abstract**

Herpes simplex virus 1 (HSV-1) latency establishment is tightly controlled by promyelocytic leukemia (PML) nuclear bodies (NBs) (or ND10), although their exact contribution is still elusive. A hallmark of HSV-1 latency is the interaction between latent viral genomes and PML NBs, leading to the formation of viral DNA-containing PML NBs (vDCP NBs), and the complete silencing of HSV-1. Using a replication-defective HSV-1-infected human primary fibroblast model reproducing the formation of vDCP NBs, combined with an immuno-FISH approach developed to detect latent/quiescent HSV-1, we show that vDCP NBs contain both histone H3.3 and its chaperone complexes, i.e., DAXX/ATRX and HIRA complex (HIRA, UBN1, CABIN1, and ASF1a). HIRA also co-localizes with vDCP NBs present in trigeminal ganglia (TG) neurons from HSV-1-infected wild type mice. ChIP and Re-ChIP show that vDCP NBs-associated latent/quiescent viral genomes are chromatinized almost exclusively with H3.3 modified on its lysine (K) 9 by trimethylation, consistent with an interaction of the H3.3 chaperones with multiple viral loci and with the transcriptional silencing of HSV-1. Only simultaneous inactivation of both H3.3 chaperone complexes has a significant impact on the deposition of H3.3 on viral genomes, suggesting a compensation mechanism. In contrast, the sole depletion of PML significantly impacts the chromatinization of the latent/quiescent viral genomes with H3.3 without any overall replacement with H3.1. vDCP NBs-associated HSV-1 genomes are not definitively silenced since the destabilization of vDCP NBs by ICP0, which is essential for HSV-1 reactivation in vivo, allows the recovery of a transcriptional lytic program and the replication of viral genomes. Consequently, the present study demonstrates a specific chromatin regulation of vDCP NBs-associated latent/quiescent HSV-1 through an H3.3-dependent HSV-1 chromatinization involving the two H3.3 chaperones DAXX/ATRX and HIRA complexes. Additionally, the study reveals that PML NBs are major actors in latent/quiescent HSV-1 H3.3 chromatinization through a PML NB/histone H3.3/H3.3 chaperone axis.

PLOS PATHOGENS

RESEARCH ARTICLE

# Promyelocytic leukemia (PML) nuclear bodies (NBs) induce latent/quiescent HSV-1 genomes chromatinization through a PML NB/Histone H3.3/H3.3 Chaperone Axis

**Camille Cohen[1], Armelle Corpet[1], Simon Roubille[1], Mohamed Ali Maroui[1], Nolwenn Poccardi[2], Antoine Rousseau[2,3¤], Constance Kleijwegt[1], Olivier Binda[1], Pascale Texier[1], Nancy Sawtell[4], Marc Labetoulle[2,3¤], Patrick Lomonte[1]***

**1** Univ Lyon, Université Claude Bernard Lyon 1, CNRS UMR 5310, INSERM U 1217, LabEx DEVweCAN, Institut NeuroMyoGène (INMG), team Chromatin Assembly, Nuclear Domains, Virus, Lyon, France, **2** Institut de Biologie Intégrative de la Cellule (I2BC), Département de Virologie, Gif-sur-Yvette, France, **3** Université Paris Sud, Centre Hospitalier Universitaire de Bicêtre, Service d'Ophthalmologie, Le Kremlin-Bicêtre, France, **4** Division of Infectious Diseases, Cincinnati Children's Hospital Medical Center, Cincinnati, Ohio, United States of America

¤ Current address: Université Paris Sud, UMR 1184, Commissariat à l'énergie atomique et aux énergies alternatives (CEA), Infectious diseases models for innovative therapies (IDMIT), Immunologie des Infections Virales et des Maladies Auto-immunes (IMVA), France
* patrick.lomonte@univ-lyon1.fr





**Citation:** Cohen C, Corpet A, Roubille S, Maroui MA, Poccardi N, Rousseau A, et al. (2018) Promyelocytic leukemia (PML) nuclear bodies (NBs) induce latent/quiescent HSV-1 genomes chromatinization through a PML NB/Histone H3.3/H3.3 Chaperone Axis. PLoS Pathog 14(9): e1007313. https://doi.org/10.1371/journal.ppat.1007313

**Editor:** Robert F. Kalejta, University of Wisconsin-Madison, UNITED STATES

**Received:** August 9, 2018

**Accepted:** August 31, 2018

**Published:** September 20, 2018



**Data Availability Statement:** All relevant data are within the paper and its Supporting Information files.

**Funding:** This work was funded by grants from CNRS (http://www.cnrs.fr), INSERM (https://www.inserm.fr), University Claude Bernard Lyon 1 (https://www.univ-lyon1.fr), French National Agency for Research-ANR (PL, ML, VIRUCEPTION, ANR-13-BSV3- 0001-01, http://www.agence-

## Abstract

Herpes simplex virus 1 (HSV-1) latency establishment is tightly controlled by promyelocytic leukemia (PML) nuclear bodies (NBs) (or ND10), although their exact contribution is still elusive. A hallmark of HSV-1 latency is the interaction between latent viral genomes and PML NBs, leading to the formation of viral DNA-containing PML NBs (vDCP NBs), and the complete silencing of HSV-1. Using a replication-defective HSV-1-infected human primary fibroblast model reproducing the formation of vDCP NBs, combined with an immuno-FISH approach developed to detect latent/quiescent HSV-1, we show that vDCP NBs contain both histone H3.3 and its chaperone complexes, i.e., DAXX/ATRX and HIRA complex (HIRA, UBN1, CABIN1, and ASF1a). HIRA also co-localizes with vDCP NBs present in trigeminal ganglia (TG) neurons from HSV-1-infected wild type mice. ChIP and Re-ChIP show that vDCP NBs-associated latent/quiescent viral genomes are chromatinized almost exclusively with H3.3 modified on its lysine (K) 9 by trimethylation, consistent with an interaction of the H3.3 chaperones with multiple viral loci and with the transcriptional silencing of HSV-1. Only simultaneous inactivation of both H3.3 chaperone complexes has a significant impact on the deposition of H3.3 on viral genomes, suggesting a compensation mechanism. In contrast, the sole depletion of PML significantly impacts the chromatinization of the latent/quiescent viral genomes with H3.3 without any overall replacement with H3.1. vDCP NBs-associated HSV-1 genomes are not definitively silenced since the destabilization of vDCP NBs by ICP0, which is essential for HSV-1 reactivation in vivo, allows the recovery of a transcriptional lytic program and the replication of viral genomes. Consequently, the present study demonstrates a specific chromatin regulation of vDCP NBs-associated latent/

nationale-recherche.fr), LabEX DEVweCAN (PL, CC, ANR-10-LABX-61, http://www.agence-nationale-recherche.fr), La Ligue contre le cancer and the FINOVI foundation (grant #142690). PL is a CNRS Research Director. The funders had no role in the study design, data collection and analysis, decision to publish, or preparation of the manuscript.

**Competing interests:** The authors have declared that no competing interests exist.

quiescent HSV-1 through an H3.3-dependent HSV-1 chromatinization involving the two H3.3 chaperones DAXX/ATRX and HIRA complexes. Additionally, the study reveals that PML NBs are major actors in latent/quiescent HSV-1 H3.3 chromatinization through a PML NB/histone H3.3/H3.3 chaperone axis.

## Author summary

An understanding of the molecular mechanisms contributing to the persistence of a virus in its host is essential to be able to control viral reactivation and its associated diseases. Herpes simplex virus 1 (HSV-1) is a human pathogen that remains latent in the PNS and CNS of the infected host. The latency is unstable, and frequent reactivations of the virus are responsible for PNS and CNS pathologies. It is thus crucial to understand the physiological, immunological and molecular levels of interplay between latent HSV-1 and the host. Promyelocytic leukemia (PML) nuclear bodies (NBs) control viral infections by preventing the onset of lytic infection. In previous studies, we showed a major role of PML NBs in favoring the establishment of a latent state for HSV-1. A hallmark of HSV-1 latency establishment is the formation of PML NBs containing the viral genome, which we called "viral DNA-containing PML NBs" (vDCP NBs). The genome entrapped in the vDCP NBs is transcriptionally silenced. This naturally occurring latent/quiescent state could, however, be transcriptionally reactivated. Therefore, understanding the role of PML NBs in controlling the establishment of HSV-1 latency and its reactivation is essential to design new therapeutic approaches based on the prevention of viral reactivation.

## Introduction

Herpes simplex virus 1 (HSV-1) is a human pathogen with neurotropic tropism and the causal agent of cold sores and more severe CNS pathologies such as encephalitis [1]. After the initial infection, HSV-1 remains latent in neuronal ganglia with the main site of latency being the trigeminal (or Gasserian) ganglion (TG). Two transcriptional programs are associated with HSV-1 infection, the lytic cycle and latency, which differ by the number and degree of viral gene transcription. The lytic cycle results from the sequential transcription of all viral genes (approximately 80) and leads to the production of viral progeny. The latency phase, occurring exclusively in neurons, is limited to the abundant expression of the so-called Latency Associated Transcripts (LATs), although physiologically a transitory expression of a limited number of lytic genes is not excluded, making latency a dynamic process[2–4].

Following lytic infection of epithelial cells at the periphery, the viral particle enters the axon termini of the innervating neurons by fusion of its envelope with the plasma membrane. The nucleocapsid is then carried into the neuron body by retrograde transport, most likely through the interaction of viral capsid components [5] with microtubule-associated proteins such as dynein and dynactin [6–10]. Once the nucleocapsid reaches the cell body, the virus phenotype changes from the one at the axon termini because most of the outer tegument proteins, including VP16, a viral transactivator that is essential for the onset of lytic infection, remain at the axonal tip [11–13]. Hence, when the viral DNA is injected into the neuron nucleus, it does not automatically benefit from the presence of VP16 to initiate transcription of lytic genes. Rather, the balance between lytic and latent transcriptional programs most likely depends on stochastic events and on undescribed neuron-associated factor(s) able to initiate the transcription of

VP16 through the activation of neuro-specific sequences present in the VP16 promoter [14]. Without VP16 synthesis, transcription of the viral genes encoding ICP4 (the major transactivator protein) and ICP0 (a positive regulator of viral and cellular gene transcription) is hampered. Hence, ICP4 and ICP0 gene transcription is unlikely to reach the required level to produce these two proteins above a threshold that would favor onset of the lytic cycle. Therefore, in neurons, commitment of the infectious process towards the lytic cycle or latency depends on a race between opposing infection-prone viral components and cellular features with antiviral activities.

Promyelocytic leukemia (PML) nuclear bodies (NBs) (also called ND10) are proteinaceous entities involved in the control of viral infection as part of the cell and nucleus-associated intrinsic antiviral response but also through innate immunity associated with the interferon (IFN) response [15]. Our recent studies have shown that PML NBs tightly associate with incoming HSV-1 genomes in the nucleus of infected TG neurons in mouse models and in primary TG neuron cultures [16,17]. Hence, PML NBs reorganize in structures called viral DNA-containing PML NBs (vDCP NBs), which are formed at early times during the process of HSV-1 latency establishment and persist during latency *per se* in a large subset of latently infected neurons in a mouse model of infection [16]. The entrapment of incoming wild type HSV-1 genomes by PML NBs is not a unique feature of latency, because it has recently been shown to occur prior to the onset of lytic infection, as part of the intrinsic antiviral response. HSV-1 genomes trapped in the vDCP NBs are transcriptionally repressed for LATs production [16]. It is known that HSV-1 latency, at least in the mouse model and possibly in humans, is heterogeneous at the single neuron level for the expression of LATs [16,18–25]. Therefore, although at the entire TG level HSV-1 latency could be a dynamic process from a transcriptional perspective, at the single neuron level, a strict, transcriptionally silent, quiescence can be observed, and vDCP NB-containing neurons are major contributors of this latent/quiescent HSV-1 state. In humans, vDCP NB-like structures have also been observed in latently infected TG neurons [17], suggesting that vDCP NBs are probably molecular hallmarks of the HSV-1 latency process, including in the natural host.

Another essential feature of HSV-1 latency is the chromatinization of its 150-kb genome, which enters the nucleus of the infected cells as a naked/non-nucleosomal dsDNA [26–28]. Once the viral genome is injected into the nucleus of the infected neuron, it circularizes, associates with nucleosomes to become chromatinized, and remains as an episome that is unintegrated into the host cell genome [29]. Although latent viral genomes sustain chromatin regulation, essentially through post-translational modifications of associated histones [30–34] not much is known about the mechanisms that induce their chromatinization and which specific histone variants are associated with these latent genomes. In mammals, specific H3 histone variants that differ by a few amino acid residues can influence chromatin compaction and transcriptional activity of the genome. The histone variant H3.3, a specific variant of the histone H3 that is expressed throughout the cell cycle, is deposited in a replication-independent manner, in contrast to H3.1 ([35] and for review [36]). Interestingly, death domain associated protein 6 (DAXX) and α-thalassemia mental retardation X-linked protein (ATRX), initially identified as a transcriptional repressor and a chromatin remodeler, respectively, are constitutively present in PML NBs, and have now been identified as H3.3-specific histone chaperones [37–39]. The other histone H3.3 specific chaperone complex is called the HIRA complex, which is composed of Histone cell cycle regulator (HIRA), Ubinuclein 1 (UBN1), Calcineurin-binding protein 1 (CABIN1), and Anti-silencing function protein 1 homolog A (ASF1a) [35]. The HIRA complex does not normally accumulate in PML NBs except upon entry of the cell into senescence [40,41]. The histone variant H3.3 itself localizes in PML NBs in proliferating and senescent cells, linking PML NBs with the chromatin assembly pathway independently of

replication [42–44]. Because vDCP NBs contain DAXX and ATRX [16,17,45], their involvement in the chromatinization of incoming HSV-1 genomes and/or long-term maintenance of chromatinized HSV-1 genomes is thus plausible.

Human primary fibroblasts or adult mouse primary TG neuron cultures infected through their cell body with a replication-defective HSV-1 virus, *in*1374, which is unable to synthesize functional ICP4 and ICP0 under specific temperature conditions, enable the establishment of a latent/quiescent state for HSV-1 [17,45–47]. The latent/quiescent state of HSV-1 in human primary fibroblasts has also been reproduced using engineered HSV-1 unable to express major immediate early genes [48,49]. We have shown that this latent/quiescent state is linked to the formation of vDCP NBs, mimicking, at least concerning this particular structural aspect, the latency observed in a subset of neurons in mouse models and in humans [16,17]. Here, using the *in*1374-based *in cellula* model of infection, we showed that vDCP NBs contained not only the DAXX and ATRX proteins but also all the components of the HIRA complex and H3.3 itself. HIRA was also found to co-localize with vDCP NBs in neurons of TG harvested from HSV-1 wild type infected mice. Both DAXX/ATRX and HIRA complex components were found to interact with multiple viral loci by chromatin immunoprecipitation (ChIP). Using the same approaches, we showed that latent/quiescent viral genomes were almost exclusively chromatinized with H3.3, itself modified on its lysine (K) 9 by trimethylation (H3.3K9me3). Most interestingly, we found that H3.3 chromatinization of the viral genomes was dependent on intact PML NBs, demonstrating that PML NBs contribute to an essential part of the chromatinization of the latent/quiescent HSV-1 genomes. Overall, this study shows that the chromatinization of latent HSV-1 involves a PML NB/histone H3.3/histone H3.3 chaperone axis that confers and probably maintains chromatin marks on viral genomes.

## Results

### The HIRA complex components accumulate in the vDCP NBs

The formation of vDCP NBs is a molecular hallmark of HSV-1 latency, and vDCP NBs are present in infected neurons from the initial stages of latency establishment to latency *per se* in mouse models [16,17]. Using a previously established *in vitro* latency system [46] consisting of human primary fibroblast cultures infected with a replication-deficient virus (hereafter called *in*1374) unable to express functional VP16, ICP4 and ICP0, we and others were able to reproduce the formation of vDCP NBs [17,45]. We first verified that vDCP NBs induced in BJ and other human primary cells infected with *in*1374 at a non-permissive temperature of 38.5˚C, contained, in addition to PML, the proteins constitutively found in the PML NBs, i.e., Sp100, DAXX, ATRX, SUMO-1 and SUMO-2/3 (S1Ai to S1vi Fig, and S1 Table). The DAXX/ATRX complex is one of the two chaperones of the histone variant H3.3 involved in the replication-independent chromatinization of specific, mostly heterochromatic, genome loci [39]. Interestingly, HSV-1 enters the nucleus of the infected cell as a naked/non-nucleosomal dsDNA and remains during latency as a circular chromatinized episome unintegrated in the host genome [29,50]. It is thus tempting to speculate that the presence of DAXX/ATRX in the vDCP NBs could be linked to a process of initiation and/or maintenance of chromatinization of the latent/quiescent viral genome. The other H3.3 chaperone is known as the HIRA complex and was initially described as specific for the replication-independent chromatinization of euchromatin regions [35,51]. Remarkably, proteins of the HIRA complex are able to bind in a sequence-independent manner to a naked/non-nucleosomal DNA [52], suggesting that the HIRA complex could also participate in the recognition and chromatinization of the incoming naked HSV-1 genome. We thus investigated the localization of all members of the HIRA complex and found that they co-localized with the latent/quiescent HSV-1 genomes at 2 days post-

infection (dpi) in BJ and other human primary cells (Fig 1Ai to 1iv, S1 Table). To confirm that the co-localization of members of the HIRA complex with the latent/quiescent HSV-1 could be reproduced in neuronal cells, adult mouse TG neuron cultures were infected with *in*1374 for 2 days before performing immuno-FISH. Mouse Hira, which was the only protein of the HIRA complex detectable in mouse cells, showed a clear co-localization with a subset of viral genomes (Fig 1B). To analyze whether this co-localization was also reproducible *in vivo*, immuno-FISH was performed on TG samples from HSV-1-infected mice. Hira was found to co-localize with HSV-1 genomes with the "multiple acute"/vDCP NB pattern (see [17,53,54]) in TG neurons from infected mice at 6 dpi (Fig 1C) but not with the "single"/vDCP NB pattern (see [16,53,54]) at 28 dpi (Fig 1D), suggesting a dynamic association of this protein with the vDCP NBs.

To analyze this dynamic association, co-localization between incoming HSV-1 genomes and proteins of the PML NBs or of the HIRA complex was quantified at early times from 30 min pi to 6 hpi using a synchronized infection procedure (Fig 1E and S2 Table). Except for the proteins of the HIRA complex, the percentages of co-localization increased with time. Interestingly, at 30 min pi, the percentage of co-localization of HSV-1 genomes with HIRA was significantly higher than with PML (41±7% vs 23±5%, p value = 0.03, Student's *t-test*, S2 Table). Although DAXX and ATRX also showed, on average, a greater percentage of co-localization with HSV-1 genomes (36±7% and 34±5% at 30 min, respectively) compared with PML, the data were not significant (S2 Table). Moreover, a recent study showed the interaction of at least PML, SUMO-2, and Sp100 with incoming HSV-1 genomes as soon as 1 hpi, which supports our data [55]. The absence of co-localization of mouse Hira with viral genomes with the "single"/vDCP NB pattern in mouse TG neurons at 28 dpi suggested that longer infection times could lead to loss of proteins of the HIRA complex from the vDCP NBs. Infection of BJ cells were reiterated as above, but this time quantifications were performed from 24 hpi to 7 dpi. Strikingly, whereas all the proteins permanently present in the PML NBs remained co-localized with a maximum of 100% of the latent/quiescent HSV-1 genome from 2 dpi until 7 dpi, proteins of the HIRA complex peaked at 2 dpi, and then their co-localization decreased at longer times pi, confirming the temporary association of the HIRA complex with the vDCP NBs (Fig 1F, and S3 Table).

To definitively show that proteins of the HIRA complex were present in vDCP NBs, immuno-FISH were performed on BJ cells infected for 2 days with *in*1374 to detect a member of the HIRA complex, HSV-1 genomes, and PML. Strikingly, while proteins of the HIRA complex showed predominant nucleoplasmic staining in non-infected cells (Fig 2i, 2iii, 2v and 2vii), in infected cells all the proteins clearly and systematically accumulated in PML NBs (Fig 2ii, 2iv, 2vi and 2viii). The accumulation of HIRA in PML NBs following infection by HSV-1 has recently been suggested to be part of an interferon-induced antiviral mechanism [56]. Consequently, HIRA, UBN1, CABIN1 and ASF1a co-localized with the latent/quiescent HSV-1 genomes in vDCP NBs (arrows in Fig 2ii, 2iv, 2vi and 2viii). Altogether, these data show that both DAXX/ATRX and HIRA complexes are present within vDCP NBs in neuronal and non-neuronal cells, suggesting a role for these two complexes in latent/quiescent HSV-1 chromatinization.

## Histone H3.3 chaperones interact with incoming viral genome

The co-localization of proteins of the DAXX/ATRX and HIRA complexes with the incoming HSV-1 genomes and their presence in the vDCP NBs suggested an interaction of these proteins with the viral genome, as shown recently for HIRA on a small subset of viral loci [56]. Since DAXX, HIRA, and UBN1 antibodies were not efficient in the ChIP experiments, we

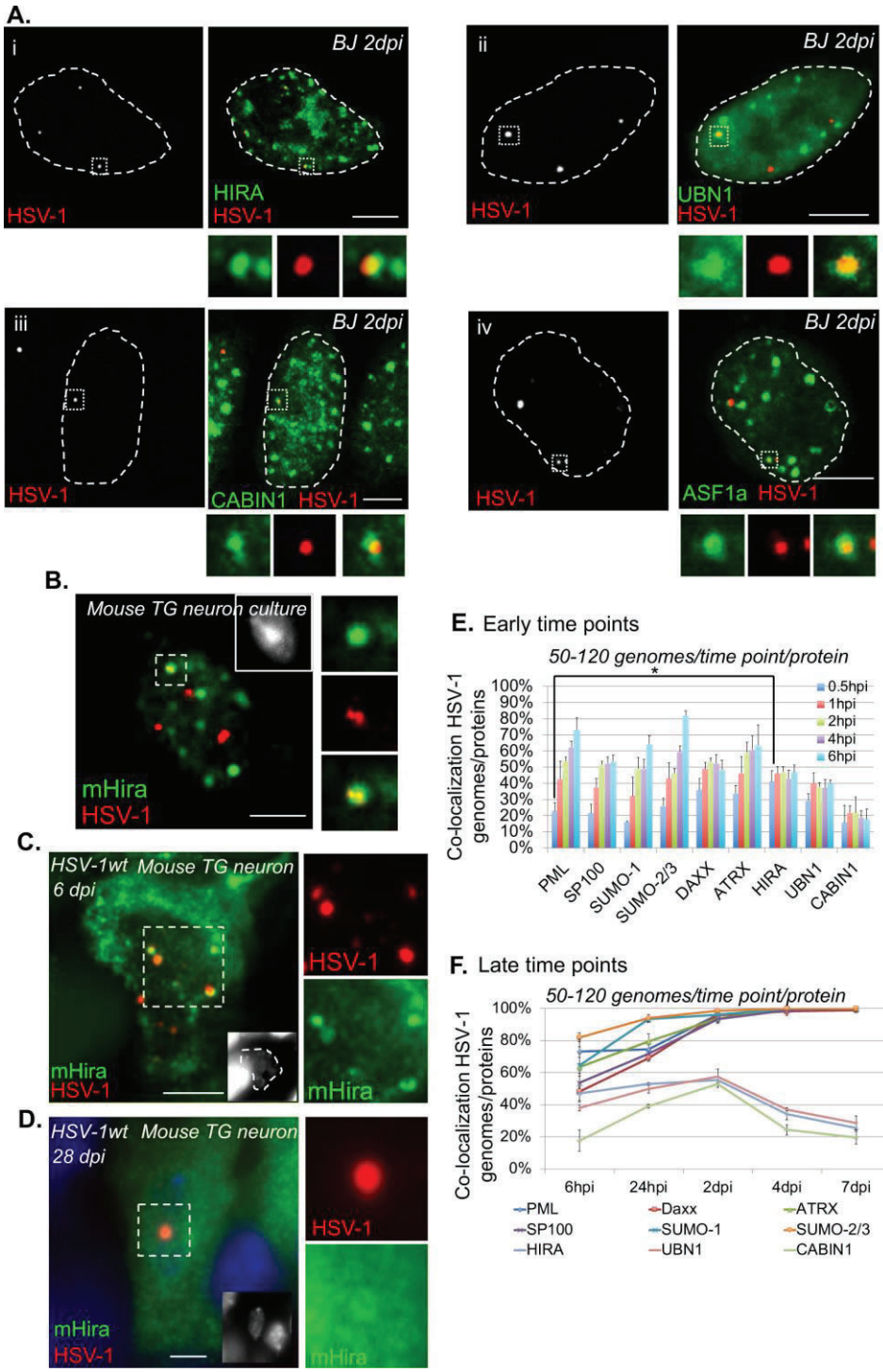
A.
i
BJ 2dpi
HSV-1
HIRA
HSV-1
ii
BJ 2dpi
HSV-1
UBN1
HSV-1
iii
BJ 2dpi
HSV-1
CABIN1 HSV-1
iv
BJ 2dpi
HSV-1
ASF1a HSV-1
B.
Mouse TG neuron culture
mHira
HSV-1
C.
HSV-1wt Mouse TG neuron
6 dpi
mHira
HSV-1
HSV-1
mHira
D.
HSV-1wt Mouse TG neuron
28 dpi
mHira
HSV-1
HSV-1
mHira
E. Early time points
50-120 genomes/time point/protein
Co-localization HSV-1 genomes/proteins
100%
90%
80%
70%
60%
50%
40%
30%
20%
10%
0%
0.5hpi
1hpi
2hpi
4hpi
6hpi
PML
SP100
SUMO-1
SUMO-2/3
DAXX
ATRX
HIRA
UBN1
CABIN1
F. Late time points
50-120 genomes/time point/protein
Co-localization HSV-1 genomes/proteins
100%
80%
60%
40%
20%
0%
6hpi
24hpi
2dpi
4dpi
7dpi
PML
Daxx
ATRX
SP100
SUMO-1
SUMO-2/3
HIRA
UBN1
CABIN1

**Fig 1. Latent/quiescent HSV-1 genomes co-localize with the HIRA complex.** (A) Immuno-FISH performed in human primary fibroblasts (BJ cells) infected for 2 days with the replication-defective HSV-1 virus *in*1374. HIRA (i), UBN1 (ii), CABIN1 (iii), ASF1a (iv) (green), and HSV-1 genomes (red) were detected. Scale bars = 5 μm. (B) Immuno-FISH performed in adult mouse primary TG neuron cultures infected for 2 days with *in*1374. Mouse Hira (mHira, green), HSV-1 genomes (red), and nucleus (inset, gray) are detected. Scale bar = 5 μm. (C) Same as (B) but in TG neurons from 6-day HSV-1wt-infected mice. Scale bars = 10 μm. (D) Same as (B) in TG neurons of 28-day HSV-1wt-infected mice. Scale bars = 10 μm. (E) Quantifications of immuno-FISH performed in BJ cells infected with *in*1374 at early times pi. Data represent the percentage of co-localization between incoming HSV-1 genomes and representative proteins of the PML NBs (PML, Sp100, SUMO-1, SUMO 2/3) or H3.3 chaperone complex proteins (DAXX, ATRX, HIRA, UBN1, CABIN1). Means from three independent experiments ± SD. The Student's *t*-test was applied to assess the significance of the results. * = $p < 0.05$ (see S2 Table for data). (F) Same as (E) but at late times pi. Means from three independent experiments ± SD (see S3 Table for data).

https://doi.org/10.1371/journal.ppat.1007313.g001

constructed cell lines stably expressing myc-DAXX, HIRA-HA, or HA-UBN1 by transduction of BJ cells with lentiviral- vectors (S2 Fig). Cells were infected with *in*1374 at 38.5˚C and harvested 24 hpi to perform ChIP-qPCR on multiple loci spread over the entire HSV-1 genome, representing promoter or core regions (CDS) of genes of all kinetics (IE/α, E/β, L/γ) (Fig 3A). Cellular glyceraldehyde 3-phosphate dehydrogenase (GAPDH) locus was used as a positive control for enrichment. Significant enrichments compared to controls were detected for all proteins on several viral loci independently of their promoter or CDS status, and with no obvious discrepancy regarding the gene kinetic, confirming the potential interaction of these proteins all along the latent/quiescent HSV-1 genomes. Our immuno-FISH data anticipated a gradual interaction of the four proteins with the incoming viral genomes at early times post infection (see Fig 1E). To verify if this could be measured, ChIP-qPCR were performed at 30 min pi, 2 hpi and 6 hpi, using the same experimental conditions as for the immuno-FISH at early times pi (with synchronization of the infection, see Materials and Methods). The data showed a tendency for a weak interaction with the viral genomes at 30 min pi then an increase at 2 hpi and 6 hpi, although with a lot of variability, probably highlighting the dynamic of the biological events occurring during the initial stages of the infection process (S3B Fig). ATRX showed the more regular increase in its interaction with viral genomes from 30 min to 24 hpi. Overall, the ChIP data correlate with the immuno-FISH, and suggest a dynamic process for the interaction between HSV-1 genomes and proteins of the DAXX/ATRX and HIRA complexes, initiating early after the viral DNA enters the nucleus, and remaining at later times when vDCP NBs are structured.

## H3.3 is present in the vDCP NBs and interacts with latent/quiescent HSV-1 genomes

The co-localization of the two histone H3.3 chaperone complexes with viral genomes suggested the chromatinization of HSV-1 latent/quiescent genomes with the histone variant H3.3. Histones H3.1 and H3.3 differ by only 5 amino acids, and, in our hands, no suitable antibody is available that can distinguish both histones by IF or IF-FISH. We thus constructed lentivirus-transduced BJ cell lines expressing a tagged version of either histone (e-H3.1 and e-H3.3) (see Materials and Methods, and [43], S4A and S4B Fig). We confirmed that ectopic expression of e-H3.3 led to its accumulation in PML NBs unlike e-H3.1 (S4C Fig) [42,43]. *In*1374 infection of BJ e-H3.1/3-expressing cells led to the co-localization of viral genomes almost exclusively with e-H3.3 (Fig 4Ai, 4ii and 4B). Importantly, e-H3.3 co-localized with HSV-1 genomes together with PML in vDCP NBs (Fig 4C). The lack of co-localization of viral genomes with e-H3.1 was in agreement with the absence of any of the H3.1 CAF-1 chaperone subunits (p150, p60, p48) in the vDCP NBs (Fig 4D, S1 Table). To confirm that e-H3.3, unlike e-H3.1, interacted with HSV-1 genomes, ChIP-qPCR were conducted on the same loci as those analyzed above. As expected, e-H3.3, but not e-H3.1, was highly enriched on the viral genome

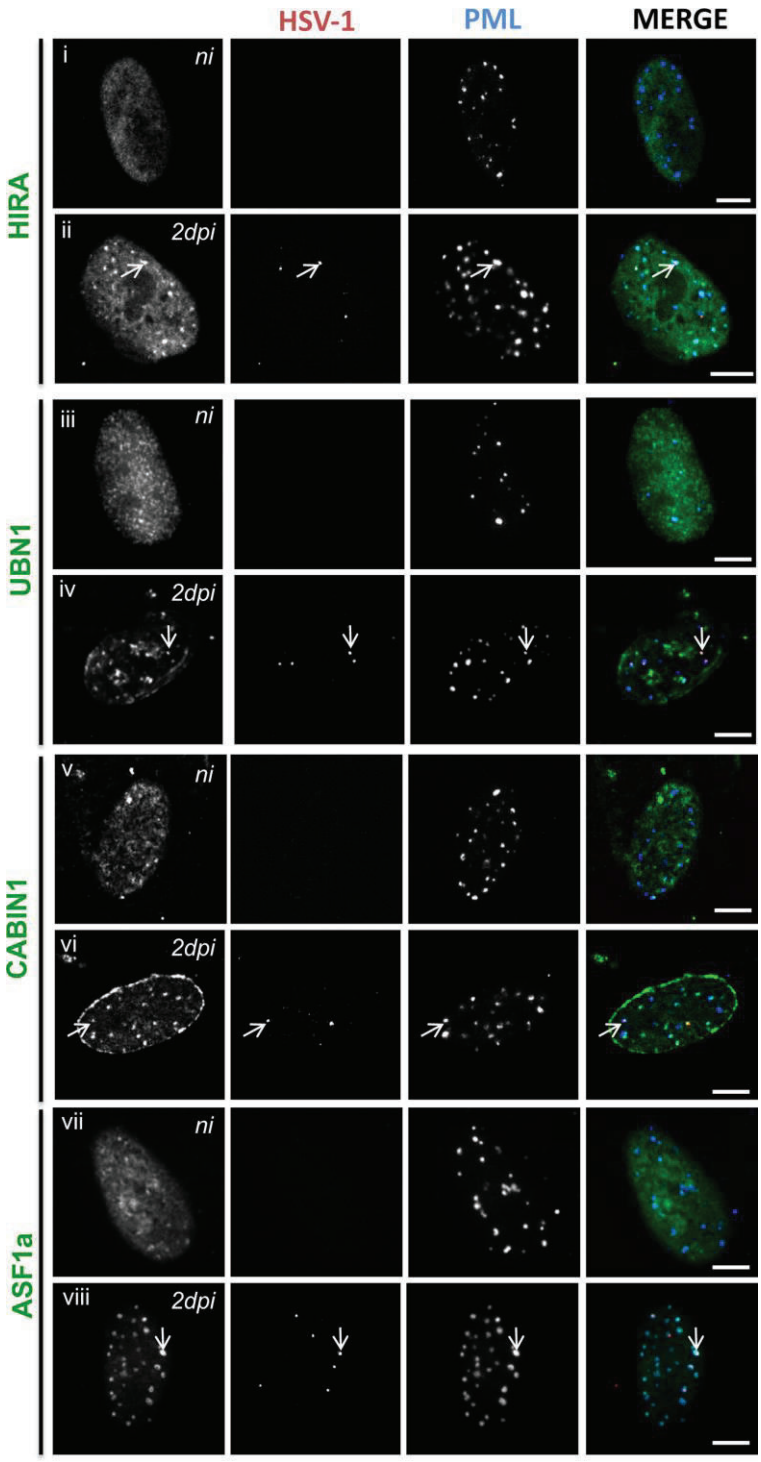
HSV-1
PML
MERGE
HIRA
UBN1
CABIN1
ASF1a
i ni
ii 2dpi
iii ni
iv 2dpi
v ni
vi 2dpi
vii ni
viii 2dpi

**Fig 2. HSV-1 infection induces the accumulation of HIRA complex proteins in PML NBs and co-localization with latent/quiescent HSV-1 genomes in vDCP NBs.** Immuno-FISH performed in BJ cells not infected (ni) (i, iii, v, vii) or infected for 2 days (ii, iv, vi, viii) with *in*1374. HIRA (i and ii), UBN1 (iii and vi), CABIN1 (v and vi), ASF1a (vii and viii) (gray, green), HSV-1 genomes (gray, red), and PML (gray, blue) were detected. Arrows indicate examples of the detection of HIRA complex proteins in vDCP NBs. Scale bars = 5 μm.

https://doi.org/10.1371/journal.ppat.1007313.g002

independently of the examined locus (Fig 4E). Several cellular loci were analyzed as controls for specific enrichments with H3.3 (Enhancer 1 (Enh.1) on chromosome 9, [57]), or H3.1 (leucine-zipper-like transcriptional regulator 1 (LZTR1) on chromosome 22, GEO accession number GSM1135044). Similar data were obtained for all other canonical histones (S5 Fig), confirming that H3.3 association with latent/quiescent HSV-1 genomes is in a nucleosomal context. To confirm that the discrepancy between the binding of e-H3.3 and e-H3.1 to viral genomes was not due to the ectopic expression of histones, we performed similar experiments using antibodies against native proteins. One specific antibody for H3.3, and suitable for ChIP experiments has previously been described [58]. We performed ChIP using antibodies against native H3.1/2 or H3.3 in normal BJ cells infected for 24 h by *in*1374. The results were similar to those obtained in infected BJ e-H3.3 using the anti-HA antibody (S6 Fig). These data confirmed that no bias was introduced in the ChIP experiments due to the use of tagged histones, and that latent/quiescent HSV-1 genomes are chromatinized with H3.3. The gradual interaction of the four proteins of the H3.3 chaperone complexes with the incoming viral genomes anticipated similar changes in the interaction of H3.3. ChIP-qPCR were performed at 30 min pi, 2 hpi and 6 hpi, using the same experimental conditions as above. The data showed an overall weak or lack of, H3.3 association with the viral genomes at 30 min pi, followed by an increased interaction at 2 hpi and 6 hpi. These data show that the H3.3 chromatinization of the incoming HSV-1 genomes is progressive and follows a kinetic that matches that observed with the proteins of the H3.3 chaperone complexes. The data also fit with recently published data showing the interaction of incoming viral genomes with canonical histones by 2 hpi [55].

## The H3.3K9me3 chromatin mark is predominantly found on vDCP NBs-associated latent/quiescent HSV-1 genomes

Both constitutive (H3K9me2, H3K9me3) and facultative (H3K27me3) heterochromatin marks have been found on various loci on latent HSV-1 genomes *in vivo* [31,33,34]. To analyze the association of these marks with vDCP NBs-associated latent/quiescent HSV-1 genomes, ChIP were performed targeting H3K9me3, H3K27me3 and one euchromatic mark H3K4me2 as a control (Fig 5). HSV-1 genomes were exclusively associated with H3K9me3 (Fig 5A), matching previous results obtained using quiescent viruses [59,60]. In contrast H3K27me3 (Fig 5B) or H3K4me2 (Fig 5C) marks were not detected. Cellular genes previously described for their association with either marks were analyzed for the specificity of the antibodies used (Zinc-finger protein 554 (ZNF554)/H3K9me3 [61]); myelin transcription factor 1 (MYT1)/H3K27me3 ([62]; Actin/H3K4me2). To confirm that the K9me3 modification is present on H3.3 associated with the HSV-1 genomes, Re-ChIP was performed targeting first H3K9me3 then e-H3.3 in infected BJ and BJ e-H3.3 (Fig 5D). An overall enrichment for H3.3 from samples initially ChIPed with the H3K9me3 antibody was detected only in BJ e-H3.3 and not BJ cells, with 17 viral loci over 31 (55%) showing significant enrichment. The cellular locus, family with sequence similarity 19 member A2 (FAM19A2) specifically enriched with H3.3K9me3 (GEO accession numbers: GSM1358809 (H3.3), and GSM1289412 (H3K9me3)) was used as positive control. These data show that (i) the Re-ChIP experiment is specific of e-H3.3 and (ii) H3.3K9me3 is indeed associated with the vDCP NB-associated HSV-1 latent/quiescent genomes.

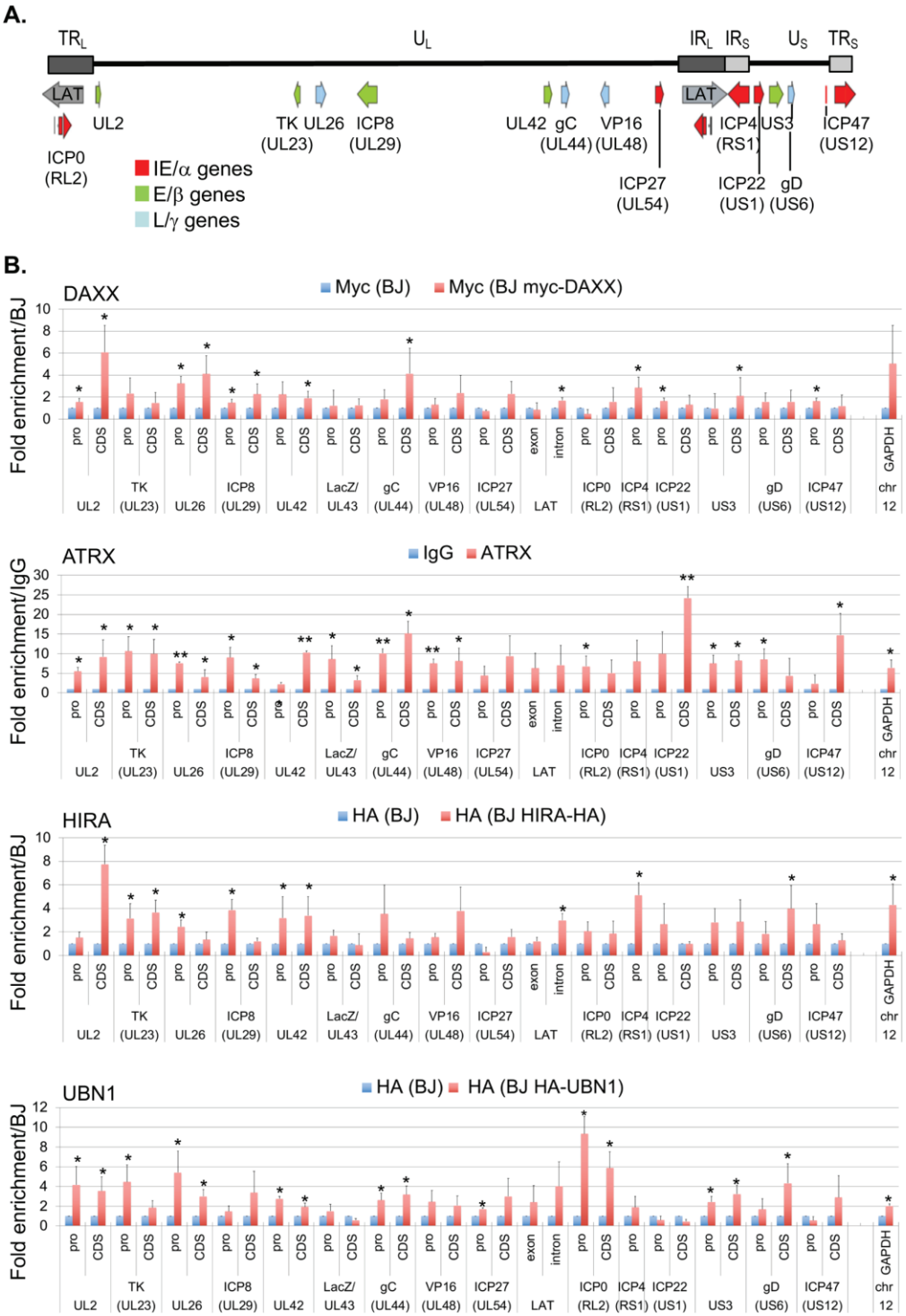
A.
TRL
UL
IRL IRS
US
TRS
LAT
UL2
TK UL26 ICP8
(UL23) (UL29)
UL42 gC VP16
(UL44) (UL48)
ICP4 US3 ICP47
(RS1) (US12)
ICP0
(RL2)
IE/α genes
E/β genes
L/γ genes
ICP27
(UL54)
ICP22 gD
(US1) (US6)
B.
DAXX
Myc (BJ)
Myc (BJ myc-DAXX)
Fold enrichment/BJ
ATRX
IgG
ATRX
Fold enrichment/IgG
HIRA
HA (BJ)
HA (BJ HIRA-HA)
Fold enrichment/BJ
UBN1
HA (BJ)
HA (BJ HA-UBN1)
Fold enrichment/BJ
pro
CDS
exon
intron
UL2
TK (UL23)
UL26
ICP8 (UL29)
UL42
LacZ/ UL43
gC (UL44)
VP16 (UL48)
ICP27 (UL54)
LAT
ICP0 (RL2)
ICP4 (RS1)
ICP22 (US1)
US3
gD (US6)
ICP47 (US12)
GAPDH
chr 12

**Fig 3. Components of the DAXX/ATRX and HIRA complexes associate with latent/quiescent HSV-1 genomes.** (A) Schematic localization of the HSV-1 genome and of the loci analyzed by quantitative PCR (qPCR). UL: Unit Long, US: Unit Short, TRL: Terminal Repeat Long, TRS: Terminal Repeat Short, IRL: Inverted Repeat Long, IRS: Inverted Repeat Short. Immediate early (IE/α) genes (red), early (E/β) genes (green), late (L/γ) genes (blue). (B) Chromatin immunoprecipitation (ChIP) associated with qPCR performed in *in*1374-infected normal BJ cells or *in*1374-infected BJ cells expressing tagged versions of DAXX, HIRA, or UBN1. Infections were performed for 24 h. Anti-myc (DAXX) or anti-HA (HIRA and UBN1) antibodies were used. For ATRX, a native antibody was used, and the results were compared to ChIP with IgG as control. Means from three independent experiments ± SD. Student's *t*-test was applied to assess the significance of the results. * = $p < 0.05$.

https://doi.org/10.1371/journal.ppat.1007313.g003

## Simultaneous inactivation of DAXX/ATRX and HIRA complexes affects HSV-1 genomes chromatinization with H3.3

To analyze the requirement of the histone H3.3 chaperones for the formation of the vDCP NBs and HSV-1 chromatinization, DAXX, ATRX, HIRA or UBN1 were depleted by shRNAs in normal BJ cells or cells constitutively expressing e-H3.3 prior to infection with *in*1374 and completion of the experiments. The two tested shRNAs for each protein significantly diminished mRNA and protein quantities in BJ cells (S7A and S7B Fig). None of the shRNA impacted the detection of PML NBs, suggesting that PML NBs were potentially functional when the proteins were individually inactivated (S8 Fig). We first measured the impact of the depletion of each protein on the co-localization of HSV-1 genomes with PML. Both shRNAs for each protein gave similar results, i.e., a significant decrease in the co-localization between HSV-1 genomes and PML and thus a decrease in the formation and/or stability of the vDCP NBs (Fig 6A and 6B, S4 Table). These data show that the inactivation of any of the H3.3 chaperone complex affects to a certain extent the fate of vDCP NBs suggesting a connection between the activity of each H3.3 chaperone complex and the formation and/or maintenance of the vDCP NBs.

We then analyzed the potential impact of the loss of vDCP NB stability on the H3.3-dependent HSV-1 chromatinization. We performed H3.3 ChIP in *in*1374-infected BJ e-H3.3 cells that had been previously depleted for HIRA, UBN1, DAXX or ATRX using one of the previously validated shRNAs (S9A and S9B Fig). The data showed that overall the inactivation of UBN1, DAXX or ATRX, had a weak impact on the association of H3.3 with the viral loci (1 to 3 loci significantly affected over 31, 3.2 to 9.6%) (Fig 6C). The depletion of HIRA had a relatively greater effect (6/31, 19.4%). To analyze if simultaneous inactivation of both complexes would significantly impact on HSV-1 chromatinization with H3.3, one protein of each complex was inactivated at the same time before performing HSV-1 infection (Fig 7A). Individual inactivation of HIRA and ATRX is known to lead to the functional inactivation of the HIRA and DAXX/ATRX complexes, respectively [35,52,63,64]. We noticed that the inactivation of HIRA by a siRNA was not as efficient as the shRNA on preventing the association of H3.3 with viral genomes (Fig 7B). This is likely due to differences in the efficiency of the siRNA compared to the shRNA (compare WBs of Figs S7B and 7A), and to the transitory effect of the siRNA compared to the stable effect of the shRNA at the time of the infection (see Materials and Methods). Nonetheless, a significant decrease of the association of H3.3 with a large number of viral loci (20/31, 64.5%) was measured by the simultaneous inactivation of HIRA and ATRX compared to their individual inactivation (Fig 7B). These results indicate that the DAXX/ATRX complex may compensate for the loss of the HIRA complex on the chromatinization of latent/quiescent HSV-1 genomes with H3.3, and conversely.

## PML NBs are essential for H3.3 chromatinization of latent/quiescent HSV-1 genomes

The above experiments were conducted in a context where the cells, although deficient for the activity of one H3.3 chaperone complex at a time, still contained intact PML NBs accumulating

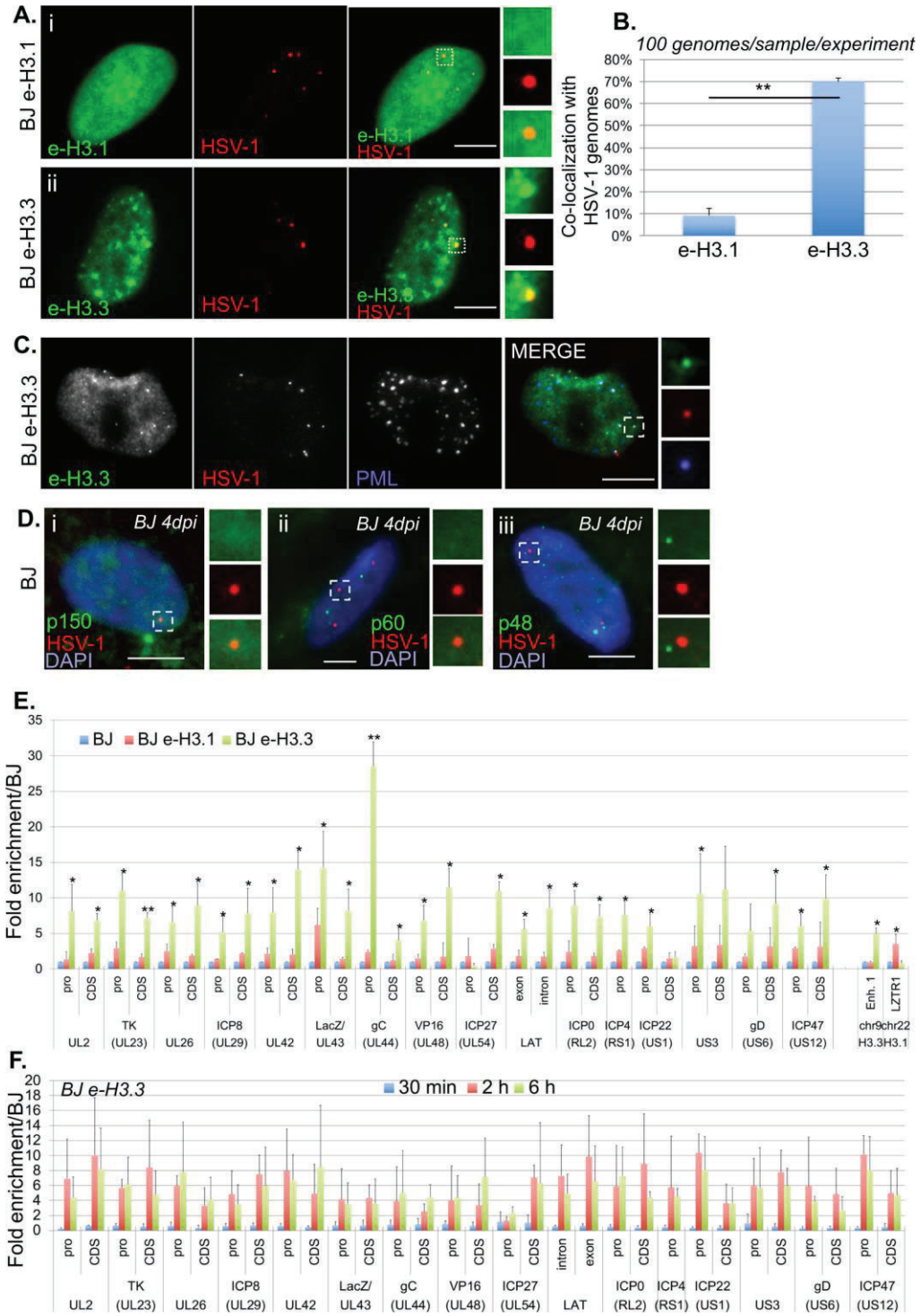
A.
BJ e-H3.1
e-H3.1
HSV-1
e-H3.1 HSV-1
BJ e-H3.3
e-H3.3
HSV-1
e-H3.3 HSV-1
B.
100 genomes/sample/experiment
Co-localization with HSV-1 genomes
80%
70%
60%
50%
40%
30%
20%
10%
0%
**
e-H3.1
e-H3.3
C.
BJ e-H3.3
e-H3.3
HSV-1
PML
MERGE
D.
BJ
i BJ 4dpi
p150
HSV-1
DAPI
ii BJ 4dpi
p60
HSV-1
DAPI
iii BJ 4dpi
p48
HSV-1
DAPI
E.
BJ BJ e-H3.1 BJ e-H3.3
Fold enrichment/BJ
pro CDS exon intron
UL2 TK (UL23) UL26 ICP8 (UL29) UL42 LacZ/ UL43 gC (UL44) VP16 (UL48) ICP27 (UL54) LAT ICP0 (RL2) ICP4 (RS1) ICP22 (US1) US3 gD (US6) ICP47 (US12) Enh. 1 chr9chr22 H3.3H3.1 LZTR1
F.
BJ e-H3.3
30 min 2 h 6 h
Fold enrichment/BJ
UL2 TK (UL23) UL26 ICP8 (UL29) UL42 LacZ/ UL43 gC (UL44) VP16 (UL48) ICP27 (UL54) LAT ICP0 (RL2) ICP4 (RS1) ICP22 (US1) US3 gD (US6) ICP47 (US12)

**Fig 4. The histone variant H3.3 co-localizes and interacts with latent/quiescent HSV-1 genomes.** (A) Immuno-FISH performed in e-H3.1 (i) or e-H3.3 (ii)-expressing BJ cells infected for 2 days with *in*1374. E-H3.1 or e-H3.3 (green), and HSV-1 genomes (red) were detected. Scale bars = 5 μm. (B) Quantification of the immuno-FISH performed in (A). Means from three independent experiments ± SD. The Student's *t*-test was applied to assess the significance of the results. ** = $p < 0.01$. (C) Immuno-FISH performed in e-H3.3-expressing BJ cells infected for 2 days with *in*1374. E-H3.3 (gray, green), HSV-1 (gray, red), and PML (gray, blue) were detected. Scale bar = 5 μm. (D) Immuno-FISH performed in normal BJ cells infected for 2 days with *in*1374. H3.1 CAF chaperone complex proteins p150 (i), p60 (ii), and p48 (iii) (green), and HSV-1 genomes (red) were detected. Nuclei were detected with DAPI (blue). Scale bars = 5 μm. (E) ChIP performed in *in*1374-infected normal BJ cells (blue), *in*1374-infected e-H3.1 (red) or e-H3.3 (green) expressing BJ cells. Infections were performed for 24 h. Anti-HA antibody was used for ChIP experiments. Analyzed viral loci were described previously. Cellular loci Enhancer 1 (Enh.1), and leucine-zipper-like transcriptional regulator 1 (LZTR1) are positive controls for deposition of H3.3 and H3.1, respectively. Means from three independent experiments ± SD. The Student's t-test was applied to assess the significance of the results. * = $p < 0.05$, ** = $p < 0.01$. (F) ChIP performed in *in*1374-infected e-H3.3-expressing BJ cells at early times pi, 30 min (blue), 2 h (red), 6 h (green). Anti-HA antibody was used for ChIP experiments. Analyzed viral loci were described previously. Means from three independent experiments ± SD.

https://doi.org/10.1371/journal.ppat.1007313.g004

e-H3.3 (S7 and S10 Fig). Therefore, we hypothesized that the accumulation of H3.3 within the PML NBs could be one of the key events acting upstream of the H3.3 chaperone complex activity for the induction of chromatinization of the latent/quiescent HSV-1 by H3.3. We analyzed the HSV-1 chromatinization in cells lacking PML NBs. In a previous study conducted in HSV-1 latently infected PML KO mice, we showed that the absence of PML significantly impacted the number of latently infected TG neurons showing the "single"/vDCP NB HSV-1 pattern and favored the detection of neurons containing the "multiple-latency" pattern prone to LAT expression [16,53]. We analyzed the very few neurons showing a "single"/vDCP NB-like pattern in the latently infected PML KO mice for the co-localization of DAXX and ATRX with the viral genomes. We could not detect any of the two proteins co-localizing with the latent HSV-1 genomes (Fig 8Ai to 8vi). Although informative, these *in vivo* studies did not allow the analysis of the real impact of the absence of PML on the co-localization of the other PML NB-associated proteins with latent HSV-1 genomes, because the neurons showing the "single"/vDCP NB-like pattern were too few to quantify the effect. We thus depleted PML in normal BJ cells using a PML shRNA-expressing lentiviral transduction approach. We verified the efficiency of the shRNAs against PML in normal BJ cells by IF, RT-qPCR and WB (S11A–S11C Fig). PML-depleted BJ cells were superinfected with *in*1374, and immuno-FISH was performed at 2 dpi to analyze the co-localization of HSV-1 genomes with DAXX, ATRX, HIRA, and UBN1 (Fig 8B). Notably, both PML shRNAs gave similar results. The quantification of the data showed that, similarly to the *in vivo* situation, the depletion of PML significantly decreased the co-localization of DAXX and ATRX with latent/quiescent HSV-1 genomes, leaving HIRA and UBN1 unaffected for their co-localization (Fig 8C, and S5 Table). Thus, we analyzed whether the failure of DAXX/ATRX to co-localize with the latent/quiescent HSV-1 genomes in the absence of PML NBs, could impact the chromatinization of HSV-1 with H3.3.

We first generated BJ e-H3.3 cells depleted for PML by shRNA-expressing lentiviral transduction similarly to the BJ cells (S11D and S11E Fig). BJ e-H3.3 control or PML-depleted cells were superinfected with *in*1374 to perform immuno-FISH and analyze the co-localization of HSV-1 genomes with H3.3 (Fig 9A). Quantification of the data showed a significant decrease in the co-localization of latent/quiescent HSV-1 genomes with H3.3 compared with controls (Fig 9B), suggesting an impact of the absence of PML NBs on the latent/quiescent HSV-1 association with H3.3. To complement these results at a more quantitative level, we performed ChIP on e-H3.3. The data showed a major impact of the absence of PML NBs on the H3.3 association with viral genomes, with a significant depletion of H3.3 on multiple loci (21/31, 68%) (Fig 9C). This could not be due to an indirect effect of PML depletion on H3.3 stability because e-H3.3 protein levels were similar in control cells and cells depleted for PML (Fig 9D). Both PML shRNAs gave similar results. To confirm that the absence of PML had an impact on

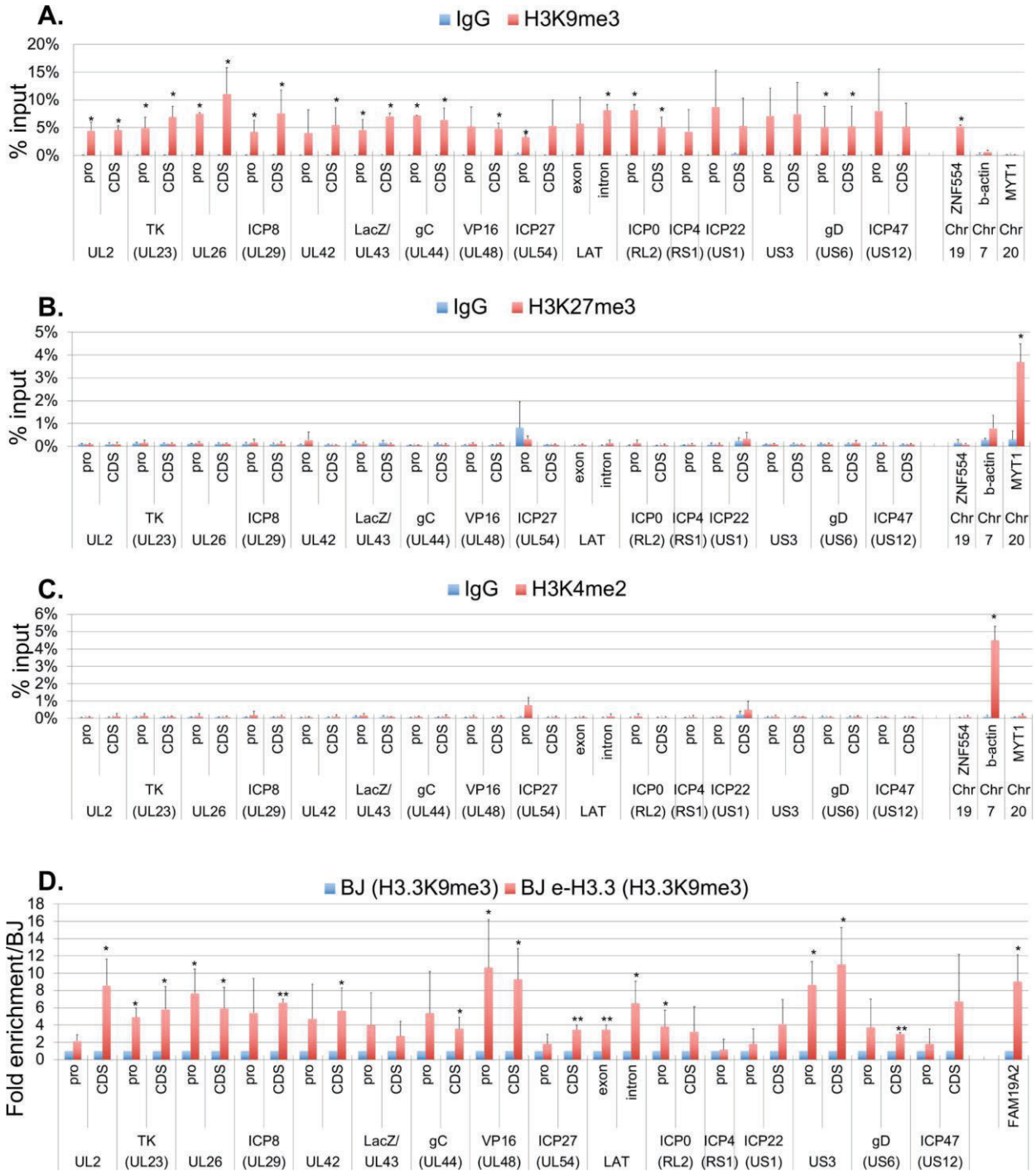


**Fig 5. The H3.3K9me3 chromatin mark is present on vDCP NBs-associated latent/quiescent HSV-1 genomes.** (A-C) ChIP against H3K9me3 (A), H3K27me3 (B), and H3K4me2 (C) performed in *in*1374-infected e-H3.3-expressing BJ cells at 24 hpi. Cellular loci zinc-finger protein 554 (ZNF554), ß-actin, and myelin transcription factor 1(MYT1) are positive controls for association with H3K9me3, H3K4me2 and H3K27me3, respectively. Means from three independent experiments ± SD. The

Student's t-test was applied to assess the significance of the results. * = p< 0.05, ** = p< 0.01. (D) Re-ChIP performed in in1374-infected normal BJ cells (blue), and e-H3.3-expressing BJ cells (red) at 24 hpi. First antibody: anti-H3K9me3, and second antibody: anti-HA against e-H3.3. Cellular locus, family with sequence similarity 19 member A2 (FAM19A2) is a positive control for association with H3.3K9me3 (GEO accession numbers: GSM1358809 (H3.3), and GSM1289412 (H3K9me3)). Means from three independent experiments ± SD. The Student's t-test was applied to assess the significance of the results. * = p< 0.05, ** = p< 0.01.

https://doi.org/10.1371/journal.ppat.1007313.g005

the H3.3 association with latent/quiescent viral genomes, we performed ChIP on *in*1374-infected control MEF $pml^{+/+}$ or MEF $pml^{-/-}$ cells previously engineered by lentiviral transduction to express e-H3.3 (Fig 9E). The data confirmed the impaired association of e-H3.3 with latent/quiescent HSV-1 genomes in the absence of PML, with 26/31 (84%) viral loci significantly impacted (Fig 9F). Cellular loci acid Sensing Ion Channel Subunit 2 (Asic2), and Heme Oxygenase 1 (Hmox1) were used respectively as positive and negative controls for deposition of H3.3 in the absence of Pml as described in [44]. To definitively attribute the lack of deposition of H3.3 on viral loci to the absence of PML, MEF $pml^{-/-}$;e-H3.3 cells were engineered to allow re-expression, under doxycycline induction, of the isoform I of human PML (PML.I) (Fig9G), which was shown to participate to the HSV-1 antiviral restriction mechanism [65]. The formation of PML NBs after induction of PML.I was visualized by IF (Fig 9H). ChIPs were then performed on *in*1374-infected MEF $pml^{-/-}$;e-H3.3;myc-PML.I cells previously treated or not with doxycycline (Fig 9I). The data showed that the re-expression of PML.I allowed the re-loading of H3.3 on all the analyzed loci of the latent/quiescent viral genomes with significant results obtained for 21 loci over 31 (68%), demonstrating the essential role of PML/PML NBs in the association of H3.3 with incoming viral genomes. Finally, we wanted to analyze whether the deficit of the H3.3 association with the viral genome in the absence of PML could be compensated by an increase of H3.1 on viral loci. The data from BJ e-H3.1 cells depleted for PML or MEF $pml^{-/-}$;e-H3.1 cells, and infected with *in*1374 showed that H3.1 did not replace H3.3 on the viral loci (S12A and S12B Fig). Altogether, these data demonstrate the essential role of PML NBs, probably through the DAXX/ATRX complex activity, in the exclusive H3.3 chromatinization of incoming viral genomes forced to adopt a vDCP NB-associated latent/quiescent pattern due to a deficit in the onset of lytic cycle.

## The destabilization of vDCP NBs induces the recovery of HSV-1 transcriptional activity and the formation of replication compartments

vDCP NB-associated latent genomes have been shown to be transcriptionally silent for the LAT expression *in vivo* [16], and for the expression of a reporter gene *in vitro* in mouse TG neuron cultures [17], and in human primary fibroblasts [45]. Moreover, it is known that the viral protein ICP0 induces the destabilization of PML NBs [66] and is essential for HSV-1 reactivation *in vivo* [67], and for the transcriptional de-repression of a silenced viral genome *in vitro* [45,59,60]. However, it is not known if the transcriptional recovery is correlated to the destabilization of the vDCP NBs. We analyzed if latent HSV-1 genomes trapped in vDCP NBs were definitively silenced or could resume a transcriptional program leading to replication of viral genomes provided that vDCP NBs were destabilized. ICP0 or its non-functional RING finger mutant (ICP0ΔRF) were expressed from BJ-eTetR/cICP0 or BJ-eTetR/cICP0ΔRF cells harboring vDCP NBs for 4 days (Fig 10). HSV-1 *in*1374 infected BJ-eTetR cells were used as controls. Expression of ICP0 or ICP0ΔRF was induced for 24 h, 48 h or 72h at the permissive temperature for *in*1374 replication (32˚C) (S13 Fig). Transcription of the reporter (LacZ) gene was measured by RT-qPCR to analyze the transcriptional recovery of the vDCP NB-associated latent/quiescent viral genomes (Fig 10A). The addition of doxycycline in infected BJ-eTetR or BJ-eTetR/c ICP0ΔRF cells did not lead to any significant transcription of the LacZ gene. Only infected BJ-eTetR/cICP0 showed the recovery of LacZ mRNA transcription from 24 h post

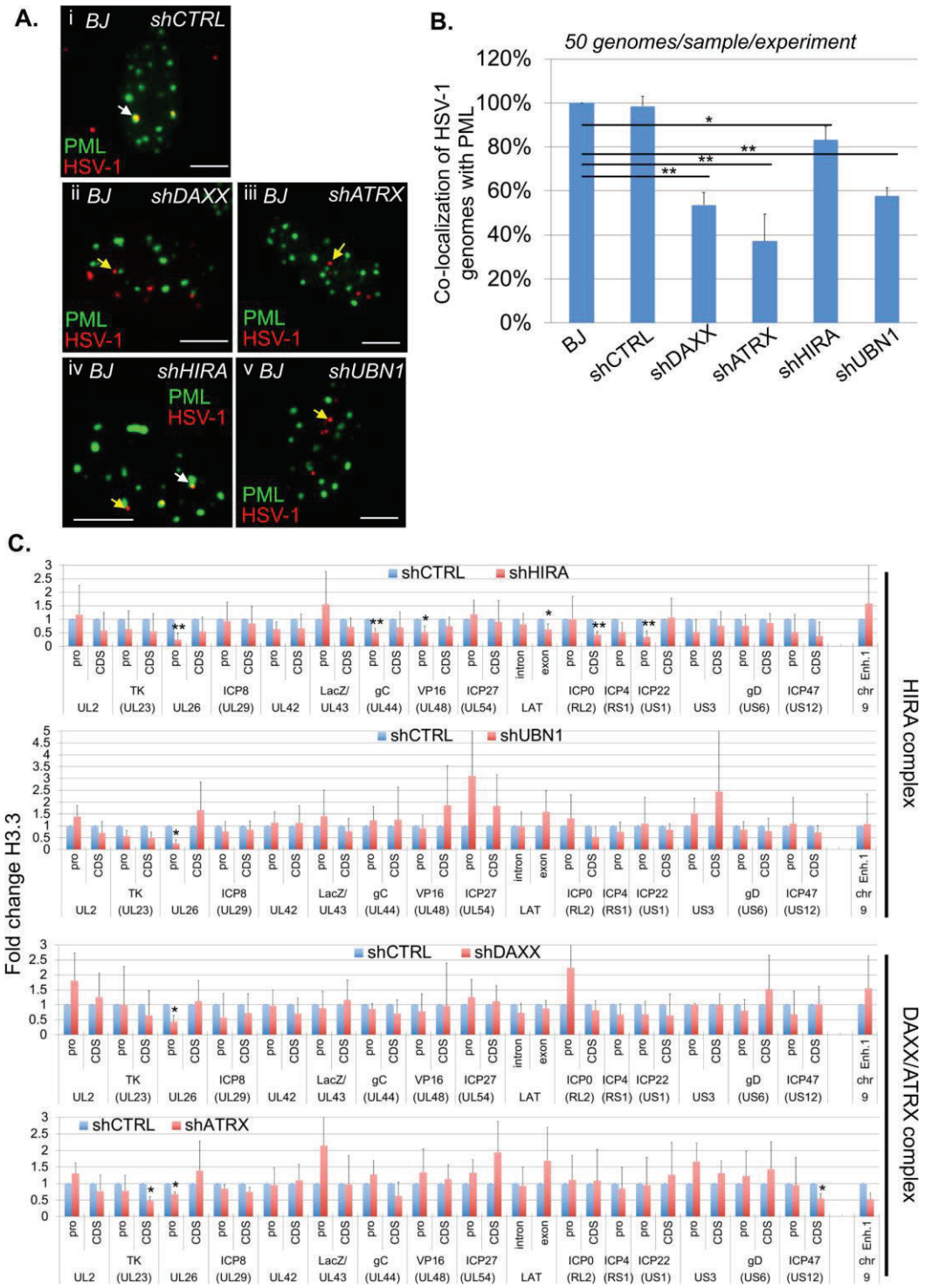
A.
i BJ shCTRL
PML
HSV-1
ii BJ shDAXX
iii BJ shATRX
iv BJ shHIRA
v BJ shUBN1
B.
50 genomes/sample/experiment
Co-localization of HSV-1 genomes with PML
120%
100%
80%
60%
40%
20%
0%
BJ
shCTRL
shDAXX
shATRX
shHIRA
shUBN1
C.
shCTRL
shHIRA
shUBN1
shDAXX
shATRX
Fold change H3.3
HIRA complex
DAXX/ATRX complex
pro
CDS
intron
exon
TK (UL23)
UL26
ICP8 (UL29)
UL42
LacZ/ UL43
gC (UL44)
VP16 (UL48)
ICP27 (UL54)
LAT
ICP0 (RL2)
ICP4 (RS1)
ICP22 (US1)
US3
gD (US6)
ICP47 (US12)
Enh.1
chr 9

**Fig 6. Individual inactivation of DAXX, ATRX, HIRA, or UBN1 significantly affects the formation of vDCP NBs, but only mildly affects the association of H3.3 with the latent/quiescent HSV-1 genome.** Normal or e-H3.3-expressing BJ cells were first transduced with shRNA-expressing lentiviruses before *in*1374 infection. (A) Immuno-FISH performed in BJ cells infected with *in*1374 for 24 h. PML (green) and HSV-1 genomes (red) were detected in lentivirus-transduced BJ cells expressing control (shCTRL) or targeted shRNAs. Scale bars = 5 μm. (B) Quantifications of the immuno-FISH performed in (A). Means from three independent experiments ± SD. The Student's *t*-test was applied to assess the significance of the results. * = p< 0.05, ** = p< 0.01 (see S4 Table for data). (C) ChIP for the detection of e-H3.3 associated with HSV-1 genomes and performed in e-H3.3-expressing BJ cells infected with *in*1374 for 24 h and previously transduced with a lentivirus expressing a control shRNA (shCTRL, blue) or a targeted shRNA (red). Anti-HA antibody was used for the ChIP experiments. The analyzed viral loci were described previously. Means from three independent experiments ± SD. The Student's *t*-test was applied to assess the significance of the results. * = p< 0.05.

https://doi.org/10.1371/journal.ppat.1007313.g006

addition of doxycycline. To analyze if the virus could sustain replication, as suggested by the observation of the BJ-eTetR/cICP0 cell monolayer (S14 Fig), following vDCP NB destabilization, immuno-FISH were performed at 24 h and 48 h post-addition of doxycycline. BJ-eTetR/

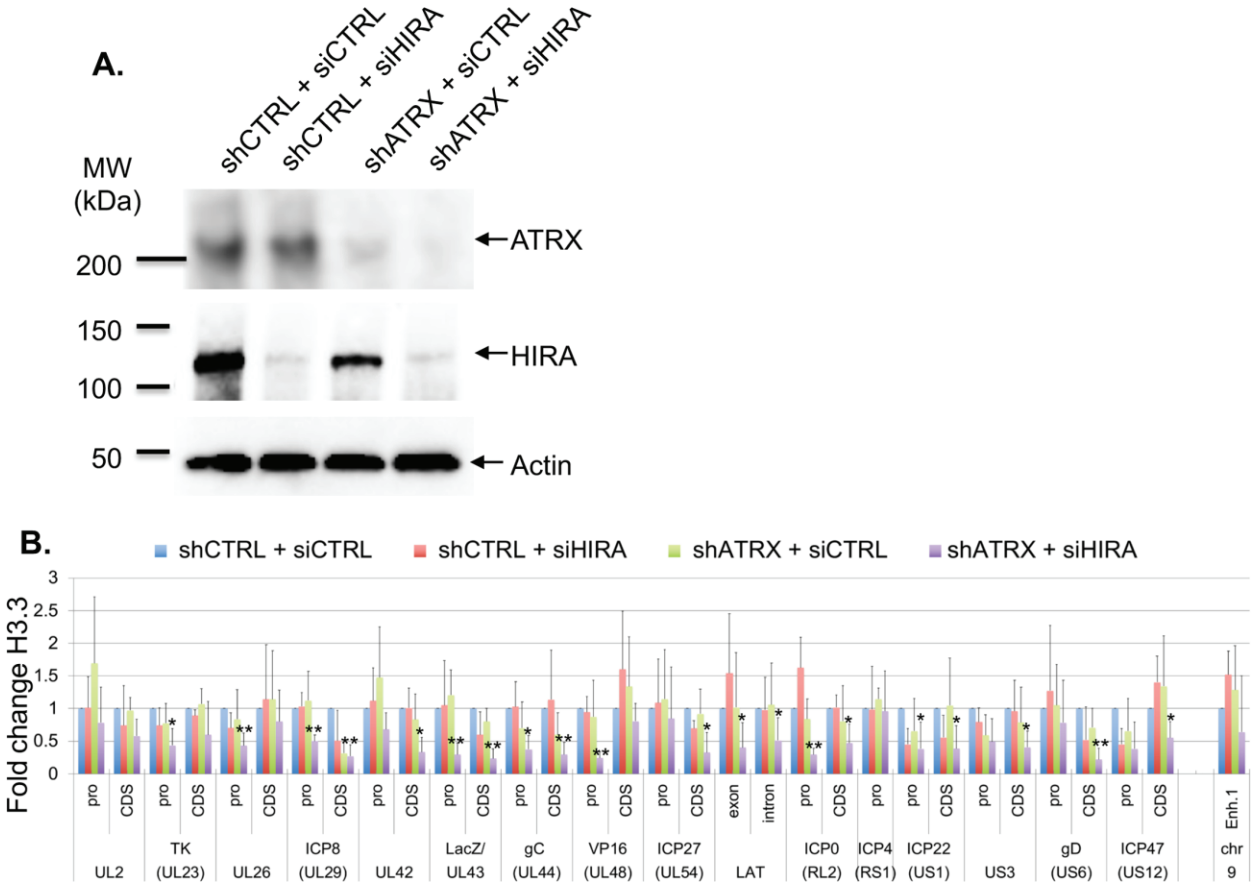


**Fig 7. Functional inactivation of both DAXX/ATRX and HIRA complexes significantly affects the association of H3.3 with multiple loci of the latent/quiescent HSV-1 genome.** (A) WB for the detection of ATRX and HIRA proteins in e-H3.3-expressing BJ cells. Cells were first transduced with a lentivirus expressing a control shRNA (shCTRL) or a shRNA against ATRX (shATRX) for 4 days. Then control siRNA (siCTRL) or HIRA siRNA (siHIRA) was transfected for 36 h. Actin was detected as a loading control. (B) ChIP for the detection of e-H3.3 associated with HSV-1 genomes and performed in e-H3.3-expressing BJ cells infected with *in*1374 for 24 h. Cells were processed with shRNAs-expressing lentiviruses then siRNAs similarly to (A), then infected with *in*1374 for 24 h. Anti-HA antibody was used for the ChIP experiments. The analyzed viral loci were described previously. Cellular loci Enhancer 1 (Enh.1) is a cellular control for deposition of H3.3. Means from three independent experiments ± SD. The Student's *t*-test was applied to assess the significance of the results. * = p< 0.05, ** = p< 0.01.

https://doi.org/10.1371/journal.ppat.1007313.g007

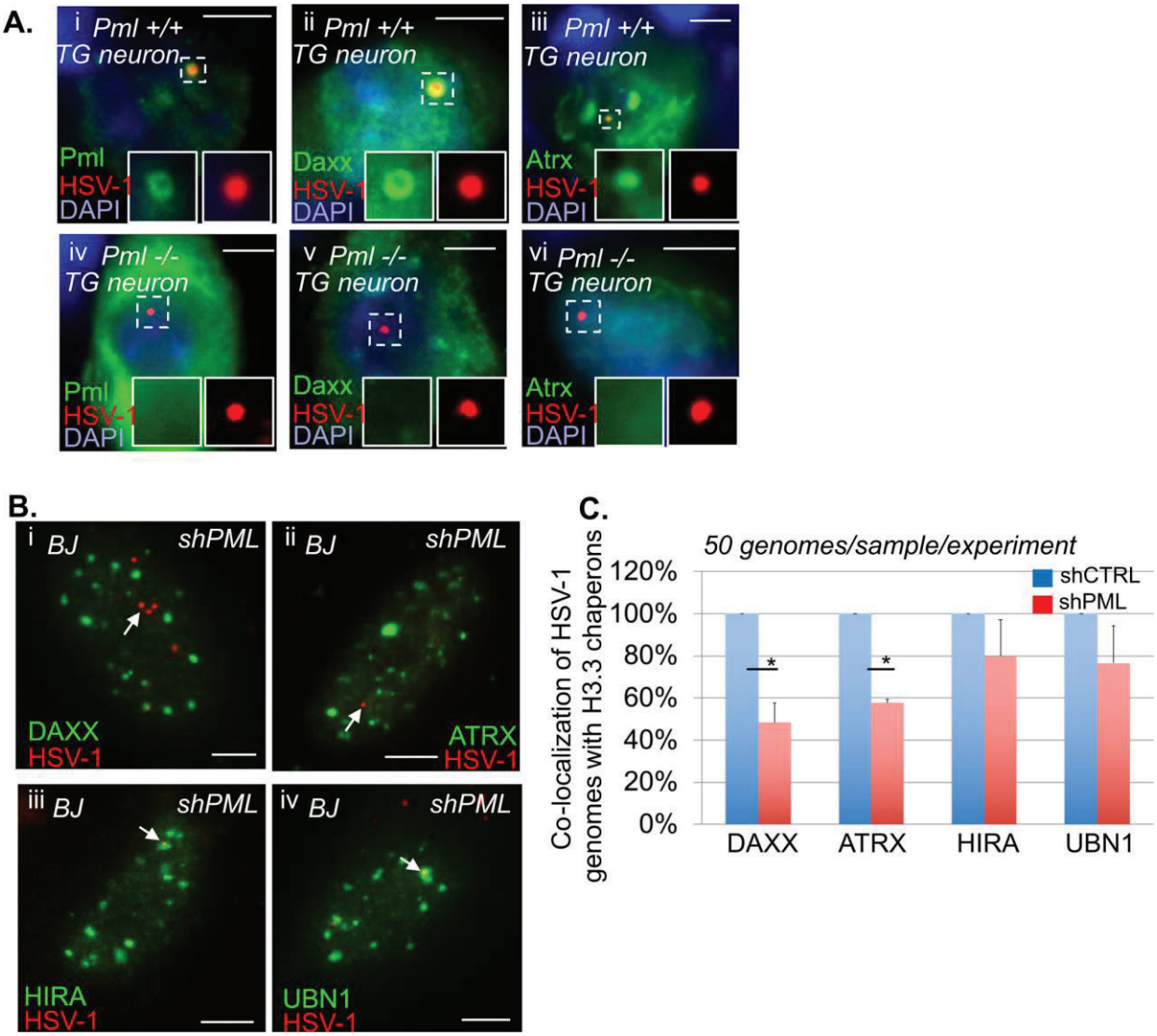


**Fig 8. Absence of PML decreases the co-localization of DAXX and ATRX but not HIRA and UBN1 with latent/quiescent HSV-1 genomes.** (A) Immuno-FISH performed in TG tissues from *pml*$^{+/+}$ and *pml*$^{-/-}$ infected mice at 28 dpi. Pml, Daxx, Atrx (green), and HSV-1 genomes (red) were detected. Nuclei were detected with DAPI (blue). Scale bars = 10 μm. (B) Immuno-FISH performed in BJ cells depleted of PML by transduction with a PML-targeted shRNA-expressing lentivirus, and subsequently infected with *in*1374 for 2 days. DAXX, ATRX, HIRA or UBN1 (green), and HSV-1 genomes (red) were detected. Scale bars = 5 μm. (C) Quantification of the immuno-FISH performed in (B). Means from three independent experiments ± SD. The Student's *t*-test was applied to assess the significance of the results. * = $p < 0.05$ (See S5 Table for data).

https://doi.org/10.1371/journal.ppat.1007313.g008

cICP0 cells (Fig 10B) but not BJ-eTetR/cICP0ΔRF (S15 Fig) showed a clear disappearance of the vDCP NBs. Concomitantly, only BJ-eTetR/cICP0 cells showed the formation of replication compartments (RCs) indicating that the virus is in the process of lytic phase following vDCP NBs destruction by ICP0. To confirm that the lytic transcriptional program was indeed occurring, viral transcripts of all kinetics were analyzed (Fig 10C). Twenty four and 48 h post ICP0

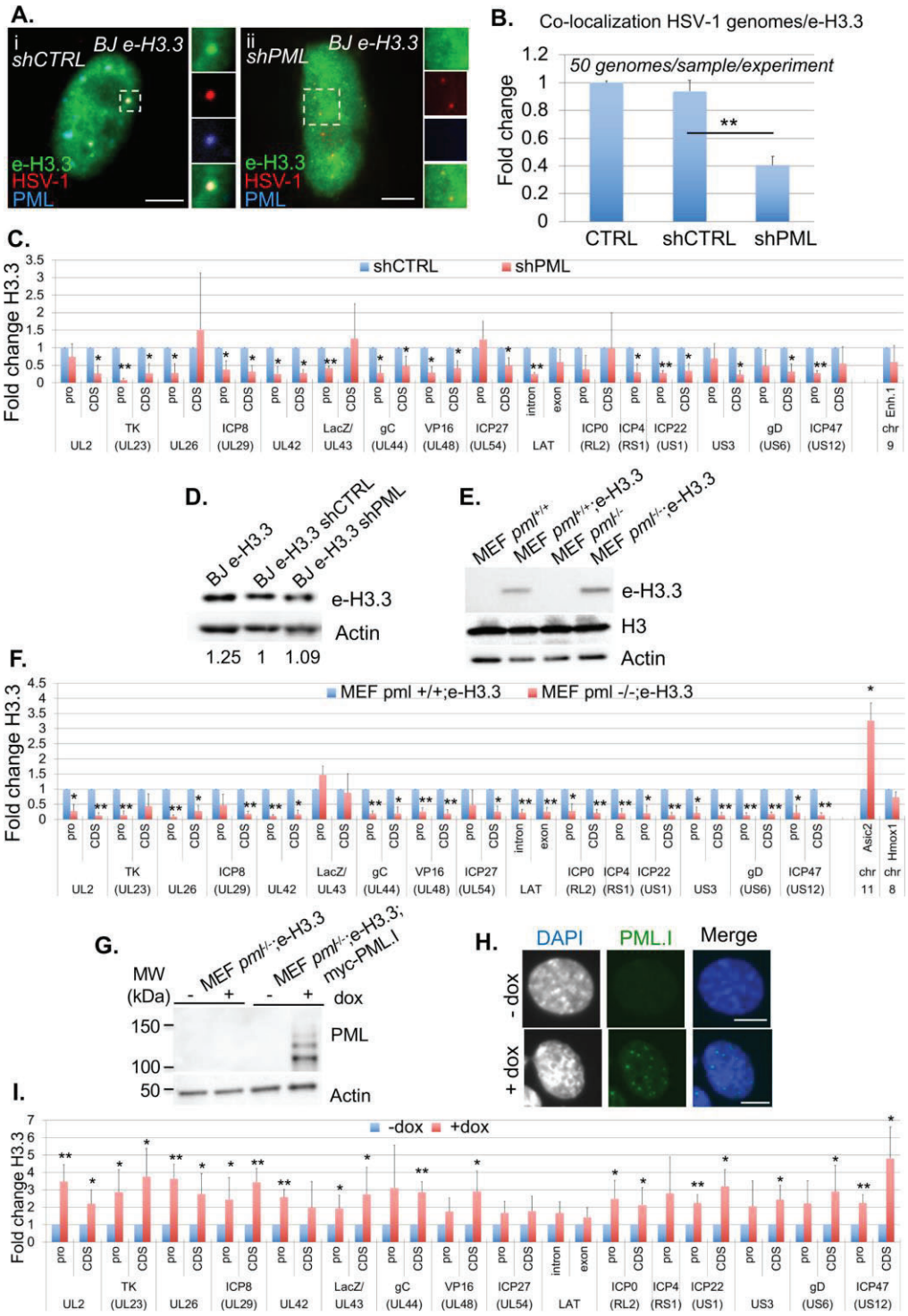
A.
i shCTRL BJ e-H3.3
ii shPML BJ e-H3.3
e-H3.3
HSV-1
PML
B. Co-localization HSV-1 genomes/e-H3.3
50 genomes/sample/experiment
Fold change
CTRL shCTRL shPML
C.
Fold change H3.3
shCTRL shPML
UL2 TK (UL23) UL26 ICP8 (UL29) UL42 LacZ/ UL43 gC (UL44) VP16 (UL48) ICP27 (UL54) LAT ICP0 (RL2) ICP4 (RS1) ICP22 (US1) US3 gD (US6) ICP47 (US12) chr 9
D.
BJ e-H3.3
BJ e-H3.3 shCTRL
BJ e-H3.3 shPML
e-H3.3
Actin
1.25 1 1.09
E.
MEF pml+/+
MEF pml+/+;e-H3.3
MEF pml-/-
MEF pml-/-;e-H3.3
e-H3.3
H3
Actin
F.
Fold change H3.3
MEF pml +/+;e-H3.3
MEF pml -/-;e-H3.3
UL2 TK (UL23) UL26 ICP8 (UL29) UL42 LacZ/ UL43 gC (UL44) VP16 (UL48) ICP27 (UL54) LAT ICP0 (RL2) ICP4 (RS1) ICP22 (US1) US3 gD (US6) ICP47 (US12) chr 11 chr 8
G.
MW (kDa)
MEF pml-/-;e-H3.3
MEF pml-/-;e-H3.3; myc-PML.I
dox
150
100
50
PML
Actin
H.
DAPI
PML.I
Merge
- dox
+ dox
I.
Fold change H3.3
-dox +dox
UL2 TK (UL23) UL26 ICP8 (UL29) UL42 LacZ/ UL43 gC (UL44) VP16 (UL48) ICP27 (UL54) LAT ICP0 (RL2) ICP4 (RS1) ICP22 (US1) US3 gD (US6) ICP47 (US12)

**Fig 9. Depletion of PML significantly impacts the association of H3.3 with latent/quiescent HSV-1 genomes.** (A) Immuno-FISH performed in e-H3.3-expressing BJ cells transduced with a control (shCTRL) or PML (shPML) shRNA-expressing lentivirus and subsequently infected with *in*1374 for 2 days. E-H3.3 (green), HSV-1 genomes (red), and PML (blue) were detected. Scale bars = 5 μm. (B) Quantification of the immuno-FISH performed in (A). Means from three independent experiments ± SD. The Student's *t*-test was applied to assess the significance of the results. ** = p< 0.01. (C) ChIP for the detection of e-H3.3 associated with HSV-1 genomes and performed in e-H3.3-expressing BJ cells infected with *in*1374 for 24 h and previously transduced with a lentivirus expressing a control shRNA (shCTRL, blue) or a PML shRNA (shPML, red). Anti-HA antibody was used for the ChIP experiments. The analyzed viral loci were described previously. Means from three independent experiments ± SD. The Student's *t*-test was applied to assess the significance of the results. * = p< 0.05 (D) WB for the detection of e-H3.3 in control e-H3.3-expressing BJ cells (CTRL) or e-H3.3-expressing BJ cells transduced with a lentivirus expressing a control shRNA (shCTRL) or a PML shRNA (shPML). Actin was detected as a loading control. (E) WB for the detection of e-H3.3 in control and e-H3.3-expressing MEF $pml^{+/+}$ or $pml^{-/-}$ cells. Actin and total histone H3 were detected as loading controls. (F) ChIP for the detection of e-H3.3 associated with HSV-1 genomes, and performed in e-H3.3-expressing $pml^{+/+}$ (blue) or $pml^{-/-}$ (red) MEF cells infected with *in*1374 for 24 h. Anti-HA antibody was used for the ChIP experiments. Analyzed viral loci were described previously. Cellular loci acid Sensing Ion Channel Subunit 2 (Asic2) and Heme Oxygenase 1 (Hmox1) are positive and negative controls for deposition of H3.3 in the absence of Pml, respectively (see *[44]*). Means from three independent experiments ± SD. The Student's *t*-test was applied to assess the significance of the results. * = p< 0.05, ** = p< 0.01. (G) WB for the detection of ectopically-expressed human PML in MEF $pml^{-/-}$;e-H3.3 or MEF $pml^{-/-}$;e-H3.3;myc-PML.I cells not treated (-) or treated (+) with doxycycline for 24 h. Anti-human PML was used for the detection of PML. Actin was detected as a loading control. (H) IF for the detection of PML NBs (green) and nuclei (gray/blue) in MEF $pml^{-/-}$;e-H3.3;myc-PML.I cells not treated (- dox) or treated (+ dox) with doxycycline for 24 h. PML was detected using the anti myc antibody. Scale bars = 5 μm. (I) ChIP for the detection of e-H3.3 associated with HSV-1 genomes and performed in MEF $pml^{-/-}$;e-H3.3;myc-PML.I cells not treated (- dox) or treated (+ dox) with doxycycline for 24 h then infected with in1374 for 24 h in the presence of dox. Anti-HA antibody was used for the ChIP experiments. Analyzed viral loci were described previously. Means from three independent experiments ± SD. Student's t-test was applied to assess the significance of the results. * = p< 0.05, ** = p < 0.01.

https://doi.org/10.1371/journal.ppat.1007313.g009

induction, lytic genes were expressed with a clear switch towards the γ genes (UL44/gC and US6/gD) at 48 h confirming the onset of the lytic transcriptional program. Expression of ICP0ΔRF did not enable the re-expression of viral genes. These data show that vDCP NBs-associated latent/quiescent HSV-1 genomes can resume transcription and a lytic program provided that the vDCP NBs are destabilized, suggesting that these genomes are not definitively silenced, and could participate to the reactivation process of HSV-1.

## Discussion

The HSV-1 genome enters the nucleus of infected neurons, which support HSV-1 latency as a naked/non-nucleosomal DNA. Many studies have described the acquisition of chromatin marks on the viral genome concomitantly to the establishment, and during the whole process, of latency. Paradoxically, although it is undisputable that these chromatin marks will predominantly be associated with latency and reactivation, few data are available for the initiation of the chromatinization of the incoming viral genome. Here, we demonstrate the essential contribution of PML NBs in the process of chromatinization of incoming HSV-1 genomes meant to remain in a latent/quiescent state. We showed that PML NBs are essential for the association of the histone variant H3.3 with the latent/quiescent HSV-1.

Two members of the HIRA complex, HIRA and ASF1a, were previously shown to be involved in H3.3-dependent chromatinization of HSV-1 genomes at early times after infection in non-neuronal and non-primary cells favoring the onset of the lytic cycle [68,69]. Moreover a recent study highlighted the interaction of HIRA with quiescent HSV-1 and plasmid DNA in primary human fibroblasts [56]. Our *in vivo* data in TG neurons and *in vitro* data in infected human primary fibroblasts or adult mice TG neuron cultures, show that all the proteins of the HIRA complex accumulate within specific nucleoprotein structures called the viral DNA-containing PML NBs or vDCP NBs. vDCP NBs contain transcriptionally silent HSV-1 genome that we previously demonstrated *in vivo* to be associated with the establishment of latency from the early steps of neuron infection [17]. Additionally, our data show that: (i) the mouse Hira protein, *in vivo*, and all the components of the HIRA complex, in cultured cells, temporarily accumulate in vDCP NBs, and (ii) significantly greater amount of incoming HSV-1

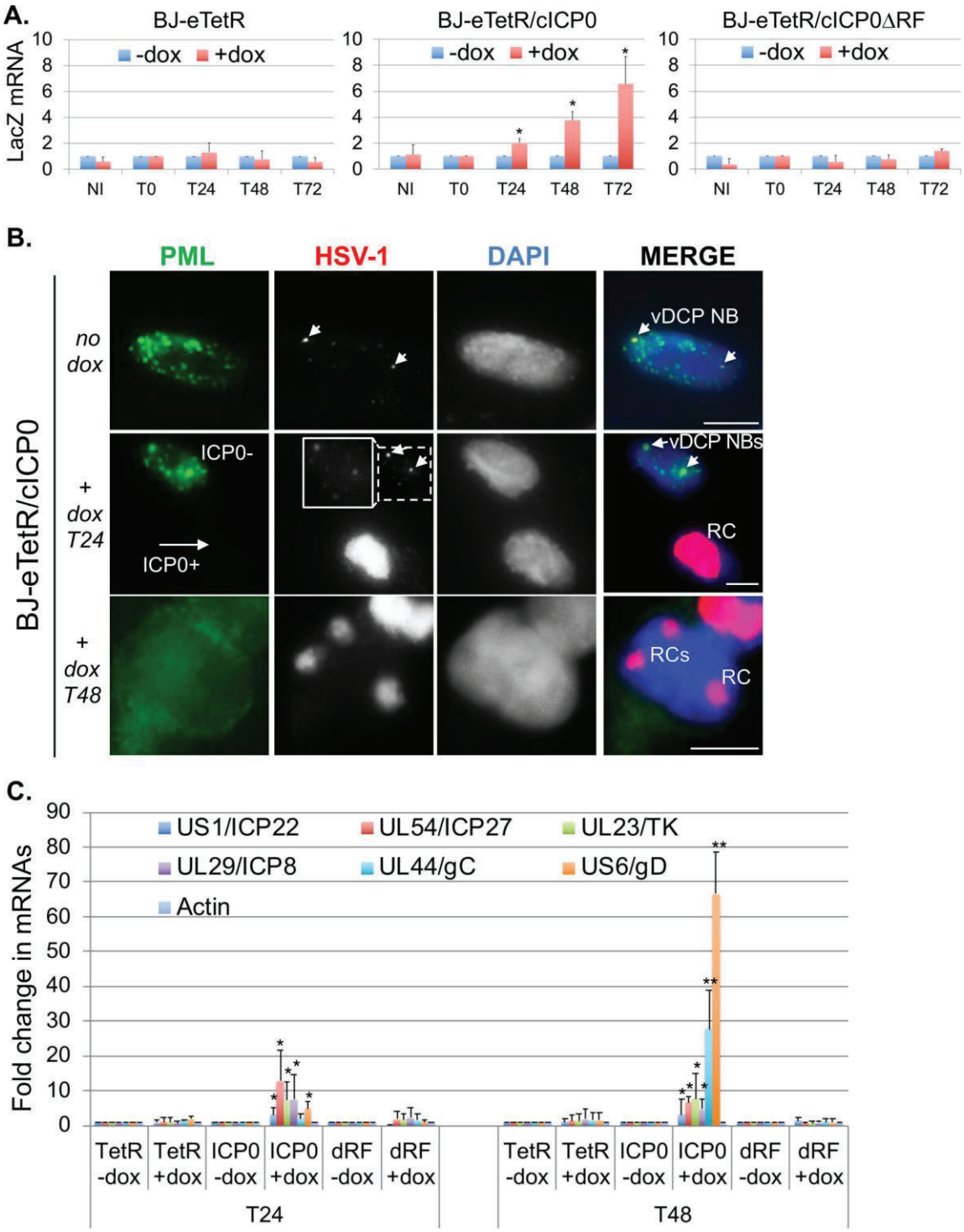
A.
BJ-eTetR
BJ-eTetR/cICP0
BJ-eTetR/cICP0ΔRF
-dox
+dox
LacZ mRNA
NI
T0
T24
T48
T72
B.
PML
HSV-1
DAPI
MERGE
BJ-eTetR/cICP0
no dox
+ dox T24
+ dox T48
vDCP NB
ICP0-
ICP0+
vDCP NBs
RC
RCs
C.
US1/ICP22
UL54/ICP27
UL23/TK
UL29/ICP8
UL44/gC
US6/gD
Actin
Fold change in mRNAs
TetR -dox
TetR +dox
ICP0 -dox
ICP0 +dox
dRF -dox
dRF +dox
T24
T48

**Fig 10. The destabilization of vDCP NBs induces the transcriptional recovery, and replication of vDCP NB-associated latent/quiescent HSV-1 genomes.** (A) RT-qPCR performed in BJ-eTetR, BJ-eTetR/cICP0 or BJ-eTetR/cICP0ΔRF cells infected with *in*1374 for 4 d at 38.5˚C, then treated (red) or not (blue) with doxycycline for 0 h (T0), 24 h (T24), 48 h (T48), or 72h (T72) at the permissive temperature (32˚C) for *in*1374 replication. Transcription of the LacZ reporter gene was analyzed. Means from three independent experiments ± SD. Student's *t*-test was applied to assess the significance of the results. * = $p < 0.05$. (B) Immuno-FISH performed in BJ-eTetR/cICP0 cells infected with *in*1374 for 4 d at 38.5˚C, then treated or not with doxycycline for 24 h (T24), or 48 h (T48) at 32˚C. PML (green), HSV-1 genomes (gray/red), and nuclei (DAPI, gray/blue) are detected. ICP0- and ICP0+ are detectable by the presence or not of PML NBs, respectively. The HSV-1 signal of the ICP0- cell in the + dox T24 is shown with two different set up to highlight the vDCP NBs-associated HSV-1 genomes compared to the cell showing the replication compartment (RC). Scale bars = 5 μm. (C) RT-qPCR performed in BJ-eTetR (TetR), BJ-eTetR/cICP0 (ICP0) or BJ-eTetR/cICP0ΔRF (dRF) cells infected with *in*1374 for 4 d at 38.5˚C, then treated (+dox) or not (-dox) with doxycycline for 24 h (T24), or 48 h (T48), at the permissive temperature (32˚C) for *in*1374 replication. Transcription of viral genes of different kinetics US1/ICP22, UL54/ICP27 (IE/α); UL23/TK, UL29/ICP8 (E/β); UL44/gC, US6/gD (L/γ) was analyzed. Actin gene was analyzed as a control. Means from three independent experiments ± SD. Student's *t*-test was applied to assess the significance of the results. * = $p < 0.05$, ** = $p < 0.01$.

https://doi.org/10.1371/journal.ppat.1007313.g010

genomes co-localize with HIRA compared with PML at very early times pi (30 min). These data suggest that the HIRA complex could also be involved to some extent in the establishment of HSV-1 latency by the initial recognition of the incoming naked/non-nucleosomal viral DNA and the chromatinization of non-replicative HSV-1 genomes intended to become latent. In this respect, a recent study suggested an anti-viral activity associated with HIRA against HSV-1 and murine cytomegalovirus lytic cycles [56]. To that extent, although they are both functionally essential for the activity of the HIRA complex [35,51,64,70], our data show that the depletion of HIRA has a greater effect compared to the UBN1 depletion, on the H3.3 association with the viral genomes. This could be simply explained by a better efficiency of the HIRA, compared to the UBN1, shRNAs. Alternatively, HIRA was shown to be recruited to UV-induced DNA damage independently of UBN1 (see figure S2D in [71]), and to participate to the loading of newly synthesized H3.3 on chromatin [72]. Therefore, the depletion of HIRA could indirectly and/or directly impact on two initial events occurring concomitantly to the entry of the viral genomes in the nucleus; first a signaling pathway associated to the detection of DNA breaks present in incoming viral DNA as suggested in [55,73]; and second the chromatinization process *per se*. If these two events are linked it could explain the differences observed between the HIRA and UBN1 depletion on the loading of H3.3 on the viral genomes. Experiments are in progress to investigate this.

Interestingly, proteins of the HIRA complex have been previously shown to be able to directly bind to naked DNA in a sequence-independent manner, in contrast to DAXX and ATRX [52]. Nevertheless, our ChIP data highlight the interaction of viral genomes with DAXX and ATRX, but we cannot assert that the two proteins directly interact with naked DNA. The gamma-interferon-inducible protein 16 (IFI16), a member of the PYHIN protein family, has been described as a nuclear sensor of incoming herpesviruses genomes, and suggested to promote the addition of specific chromatin marks that contribute to viral genome silencing [74–81]. A proteomic study determining the functional interactome of human PYHIN proteins revealed the possible interaction between ATRX and IFI16 [82]. Thus, it will be interesting to determine in future studies if IFI16 and H3.3 chaperone complexes physically and functionally cooperate in the process of chromatinization of the latent/quiescent HSV-1 genome.

One of the main finding of our study is the demonstration of the essential contribution of PML NBs in the H3.3-dependent chromatinization of the latent/quiescent HSV-1 genomes. A close link between PML NBs and H3.3 in chromatin dynamics has been demonstrated during oncogene-induced senescence (OIS). In OIS, expression of the oncogene H-RasV12 induces DAXX-dependent relocalization of neo-synthesized H3.3 in the PML NBs before a drastic reorganization of the chromatin to form senescence-associated heterochromatin foci [42,43]. Hence, the contribution of the PML NBs in the deposition of H3.3 on specific cellular chromatin loci has also been reported [43,44]. The present study shows that the absence of Pml in

HSV-1wt latently infected Pml KO mice, or the depletion of PML by shRNA in BJ cells infected with *in*1374, significantly affects the co-localization of DAXX and ATRX, but not HIRA and UBN1, with latent/quiescent HSV-1 genomes, confirming previous studies for DAXX and ATRX [45]. Taken together with the impaired association of H3.3 with the viral genomes in the absence of PML NBs, these data suggest that a significant part of the latent/quiescent HSV-1 genome chromatinization by H3.3 could occur through the activity of the DAXX/ATRX complex in association with the PML NBs.

Given the particular structure formed by the latent/quiescent HSV-1 genome with the PML NBs, our study raises the question of the possible acquisition of a chromatin structure within the vDCP NBs. The individual inactivation of DAXX, ATRX, HIRA, or UBN1 significantly impacts the co-localization of the latent/quiescent HSV-1 genomes with PML, and hence the formation of vDCP NBs. However, it only mildly affects the association of H3.3 with viral genomes, suggesting an absence of correlation between the formation of vDCP NBs and H3.3 chromatinization. However, our data show that the depletion of DAXX, ATRX, HIRA, or UBN1 does not modify the accumulation of e-H3.3 at PML NBs, leaving intact the upstream requirement of H3.3 accumulation in PML NBs for H3.3-dependent viral chromatin assembly. We have recently shown that vDCP NBs are dynamic structures that can fuse during the course of a latent infection [17]. It is thus possible that incoming viral genomes can be dynamically associated with vDCP NBs to be chromatinized, and in the absence of any of the H3.3 chaperone complex subunit, this dynamic can be perturbed, resulting in some viral genomes that do not show a co-localization with PML. Given that depletion of none of the four proteins affects the structure of the PML NBs, and considering the essential role of PML NBs in the H3.3 chromatinization of the viral genomes, this possibility cannot be ruled out. The depletion of H3.3, which almost exclusively participates in latent/quiescent HSV-1 genome chromatinization compared to H3.1/2, does not prevent the formation of vDCP NBs (S16 Fig), and is rather in favor of a chromatinization of the viral genome in the vDCP NBs. It is unlikely that canonical H3.1/2 could replace H3.3 for the chromatinization of the incoming HSV-1 genomes prior to the formation of the vDCP NBs. Indeed, our multiple immuno-FISH and ChIP assays failed to detect H3.1/2 and/or H3.1/2 chaperones that associate or co-localize with viral genomes. Nonetheless, we cannot rule out a possible replacement of H3.3 with another H3 variant for the chromatinization of viral genomes before their entrapment by the PML NBs to form vDCP NBs.

Our data show that the vDCP NBs-associated HSV-1 genomes are chromatinized with H3K9me3, and the Re-ChIP assays confirm an association with H3.3K9me3, but not H3K27me3. *In vivo*, it has been shown that both H3 modifications could be found on latent HSV-1 genomes [31,33,34]. One simple explanation could reside in the heterogeneity of latent genomes distribution within the nuclei of the infected neurons in the *in vivo* mouse and/or rabbit models of latency [16,17,54], however this would need to be formally demonstrated. Though, vDCP NBs-associated HSV-1 genomes remain compatible with the transcription of lytic genes provided that the vDCP NBs are destabilized by ICP0, a viral protein known to be required for full *in vivo* reactivation [67], and to erase chromatin marks associated with latent/quiescent viral genomes *in vitro* [59]. Therefore, vDCP NBs are not a dead end for the virus life cycle, and HSV-1 latently infected neurons containing vDCP NBs are likely to contribute to the process of reactivation.

Altogether, our study demonstrates the essential role of a PML NB/H3.3/H3.3 chaperone axis in the process of chromatinization of viral genomes adopting a vDCP NB pattern, which represents an essential structural and functional aspect of HSV-1 latency establishment. Given the involvement of H3.3 in the chromatinization of other latent herpesviruses belonging to different sub-families than HSV-1, such as EBV [83] and HCMV [58], as well as adenovirus type

5 [84], this pathway of chromatinization is likely to play a major role in the biology of the whole *Herpesviridae* family, and possibly of other DNA viruses such as adenoviruses, papillomaviruses, hepatitis B virus, and retroviruses.

## Materials and methods

### Ethics statement

All procedures involving experimental animals conformed to the ethical standards of the Association for Research in Vision and Ophthalmology (ARVO) statement for the use of animals in research and were approved by the local Ethics Committee of the Institute for Integrative Biology of the Cell (I2BC) and the Ethics Committee for Animal Experimentation (CEEA) 59 (Paris I) under number 2012–0047 and in accordance with European Community Council Directive 2010/63/EU. For animal experiments performed in the USA: animals were housed in American Association for Laboratory Animal Care-approved housing with unlimited access to food and water. All procedures involving animals were approved by the Children's Hospital Animal Care and Use Committee and were in compliance with the Guide for the Care and Use of Laboratory Animals (protocol number: IAUC2013-0162 of 2/28/2107).

### Virus strains, mice and virus inoculation, primary mouse TG neuron cultures, cells

The HSV-1 SC16 strain was used for mouse infections and has been characterized previously [85]. The HSV-1 mutant *in*1374 is derived from the 17 *syn* + strain and expresses a temperature-sensitive variant of the major viral transcriptional activator ICP4 [86] and is derived from *in*1312, a virus derived from the VP16 insertion mutant *in*1814 [87], which also carries a deletion/frameshift mutation in the ICP0 open reading frame [88] and contains an HCMV-*lacZ* reporter cassette inserted into the UL43 gene of *in*1312 [89]. This virus has been used and described previously [17,45]. All HSV-1 strains were grown in baby hamster kidney cell (BHK-21, ATCC, CCL-10) and titrated in human bone osteosarcoma epithelial cells (U2OS, ATCC, HTB-96). *In*1374 was grown and titrated at 32˚C in the presence of 3 mM hexamethylene bisacetamide [90].

PML wild-type, and knockout mice were obtained from the NCI Mouse Repository (NIH, http://mouse.ncifcrf.gov; strain, 129/Sv-*Pml*$^{tm1Ppp}$) [91]. Genotypes were confirmed by PCR, according to the NCI Mouse Repository guidelines with primers described in [16].

Mice were inoculated and TG processed as described previously [16]. Briefly, for the lip model: 6-week-old inbred female BALB/c mice (Janvier Labs, France) were inoculated with $10^6$ PFU of SC16 virus into the upper-left lip. Mice were sacrificed at 6 or 28 dpi. Frozen sections of mouse TG were prepared as described previously [16,92]. For the eye model: inoculation was performed as described previously [93]. Briefly, prior to inoculation, mice were anesthetized by intra-peritoneal injection of sodium pentobarbital (50 mg/kg of body weight). A 10-μL drop of inoculum containing $10^5$ PFU of 17syn+ was placed onto each scarified corneal surface. This procedure results in ~80% mouse survival and 100% infected TG.

Primary mouse TG neuron cultures were established from OF1 male mice (Janvier lab), following a previously described procedure [17]. Briefly, 6–8-week-old mice were sacrificed before TG removal. TG were incubated at 37˚C for 20 min in papain (25 mg) (Worthington) reconstituted with 5 mL Neurobasal A medium (Invitrogen) and for 20 min in Hank's balanced salt solution (HBSS) containing dispase (4.67 mg/mL) and collagenase (4 mg/mL) (Sigma) on a rotator, and mechanically dissociated. The cell suspension was layered twice on a five-step OptiPrep (Sigma) gradient, followed by centrifugation for 20 min at 800 *g*. The lower

ends of the centrifuged gradient were transferred to a new tube and washed twice with Neurobasal A medium supplemented with 2% B27 supplement (Invitrogen) and 1% penicillin–streptomycin (PS). Cells were counted and plated on poly-D-lysine (Sigma)- and laminin (Sigma)-coated, eight-well chamber slides (Millipore) at a density of 8,000 cells per well. Neuronal cultures were maintained in complete neuronal medium consisting of Neurobasal A medium supplemented with 2% B27 supplement, 1% PS, L-glutamine (500 μM), nerve growth factor (NGF; 50 ng/mL, Invitrogen), glial cell-derived neurotrophic factor (GDNF; 50 ng/mL, PeproTech), and the mitotic inhibitors fluorodeoxyuridine (40 μM, Sigma) and aphidicolin (16.6 μg/mL, Sigma) for the first 3 days. The medium was then replaced with fresh medium without fluorodeoxyuridine and aphidicolin.

Primary human foreskin (BJ, ATCC, CRL-2522), lung (IMR-90, Sigma, 85020204), fetal foreskin (HFFF-2, European Collection of Authenticated Cell Cultures, ECACC 86031405, kind gift from Roger Everett, CVR-University of Glasgow) fibroblast cells, primary human hepatocyte (HepaRG, HPR101, kind gift from Olivier Hantz & Isabelle Chemin, CRCL, Lyon, France) cells, human embryonic kidney (HEK 293T, ATCC CRL-3216, kind gift from M. Stucki, University Hospital Zürich) cells, U2OS, mouse embryonic fibroblast (MEF) $pml^{+/+}$, MEF $pml^{-/-}$ cells (kind gift from Valérie Lallemand, Hopital St Louis, Paris), and BHK-21 cells were grown in Dulbecco's Modified Eagle's Medium (DMEM) supplemented with 10% fetal bovine serum (Sigma, F7524), L-glutamine (1% v/v), 10 U/mL penicillin, and 100 mg/mL streptomycin. BJ cell division is stopped by contact inhibition. Therefore, to limit their division, cells were seeded at confluence before being infected at a multiplicity of infection (m.o.i.) of 3, and then maintained in 2% serum throughout the experiment. Infections of BJ cells for short times (from 30 min to 6 h) were performed by synchronizing the infection process with a pre-step of virus attachment to the cells at 4˚C for one hour. The infection medium was then removed, and the temperature was shifted to 37˚C to allow a maximum of viruses to simultaneously penetrate into the cells.

## Frozen sections

Frozen sections of mouse TG were generated as previously described [92]. Mice were anesthetized at 6 or 28 d.p.i., and before tissue dissection, mice were perfused intracardially with a solution of 4% formaldehyde, 20% sucrose in 1X PBS. Individual TG were prepared as previously described [92], and 10-μm frontal sections were collected in three parallel series and stored at -80˚C.

## DNA-FISH and immuno-DNA FISH

HSV-1 DNA FISH probes consisting of cosmids 14, 28 and 56 [94] comprising a total of ~90 kb of the HSV-1 genome were labeled by nick-translation (Invitrogen) with dCTP-Cy3 (GE Healthcare) and stored in 100% formamide (Sigma). The DNA-FISH and immuno-DNA FISH procedures have been described previously [16,92]. Briefly, infected cells or frozen sections were thawed, rehydrated in 1x PBS and permeabilized in 0.5% Triton X-100. Heat-based unmasking was performed in 100 mM citrate buffer, and sections were post-fixed using a standard methanol/acetic acid procedure and dried for 10 min at RT. DNA denaturation of the section and probe was performed for 5 min at 80˚C, and hybridization was carried out overnight at 37˚C. Sections were washed 3 x 10 min in 2 x SSC and for 3 x 10 min in 0.2 x SSC at 37˚C, and nuclei were stained with Hoechst 33258 (Invitrogen). All sections were mounted under coverslips using Vectashield mounting medium (Vector Laboratories) and stored at 4˚C until observation.

For immuno-DNA FISH, cells or frozen sections were treated as described for DNA-FISH up to the antigen-unmasking step. Tissues were then incubated for 24 h with the primary

antibody. After three washes, secondary antibody was applied for 1 h. Following immunostaining, the cells were post-fixed in 1% PFA, and DNA FISH was carried out from the methanol/acetic acid step onward.

The same procedures were used for infected neuronal cultures except that the cells were fixed in 2% PFA before permeabilization.

## Western blotting

Cells were collected in lysis buffer (10 mM Tris-EDTA, pH 8.0) containing a protease inhibitor cocktail (Complete EDTA-free; Roche) and briefly sonicated. Protein extracts were homogenized using QiaShredders (Qiagen). The protein concentration was estimated by the Bradford method. Extracted proteins were analyzed by Western blotting using appropriate antibodies (see below).

## Microscopy, imaging, and quantification

Observations and most image collections were performed using an inverted Cell Observer microscope (Zeiss) with a Plan-Apochromat ×100 N.A. 1.4 objective and a CoolSnap HQ2 camera from Molecular Dynamics (Ropper Scientific) or a Zeiss LSM 800 confocal microscope. Raw images were processed using ImageJ software (NIH).

## Lentivirus and retrovirus production and establishment of cell lines

BJ or MEF cell lines expressing H3.1-SNAP-HAx3 (e-H3.1), H3.3-SNAP-HAx3 (e-H3.3), or Myc-hDAXX were established by retroviral transduction [95]. Briefly, pBABE plasmids encoding H3.1-SNAP-HAx3 or H3.3-SNAP-HAx3 (gift from Dr L. Jansen), pLNCX2 encoding Myc-hDAXX [43], were co-transfected with pCL-ampho (for subsequent transduction of BJ cells, kind gift from M. Stucki, University Hospital Zürich) or pCL-eco (for subsequent transduction of MEF cells, kind gift from M. Stucki, University Hospital Zürich) plasmids [96] by the calcium phosphate method into HEK 293T cells to package retroviral particles [97]. BJ cells stably expressing HIRA-HA and HA-UBN1 or transiently expressing the shRNAs were established by lentiviral transduction. Briefly, pLenti encoding HIRA-HA or HA-UBN1, pLKOneo.CMV.EGFPnlsTetR, pLKO.DCMV.TetO.cICP0, pLKO.DCMV.TetO.cICP0ΔRF (gift from Dr. R. D. Everett, [98]), pLVX-TetOne-Myc-PML.I (issued from pLNGY-PML.I, gift from Dr. R. D. Everett [65]), pLKO empty, pLKO shPML_01, 02, shDAXX_01, 02, shATRX_01, 02, shHIRA_01, 02, shUBN1_01, 02, were co-transfected with psPAX.2 (Addgene #12260) and pMD2.G (Addgene #12259) plasmids by the calcium phosphate method into HEK 293T cells to package lentiviral particles. After 48 h, supernatant containing replication-incompetent retroviruses or lentiviruses was filtered and applied for 24 h on the target BJ or MEF cells in a medium containing polybrene 8 μg/mL (Sigma) [95]. Stable transfectants were selected with Blasticidin S (5 μg/mL, Invivogen), puromycin (1 μg/mL, Invivogen), or neomycin (G418, 1 mg/mL, Millipore) for 3 days, and a polyclonal population of cells was used for all experiments. Target sequences of the shRNA-expressing plasmids are provided in Table 1.

## ChIP and quantitative PCR

Cells were fixed with methanol-free formaldehyde (#28908, Thermo Fisher Scientific) 1% for 5 min at RT, and then glycine 125 mM was added to arrest fixation for 5 min. After two washes with ice-cold PBS, the cells were scraped and resuspended in "Lysis Buffer" (10% glycerol, 50mM HEPES pH7,5; 140mM NaCl; 0,8% NP40;0,25% Triton; 1mM EDTA, Protease Inhibitor Cocktail 1X (PIC) (Complete EDTA-free; Roche) and incubated for 10 min at 4˚C under

**Table 1. Characteristics of the shRNA-expressing plasmids.**

| Plasmids | Origin | Target sequences |
|---|---|---|
| pLKO1-puro shCTRL | Sigma SHC002 lot 01181209MN | CCGGCAACAAGATGAAGAGCACCAA |
| pLKO1-puro shPML_01 | Sigma TRCN 0000003867 NM_002675 x-1497s1c1 | GCCAGTGTACGCCTTCTCCAT |
| pLKO1-puro shPML_02 | Sigma TRCN 0000003869 NM_002675 x-1501s1c1 | GTGTACGCCTTCTCCATCAAA |
| pLKO1-puro shATRX_01 | Sigma TRCN 0000013590 NM_00489 2-2215s1c1 | CGACAGAAACTAACCCTGTAA |
| pLKO1-puro shATRX_02 | Sigma TRCN 0000342811 NM_00489 3-2357s21c1 | GATAATCCTAAGCCTAATAAA |
| pSuper.retro.puro-shDAXX_01 | [99] | GGAGUUGGAUCUCUCAGAA |
| pLKO1-puro shDAXX_02 | Sigma TRCN 0000003802 NM-001350 x-2285s1c1 | GCCACACAATGCGATCCAGAA |
| pLKO1-puro shHIRA_01 | Sigma TRCN 0000232156 NM_003325 3-592s21c1 | CTCTATCCTCCGGAATCATTC |
| pLKO1-puro shHIRA_02 | Sigma TRCN 0000232159 NM_003325 3-3073s21c1 | TGAATACCGACTTCGAGAAAT |
| pLKO1-puro shUBN1_01 | Sigma TRCN 0000235872 NM_016936 3-1764s21c1 | ATGGACTCGCTGACGGATTTG |
| pLKO1-puro shUBN1_02 | Sigma TRCN 0000235871 NM_016936 3-1244s21c1 | ATCCGACTCCTTCATCGATAA |

https://doi.org/10.1371/journal.ppat.1007313.t001

shaking. The cells were subsequently washed in "Wash buffer"(200mM NaCl; 20mM Tris pH8; 0,5mM EGTA; 1mM EDTA, PIC 1X) for 10 min at 4˚C under shaking then were resuspended and centrifuged twice during 5 min 1700g at 4˚C in "Shearing Buffer" (10mM Tris pH7,6; 1mM EDTA; 0,1%SDS; PIC 1X). Finally, nuclei were resuspended in 1mL of "Shearing Buffer" and were sonicated with a S220 Focused-ultrasonicator (Covaris) (Power 140W; Duty Off 10%; Burst Cycle 200). Eighty-five μL of the sonication product were kept for the input, 50 μL for analyzes of the sonication efficiency, and 850 μL diluted twice in IP buffer 2X (300mM NaCl, 10mM Tris pH8; 1mM EDTA; 0,1% SDS; 2% Triton) for ChIP. Two micrograms of Ab were added and incubated overnight at 4˚C. Fifty microliters of agarose beads coupled to protein A (Millipore 16–157) or G (Millipore 16–201) were added for 2 h at 4˚C under constant shaking. Beads were then successively washed for 5 min at 4˚C under constant shaking once in "low salt" (0.1% SDS, 1% Triton X-100, 2 mM EDTA, 20 mM Tris HCl pH 8.0, 150 mM NaCl) buffer, once in "high salt" (0.1% SDS, 1% Triton X-100, 2 mM EDTA, 20 mM Tris HCl pH 8.0, 500 mM NaCl) buffer, once in "LiCl" (0.25 mM LiCL, 1% NP40, 1% NaDOC, 1 mM EDTA, 10 mM Tris HCl pH 8.0) buffer, and twice in TE (10 mM Tris pH 8.0, 1 mM EDTA) buffer. Chromatin-antibody complexes are then eluted at 65˚C for 30 min under constant shaking with 200 μL of elution buffer (1% SDS, 0.1 M NaHCO3). Input and IP products were de-crosslinked overnight at 65˚C with 20 mg/mL of proteinase K (Sigma) and 10 mg/mL of RNAse A (Sigma). DNA was then purified by phenol-chloroform/ethanol precipitation, resuspended in water, and kept at -20˚C until use for qPCR.

Quantitative PCR was performed using Quantifast SYBR Green mix (Qiagen) and the MX3005P apparatus (Agilent/Stratagene). Primers were used at a final concentration of 1 μM. Their sequences and target genes are provided in Tables 2 and 3.

## Re-ChIP

Cells were processed similarly to ChIP until addition of the antibody. Two μg of the first antibody were pre-incubating with agarose beads coupled to protein A (Millipore 16–157) in PBS-0.5% BSA overnight at 4˚C under shaking. The beads were washed twice with IP Buffer 1X (150mM NaCl, 5mM Tris pH8; 0.5mM EDTA; 0.1% SDS; 1% Triton), then the chromatin was incubated with the antibody/beads overnight at 4˚C. Beads were then successively washed for 5 min at 4˚C under constant shaking once in "low salt" buffer, once in "high salt" buffer, once in "LiCl" buffer and twice in TE buffer. Chromatin-antibody complexes were eluted at 37˚C for 30 min with 100 μL of Re-ChIP elution buffer (1% SDS, 0.1M NaHCO3, 10mM DTT). Fifty μL were kept for analysis of the first capture efficiency, then the other 50 μL were diluted

**Table 2. Primer sequences and target HSV-1 genes.**

| Genes | Proteins | | Forward primers (5'-> 3') | Reverse primers (5'-> 3') |
|---|---|---|---|---|
| UL2 | Uracil DNA glycosylase | promoter | TAAACCAACGAAAAGCGCGG | 5' GGCACCCACAGAAACCTACA 3' |
| | | CDS | CCCTCTCCAAGGTTCCGTTC | CGACCAGTCGATGGGTGAAA |
| UL23 | TK | promoter | CAGCTGCTTCATCCCCGTGG | AGATCTGCGGCACGCTGTTG |
| | | CDS | ATGCTGCCCATAAGGTATCG | GTAATGACAAGCGCCCAGAT |
| UL26 | VP21 | promoter | AGAACAAGAGCCTCCGTTGG | AGGCGAGAGCGAATGCTAAA |
| | | CDS | CCCATTTACGTGGCTGGGTT | TCCGGATCCAATGCCAACTC |
| UL29 | ICP8 | promoter | CCTTTTGTCAATCGGTCCGC | CGGGAGACATACCTTGTCGG |
| | | CDS | TGTTCACCACGAGTACCTGC | ACCTATGCACCTTCGACACG |
| UL42 | DNA polymerase | promoter | CGTAGTTTCTGGCTCGGTGA | GAACACCCCACAGTGACGAG |
| | | CDS | TGTTCACCACGAGTACCTGC | TTTCCCCGTACACCGTCTTG |
| LacZ/UL43 (HCMV-lacZ reporter cassette) | β-Galactosidase | Promoter (CMV) | TTCCTACTTGGCAGTACATCTACG | GTCAATGGGGTGGAGACTTGG |
| | | CDS (LacZ) | GCAGCAACGAGACGTCA | GAAAGCTGGCTACAGGAAG |
| UL44 | gC | promoter | CGCCGGTGTGTGATGATTT | TTTATACCCGGGCCCCAT |
| | | CDS | GGGTCCGTCCCCCCCAAT | CGTTAGGTTGGGGGCGCT |
| UL48 | VP16 | promoter | GCGTTCATGTCGGCAAACAG | CCCGTATCAACCCCACCCAAT |
| | | CDS | TGCGGGAGCTAAACCACATT | TCCAACTTCGCCCGAATCAA |
| UL54 | ICP27 | promoter | CCACGGGTATAAGGACATCCA | GGATATGGCCTCTGGTGGTG |
| | | CDS | GGCGACTGACATTGA | CTGCTGTCCGATTCCAGGTC |
| LAT | Latency Associated transcript | exon | GGCTCCATCGCCTTTCCT | AAGGGAGGGAGGAGGGTACTG |
| | | intron | CCCACGTACTCCAAGAAGGC | AGACCCAAGCATAGAGAGCCAG |
| RL2 | ICP0 | promoter | CCGCCGACGCAACAG | CCGCCGACGCAACAG |
| | | CDS | CGTGTGCACGGATGAGATCG | GCGCAATTGCATCCAGGTTT |
| RS1 | ICP4 | promoter | CGTGGTGGTGCTGTACTCG | GCTCGGCGGACCACTC |
| US1 | ICP22 | promoter | GATCGCATCGGAAAGGGACA | GGTGCTTACCCGTGCAAAAA |
| | | CDS | GTTACGCTGGAAACCCCAGA | CCAGACACTTGCGGTCTTCT |
| US3 | Protein kinase US3 | promoter | GCGGGGGCTGCTCTAAAAAT | GGGTTTTAAGGAGCGGCAGT |
| | | CDS | ACTGGCATGGGCTTTACGAT | TTCACGATTACCCGTTGGGG |
| US6 | gD | promoter | GGGGTTAGGGAGTTGTTCGG | CGCACCACACAAAAGAGACC |
| | | CDS | ACGGTTTACTACGCCGTGTT | TGTAGGGTTGTTTCCGGACG |
| US12 | ICP47 | promoter | GATCGCATCGGAAAGGGACA | GGTGCTTACCCGTGCAAAAA |
| | | CDS | TACCGGATTACGGGGACTGT | ATAAAAGGGGGCGTGAGGAC |

https://doi.org/10.1371/journal.ppat.1007313.t002

**Table 3. Primer sequences and target cellular genes.**

| Genes | Forward primers (5'-> 3') | Reverse primers (5'-> 3') |
|---|---|---|
| Glyceraldehyde 3-phosphate dehydrogenase (GAPDH) | GAGTCAACGGATTTGGTCGT | TTGATTTTGGAGGGATCTCG |
| Enhancer 1 (Enh.1) | GCATGGTAGTCTCCCACTGATTT | CTGCAAATTCCTGCTGACTCAC |
| leucine-zipper-like transcriptional regulator 1 (LTZR1) | GTGGGAAATGGGGGACCTTC | GCAGGAGGCCATCTTTCTTTG |
| Myelin transcription factor 1 (MYT1) | CAGGAAGACACCTCTCACAC | ACAGTGTCCAGGGGCTTTGC |
| Zinc-finger protein 554 (ZNF554) | CGGGGAAAAGCCCTATAAA | TCCACATTCACTGCATTCGT |
| Family with sequence similarity 19 member A2 (FAM19A2) | TGCAATATACAGTGTGAGCAGTC | GCCCCTTCCCAGCTTATGAA |
| Actin | CGGGAAATCGTGCGTGACATTAAG | GAACCGCTCATTGCCAATGGTGAT |

https://doi.org/10.1371/journal.ppat.1007313.t003

20 times with IP buffer 1X and incubated overnight at 4˚C with the second antibody pre-incubated with agarose beads coupled to protein A. The beads were washed twice with IP Buffer 1X, then successively washed for 5 min at 4˚C under constant shaking, once in "low salt" buffer, once in "high salt" buffer, once in "LiCl" buffer and twice in TE buffer. Chromatin-antibody complexes were then eluted at 65˚C for 30 min under constant shaking with 200 μL of elution buffer (1% SDS, 0.1M NaHCO3). Input and IP products were de-crosslinked overnight at 65˚C a with 20 mg/mL of proteinase K (Sigma) and 10 mg/mL of RNAse A (Sigma). DNA was then purified by phenol-chloroform/ethanol precipitation, resuspended in water, and kept at -20˚C until use for qPCR.

## siRNA transfections

Transfections of BJ cells with siRNAs was performed using Lipofectamine RNAiMAX and following the supplier's procedure (Thermo Fisher Scientific). The following siRNAs were used at a final concentration of 40 nM for 48 h: siRNA_negative control (EUROGENTEC, FR-CL000-005), siHIRA 5'–GGAUAACACUGUCGUCAUC (Dharmacon: J-013610-07) [52]; siH3F3A: 5′-CUACAAAAGCCGCUCGCAA [100]; siH3F3B: 5′-GCUAAGAGAGUCACCA UCA [100].

## Antibodies

The antibodies used for immunofluorescence, ChIP and WB are provided in Tables 4–6.

**Table 4. Antibodies used in immunofluorescence [(1)].**

| Proteins | Origin | References | Species | Dilution |
|---|---|---|---|---|
| Asf1a | Geneviève Almouzni (Institut Curie, Paris) | #28134 | Rabbit polyclonal | 1/1000 |
| ATRX (h-300) | Santa Cruz | sc-15408 | Rabbit polyclonal | 1/100 |
| c-Myc (9E10) | Santa cruz | sc-40 | Mouse monoclonal | 1/200 |
| Cabin1 | Sigma | HPA043296 | Rabbit polyclonal | 1/100 |
| DAXX (M-112) | Santa Cruz | sc-7152 | Rabbit polyclonal | 1/100 |
| HA | Abcam | ab9110 | Rabbit polyclonal | 1/500-1000 |
| HA (3F10) | Roche | 1867423 | Rat monoclonal | (1/1000) |
| HIRA | Abcam | ab20655 | Rabbit polyclonal | 1/100 |
| HIRA (WC119) | Millipore | 04–1488 | Mouse monoclonal | 1/100 |
| p48 (CAF-1) | Abcam | ab1765 | Rabbit polyclonal | 1/100 |
| p60 (CAF-1) | Novus | 500–207 | Mouse monoclonal | 1/100 |
| p150 (CAF-1) | Novus | 500–212 | Mouse monoclonal | 1/100 |
| human PML (H-238) | Santa Cruz | sc-5621 | Rabbit polyclonal | 1/500 |
| human PML(PG-M3) | Santa Cruz | sc-966 | Mouse monoclonal | 1/500 |
| human PML 5E10 | Roel Van Driel (University of Amsterdam) | | Mouse monoclonal | 1/500 |
| mouse PML | Millipore | MAB3738 | Mouse monoclonal | 1/100 |
| Sp100 | Thomas Sternsdorf (University of Hamburg) | SpGH | Rabbit polyclonal | 1/500 |
| SUMO-1 | Cell Signaling | 4930 | Rabbit polyclonal | 1/500 |
| SUMO-1 (5B12) | MBL | M113-3 | Mouse monoclonal | 1/500 |
| SUMO-2/3 (18H8) | Cell Signaling | 4971 | Rabbit monoclonal | 1/500 |
| SUMO-2/3 (1E7) | MBL | M114-3 | Mouse monoclonal | 1/500 |
| UBN1 Zap1 | Henri Gruffat (CIRI, ENS, Lyon) | | Mouse monoclonal | 1/100 |

(1) All secondary antibodies were Alexa Fluor-conjugated and were raised in goats (Invitrogen).

https://doi.org/10.1371/journal.ppat.1007313.t004

**Table 5. Antibodies used in ChIP.**

| Proteins | Origin | References | Species |
|---|---|---|---|
| ATRX (h-300) | Santa Cruz | sc-15408 | Rabbit polyclonal |
| c-Myc (9E10) | Millipore | MABE282 | Mouse monoclonal |
| H3.1/2 | Millipore | ABE154 | Rabbit polyclonal |
| H3.3 | Millipore | 09–838 | Rabbit polyclonal |
| HA | Abcam | ab9110 | Rabbit polyclonal |
| H3 | Abcam | ab1791 | Rabbit polyclonal |
| H4 | Millipore | 05–858 | Rabbit monoclonal |
| H2A | Millipore | 07–146 | Rabbit polyclonal |
| H2B | Millipore | 07–371 | Rabbit polyclonal |
| H3K9me3 | Abcam | ab8898 | Rabbit polyclonal |
| H3K27me3 | Abcam | ab6002 | Mouse monoclonal |
| H3K4me2 | Abcam | ab7766 | Mouse monoclonal |
| IgG Mouse | Diagenode | Kch-819-015 | Mouse monoclonal |
| IgG Rabbit | Diagenode | Kch-504-250 | Rabbit polyclonal |

https://doi.org/10.1371/journal.ppat.1007313.t005

**Table 6. Antibodies used in WB [(1)].**

| Proteins | Origin | References | Species | Dilution |
|---|---|---|---|---|
| human PML (H-238) | Santa Cruz | sc-5621 | Rabbit polyclonal | 1/1000 |
| ATRX (h-300) | Santa Cruz | sc-15408 | Rabbit polyclonal | 1/1000 |
| DAXX (25C12) | Cell Signaling | #4533 | Rabbit monoclonal | 1/1000 |
| HIRA (WC119) | Millipore | 04–1488 | Mouse monoclonal | 1/1000 |
| UBN1 Zap1 | Henri Gruffat (CIRI, ENS, Lyon) | | Mouse monoclonal | 1/250 |
| c-Myc (9E10) | Millipore | MABE282 | Mouse monoclonal | 1/1000 |
| HA | Abcam | ab9110 | Rabbit polyclonal | 1/1000 |
| Actin | Sigma | A2066 | Rabbit polyclonal | 1/1000 |

(1) All secondary antibodies were HRP-conjugated and were raised in goats (Sigma).

https://doi.org/10.1371/journal.ppat.1007313.t006

## Transcriptional reactivation procedure

BJ cells were transduced first with pLKOneo.CMV.EGFPnlsTetR to produce BJ-eTetR cell lines stably and constitutively expressing the EGFPnlsTetR protein (selection G418 1 mg/mL). BJ-eTetR cells were then transduced with pLKO.DCMV.TetO.cICP0 or pLKO.DCMV.TetO. cICP0ΔRF to produce BJ-eTetR/cICP0 or BJ-eTetR/cICP0ΔRF expressing ICP0 or its RING finger mutant FXE, respectively (selection puromycin 1 μg/mL). The expression of ICP0 or ICP0ΔRF was induced by the addition of doxycycline (100ng/μL) in the medium. BJ-eTetR, BJ-eTetR/cICP0 or BJ-eTetR/cICP0ΔRF were infected with HSV-1 *in*1374 for 4 days at 38.5˚C to stabilize the formation of vDCP NBs. Then doxycycline was added or not in the medium to induce the expression of ICP0 or ICP0ΔRF. Cells were incubated at 32˚C the permissive temperature for *in*1374 (see section virus). Twenty four hours, 48h or 72h after addition of doxycycline, the cells were fixed to proceed to IF or IF-FISH analyses or treated with FastLane cell SYBR Green RT-PCR (Qiagen 204243) to analyze the LacZ and viral transcripts by RT-qPCR.

## Supporting information

**S1 Fig. Latent/quiescent HSV-1 genomes co-localize with PML and PML NB-associated proteins in vDCP NBs.** figImmuno-FISH performed in human primary fibroblasts (BJ cells)

infected for 2 days with the replication-defective HSV-1 virus *in*1374. PML (i), Sp100 (ii), SUMO-1 (iii), SUMO 2/3 (iv), ATRX (v), DAXX (vi) (green), and HSV-1 genomes (red) were detected. Scale bars = 5 $\mu$m.
(TIF)

**S2 Fig. Expression of tagged versions of DAXX (Myc), HIRA and UBN1 (HA) in BJ cells.** Normal BJ cells were transduced with lentiviruses expressing Myc-DAXX, HIRA-HA, or HA-UBN1, and stable cell lines expressing the tagged proteins were selected by puromycin selection. Expression of the tagged proteins was detected by immunofluorescence (A) and Western blotting (B). For WB, actin was used as a loading control. Scale bars = 5 $\mu$m.
(TIF)

**S3 Fig. Components of the DAXX/ATRX and HIRA complexes associate with latent/quiescent HSV-1 genomes at early times pi.** (A) Schematic localization of the HSV-1 genome and of the loci analyzed by quantitative PCR (qPCR). UL: Unit Long, US: Unit Short, TRL: Terminal Repeat Long, TRS: Terminal Repeat Short, IRL: Inverted Repeat Long, IRS: Inverted Repeat Short. Immediate early (IE/α) genes (red), early (E/β) genes (green), late (L/γ) genes (blue).
(B) ChIP performed in *in*1374-infected normal BJ cells or *in*1374-infected BJ cells expressing tagged versions of DAXX, HIRA, or UBN1. Anti-myc (DAXX) or anti-HA (HIRA and UBN1) antibodies were used. Infections were performed for 30 min (blue), 2 h (red), 6 h (green). For ATRX, a native antibody was used, and the results were compared to ChIP with IgG as control. Analyzed viral loci were described previously. Means from three independent experiments ± SD.
(TIF)

**S4 Fig. Expression of the tagged H3.3 (e-H3.3) and H3.1 (e-H3.1) in BJ cells.** (A) Detection of the protein expression by WB using the anti-HA antibody. Endogenous histone H3 was detected as a control. Actin was detected as a loading control.
(B) Detection of e-H3.1 (i) and e-H3.3 (ii) by immunofluorescence.
(C) Co-detection of e-H3.1 (i) and e-H3.3 (ii) (green) with PML (red). Nuclei are detected with DAPI (insets, gray) E-H3.3, unlike e-H3.1, co-localizes with PML NBs. Scale bars = 5 $\mu$m.
(D) Quantification of the immunofluorescence experiments performed in (C). Means from two independent experiments.
(TIF)

**S5 Fig. Canonical histones associate with latent/quiescent HSV-1 genomes.** ChIP performed in *in*1374-infected BJ cells at 24 hpi. Anti-H3, H4, H2A and H2B antibodies were used for ChIP experiments. Analyzed viral loci were described previously. Cellular locus glyceraldehyde 3-phosphate dehydrogenase (GAPDH) was analyzed as control.
(TIF)

**S6 Fig. The endogenous histone variant H3.3, but not the canonical H3.1/2, associates with latent/quiescent HSV-1 genomes.** ChIP performed in *in*1374-infected BJ cells using control IgG (blue), anti-H3.1/2 (red), or anti-H3.3 (green) antibodies. Infections were performed for 24 h. Analyzed viral loci were described previously. Cellular loci Enhancer 1 (Enh.1), and leucine-zipper-like transcriptional regulator 1 (LZTR1) are positive controls for deposition of H3.3 and H3.1, respectively.
(TIF)

**S7 Fig. Validation of the shRNAs against DAXX, ATRX, HIRA, and UBN1.** (A) BJ cells were transduced with shRNA-expressing lentiviruses before analysis 48 h post-transduction.

RT-qPCR to detect DAXX, ATRX, HIRA, and UBN1 mRNA was performed, and the results were compared to a control shRNA (shCTRL). Means from three independent experiments ± SD. The Student's *t*-test was applied to assess the significance of the results. * = $p < 0.05$, ** = $p < 0.01$.
(B) WB for detection of decreases in DAXX, ATRX, HIRA, and UBN1 proteins in normal BJ cells or BJ cells transduced with shRNA-expressing lentiviruses (48 h post-transduction). Actin was detected as a loading control. Two shRNAs were tested for each protein.
(TIF)

**S8 Fig. Effects of the depletion of DAXX, ATRX, HIRA or UBN1 on PML NB detection.** BJ cells were transduced with shRNA-expressing lentiviruses before analysis 48 h post-transduction. Immunofluorescences were performed to detect DAXX, ATRX, HIRA, and UBN1 (green) and PML (gray, red). Two shRNAs were tested for each protein. Scale bars = 5 $\mu$m.
(TIF)

**S9 Fig. Validation of the shRNAs against DAXX, ATRX, HIRA, and UBN1 in e-H3.3-expressing BJ cells.** H3.3-expressing BJ cells were transduced with shRNA-expressing lentiviruses before analysis 48 h post-transduction.
(A) RT-qPCR to quantify DAXX, ATRX, HIRA, and UBN1 mRNA was performed, and the results were compared to a control shRNA (shCTRL). Data represent means from two independent experiments.
(B) WB for detection of decreases in ATRX, HIRA, and UBN1 proteins (48 h post-transduction) in normal e-H3.3-expressing BJ cells or e-H3.3-expressing BJ cells transduced with shRNA-expressing lentiviruses. Actin was detected as a loading control.
(TIF)

**S10 Fig. Inactivation of DAXX, ATRX, HIRA, or UBN1 does not affect the accumulation of e-H3.3 in PML NBs.** Immunofluorescence experiments performed in e-H3.3-expressing BJ cells transduced with a lentivirus expressing a control shRNA (shCTRL, i, iii, v, vii) or a shRNA targeting DAXX (ii), ATRX (iv), HIRA (vi), or UBN1 (viii). E-H3.3 (gray, green); DAXX, ATRX, HIRA, UBN1 (gray, red); and PML (gray, blue) were detected. For the staining, a rat anti-HA mAb was used to detect e-H3.3, a rabbit polyclonal for the detection of DAXX, ATRX (i-iv), or PML (v-viii), and a mouse mAb for the detection of HIRA, UBN1 (v-viii) or PML (i-iv). Arrowheads point out examples of e-H3.3 co-localization with PML NBs in each sample. Scale bars = 5 $\mu$m.
(TIF)

**S11 Fig. Validation of the shRNAs against PML in normal and e-H3.3-expressing BJ cells.** Normal (A-C) or e-H3.3-expressing (D and E) BJ cells were transduced with a lentivirus expressing a control shRNA (shCTRL) or PML shRNAs (shPML) before analysis. Two different shRNAs were validated in normal BJ cells.
(A) Immunofluorescence to detect the PML NB signal. Scale bars = 5 $\mu$m.
(B) RT-qPCR to quantify PML mRNA. Means from three independent experiments ± SD. The Student's *t*-test was applied to assess the significance of the results. * = $p < 0.05$, ** = $p < 0.01$.
(C) WB to detect PML protein.
(D) RT-qPCR to quantify PML mRNA. Means from two independent experiments.
(E) WB to detect PML protein.
(TIF)

**S12 Fig. The decrease in the H3.3 association with latent/quiescent HSV-1 genomes is not compensated by H3.1.** ChIP for the detection of e-H3.1 associated with HSV-1 in e-

H3.1-expressing BJ cells previously transduced with a lentivirus expressing a shRNA control (shCTRL, blue) or a PML shRNA (shPML, red) (A) or e-H3.1-expressing MEF pml$^{-/-}$ cells (B). Cells were infected with *in*1374 for 24 h. Anti-HA antibody was used for the ChIP experiments. The analyzed viral loci were described previously. Data represent means from two independent experiments ± SD.
(TIF)

**S13 Fig. IF for the detection of ICP0 or ICP0ΔRF (green) and PML (red) in BJ-eTetR, BJ-eTetR/cICP0 or BJ-eTetR/cICP0*μ*RF cells treated (+ dox) or not (no dox) with doxycycline for 24 h.** ICP0 or ICP0*μ*RF (green), PML (red), and nuclei (DAPI, gray/blue) are detected. Expression of ICP0 but not ICP0*μ*RF induces the disappearance of PML-NBs. Scale bars = 5 *μ*m.
(TIF)

**S14 Fig. Phase contrast images showing the state of the cell monolayers in BJ-eTetR, BJ-eTetR/cICP0 or BJ-eTetR/cICP0*μ*RF cells not infected (NI) or infected with *in*1374 for 4 d at 38.5˚C, then treated (+ dox) or not (no dox) with doxycycline for 0 h (T0), 24 h (T24), or 48 h (T48) at the permissive temperature (32˚C) for in1374 replication.** Expression of ICP0, but not ICP0*μ*RF or doxycycline alone, induces a cytopathic effect from T24. Scale bars = 50 *μ*m.
(TIF)

**S15 Fig. Immuno-FISH performed in BJ-eTetR or BJ-eTetR/cICP0ΔRF cells infected with *in*1374 for 4 d at 38.5˚C, then treated (+ dox) or not (no dox) with doxycycline for 24 h (T24), or 48 h (T48), at 32˚C.** PML (green), HSV-1 genomes (gray/red), and nuclei (DAPI, gray/blue) are detected. Scale bars = 5 *μ*m.
(TIF)

**S16 Fig. The specific depletion of H3.3 does not affect the formation of vDCP NBs.** (A) WB to visualize the depletion of H3.3 in e-H3.3-expressing BJ cells. A combination of two siRNAs targeting H3.3 transcripts from both H3.3-encoding genes (H3F3A and H3F3B) were used for the depletion of H3.3. Actin was detected as a loading control.
(B) Immunofluorescence performed in e-H3.3-expressing BJ cells transfected with control (siCTRL) or H3.3 (siH3F3A+3B) siRNAs. E-H3.3 (green), and PML (red) were detected. Nuclei were detected with DAPI (gray). Scale bars = 5 *μ*m.
(C) Quantifications of co-localizations of HSV-1 genomes with PML issued from immuno-FISH experiments performed in *in*1374-infected BJ cells (2 dpi) previously transfected with control (siCTRL) or H3.3 (siH3F3A+3B) siRNAs. Means from three independent experiments ± SD. The data suggest that vDCP-NBs are independent of H3.3 chromatinization of the latent/quiescent HSV-1 genomes for their formation.
(TIF)

**S1 Table. Co-localization between HSV-1 genomes and proteins in different cell types at 2 dpi.**
(TIF)

**S2 Table. Co-localization between HSV-1 genomes and PML-NBs-associated proteins/H3.3 chaperones.** Short times pi (Means % ± SD).
(TIF)

**S3 Table. Co-localization between HSV-1 genomes and PML-NBs-associated proteins/H3.3 chaperones.** Long times pi (Means % ± SD).
(TIF)

**S4 Table. Co-localization between HSV-1 genomes and PML in cells depleted for PML-NBs-associated proteins/ H3.3 chaperones (Means % ± SD).**
(TIF)

**S5 Table. Co-localization of latent/quiescent HSV-1 with DAXX, ATRX, HIRA, UBN1 in BJ cells depleted for PML (Means % ± SD).**
(TIF)

## Acknowledgments

We thank Roel van Driel (University of Amsterdam, Netherland) for the PML antibody (mAb 5E10), Henri Gruffat (CIRI, ENS Lyon, France) for the UBN1 antibody, Geneviève Almouzni (Institut Curie, Paris, France) for the ASF1a antibody, Thomas Sternsdorf (University of Hamburg, Germany) for the Sp100 antibody, Roger Everett and Chris Preston (Center for Virus Research, University of Glasgow, UK) for the *in*1374 virus and various lentivirus vectors, Wade Bresnahan (University of Texas, USA) for the pSuper.retro.puro-shDAXX_01, Lars Jansen (Instituto Gulbenkian de Ciencia, Portugal) for the pBABE plasmids encoding H3.1-SNAP-HAx3 and H3.3-SNAP-HAx3, Manuel Stucki (University Hospital Zürich) for the pCL-ampho and pCL-eco plasmids, Olivier Hantz and Isabelle Chemin (CRCL, Lyon) for the HepaRG cells, Valérie Lallemand-Breitenbach (Hopital Saint Louis, Paris, France) for the MEF $pml^{+/+}$ and $pml^{-/-}$ cells, Gérard Benoit (LBMC, ENS Lyon, France) for technical advice for the ChIP experiments, the Centre Technologique des Microstructures (CTμ) and the Centre d'Imagerie Quantitative Lyon Est (CIQLE) of the Université Claude Bernard Lyon 1 for the confocal microscopy facilities.

## Author Contributions

**Conceptualization:** Camille Cohen, Armelle Corpet, Marc Labetoulle, Patrick Lomonte.

**Data curation:** Camille Cohen, Patrick Lomonte.

**Formal analysis:** Camille Cohen, Patrick Lomonte.

**Funding acquisition:** Armelle Corpet, Marc Labetoulle, Patrick Lomonte.

**Investigation:** Camille Cohen, Armelle Corpet, Simon Roubille, Mohamed Ali Maroui, Nolwenn Poccardi, Antoine Rousseau, Constance Kleijwegt, Olivier Binda, Pascale Texier, Nancy Sawtell, Marc Labetoulle, Patrick Lomonte.

**Methodology:** Camille Cohen, Armelle Corpet, Marc Labetoulle, Patrick Lomonte.

**Project administration:** Patrick Lomonte.

**Resources:** Patrick Lomonte.

**Supervision:** Marc Labetoulle, Patrick Lomonte.

**Validation:** Camille Cohen, Marc Labetoulle, Patrick Lomonte.

**Visualization:** Camille Cohen, Marc Labetoulle, Patrick Lomonte.

**Writing – original draft:** Camille Cohen, Armelle Corpet, Patrick Lomonte.

**Writing – review & editing:** Camille Cohen, Patrick Lomonte.

## References

1. Whitley RJ, Roizman B. Herpes simplex virus infections. Lancet. 2001; 357: 1513–1518. https://doi.org/10.1016/S0140-6736(00)04638-9 PMID: 11377626

2. Efstathiou S, Preston CM. Towards an understanding of the molecular basis of herpes simplex virus latency. Virus Res. 2005; 111: 108–119. https://doi.org/10.1016/j.virusres.2005.04.017 PMID: 15951043
3. St Leger AJ, Peters B, Sidney J, Sette A, Hendricks RL. Defining the herpes simplex virus-specific CD8+ T cell repertoire in C57BL/6 mice. J Immunol. 2011; 186: 3927–3933. https://doi.org/10.4049/jimmunol.1003735 PMID: 21357536
4. van Velzen M, Jing L, Osterhaus ADME, Sette A, Koelle DM, Verjans GMGM. Local CD4 and CD8 T-cell reactivity to HSV-1 antigens documents broad viral protein expression and immune competence in latently infected human trigeminal ganglia. PLoS Pathog. 2013; 9.
5. Douglas MW, Diefenbach RJ, Homa FL, Miranda-Saksena M, Rixon FJ, Vittone V, et al. Herpes simplex virus type 1 capsid protein VP26 interacts with dynein light chains RP3 and Tctex1 and plays a role in retrograde cellular transport. The Journal of biological chemistry. American Society for Biochemistry and Molecular Biology; 2004; 279: 28522–28530. https://doi.org/10.1074/jbc.M311671200 PMID: 15117959
6. Sodeik B, Ebersold MW, Helenius A. Microtubule-mediated transport of incoming herpes simplex virus 1 capsids to the nucleus. J Cell Biol. 1997; 136: 1007–1021. PMID: 9060466
7. Döhner K, Radtke K, Schmidt S, Sodeik B. Eclipse phase of herpes simplex virus type 1 infection: Efficient dynein-mediated capsid transport without the small capsid protein VP26. J Virol. 2006; 80: 8211–8224. https://doi.org/10.1128/JVI.02528-05 PMID: 16873277
8. Koyuncu OO, Hogue IB, Enquist LW. Virus infections in the nervous system. Cell Host Microbe. Elsevier; 2013; 13: 379–393.
9. Kramer T, Enquist LW. Directional spread of alphaherpesviruses in the nervous system. Viruses. 2013; 5: 678–707. https://doi.org/10.3390/v5020678 PMID: 23435239
10. Taylor MP, Enquist LW. Axonal spread of neuroinvasive viral infections. Trends Microbiol. 2015; 23: 288.
11. Sears AE, Hukkanen V, Labow MA, Levine AJ, Roizman B. Expression of the herpes simplex virus 1 alpha transinducing factor (VP16) does not induce reactivation of latent virus or prevent the establishment of latency in mice. J Virol. American Society for Microbiology (ASM); 1991; 65: 2929–2935. PMID: 1851865
12. Luxton GWG, Haverlock S, Coller KE, Antinone SE, Pincetic A, Smith GA. Targeting of herpesvirus capsid transport in axons is coupled to association with specific sets of tegument proteins. Proc Natl Acad Sci USA. 2005; 102: 5832–5837. https://doi.org/10.1073/pnas.0500803102 PMID: 15795370
13. Aggarwal A, Miranda-Saksena M, Boadle RA, Kelly BJ, Diefenbach RJ, Alam W, et al. Ultrastructural visualization of individual tegument protein dissociation during entry of herpes simplex virus 1 into human and rat dorsal root ganglion neurons. J Virol. 2012; 86: 6123–6137. https://doi.org/10.1128/JVI.07016-11 PMID: 22457528
14. Sawtell NM, Thompson RL. De Novo Herpes Simplex Virus VP16 Expression Gates a Dynamic Programmatic Transition and Sets the Latent/Lytic Balance during Acute Infection in Trigeminal Ganglia. PLoS Pathog. Public Library of Science; 2016; 12: e1005877. https://doi.org/10.1371/journal.ppat.1005877 PMID: 27607440
15. Alandijany T, Roberts APE, Conn KL, Loney C, McFarlane S, Orr A, et al. Distinct temporal roles for the promyelocytic leukaemia (PML) protein in the sequential regulation of intracellular host immunity to HSV-1 infection. Hutt-Fletcher L, editor. PLoS Pathog. Public Library of Science; 2018; 14: e1006769. https://doi.org/10.1371/journal.ppat.1006769 PMID: 29309427
16. Catez F, Picard C, Held K, Gross S, Rousseau A, Theil D, et al. HSV-1 Genome Subnuclear Positioning and Associations with Host-Cell PML-NBs and Centromeres Regulate LAT Locus Transcription during Latency in Neurons. PLoS Pathog. 2012; 8: e1002852. https://doi.org/10.1371/journal.ppat.1002852 PMID: 22912575
17. Maroui M-A, Callé A, Cohen C, Streichenberger N, Texier P, Takissian J, et al. Latency Entry of Herpes Simplex Virus 1 Is Determined by the Interaction of Its Genome with the Nuclear Environment. PLoS Pathog. Public Library of Science; 2016; 12: e1005834. https://doi.org/10.1371/journal.ppat.1005834 PMID: 27618691
18. Mehta A, Maggioncalda J, Bagasra O, Thikkavarapu S, Saikumari P, Valyi-Nagy T, et al. In situ DNA PCR and RNA hybridization detection of herpes simplex virus sequences in trigeminal ganglia of latently infected mice. Virology. 1995; 206: 633–640. PMID: 7831818
19. Sawtell NM. Comprehensive quantification of herpes simplex virus latency at the single-cell level. J Virol. 1997 ed. 1997; 71: 5423–5431. PMID: 9188614
20. Sawtell NM, Poon DK, Tansky CS, Thompson RL. The latent herpes simplex virus type 1 genome copy number in individual neurons is virus strain specific and correlates with reactivation. J Virol. 1998 ed. 1998; 72: 5343–5350. PMID: 9620987

21. Chen X-P, Mata M, Kelley M, Glorioso JC, Fink DJ. The relationship of herpes simplex virus latency associated transcript expression to genome copy number: a quantitative study using laser capture microdissection. J Neurovirol. 2002; 8: 204–210. https://doi.org/10.1080/13550280290049642 PMID: 12053275

22. Wang K, Lau TY, Morales M, Mont EK, Straus SE. Laser-capture microdissection: refining estimates of the quantity and distribution of latent herpes simplex virus 1 and varicella-zoster virus DNA in human trigeminal Ganglia at the single-cell level. J Virol. 2005 ed. 2005; 79: 14079–14087. https://doi.org/10.1128/JVI.79.22.14079-14087.2005 PMID: 16254342

23. Proenca JT, Coleman HM, Connor V, Winton DJ, Efstathiou S. A historical analysis of herpes simplex virus promoter activation in vivo reveals distinct populations of latently infected neurones. The Journal of general virology. 2008; 89: 2965–2974. https://doi.org/10.1099/vir.0.2008/005066-0 PMID: 19008381

24. Proenca JT, Coleman HM, Nicoll MP, Connor V, Preston CM, Arthur J, et al. An investigation of HSV promoter activity compatible with latency establishment reveals VP16 independent activation of HSV immediate early promoters in sensory neurones. The Journal of general virology. 2011; 92: 2575–2585. https://doi.org/10.1099/vir.0.034728-0 PMID: 21752961

25. Held K, Junker A, Dornmair K, Meinl E, Sinicina I, Brandt T, et al. Expression of herpes simplex virus 1-encoded microRNAs in human trigeminal ganglia and their relation to local T-cell infiltrates. J Virol. 2011; 85: 9680–9685. https://doi.org/10.1128/JVI.00874-11 PMID: 21795359

26. Bloom DC, Giordani NV, Kwiatkowski DL. Epigenetic regulation of latent HSV-1 gene expression. Biochimica et biophysica acta. 2010 ed. 2010; 1799: 246–256. https://doi.org/10.1016/j.bbagrm.2009.12.001 PMID: 20045093

27. Kristie TM, Liang Y, Vogel JL. Control of alpha-herpesvirus IE gene expression by HCF-1 coupled chromatin modification activities. Biochimica et biophysica acta. 2009 ed. 2010; 1799: 257–265. https://doi.org/10.1016/j.bbagrm.2009.08.003 PMID: 19682612

28. Knipe DM, Lieberman PM, Jung JU, McBride AA, Morris KV, Ott M, et al. Snapshots: chromatin control of viral infection. Virology. 2013; 435: 141–156. https://doi.org/10.1016/j.virol.2012.09.023 PMID: 23217624

29. Deshmane SL, Fraser NW. During latency, herpes simplex virus type 1 DNA is associated with nucleosomes in a chromatin structure. J Virol. 1989; 63: 943–947. PMID: 2536115

30. Kubat NJ, Tran RK, McAnany P, Bloom DC. Specific histone tail modification and not DNA methylation is a determinant of herpes simplex virus type 1 latent gene expression. J Virol. 2004 ed. 2004; 78: 1139–1149. https://doi.org/10.1128/JVI.78.3.1139-1149.2004 PMID: 14722269

31. Wang Q-Y, Zhou C, Johnson KE, Colgrove RC, Coen DM, Knipe DM. Herpesviral latency-associated transcript gene promotes assembly of heterochromatin on viral lytic-gene promoters in latent infection. Proc Natl Acad Sci USA. 2005; 102: 16055–16059. https://doi.org/10.1073/pnas.0505850102 PMID: 16247011

32. Knipe DM, Cliffe A. Chromatin control of herpes simplex virus lytic and latent infection. Nature reviews. 2008; 6: 211–221. https://doi.org/10.1038/nrmicro1794 PMID: 18264117

33. Cliffe AR, Garber DA, Knipe DM. Transcription of the herpes simplex virus latency-associated transcript promotes the formation of facultative heterochromatin on lytic promoters. J Virol. 2009 ed. American Society for Microbiology; 2009; 83: 8182–8190. https://doi.org/10.1128/JVI.00712-09 PMID: 19515781

34. Kwiatkowski DL, Thompson HW, Bloom DC. The polycomb group protein Bmi1 binds to the herpes simplex virus 1 latent genome and maintains repressive histone marks during latency. J Virol. 2009 ed. American Society for Microbiology; 2009; 83: 8173–8181. https://doi.org/10.1128/JVI.00686-09 PMID: 19515780

35. Tagami H, Ray-Gallet D, Almouzni G, Nakatani Y. Histone H3.1 and H3.3 complexes mediate nucleosome assembly pathways dependent or independent of DNA synthesis. Cell. 2004; 116: 51–61. PMID: 14718166

36. Szenker E, Ray-Gallet D, Almouzni G. The double face of the histone variant H3.3. Cell Res. 2011; 21: 421–434. https://doi.org/10.1038/cr.2011.14 PMID: 21263457

37. Wong LH, McGhie JD, Sim M, Anderson MA, Ahn S, Hannan RD, et al. ATRX interacts with H3.3 in maintaining telomere structural integrity in pluripotent embryonic stem cells. Genome Res. 2010; 20: 351–360. https://doi.org/10.1101/gr.101477.109 PMID: 20110566

38. Goldberg AD, Banaszynski LA, Noh K-M, Lewis PW, Elsaesser SJ, Stadler S, et al. Distinct factors control histone variant H3.3 localization at specific genomic regions. Cell. 2010; 140: 678–691. https://doi.org/10.1016/j.cell.2010.01.003 PMID: 20211137

39. Drané P, Ouararhni K, Depaux A, Shuaib M, Hamiche A. The death-associated protein DAXX is a novel histone chaperone involved in the replication-independent deposition of H3.3. Genes & development. 2010; 24: 1253–1265.

40. Banumathy G, Somaiah N, Zhang R, Tang Y, Hoffmann J, Andrake M, et al. Human UBN1 is an ortholog of yeast Hpc2p and has an essential role in the HIRA/ASF1a chromatin-remodeling pathway in senescent cells. Molecular and cellular biology. 2009; 29: 758–770. https://doi.org/10.1128/MCB.01047-08 PMID: 19029251

41. Rai TS, Puri A, McBryan T, Hoffman J, Tang Y, Pchelintsev NA, et al. Human CABIN1 is a functional member of the human HIRA/UBN1/ASF1a histone H3.3 chaperone complex. Molecular and cellular biology. 2011; 31: 4107–4118. https://doi.org/10.1128/MCB.05546-11 PMID: 21807893

42. Delbarre E, Ivanauskiene K, Küntziger T, Collas P. DAXX-dependent supply of soluble (H3.3-H4) dimers to PML bodies pending deposition into chromatin. Genome Res. 2013; 23: 440–451. https://doi.org/10.1101/gr.142703.112 PMID: 23222847

43. Corpet A, Olbrich T, Gwerder M, Fink D, Stucki M. Dynamics of histone H3.3 deposition in proliferating and senescent cells reveals a DAXX-dependent targeting to PML-NBs important for pericentromeric heterochromatin organization. Cell cycle (Georgetown), Tex. 2013; 13: 249–267.

44. Delbarre E, Ivanauskiene K, Spirkoski J, Shah A, Vekterud K, Moskaug JØ, et al. PML protein organizes heterochromatin domains where it regulates histone H3.3 deposition by ATRX/DAXX. Genome Res. Cold Spring Harbor Lab; 2017;: gr.215830.116.

45. Everett RD, Murray J, Orr A, Preston CM. Herpes simplex virus type 1 genomes are associated with ND10 nuclear substructures in quiescently infected human fibroblasts. J Virol. 2007 ed. American Society for Microbiology; 2007; 81: 10991–11004. https://doi.org/10.1128/JVI.00705-07 PMID: 17670833

46. Jamieson DR, Robinson LH, Daksis JI, Nicholl MJ, Preston CM. Quiescent viral genomes in human fibroblasts after infection with herpes simplex virus type 1 Vmw65 mutants. The Journal of general virology. 1995 ed. 1995; 76 (Pt 6): 1417–1431.

47. Preston CM, Nicholl MJ. Repression of gene expression upon infection of cells with herpes simplex virus type 1 mutants impaired for immediate-early protein synthesis. J Virol. 1997; 71: 7807–13. PMID: 9311867

48. Samaniego LA, Neiderhiser L, DeLuca NA. Persistence and expression of the herpes simplex virus genome in the absence of immediate-early proteins. J Virol. 1998; 72: 3307–20. PMID: 9525658

49. Ferenczy MW, Deluca NA. Epigenetic modulation of gene expression from quiescent herpes simplex virus genomes. J Virol. 2009 ed. American Society for Microbiology; 2009; 83: 8514–8524. https://doi.org/10.1128/JVI.00785-09 PMID: 19535445

50. Jackson SA, DeLuca NA. Relationship of herpes simplex virus genome configuration to productive and persistent infections. Proc Natl Acad Sci USA. 2003; 100: 7871–7876. https://doi.org/10.1073/pnas.1230643100 PMID: 12796511

51. Ray-Gallet D, Quivy J-P, Scamps C, Martini EM-D, Lipinski M, Almouzni G. HIRA is critical for a nucleosome assembly pathway independent of DNA synthesis. Molecular cell. 2002; 9: 1091–1100. PMID: 12049744

52. Ray-Gallet D, Woolfe A, Vassias I, Pellentz C, Lacoste N, Puri A, et al. Dynamics of histone h3 deposition in vivo reveal a nucleosome gap-filling mechanism for h3.3 to maintain chromatin integrity. Molecular cell. 2011; 44: 928–941. https://doi.org/10.1016/j.molcel.2011.12.006 PMID: 22195966

53. Lomonte P. The interaction between herpes simplex virus 1 genome and promyelocytic leukemia nuclear bodies (PML-NBs) as a hallmark of the entry in latency. Microb Cell. 2016; 3: 569–572. https://doi.org/10.15698/mic2016.11.541 PMID: 28357326

54. Lomonte P. Herpesvirus Latency: On the Importance of Positioning Oneself. Adv Anat Embryol Cell Biol. Cham: Springer International Publishing; 2017; 223: 95–117. https://doi.org/10.1007/978-3-319-53168-7_5 PMID: 28528441

55. Dembowski JA, Deluca NA. Temporal Viral Genome-Protein Interactions Define Distinct Stages of Productive Herpesviral Infection. Imperiale MJ, editor. MBio. 2018; 9: 90.

56. Rai TS, Glass M, Cole JJ, Rather MI, Marsden M, Neilson M, et al. Histone chaperone HIRA deposits histone H3.3 onto foreign viral DNA and contributes to anti-viral intrinsic immunity. Nucleic acids research. 2017.

57. Zhang H, Gan H, Wang Z, Lee J-H, Zhou H, Ordog T, et al. RPA Interacts with HIRA and Regulates H3.3 Deposition at Gene Regulatory Elements in Mammalian Cells. Molecular cell. Elsevier; 2017; 65: 272–284. https://doi.org/10.1016/j.molcel.2016.11.030 PMID: 28107649

58. Albright ER, Kalejta RF. Canonical and variant forms of histone H3 are deposited onto the human cytomegalovirus genome during lytic and latent infections. J Virol. 2016.

59. Ferenczy MW, Deluca NA. Reversal of Heterochromatic Silencing of Quiescent Herpes Simplex Virus Type 1 by ICP0. J Virol. 2011; 85: 3424–3435. https://doi.org/10.1128/JVI.02263-10 PMID: 21191021

60. Ferenczy MW, Ranayhossaini DJ, DeLuca NA. Activities of Icp0 Involved in the Reversal of Silencing of Quiescent Hsv-1. J Virol. 2011 ed. 2011.

61. Blahnik KR, Dou L, Echipare L, Iyengar S, O'Geen H, Sanchez E, et al. Characterization of the contradictory chromatin signatures at the 3' exons of zinc finger genes. Wutz A, editor. PloS one. Public Library of Science; 2011; 6: e17121. https://doi.org/10.1371/journal.pone.0017121 PMID: 21347206

62. Kirmizis A, Bartley SM, Kuzmichev A, Margueron R, Reinberg D, Green R, et al. Silencing of human polycomb target genes is associated with methylation of histone H3 Lys 27. Genes & development. Cold Spring Harbor Lab; 2004; 18: 1592–1605.

63. Banumathy G, Somaiah N, Zhang R, Tang Y, Hoffmann J, Andrake M, et al. Human UBN1 Is an Ortholog of Yeast Hpc2p and Has an Essential Role in the HIRA/ASF1a Chromatin-Remodeling Pathway in Senescent Cells. Molecular and cellular biology. 2009; 29: 758–770. https://doi.org/10.1128/MCB.01047-08 PMID: 19029251

64. Ricketts MD, Frederick B, Hoff H, Tang Y, Schultz DC, Singh Rai T, et al. Ubinuclein-1 confers histone H3.3-specific-binding by the HIRA histone chaperone complex. Nat Commun. 2015; 6: 7711–11. https://doi.org/10.1038/ncomms8711 PMID: 26159857

65. Cuchet-Lourenço D, Vanni E, Glass M, Orr A, Everett RD. Herpes simplex virus 1 ubiquitin ligase ICP0 interacts with PML isoform I and induces its SUMO-independent degradation. J Virol. 2012; 86: 11209–11222. https://doi.org/10.1128/JVI.01145-12 PMID: 22875967

66. Everett RD, Maul GG. HSV-1 IE protein Vmw110 causes redistribution of PML. The EMBO journal. 1994; 13: 5062–5069. PMID: 7957072

67. Halford WP, Schaffer PA. ICP0 is required for efficient reactivation of herpes simplex virus type 1 from neuronal latency. J Virol. 2001; 75: 3240–9. https://doi.org/10.1128/JVI.75.7.3240-3249.2001 PMID: 11238850

68. Placek BJ, Huang J, Kent JR, Dorsey J, Rice L, Fraser NW, et al. The histone variant H3.3 regulates gene expression during lytic infection with herpes simplex virus type 1. J Virol. 2008 ed. 2009; 83: 1416–1421. https://doi.org/10.1128/JVI.01276-08 PMID: 19004946

69. Oh J, Ruskoski N, Fraser NW. Chromatin assembly on herpes simplex virus 1 DNA early during a lytic infection is Asf1a dependent. J Virol. 2012; 86: 12313–12321. https://doi.org/10.1128/JVI.01570-12 PMID: 22951827

70. Tang Y, Puri A, Ricketts MD, Rai TS, Hoffmann J, Hoi E, et al. Identification of an ubinuclein 1 region required for stability and function of the human HIRA/UBN1/CABIN1/ASF1a histone H3.3 chaperone complex. Biochemistry. American Chemical Society; 2012; 51: 2366–2377.

71. Adam S, Polo SE, Almouzni G. Transcription Recovery after DNA Damage Requires Chromatin Priming by the H3.3 Histone Chaperone HIRA. Cell. 2013; 155: 94–106. https://doi.org/10.1016/j.cell.2013.08.029 PMID: 24074863

72. Adam S, Dabin J, Chevallier O, Leroy O, Baldeyron C, Corpet A, et al. Real-Time Tracking of Parental Histones Reveals Their Contribution to Chromatin Integrity Following DNA Damage. Molecular cell. 2016; 64: 65–78. https://doi.org/10.1016/j.molcel.2016.08.019 PMID: 27642047

73. Wilkie NM. The synthesis and substructure of herpesvirus DNA: the distribution of alkali-labile single strand interruptions in HSV-1 DNA. The Journal of general virology. Microbiology Society; 1973; 21: 453–467. https://doi.org/10.1099/0022-1317-21-3-453 PMID: 4357936

74. Orzalli MH, Conwell SE, Berrios C, DeCaprio JA, Knipe DM. Nuclear interferon-inducible protein 16 promotes silencing of herpesviral and transfected DNA. Proc Natl Acad Sci USA. 2013; 110: 501. https://doi.org/10.1073/pnas.1201390110 PMID: 23267076

75. Unterholzner L, Keating SE, Baran M, Horan KA, Jensen SB, Sharma S, et al. IFI16 is an innate immune sensor for intracellular DNA. Nat Immunol. 2010; 11: 997–1004. https://doi.org/10.1038/ni.1932 PMID: 20890285

76. Kerur N, Veettil MV, Sharma-Walia N, Bottero V, Sadagopan S, Otageri P, et al. IFI16 acts as a nuclear pathogen sensor to induce the inflammasome in response to Kaposi Sarcoma-associated herpesvirus infection. Cell Host Microbe. 2011; 9: 363–375. https://doi.org/10.1016/j.chom.2011.04.008 PMID: 21575908

77. Gariano GR, Dell'Oste V, Bronzini M, Gatti D, Luganini A, De Andrea M, et al. The intracellular DNA sensor IFI16 gene acts as restriction factor for human cytomegalovirus replication. PLoS Pathog. 2012; 8: e1002498. https://doi.org/10.1371/journal.ppat.1002498 PMID: 22291595

78. Orzalli MH, Deluca NA, Knipe DM. Nuclear IFI16 induction of IRF-3 signaling during herpesviral infection and degradation of IFI16 by the viral ICP0 protein. Proc Natl Acad Sci USA. National Acad Sciences; 2012; 109: E3008–17. https://doi.org/10.1073/pnas.1211302109 PMID: 23027953

79. Johnson KE, Chikoti L, Chandran B. Herpes simplex virus 1 infection induces activation and subsequent inhibition of the IFI16 and NLRP3 inflammasomes. J Virol. 2013; 87: 5005–5018. https://doi.org/10.1128/JVI.00082-13 PMID: 23427152

80. Ansari MA, Singh VV, Dutta S, Veettil MV, Dutta D, Chikoti L, et al. Constitutive interferon-inducible protein 16-inflammasome activation during Epstein-Barr virus latency I, II, and III in B and epithelial cells. J Virol. 2013; 87: 8606–8623. https://doi.org/10.1128/JVI.00805-13 PMID: 23720728

81. Dutta D, Dutta S, Veettil MV, Roy A, Ansari MA, Iqbal J, et al. BRCA1 Regulates IFI16 Mediated Nuclear Innate Sensing of Herpes Viral DNA and Subsequent Induction of the Innate Inflammasome and Interferon-β Responses. Feng P, editor. PLoS Pathog. 2015; 11: e1005030. https://doi.org/10.1371/journal.ppat.1005030 PMID: 26121674

82. Diner BA, Li T, Greco TM, Crow MS, Fuesler JA, Wang J, et al. The functional interactome of PYHIN immune regulators reveals IFIX is a sensor of viral DNA. Mol Syst Biol. European Molecular Biology Organization; 2015; 11: 787–787. https://doi.org/10.15252/msb.20145808 PMID: 25665578

83. Tsai K, Chan L, Gibeault R, Conn K, Dheekollu J, Domsic J, et al. Viral Reprogramming of the Daxx-Histone H3.3 Chaperone During EBV Early Infection. J Virol. American Society for Microbiology; 2014; 88: 14350–14363. https://doi.org/10.1128/JVI.01895-14 PMID: 25275136

84. Schreiner S, Bürck C, Glass M, Groitl P, Wimmer P, Kinkley S, et al. Control of human adenovirus type 5 gene expression by cellular Daxx/ATRX chromatin-associated complexes. Nucleic acids research. 2013.

85. Labetoulle M, Maillet S, Efstathiou S, Dezelee S, Frau E, Lafay F. HSV1 latency sites after inoculation in the lip: assessment of their localization and connections to the eye. Invest Ophthalmol Vis Sci. 2003; 44: 217–225. PMID: 12506078

86. Preston CM. Abnormal properties of an immediate early polypeptide in cells infected with the herpes simplex virus type 1 mutant tsK. J Virol. 1979; 32: 357–369. PMID: 228063

87. Ace CI, McKee TA, Ryan JM, Cameron JM, Preston CM. Construction and characterization of a herpes simplex virus type 1 mutant unable to transinduce immediate-early gene expression. J Virol. 1989; 63: 2260–2269. PMID: 2539517

88. Preston CM, Rinaldi A, Nicholl MJ. Herpes simplex virus type 1 immediate early gene expression is stimulated by inhibition of protein synthesis. The Journal of general virology. 1998; 79 (Pt 1): 117–124.

89. Preston CM, Nicholl MJ. Human Cytomegalovirus Tegument Protein pp71 Directs Long-Term Gene Expression from Quiescent Herpes Simplex Virus Genomes. J Virol. 2005; 79: 525–535. https://doi.org/10.1128/JVI.79.1.525-535.2005 PMID: 15596845

90. McFarlane M, Daksis JI, Preston CM. Hexamethylene bisacetamide stimulates herpes simplex virus immediate early gene expression in the absence of trans-induction by Vmw65. The Journal of general virology. 1992; 73 (Pt 2): 285–292.

91. Wang ZG, Ruggero D, Ronchetti S, Zhong S, Gaboli M, Rivi R, et al. PML is essential for multiple apoptotic pathways. Nat Genet. 1998; 20: 266–272. https://doi.org/10.1038/3073 PMID: 9806545

92. Catez F, Rousseau A, Labetoulle M, Lomonte P. Detection of the genome and transcripts of a persistent DNA virus in neuronal tissues by fluorescent in situ hybridization combined with immunostaining. J Vis Exp. 2014;: e51091. https://doi.org/10.3791/51091 PMID: 24514006

93. Sawtell NM, Thompson RL. Comparison of herpes simplex virus reactivation in ganglia in vivo and in explants demonstrates quantitative and qualitative differences. J Virol. 2004 ed. 2004; 78: 7784–7794. https://doi.org/10.1128/JVI.78.14.7784-7794.2004 PMID: 15220452

94. Cunningham C, Davison AJ. A cosmid-based system for constructing mutants of herpes simplex virus type 1. Virology. 1993; 197: 116–124. https://doi.org/10.1006/viro.1993.1572 PMID: 8212547

95. Pear W. Transient transfection methods for preparation of high-titer retroviral supernatants. Curr Protoc Mol Biol. Hoboken, NJ, USA: John Wiley & Sons, Inc; 2001;Chapter 9: Unit9.11.

96. Naviaux RK, Costanzi E, Haas M, Verma IM. The pCL vector system: rapid production of helper-free, high-titer, recombinant retroviruses. J Virol. 1996; 70: 5701–5705. PMID: 8764092

97. Sambrook J, Russell DW. Calcium-phosphate-mediated Transfection of Eukaryotic Cells with Plasmid DNAs. Sambrook JRussell D, editors. CSH Protoc. 2006;2006: pdb.prot3871.

98. Everett RD, Parsy M-L, Orr A. Analysis of the functions of herpes simplex virus type 1 regulatory protein ICP0 that are critical for lytic infection and derepression of quiescent viral genomes. J Virol. 2009 ed. American Society for Microbiology; 2009; 83: 4963–4977. https://doi.org/10.1128/JVI.02593-08 PMID: 19264778

99. Cantrell SR, Bresnahan WA. Human cytomegalovirus (HCMV) UL82 gene product (pp71) relieves hDaxx-mediated repression of HCMV replication. J Virol. 2006; 80: 6188–6191. https://doi.org/10.1128/JVI.02676-05 PMID: 16731959

100. Zhang R, Liu S-T, Chen W, Bonner M, Pehrson J, Yen TJ, et al. HP1 proteins are essential for a dynamic nuclear response that rescues the function of perturbed heterochromatin in primary human cells. Molecular and cellular biology. 2007; 27: 949–962. https://doi.org/10.1128/MCB.01639-06 PMID: 17101789

# Bibliographie


A, P., and Weber, S.C. (2019). Evidence for and against Liquid-Liquid Phase Separation in the Nucleus. Non-Coding RNA *5*, 50.

Abu-Zhayia, E.R., Awwad, S.W., Ben-Oz, B.M., Khoury-Haddad, H., and Ayoub, N. (2018). CDYL1 fosters double-strand break-induced transcription silencing and promotes homology-directed repair. J. Mol. Cell Biol. *10*, 341–357.

Adam, S., Polo, S.E., and Almouzni, G. (2013). Transcription Recovery after DNA Damage Requires Chromatin Priming by the H3.3 Histone Chaperone HIRA. Cell *155*, 94–106.

Ahmad, K., and Henikoff, S. (2002). The histone variant H3.3 marks active chromatin by replication-independent nucleosome assembly. Mol. Cell *9*, 1191–1200.

Alandijany, T., Roberts, A.P.E., Conn, K.L., Loney, C., McFarlane, S., Orr, A., and Boutell, C. (2018). Distinct temporal roles for the promyelocytic leukaemia (PML) protein in the sequential regulation of intracellular host immunity to HSV-1 infection. PLOS Pathog. *14*, e1006769.

Aleksandrov, R., Hristova, R., Stoynov, S., and Gospodinov, A. (2020). The Chromatin Response to Double-Strand DNA Breaks and Their Repair. Cells *9*.

Allfrey, V.G., Faulkner, R., and Mirsky, A.E. (1964). Acetylation and Methylation of Histones and Their Possible Role in the Regulation of Rna Synthesis. Proc. Natl. Acad. Sci. *51*, 786–794.

Allis, C.D., and Jenuwein, T. (2016). The molecular hallmarks of epigenetic control. Nat. Rev. Genet. *17*, 487–500.

Alvarez, F., Muñoz, F., Schilcher, P., Imhof, A., Almouzni, G., and Loyola, A. (2011). Sequential Establishment of Marks on Soluble Histones H3 and H4 *. J. Biol. Chem. *286*, 17714–17721.

Ambrosi, C., Manzo, M., and Baubec, T. (2017). Dynamics and Context-Dependent Roles of DNA Methylation. J. Mol. Biol. *429*, 1459–1475.

Amin, A.D., Vishnoi, N., and Prochasson, P. (2012). A global requirement for the HIR complex in the assembly of chromatin. Biochim. Biophys. Acta BBA - Gene Regul. Mech. *1819*, 264–276.

Arimura, Y., Kimura, H., Oda, T., Sato, K., Osakabe, A., Tachiwana, H., Sato, Y., Kinugasa, Y., Ikura, T., Sugiyama, M., et al. (2013). Structural basis of a nucleosome containing histone H2A.B/H2A.Bbd that transiently associates with reorganized chromatin. Sci. Rep. *3*, 3510.

Armache, A., Yang, S., de Paz, A.M., Robbins, L.E., Durmaz, C., Jeong, J.Q., Ravishankar, A., Daman, A.W., Ahimovic, D.J., Klevorn, T., et al. (2020). Histone H3.3 phosphorylation amplifies stimulation-induced transcription. Nature *583*, 852–857.

Arnaudo, A.M., and Garcia, B.A. (2013). Proteomic characterization of novel histone post-translational modifications. Epigenetics Chromatin *6*, 24.

Arnould, C., Rocher, V., Finoux, A.-L., Clouaire, T., Li, K., Zhou, F., Caron, P., Mangeot, P.E., Ricci, E.P., Mourad, R., et al. (2021). Loop extrusion as a mechanism for formation of DNA damage repair foci. Nature 1–6.

Atianand, M.K., Hu, W., Satpathy, A.T., Shen, Y., Ricci, E.P., Alvarez-Dominguez, J.R., Bhatta, A., Schattgen, S.A., McGowan, J.D., Blin, J., et al. (2016). A Long Noncoding RNA lincRNA-EPS Acts as a Transcriptional Brake to Restrain Inflammation. Cell *165*, 1672–1685.

van Attikum, H., Fritsch, O., and Gasser, S.M. (2007). Distinct roles for SWR1 and INO80 chromatin remodeling complexes at chromosomal double-strand breaks. EMBO J. *26*, 4113–4125.

Awasthi, P., Foiani, M., and Kumar, A. (2015). ATM and ATR signaling at a glance. J. Cell Sci. *128*, 4255–4262.

Aymard, F., Bugler, B., Schmidt, C.K., Guillou, E., Caron, P., Briois, S., Iacovoni, J.S., Daburon, V., Miller, K.M., Jackson, S.P., et al. (2014). Transcriptionally active chromatin recruits homologous recombination at DNA double strand breaks. Nat. Struct. Mol. Biol. *21*, 366–374.

Baker, D.J., Childs, B.G., Durik, M., Wijers, M.E., Sieben, C.J., Zhong, J., Saltness, R.A., Jeganathan, K.B., Verzosa, G.C., Pezeshki, A., et al. (2016). Naturally occurring p16(Ink4a)-positive cells shorten healthy lifespan. Nature *530*, 184–189.

Balas, M.M., and Johnson, A.M. (2018). Exploring the mechanisms behind long noncoding RNAs and cancer. Non-Coding RNA Res. *3*, 108–117.

Balbo Pogliano, C., Gatti, M., Rüthemann, P., Garajovà, Z., Penengo, L., and Naegeli, H. (2017). ASH1L histone methyltransferase regulates the handoff between damage recognition factors in global-genome nucleotide excision repair. Nat. Commun. *8*, 1333.

Banani, S.F., Rice, A.M., Peeples, W.B., Lin, Y., Jain, S., Parker, R., and Rosen, M.K. (2016). Compositional Control of Phase-Separated Cellular Bodies. Cell *166*, 651–663.

Banani, S.F., Lee, H.O., Hyman, A.A., and Rosen, M.K. (2017). Biomolecular condensates: Organizers of cellular biochemistry. Nat. Rev. Mol. Cell Biol. *18*, 285–298.

Banigan, E.J., and Mirny, L.A. (2020). Loop extrusion: theory meets single-molecule experiments. Curr. Opin. Cell Biol. *64*, 124–138.

Banin, S., Moyal, L., Shieh, S., Taya, Y., Anderson, C.W., Chessa, L., Smorodinsky, N.I., Prives, C., Reiss, Y., Shiloh, Y., et al. (1998). Enhanced phosphorylation of p53 by ATM in response to DNA damage. Science *281*, 1674–1677.

Bannister, A.J., and Kouzarides, T. (2011). Regulation of chromatin by histone modifications. Cell Res. *21*, 381–395.

Bannister, A.J., Zegerman, P., Partridge, J.F., Miska, E.A., Thomas, J.O., Allshire, R.C., and Kouzarides, T. (2001). Selective recognition of methylated lysine 9 on histone H3 by the HP1 chromo domain. Nature *410*, 120–124.

Banumathy, G., Somaiah, N., Zhang, R., Tang, Y., Hoffmann, J., Andrake, M., Ceulemans, H., Schultz, D., Marmorstein, R., and Adams, P.D. (2009). Human UBN1 is an ortholog of yeast Hpc2p and has an essential role in the HIRA/ASF1a chromatin-remodeling pathway in senescent cells. Mol. Cell. Biol. *29*, 758–770.

Barr, S.M., Leung, C.G., Chang, E.E., and Cimprich, K.A. (2003). ATR kinase activity regulates the intranuclear translocation of ATR and RPA following ionizing radiation. Curr. Biol. CB *13*, 1047–1051.

Barrat, F.J., Crow, M.K., and Ivashkiv, L.B. (2019). Interferon target-gene expression and epigenomic signatures in health and disease. Nat. Immunol. *20*, 1574–1583.

Bartkova, J., Rezaei, N., Liontos, M., Karakaidos, P., Kletsas, D., Issaeva, N., Vassiliou, L.-V.F., Kolettas, E., Niforou, K., Zoumpourlis, V.C., et al. (2006). Oncogene-induced senescence is part of the tumorigenesis barrier imposed by DNA damage checkpoints. Nature *444*, 633–637.

Battu, A., Ray, A., and Wani, A.A. (2011). ASF1A and ATM regulate H3K56-mediated cell-cycle checkpoint recovery in response to UV irradiation. Nucleic Acids Res. *39*, 7931–7945.

Beauclair, G., Bridier-Nahmias, A., Zagury, J.-F., Saïb, A., and Zamborlini, A. (2015). JASSA: a comprehensive tool for prediction of SUMOylation sites and SIMs. Bioinformatics *31*, 3483–3491.

Behjati, S., Tarpey, P.S., Presneau, N., Scheipl, S., Pillay, N., Van Loo, P., Wedge, D.C., Cooke, S.L., Gundem, G., Davies, H., et al. (2013). Distinct H3F3A and H3F3B driver variants define chondroblastoma and giant cell tumour of bone. Nat. Genet. *45*.

Bell, P., Lieberman, P.M., and Maul, G.G. (2000a). Lytic but not latent replication of epstein-barr virus is associated with PML and induces sequential release of nuclear domain 10 proteins. J.

Virol. *74*, 11800–11810.

Bell, P., Brazas, R., Ganem, D., and Maul, G.G. (2000b). Hepatitis Delta Virus Replication Generates Complexes of Large Hepatitis Delta Antigen and Antigenomic RNA That Affiliate with and Alter Nuclear Domain 10. J. Virol. *74*, 5329–5336.

Bergink, S., and Jentsch, S. (2009). Principles of ubiquitin and SUMO modifications in DNA repair. Nature *458*, 461–467.

Bergink, S., Salomons, F.A., Hoogstraten, D., Groothuis, T.A.M., de Waard, H., Wu, J., Yuan, L., Citterio, E., Houtsmuller, A.B., Neefjes, J., et al. (2006). DNA damage triggers nucleotide excision repair-dependent monoubiquitylation of histone H2A. Genes Dev. *20*, 1343–1352.

Bernardi, R., and Pandolfi, P.P. (2007). Structure, dynamics and functions of promyelocytic leukaemia nuclear bodies. Nat. Rev. Mol. Cell Biol. *8*, 1006–1016.

Bernardi, R., Scaglioni, P.P., Bergmann, S., Horn, H.F., Vousden, K.H., and Pandolfi, P.P. (2004). PML regulates p53 stability by sequestering Mdm2 to the nucleolus. Nat. Cell Biol. *6*, 665–672.

Bernardi, R., Guernah, I., Jin, D., Grisendi, S., Alimonti, A., Teruya-Feldstein, J., Cordon-Cardo, C., Celeste Simon, M., Rafii, S., and Pandolfi, P.P. (2006). PML inhibits HIF-1α translation and neoangiogenesis through repression of mTOR. Nature *442*, 779–785.

Bischof, O., Kim, S.-H., Irving, J., Beresten, S., Ellis, N.A., and Campisi, J. (2001). Regulation and Localization of the Bloom Syndrome Protein in Response to DNA Damage. J. Cell Biol. *153*, 367–380.

Blackford, A.N., and Jackson, S.P. (2017). ATM, ATR, and DNA-PK: The Trinity at the Heart of the DNA Damage Response. Mol. Cell *66*, 801–817.

Blondel, D., Regad, T., Poisson, N., Pavie, B., Harper, F., Pandolfi, P.P., De Thé, H., and Chelbi-Alix, M.K. (2002). Rabies virus P and small P products interact directly with PML and reorganize PML nuclear bodies. Oncogene *21*, 7957–7970.

Bloom, D.C., Giordani, N.V., and Kwiatkowski, D.L. (2010). Epigenetic regulation of latent HSV-1 gene expression. Biochim. Biophys. Acta *1799*, 246–256.

Boddy, M.N., Howe, K., Etkin, L.D., Solomon, E., and Freemont, P.S. (1996). PIC 1, a novel ubiquitin-like protein which interacts with the PML component of a multiprotein complex that is disrupted in acute promyelocytic leukaemia. Oncogene *13*, 971–982.

Boeren, J., and Gribnau, J. (2021). Xist-mediated chromatin changes that establish silencing of an entire X chromosome in mammals. Curr. Opin. Cell Biol. *70*, 44–50.

Bohren, K.M., Nadkarni, V., Song, J.H., Gabbay, K.H., and Owerbach, D. (2004). A M55V polymorphism in a novel SUMO gene (SUMO-4) differentially activates heat shock transcription factors and is associated with susceptibility to type I diabetes mellitus. J. Biol. Chem. *279*, 27233–27238.

Boisvert, F.M., Kruhlak, M.J., Box, A.K., Hendzel, M.J., and Bazett-Jones, D.P. (2001). The transcription coactivator CBP is a dynamic component of the promyelocytic leukemia nuclear body. J. Cell Biol. *152*, 1099–1106.

Bonilla, W.V., Pinschewer, D.D., Klenerman, P., Rousson, V., Gaboli, M., Pandolfi, P.P., Zinkernagel, R.M., Salvato, M.S., and Hengartner, H. (2002). Effects of promyelocytic leukemia protein on virus-host balance. J. Virol. *76*, 3810–3818.

Bonnefoy, E., Orsi, G.A., Couble, P., and Loppin, B. (2007). The essential role of Drosophila HIRA for de novo assembly of paternal chromatin at fertilization. Plos Genet. *3*, 1991–2006.

Borden, K.L. (1998). RING fingers and B-boxes: zinc-binding protein-protein interaction domains. Biochem. Cell Biol. Biochim. Biol. Cell. *76*, 351–358.

Bostick, M., Kim, J.K., Estève, P.-O., Clark, A., Pradhan, S., and Jacobsen, S.E. (2007). UHRF1 plays a role in maintaining DNA methylation in mammalian cells. Science *317*, 1760–1764.

Botuyan, M.V., Lee, J., Ward, I.M., Kim, J.-E., Thompson, J.R., Chen, J., and Mer, G. (2006). Structural basis for the methylation state-specific recognition of histone H4-K20 by 53BP1 and Crb2 in DNA repair. Cell *127*, 1361–1373.

Boyer, J.A., Spangler, C.J., Strauss, J.D., Cesmat, A.P., Liu, P., McGinty, R.K., and Zhang, Q. (2020). Structural basis of nucleosome-dependent cGAS inhibition. Science *370*, 450–454.

Bradley, J.R. (2008). TNF-mediated inflammatory disease. J. Pathol. *214*, 149–160.

Braig, M., Lee, S., Loddenkemper, C., Rudolph, C., Peters, A.H.F.M., Schlegelberger, B., Stein, H., Dörken, B., Jenuwein, T., and Schmitt, C.A. (2005). Oncogene-induced senescence as an initial barrier in lymphoma development. Nature *436*, 660–665.

Brand, P., Lenser, T., and Hemmerich, P. (2010). Assembly dynamics of PML nuclear bodies in living cells. PMC Biophys. *3*, 3.

Braunschweig, U., Hogan, G.J., Pagie, L., and van Steensel, B. (2009). Histone H1 binding is inhibited by histone variant H3.3. EMBO J. *28*, 3635–3645.

Brubaker, S.W., Bonham, K.S., Zanoni, I., and Kagan, J.C. (2015). Innate Immune Pattern Recognition: A Cell Biological Perspective. Annu. Rev. Immunol. *33*, 257–290.

Brzostek-Racine, S., Gordon, C., Van Scoy, S., and Reich, N.C. (2011). The DNA Damage Response Induces Interferon. J. Immunol. Baltim. Md 1950 *187*, 5336–5345.

Buczek, M.E., Miles, A.K., Green, W., Johnson, C., Boocock, D.J., Pockley, A.G., Rees, R.C., Hulman, G., van Schalkwyk, G., Parkinson, R., et al. (2016). Cytoplasmic PML promotes TGF-β-associated epithelial–mesenchymal transition and invasion in prostate cancer. Oncogene *35*, 3465–3475.

Buschbeck, M., and Hake, S.B. (2017). Variants of core histones and their roles in cell fate decisions, development and cancer. Nat. Rev. Mol. Cell Biol. *18*, 299–314.

Cadet, J., Berger, M., Douki, T., and Ravanat, J.-L. (1997). Oxidative damage to DNA: Formation, measurement, and biological significance. In Reviews of Physiology Biochemistry and Pharmacology, Volume 131: Special Issue on Membrane-Mediated Cellular Responses: The Roles of Reactive Oxygens, NO, CO, II, (Berlin, Heidelberg: Springer), pp. 1–87.

Campisi, J. (2005). Senescent Cells, Tumor Suppression, and Organismal Aging: Good Citizens, Bad Neighbors. Cell *120*, 513–522.

Canman, C.E., Lim, D.S., Cimprich, K.A., Taya, Y., Tamai, K., Sakaguchi, K., Appella, E., Kastan, M.B., and Siliciano, J.D. (1998). Activation of the ATM kinase by ionizing radiation and phosphorylation of p53. Science *281*, 1677–1679.

Cappadocia, L., Mascle, X.H., Bourdeau, V., Tremblay-Belzile, S., Chaker-Margot, M., Lussier-Price, M., Wada, J., Sakaguchi, K., Aubry, M., Ferbeyre, G., et al. (2015). Structural and Functional Characterization of the Phosphorylation-Dependent Interaction between PML and SUMO1. Structure *23*, 126–138.

Carbone, R., Pearson, M., Minucci, S., and Pelicci, P.G. (2002). PML NBs associate with the hMre11 complex and p53 at sites of irradiation induced DNA damage. Oncogene *21*, 1633–1640.

Carpenter, S., Atianand, M., Aiello, D., Ricci, E., Gandhi, P., Hall, L.L., Byron, M., Monks, B., Henry-Bezy, M., O'Neill, L.A.J., et al. (2013). A long noncoding RNA induced by TLRs mediates both activation and repression of immune response genes. Science *341*, 789–792.

Carracedo, A., Weiss, D., Leliaert, A.K., Bhasin, M., de Boer, V.C.J., Laurent, G., Adams, A.C., Sundvall, M., Song, S.J., Ito, K., et al. (2012). A metabolic prosurvival role for PML in breast cancer. J. Clin. Invest. *122*, 3088–3100.

Carvalho, S., Vítor, A.C., Sridhara, S.C., Martins, F.B., Raposo, A.C., Desterro, J.M.P., Ferreira, J., and de Almeida, S.F. (2014). SETD2 is required for DNA double-strand break repair and activation of the p53-mediated checkpoint. ELife *3*, e02482.

Catez, F., Picard, C., Held, K., Gross, S., Rousseau, A., Theil, D., Sawtell, N., Labetoulle, M., and Lomonte, P. (2012). HSV-1 Genome Subnuclear Positioning and Associations with Host-Cell PML-NBs and Centromeres Regulate LAT Locus Transcription during Latency in Neurons. PLOS Pathog. *8*, e1002852.

Cavalli, G., and Heard, E. (2019). Advances in epigenetics link genetics to the environment and disease. Nature *571*, 489–499.

Ceccaldi, R., Sarangi, P., and D'Andrea, A.D. (2016a). The Fanconi anaemia pathway: new players and new functions. Nat. Rev. Mol. Cell Biol. *17*, 337–349.

Ceccaldi, R., Rondinelli, B., and D'Andrea, A.D. (2016b). Repair Pathway Choices and Consequences at the Double-Strand Break. Trends Cell Biol. *26*, 52–64.

Cecco, M.D., Ito, T., Petrashen, A.P., Elias, A.E., Skvir, N.J., Criscione, S.W., Caligiana, A., Brocculi, G., Adney, E.M., Boeke, J.D., et al. (2019). LINE-1 derepression in senescent cells triggers interferon and inflammaging. Nature *566*, 73–78.

Chang, H.-M., and Yeh, E.T.H. (2020). SUMO: From Bench to Bedside. Physiol. Rev. *100*, 1599–1619.

Chang, C.-C., Naik, M.T., Huang, Y.-S., Jeng, J.-C., Liao, P.-H., Kuo, H.-Y., Ho, C.-C., Hsieh, Y.-L., Lin, C.-H., Huang, N.-J., et al. (2011). Structural and Functional Roles of Daxx SIM Phosphorylation in SUMO Paralog-Selective Binding and Apoptosis Modulation. Mol. Cell *42*, 62–74.

Chang, F.T.M., Chan, F.L., R McGhie, J.D., Udugama, M., Mayne, L., Collas, P., Mann, J.R., and Wong, L.H. (2015). CHK1-driven histone H3.3 serine 31 phosphorylation is important for chromatin maintenance and cell survival in human ALT cancer cells. Nucleic Acids Res. *43*, 2603–2614.

Chang, H.R., Munkhjargal, A., Kim, M.-J., Park, S.Y., Jung, E., Ryu, J.-H., Yang, Y., Lim, J.-S., and Kim, Y. (2018). The functional roles of PML nuclear bodies in genome maintenance. Mutat. Res. Mol. Mech. Mutagen. *809*, 99–107.

Channappanavar, R., and Perlman, S. (2017). Pathogenic human coronavirus infections: causes and consequences of cytokine storm and immunopathology. Semin. Immunopathol. *39*, 529–539.

Chapman, J.R., and Jackson, S.P. (2008). Phospho-dependent interactions between NBS1 and MDC1 mediate chromatin retention of the MRN complex at sites of DNA damage. EMBO Rep. *9*, 795–801.

Chatterjee, N., and Walker, G.C. (2017). Mechanisms of DNA damage, repair and mutagenesis. Environ. Mol. Mutagen. *58*, 235–263.

Chaturvedi, P., Eng, W.K., Zhu, Y., Mattern, M.R., Mishra, R., Hurle, M.R., Zhang, X., Annan, R.S., Lu, Q., Faucette, L.F., et al. (1999). Mammalian Chk2 is a downstream effector of the ATM-dependent DNA damage checkpoint pathway. Oncogene *18*, 4047–4054.

Chelbi-Alix, M.K., Pelicano, L., Quignon, F., Koken, M.H., Venturini, L., Stadler, M., Pavlovic, J., Degos, L., and de Thé, H. (1995). Induction of the PML protein by interferons in normal and APL cells. Leukemia *9*, 2027–2033.

Chen, Y., and Belmont, A.S. (2019). Genome Organization around Nuclear Speckles. Curr. Opin. Genet. Dev. *55*, 91–99.

Chen, C., Sun, M., Warzecha, C., Bachu, M., Dey, A., Wu, T., Adams, P.D., Macfarlan, T., Love, P., and Ozato, K. (2020). HIRA, a DiGeorge Syndrome Candidate Gene, Confers Proper Chromatin Accessibility on HSCs and Supports All Stages of Hematopoiesis. Cell Rep. *30*, 2136-

2149.e4.

Chen, K., Liu, J., and Cao, X. (2017). Regulation of type I interferon signaling in immunity and inflammation: A comprehensive review. J. Autoimmun. *83*, 1–11.

Chen, P., Zhao, J., Wang, Y., Wang, M., Long, H., Liang, D., Huang, L., Wen, Z., Li, W., Li, X., et al. (2013). H3.3 actively marks enhancers and primes gene transcription via opening higher-ordered chromatin. Genes Dev. *27*, 2109–2124.

Chen, Z., Trotman, L.C., Shaffer, D., Lin, H.-K., Dotan, Z.A., Niki, M., Koutcher, J.A., Scher, H.I., Ludwig, T., Gerald, W., et al. (2005). Crucial role of p53-dependent cellular senescence in suppression of Pten-deficient tumorigenesis. Nature *436*, 725–730.

Cheng, X., and Kao, H.-Y. (2013). Post-translational modifications of PML: consequences and implications. Front. Oncol. *2*.

Cheng, X., Liu, Y., Chu, H., and Kao, H.-Y. (2012). Promyelocytic leukemia protein (PML) regulates endothelial cell network formation and migration in response to tumor necrosis factor α (TNFα) and interferon α (IFNα). J. Biol. Chem. *287*, 23356–23367.

Cheng, X., Guo, S., Liu, Y., Chu, H., Hakimi, P., Berger, N.A., Hanson, R.W., and Kao, H.-Y. (2013). Ablation of promyelocytic leukemia protein (PML) re-patterns energy balance and protects mice from obesity induced by a Western diet. J. Biol. Chem. *288*, 29746–29759.

Chou, D.M., Adamson, B., Dephoure, N.E., Tan, X., Nottke, A.C., Hurov, K.E., Gygi, S.P., Colaiácovo, M.P., and Elledge, S.J. (2010). A chromatin localization screen reveals poly (ADP ribose)-regulated recruitment of the repressive polycomb and NuRD complexes to sites of DNA damage. Proc. Natl. Acad. Sci. U. S. A. *107*, 18475–18480.

Chowdhury, D., Keogh, M.-C., Ishii, H., Peterson, C.L., Buratowski, S., and Lieberman, J. (2005). gamma-H2AX dephosphorylation by protein phosphatase 2A facilitates DNA double-strand break repair. Mol. Cell *20*, 801–809.

Chowdhury, D., Xu, X., Zhong, X., Ahmed, F., Zhong, J., Liao, J., Dykxhoorn, D.M., Weinstock, D.M., Pfeifer, G.P., and Lieberman, J. (2008). A PP4-phosphatase complex dephosphorylates gamma-H2AX generated during DNA replication. Mol. Cell *31*, 33–46.

Chung, I., Leonhardt, H., and Rippe, K. (2011). De novo assembly of a PML nuclear subcompartment occurs through multiple pathways and induces telomere elongation. J. Cell Sci. *124*, 3603–3618.

Ciccia, A., and Elledge, S.J. (2010). The DNA Damage Response: Making it safe to play with knives. Mol. Cell *40*, 179–204.

Clapier, C.R., Iwasa, J., Cairns, B.R., and Peterson, C.L. (2017). Mechanisms of action and regulation of ATP-dependent chromatin-remodelling complexes. Nat. Rev. Mol. Cell Biol. *18*, 407–422.

Cliffe, A.R., Garber, D.A., and Knipe, D.M. (2009). Transcription of the Herpes Simplex Virus Latency-Associated Transcript Promotes the Formation of Facultative Heterochromatin on Lytic Promoters. J. Virol. *83*, 8182–8190.

Clouaire, T., Rocher, V., Lashgari, A., Arnould, C., Aguirrebengoa, M., Biernacka, A., Skrzypczak, M., Aymard, F., Fongang, B., Dojer, N., et al. (2018). Comprehensive Mapping of Histone Modifications at DNA Double-Strand Breaks Deciphers Repair Pathway Chromatin Signatures. Mol. Cell *72*, 250-262.e6.

Clynes, D., Higgs, D.R., and Gibbons, R.J. (2013). The chromatin remodeller ATRX: a repeat offender in human disease. Trends Biochem. Sci. *38*, 461–466.

Cohen, C., Corpet, A., Roubille, S., Maroui, M.A., Poccardi, N., Rousseau, A., Kleijwegt, C., Binda, O., Texier, P., Sawtell, N., et al. (2018). Promyelocytic leukemia (PML) nuclear bodies (NBs) induce latent/quiescent HSV-1 genomes chromatinization through a PML NB/Histone

H3.3/H3.3 Chaperone Axis. PLoS Pathog. *14*, e1007313.

Coit, P., Jeffries, M., Altorok, N., Dozmorov, M.G., Koelsch, K.A., Wren, J.D., Merrill, J.T., McCune, W.J., and Sawalha, A.H. (2013). Genome-wide DNA methylation study suggests epigenetic accessibility and transcriptional poising of interferon-regulated genes in naïve CD4+ T cells from lupus patients. J. Autoimmun. *43*, 78–84.

Coit, P., Yalavarthi, S., Ognenovski, M., Zhao, W., Hasni, S., Wren, J.D., Kaplan, M.J., and Sawalha, A.H. (2015). Epigenome profiling reveals significant DNA demethylation of interferon signature genes in lupus neutrophils. J. Autoimmun. *58*, 59–66.

Condemine, W., Takahashi, Y., Zhu, J., Puvion-Dutilleul, F., Guegan, S., Janin, A., and Thé, H. de (2006). Characterization of Endogenous Human Promyelocytic Leukemia Isoforms. Cancer Res. *66*, 6192–6198.

Cook, A.J.L., Gurard-Levin, Z.A., Vassias, I., and Almouzni, G. (2011). A specific function for the histone chaperone NASP to fine-tune a reservoir of soluble H3-H4 in the histone supply chain. Mol. Cell *44*, 918–927.

Coperchini, F., Chiovato, L., Croce, L., Magri, F., and Rotondi, M. (2020). The cytokine storm in COVID-19: An overview of the involvement of the chemokine/chemokine-receptor system. Cytokine Growth Factor Rev. *53*, 25–32.

Coppé, J.-P., Patil, C.K., Rodier, F., Sun, Y., Muñoz, D.P., Goldstein, J., Nelson, P.S., Desprez, P.-Y., and Campisi, J. (2008). Senescence-Associated Secretory Phenotypes Reveal Cell-Nonautonomous Functions of Oncogenic RAS and the p53 Tumor Suppressor. PLoS Biol. *6*.

Corpet, A., Olbrich, T., Gwerder, M., Fink, D., and Stucki, M. (2014). Dynamics of histone H3.3 deposition in proliferating and senescent cells reveals a DAXX-dependent targeting to PML-NBs important for pericentromeric heterochromatin organization. Cell Cycle *13*, 249–267.

Corpet, A., Kleijwegt, C., Roubille, S., Juillard, F., Jacquet, K., Texier, P., and Lomonte, P. (2020). PML nuclear bodies and chromatin dynamics: catch me if you can! Nucleic Acids Res. *48*, 11890–11912.

Courilleau, C., Chailleux, C., Jauneau, A., Grimal, F., Briois, S., Boutet-Robinet, E., Boudsocq, F., Trouche, D., and Canitrot, Y. (2012). The chromatin remodeler p400 ATPase facilitates Rad51-mediated repair of DNA double-strand breaks. J. Cell Biol. *199*, 1067–1081.

Crosetto, N., and Bienko, M. (2020). Radial Organization in the Mammalian Nucleus. Front. Genet. *11*, 33.

Cuchet-Lourenço, D., Boutell, C., Lukashchuk, V., Grant, K., Sykes, A., Murray, J., Orr, A., and Everett, R.D. (2011). SUMO Pathway Dependent Recruitment of Cellular Repressors to Herpes Simplex Virus Type 1 Genomes. PLoS Pathog. *7*.

Cutter, A.R., and Hayes, J.J. (2017). Linker histones: Novel insights into structure-specific recognition of the nucleosome. Biochem. Cell Biol. Biochim. Biol. Cell. *95*, 171–178.

Daugaard, M., Baude, A., Fugger, K., Povlsen, L.K., Beck, H., Sørensen, C.S., Petersen, N.H.T., Sorensen, P.H.B., Lukas, C., Bartek, J., et al. (2012). LEDGF (p75) promotes DNA-end resection and homologous recombination. Nat. Struct. Mol. Biol. *19*, 803–810.

Day, P.M., Baker, C.C., Lowy, D.R., and Schiller, J.T. (2004). Establishment of papillomavirus infection is enhanced by promyelocytic leukemia protein (PML) expression. Proc. Natl. Acad. Sci. U. S. A. *101*, 14252–14257.

Delbarre, E., Ivanauskiene, K., Küntziger, T., and Collas, P. (2013). DAXX-dependent supply of soluble (H3.3-H4) dimers to PML bodies pending deposition into chromatin. Genome Res. *23*, 440–451.

Delbarre, E., Ivanauskiene, K., Spirkoski, J., Shah, A., Vekterud, K., Moskaug, J.Ø., Bøe, S.O., Wong, L., Küntziger, T., and Collas, P. (2017). PML protein organizes heterochromatin domains

where it regulates histone H3.3 deposition by ATRX/DAXX. Genome Res.

Dellaire, G., and Bazett-Jones, D.P. (2004). PML nuclear bodies: dynamic sensors of DNA damage and cellular stress. BioEssays *26*, 963–977.

Dellaire, G., Ching, R.W., Ahmed, K., Jalali, F., Tse, K.C.K., Bristow, R.G., and Bazett-Jones, D.P. (2006a). Promyelocytic leukemia nuclear bodies behave as DNA damage sensors whose response to DNA double-strand breaks is regulated by NBS1 and the kinases ATM, Chk2, and ATR. J. Cell Biol. *175*, 55–66.

Dellaire, G., Ching, R.W., Dehghani, H., Ren, Y., and Bazett-Jones, D.P. (2006b). The number of PML nuclear bodies increases in early S phase by a fission mechanism. J. Cell Sci. *119*, 1026–1033.

Der, S.D., Zhou, A., Williams, B.R.G., and Silverman, R.H. (1998). Identification of genes differentially regulated by interferon α, β, or γ using oligonucleotide arrays. Proc. Natl. Acad. Sci. U. S. A. *95*, 15623–15628.

Deshmane, S.L., and Fraser, N.W. (1989). During latency, herpes simplex virus type 1 DNA is associated with nucleosomes in a chromatin structure. J. Virol. *63*, 943–947.

Dexheimer, T.S. (2013). DNA Repair Pathways and Mechanisms. In DNA Repair of Cancer Stem Cells, L.A. Mathews, S.M. Cabarcas, and E.M. Hurt, eds. (Dordrecht: Springer Netherlands), pp. 19–32.

Dinant, C., Ampatziadis-Michailidis, G., Lans, H., Tresini, M., Lagarou, A., Grosbart, M., Theil, A.F., van Cappellen, W.A., Kimura, H., Bartek, J., et al. (2013). Enhanced chromatin dynamics by FACT promotes transcriptional restart after UV-induced DNA damage. Mol. Cell *51*, 469–479.

Dinarello, C.A. (2009). Immunological and Inflammatory Functions of the Interleukin-1 Family. Annu. Rev. Immunol. *27*, 519–550.

Dixon, J.R., Selvaraj, S., Yue, F., Kim, A., Li, Y., Shen, Y., Hu, M., Liu, J.S., and Ren, B. (2012). Topological domains in mammalian genomes identified by analysis of chromatin interactions. Nature *485*, 376–380.

D'Orazi, G., Cecchinelli, B., Bruno, T., Manni, I., Higashimoto, Y., Saito, S., Gostissa, M., Coen, S., Marchetti, A., Del Sal, G., et al. (2002). Homeodomain-interacting protein kinase-2 phosphorylates p53 at Ser 46 and mediates apoptosis. Nat. Cell Biol. *4*, 11–19.

Dou, Z., Ghosh, K., Vizioli, M.G., Zhu, J., Sen, P., Wangensteen, K.J., Simithy, J., Lan, Y., Lin, Y., Zhou, Z., et al. (2017). Cytoplasmic chromatin triggers inflammation in senescence and cancer. Nature *550*, 402–406.

Drané, P., Ouararhni, K., Depaux, A., Shuaib, M., and Hamiche, A. (2010). The death-associated protein DAXX is a novel histone chaperone involved in the replication-independent deposition of H3.3. Genes Dev. *24*, 1253–1265.

Du, M., and Chen, Z.J. (2018). DNA-induced liquid phase condensation of cGAS activates innate immune signaling. Science *361*, 704–709.

Du, Q., Luu, P.-L., Stirzaker, C., and Clark, S.J. (2015). Methyl-CpG-binding domain proteins: readers of the epigenome. Epigenomics *7*, 1051–1073.

Dutrieux, J., Maarifi, G., Portilho, D.M., Arhel, N.J., Chelbi-Alix, M.K., and Nisole, S. (2015). PML/TRIM19-Dependent Inhibition of Retroviral Reverse-Transcription by Daxx. PLOS Pathog. *11*, e1005280.

Dyer, M.A., Qadeer, Z.A., Valle-Garcia, D., and Bernstein, E. (2017). ATRX and DAXX: Mechanisms and Mutations. Cold Spring Harb. Perspect. Med. *7*.

El Asmi, F., Maroui, M.A., Dutrieux, J., Blondel, D., Nisole, S., and Chelbi-Alix, M.K. (2014). Implication of PMLIV in Both Intrinsic and Innate Immunity. PLoS Pathog. *10*.

El Bougrini, J., Dianoux, L., and Chelbi-Alix, M.K. (2011). PML positively regulates interferon gamma signaling. Biochimie *93*, 389–398.

El Mchichi, B., Regad, T., Maroui, M.-A., Rodriguez, M.S., Aminev, A., Gerbaud, S., Escriou, N., Dianoux, L., and Chelbi-Alix, M.K. (2010). SUMOylation Promotes PML Degradation during Encephalomyocarditis Virus Infection. J. Virol. *84*, 11634–11645.

Elsässer, S.J., Huang, H., Lewis, P.W., Chin, J.W., Allis, C.D., and Patel, D.J. (2012). DAXX envelops a histone H3.3–H4 dimer for H3.3-specific recognition. Nature *491*, 560–565.

Elsässer, S.J., Noh, K.-M., Diaz, N., Allis, C.D., and Banaszynski, L.A. (2015). Histone H3.3 is required for endogenous retroviral element silencing in embryonic stem cells. Nature *522*, 240–244.

Erdel, F., Rademacher, A., Vlijm, R., Tünnermann, J., Frank, L., Weinmann, R., Schweigert, E., Yserentant, K., Hummert, J., Bauer, C., et al. (2020). Mouse Heterochromatin Adopts Digital Compaction States without Showing Hallmarks of HP1-Driven Liquid-Liquid Phase Separation. Mol. Cell *78*, 236-249.e7.

Erker, Y., Neyret-Kahn, H., Seeler, J.S., Dejean, A., Atfi, A., and Levy, L. (2013). Arkadia, a novel SUMO-targeted ubiquitin ligase involved in PML degradation. Mol. Cell. Biol. *33*, 2163–2177.

Evangelista, F.M., Maglott-Roth, A., Stierle, M., Brino, L., Soutoglou, E., and Tora, L. (2018). Transcription and mRNA export machineries SAGA and TREX-2 maintain monoubiquitinated H2B balance required for DNA repair. J. Cell Biol. *217*, 3382–3397.

Everett, R.D. (2006). Interactions between DNA viruses, ND10 and the DNA damage response. Cell. Microbiol. *8*, 365–374.

Everett, R.D., and Chelbi-Alix, M.K. (2007). PML and PML nuclear bodies: implications in antiviral defence. Biochimie *89*, 819–830.

Everett, R.D., Murray, J., Orr, A., and Preston, C.M. (2007). Herpes simplex virus type 1 genomes are associated with ND10 nuclear substructures in quiescently infected human fibroblasts. J. Virol. *81*, 10991–11004.

Falkenberg, K.J., and Johnstone, R.W. (2014). Histone deacetylases and their inhibitors in cancer, neurological diseases and immune disorders. Nat. Rev. Drug Discov. *13*, 673–691.

Fang, T.C., Schaefer, U., Mecklenbrauker, I., Stienen, A., Dewell, S., Chen, M.S., Rioja, I., Parravicini, V., Prinjha, R.K., Chandwani, R., et al. (2012). Histone H3 lysine 9 di-methylation as an epigenetic signature of the interferon response. J. Exp. Med. *209*, 661–669.

Ferbeyre, G., de Stanchina, E., Querido, E., Baptiste, N., Prives, C., and Lowe, S.W. (2000). PML is induced by oncogenic ras and promotes premature senescence. Genes Dev. *14*, 2015–2027.

Ferrand, J., Plessier, A., and Polo, S.E. (2021). Control of the chromatin response to DNA damage: Histone proteins pull the strings. Semin. Cell Dev. Biol. *113*, 75–87.

Filion, G.J.P., Zhenilo, S., Salozhin, S., Yamada, D., Prokhortchouk, E., and Defossez, P.-A. (2006). A Family of Human Zinc Finger Proteins That Bind Methylated DNA and Repress Transcription. Mol. Cell. Biol. *26*, 169–181.

Finlan, L.E., Sproul, D., Thomson, I., Boyle, S., Kerr, E., Perry, P., Ylstra, B., Chubb, J.R., and Bickmore, W.A. (2008). Recruitment to the Nuclear Periphery Can Alter Expression of Genes in Human Cells. PLoS Genet. *4*.

Fnu, S., Williamson, E.A., De Haro, L.P., Brenneman, M., Wray, J., Shaheen, M., Radhakrishnan, K., Lee, S.-H., Nickoloff, J.A., and Hromas, R. (2011). Methylation of histone H3 lysine 36 enhances DNA repair by nonhomologous end-joining. Proc. Natl. Acad. Sci. U. S. A. *108*, 540–545.

Fortuny, A., Chansard, A., Caron, P., Chevallier, O., Leroy, O., Renaud, O., and Polo, S.E.

(2021). Imaging the response to DNA damage in heterochromatin domains reveals core principles of heterochromatin maintenance. Nat. Commun. *12*, 2428.

Fradet-Turcotte, A., Canny, M.D., Escribano-Díaz, C., Orthwein, A., Leung, C.C.Y., Huang, H., Landry, M.-C., Kitevski-LeBlanc, J., Noordermeer, S.M., Sicheri, F., et al. (2013). 53BP1 is a reader of the DNA-damage-induced H2A Lys 15 ubiquitin mark. Nature *499*, 50–54.

Fu, D., Calvo, J.A., and Samson, L.D. (2012). SERIES: Genomic instability in cancer Balancing repair and tolerance of DNA damage caused by alkylating agents. Nat. Rev. Cancer *12*, 104–120.

Fyodorov, D.V., Zhou, B.-R., Skoultchi, A.I., and Bai, Y. (2018). Emerging roles of linker histones in regulating chromatin structure and function. Nat. Rev. Mol. Cell Biol. *19*, 192–206.

Galvani, A., Courbeyrette, R., Agez, M., Ochsenbein, F., Mann, C., and Thuret, J.-Y. (2008). In vivo study of the nucleosome assembly functions of ASF1 histone chaperones in human cells. Mol. Cell. Biol. *28*, 3672–3685.

Gao, C., Ho, C.-C., Reineke, E., Lam, M., Cheng, X., Stanya, K.J., Liu, Y., Chakraborty, S., Shih, H.-M., and Kao, H.-Y. (2008). Histone deacetylase 7 promotes PML sumoylation and is essential for PML nuclear body formation. Mol. Cell. Biol. *28*, 5658–5667.

Gareau, J.R., and Lima, C.D. (2010). The SUMO pathway: emerging mechanisms that shape specificity, conjugation and recognition. Nat. Rev. Mol. Cell Biol. *11*, 861–871.

Garrick, D., Sharpe, J.A., Arkell, R., Dobbie, L., Smith, A.J.H., Wood, W.G., Higgs, D.R., and Gibbons, R.J. (2006). Loss of Atrx Affects Trophoblast Development and the Pattern of X-Inactivation in Extraembryonic Tissues. PLoS Genet. *2*.

Gatti, M., Pinato, S., Maiolica, A., Rocchio, F., Prato, M.G., Aebersold, R., and Penengo, L. (2015). RNF168 promotes noncanonical K27 ubiquitination to signal DNA damage. Cell Rep. *10*, 226–238.

Gee, K., Guzzo, C., Che Mat, N.F., Ma, W., and Kumar, A. (2009). The IL-12 family of cytokines in infection, inflammation and autoimmune disorders. Inflamm. Allergy Drug Targets *8*, 40–52.

Geijtenbeek, T.B.H., and Gringhuis, S.I. (2009). Signalling through C-type lectin receptors: shaping immune responses. Nat. Rev. Immunol. *9*, 465–479.

Geoffroy, M.-C., and Chelbi-Alix, M.K. (2011). Role of Promyelocytic Leukemia Protein in Host Antiviral Defense. J. Interferon Cytokine Res. *31*, 145–158.

Gialitakis, M., Arampatzi, P., Makatounakis, T., and Papamatheakis, J. (2010). Gamma Interferon-Dependent Transcriptional Memory via Relocalization of a Gene Locus to PML Nuclear Bodies. Mol. Cell. Biol. *30*, 2046–2056.

Gibcus, J.H., Samejima, K., Goloborodko, A., Samejima, I., Naumova, N., Nuebler, J., Kanemaki, M., Xie, L., Paulson, J.R., Earnshaw, W.C., et al. (2018). A pathway for mitotic chromosome formation. Science *359*.

Glück, S., Guey, B., Gulen, M.F., Wolter, K., Kang, T.-W., Schmacke, N.A., Bridgeman, A., Rehwinkel, J., Zender, L., and Ablasser, A. (2017). Innate immune sensing of cytosolic chromatin fragments through cGAS promotes senescence. Nat. Cell Biol. *19*, 1061–1070.

Goldberg, A.D., Banaszynski, L.A., Noh, K.-M., Lewis, P.W., Elsaesser, S.J., Stadler, S., Dewell, S., Law, M., Guo, X., Li, X., et al. (2010). Distinct Factors Control Histone Variant H3.3 Localization at Specific Genomic Regions. Cell *140*, 678–691.

Goldstein, M., Derheimer, F.A., Tait-Mulder, J., and Kastan, M.B. (2013). Nucleolin mediates nucleosome disruption critical for DNA double-strand break repair. Proc. Natl. Acad. Sci. U. S. A. *110*, 16874–16879.

Gomez, J.A., Wapinski, O.L., Yang, Y.W., Bureau, J.-F., Gopinath, S., Monack, D.M., Chang, H.Y., Brahic, M., and Kirkegaard, K. (2013). The NeST long ncRNA controls microbial

susceptibility and epigenetic activation of the interferon-γ locus. Cell *152*, 743–754.

Gong, F., Chiu, L.-Y., Cox, B., Aymard, F., Clouaire, T., Leung, J.W., Cammarata, M., Perez, M., Agarwal, P., Brodbelt, J.S., et al. (2015). Screen identifies bromodomain protein ZMYND8 in chromatin recognition of transcription-associated DNA damage that promotes homologous recombination. Genes Dev. *29*, 197–211.

Gong, F., Clouaire, T., Aguirrebengoa, M., Legube, G., and Miller, K.M. (2017). Histone demethylase KDM5A regulates the ZMYND8-NuRD chromatin remodeler to promote DNA repair. J. Cell Biol. *216*, 1959–1974.

González-Navajas, J.M., Lee, J., David, M., and Raz, E. (2012). Immunomodulatory functions of type I interferons. Nat. Rev. Immunol. *12*, 125–135.

Goodarzi, A.A., Noon, A.T., Deckbar, D., Ziv, Y., Shiloh, Y., Löbrich, M., and Jeggo, P.A. (2008). ATM Signaling Facilitates Repair of DNA Double-Strand Breaks Associated with Heterochromatin. Mol. Cell *31*, 167–177.

Green, E.M., Antczak, A.J., Bailey, A.O., Franco, A.A., Wu, K.J., Yates, J.R., and Kaufman, P.D. (2005). Replication-Independent Histone Deposition by the HIR Complex and Asf1. Curr. Biol. *15*, 2044–2049.

Guelen, L., Pagie, L., Brasset, E., Meuleman, W., Faza, M.B., Talhout, W., Eussen, B.H., de Klein, A., Wessels, L., de Laat, W., et al. (2008). Domain organization of human chromosomes revealed by mapping of nuclear lamina interactions. Nature *453*, 948–951.

Guo, J.U., Su, Y., Zhong, C., Ming, G., and Song, H. (2011). Hydroxylation of 5-Methylcytosine by TET1 Promotes Active DNA Demethylation in the Adult Brain. Cell *145*, 423–434.

Guo, L., Giasson, B.I., Glavis-Bloom, A., Brewer, M.D., Shorter, J., Gitler, A.D., and Yang, X. (2014a). A cellular system that degrades misfolded proteins and protects against neurodegeneration. Mol. Cell *55*, 15–30.

Guo, Q., Wang, Y., Xu, D., Nossent, J., Pavlos, N.J., and Xu, J. (2018). Rheumatoid arthritis: pathological mechanisms and modern pharmacologic therapies. Bone Res. *6*.

Guo, R., Zheng, L., Park, J.W., Lv, R., Chen, H., Jiao, F., Xu, W., Mu, S., Wen, H., Qiu, J., et al. (2014b). BS69/ZMYND11 reads and connects histone H3.3 lysine 36 trimethylation-decorated chromatin to regulated pre-mRNA processing. Mol. Cell *56*, 298–310.

Guo, S., Cheng, X., Lim, J.-H., Liu, Y., and Kao, H.-Y. (2014c). Control of antioxidative response by the tumor suppressor protein PML through regulating Nrf2 activity. Mol. Biol. Cell *25*, 2485–2498.

Guo, Z., Kumagai, A., Wang, S.X., and Dunphy, W.G. (2000). Requirement for Atr in phosphorylation of Chk1 and cell cycle regulation in response to DNA replication blocks and UV-damaged DNA in Xenopus egg extracts. Genes Dev. *14*, 2745–2756.

Gupta, R., Somyajit, K., Narita, T., Maskey, E., Stanlie, A., Kremer, M., Typas, D., Lammers, M., Mailand, N., Nussenzweig, A., et al. (2018). DNA Repair Network Analysis Reveals Shieldin as a Key Regulator of NHEJ and PARP Inhibitor Sensitivity. Cell *173*, 972-988.e23.

Gurard-Levin, Z.A., Quivy, J.-P., and Almouzni, G. (2014). Histone chaperones: assisting histone traffic and nucleosome dynamics. Annu. Rev. Biochem. *83*, 487–517.

Gursoy-Yuzugullu, O., Ayrapetov, M.K., and Price, B.D. (2015). Histone chaperone Anp32e removes H2A.Z from DNA double-strand breaks and promotes nucleosome reorganization and DNA repair. Proc. Natl. Acad. Sci. U. S. A. *112*, 7507–7512.

Ha, H., Debnath, B., and Neamati, N. (2017). Role of the CXCL8-CXCR1/2 Axis in Cancer and Inflammatory Diseases. Theranostics *7*, 1543–1588.

Hake, S.B., Garcia, B.A., Kauer, M., Baker, S.P., Shabanowitz, J., Hunt, D.F., and Allis, C.D.

(2005). Serine 31 phosphorylation of histone variant H3.3 is specific to regions bordering centromeres in metaphase chromosomes. Proc. Natl. Acad. Sci. *102*, 6344–6349.

Hancock, R. (2004). A role for macromolecular crowding effects in the assembly and function of compartments in the nucleus. J. Struct. Biol. *146*, 281–290.

Harada, A., Okada, S., Konno, D., Odawara, J., Yoshimi, T., Yoshimura, S., Kumamaru, H., Saiwai, H., Tsubota, T., Kurumizaka, H., et al. (2012). Chd2 interacts with H3.3 to determine myogenic cell fate. EMBO J. *31*, 2994–3007.

Hardeland, U., Steinacher, R., Jiricny, J., and Schär, P. (2002). Modification of the human thymine-DNA glycosylase by ubiquitin-like proteins facilitates enzymatic turnover. EMBO J. *21*, 1456–1464.

Harding, S.M., Benci, J.L., Irianto, J., Discher, D.E., Minn, A.J., and Greenberg, R.A. (2017). Mitotic progression following DNA damage enables pattern recognition within micronuclei. Nature *548*, 466–470.

Hassan, A.H., Prochasson, P., Neely, K.E., Galasinski, S.C., Chandy, M., Carrozza, M.J., and Workman, J.L. (2002). Function and Selectivity of Bromodomains in Anchoring Chromatin-Modifying Complexes to Promoter Nucleosomes. Cell *111*, 369–379.

Hauer, M.H., Seeber, A., Singh, V., Thierry, R., Sack, R., Amitai, A., Kryzhanovska, M., Eglinger, J., Holcman, D., Owen-Hughes, T., et al. (2017). Histone degradation in response to DNA damage enhances chromatin dynamics and recombination rates. Nat. Struct. Mol. Biol. *24*, 99–107.

Hayflick, L. (1965). The limited in vitro lifetime of human diploid cell strains. Exp. Cell Res. *37*, 614–636.

Hayflick, L., and Moorhead, P.S. (1961). The serial cultivation of human diploid cell strains. Exp. Cell Res. *25*, 585–621.

Hecker, C.-M., Rabiller, M., Haglund, K., Bayer, P., and Dikic, I. (2006). Specification of SUMO1- and SUMO2-interacting Motifs *. J. Biol. Chem. *281*, 16117–16127.

Heinrich, P.C., Behrmann, I., Haan, S., Hermanns, H.M., Müller-Newen, G., and Schaper, F. (2003). Principles of interleukin (IL)-6-type cytokine signalling and its regulation. Biochem. J. *374*, 1–20.

Hekmat-Nejad, M., You, Z., Yee, M.C., Newport, J.W., and Cimprich, K.A. (2000). Xenopus ATR is a replication-dependent chromatin-binding protein required for the DNA replication checkpoint. Curr. Biol. CB *10*, 1565–1573.

Hendriks, I.A., D'Souza, R.C., Chang, J.-G., Mann, M., and Vertegaal, A.C.O. (2015). System-wide identification of wild-type SUMO-2 conjugation sites. Nat. Commun. *6*, 7289.

Hermann, A., Goyal, R., and Jeltsch, A. (2004). The Dnmt1 DNA-(cytosine-C5)-methyltransferase methylates DNA processively with high preference for hemimethylated target sites. J. Biol. Chem. *279*, 48350–48359.

Hertzog, P., Forster, S., and Samarajiwa, S. (2011). Systems Biology of Interferon Responses. J. Interferon Cytokine Res. *31*, 5–11.

Heuser, M., van der Kuip, H., Falini, B., Peschel, C., Huber, C., and Fischer, T. (1998). Induction of the pro-myelocytic leukaemia gene by type I and type II interferons. Mediators Inflamm. *7*, 319–325.

Hinchcliffe, E.H., Day, C.A., Karanjeet, K.B., Fadness, S., Langfald, A., Vaughan, K.T., and Dong, Z. (2016). Chromosome missegregation during anaphase triggers p53 cell cycle arrest through histone H3.3 Ser31 phosphorylation. Nat. Cell Biol. *18*, 668–675.

Hödl, M., and Basler, K. (2009). Transcription in the Absence of Histone H3.3. Curr. Biol. *19*,

1221–1226.

Hoelper, D., Huang, H., Jain, A.Y., Patel, D.J., and Lewis, P.W. (2017). Structural and mechanistic insights into ATRX-dependent and -independent functions of the histone chaperone DAXX. Nat. Commun. *8*, 1193.

Hofmann, T.G., Möller, A., Sirma, H., Zentgraf, H., Taya, Y., Dröge, W., Will, H., and Schmitz, M.L. (2002). Regulation of p53 activity by its interaction with homeodomain-interacting protein kinase-2. Nat. Cell Biol. *4*, 1–10.

Hoischen, C., Monajembashi, S., Weisshart, K., and Hemmerich, P. (2018). Multimodal Light Microscopy Approaches to Reveal Structural and Functional Properties of Promyelocytic Leukemia Nuclear Bodies. Front. Oncol. *8*, 125.

Holbrook, J., Lara-Reyna, S., Jarosz-Griffiths, H., and McDermott, M.F. (2019). Tumour necrosis factor signalling in health and disease. F1000Research *8*.

Holliday, R. (1994). Epigenetics: An overview. Dev. Genet. *15*, 453–457.

Holliday, R., and Pugh, J.E. (1975). DNA modification mechanisms and gene activity during development. Science *187*, 226–232.

Hopfner, K.-P., and Hornung, V. (2020). Molecular mechanisms and cellular functions of cGAS–STING signalling. Nat. Rev. Mol. Cell Biol. *21*, 501–521.

Hotchkiss, R.D. (1948). The Quantitative Separation of Purines, Pyrimidines, and Nucleosides by Paper Chromatography. J. Biol. Chem. *175*, 315–332.

Hsiao, K.-Y., and Mizzen, C.A. (2013). Histone H4 deacetylation facilitates 53BP1 DNA damage signaling and double-strand break repair. J. Mol. Cell Biol. *5*, 157–165.

Hsu, K.-S., and Kao, H.-Y. (2018). PML: Regulation and multifaceted function beyond tumor suppression. Cell Biosci. *8*.

Hsu, K.-S., Zhao, X., Cheng, X., Guan, D., Mahabeleshwar, G.H., Liu, Y., Borden, E., Jain, M.K., and Kao, H.-Y. (2017). Dual regulation of Stat1 and Stat3 by the tumor suppressor protein PML contributes to interferon α-mediated inhibition of angiogenesis. J. Biol. Chem. *292*, 10048–10060.

Huang, M., Qian, F., Hu, Y., Ang, C., Li, Z., and Wen, Z. (2002). Chromatin-remodelling factor BRG1 selectively activates a subset of interferon-alpha-inducible genes. Nat. Cell Biol. *4*, 774–781.

Hubackova, S., Krejcikova, K., Bartek, J., and Hodny, Z. (2012). Interleukin 6 Signaling Regulates Promyelocytic Leukemia Protein Gene Expression in Human Normal and Cancer Cells. J. Biol. Chem. *287*, 26702–26714.

Huen, M.S.Y., Grant, R., Manke, I., Minn, K., Yu, X., Yaffe, M.B., and Chen, J. (2007). RNF8 transduces the DNA-damage signal via histone ubiquitylation and checkpoint protein assembly. Cell *131*, 901–914.

Hung, T., Wang, Y., Lin, M.F., Koegel, A.K., Kotake, Y., Grant, G.D., Horlings, H.M., Shah, N., Umbricht, C., Wang, P., et al. (2011). Extensive and coordinated transcription of noncoding RNAs within cell-cycle promoters. Nat. Genet. *43*, 621–629.

Hurley, J. (1972). Acute Inflamm.

Iacovoni, J.S., Caron, P., Lassadi, I., Nicolas, E., Massip, L., Trouche, D., and Legube, G. (2010). High-resolution profiling of gammaH2AX around DNA double strand breaks in the mammalian genome. EMBO J. *29*, 1446–1457.

Ishov, A.M., Sotnikov, A.G., Negorev, D., Vladimirova, O.V., Neff, N., Kamitani, T., Yeh, E.T., Strauss, J.F., and Maul, G.G. (1999). PML is critical for ND10 formation and recruits the PML-interacting protein daxx to this nuclear structure when modified by SUMO-1. J. Cell Biol. *147*,

221–234.

Ismail, I.H., Andrin, C., McDonald, D., and Hendzel, M.J. (2010). BMI1-mediated histone ubiquitylation promotes DNA double-strand break repair. J. Cell Biol. *191*, 45–60.

Ito, K., Bernardi, R., Morotti, A., Matsuoka, S., Saglio, G., Ikeda, Y., Rosenblatt, J., Avigan, D.E., Teruya-Feldstein, J., and Pandolfi, P.P. (2008). PML targeting eradicates quiescent leukaemia-initiating cells. Nature *453*, 1072–1078.

Ito, K., Carracedo, A., Weiss, D., Arai, F., Ala, U., Avigan, D.E., Schafer, Z.T., Evans, R.M., Suda, T., Lee, C.-H., et al. (2012). A PML-PPARδ pathway for fatty acid oxidation regulates haematopoietic stem cell maintenance. Nat. Med. *18*, 1350–1358.

Ivanauskiene, K., Delbarre, E., McGhie, J.D., Küntziger, T., Wong, L.H., and Collas, P. (2014). The PML-associated protein DEK regulates the balance of H3.3 loading on chromatin and is important for telomere integrity. Genome Res. *24*, 1584–1594.

Ivashkiv, L.B. (2018). IFNγ: signalling, epigenetics and roles in immunity, metabolism, disease and cancer immunotherapy. Nat. Rev. Immunol. *18*, 545–558.

Iwanami, A., Gini, B., Zanca, C., Matsutani, T., Assuncao, A., Nael, A., Dang, J., Yang, H., Zhu, S., Kohyama, J., et al. (2013). PML mediates glioblastoma resistance to mammalian target of rapamycin (mTOR)-targeted therapies. Proc. Natl. Acad. Sci.

Iwasaki, W., Tachiwana, H., Kawaguchi, K., Shibata, T., Kagawa, W., and Kurumizaka, H. (2011). Comprehensive Structural Analysis of Mutant Nucleosomes Containing Lysine to Glutamine (KQ) Substitutions in the H3 and H4 Histone-Fold Domains. Biochemistry *50*, 7822–7832.

Iyer, L.M., Zhang, D., and Aravind, L. (2016). Adenine methylation in eukaryotes: Apprehending the complex evolutionary history and functional potential of an epigenetic modification. Bioessays *38*, 27–40.

Janer, A., Martin, E., Muriel, M.-P., Latouche, M., Fujigasaki, H., Ruberg, M., Brice, A., Trottier, Y., and Sittler, A. (2006). PML clastosomes prevent nuclear accumulation of mutant ataxin-7 and other polyglutamine proteins. J. Cell Biol. *174*, 65–76.

Jang, C.-W., Shibata, Y., Starmer, J., Yee, D., and Magnuson, T. (2015). Histone H3.3 maintains genome integrity during mammalian development. Genes Dev. *29*, 1377–1392.

Jasencakova, Z., Scharf, A.N.D., Ask, K., Corpet, A., Imhof, A., Almouzni, G., and Groth, A. (2010). Replication Stress Interferes with Histone Recycling and Predeposition Marking of New Histones. Mol. Cell *37*, 736–743.

Jeanne, M., Lallemand-Breitenbach, V., Ferhi, O., Koken, M., Le Bras, M., Duffort, S., Peres, L., Berthier, C., Soilihi, H., Raught, B., et al. (2010). PML/RARA Oxidation and Arsenic Binding Initiate the Antileukemia Response of As2O3. Cancer Cell *18*, 88–98.

Jensen, K., Shiels, C., and Freemont, P.S. (2001). PML protein isoforms and the RBCC/TRIM motif. Oncogene *20*, 7223–7233.

Jenuwein, T., and Allis, C.D. (2001). Translating the Histone Code. Science *293*, 1074–1080.

Jiang, H., Xue, X., Panda, S., Kawale, A., Hooy, R.M., Liang, F., Sohn, J., Sung, P., and Gekara, N.O. (2019). Chromatin-bound cGAS is an inhibitor of DNA repair and hence accelerates genome destabilization and cell death. EMBO J. *38*, e102718.

Jin, C., and Felsenfeld, G. (2007). Nucleosome stability mediated by histone variants H3.3 and H2A.Z. Genes Dev. *21*, 1519–1529.

Jones, P.A. (2012). Functions of DNA methylation: islands, start sites, gene bodies and beyond. Nat. Rev. Genet. *13*, 484–492.

Juhász, S., Elbakry, A., Mathes, A., and Löbrich, M. (2018). ATRX Promotes DNA Repair

Synthesis and Sister Chromatid Exchange during Homologous Recombination. Mol. Cell *71*, 11-24.e7.

Kahle, T., Volkmann, B., Eissmann, K., Herrmann, A., Schmitt, S., Wittmann, S., Merkel, L., Reuter, N., Stamminger, T., and Gramberg, T. (2015). TRIM19/PML Restricts HIV Infection in a Cell Type-Dependent Manner. Viruses *8*.

Kaiser, T.E., Intine, R.V., and Dundr, M. (2008). De Novo Formation of a Subnuclear Body. Science *322*, 1713–1717.

Kakarougkas, A., Ismail, A., Chambers, A.L., Riballo, E., Herbert, A.D., Künzel, J., Löbrich, M., Jeggo, P.A., and Downs, J.A. (2014). Requirement for PBAF in transcriptional repression and repair at DNA breaks in actively transcribed regions of chromatin. Mol. Cell *55*, 723–732.

Kakumu, E., Nakanishi, S., Shiratori, H.M., Kato, A., Kobayashi, W., Machida, S., Yasuda, T., Adachi, N., Saito, N., Ikura, T., et al. (2017). Xeroderma pigmentosum group C protein interacts with histones: regulation by acetylated states of histone H3. Genes Cells Devoted Mol. Cell. Mech. *22*, 310–327.

Kamada, R., Yang, W., Zhang, Y., Patel, M.C., Yang, Y., Ouda, R., Dey, A., Wakabayashi, Y., Sakaguchi, K., Fujita, T., et al. (2018). Interferon stimulation creates chromatin marks and establishes transcriptional memory. Proc. Natl. Acad. Sci. *115*, E9162–E9171.

Kamitani, T., Kito, K., Nguyen, H.P., Fukuda-Kamitani, T., and Yeh, E.T. (1998a). Characterization of a second member of the sentrin family of ubiquitin-like proteins. J. Biol. Chem. *273*, 11349–11353.

Kamitani, T., Kito, K., Nguyen, H.P., Wada, H., Fukuda-Kamitani, T., and Yeh, E.T.H. (1998b). Identification of Three Major Sentrinization Sites in PML *. J. Biol. Chem. *273*, 26675–26682.

Kerscher, O. (2007). SUMO junction—what's your function? New insights through SUMO-interacting motifs. EMBO Rep. *8*, 550–555.

Khalfin-Rabinovich, Y., Weinstein, A., and Levi, B.-Z. (2011). PML is a key component for the differentiation of myeloid progenitor cells to macrophages. Int. Immunol. *23*, 287–296.

Khurana, S., Kruhlak, M.J., Kim, J., Tran, A.D., Liu, J., Nyswaner, K., Shi, L., Jailwala, P., Sung, M.-H., Hakim, O., et al. (2014). A macrohistone variant links dynamic chromatin compaction to BRCA1-dependent genome maintenance. Cell Rep. *8*, 1049–1062.

Kim, Y.-E., and Ahn, J.-H. (2015). Positive Role of Promyelocytic Leukemia Protein in Type I Interferon Response and Its Regulation by Human Cytomegalovirus. PLoS Pathog. *11*.

Kim, H., Chen, J., and Yu, X. (2007). Ubiquitin-binding protein RAP80 mediates BRCA1-dependent DNA damage response. Science *316*, 1202–1205.

Kim, J., Sturgill, D., Sebastian, R., Khurana, S., Tran, A.D., Edwards, G.B., Kruswick, A., Burkett, S., Hosogane, E.K., Hannon, W.W., et al. (2018). Replication Stress Shapes a Protective Chromatin Environment across Fragile Genomic Regions. Mol. Cell *69*, 36-47.e7.

Kim, J.J., Lee, S.Y., Gong, F., Battenhouse, A.M., Boutz, D.R., Bashyal, A., Refvik, S.T., Chiang, C.-M., Xhemalce, B., Paull, T.T., et al. (2019). Systematic bromodomain protein screens identify homologous recombination and R-loop suppression pathways involved in genome integrity. Genes Dev. *33*, 1751–1774.

Kim, M.K., Yang, S., Lee, K.-H., Um, J.-H., Liu, M., Kang, H., Park, S.J., and Chung, J.H. (2011). Promyelocytic leukemia inhibits adipogenesis, and loss of promyelocytic leukemia results in fat accumulation in mice. Am. J. Physiol. - Endocrinol. Metab. *301*, E1130–E1142.

Kireeva, N., Lakonishok, M., Kireev, I., Hirano, T., and Belmont, A.S. (2004). Visualization of early chromosome condensation. J. Cell Biol. *166*, 775–785.

Kitamura, Y.I., Kitamura, T., Kruse, J.-P., Raum, J.C., Stein, R., Gu, W., and Accili, D. (2005).

FoxO1 protects against pancreatic β cell failure through NeuroD and MafA induction. Cell Metab. *2*, 153–163.

Koch, A.E., Polverini, P.J., Kunkel, S.L., Harlow, L.A., DiPietro, L.A., Elner, V.M., Elner, S.G., and Strieter, R.M. (1992). Interleukin-8 as a macrophage-derived mediator of angiogenesis. Science *258*, 1798–1801.

Kolas, N.K., Chapman, J.R., Nakada, S., Ylanko, J., Chahwan, R., Sweeney, F.D., Panier, S., Mendez, M., Wildenhain, J., Thomson, T.M., et al. (2007). Orchestration of the DNA-damage response by the RNF8 ubiquitin ligase. Science *318*, 1637–1640.

Konev, A.Y., Tribus, M., Park, S.Y., Podhraski, V., Lim, C.Y., Emelyanov, A.V., Vershilova, E., Pirrotta, V., Kadonaga, J.T., Lusser, A., et al. (2007). CHD1 Motor Protein Is Required for Deposition of Histone Variant H3.3 into Chromatin in Vivo. Science *317*, 1087–1090.

Korb, E., Wilkinson, C.L., Delgado, R.N., Lovero, K.L., and Finkbeiner, S. (2013). Arc in the nucleus regulates PML dependent GluA1 transcription and homeostatic plasticity. Nat. Neurosci. *16*, 874–883.

Kornberg, R.D. (1974). Chromatin Structure: A Repeating Unit of Histones and DNA. Science *184*, 868–871.

Kornberg, R.D. (1977). Structure of chromatin. Annu. Rev. Biochem. *46*, 931–954.

Kouzarides, T. (2007). Chromatin Modifications and Their Function. Cell *128*, 693–705.

Koyama, M., and Kurumizaka, H. (2018). Structural diversity of the nucleosome. J. Biochem. (Tokyo) *163*, 85–95.

Krimer, D.B., Cheng, G., and Skoultchi, A.I. (1993). Induction of H3.3 replacement histone mRNAs during the precommitment period of murine erythroleukemia cell differentiation. Nucleic Acids Res. *21*, 2873–2879.

Krizhanovsky, V., Yon, M., Dickins, R.A., Hearn, S., Simon, J., Miething, C., Yee, H., Zender, L., and Lowe, S.W. (2008). Senescence of activated stellate cells limits liver fibrosis. Cell *134*, 657–667.

Kroetz, D.N., Allen, R.M., Schaller, M.A., Cavallaro, C., Ito, T., and Kunkel, S.L. (2015). Type I Interferon Induced Epigenetic Regulation of Macrophages Suppresses Innate and Adaptive Immunity in Acute Respiratory Viral Infection. PLoS Pathog. *11*, e1005338.

Kujirai, T., Zierhut, C., Takizawa, Y., Kim, R., Negishi, L., Uruma, N., Hirai, S., Funabiki, H., and Kurumizaka, H. (2020). Structural basis for the inhibition of cGAS by nucleosomes. Science *370*, 455–458.

Kumar, S., Cheng, X., Klimasauskas, S., Mi, S., Posfai, J., Roberts, R.J., and Wilson, G.G. (1994). The DNA (cytosine-5) methyltransferases. Nucleic Acids Res. *22*, 1–10.

Kumaran, R.I., and Spector, D.L. (2008). A genetic locus targeted to the nuclear periphery in living cells maintains its transcriptional competence. J. Cell Biol. *180*, 51–65.

Kurihara, M., Kato, K., Sanbo, C., Shigenobu, S., Ohkawa, Y., Fuchigami, T., and Miyanari, Y. (2020). Genomic Profiling by ALaP-Seq Reveals Transcriptional Regulation by PML Bodies through DNMT3A Exclusion. Mol. Cell *78*, 493-505.e8.

Kwiatkowski, D.L., Thompson, H.W., and Bloom, D.C. (2009). The polycomb group protein Bmi1 binds to the herpes simplex virus 1 latent genome and maintains repressive histone marks during latency. J. Virol. *83*, 8173–8181.

Laane, E., Tamm, K.P., Buentke, E., Ito, K., Khahariza, P., Oscarsson, J., Corcoran, M., Björklund, A.-C., Hultenby, K., Lundin, J., et al. (2009). Cell death induced by dexamethasone in lymphoid leukemia is mediated through initiation of autophagy. Cell Death Differ. *16*, 1018–1029.

Lachner, M., O'Carroll, D., Rea, S., Mechtler, K., and Jenuwein, T. (2001). Methylation of histone H3 lysine 9 creates a binding site for HP1 proteins. Nature *410*, 116–120.

Lallemand-Breitenbach, V., and de Thé, H. (2010). PML nuclear bodies. Cold Spring Harb. Perspect. Biol. *2*, a000661.

Lallemand-Breitenbach, V., and de Thé, H. (2018). PML nuclear bodies: from architecture to function. Curr. Opin. Cell Biol. *52*, 154–161.

Lallemand-Breitenbach, V., Zhu, J., Puvion, F., Koken, M., Honoré, N., Doubeikovsky, A., Duprez, E., Pandolfi, P.P., Puvion, E., Freemont, P., et al. (2001). Role of Promyelocytic Leukemia (Pml) Sumolation in Nuclear Body Formation, 11s Proteasome Recruitment, and as2O3-Induced Pml or Pml/Retinoic Acid Receptor α Degradation. J. Exp. Med. *193*, 1361–1372.

Lang, M., Jegou, T., Chung, I., Richter, K., Münch, S., Udvarhelyi, A., Cremer, C., Hemmerich, P., Engelhardt, J., Hell, S.W., et al. (2010). Three-dimensional organization of promyelocytic leukemia nuclear bodies. J. Cell Sci. *123*, 392–400.

Laurent, L., Wong, E., Li, G., Huynh, T., Tsirigos, A., Ong, C.T., Low, H.M., Kin Sung, K.W., Rigoutsos, I., Loring, J., et al. (2010). Dynamic changes in the human methylome during differentiation. Genome Res. *20*, 320–331.

Lavau, C., Marchio, A., Fagioli, M., Jansen, J., Falini, B., Lebon, P., Grosveld, F., Pandolfi, P.P., Pelicci, P.G., and Dejean, A. (1995). The acute promyelocytic leukaemia-associated PML gene is induced by interferon. Oncogene *11*, 871–876.

Law, M.J., Lower, K.M., Voon, H.P.J., Hughes, J.R., Garrick, D., Viprakasit, V., Mitson, M., Gobbi, M.D., Marra, M., Morris, A., et al. (2010). ATR-X Syndrome Protein Targets Tandem Repeats and Influences Allele-Specific Expression in a Size-Dependent Manner. Cell *143*, 367–378.

Lewis, P.W., Elsaesser, S.J., Noh, K.-M., Stadler, S.C., and Allis, C.D. (2010). Daxx is an H3.3-specific histone chaperone and cooperates with ATRX in replication-independent chromatin assembly at telomeres. Proc. Natl. Acad. Sci. U. S. A. *107*, 14075–14080.

Lewis, P.W., Müller, M.M., Koletsky, M.S., Cordero, F., Lin, S., Banaszynski, L.A., Garcia, B.A., Muir, T.W., Becher, O.J., and Allis, C.D. (2013). Inhibition of PRC2 Activity by a Gain-of-Function H3 Mutation Found in Pediatric Glioblastoma. Science *340*, 857–861.

Li, X., and Tyler, J.K. (2016). Nucleosome disassembly during human non-homologous end joining followed by concerted HIRA- and CAF-1-dependent reassembly. ELife *5*.

Li, F., Mao, G., Tong, D., Huang, J., Gu, L., Yang, W., and Li, G.-M. (2013). The histone mark H3K36me3 regulates human DNA mismatch repair through its interaction with MutSα. Cell *153*, 590–600.

Li, F., Deng, Z., Zhang, L., Wu, C., Jin, Y., Hwang, I., Vladimirova, O., Xu, L., Yang, L., Lu, B., et al. (2019). ATRX loss induces telomere dysfunction and necessitates induction of alternative lengthening of telomeres during human cell immortalization. EMBO J. *38*, e96659.

Li, H., Leo, C., Zhu, J., Wu, X., O'Neil, J., Park, E.-J., and Chen, J.D. (2000). Sequestration and Inhibition of Daxx-Mediated Transcriptional Repression by PML. Mol. Cell. Biol. *20*, 1784–1796.

Li, W., Ferguson, B.J., Khaled, W.T., Tevendale, M., Stingl, J., Poli, V., Rich, T., Salomoni, P., and Watson, C.J. (2009). PML depletion disrupts normal mammary gland development and skews the composition of the mammary luminal cell progenitor pool. Proc. Natl. Acad. Sci. U. S. A. *106*, 4725–4730.

Liang, Y.-C., Lee, C.-C., Yao, Y.-L., Lai, C.-C., Schmitz, M.L., and Yang, W.-M. (2016). SUMO5, a Novel Poly-SUMO Isoform, Regulates PML Nuclear Bodies. Sci. Rep. *6*.

Lieberman-Aiden, E., Berkum, N.L. van, Williams, L., Imakaev, M., Ragoczy, T., Telling, A., Amit, I., Lajoie, B.R., Sabo, P.J., Dorschner, M.O., et al. (2009). Comprehensive Mapping of Long-Range Interactions Reveals Folding Principles of the Human Genome. Science *326*, 289–293.

Lim, B., Mun, J., Kim, Y.S., and Kim, S.-Y. (2017). Variability in Chromatin Architecture and Associated DNA Repair at Genomic Positions Containing Somatic Mutations. Cancer Res. *77*, 2822–2833.

Lin, H.-K., Bergmann, S., and Pandolfi, P.P. (2004). Cytoplasmic PML function in TGF-beta signalling. Nature *431*, 205–211.

Lindahl, T. (1993). Instability and decay of the primary structure of DNA. Nature *362*, 709–715.

Lister, R., Pelizzola, M., Dowen, R.H., Hawkins, R.D., Hon, G., Tonti-Filippini, J., Nery, J.R., Lee, L., Ye, Z., Ngo, Q.-M., et al. (2009). Human DNA methylomes at base resolution show widespread epigenomic differences. Nature *462*, 315–322.

Liu, C.-P., Xiong, C., Wang, M., Yu, Z., Yang, N., Chen, P., Zhang, Z., Li, G., and Xu, R.-M. (2012). Structure of the variant histone H3.3–H4 heterodimer in complex with its chaperone DAXX. Nat. Struct. Mol. Biol. *19*, 1287–1292.

Liu, D., Keijzers, G., and Rasmussen, L.J. (2017). DNA mismatch repair and its many roles in eukaryotic cells. Mutat. Res. Mutat. Res. *773*, 174–187.

Liu, H., Kang, H., Liu, R., Chen, X., and Zhao, K. (2002). Maximal induction of a subset of interferon target genes requires the chromatin-remodeling activity of the BAF complex. Mol. Cell. Biol. *22*, 6471–6479.

Liu, H., Zhang, H., Wu, X., Ma, D., Wu, J., Wang, L., Jiang, Y., Fei, Y., Zhu, C., Tan, R., et al. (2018). Nuclear cGAS suppresses DNA repair and promotes tumorigenesis. Nature *563*, 131.

Liu, Q., Guntuku, S., Cui, X.S., Matsuoka, S., Cortez, D., Tamai, K., Luo, G., Carattini-Rivera, S., DeMayo, F., Bradley, A., et al. (2000). Chk1 is an essential kinase that is regulated by Atr and required for the G(2)/M DNA damage checkpoint. Genes Dev. *14*, 1448–1459.

Lo, Y.-H., Huang, Y.-W., Wu, Y.-H., Tsai, C.-S., Lin, Y.-C., Mo, S.-T., Kuo, W.-C., Chuang, Y.-T., Jiang, S.-T., Shih, H.-M., et al. (2013). Selective inhibition of the NLRP3 inflammasome by targeting to promyelocytic leukemia protein in mouse and human. Blood *121*, 3185–3194.

Loe, T.K., Li, J.S.Z., Zhang, Y., Azeroglu, B., Boddy, M.N., and Denchi, E.L. (2020). Telomere length heterogeneity in ALT cells is maintained by PML-dependent localization of the BTR complex to telomeres. Genes Dev. *34*, 650–662.

Lomonte, P. (2017). Herpesvirus Latency: On the Importance of Positioning Oneself. Adv. Anat. Embryol. Cell Biol. *223*, 95–117.

Lopes, E.C., Valls, E., Figueroa, M.E., Mazur, A., Meng, F.-G., Chiosis, G., Laird, P.W., Schreiber-Agus, N., Greally, J.M., Prokhortchouk, E., et al. (2008). Kaiso Contributes to DNA Methylation-Dependent Silencing of Tumor Suppressor Genes in Colon Cancer Cell Lines. Cancer Res. *68*, 7258–7263.

Loppin, B., Bonnefoy, E., Anselme, C., Laurençon, A., Karr, T.L., and Couble, P. (2005). The histone H3.3 chaperone HIRA is essential for chromatin assembly in the male pronucleus. Nature *437*, 1386–1390.

Lowe, B.R., Maxham, L.A., Hamey, J.J., Wilkins, M.R., and Partridge, J.F. (2019). Histone H3 Mutations: An Updated View of Their Role in Chromatin Deregulation and Cancer. Cancers *11*.

Lu, C., Jain, S.U., Hoelper, D., Bechet, D., Molden, R.C., Ran, L., Murphy, D., Venneti, S., Hameed, M., Pawel, B.R., et al. (2016). Histone H3K36 mutations promote sarcomagenesis through altered histone methylation landscape. Science *352*, 844–849.

Luger, K., and Richmond, T.J. (1998). The histone tails of the nucleosome. Curr. Opin. Genet. Dev. *8*, 140–146.

Luger, K., Mäder, A.W., Richmond, R.K., Sargent, D.F., and Richmond, T.J. (1997). Crystal structure of the nucleosome core particle at 2.8 Å resolution. Nature *389*, 251–260.

Luijsterburg, M.S., de Krijger, I., Wiegant, W.W., Shah, R.G., Smeenk, G., de Groot, A.J.L., Pines, A., Vertegaal, A.C.O., Jacobs, J.J.L., Shah, G.M., et al. (2016). PARP1 Links CHD2-Mediated Chromatin Expansion and H3.3 Deposition to DNA Repair by Non-homologous End-Joining. Mol. Cell *61*, 547–562.

Lunardi, A., Gaboli, M., Giorgio, M., Rivi, R., Bygrave, A., Antoniou, M., Drabek, D., Dzierzak, E., Fagioli, M., Salmena, L., et al. (2011). A Role for PML in Innate Immunity. Genes Cancer *2*, 10–19.

Lusic, M., Marini, B., Ali, H., Lucic, B., Luzzati, R., and Giacca, M. (2013). Proximity to PML Nuclear Bodies Regulates HIV-1 Latency in CD4+ T Cells. Cell Host Microbe *13*, 665–677.

Maarifi, G., Chelbi-Alix, M.K., and Nisole, S. (2014). PML control of cytokine signaling. Cytokine Growth Factor Rev. *25*, 551–561.

Mackenzie, K.J., Carroll, P., Martin, C.-A., Murina, O., Fluteau, A., Simpson, D.J., Olova, N., Sutcliffe, H., Rainger, J.K., Leitch, A., et al. (2017). cGAS surveillance of micronuclei links genome instability to innate immunity. Nature *548*, 461–465.

Maeshima, K., Ide, S., and Babokhov, M. (2019). Dynamic chromatin organization without the 30-nm fiber. Curr. Opin. Cell Biol. *58*, 95–104.

Mahmudpour, M., Roozbeh, J., Keshavarz, M., Farrokhi, S., and Nabipour, I. (2020). COVID-19 cytokine storm: The anger of inflammation. Cytokine *133*, 155151.

Mailand, N., Bekker-Jensen, S., Faustrup, H., Melander, F., Bartek, J., Lukas, C., and Lukas, J. (2007). RNF8 ubiquitylates histones at DNA double-strand breaks and promotes assembly of repair proteins. Cell *131*, 887–900.

Mantovani, A., Dinarello, C.A., Molgora, M., and Garlanda, C. (2019). Interleukin-1 and Related Cytokines in the Regulation of Inflammation and Immunity. Immunity *50*, 778–795.

Mao, Y.S., Zhang, B., and Spector, D.L. (2011). Biogenesis and function of nuclear bodies. Trends Genet. *27*, 295–306.

Maor, G.L., Yearim, A., and Ast, G. (2015). The alternative role of DNA methylation in splicing regulation. Trends Genet. *31*, 274–280.

Mariathasan, S., and Monack, D.M. (2007). Inflammasome adaptors and sensors: intracellular regulators of infection and inflammation. Nat. Rev. Immunol. *7*, 31–40.

Maroui, M.A., Pampin, M., and Chelbi-Alix, M.K. (2011). Promyelocytic Leukemia Isoform IV Confers Resistance to Encephalomyocarditis Virus via the Sequestration of 3D Polymerase in Nuclear Bodies ▿. J. Virol. *85*, 13164–13173.

Maroui, M.A., Callé, A., Cohen, C., Streichenberger, N., Texier, P., Takissian, J., Rousseau, A., Poccardi, N., Welsch, J., Corpet, A., et al. (2016). Latency Entry of Herpes Simplex Virus 1 Is Determined by the Interaction of Its Genome with the Nuclear Environment. PLoS Pathog. *12*.

Martín-Martín, N., Piva, M., Urosevic, J., Aldaz, P., Sutherland, J.D., Fernández-Ruiz, S., Arreal, L., Torrano, V., Cortazar, A.R., Planet, E., et al. (2016). Stratification and therapeutic potential of PML in metastatic breast cancer. Nat. Commun. *7*.

Martire, S., and Banaszynski, L.A. (2020). The roles of histone variants in fine-tuning chromatin organization and function. Nat. Rev. Mol. Cell Biol. *21*, 522–541.

Martire, S., Gogate, A.A., Whitmill, A., Tafessu, A., Nguyen, J., Teng, Y.-C., Tastemel, M., and Banaszynski, L.A. (2019). Phosphorylation of histone H3.3 at serine 31 promotes p300 activity and enhancer acetylation. Nat. Genet. *51*, 941–946.

Marzluff, W.F., Gongidi, P., Woods, K.R., Jin, J., and Maltais, L.J. (2002). The Human and Mouse Replication-Dependent Histone Genes. Genomics *80*, 487–498.

di Masi, A., Cilli, D., Berardinelli, F., Talarico, A., Pallavicini, I., Pennisi, R., Leone, S., Antoccia, A., Noguera, N.I., Lo-Coco, F., et al. (2016). PML nuclear body disruption impairs DNA double-strand break sensing and repair in APL. Cell Death Dis. *7*, e2308–e2308.

Massip, L., Caron, P., Iacovoni, J.S., Trouche, D., and Legube, G. (2010). Deciphering the chromatin landscape induced around DNA double strand breaks. Cell Cycle Georget. Tex *9*, 2963–2972.

Matsuoka, S., Huang, M., and Elledge, S.J. (1998). Linkage of ATM to cell cycle regulation by the Chk2 protein kinase. Science *282*, 1893–1897.

Matsuoka, S., Rotman, G., Ogawa, A., Shiloh, Y., Tamai, K., and Elledge, S.J. (2000). Ataxia telangiectasia-mutated phosphorylates Chk2 in vivo and in vitro. Proc. Natl. Acad. Sci. U. S. A. *97*, 10389–10394.

Mattiroli, F., Vissers, J.H.A., van Dijk, W.J., Ikpa, P., Citterio, E., Vermeulen, W., Marteijn, J.A., and Sixma, T.K. (2012). RNF168 ubiquitinates K13-15 on H2A/H2AX to drive DNA damage signaling. Cell *150*, 1182–1195.

Matunis, M.J., Coutavas, E., and Blobel, G. (1996). A novel ubiquitin-like modification modulates the partitioning of the Ran-GTPase-activating protein RanGAP1 between the cytosol and the nuclear pore complex. J. Cell Biol. *135*, 1457–1470.

Mazewski, C., Perez, R.E., Fish, E.N., and Platanias, L.C. (2020). Type I Interferon (IFN)-Regulated Activation of Canonical and Non-Canonical Signaling Pathways. Front. Immunol. *11*.

McCulloch, S.D., and Kunkel, T.A. (2008). The fidelity of DNA synthesis by eukaryotic replicative and translesion synthesis polymerases. Cell Res. *18*, 148–161.

McFarlane, S., Orr, A., Roberts, A.P.E., Conn, K.L., Iliev, V., Loney, C., Filipe, A. da S., Smollett, K., Gu, Q., Robertson, N., et al. (2019). The histone chaperone HIRA promotes the induction of host innate immune defences in response to HSV-1 infection. PLOS Pathog. *15*, e1007667.

McSwiggen, D.T., Mir, M., Darzacq, X., and Tjian, R. (2019). Evaluating phase separation in live cells: diagnosis, caveats, and functional consequences. Genes Dev.

Medzhitov, R. (2008). Origin and physiological roles of inflammation. Nature *454*, 428–435.

Melander, F., Bekker-Jensen, S., Falck, J., Bartek, J., Mailand, N., and Lukas, J. (2008). Phosphorylation of SDT repeats in the MDC1 N terminus triggers retention of NBS1 at the DNA damage-modified chromatin. J. Cell Biol. *181*, 213–226.

Melters, D.P., Pitman, M., Rakshit, T., Dimitriadis, E.K., Bui, M., Papoian, G.A., and Dalal, Y. (2019). Intrinsic elasticity of nucleosomes is encoded by histone variants and calibrated by their binding partners. Proc. Natl. Acad. Sci. *116*, 24066–24074.

Micco, R.D., Fumagalli, M., Cicalese, A., Piccinin, S., Gasparini, P., Luise, C., Schurra, C., Garre', M., Nuciforo, P.G., Bensimon, A., et al. (2006). Oncogene-induced senescence is a DNA damage response triggered by DNA hyper-replication. Nature *444*, 638–642.

Michaelson, J.S., Bader, D., Kuo, F., Kozak, C., and Leder, P. (1999). Loss of Daxx, a promiscuously interacting protein, results in extensive apoptosis in early mouse development. Genes Dev. *13*, 1918–1923.

Michalski, S., Mann, C.C. de O., Stafford, C.A., Witte, G., Bartho, J., Lammens, K., Hornung, V., and Hopfner, K.-P. (2020). Structural basis for sequestration and autoinhibition of cGAS by chromatin. Nature *587*, 678–682.

Michod, D., Bartesaghi, S., Khelifi, A., Bellodi, C., Berliocchi, L., Nicotera, P., and Salomoni, P. (2012). Calcium-Dependent Dephosphorylation of the Histone Chaperone DAXX Regulates H3.3 Loading and Transcription upon Neuronal Activation. Neuron *74*, 122–135.

Miki, T., Xu, Z., Chen-Goodspeed, M., Liu, M., Van Oort-Jansen, A., Rea, M.A., Zhao, Z., Lee,

C.C., and Chang, K.-S. (2012). PML regulates PER2 nuclear localization and circadian function. EMBO J. *31*, 1427–1439.

Miller, K.M., Tjeertes, J.V., Coates, J., Legube, G., Polo, S.E., Britton, S., and Jackson, S.P. (2010). Human HDAC1 and HDAC2 function in the DNA-damage response to promote DNA nonhomologous end-joining. Nat. Struct. Mol. Biol. *17*, 1144–1151.

Mirzoeva, O.K., and Petrini, J.H.J. (2001). DNA Damage-Dependent Nuclear Dynamics of the Mre11 Complex. Mol. Cell. Biol. *21*, 281–288.

Missiroli, S., Bonora, M., Patergnani, S., Poletti, F., Perrone, M., Gafà, R., Magri, E., Raimondi, A., Lanza, G., Tacchetti, C., et al. (2016). PML at Mitochondria-Associated Membranes Is Critical for the Repression of Autophagy and Cancer Development. Cell Rep. *16*, 2415–2427.

Misteli, T. (2020). The Self-Organizing Genome: Principles of Genome Architecture and Function. Cell *183*, 28–45.

Mito, Y., Henikoff, J.G., and Henikoff, S. (2005). Genome-scale profiling of histone H3.3 replacement patterns. Nat. Genet. *37*, 1090–1097.

Moiseeva, O., Mallette, F.A., Mukhopadhyay, U.K., Moores, A., and Ferbeyre, G. (2006). DNA damage signaling and p53-dependent senescence after prolonged beta-interferon stimulation. Mol. Biol. Cell *17*, 1583–1592.

Moore, L.D., Le, T., and Fan, G. (2013). DNA Methylation and Its Basic Function. Neuropsychopharmacology *38*, 23–38.

Mousavi, K., Zare, H., Dell'Orso, S., Grontved, L., Gutierrez-Cruz, G., Derfoul, A., Hager, G.L., and Sartorelli, V. (2013). eRNAs Promote Transcription by Establishing Chromatin Accessibility at Defined Genomic Loci. Mol. Cell *51*, 606–617.

Moyal, L., Lerenthal, Y., Gana-Weisz, M., Mass, G., So, S., Wang, S.-Y., Eppink, B., Chung, Y.M., Shalev, G., Shema, E., et al. (2011). Requirement of ATM-dependent monoubiquitylation of histone H2B for timely repair of DNA double-strand breaks. Mol. Cell *41*, 529–542.

Mukhopadhyay, D., and Dasso, M. (2007). Modification in reverse: the SUMO proteases. Trends Biochem. Sci. *32*, 286–295.

Müller, S., Matunis, M.J., and Dejean, A. (1998). Conjugation with the ubiquitin-related modifier SUMO-1 regulates the partitioning of PML within the nucleus. EMBO J. *17*, 61–70.

Muñoz-Espín, D., Cañamero, M., Maraver, A., Gómez-López, G., Contreras, J., Murillo-Cuesta, S., Rodríguez-Baeza, A., Varela-Nieto, I., Ruberte, J., Collado, M., et al. (2013). Programmed Cell Senescence during Mammalian Embryonic Development. Cell *155*, 1104–1118.

Murr, R., Loizou, J.I., Yang, Y.-G., Cuenin, C., Li, H., Wang, Z.-Q., and Herceg, Z. (2006). Histone acetylation by Trrap–Tip60 modulates loading of repair proteins and repair of DNA double-strand breaks. Nat. Cell Biol. *8*, 91–99.

Nakada, S., Chen, G.I., Gingras, A.-C., and Durocher, D. (2008). PP4 is a gamma H2AX phosphatase required for recovery from the DNA damage checkpoint. EMBO Rep. *9*, 1019–1026.

Nakamura, K., Kato, A., Kobayashi, J., Yanagihara, H., Sakamoto, S., Oliveira, D.V.N.P., Shimada, M., Tauchi, H., Suzuki, H., Tashiro, S., et al. (2011). Regulation of homologous recombination by RNF20-dependent H2B ubiquitination. Mol. Cell *41*, 515–528.

Nakamura, K., Saredi, G., Becker, J.R., Foster, B.M., Nguyen, N.V., Beyer, T.E., Cesa, L.C., Faull, P.A., Lukauskas, S., Frimurer, T., et al. (2019). H4K20me0 recognition by BRCA1-BARD1 directs homologous recombination to sister chromatids. Nat. Cell Biol. *21*, 311–318.

Nanney, D.L. (1958). Epigenetic Control Systems. Proc. Natl. Acad. Sci. *44*, 712–717.

Nazarov, I.B., Smirnova, A.N., Krutilina, R.I., Svetlova, M.P., Solovjeva, L.V., Nikiforov, A.A., Oei,

S.-L., Zalenskaya, I.A., Yau, P.M., Bradbury, E.M., et al. (2003). Dephosphorylation of histone gamma-H2AX during repair of DNA double-strand breaks in mammalian cells and its inhibition by calyculin A. Radiat. Res. *160*, 309–317.

Nicoglou, A., and Merlin, F. (2017). Epigenetics: A way to bridge the gap between biological fields. Stud. Hist. Philos. Sci. Part C Stud. Hist. Philos. Biol. Biomed. Sci. *66*, 73–82.

Nisole, S., Maroui, M.A., Mascle, X.H., Aubry, M., and Chelbi-Alix, M.K. (2013). Differential Roles of PML Isoforms. Front. Oncol. *3*.

Niu, C., Livingston, C.M., Li, L., Beran, R.K., Daffis, S., Ramakrishnan, D., Burdette, D., Peiser, L., Salas, E., Ramos, H., et al. (2017). The Smc5/6 Complex Restricts HBV when Localized to ND10 without Inducing an Innate Immune Response and Is Counteracted by the HBV X Protein Shortly after Infection. PLOS ONE *12*, e0169648.

Niwa-Kawakita, M., Ferhi, O., Soilihi, H., Le Bras, M., Lallemand-Breitenbach, V., and de Thé, H. (2017). PML is a ROS sensor activating p53 upon oxidative stress. J. Exp. Med. *214*, 3197–3206.

Nora, E.P., Lajoie, B.R., Schulz, E.G., Giorgetti, L., Okamoto, I., Servant, N., Piolot, T., Berkum, N.L. van, Meisig, J., Sedat, J., et al. (2012). Spatial partitioning of the regulatory landscape of the X-inactivation centre. Nature *485*, 381–385.

Novakova, Z., Hubackova, S., Kosar, M., Janderova-Rossmeislova, L., Dobrovolna, J., Vasicova, P., Vancurova, M., Horejsi, Z., Hozak, P., Bartek, J., et al. (2010). Cytokine expression and signaling in drug-induced cellular senescence. Oncogene *29*, 273–284.

O'Hagan, H.M., Mohammad, H.P., and Baylin, S.B. (2008). Double strand breaks can initiate gene silencing and SIRT1-dependent onset of DNA methylation in an exogenous promoter CpG island. PLoS Genet. *4*, e1000155.

O'Hagan, H.M., Wang, W., Sen, S., Destefano Shields, C., Lee, S.S., Zhang, Y.W., Clements, E.G., Cai, Y., Van Neste, L., Easwaran, H., et al. (2011). Oxidative damage targets complexes containing DNA methyltransferases, SIRT1, and polycomb members to promoter CpG Islands. Cancer Cell *20*, 606–619.

Ohgiya, D., Matsushita, H., Onizuka, M., Nakamura, N., Amaki, J., Aoyama, Y., Kawai, H., Ogawa, Y., Kawada, H., and Ando, K. (2012). Association of promyelocytic leukemia protein with expression of IL-6 and resistance to treatment in multiple myeloma. Acta Haematol. *128*, 213–222.

Okano, M., Bell, D.W., Haber, D.A., and Li, E. (1999). DNA Methyltransferases Dnmt3a and Dnmt3b Are Essential for De Novo Methylation and Mammalian Development. Cell *99*, 247–257.

Okura, T., Gong, L., Kamitani, T., Wada, T., Okura, I., Wei, C.F., Chang, H.M., and Yeh, E.T. (1996). Protection against Fas/APO-1- and tumor necrosis factor-mediated cell death by a novel protein, sentrin. J. Immunol. Baltim. Md 1950 *157*, 4277–4281.

Oliveira, D.V., Kato, A., Nakamura, K., Ikura, T., Okada, M., Kobayashi, J., Yanagihara, H., Saito, Y., Tauchi, H., and Komatsu, K. (2014). Histone chaperone FACT regulates homologous recombination by chromatin remodeling through interaction with RNF20. J. Cell Sci. *127*, 763–772.

de Oliveira Mann, C.C., Orzalli, M.H., King, D.S., Kagan, J.C., Lee, A.S.Y., and Kranzusch, P.J. (2019). Modular Architecture of the STING C-Terminal Tail Allows Interferon and NF-κB Signaling Adaptation. Cell Rep. *27*, 1165-1175.e5.

Osley, M.A. (1991). The regulation of histone synthesis in the cell cycle. Annu. Rev. Biochem. *60*, 827–861.

Osley, M.A., and Lycan, D. (1987). Trans-acting regulatory mutations that alter transcription of Saccharomyces cerevisiae histone genes. Mol. Cell. Biol. *7*, 4204–4210.

Osterwald, S., Deeg, K.I., Chung, I., Parisotto, D., Wörz, S., Rohr, K., Erfle, H., and Rippe, K.

(2015). PML induces compaction, TRF2 depletion and DNA damage signaling at telomeres and promotes their alternative lengthening. J. Cell Sci. *128*, 1887–1900.

Ostuni, R., Piccolo, V., Barozzi, I., Polletti, S., Termanini, A., Bonifacio, S., Curina, A., Prosperini, E., Ghisletti, S., and Natoli, G. (2013). Latent Enhancers Activated by Stimulation in Differentiated Cells. Cell *152*, 157–171.

Ou, H.D., Phan, S., Deerinck, T.J., Thor, A., Ellisman, M.H., and O'Shea, C.C. (2017). ChromEMT: Visualizing 3D chromatin structure and compaction in interphase and mitotic cells. Science *357*.

Owerbach, D., McKay, E.M., Yeh, E.T.H., Gabbay, K.H., and Bohren, K.M. (2005). A proline-90 residue unique to SUMO-4 prevents maturation and sumoylation. Biochem. Biophys. Res. Commun. *337*, 517–520.

Padeken, J., and Heun, P. (2014). Nucleolus and nuclear periphery: Velcro for heterochromatin. Curr. Opin. Cell Biol. *28*, 54–60.

Pandey, R.R., Mondal, T., Mohammad, F., Enroth, S., Redrup, L., Komorowski, J., Nagano, T., Mancini-DiNardo, D., and Kanduri, C. (2008). Kcnq1ot1 Antisense Noncoding RNA Mediates Lineage-Specific Transcriptional Silencing through Chromatin-Level Regulation. Mol. Cell *32*, 232–246.

Pannunzio, N.R., Watanabe, G., and Lieber, M.R. (2018). Nonhomologous DNA end-joining for repair of DNA double-strand breaks. J. Biol. Chem. *293*, 10512–10523.

Park, S.H., Kang, K., Giannopoulou, E., Qiao, Y., Kang, K., Kim, G., Park-Min, K.-H., and Ivashkiv, L.B. (2017). Type I interferons and the cytokine TNF cooperatively reprogram the macrophage epigenome to promote inflammatory activation. Nat. Immunol. *18*, 1104–1116.

Patel, M.C., Debrosse, M., Smith, M., Dey, A., Huynh, W., Sarai, N., Heightman, T.D., Tamura, T., and Ozato, K. (2013). BRD4 Coordinates Recruitment of Pause Release Factor P-TEFb and the Pausing Complex NELF/DSIF To Regulate Transcription Elongation of Interferon-Stimulated Genes. Mol. Cell. Biol. *33*, 2497–2507.

Pathare, G.R., Decout, A., Glück, S., Cavadini, S., Makasheva, K., Hovius, R., Kempf, G., Weiss, J., Kozicka, Z., Guey, B., et al. (2020). Structural mechanism of cGAS inhibition by the nucleosome. Nature *587*, 668–672.

Paul, A., and Wang, B. (2017). RNF8- and Ube2S-dependent ubiquitin lysine 11-linkage modification in response to DNA damage. Mol. Cell *66*, 458-472.e5.

Paulson, M., Press, C., Smith, E., Tanese, N., and Levy, D.E. (2002). IFN-Stimulated transcription through a TBP-free acetyltransferase complex escapes viral shutoff. Nat. Cell Biol. *4*, 140–147.

Pearson, M., Carbone, R., Sebastiani, C., Cioce, M., Fagioli, M., Saito, S., Higashimoto, Y., Appella, E., Minucci, S., Pandolfi, P.P., et al. (2000). PML regulates p53 acetylation and premature senescence induced by oncogenic Ras. Nature *406*, 207–210.

Pei, H., Zhang, L., Luo, K., Qin, Y., Chesi, M., Fei, F., Bergsagel, P.L., Wang, L., You, Z., and Lou, Z. (2011). MMSET regulates histone H4K20 methylation and 53BP1 accumulation at DNA damage sites. Nature *470*, 124–128.

Peric-Hupkes, D., Meuleman, W., Pagie, L., Bruggeman, S.W.M., Solovei, I., Brugman, W., Gräf, S., Flicek, P., Kerkhoven, R.M., van Lohuizen, M., et al. (2010). Molecular maps of the reorganization of genome – nuclear lamina interactions during differentiation. Mol. Cell *38*, 603–613.

Pfister, S.X., Ahrabi, S., Zalmas, L.-P., Sarkar, S., Aymard, F., Bachrati, C.Z., Helleday, T., Legube, G., La Thangue, N.B., Porter, A.C.G., et al. (2014). SETD2-dependent histone H3K36 trimethylation is required for homologous recombination repair and genome stability. Cell Rep. *7*, 2006–2018.

Philpott, D.J., and Girardin, S.E. (2010). Nod-like receptors: sentinels at host membranes. Curr. Opin. Immunol. *22*, 428–434.

Pichler, A., Knipscheer, P., Oberhofer, E., van Dijk, W.J., Körner, R., Olsen, J.V., Jentsch, S., Melchior, F., and Sixma, T.K. (2005). SUMO modification of the ubiquitin-conjugating enzyme E2-25K. Nat. Struct. Mol. Biol. *12*, 264–269.

Piquet, S., Le Parc, F., Bai, S.-K., Chevallier, O., Adam, S., and Polo, S.E. (2018). The Histone Chaperone FACT Coordinates H2A.X-Dependent Signaling and Repair of DNA Damage. Mol. Cell *72*, 888-901.e7.

Platanias, L.C. (2005). Mechanisms of type-I- and type-II-interferon-mediated signalling. Nat. Rev. Immunol. *5*, 375–386.

Polo, S.E., Roche, D., and Almouzni, G. (2006). New histone incorporation marks sites of UV repair in human cells. Cell *127*, 481–493.

Ponente, M., Campanini, L., Cuttano, R., Piunti, A., Delledonne, G.A., Coltella, N., Valsecchi, R., Villa, A., Cavallaro, U., Pattini, L., et al. (2017). PML promotes metastasis of triple-negative breast cancer through transcriptional regulation of HIF1A target genes. JCI Insight *2*.

Pope, B.D., Ryba, T., Dileep, V., Yue, F., Wu, W., Denas, O., Vera, D.L., Wang, Y., Hansen, R.S., Canfield, T.K., et al. (2014). Topologically associating domains are stable units of replication-timing regulation. Nature *515*, 402–405.

Probst, A.V., Dunleavy, E., and Almouzni, G. (2009). Epigenetic inheritance during the cell cycle. Nat. Rev. Mol. Cell Biol. *10*, 192–206.

Prochasson, P., Florens, L., Swanson, S.K., Washburn, M.P., and Workman, J.L. (2005). The HIR corepressor complex binds to nucleosomes generating a distinct protein/DNA complex resistant to remodeling by SWI/SNF. Genes Dev. *19*, 2534–2539.

Prokhortchouk, A., Hendrich, B., Jørgensen, H., Ruzov, A., Wilm, M., Georgiev, G., Bird, A., and Prokhortchouk, E. (2001). The p120 catenin partner Kaiso is a DNA methylation-dependent transcriptional repressor. Genes Dev. *15*, 1613–1618.

Punchard, N.A., Whelan, C.J., and Adcock, I. (2004). The Journal of Inflammation. J. Inflamm. Lond. Engl. *1*, 1.

Qiao, Y., Giannopoulou, E.G., Chan, C.H., Park, S., Gong, S., Chen, J., Hu, X., Elemento, O., and Ivashkiv, L.B. (2013). Synergistic Activation of Inflammatory Cytokine Genes by Interferon-γ-induced Chromatin Remodeling and Toll-like Receptor Signaling. Immunity *39*.

Qiu, L., Hu, X., Jing, Q., Zeng, X., Chan, K.-M., and Han, J. (2018). Mechanism of cancer: Oncohistones in action. J. Genet. Genomics *45*, 227–236.

Queen, D., Ediriweera, C., and Liu, L. (2019). Function and Regulation of IL-36 Signaling in Inflammatory Diseases and Cancer Development. Front. Cell Dev. Biol. *7*.

Rai, T.S., and Adams, P.D. (2012). Lessons from senescence: Chromatin maintenance in non-proliferating cells. Biochim. Biophys. Acta *1819*, 322–331.

Rai, T.S., Puri, A., McBryan, T., Hoffman, J., Tang, Y., Pchelintsev, N.A., van Tuyn, J., Marmorstein, R., Schultz, D.C., and Adams, P.D. (2011). Human CABIN1 is a functional member of the human HIRA/UBN1/ASF1a histone H3.3 chaperone complex. Mol. Cell. Biol. *31*, 4107–4118.

Rai, T.S., Cole, J.J., Nelson, D.M., Dikovskaya, D., Faller, W.J., Vizioli, M.G., Hewitt, R.N., Anannya, O., McBryan, T., Manoharan, I., et al. (2014). HIRA orchestrates a dynamic chromatin landscape in senescence and is required for suppression of neoplasia. Genes Dev. *28*, 2712–2725.

Rai, T.S., Glass, M., Cole, J.J., Rather, M.I., Marsden, M., Neilson, M., Brock, C., Humphreys,

I.R., Everett, R.D., and Adams, P.D. (2017). Histone chaperone HIRA deposits histone H3.3 onto foreign viral DNA and contributes to anti-viral intrinsic immunity. Nucleic Acids Res. *45*, 11673–11683.

Ramachandran, S., Haddad, D., Li, C., Le, M.X., Ling, A.K., So, C.C., Nepal, R.M., Gommerman, J.L., Yu, K., Ketela, T., et al. (2016). The SAGA Deubiquitination Module Promotes DNA Repair and Class Switch Recombination through ATM and DNAPK-Mediated γH2AX Formation. Cell Rep. *15*, 1554–1565.

Rao, S.S.P., Huntley, M.H., Durand, N.C., Stamenova, E.K., Bochkov, I.D., Robinson, J.T., Sanborn, A.L., Machol, I., Omer, A.D., Lander, E.S., et al. (2014). A 3D Map of the Human Genome at Kilobase Resolution Reveals Principles of Chromatin Looping. Cell *159*, 1665–1680.

Rayavarapu, S., Coley, W., Kinder, T.B., and Nagaraju, K. (2013). Idiopathic inflammatory myopathies: pathogenic mechanisms of muscle weakness. Skelet. Muscle *3*, 13.

Ray-Gallet, D., Quivy, J.-P., Silljé, H.W.W., Nigg, E.A., and Almouzni, G. (2007). The histone chaperone Asf1 is dispensable for direct de novo histone deposition in Xenopus egg extracts. Chromosoma *116*, 487–496.

Ray-Gallet, D., Woolfe, A., Vassias, I., Pellentz, C., Lacoste, N., Puri, A., Schultz, D.C., Pchelintsev, N.A., Adams, P.D., Jansen, L.E.T., et al. (2011). Dynamics of histone H3 deposition in vivo reveal a nucleosome gap-filling mechanism for H3.3 to maintain chromatin integrity. Mol. Cell *44*, 928–941.

Ray-Gallet, D., Ricketts, M.D., Sato, Y., Gupta, K., Boyarchuk, E., Senda, T., Marmorstein, R., and Almouzni, G. (2018). Functional activity of the H3.3 histone chaperone complex HIRA requires trimerization of the HIRA subunit. Nat. Commun. *9*, 3103.

Reddy, K.L., Zullo, J.M., Bertolino, E., and Singh, H. (2008). Transcriptional repression mediated by repositioning of genes to the nuclear lamina. Nature *452*, 243–247.

Regad, T., Bellodi, C., Nicotera, P., and Salomoni, P. (2009). The tumor suppressor Pml regulates cell fate in the developing neocortex. Nat. Neurosci. *12*, 132–140.

Reichelt, M., Wang, L., Sommer, M., Perrino, J., Nour, A.M., Sen, N., Baiker, A., Zerboni, L., and Arvin, A.M. (2011). Entrapment of Viral Capsids in Nuclear PML Cages Is an Intrinsic Antiviral Host Defense against Varicella-Zoster Virus. PLOS Pathog. *7*, e1001266.

Ricci, M.A., Manzo, C., García-Parajo, M.F., Lakadamyali, M., and Cosma, M.P. (2015). Chromatin Fibers Are Formed by Heterogeneous Groups of Nucleosomes In Vivo. Cell *160*, 1145–1158.

Ricketts, M.D., and Marmorstein, R. (2016). A Molecular Prospective for HIRA Complex Assembly and H3.3-Specific Histone Chaperone Function. J. Mol. Biol.

Ricketts, M.D., Frederick, B., Hoff, H., Tang, Y., Schultz, D.C., Singh Rai, T., Grazia Vizioli, M., Adams, P.D., and Marmorstein, R. (2015). Ubinuclein-1 confers histone H3.3-specific-binding by the HIRA histone chaperone complex. Nat. Commun. *6*.

Ricketts, M.D., Dasgupta, N., Fan, J., Han, J., Gerace, M., Tang, Y., Black, B.E., Adams, P.D., and Marmorstein, R. (2019). The HIRA histone chaperone complex subunit UBN1 harbors H3/H4- and DNA-binding activity. J. Biol. Chem. *294*, 9239–9259.

Riggs, A.D. (1975). X inactivation, differentiation, and DNA methylation. Cytogenet. Cell Genet. *14*, 9–25.

Riggs, A., Martienssen, R., and Russo, V. (1996). Introduction. In Epigenetic mechanisms of gene regulation. In Epigenetic Mechanisms of Gene Regulation, (Cold Spring Harbor, NY: Cold Spring Harbor Laboratory Press), pp. 1–4.

Roberts, C., Sutherland, H.F., Farmer, H., Kimber, W., Halford, S., Carey, A., Brickman, J.M., Wynshaw-Boris, A., and Scambler, P.J. (2002). Targeted Mutagenesis of the Hira Gene Results

in Gastrulation Defects and Patterning Abnormalities of Mesoendodermal Derivatives Prior to Early Embryonic Lethality. Mol. Cell. Biol. *22*, 2318–2328.

Robson, M.I., Heras, J.I. de las, Czapiewski, R., Sivakumar, A., Kerr, A.R.W., and Schirmer, E.C. (2017). Constrained release of lamina-associated enhancers and genes from the nuclear envelope during T-cell activation facilitates their association in chromosome compartments. Genome Res. *27*, 1126–1138.

Rogakou, E.P., Pilch, D.R., Orr, A.H., Ivanova, V.S., and Bonner, W.M. (1998). DNA Double-stranded Breaks Induce Histone H2AX Phosphorylation on Serine 139*. J. Biol. Chem. *273*, 5858–5868.

Roque, A., Ponte, I., and Suau, P. (2016). Interplay between histone H1 structure and function. Biochim. Biophys. Acta BBA - Gene Regul. Mech. *1859*, 444–454.

Roy, A., Ghosh, A., Kumar, B., and Chandran, B. (2019). IFI16, a nuclear innate immune DNA sensor, mediates epigenetic silencing of herpesvirus genomes by its association with H3K9 methyltransferases SUV39H1 and GLP. ELife *8*.

Rubbi, C.P., and Milner, J. (2003). p53 is a chromatin accessibility factor for nucleotide excision repair of DNA damage. EMBO J. *22*, 975–986.

Rusinova, I., Forster, S., Yu, S., Kannan, A., Masse, M., Cumming, H., Chapman, R., and Hertzog, P.J. (2013). INTERFEROME v2.0: an updated database of annotated interferon-regulated genes. Nucleic Acids Res. *41*, D1040–D1046.

Russo, R.C., Garcia, C.C., Teixeira, M.M., and Amaral, F.A. (2014). The CXCL8/IL-8 chemokine family and its receptors in inflammatory diseases. Expert Rev. Clin. Immunol. *10*, 593–619.

Sadic, D., Schmidt, K., Groh, S., Kondofersky, I., Ellwart, J., Fuchs, C., Theis, F.J., and Schotta, G. (2015). Atrx promotes heterochromatin formation at retrotransposons. EMBO Rep. *16*, 836–850.

Sahin, U., Ferhi, O., Jeanne, M., Benhenda, S., Berthier, C., Jollivet, F., Niwa-Kawakita, M., Faklaris, O., Setterblad, N., de Thé, H., et al. (2014a). Oxidative stress-induced assembly of PML nuclear bodies controls sumoylation of partner proteins. J. Cell Biol. *204*, 931–945.

Sahin, U., Ferhi, O., Carnec, X., Zamborlini, A., Peres, L., Jollivet, F., Vitaliano-Prunier, A., Thé, H. de, and Lallemand-Breitenbach, V. (2014b). Interferon controls SUMO availability via the Lin28 and let-7 axis to impede virus replication. Nat. Commun. *5*, 4187.

Saitoh, H., and Hinchey, J. (2000). Functional heterogeneity of small ubiquitin-related protein modifiers SUMO-1 versus SUMO-2/3. J. Biol. Chem. *275*, 6252–6258.

Sale, J.E. (2013). Translesion DNA Synthesis and Mutagenesis in Eukaryotes. Cold Spring Harb. Perspect. Biol. *5*.

Sallmyr, A., and Tomkinson, A.E. (2018). Repair of DNA double-strand breaks by mammalian alternative end-joining pathways. J. Biol. Chem. *293*, 10536–10546.

Sanchez, A., De Vivo, A., Uprety, N., Kim, J., Stevens, S.M., and Kee, Y. (2016). BMI1-UBR5 axis regulates transcriptional repression at damaged chromatin. Proc. Natl. Acad. Sci. U. S. A. *113*, 11243–11248.

Sarai, N., Nimura, K., Tamura, T., Kanno, T., Patel, M.C., Heightman, T.D., Ura, K., and Ozato, K. (2013). WHSC1 links transcription elongation to HIRA-mediated histone H3.3 deposition. EMBO J. *32*, 2392–2406.

Saredi, G., Huang, H., Hammond, C.M., Alabert, C., Bekker-Jensen, S., Forne, I., Reverón-Gómez, N., Foster, B.M., Mlejnkova, L., Bartke, T., et al. (2016). H4K20me0 marks post-replicative chromatin and recruits the TONSL–MMS22L DNA repair complex. Nature *534*, 714–718.

Satoh, T., Kato, H., Kumagai, Y., Yoneyama, M., Sato, S., Matsushita, K., Tsujimura, T., Fujita, T., Akira, S., and Takeuchi, O. (2010). LGP2 is a positive regulator of RIG-I- and MDA5-mediated antiviral responses. Proc. Natl. Acad. Sci. U. S. A. *107*, 1512–1517.

Saurin, A.J., Borden, K.L., Boddy, M.N., and Freemont, P.S. (1996). Does this have a familiar RING? Trends Biochem. Sci. *21*, 208–214.

Sawatsubashi, S., Murata, T., Lim, J., Fujiki, R., Ito, S., Suzuki, E., Tanabe, M., Zhao, Y., Kimura, S., Fujiyama, S., et al. (2010). A histone chaperone, DEK, transcriptionally coactivates a nuclear receptor. Genes Dev. *24*, 159–170.

Schärer, O.D. (2013). Nucleotide Excision Repair in Eukaryotes. Cold Spring Harb. Perspect. Biol. *5*.

Scheller, J., Chalaris, A., Schmidt-Arras, D., and Rose-John, S. (2011). The pro- and anti-inflammatory properties of the cytokine interleukin-6. Biochim. Biophys. Acta BBA - Mol. Cell Res. *1813*, 878–888.

Scherer, M., and Stamminger, T. (2016). Emerging Role of PML Nuclear Bodies in Innate Immune Signaling. J. Virol. *90*, 5850–5854.

Schmidl, C., Klug, M., Boeld, T.J., Andreesen, R., Hoffmann, P., Edinger, M., and Rehli, M. (2009). Lineage-specific DNA methylation in T cells correlates with histone methylation and enhancer activity. Genome Res. *19*, 1165–1174.

Schmitz, M.L., and Grishina, I. (2012). Regulation of the tumor suppressor PML by sequential post-translational modifications. Front. Oncol. *2*.

Schneider, W.M., Chevillotte, M.D., and Rice, C.M. (2014). Interferon-Stimulated Genes: A Complex Web of Host Defenses. Annu. Rev. Immunol. *32*, 513–545.

Schneider, W.M., Luna, J.M., Hoffmann, H.-H., Sánchez-Rivera, F.J., Leal, A.A., Ashbrook, A.W., Le Pen, J., Ricardo-Lax, I., Michailidis, E., Peace, A., et al. (2021). Genome-Scale Identification of SARS-CoV-2 and Pan-coronavirus Host Factor Networks. Cell *184*, 120-132.e14.

Schneiderman, J.I., Orsi, G.A., Hughes, K.T., Loppin, B., and Ahmad, K. (2012). Nucleosome-depleted chromatin gaps recruit assembly factors for the H3.3 histone variant. Proc. Natl. Acad. Sci. *109*, 19721–19726.

Schreiber, G. (2017). The molecular basis for differential type I interferon signaling. J. Biol. Chem. *292*, 7285–7294.

Schwartz, B.E., and Ahmad, K. (2005). Transcriptional activation triggers deposition and removal of the histone variant H3.3. Genes Dev. *19*, 804–814.

Schwartzentruber, J., Korshunov, A., Liu, X.-Y., Jones, D.T.W., Pfaff, E., Jacob, K., Sturm, D., Fontebasso, A.M., Quang, D.-A.K., Tönjes, M., et al. (2012). Driver mutations in histone H3.3 and chromatin remodelling genes in paediatric glioblastoma. Nature *482*, 226–231.

Scionti, I., Hayashi, S., Mouradian, S., Girard, E., Lima, J.E. de, Morel, V., Simonet, T., Wurmser, M., Maire, P., Ancelin, K., et al. (2017). LSD1 Controls Timely MyoD Expression via MyoD Core Enhancer Transcription. Cell Rep. *18*, 1996–2006.

Scully, R., Panday, A., Elango, R., and Willis, N.A. (2019). DNA double strand break repair pathway choice in somatic mammalian cells. Nat. Rev. Mol. Cell Biol. *20*, 698–714.

Seker, H., Rubbi, C., Linke, S.P., Bowman, E.D., Garfield, S., Hansen, L., Borden, K.L., Milner, J., and Harris, C.C. (2003). UV-C-induced DNA damage leads to p53-dependent nuclear trafficking of PML. Oncogene *22*, 1620–1628.

Sellou, H., Lebeaupin, T., Chapuis, C., Smith, R., Hegele, A., Singh, H.R., Kozlowski, M., Bultmann, S., Ladurner, A.G., Timinszky, G., et al. (2016). The poly(ADP-ribose)-dependent chromatin remodeler Alc1 induces local chromatin relaxation upon DNA damage. Mol. Biol. Cell

*27*, 3791–3799.

Semba, Y., Harada, A., Maehara, K., Oki, S., Meno, C., Ueda, J., Yamagata, K., Suzuki, A., Onimaru, M., Nogami, J., et al. (2017). Chd2 regulates chromatin for proper gene expression toward differentiation in mouse embryonic stem cells. Nucleic Acids Res. *45*, 8758–8772.

Shalginskikh, N., Poleshko, A., Skalka, A.M., and Katz, R.A. (2013). Retroviral DNA Methylation and Epigenetic Repression Are Mediated by the Antiviral Host Protein Daxx. J. Virol. *87*, 2137–2150.

Shanbhag, N.M., Rafalska-Metcalf, I.U., Balane-Bolivar, C., Janicki, S.M., and Greenberg, R.A. (2010). ATM-dependent chromatin changes silence transcription in cis to DNA double-strand breaks. Cell *141*, 970–981.

Sharif, J., Muto, M., Takebayashi, S., Suetake, I., Iwamatsu, A., Endo, T.A., Shinga, J., Mizutani-Koseki, Y., Toyoda, T., Okamura, K., et al. (2007). The SRA protein Np95 mediates epigenetic inheritance by recruiting Dnmt1 to methylated DNA. Nature *450*, 908–912.

Shastrula, P.K., Sierra, I., Deng, Z., Keeney, F., Hayden, J.E., Lieberman, P.M., and Janicki, S.M. (2019). PML is recruited to heterochromatin during S phase and represses DAXX-mediated histone H3.3 chromatin assembly. J. Cell Sci. *132*.

Shaw, A.E., Hughes, J., Gu, Q., Behdenna, A., Singer, J.B., Dennis, T., Orton, R.J., Varela, M., Gifford, R.J., Wilson, S.J., et al. (2017). Fundamental properties of the mammalian innate immune system revealed by multispecies comparison of type I interferon responses. PLOS Biol. *15*, e2004086.

Shen, T.H., Lin, H.-K., Scaglioni, P.P., Yung, T.M., and Pandolfi, P.P. (2006). The Mechanisms of PML-Nuclear Body Formation. Mol. Cell *24*, 331–339.

Shen, Z., Pardington-Purtymun, P.E., Comeaux, J.C., Moyzis, R.K., and Chen, D.J. (1996). UBL1, a human ubiquitin-like protein associating with human RAD51/RAD52 proteins. Genomics *36*, 271–279.

Shi, L., Wen, H., and Shi, X. (2017). The Histone Variant H3.3 in Transcriptional Regulation and Human Disease. J. Mol. Biol. *429*, 1934–1945.

Shi, L., Shi, J., Shi, X., Li, W., and Wen, H. (2018). Histone H3.3 G34 mutations alter histone H3K36 and H3K27 methylation in cis. J. Mol. Biol. *430*, 1562–1565.

Shi, X., Hong, T., Walter, K.L., Ewalt, M., Michishita, E., Hung, T., Carney, D., Peña, P., Lan, F., Kaadige, M.R., et al. (2006). ING2 PHD domain links histone H3 lysine 4 methylation to active gene repression. Nature *442*, 96–99.

Shimada, N., Shinagawa, T., and Ishii, S. (2008). Modulation of M2-type pyruvate kinase activity by the cytoplasmic PML tumor suppressor protein. Genes Cells *13*, 245–254.

Siggens, L., Cordeddu, L., Rönnerblad, M., Lennartsson, A., and Ekwall, K. (2015). Transcription-coupled recruitment of human CHD1 and CHD2 influences chromatin accessibility and histone H3 and H3.3 occupancy at active chromatin regions. Epigenetics Chromatin *8*, 4.

Siliciano, J.D., Canman, C.E., Taya, Y., Sakaguchi, K., Appella, E., and Kastan, M.B. (1997). DNA damage induces phosphorylation of the amino terminus of p53. Genes Dev. *11*, 3471–3481.

Simpson, R.T. (1978). Structure of the chromatosome, a chromatin particle containing 160 base pairs of DNA and all the histones. Biochemistry *17*, 5524–5531.

Sitbon, D., Boyarchuk, E., Dingli, F., Loew, D., and Almouzni, G. (2020). Histone variant H3.3 residue S31 is essential for Xenopus gastrulation regardless of the deposition pathway. Nat. Commun. *11*, 1256.

Siwek, W., Tehrani, S.S.H., Mata, J.F., and Jansen, L.E.T. (2020). Activation of Clustered IFNγ Target Genes Drives Cohesin-Controlled Transcriptional Memory. Mol. Cell *80*, 396-409.e6.

Smerdon, M.J. (1991). DNA repair and the role of chromatin structure. Curr. Opin. Cell Biol. *3*, 422–428.

Smith, R., Sellou, H., Chapuis, C., Huet, S., and Timinszky, G. (2018). CHD3 and CHD4 recruitment and chromatin remodeling activity at DNA breaks is promoted by early poly(ADP-ribose)-dependent chromatin relaxation. Nucleic Acids Res. *46*, 6087–6098.

Sobhian, B., Shao, G., Lilli, D.R., Culhane, A.C., Moreau, L.A., Xia, B., Livingston, D.M., and Greenberg, R.A. (2007). RAP80 targets BRCA1 to specific ubiquitin structures at DNA damage sites. Science *316*, 1198–1202.

Soll, J.M., Sobol, R.W., and Mosammaparast, N. (2017). Regulation of DNA Alkylation Damage Repair: Lessons and Therapeutic Opportunities. Trends Biochem. Sci. *42*, 206–218.

Song, F., Smith, J.F., Kimura, M.T., Morrow, A.D., Matsuyama, T., Nagase, H., and Held, W.A. (2005a). Association of tissue-specific differentially methylated regions (TDMs) with differential gene expression. Proc. Natl. Acad. Sci. *102*, 3336–3341.

Song, J., Zhang, Z., Hu, W., and Chen, Y. (2005b). Small Ubiquitin-like Modifier (SUMO) Recognition of a SUMO Binding Motif: A REVERSAL OF THE BOUND ORIENTATION *. J. Biol. Chem. *280*, 40122–40129.

Soni, S., Pchelintsev, N., Adams, P.D., and Bieker, J.J. (2014). Transcription factor EKLF (KLF1) recruitment of the histone chaperone HIRA is essential for β-globin gene expression. Proc. Natl. Acad. Sci. U. S. A. *111*, 13337–13342.

Soria, G., Polo, S.E., and Almouzni, G. (2012). Prime, Repair, Restore: The Active Role of Chromatin in the DNA Damage Response. Mol. Cell *46*, 722–734.

Sourvinos, G., and Everett, R.D. (2002). Visualization of parental HSV-1 genomes and replication compartments in association with ND10 in live infected cells. EMBO J. *21*, 4989–4997.

Spycher, C., Miller, E.S., Townsend, K., Pavic, L., Morrice, N.A., Janscak, P., Stewart, G.S., and Stucki, M. (2008). Constitutive phosphorylation of MDC1 physically links the MRE11-RAD50-NBS1 complex to damaged chromatin. J. Cell Biol. *181*, 227–240.

Stadler, M., Chelbi-Alix, M.K., Koken, M.H., Venturini, L., Lee, C., Saïb, A., Quignon, F., Pelicano, L., Guillemin, M.C., and Schindler, C. (1995). Transcriptional induction of the PML growth suppressor gene by interferons is mediated through an ISRE and a GAS element. Oncogene *11*, 2565–2573.

de Stanchina, E., Querido, E., Narita, M., Davuluri, R.V., Pandolfi, P.P., Ferbeyre, G., and Lowe, S.W. (2004). PML Is a Direct p53 Target that Modulates p53 Effector Functions. Mol. Cell *13*, 523–535.

Storer, M., Mas, A., Robert-Moreno, A., Pecoraro, M., Ortells, M.C., Di Giacomo, V., Yosef, R., Pilpel, N., Krizhanovsky, V., Sharpe, J., et al. (2013). Senescence is a developmental mechanism that contributes to embryonic growth and patterning. Cell *155*, 1119–1130.

Strahl, B.D., and Allis, C.D. (2000). The language of covalent histone modifications. Nature *403*, 41–45.

Stucki, M., Clapperton, J.A., Mohammad, D., Yaffe, M.B., Smerdon, S.J., and Jackson, S.P. (2005). MDC1 directly binds phosphorylated histone H2AX to regulate cellular responses to DNA double-strand breaks. Cell *123*, 1213–1226.

Sun, H., Huang, Y., Mei, S., Xu, F., Liu, X., Zhao, F., Yin, L., Zhang, D., Wei, L., Wu, C., et al. (2021). A Nuclear Export Signal Is Required for cGAS to Sense Cytosolic DNA. Cell Rep. *34*, 108586.

Sun, L., Wu, J., Du, F., Chen, X., and Chen, Z.J. (2013). Cyclic GMP-AMP Synthase is a Cytosolic DNA Sensor that Activates the Type-I Interferon Pathway. Science *339*.

Sun, Y., Jiang, X., Xu, Y., Ayrapetov, M.K., Moreau, L.A., Whetstine, J.R., and Price, B.D. (2009). Histone H3 methylation links DNA damage detection to activation of the tumour suppressor Tip60. Nat. Cell Biol. *11*, 1376–1382.

Swindle, C.S., Zou, N., Van Tine, B.A., Shaw, G.M., Engler, J.A., and Chow, L.T. (1999). Human Papillomavirus DNA Replication Compartments in a Transient DNA Replication System. J. Virol. *73*, 1001–1009.

Szenker, E., Ray-Gallet, D., and Almouzni, G. (2011). The double face of the histone variant H3.3. Cell Res. *21*, 421–434.

Szenker, E., Lacoste, N., and Almouzni, G. (2012). A developmental requirement for HIRA-dependent H3.3 deposition revealed at gastrulation in Xenopus. Cell Rep. *1*, 730–740.

Tachiwana, H., Kagawa, W., Shiga, T., Osakabe, A., Miya, Y., Saito, K., Hayashi-Takanaka, Y., Oda, T., Sato, M., Park, S.-Y., et al. (2011). Crystal structure of the human centromeric nucleosome containing CENP-A. Nature *476*, 232–235.

Tagami, H., Ray-Gallet, D., Almouzni, G., and Nakatani, Y. (2004). Histone H3.1 and H3.3 Complexes Mediate Nucleosome Assembly Pathways Dependent or Independent of DNA Synthesis. Cell *116*, 51–61.

Takeuchi, O., and Akira, S. (2010). Pattern Recognition Receptors and Inflammation. Cell *140*, 805–820.

Talbert, P.B., and Henikoff, S. (2010). Histone variants — ancient wrap artists of the epigenome. Nat. Rev. Mol. Cell Biol. *11*, 264–275.

Tang, J., Cho, N.W., Cui, G., Manion, E.M., Shanbhag, N.M., Botuyan, M.V., Mer, G., and Greenberg, R.A. (2013). Acetylation limits 53BP1 association with damaged chromatin to promote homologous recombination. Nat. Struct. Mol. Biol. *20*, 317–325.

Tang, Q., Li, L., Ishov, A.M., Revol, V., Epstein, A.L., and Maul, G.G. (2003). Determination of Minimum Herpes Simplex Virus Type 1 Components Necessary To Localize Transcriptionally Active DNA to ND10. J. Virol. *77*, 5821–5828.

Tang, Y., Poustovoitov, M.V., Zhao, K., Garfinkel, M., Canutescu, A.A., Dunbrack, R., Adams, P.D., and Marmorstein, R. (2006). Structure of a human ASF1a-HIRA complex and insights into specificity of histone chaperone complex assembly. Nat. Struct. Mol. Biol. *13*, 921–929.

Tatham, M.H., Jaffray, E., Vaughan, O.A., Desterro, J.M., Botting, C.H., Naismith, J.H., and Hay, R.T. (2001). Polymeric chains of SUMO-2 and SUMO-3 are conjugated to protein substrates by SAE1/SAE2 and Ubc9. J. Biol. Chem. *276*, 35368–35374.

Tatham, M.H., Geoffroy, M.-C., Shen, L., Plechanovova, A., Hattersley, N., Jaffray, E.G., Palvimo, J.J., and Hay, R.T. (2008). RNF4 is a poly-SUMO-specific E3 ubiquitin ligase required for arsenic-induced PML degradation. Nat. Cell Biol. *10*, 538–546.

de Thé, H., Chomienne, C., Lanotte, M., Degos, L., and Dejean, A. (1990). The t(15;17) translocation of acute promyelocytic leukaemia fuses the retinoic acid receptor alpha gene to a novel transcribed locus. Nature *347*, 558–561.

de Thé, H., Le Bras, M., and Lallemand-Breitenbach, V. (2012). Acute promyelocytic leukemia, arsenic, and PML bodies. J. Cell Biol. *198*, 11–21.

Thorslund, T., Ripplinger, A., Hoffmann, S., Wild, T., Uckelmann, M., Villumsen, B., Narita, T., Sixma, T.K., Choudhary, C., Bekker-Jensen, S., et al. (2015). Histone H1 couples initiation and amplification of ubiquitin signalling after DNA damage. Nature *527*, 389–393.

Timinszky, G., Till, S., Hassa, P.O., Hothorn, M., Kustatscher, G., Nijmeijer, B., Colombelli, J., Altmeyer, M., Stelzer, E.H.K., Scheffzek, K., et al. (2009). A macrodomain-containing histone rearranges chromatin upon sensing PARP1 activation. Nat. Struct. Mol. Biol. *16*, 923–929.

Toiber, D., Erdel, F., Bouazoune, K., Silberman, D.M., Zhong, L., Mulligan, P., Sebastian, C., Cosentino, C., Martinez-Pastor, B., Giacosa, S., et al. (2013). SIRT6 recruits SNF2H to DNA break sites, preventing genomic instability through chromatin remodeling. Mol. Cell *51*, 454–468.

Torné, J., Ray-Gallet, D., Boyarchuk, E., Garnier, M., Le Baccon, P., Coulon, A., Orsi, G.A., and Almouzni, G. (2020). Two HIRA-dependent pathways mediate H3.3 de novo deposition and recycling during transcription. Nat. Struct. Mol. Biol. *27*, 1057–1068.

Torres-Padilla, M.-E., Bannister, A.J., Hurd, P.J., Kouzarides, T., and Zernicka-Goetz, M. (2006). Dynamic distribution of the replacement histone variant H3.3 in the mouse oocyte and preimplantation embryos. Int. J. Dev. Biol. *50*, 455–461.

Trojer, P., Li, G., Sims, R.J., Vaquero, A., Kalakonda, N., Boccuni, P., Lee, D., Erdjument-Bromage, H., Tempst, P., Nimer, S.D., et al. (2007). L3MBTL1, a Histone-Methylation-Dependent Chromatin Lock. Cell *129*, 915–928.

Tuzon, C.T., Spektor, T., Kong, X., Congdon, L.M., Wu, S., Schotta, G., Yokomori, K., and Rice, J.C. (2014). Concerted activities of distinct H4K20 methyltransferases at DNA double-strand breaks regulate 53BP1 nucleation and NHEJ-directed repair. Cell Rep. *8*, 430–438.

Ui, A., Nagaura, Y., and Yasui, A. (2015). Transcriptional elongation factor ENL phosphorylated by ATM recruits polycomb and switches off transcription for DSB repair. Mol. Cell *58*, 468–482.

Ulbricht, T., Alzrigat, M., Horch, A., Reuter, N., von Mikecz, A., Steimle, V., Schmitt, E., Krämer, O.H., Stamminger, T., and Hemmerich, P. (2012). PML promotes MHC class II gene expression by stabilizing the class II transactivator. J. Cell Biol. *199*, 49–63.

Van Damme, E., Laukens, K., Dang, T.H., and Van Ostade, X. (2010). A manually curated network of the PML nuclear body interactome reveals an important role for PML-NBs in SUMOylation dynamics. Int. J. Biol. Sci. *6*, 51–67.

Vancurova, M., Hanzlikova, H., Knoblochova, L., Kosla, J., Majera, D., Mistrik, M., Burdova, K., Hodny, Z., and Bartek, J. (2019). PML nuclear bodies are recruited to persistent DNA damage lesions in an RNF168-53BP1 dependent manner and contribute to DNA repair. DNA Repair *78*, 114–127.

Veer, M.J. de, Holko, M., Frevel, M., Walker, E., Der, S., Paranjape, J.M., Silverman, R.H., and Williams, B.R.G. (2001). Functional classification of interferon-stimulated genes identified using microarrays. J. Leukoc. Biol. *69*, 912–920.

Vernier, M., Bourdeau, V., Gaumont-Leclerc, M.-F., Moiseeva, O., Bégin, V., Saad, F., Mes-Masson, A.-M., and Ferbeyre, G. (2011). Regulation of E2Fs and senescence by PML nuclear bodies. Genes Dev. *25*, 41–50.

Vertegaal, A.C.O., Andersen, J.S., Ogg, S.C., Hay, R.T., Mann, M., and Lamond, A.I. (2006). Distinct and Overlapping Sets of SUMO-1 and SUMO-2 Target Proteins Revealed by Quantitative Proteomics * S. Mol. Cell. Proteomics *5*, 2298–2310.

Volkman, H.E., Cambier, S., Gray, E.E., and Stetson, D.B. (2019). Tight nuclear tethering of cGAS is essential for preventing autoreactivity. ELife *8*.

Voon, H.P.J., Hughes, J.R., Rode, C., De La Rosa-Velázquez, I.A., Jenuwein, T., Feil, R., Higgs, D.R., and Gibbons, R.J. (2015). ATRX Plays a Key Role in Maintaining Silencing at Interstitial Heterochromatic Loci and Imprinted Genes. Cell Rep. *11*, 405–418.

Voon, H.P.J., Udugama, M., Lin, W., Hii, L., Law, R.H.P., Steer, D.L., Das, P.P., Mann, J.R., and Wong, L.H. (2018). Inhibition of a K9/K36 demethylase by an H3.3 point mutation found in paediatric glioblastoma. Nat. Commun. *9*, 3142.

Waddington, C.H. (1940). Organisers and Genes. Camb. Camb. Univ. Press.

Wajant, H., Pfizenmaier, K., and Scheurich, P. (2003). Tumor necrosis factor signaling. Cell Death Differ. *10*, 45–65.

Wang, K.C., and Chang, H.Y. (2011). Molecular Mechanisms of Long Noncoding RNAs. Mol. Cell *43*, 904–914.

Wang, H., Xu, X., Nguyen, C.M., Liu, Y., Gao, Y., Lin, X., Daley, T., Kipniss, N.H., Russa, M.L., and Qi, L.S. (2018a). CRISPR-Mediated Programmable 3D Genome Positioning and Nuclear Organization. Cell *175*, 1405-1417.e14.

Wang, J., Shiels, C., Sasieni, P., Wu, P.J., Islam, S.A., Freemont, P.S., and Sheer, D. (2004). Promyelocytic leukemia nuclear bodies associate with transcriptionally active genomic regions. J. Cell Biol. *164*, 515–526.

Wang, P., Benhenda, S., Wu, H., Lallemand-Breitenbach, V., Zhen, T., Jollivet, F., Peres, L., Li, Y., Chen, S.-J., Chen, Z., et al. (2018b). RING tetramerization is required for nuclear body biogenesis and PML sumoylation. Nat. Commun. *9*, 1277.

Wang, X.W., Tseng, A., Ellis, N.A., Spillare, E.A., Linke, S.P., Robles, A.I., Seker, H., Yang, Q., Hu, P., Beresten, S., et al. (2001). Functional interaction of p53 and BLM DNA helicase in apoptosis. J. Biol. Chem. *276*, 32948–32955.

Wang, Z.G., Delva, L., Gaboli, M., Rivi, R., Giorgio, M., Cordon-Cardo, C., Grosveld, F., and Pandolfi, P.P. (1998a). Role of PML in Cell Growth and the Retinoic Acid Pathway. Science *279*, 1547–1551.

Wang, Z.-G., Ruggero, D., Ronchetti, S., Zhong, S., Gaboli, M., Rivi, R., and Pandolfi, P.P. (1998b). Pml is essential for multiple apoptotic pathways. Nat. Genet. *20*, 266–272.

Wei, J., Alfajaro, M.M., DeWeirdt, P.C., Hanna, R.E., Lu-Culligan, W.J., Cai, W.L., Strine, M.S., Zhang, S.-M., Graziano, V.R., Schmitz, C.O., et al. (2021). Genome-wide CRISPR Screens Reveal Host Factors Critical for SARS-CoV-2 Infection. Cell *184*, 76-91.e13.

Weidtkamp-Peters, S., Lenser, T., Negorev, D., Gerstner, N., Hofmann, T.G., Schwanitz, G., Hoischen, C., Maul, G., Dittrich, P., and Hemmerich, P. (2008). Dynamics of component exchange at PML nuclear bodies. J. Cell Sci. *121*, 2731–2743.

Wen, H., Li, Y., Xi, Y., Jiang, S., Stratton, S., Peng, D., Tanaka, K., Ren, Y., Xia, Z., Wu, J., et al. (2014). ZMYND11 links histone H3.3K36me3 to transcription elongation and tumour suppression. Nature *508*, 263–268.

Wilkinson, K.A., and Henley, J.M. (2010). Mechanisms, regulation and consequences of protein SUMOylation. Biochem. J. *428*, 133–145.

Wilson, V.G. (2017). Introduction to Sumoylation. Adv. Exp. Med. Biol. *963*, 1–12.

Wong, L.H., Ren, H., Williams, E., McGhie, J., Ahn, S., Sim, M., Tam, A., Earle, E., Anderson, M.A., Mann, J., et al. (2009). Histone H3.3 incorporation provides a unique and functionally essential telomeric chromatin in embryonic stem cells. Genome Res. *19*, 404–414.

Wright, W.D., Shah, S.S., and Heyer, W.-D. (2018). Homologous recombination and the repair of DNA double-strand breaks. J. Biol. Chem. *293*, 10524–10535.

Wu, J., and Chen, Z.J. (2014). Innate Immune Sensing and Signaling of Cytosolic Nucleic Acids. Annu. Rev. Immunol. *32*, 461–488.

Wu, J., Sun, L., Chen, X., Du, F., Shi, H., Chen, C., and Chen, Z.J. (2013). Cyclic-GMP-AMP Is An Endogenous Second Messenger in Innate Immune Signaling by Cytosolic DNA. Science *339*.

Wu, R.S., Tsai, S., and Bonner, W.M. (1982). Patterns of histone variant synthesis can distinguish G0 from G1 cells. Cell *31*, 367–374.

Wutz, A., Smrzka, O.W., Schweifer, N., Schellander, K., Wagner, E.F., and Barlow, D.P. (1997). Imprinted expression of the Igf2r gene depends on an intronic CpG island. Nature *389*, 745–749.

Xiong, C., Wen, Z., and Li, G. (2016). Histone Variant H3.3: A versatile H3 variant in health and in

disease. Sci. China Life Sci. *59*, 245–256.

Xu, C., Xu, Y., Gursoy-Yuzugullu, O., and Price, B.D. (2012). The histone variant macroH2A1.1 is recruited to DSBs through a mechanism involving PARP1. FEBS Lett. *586*, 3920–3925.

Xu, H., Kim, U.J., Schuster, T., and Grunstein, M. (1992). Identification of a new set of cell cycle-regulatory genes that regulate S-phase transcription of histone genes in Saccharomyces cerevisiae. Mol. Cell. Biol. *12*, 5249–5259.

Xu, Z.-X., Timanova-Atanasova, A., Zhao, R.-X., and Chang, K.-S. (2003). PML Colocalizes with and Stabilizes the DNA Damage Response Protein TopBP1. Mol. Cell. Biol. *23*, 4247–4256.

Yan, J., Kim, Y.-S., Yang, X.-P., Li, L.-P., Liao, G., Xia, F., and Jetten, A.M. (2007). The ubiquitin-interacting motif containing protein RAP80 interacts with BRCA1 and functions in DNA damage repair response. Cancer Res. *67*, 6647–6656.

Yang, G., Chen, Y., Wu, J., Chen, S.-H., Liu, X., Singh, A.K., and Yu, X. (2020). Poly(ADP-ribosyl)ation mediates early phase histone eviction at DNA lesions. Nucleic Acids Res. *48*, 3001–3013.

Yang, H., Wang, H., Ren, J., Chen, Q., and Chen, Z.J. (2017). cGAS is essential for cellular senescence. Proc. Natl. Acad. Sci. U. S. A. *114*, E4612–E4620.

Yang, J.-H., Choi, J.-H., Jang, H., Park, J.-Y., Han, J.-W., Youn, H.-D., and Cho, E.-J. (2011a). Histone chaperones cooperate to mediate Mef2-targeted transcriptional regulation during skeletal myogenesis. Biochem. Biophys. Res. Commun. *407*, 541–547.

Yang, J.-H., Song, Y., Seol, J.-H., Park, J.Y., Yang, Y.-J., Han, J.-W., Youn, H.-D., and Cho, E.-J. (2011b). Myogenic transcriptional activation of MyoD mediated by replication-independent histone deposition. Proc. Natl. Acad. Sci. U. S. A. *108*, 85–90.

Yang, J.-H., Song, T.-Y., Jo, C., Park, J., Lee, H.-Y., Song, I., Hong, S., Jung, K.Y., Kim, J., Han, J.-W., et al. (2016). Differential regulation of the histone chaperone HIRA during muscle cell differentiation by a phosphorylation switch. Exp. Mol. Med. *48*, e252.

Yang, S., Kuo, C., Bisi, J.E., and Kim, M.K. (2002). PML-dependent apoptosis after DNA damage is regulated by the checkpoint kinase hCds1/Chk2. Nat. Cell Biol. *4*, 865–870.

Yang, S., Jeong, J.-H., Brown, A.L., Lee, C.-H., Pandolfi, P.P., Chung, J.H., and Kim, M.K. (2006). Promyelocytic Leukemia Activates Chk2 by Mediating Chk2 Autophosphorylation *. J. Biol. Chem. *281*, 26645–26654.

Yarilina, A., and Ivashkiv, L.B. (2010). Type I Interferon: A New Player in TNF Signaling. Curr. Dir. Autoimmun. *11*, 94–104.

Ye, X., Zerlanko, B., Zhang, R., Somaiah, N., Lipinski, M., Salomoni, P., and Adams, P.D. (2007a). Definition of pRB- and p53-dependent and -independent steps in HIRA/ASF1a-mediated formation of senescence-associated heterochromatin foci. Mol. Cell. Biol. *27*, 2452–2465.

Ye, X., Zerlanko, B., Kennedy, A., Banumathy, G., Zhang, R., and Adams, P.D. (2007b). Downregulation of Wnt signaling is a trigger for formation of facultative heterochromatin and onset of cell senescence in primary human cells. Mol. Cell *27*, 183–196.

Yeager, T.R., Neumann, A.A., Englezou, A., Huschtscha, L.I., Noble, J.R., and Reddel, R.R. (1999). Telomerase-negative Immortalized Human Cells Contain a Novel Type of Promyelocytic Leukemia (PML) Body. Cancer Res. *59*, 4175–4179.

Yeung, P.L., Denissova, N.G., Nasello, C., Hakhverdyan, Z., Chen, J.D., and Brenneman, M.A. (2012). Promyelocytic leukemia nuclear bodies support a late step in DNA double-strand break repair by homologous recombination. J. Cell. Biochem. *113*, 1787–1799.

Yoon, H.-G., Chan, D.W., Reynolds, A.B., Qin, J., and Wong, J. (2003). N-CoR Mediates DNA Methylation-Dependent Repression through a Methyl CpG Binding Protein Kaiso. Mol. Cell *12*,

723–734.

Yu, Q., Katlinskaya, Y.V., Carbone, C.J., Zhao, B., Katlinski, K.V., Zheng, H., Guha, M., Li, N., Chen, Q., Yang, T., et al. (2015). DNA-Damage-Induced Type I Interferon Promotes Senescence and Inhibits Stem Cell Function. Cell Rep. *11*, 785–797.

Yu, W., Zhang, L., Wei, Q., and Shao, A. (2020). O6-Methylguanine-DNA Methyltransferase (MGMT): Challenges and New Opportunities in Glioma Chemotherapy. Front. Oncol. *9*.

Zanin, N., Viaris de Lesegno, C., Lamaze, C., and Blouin, C.M. (2021). Interferon Receptor Trafficking and Signaling: Journey to the Cross Roads. Front. Immunol. *11*.

Zhang, H., Gan, H., Wang, Z., Lee, J.-H., Zhou, H., Ordog, T., Wold, M.S., Ljungman, M., and Zhang, Z. (2017). RPA Interacts with HIRA and Regulates H3.3 Deposition at Gene Regulatory Elements in Mammalian Cells. Mol. Cell *65*, 272–284.

Zhang, R., Poustovoitov, M.V., Ye, X., Santos, H.A., Chen, W., Daganzo, S.M., Erzberger, J.P., Serebriiskii, I.G., Canutescu, A.A., Dunbrack, R.L., et al. (2005). Formation of MacroH2A-containing senescence-associated heterochromatin foci and senescence driven by ASF1a and HIRA. Dev. Cell *8*, 19–30.

Zhang, T., Cooper, S., and Brockdorff, N. (2015a). The interplay of histone modifications – writers that read. EMBO Rep. *16*, 1467–1481.

Zhang, Y., Mao, D., Roswit, W.T., Jin, X., Patel, A.C., Patel, D.A., Agapov, E., Wang, Z., Tidwell, R.M., Atkinson, J.J., et al. (2015b). PARP9-DTX3L ubiquitin ligase targets host histone H2BJ and viral 3C protease to enhance interferon signaling and control viral infection. Nat. Immunol. *16*, 1215–1227.

Zhao, H., and Piwnica-Worms, H. (2001). ATR-mediated checkpoint pathways regulate phosphorylation and activation of human Chk1. Mol. Cell. Biol. *21*, 4129–4139.

Zhao, Y., and Garcia, B.A. (2015). Comprehensive Catalog of Currently Documented Histone Modifications. Cold Spring Harb. Perspect. Biol. *7*, a025064.

Zharkov, D.O. (2008). Base excision DNA repair. Cell. Mol. Life Sci. *65*, 1544–1565.

Zheng, S., Li, D., Lu, Z., Liu, G., Wang, M., Xing, P., Wang, M., Dong, Y., Wang, X., Li, J., et al. (2018). Bre1-dependent H2B ubiquitination promotes homologous recombination by stimulating histone eviction at DNA breaks. Nucleic Acids Res. *46*, 11326–11339.

Zhong, S., Hu, P., Ye, T.-Z., Stan, R., Ellis, N.A., and Pandolfi, P.P. (1999). A role for PML and the nuclear body in genomic stability. Oncogene *18*, 7941–7947.

Zhong, S., Müller, S., Ronchetti, S., Freemont, P.S., Dejean, A., and Pandolfi, P.P. (2000). Role of SUMO-1–modified PML in nuclear body formation. Blood *95*, 2748–2752.

Zhu, J., Zhou, J., Peres, L., Riaucoux, F., Honoré, N., Kogan, S., and de Thé, H. (2005). A sumoylation site in PML/RARA is essential for leukemic transformation. Cancer Cell *7*, 143–153.

Zindel, J., and Kubes, P. (2020). DAMPs, PAMPs, and LAMPs in Immunity and Sterile Inflammation. Annu. Rev. Pathol. Mech. Dis. *15*, 493–518.